CR-181503

HELICOPTERS
SELECTION OF DESIGN PARAMETERS

by

M. N. Tishchenko, A. V. Nekrasov, A. S. Radin

(NASA-CR-181503) HELICOPTERS: SELECTION OF DESIGN PARAMETERS (International Technical Associates) 294 p

N90-70426

Unclas
00/05 0121600

Edited and prepared for publication by W.Z. Stepniewski and W.L. Metz, International Technical Associates, Ltd. for U.S. Army Research & Technology Laboratories (AVRADCOM), Ames Research Center, under Contract No. NAS2-10062, April, 1979.

Mashinostroyeniye Press
Moscow, 1976

#121600

ANNOTATION

GENERAL REMARKS

The team of Mrs. Wanda L. Metz and the undersigned, representing international Technical Associates, Ltd., was awarded a contract, through NASA, by the U.S. Army Research and Technology Laboratories (AVRADCOM), Ames Research Center, to prepare for publication, both editorially and graphically, a translation of a book entitled *Helicopters, Selection of Design Parameters,* by M.N. Tishchenko, et al. In addition to the above task, a brief general evaluation of the book was to be made—examining its potential usefulness to the Western and especially, the American reader, and giving an example of Soviet vs. Western (US) approach to design methodology by concentrating attention on a particular selected problem.

A rough draft of the translated text plus a copy of the original book was supplied by the Contracting Agency. Using this draft as a basis, the text was prepared; attempting to obtain as much as possible, a presentation in conversational English, but with minimal deviations from the original style and format. Practically all the original main symbols were retained. However, subscripts and superscripts were anglicized in order to retain their descriptive character. Symbols denoting metric units were standardized with the exception that the symbol *kg* is used to signify kilogram of force (*kg = 9.8N*), and not a unit of mass, as is customarily the case. The word *ton* refers to a unit of force. This was done for the sake of simplicity since, throughout the text, *kilogram* and *ton* are uniquely used with reference to units of force, and thus, there was no necessity to use separate symbols for the kilogram-mass vs kilogram-force, and ton-mass vs. ton-force.

A considerable interest in the project was shown by Dr. R. Carlson, Director of the R&T Laboratories, as well as by Messrs W. Mosher of the Advanced Systems Research Office, who served as technical monitor of the project and F. Immen, Chief of that office, who was instrumental in making the publication of this text a reality. Thanks and appreciation are also extended to Colonel C.J. Reeder (Director) and Mr. E.R. McInturff of AFSTC in Charlottesville, for their interest and support. To these gentlemen, as well as the many others who contributed their valuable technical remarks and comments, we wish to express our sincere gratitude.

REVIEW OF TEXT AND TECHNICAL COMMENTS

The first impression one gets from glancing through the book is the abundance of up-to-date data and current technical information on Westers (especially American) designs; including the UTTAS, HLH, and S-63, which clearly points out the close surveillance by the Soviet of foreign technology. However, there is also an almost equivalent amount of data on Soviet transport designs (mainly, the Mil' family).

In spite of this abundance of reference to Western technology, the undersigned believes that the material presented here should generate interest in the technical community of the West; not only as a source of documentation reflecting the thinking of the representatives of the Soviet block, but also because of the technical merits of the book. This, in spite of the fact that one may not necessarily agree with all the presented approaches, ground rules, and the authors' ranking of the compared configurations of transport rotary-wing aircraft.

As to the scope of its appeal, this book should also be of interest and help to members of organizations responsible for the development of new types and systems of rotary-wing aircraft and preparation of their basic specifications. As a matter of fact, it perhaps should constitute a "must reading" for this particular group, as well as being of definite assistance to designers engaged in the rotary-wing aircraft industry. Finally, it should also provide useful material in teaching design courses on an academic level. This broad range of application and potential interest can be justified by a brief review of the individual chapters.

Chapter 1, dealing with establishing proper criteria for evaluating the effectiveness of rotary-wing aircraft and optimization of design parameters, reflects the well-known difficulties and frustrations encountered by students of this subject in their search toward finding an all-encompassing criterion that, on one hand, could serve as a yardstick for measuring "complete" superiority of a given type or variant of aircraft; while on the other, when applied to the selection of optimal design parameters, would lead to practically-manageable mathematical models.

It is interesting to note that similar to the Western approach, the representatives of the Soviet economy also came to the conclusion that the overall life-cycle cost of a helicopter system as represented by development and system life-long operation expenditures represents a significant criterion. This is especially true in those cases when the whole system for both military and civilian machines as in the case of the Soviets; or for military machines as in the case of the West, is financed from "cradle to grave" by a single customer (the government).

Unfortunately, both the Soviet authors and those in the West realize that translation of this criterion into a rigorous analytical tool of design parameter optimization is impractical, as this would require an overly complicated mathematical model. Consequently, in the concept-formulation and preliminary design phases, some simpler special (specific) criteria must be applied. After reviewing several approaches, the authors indicate that maximizing payload for a given range (at constant gross weight) should provide a guide for the design of transport machines. This can be supplemented with productivity criteria. Separate standards are given for crane and agricultural helicopters.

Chapter 2, encompassing over 50 percent of the text, is devoted to showing how optimum parameters (chiefly main-rotor radius and number of blades) are selected through use of the maximum-payload criterion for transport pure and compound helicopters, and how various configurations of the machines can be ranked with respect to that criterion.

To achieve this goal, methods of weight estimation of the major components are presented first. These are interesting considerations, as they point out some design philosophies which may be either somewhat different from those in the West, or simply not so strongly emphasized. One example in this respect is the authors' recommendation that the Lock number (referred to here as the blade mass characteristic) should be $\gamma_o \equiv c_y{}^a \rho_o b_{0.7} R^4/2I_{f.b} \leqslant 7.0$; preferably no higher than $\gamma_o \approx 4.0$ to 5.0.

In the above expression, $c_y{}^a$ = the lift-curve slope, ρ_o = air density at sea level, $b_{o.7}$ = blade chord at 0.7 blade radius, R = blade radius, and $I_{f.b}$ = blade moment of inertia about the flapping hinge.

With respect to the weight-prediction formulae for all major components, the differences between those presented in the book and those used in the West may be expected. One case of such difference is discussed later on an example of the main-rotor hub weights.

In the optimization process, especially when selecting an optimal variant of a given aircraft, prediction of the relative component weight variation with respect to some baseline version, may be more important than an accurate determination of the absolute weight. This method of comparing weights is widely used throughout the book.

Again it is interesting to note the level of convergence between "their" and "our" predictions in that respect. The previously-mentioned example of main-rotor hub weights will indicate that differences in this area may also be encountered.

In almost every engineering design optimization process, one encounters various constraints. Those related to the rotary-wing design are thoroughly discussed in Chapter 2. Attention should be called to the following quantities.

Disc Loading. Maximum values of disc loading recommended by the authors are shown in Table A-1. One would notice from this table that, in general, the limits are similar to those used in the West, although in the transport category, they appear higher than their Western counterparts.

TYPE OF HELICOPTER	MAXIMUM DISC LOADING	
	kg/m^2	*psf*
TRANSPORT *(no people on the ground or in the downwash)*	70 – 80	14.3 – 16.4
CRANES	50 – 60	10.2 – 12.3
RESCUE & UTILITY	30 – 35	6.1 – 7.2
TWIN-ROTOR CONFIGURATIONS	45	9.2

Table A-1 Maximum Permissible disc loading

Bevel-Gear Capacity. The authors indicate that the maximum power transmitted by a pair of bevel gears should not exceed 8000 hp which, assuming six driving gears (see Fig 2.53), establishes a 48 000-hp limit for power transmitted to a single rotor. This also leads to the necessity of using two synchronizing shafts in tandem helicopters of the 44 to 60-ton gross-weight class (Fig 2.57), and establishes a maximum installed power of 28 000 hp for this configuration. The authors realize that these power limits have been exceeded (10 600 hp per pair) in such Western projects as the HLH of Boeing Vertol; nevertheless, they believe that a degree of conservatism in that respect represents a sound design philosophy.

Shaft rpm. Maximum allowable shaft rpm represents another aspect of design conservatism advocated by the authors. They establish $n_{shaft} \leqslant 3000\ rpm$ as a constraint for helicopter shafts. This obviously places the tandem configurations at a disadvantage, where about one-half of the power developed by the engines is continuously transmitted through the synchronizing shafts. Here, again, the authors are aware that in such tandems as the Chinook, the sync shafts operate up to 7000 rpm (Fig 2.17), and in the HLH, go as high as 8000 rpm (Fig 2.55); nevertheless, they believe that accepting the 3000 rpm limit is a sound design policy, as it permits one to use grease-lubricated bearings.

As far as other constraints are concerned, much attention is devoted to limits to the maximum permissible rotor overlap (both for tandem and side-by-side configurations) as imposed by the blade-strike possibility.

Maximum permissible static blade droop as limited to 12 percent of the blade radius appears noncontroversial. Also, the most often recommended rotor thrust coefficient in hovering at sea level std, $t_{y_o} \equiv T/\frac{1}{2}\rho U_t^2 \sigma \pi R^2 \approx 0.155$, which corresponds to the average lift coefficient of $\bar{c}_{l_b} \approx 0.465$, seems close to the levels used in successful Western designs.

The section, *Determination of Data Required for Calculating Structural Weight and Selection of Helicopter Parameters* contains detailed considerations regarding the determination of wing area for side-by-side helicopters.

It should be noted that this particular configuration in the pure helicopter as well as in the compound version receives considerable attention throughout the whole text, and contains many interesting technical inputs, revealing that the authors must have directly participated in the development of this type of rotary-wing aircraft.

As far as the aerodynamics of the tandem is concerned, it appears that a high degree of agreement exists between the authors' and the Western approach, as exemplified by Figure A.1. A graph giving the thrust losses due to overlap as predicted by the authors is reproduced on the left side of the figure; while U.S. data is shown on the right. A comparison of the graphs indicates very close agreement. Also, the aerodynamic rotor-interference aspects in forward flight, as illustrated in Figure 2.65 appear to be in general agreement with theoretical and experimental Western data (see Section 6 of Chapter I of Reference 1).

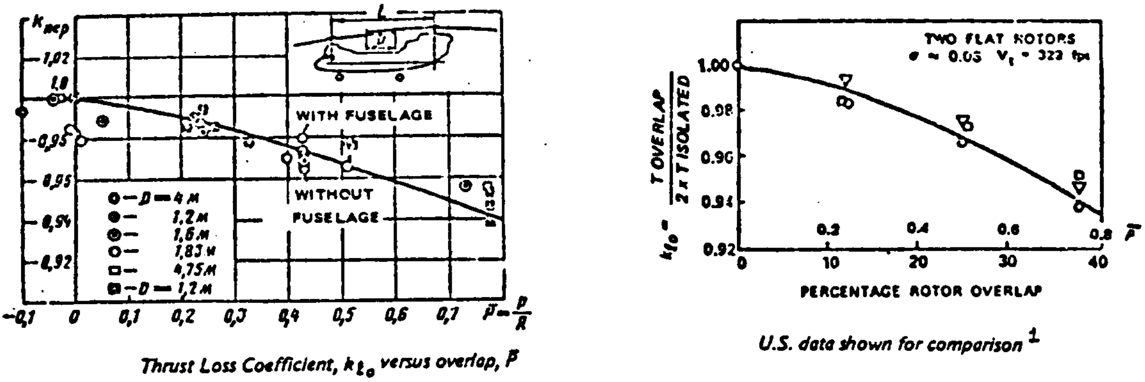

Thrust Loss Coefficient, k_{t_0} versus overlap, $\bar{\rho}$

U.S. data shown for comparison 1

Figure A.1 Comparison of graphs showing thrust losses due to overlap

The section, *Comparison of Different Helicopter Configurations and Selection of Optimal Main-Rotor Diameter and Number of Blades* is probably the most controversial, especially as far as ranking various transport helicopters is concerned.

The authors indicate that in all of the considered gross-weight classes (12–24, 44–60 tons, and very-heavy-lift rotary-wing aircraft up to 160-ton gross weight), single-rotor configurations (both pure and compound helicopters) are better regarding payload-carrying capability than the side-by-side types, and decisively superior to the tandems. This ranking is supposed to be true for very short (50-km), as well as to quite long (800 km) ranges.

It would be interesting to run a study in order to determine whether the tandem is hurt more than other configurations by such conservative assumptions as the restriction of shaft speed to 3000 rpm, and limitation of power transmitted through a pair of bevel gears to 8000 hp, and whether the ranking would remain the same after removing these restrictions.

The reader interested in compound helicopters will find valuable material at the end of Chapter 2, where these configurations are compared with pure and winged helicopters on the basis of productivity. Here, one would probably find little opposition to the authors' statement that the single-rotor type represents the most advantageous configuration for the compound helicopter

From the amount of space devoted to the subject, one gets the impression that the Soviets are definitely interested in the application of the compound helicopter configuration to heavy transports of the 50-ton weight class, which is justified by a slightly higher productivity when compared with pure helicopters (Fig 2.113), in spite of the obviously lower payload capability of the compound (Figure 2.109).

Chapter 3 is devoted to the analysis of technological factors (strength aspects, and practically possible minimal gages) influencing the blade weight, and this enables one to determine minimum obtainable blade weight. It is interesting to note that in the course of whole analysis, only two design load sources are considered: (a) the blade centrifugal force, and (b) blade weight. It is here again emphasized that having the blade mass characteristic (Lock number) $\gamma_o \leqslant 4.0$ is one of the best ways to assure dynamically undisturbed operation (free of aeroelastic instability) of the rotor throughout all regimes of flight. Consequently, a conflict may arise between the desire to achieve the lowest possible structural blade weight, and striving for a "heavy" blade as dictated by the $\gamma_o \leqslant 4.0$ requirement.

The authors advise that the blade designer should always try to achieve the lowest possible structural weight; even if this may lead to a higher γ_o value than desired. (Means other than increasing the weight should be found to cope with the dynamic problems.)

Although only blades with steel tubular and extruded aluminum D-spar and fiberglass boxes are considered in this chapter, the presented methodology can be applied to other blade designs as well.

Chapters 4 and 5, dealing with the economics of helicopter development and operation, are especially recommended to the designers of rotary-wing aircraft who, in their creative efforts, sometimes ignore, or forget, about the cost aspects of their decisions.

It should be noted that the Soviet authors appear to be as cost-conscious as procuring agencies and private operators in the West, and try to transmit their message to the designers. In that endeavor, they use an abundance of Western data, and even quote, in English, such slogans as "Design to cost or all is lost."

Chapter 4 is devoted to methods of calculating helicopter costs. Here, upon reviewing some existing approaches, the authors, probably rightly, came to the conclusion that the most reliable method of predicting cost per kg of a component destined for series production would consist of comparing it with that of another production component performing the same function, but which otherwise could be produced under different conditions and show complete dissimilarity in design. It is only necessary to properly account for those differences through suitable "economic" and "design peculiarity" coefficients. The economic coefficient would reflect such aspects as production facilities, labor and material costs, etc., while the design peculiarity coefficient would reflect such differences as number of parts per kg of component weight and manufacturing tolerances. Further improvement is achieved in this realm of design differences by taking into consideration the machined surfaces of new and baseline components.

Knowledge of the manufacturing cost of new components permits one to calculate their replacement cost as well as that of the helicopter as a whole.

The cost of major overhauls is computed similarly to that of manufacturing. Methods for calculating the cost of scheduled maintenance and technical servicing are also given. All this, together with data on the cost of fuel and lubricants plus the flight-crew wages provides the necessary inputs for estimating the direct operating cost. Thus, the influence of design parameter values on direct operating cost can be examined.

The helicopter designer, through his decisions in selecting design parameter values, exercises very little influence as far as indirect operating cost is concerned. The only exception may be the insurance cost which would increase with the number of new technical solutions intorduced into the design.

In Chapter 5, the methods presented in Chapter 4 are used to select helicopter parameters according to the minimum-cost criterion.

Finally, selection of optimal cargo-transport helicopter parameters based on minimum cost per ton-kilometer is compared with that attempting to maximize the payload transported over a given distance.

The fact that the helicopter having the highest payload-to-gross-weight ratio is not necessarily the one having the lowest cost per ton-km is shown on the example of cost vs gross weight at constant payload given in Figure 5.22.

At the conclusion of this brief review of the text, it should once more be emphasized that in the design optimization process, two parameters only; namely, rotor radius and number of blades were considered. Other quantities which come to one's mind as potential control variables such as rotor tip speed, blade planform and twist, and airfoil characteristics were assumed as invariable. (Deviation of tip speed from the standard value of $U_{t_o} = 220\ m/s$ were only reflected through proper correction factors.)

This limitation of the number of parameters definitely has the advantage of simplicity and ease of presentation of the results as simple graphs. Students of optimization who struggled to imagine and somehow represent a search for an optimum in a multi-dimensional space would definitely appreciate the simplicity of dealing with two parameters only. However, on the other hand, it would be interesting to find out, even on some selected samples only, to what extent the introduction of other design parameters as independent variables would modify the previously obtained results.

COMPARISON OF ROTOR-HUB WEIGHT TRENDS

Rotor-hub weight trends were selected to provide an example for a comparison of Tishchenko's et al structural weight prediction methods with those used in the West, as represented by a procedure described by R. Swan of Boeing Vertol[2].

In the latter approach, it is assumed that the dimensions of a hub and hence, its weight, are governed by the magnitude of the following forces and moments: (1) blade centrifugal force, N_{bl}, (2) rotor thrust, T, (3) hub (overturning) moment, M_{hub}, and (4) rotor torque, M_Q.

Starting with these premises, the functional relationships between the forces and moments, and various helicopter design and operational parameters are studied, and representative trend parameters indicated (Table A-II).

LOAD	REPRESENTATIVE TREND PARAMETERS
$N_{bl} \sim G_{bl}\bar{r}_{c.g}\, n^2$	G_{bl}, R, n
$T \sim U_t^2 A_{bl}$	n, R, z_{bl}, b
$M_Q \sim HP_R/n$	HP_R, n
$M_{hub} \sim N_{bl}\beta e$	G_{bl}, R, n

TABLE A-II Significant loads and their representative parameters

This would lead to an assumption that the weight of the hub can be expressed as a function of the product of those parameters whose importance is reflected by the power to which each of the parameters is raised:

$$G_{hub} = f(G_{bl}^a \cdot R^b \cdot n^c \cdot HP_R^d \cdot z_{bl}^e \cdot r^f \cdot const) \qquad (A.1)$$

where, using Tishchenko's notations, G_{bl} = blade weight, n = rotor rpm, HP = horsepower transmitted to the rotor, z_{bl} = number of blades, and r = hub radius.

The slope of the line along which statistical points are gathered would indicate the power to which the expression in the parentheses of Eq (A.1) should be raised.

As a result of this approach, the following formula for the hub weight was obtained:

$$G_{hub} = 61(G_{bl}\, Rn^2\, HP_R\, z_{bl}^{1.5} r^{1.82} \cdot 10^{-11})^{0.358}. \qquad (A.2)$$

Although Eq (A.2) well represents the general trend of the hub weight, there are still some hubs whose actual weight significantly differ from that given in the equation. Swan and his coworkers suspected that those discrepancies may have stemmed from such factors as (1) difference in materials, (2) design approach, and (3) stage of development. To take these factors into account, a special k_{mad} factor was introduced into the equation:

$$G_{hub} = 61(G_{bl}\, Rn^2\, HP_R z_{bl}^{1.5}\, r^{1.82} k_{mad} \cdot 10^{-11})^{0.358}. \qquad (A.3)$$

With this innovation, the agreement between the predicted and the actual hub weights became quite satisfactory as the standard deviation was less than 4.5 percent.

Tishchenko's et al approach was different. They assumed that designing load sources could be limited to the blade centrifugal force (N_{bl}) and its bending moment expressed as $N_{bl}e$.

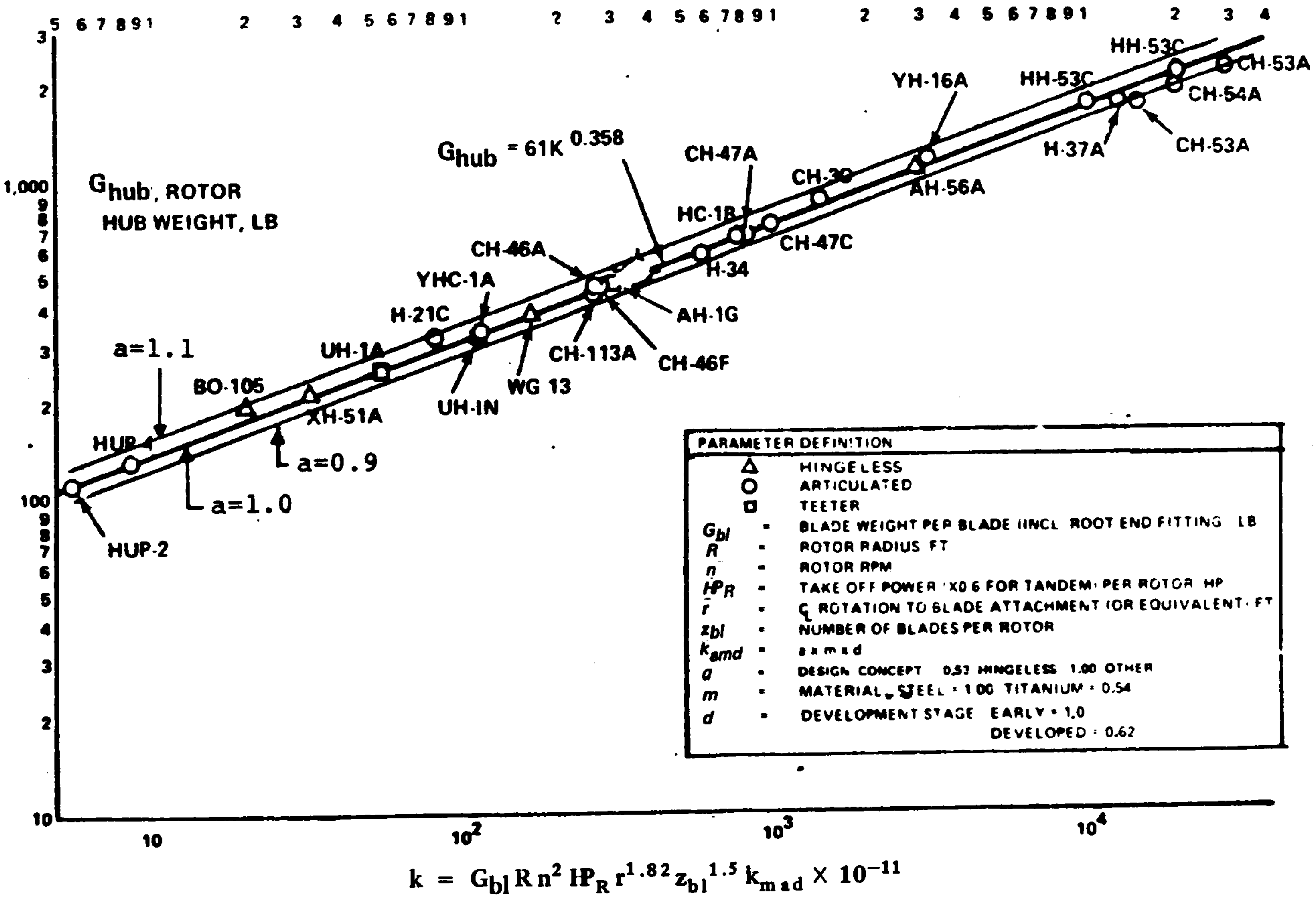

Figure A.2 Rotor hub weight trend[3]

The weight of the hub arm should be proportional to the magnitude of centrifugal force and arm radius, r:

$$G_{arm} \sim N_{bl} r. \tag{A.4}$$

Furthermore, it was indicated that for classical articulated rotor hubs with closely located hinges, $r \sim \sqrt{N_{bl}}$; thus Eq (A.9) can be rewritten as

$$G_{arm} \sim (N_{bl})^{3/2}. \tag{A.5}$$

Assuming that the weight of all hub arms will be a multiple of the number of blades while the weight of the hub center-body can be taken as a fixed fraction of the arm weight, it becomes clear that

$$G_{hub} \sim z_{bl} (N_{bl})^{3/2}. \tag{A.6}$$

Realizing that the influence of the number of blades may actually be more involved than straight proportionality, the authors introduced a special correction factor for $z_{bl} \geqslant 4$, thus obtaining the following expression for the hub weight:

$$G_{hub} = k_{hub} [1 + 0.05(z_{bl} - 4)] z_{bl} (N_{bl})^{3/2} \tag{A.7}$$

where k_{hub} is the coefficient of proportionality, whose value represents a very large scatter (see Fig 2.7).

To account for the fact that because of the necessity of maintaining some minimum wall thickness of the hubs designed for lower centrifugal forces and consequently, that such hubs are relatively heavier, an exponent of 1.35 instead of 3/2 was suggested. Now, the proposed expression for the hub weight becomes

$$G_{hub} = k^*_{hub} [1 + 0.05(z_{bl} - 4)] z_{bl} (N_{bl})^{1.35}. \tag{A.8}$$

While k^*_{hub} values computed using Eq (A.8) still represent a considerable scatter (see Fig 2.8), when comparing Eqs (A.3) and (A.8), one would notice that the product of $G_{bl} R n^2$ in Eq (A.3) actually represents the blade centrifugal force; assuming the location of the blade c.g. at the same relative blade radius $\bar{r}_{c.g} = const:$

$$N_{bl} \sim G_{bl} R n^2 .$$

However, the degree of influence of the blade centrifugal force on the hub weight will be weaker according to Boeing Vertol formulae $(N_{bl}{}^{0.358})$ than in Tishchenko's approach where $(N_{bl}{}^{1.35})$.

Also, the influence of the number of blades will be different in the two compared approaches, as indicated by the exponent of 0.539 for z_{bl} in Eq (A.3) vs z_{bl} to the first power (at least, for $z_{bl} \leqslant 4$ in Eq (A.8). Furthermore, the hub radius does not appear explicitly in

Eq (A.8), but only through the change in the N_{bl} exponent, while the influence of the rotor power is not taken into account at all. Anything similar to the k_{mad} coefficient in Eq (A.3) is also absent in Tishchenko's approach.

From the above discussion of an example of rotor-hub weight estimates, it is apparent that considerable differences in basic philosophy in the development of weight prediction methods exist between Boeing Vertol's and Tishchenko's approaches.

However, without specific detailed numerical calculations, it is impossible to pinpoint how large the differences in the predicted hub weights would actually be.

In the design optimization process, it may be more important to correctly indicate the relative weight change of the component as the considered parameters are varied than to precisely determine the weight of a particular helicopter component as a function of design parameters. Since in this book both the blade radius and the number of main-rotor blades are considered as the most important design parameters, it would consequently be interesting to compare how the Boeing Vertol and Tishchenko methods predict changes of the main-rotor hub weight referred to some baseline value, as either z_{bl} or R are independently varied, while other parameters remain constant.

To illustrate this problem, variation of the hub weight ratio (G_{hub_n}/G_{hub_o}) will be investigated:

$$(G_{hub_n}/G_{hub_o}) = f(z_{bl_n}/z_{bl_o}). \tag{A.9}$$

The problem will be simplified by assuming that $z_{bl_o} N_{bl_n} = z_{bl_n} N_{bl_n}$ and $z_{bl_o} G_{bl_o} = z_{bl_n} G_{bl_n}$, while all other parameters appearing in Eq (A.3) and (A.8) remain constant.

Under the above assumption, the ratio expressed by Eq (A.9) according to the Boeing Vertol method will be

$$(G_{hub_n}/G_{hub_o})_{B.V} = (z_{bl_n}/z_{bl_o})^{0.179} \tag{A.10}$$

and, according to Tishchenko et al,

$$(G_{hub_n}/G_{hub_o})_T = [1 + 0.05(z_n - 4)]\,(z_{bl_o}/z_{bl_n})^{0.35}. \tag{A.11}$$

It can be seen from the above formulae, as well as from Fig (A.3) that under the assumed conditions, the trends of relative hub weight variation with number of blades predicted by the Boeing Vertol method and that by Tishchenko et al are completely different.

To further investigate this relative-weight trend problem, the influence of the blade radius variation at $z_{bl} = const$ was examined.

Again, in order to simplify the problem, in Eq (A.3) it was assumed that all the parameters except R, and G_{bl} as influenced by R, remain constant; while in Eq (A.8), only the influence of R on N_{bl} is taken into consideration.

Assuming, for simplicity, that rotor solidity $\sigma = const$, as well as tip speed $U_t = const$, and that the relative radius of the blade c.g. position also remains $\bar{r}_{c.g} = const$. Then $n_n = n_o(R_o/R_n)$, while $N_{bl_n} = N_{bl_o}(R_o/R_n)$.

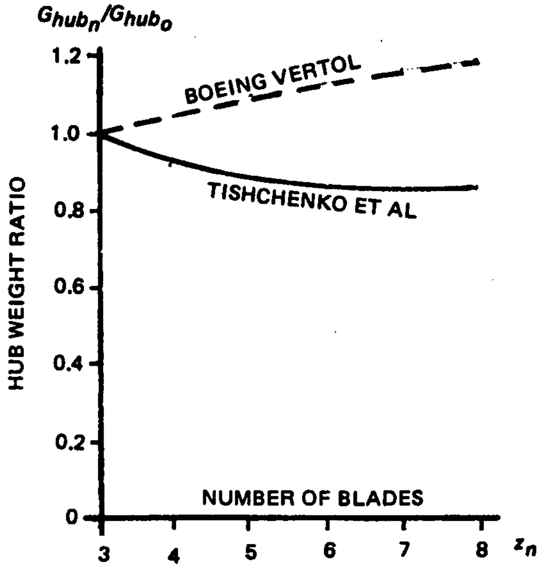

Figure A.3 Variation of the hub-weight ratio with the number of blades as predicted by the Boeing Vertol and Tishchenko methods

Consequently, the relationship $(G_{hub_n}/G_{hub_o}) = f(R_n/R_o)$, according to Eq (A.3) will be expressed as

$$(G_{hub_n}/G_{hub_o})_{V.B} = (R_o/R_n)^{0.358} \tag{A.12}$$

and, according to Eq (A.3), as

$$(G_{hub_n}/G_{hub_o})_T = (R_o/R_n)^{1.35} \tag{A.13}$$

The results of the calculations according to Eqs (A.12) and (A.13) are plotted in Fig A.4; this time, showing there is an agreement between the two approaches regarding the sign of the relative increment, but the slope of these variations as predicted by Tishchenko et al is much steeper than that anticipated by the Boeing Vertol method.

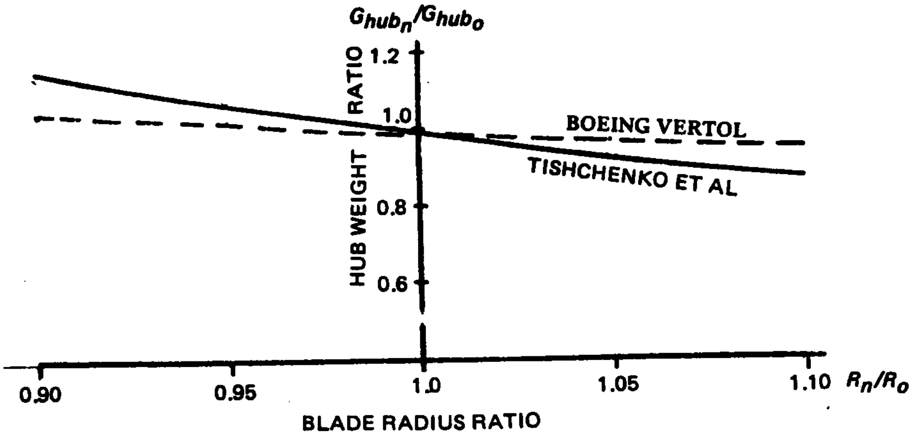

Figure A.4 Variation of the hub-weight ratio with the rotor-blade radius as predicted by the Boeing Vertol and Tichenko methods

These results further illustrate the previously made statement regarding the essential differences in the weight-prediction formulae between the Tishchenko et al approach and those developed by Boeing Vertol, and point out the need for deeper studies required to resolve which of the two approaches better reflects a reality.

CONCLUDING REMARKS

1. The book by Tishchenko et al provides a valuable insight into the Soviet design philosophy of rotary-wing aircraft and especially, transport helicopters and compounds.
2. The presented material covers a broad range of design aspects and thus, may be of direct use to the practicing engineer in both industrial and government organizations. It may also form a basis for academic courses on the design of rotary-wing aircraft.
3. In the book, there are many opinions and approaches to which one may take exception. However, since the book was written by true professionals in their fields, the encountered controversies should not be rejected, but should serve as a stimulus for further study, and a deeper insight into the discrepancies.
4. It appears, hence, that the reviewed text should be of genuine interest to the Western technical community and may be recommended as desirable reading.

REFERENCES

1. Stepniewski, W.Z. *Rotary-Wing Aerodynamics.* Vol I, NASA CR 3082, January 1979.

2. Swan, R.H. *Rotary-Wing Head Weight Prediction.* Paper No 914, presented at the 31st Annual Conference of the Society of Aeronautical Weight Engineers, Atlanta, Ga. 22-25 May 1972.

3. Davis, S.Jon and Wisniewski, J.S. *User's Manual for HESCOMP - The Helicopter Sizing and Performance Computer Program.* First Revision, U.S. Navy Contract N62269-74-C-0757 (HESCOMP Modified to Enable Analysis of Advanced Helicopter Configurations), September 1973.

W. Z. Stepniewski
Upper Darby, Pa.
April 23, 1979

FOREWORD

The areas of application of helicopters in the national economy of the USSR are broadening every year. Cargo transportation into remote regions, regular ferrying of oil workers to offshore drilling platforms, servicing geological parties, transporting passengers, construction and assembly operations, and many other types of work are performed by hundreds of these irreplaceable machines. The volume of operations performed by these vehicles is increasing each year. The constantly expanding field of rotary-wing applications is largely due to the geographic peculiarities of the USSR; and the scope of construction in both new and as yet undeveloped regions makes it possible to consider that the role of these vehicles will continue to grow steadily in the national economy. At the same time, the broad usage of helicopters leads to a situation in which construction and operation of rotary-wing aircraft on a national scale are becoming appreciable.

Because of this, the problem of improving helicopter efficiency is extremely vital and, in turn, requires a particularly careful approach to the selection of optimal parameters of new designs. The rational determination of the basic parameters of any new means of transport has always been difficult. Such selection of the parameters is particularly important in the case of flight vehicles where weight increases resulting from nonoptimal dimensions or improper design of particular components increases the gross weight (or reduces the payload that can be carried). In many cases, this leads to a significant over-expenditure of funds for mass production and subsequent operation of the fleet of such vehicles within the national economy.

The problem of developing an optimal flight vehicle is solved by simultaneous design of several variants from which is selected a compromise representing, on one hand, that which is desired while on the other, the feasibility of realization within acceptable time periods with available funds and manpower.

In selecting the final design variant of the project, the designer must take into account all the various requirements and considerations, the most important of which are as follows: meeting specified requirements for performance and payload with minimal gross and structural weights, assurance of the required structural strength and reliability, stability and control of the aircraft, safety in flight, degree of complexity of the problems that must be resolved, risk level of not meeting the specification because of previously unforeseen circumstances, and degree of complexity of manpower required in the design and manufacture of the flight vehicle; also the cost of production, operational aspects, and especially, ease of maintenance and economic efficiency of the aircraft.

At the present time, a large part of the above-mentioned problems can be examined with some degree of confidence on the basis of analytical methods which have been developed and introduced into practice. However, there still exists a series of problems and resulting tasks which cannot be solved through calculations, but can only be evaluated on the basis of knowledge, experience, and the general background of the design team. In this work, an attempt is made to interrelate the various individual problems and, using mathematical methods directed toward the use of computers, outline ways leading to optimization of the design.

The problems have not been examined in an integrated manner in either the Soviet or foreign literature to date. Therefore, the authors hope that this book will be useful to those engaged in the design ansd evaluation of new helicopters.

Chapter 1 was written by M.N. Tishchenko, Chapters 2 and 3 by A.V. Nekrasov, and Chapters 4 and 5 by A.S. Radin. The comparison of the various helicopter versions presented in Chapter 2 was based on calculations by V.G. Pashkin. The analysis and systemization of the various helicopters were performed by V.V. Kronshtadtov, L.A. Samoilov, and V.P. Nefedov. Several valuable suggestions were made by our reviewer, R.A. Mikheev. In addition, L.N. Mazure, A.I. Groznova, G.I. Zakharova, T.V. Raivich, G.P. Kuz'minova, G.N. Deleikina, S.N. Gurova, and S.D. Fedina assisted in the calculations and also the preparation of the manuscript. The authors wish to express their thanks to all these individuals.

CONTENTS

Page

Foreword iii

1 CRITERIA FOR EVALUATING HELICOPTER EFFECTIVENESS AND OPTIMIZING HELICOPTER PARAMETERS

1.1 Classification of Effectiveness Criteria 1
1.2 Functional Effectiveness 2
1.3 Production Effectiveness 17
1.4 Operational Effectiveness 19
1.5 Economic Effectiveness of Helicopter Operation 21
1.6 National Economic Effectiveness 22
1.7 Fields of Application of Criteria at the Various Levels 23

2 SELECTION OF OPTIMUM TRANSPORT HELICOPTER PARAMETERS AND CONFIGURATION BASED ON MAXIMUM USEFUL (TRANSPORTED) LOAD

2.1 Introduction 27
2.2 Weight Analysis Formulae and Brief Justification of Helicopter Weight Determination of Basic Components and Systems 28
2.3 Some Constraints Encountered in Design 89
2.4 Determination of Data Required for Calculating Structural Weight, and Selection of Design Parameters 110
2.5 Comparison of Different Helicopter Configurations, Selection of Optimal Main-Rotor Diameter and Number of Blades 124
2.6 Comparison of Pure and Compound Transport Helicopter 148

3 ANALYSIS OF WEIGHT-CONTRIBUTING STRUCTURE AND CALCULATIONS OF STRUCTURAL-TECHNOLOGICAL WEIGHT OF LIFTING-ROTOR BLADES

3.1 Some Relations Concerning Blade Weight 174

4 SOME METHODS FOR CALCULATING HELICOPTER COSTS

4.1 Helicopter Production Costs 198
4.2 Estimating Direct Operating Costs 221
4.3 Training Flight Costs. Airport and Other Costs 234

5 OPTIMAL HELICOPTER PARAMETER SELECTION BASED ON MINIMAL COST CRITERIA

5.1 Replacement Cost Dependence on Helicopter Parameters 238
5.2 Dependence of Direct and Indirect Costs on Helicopter Parameters 265
5.3 Selection of Optimal Cargo Transport Helicopter Parameters Based on Minimum Cost per Ton-Kilometer 269

References 281

1

CRITERIA FOR EVALUATING HELICOPTER EFFECTIVENESS AND OPTIMIZING HELICOPTER PARAMETERS

1.1 Classification of Effectiveness Criteria

The most universal and general criterion for gaging application effectiveness of a flight vehicle is the relationship between the useful work done by the vehicle and the overall cost of developing and operating such a machine.

However, it is not always possible to make such a broad evaluation of a flight vehicle under development. Therefore, in order to evaluate a new project, both specific and general criteria are applied.

From the practical experience of design offices and purchasing organizations, a system of ideas (concepts) and criteria has been developed, and is presently available for evaluation of the effectiveness of the considered projects. Several studies devoted to the development and justification of the effectiveness of methods for evaluating flight vehicles, primarily airplanes, have been published. These problems have been examined most completely in the works of V.M. Sheynin[20], A.A. Badyagin and E.A. Ovrutskiy[2], A.V. Glichev[6], S.A. Sarkisyan and E.S. Minaev[18], along with several other authors.

Comparisons of various flight vehicles through the application of the most general, as well as specific, criteria still does not permit one to reach a final conclusion as to which is the best flight vehicle. This is due to the fact that quite often these criteria do not evaluate certain features of the given machine being of definite operational value for the users; thus representing very important characteristics of an aircraft.

For example, one can not make a comparison between airplanes and helicopters on the basis of ton-km cost. The ability of the helicopter to take off vertically and perform many operations in the hover regime may be very important to the user, and this makes it an irreplaceable flight vehicle in spite of the fact that the cost per ton-km is higher than that of the airplane.

The same applies to the compound helicopter which has a higher flight speed than the pure helicopter even though the costs of performing transport operations are greater. Furthermore, the criteria normally used do not consider the advantages of a configurational nature nor particular features of the layout; for example, cargo-loading convenience and low-vibration level in the cockpit for helicopters of the side-by-side configuration.

Thus, a decision regarding the use of these or other criteria should be made within a group of vehicles destined for the same mission and operating under similar conditions.

Examining the presently-used specific criteria or methods of evaluation, we will group them on three levels similar to the approach taken by V.M. Sheynin and V.I. Kozlovskiy[19].

On the first level, one would group the criteria which define functional effectiveness followed by producibility and finally, operational effectiveness.

The functional effectiveness criterion (including weight aspects) characterizes how completely and at what level of technical efficiency the given vehicle performs its basic mission. For cargo and passenger vehicles, we examine the transport effectiveness; for crane helicopters, it is convenient to examine hoisting effectiveness; and finally, for agricultural helicopters, particular criteria reflecting the effectiveness of their operation will be applied.

The producibility effectiveness criteria evaluate the design from the viewpoint of manufacturing efficiency and the conditions associated with production.

Finally, the operational effectiveness criteria make it possible to evaluate variants of a given design for various vehicles from the viewpoint of their operational qualities.

Several authors have studied the problems of developing transport effectiveness criteria. A detailed review of this subject is presented in the studies cited above. It should be emphasized that although it is possible to assume that the criteria of transport effectiveness have been profoundly studied and developed, the production and operational effectiveness criteria have not been adequately worked out.

The second and higher levels include the criteria which evaluate the characteristics of the individual flight vehicle in an integrated fashion while simultaneously considering its functional, production, and operational effectiveness. Such an overall evaluation of the design becomes possible through the use of economic methods.

The cost per ton-km for transport vehicles, the cost of treating one hectare for the agricultural vehicles, or the cost per hour of operation for the crane helicopter represent the type of criteria most often used in practice.

The methods for calculating the cost per ton-km for airplanes have been developed in considerable detail by several authors; for example, by A.A. Badyagin and Ovrutskiy[2].

The third and highest level of criteria consists of methods oriented toward the overall economic evaluation of the effectiveness, not of a single airplane or helicopter, but of all aircraft of a given type developed to accomplish a particular task. Here, one should mention the work of A.V. Glichev[6] wherein the systems approach to the solution of such problems is presented in considerable detail.

The problem of selecting optimal variants of flight vehicle systems on the basis of an integrated economic evaluation was also considered in a study by S.A. Sarkisyan and E.S. Minayev[18].

1.2 Functional Effectiveness

The problem of defining the technical and economic characteristics of an aircraft with the aid of a simple and precise formula is very appealing. Therefore, considerable attention has been devoted both in the USSR and abroad to the solution of this problem. A quite detailed analysis of prewar studies containing criteria for technical and economic evaluation of flight vehicles (including the Everling number, Green criterion, Lenoir criterion, and others) was presented by E.A. Ovrutskiy[15]. These same questions, in the light of modern concepts, have also been examined in considerable detail in the previously cited studies of V.M. Sheymin[20], A.V. Glichev[6], and others.

It is possible to identify three basic factors defining the indices (measurements) of the functional effectiveness of an airplane or helicopter through examination of the considered criteria. The first of these is the productivity; i.e., the quantity characterizing the amount of useful work performed by the considered vehicle per unit time. Second is the weight efficiency of the flight vehicle, usually defined as the relationship between gross weight, payload, and structural weight. Finally, the third is the efficiency of the vehicle from the viewpoint of fuel consumption. This factor depends, on one hand, on the aerodynamic efficiency determining the power required for flight and on the other, the efficiency of the powerplant which influences the fuel consumption associated with the power required for flight.

The transport effectiveness criteria proposed by various authors reflect only individual characteristics of the flight vehicle given by one or more of the above-mentioned factors.

Obviously, the most general criterion makes it possible to simultaneously take into account all the basic factors enumerated above which define airplane or helicopter transport effectiveness.

We shall examine the basic primary criteria which are now in use.

1.2.1 Weight Ratio

The weight-ratio concept is very widely used in practice. It is defined as the difference between the gross and empty weights of the helicopter divided by the gross weight or, as the ratio of the useful load to the gross weight.

$$\overline{G} = (G_{gr} - G_e)/G_{gr} = G_{ul}/G_{gr}. \tag{1.1}$$

This criterion is often used to evaluate the efficiency of a specific flight vehicle as well as to compare several flight vehicles with one another. Actually, being very simple from a computational viewpoint, the weight ratio clearly indicates the structural weight efficiency of the considered airplane or helicopter. The designer naturally strives to achieve the highest possible weight ratio when designing a new aircraft. In addition, when working out the design of a specific vehicle where the basic parameters have already been established, the problem of obtaining minimal structural weight becomes one of the principal tasks. It should be mentioned that a gain of 5 percent in the weight ratio of the actual helicopter over its original weight would result in a first-class helicopter, while a 5-percent reduction in this ratio would lead to a very poor vehicle. Therefore, diligent effort to achieve the minimal weight of each structural element has always accompanied the creation of any flight vehicle.

To a large extent, the weight ratio of a future aircraft is determined by the parameters related to its major components, powerplant, and equipment. Therefore, in selecting the parameters of the future, it is necessary to take into account the factors which determine the characteristics of these systems.

For example, two helicopters having the same takeoff weight and exhibiting the same weight ratios will not be equivalent from the viewpoint of their transport capabilities if, because of a variance in aerodynamic efficiency and/or powerplant characteristics, the fuel consumption per kilometer is different.

As a consequence of this, the weight ratio of the vehicle, although indisputably being a parameter characterizing structural weight efficiency, can not be used during the preliminary design process as an overall criterion of transport effectiveness.

1.2.2 Productivity

If it is necessary to conduct a major transport operation requiring many flights, then in order to determine the calendar time and the number of helicopters required to perform this task, one must determine the work performed per unit of time by a single helicopter; i.e., the helicopter productivity.

The productivity of a transport helicopter is evaluated on the basis of work performed by the helicopter; defined as

$$A = \sum_i G_{pl_i} L_i, \text{ or } A = (G_{pl})_{av} L_\Sigma \tag{1.2}$$

where G_{pl_i} = payload transported in the i-th trip; L_i = length of the i-th trip; L_Σ = overall length of all the trips; and $(G_{pl})_{av}$ = average value of the payload.

Considering the basic mission of transport flight vehicles, one can evaluate them through their average productivity as represented by the work performed per unit time.

$$\Pi_{av} = A/T_{\Sigma_{cal}} \tag{1.3}$$

where $T_{\Sigma_{cal}}$ is the overall calendar time required to perform the work.

The overall calendar time expended in performing the operation includes the flight time, T_Σ ; the time expended in loading and unloading, $T_{l.u}$; the time required for performing routine maintenance, $T_{r.m}$; the idle time $T_{i.t}$, associated with medical (legal) limitation of flight crew duty time; weather conditions; duration of refueling; and finally, the time required to take care of unforeseen problems:

$$T_{\Sigma_{cal}} = T_\Sigma + T_{l.u} + T_{r.m} + T_{i.t}. \tag{1.4}$$

The idle time obviously indicates how well the operation is organized, and also reflects the degree of reliability and dependability of the flight vehicle.

The time expended on routine maintenance determines the operational qualities of the helicopter or airplane and will therefore be examined separately in Sect 1.4. Here, attention will be focused on flight productivity as determined by flight time, T_Σ . In addition to the fact that flight productivity is the most important component of the overall productivity, it also reflects performance and weight characteristics of the flight vehicle. In addition, it characterizes the overall transport capabilities of the given flight vehicle, since the service life of all accessories, systems, engines, and the vehicle itself are calculated in terms of flight hours.

The flight productivity is usually defined as

$$\Pi_{av} = (G_{pl})_{av} L_\Sigma / T_\Sigma = (G_{pl})_{av} V_b \tag{1.5}$$

where V_b is the block speed; i.e., the speed calculated, taking into account the time expended in maneuvering before takeoff and after landing, as well as during climb and descent.

Most authors examine only the flight productivity. Consequently, to retain the customary terminology, the term productivity will be used in the sense of flight productivity.

We can introduce the concept of maximum productivity of the considered flight vehicle. This quantity appears as a very important criterion of vehicle transport efficiency. It is obvious that maximum productivity is obtained as a product of the maximum payload transported over a given distance and block speed:

$$\Pi = G_{pl} V_b. \tag{1.6}$$

The block speed can usually be related to the cruise speed through the coefficient k_v ($V_b = k_v V_{cr}$) thus making it possible to write the productivity in the following form:

$$\Pi = k_v G_{pl} V_{cr}. \tag{1.7}$$

It should be noted that in the design process, when the values of cruise speed and payload transported over a given distance are specified, productivity ceases to be an optimization criterion since all the compared design variants satisfy the cruise speed—payload requirements and therefore, would have the same productivity.

This difficulty can be overcome if we examine specific productivity; defined as the ratio of productivity to the empty weight of the equipped vehicle (G_{ee}):

$$\overline{\Pi}_{e.e} = k_v G_{pl} V_{cr} / G_{e.e}. \tag{1.8}$$

The specific productivity can also be defined by referring the productivity to the gross-weight (Rowe criterion[31]):

$$\Pi = k_v G_{pl} V_{cr} / G_{gr} . \tag{1.9}$$

Thus, we can obtain a criterion which makes it possible to evaluate the design from the viewpoint of both its weight efficiency and productivity. This is a more general criterion than the weight ratio or the productivity alone. However, the level of aerodynamic efficiency and fuel economy of the powerplant are not reflected in explicit form in this criterion; rather these factors show up through the influence of the flight range, for which the productivity is determined, on the value of the maximum payload which can be transported.

1.2.3 Mil Criterion

A section of M.L. Mil's book[11] was devoted to the determination of transport helicopter efficiency from the viewpoint of fuel consumption. When examining two vehicles having the same productivity, Mil proposed, as a criterion, to use the quantity L_{eq} which would equal the hypothetical equivalent distance that the vehicle could fly if the entire useful load were replaced by fuel.

$$L_{eq} = G_{l_{max}} V_{cr} \cdot 10^3 / G_{fu/h} = G_{l_{max}} \cdot 10^3 / q , \tag{1.10}$$

where $G_{l_{max}}$ is the maximum load equal to the sum of the payload and fuel weights in tons; $G_{fu/h}$ is the hourly fuel consumption in kg/hr; and q is equal to the fuel consumption per km in kg/km.

This criterion takes the weight and aerodynamic efficiency as well as the efficiency of the powerplant into consideration. However, since this criterion can be applied only to maximum range considerations, its practical use in the above form appears difficult.

In fact, of the two helicopters having the same value of $L_{eq} = 1800\ km$ depicted in Fig 1.1, helicopter No. 2 would transport much lower payloads over shorter distances in spite of the fact that by virtue of high aerodynamic efficiency and good fuel consumption rates, it has a high value of L_{eq}.

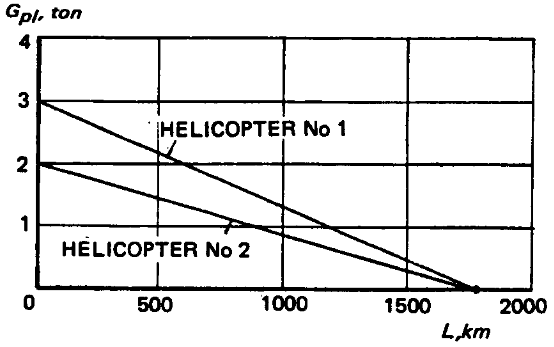

Figure 1.1 Relationship between payload and distance for two helicopters having the same L_{eq} values

In order to overcome this difficulty, Mil introduced still another criterion—the quantity C_L, which shows how much fuel must be expended per one ton-km:

$$C_L = (1000 G_{fu}/G_{pl}L) + \Delta C_{L_h} \tag{1.11}$$

where G_{fu} is the weight of fuel required to fly the distance L in km, and ΔC_{L_h} reflects the fuel expended in the hovering regime.

In this form, the criterion makes it possible to determine the effectiveness of fuel expenditure on transporting cargo for any distance, but no longer reflects the aircraft weight efficiency. Consequently, the field of application of this criterion is still limited. However, when the supply of fuel runs into major difficulties; for example, when operating in remote and inaccessible regions of the country, this criterion becomes very important. Mil realized this and considered fuel efficiency the most important parameter, indicating that this criterion takes into account, not only the economics, but also the quite realistic and important requirement under combat conditions of providing fuel supplies for transport operations[11].

Thus, although the C_L criterion evaluates helicopter characteristics which, under certain conditions (for example, during the energy crisis in the West in 1973-75) become very important, it does not fully reflect the weight advantages of the aircraft. As for the L_{eq} criterion, it fails to reflect payload aspects. Consequently, both of these criteria are not generally suitable to serve as a guide for optimization of transport helicopter parameters.

1.2.4 Weight Ratio Based on Payload Transported Over Some Distance

When studying the influence of various parameters on the basic performance characteristics of an aircraft, one very often examines how, at a constant takeoff weight, the payload varies corresponding to a given range, or how the range changes at a constant payload.

The primary convenience of this approach lies in the fact that it becomes possible to determine, in explicit form, the values of the basic parameters for which the given payload can be transported over the given distance. In fact, the transport helicopter specifications usually include this relationship as a requirement. Therefore if, during the design study, we identify those values of the variables for which a specified fixed-range value would result in a payload equal to or greater than the specified level, the obtained region of variable parameter values would assure that the objective is met.

The so-obtained result can be extended to other approximate takeoff weight values through the use of weight ratio based on payload for a fixed range:

$$\bar{G}_{pl} = G_{pl}/G_{to}.$$

The quantity $\bar{G}_{pl}$ can also be considered a criterion characterizing the weight and fuel consumption efficiency of the designed aircraft. The disadvantage of this criterion is the fact that it does not consider productivity.

In fact, flight vehicles with the same payload and flight range, but having different cruising speeds, will have different values of productivity for the same weight ratio based on the load transported over the same distance.

1.2.5 The Sheynin Criterion

In order to overcome the above-discussed drawbacks of specific criteria, Sheynin suggested making use of the relationship between basic factors which are not influenced by the operating conditions and which are entirely under the control of the airplane designer. As the magnitude of the work ($G_{pl}L$ in ton-km) performed in flight at the optimal cruise speed, minimal fuel consumption, and lowest weight empty of the equipped airplane become higher, the value of the proposed transport effectiveness also becomes higher[20].

$$t_{tr.ef} = k_v G_{pl} L V_{cr} / G_e G_{fu}$$

or

$$t_{tr.ef} = k_v G_{pl} V_{cr} / G_e q. \qquad (1.12)$$

Using Eq (1.8), this formula can be rewritten as

$$t_{tr.ef} = \bar{\Pi}_{e.e}/q \qquad (1.13)$$

Thus, the Sheynin transport effectiveness criterion is equal to the specific productivity (based on the weight empty of the equipped airplane) divided by the fuel consumption per km.

This criterion takes into account all the previously-mentioned important factors: weight and aerodynamic efficiencies and fuel economy of the powerplant. However, the field of application of this criterion is limited by the fact that it can be used only when comparing vehicles having the same gross weight.

In fact, this criterion cannot be used when comparing vehicles of different gross weights since, with an increase in weight—regardless of their having the same aerodynamic efficiencies and specific fuel consumption of the engine(s)—the sfc per km increases. Consequently, the quantity $t_{tr.ef}$ will decrease (Fig 1.2)

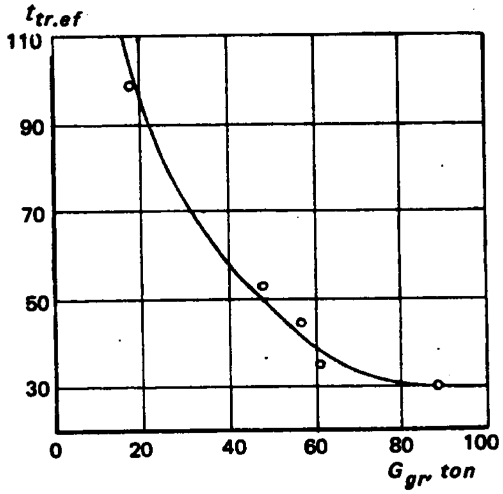

Figure 1.2 Values of the transport efficiency parameter for various airplanes used over a 1500-km distance

1.2.6 Criterion for Evaluating Effectiveness of Cargo and Passenger Helicopters

We have previously listed the basic factors which must be taken into account when establishing a criterion for transport effectiveness. With due consideration of these factors, the requirements for a generalized criterion can be formulated as follows: From various versions of cargo or passenger helicopters being designed to fulfill given specifications, it is necessary to select a variant which would have maximum productivity, best weight efficiency, and minimum fuel consumption. The relative productivity defined by Eq (1.9) as the ratio of the product of the payload and block speed to the takeoff weight was selected as the quantity characterizing productivity and weight efficiency when operating over a given distance. The selected takeoff weight determines the size of the entire flight vehicle and its basic components. Therefore, the productivity referred to unit of takeoff weight becomes an objective criterion of cargo or passenger helicopters, independent of the flight weight.

Consequently, relative fuel consumption—equal to the ratio of the fuel used per km to the flight weight—is selected to evaluate and compare helicopter designs from the viewpoint of fuel consumption.

It can be shown that the fuel consumption per km is directly proportional to the takeoff weight, power losses, and engine specific fuel consumption; and inversely proportional to the flight vehicle lift-to-drag ratio.

$$q = G'_{to} c_{e_{cr}} / 0.27 k_v K \xi \tag{1.14}$$

where G'_{to} = takeoff weight in tons; $K = Y/X$ is the lift-to-drag ratio, where $Y = G_{to}$; ξ = coefficient accounting for power utilization and engine efficiency; $c_{e_{cr}}$ = specific fuel consumption in cruise in kg/hp-hr; and q = fuel consumption in kg/km.

On the other hand, the fuel consumption per km can be defined as

$$q = G_{fu}/L \tag{1.15}$$

where G_{fu} = weight of fuel in kg; and L = flight range in km, corresponding to this quantity of fuel.

The consumption per km referred to the takeoff (gross) weight reflects the aerodynamic efficieicy, specific fuel consumption, and power losses corresponding to the considered vehicle:

$$\overline{q} = q/G_{to} = c_{e_{cr}}/0.27 k_v K \xi \tag{1.16}$$

or

$$\overline{q} = G_{fu}/G_{to} L. \tag{1.17}$$

By dividing the specific productivity by the specific fuel consumption, we can obtain a criterion for evaluating the effectiveness of transport helicopters that accounts for the three factors mentioned above. The so-defined criterion is called reduced productivity,

$$\tilde{\Pi} = \overline{\Pi}/\overline{q}. \tag{1.18}$$

In a physical sense, the proposed criterion can be interpreted as follows. It shows the productivity in tons-km/hr for a hypothetical helicopter having the same cruise speed, weight efficiency, engine specific fuel consumption, and aerodynamic efficiency as the helicopter under consideration, but differing in gross weight; as the gross weight of the hypothetical helicopter was selected on the basis of a fuel consumption of 1 kg/km.

When studying the parameters of different helicopters, or when comparing them through the use of reduced productivity, all the compared variants—in spite of varying gross weights—are reduced to the same basis of comparison expressed as the fuel consumption per km. Using the above-outlined process, the obtained productivity appears as a quantity defining the efficiency of the considered aircraft.

The reduced productivity of a helicopter with takeoff (gross) weight G_{to} transporting payload G_{pl} over a distance L at a block speed $V_{bl} = k_v V_{cr}$; having lift-to-drag ratio K; coefficient of power loss and engine efficiency ξ; sfc in cruise $c_{e_{cr}}$; and weight of available fuel G_{fu}, can be represented as follows:

$$\tilde{\Pi} = k_v G_{pl} V_{cr} L / G_{fu} \qquad (1.19)$$

or

$$\tilde{\Pi} = 0.27 k_v^2 G_{pl} V_{cr} K \xi / G_{to} c_{e_{cr}}. \qquad (1.20)$$

Eq (1.19) is convenient for calculating the reduced productivity of helicopters which have already been built or are being designed, while Eq (1.20) is more convenient for estimating the influence on $\tilde{\Pi}$ of the individual parameters which can be varied during design.

Figure 1.3 is given as an example of the reduced productivity vs stage length for the Mi-6 helicopter. We see that the curve $\tilde{\Pi}$ as a function of L reaches a maximum at the optimal range L_{opt}. For distances shorter than L_{opt}, a reduction in the block speed leads to a reduction in productivity in spite of an increase in payload. For distances greater than L_{opt}, productivity is reduced, due to the diminishing payload.

Several values of the reduced productivity for Soviet production helicopters vs the year of their introduction into service are shown in Fig 1.4. Here, we see that in addition to the fact that each new helicopter has met the specification with respect to load-carrying requirements, they also exhibit higher reduced productivity.

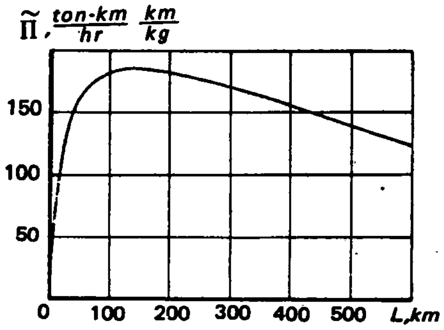

Figure 1.3 Relative productivity $\tilde{\pi}$ vs flight distance for the Mi-6 helicopter

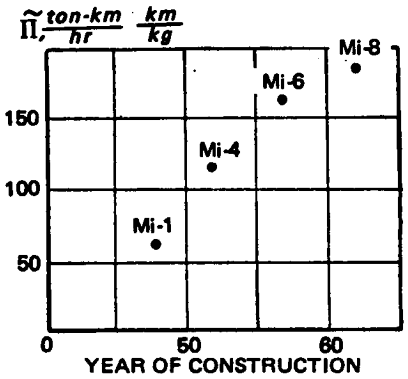

Figure 1.4 Values of relative productivity $\tilde{\pi}$ for Soviet helicopters

From this analysis, it follows that the reduced productivity can be used as a criterion for evaluating the productivity as well as structural weight efficiency of the considered helicopter while still accounting for economic fuel consumption. This criterion can be used when examining different variants of transport helicopter designs, and further evaluation of the selected variant when comparing cargo or passenger helicopters of different gross-weight categories.

1.2.7 Criterion for Evaluating Operating Effectiveness of Crane Helicopters

Before examining the method for evaluating the operating effectiveness of a crane helicopter, we should note that such helicopters can be used in operations of varied nature.

Frequently, when performing installation work, hovering with a load represents the primary regime of flight, and thus makes up a large part of the operating time. An example of such application is the scrubber installation performed by the Mi-10K helicopter (Fig 1.5).

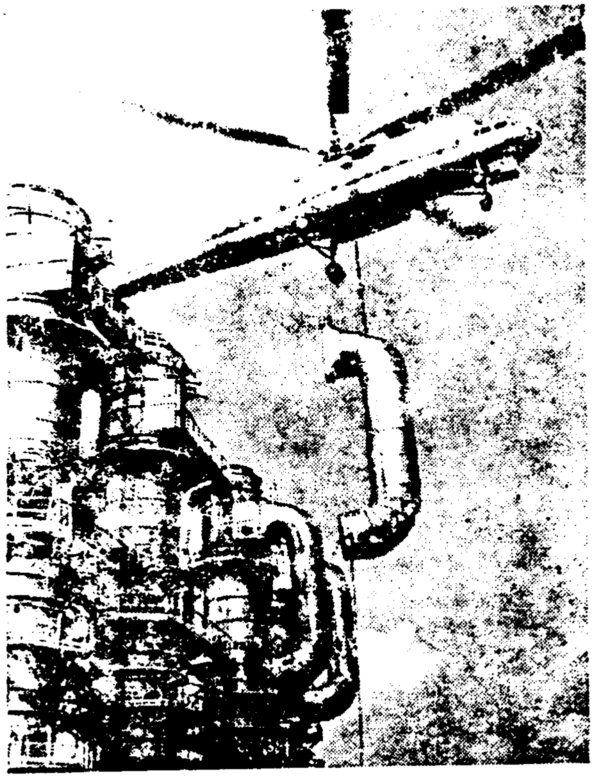

Figure 1.5 Assembly of scrubber by the Mi-10K helicopter

In addition, crane helicopters find wide use in transporting oversized loads which will not fit in the fuselages of cargo helicopters. A well-known example of such operation is transportation of the wings of the Tu-144 supersonic airliner by the Mi-10 helicopter (Fig 1.6). It is obvious that the elements and performance of operations involved with transporting loads do not differ in nature from those of passenger transports; therefore, the effectiveness of crane helicopter utilization in such operations can be evaluated by the magnitude of reduced productivity as determined in Eqs (1.19) and (1.20).

Here, we shall examine only those aspects of crane helicopter operations which are basically related to the hover regime.

When determining the lifting capacity of the crane helicopter, it is necessary to take into account several characteristics associated with the conditions encountered in the performance of assembly and erection tasks. There are two such basic conditions: ensuring the required hovering duration when performing the specified operation, and operational safety in the case of failure of one engine.

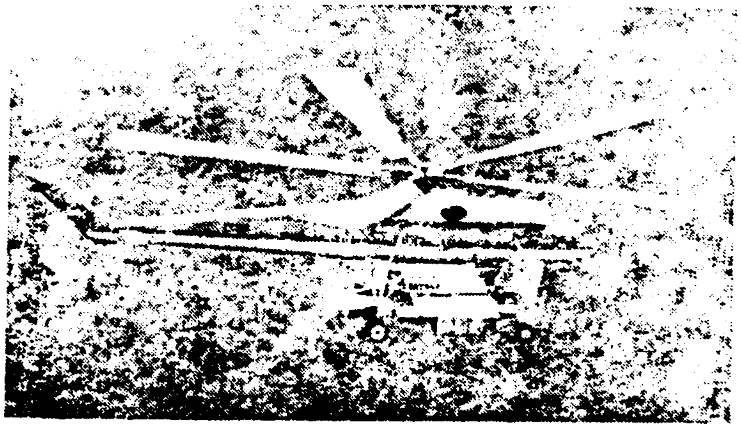

Figure 1.6 Transportation of the wings of the supersonic airliner Tu-144 by the Mi-10 helicopter

The first condition is used to determine the possible gross weight as a function of engine rating. Gross weight becomes maximal if anticipated time of assembly or installation cycle is short enough to allow the engines to oprate at their takeoff power setting. However, if the time required for performing the given task is longer than that permitted by the takeoff setting, the gross weight and magnitude of the useful load are determined by the thrust corresponding to engine operation at lower power. For example, at normal rated power. In the second case, it is obvious that both the gross and hoisted cargo weights will be lower than when using takeoff power.

A still further reduction in the gross weight and therefore, that of the hoisted load may take place if, in order to ensure safety during crane operations, it is not possible for the pilot to drop the load in case of an engine failure. This situation may arise during tasks performed over operating facilities, or when people are under the load. In this case, the gross weight and useful cargo load are determined by performance corresponding to operation with the remaining engine (or engines) at the maximum possible power; often called emergency power. These requirements are so difficult to satisfy that on a helicopter which is not specifically designed with a large power reserve for crane operations, the hoisted load may be close to zero.

Thus, depending on the operating conditions, there are three values of gross and consequently, hoisted, weights which are possible for a crane helicopter.

First—the load which can be lifted when using takeoff power of the installed engines. The load corresponding to these conditions is the maximum load. Second—the load which can be lifted when using normal rated engine power. In this case, the load is lower than the first. Third—the load which the helicopter can maintain in the case of an engine failure. In this case, the load is still lower than in the two preceding cases. Considering these facts in examining crane operations, we must consider the particular takeoff and cargo weights corresponding to the specific operating conditions.

The magnitude of the load which can be lifted, transported, and placed within a definite time period should be used as the quantity characterizing useful work performed by the crane helicopter.

As is well known, the product of a force and its time of action is called the impulse, or momentum. Therefore, in order to perform an assembly operation in which it is necessary to place N loads weighing G_{pl_i}, with time T_i required for each operation, the total impulse becomes:

$$I_{\Sigma} = \sum_{i=1}^{N} G_{pl_i} T_i \tag{1.21}$$

Consequently, we shall use this total impulse as a quantity analytically denoting the amount of useful work performed by the crane helicopter.

The average productivity of the crane helicopter(s) performing this work can be defined as the ratio of the total impulse to the time T_{Σ} expended on the entire operation.

$$\Pi_{cre_{av}} = I_{\Sigma}/T_{\Sigma} = \sum_{i} G_{pl_i} T_i/T_{\Sigma} \tag{1.22}$$

When we consider a single operation of one helicopter, the productivity can be defined as

$$\Pi_{cre} = G_{pl} T_{ass}/T_{ft} = k_T G_{pl} \tag{1.23}$$

Here, the coefficient k_T takes into consideration the difference between the time T_{ass} expended on assembly proper and the flight time T_{ft} which also includes the time expended in maneuvering before takeoff and after landing, and also the time required for flight to the point of operation and return.

The relative productivity of the crane helicopter can be defined as the ratio of productivity to the takeoff (gross) weight:

$$\bar{\Pi}_{cre} = k_T G_{pl}/G_{to} = k_T \bar{G}_{pl}. \tag{1.24}$$

V.P. Petruchik[17] proposes the use of the weight output of the crane helicopter as the criterion for optimizing the parameters. We can see from Eq (1.24) that this approach is close to that in which the relative productivity is taken as the criterion without accounting for the time losses T_{ft} and the amount of fuel required to perform the operation. However, the weight of the fuel consumed in crane operations must be considered as it may account for 15 to 40 percent of the transported load weight.

As in the case of helicopter transport operations, the specific productivity can be used as an optimization criterion for crane helicopters. However, in this case, the fuel economy aspects are expressed indirectly through reduction of the load carried with an increase in the operating time.

To obtain a criterion analogous to the reduced productivity of transport helicopters, it becomes necessary to find the relationship between hourly fuel consumption and takeoff (gross) weight in order to divide the relative productivity by the relative hourly fuel consumption, which is independent of the gross weight.

Using the well-known Vel'ner formula, we can obtain the following relationship between power and weight in hover:

$$N = \sqrt{P} G_{gr}/37.5 \eta_o \xi \sqrt{\Delta}. \tag{1.25}$$

From this, the hourly fuel consumption can be presented as follows:

$$G_{fu/h} = \sqrt{P} c_e G_{gr}/37.5 \eta_o \xi \sqrt{\Delta}.$$

The relative hourly consumption (1/hr-unit) becomes

$$\bar{G}_{fu/h} = \sqrt{P}c_e/37.5\eta_o\xi\sqrt{\Delta}. \tag{1.26}$$

Here, P = main-rotor disc loading in kg/m^2; η_o = Figure-of-Merit of the main rotor (or rotors); ξ = power utilization factor; c_e = sfc in kg/hp-hr; and Δ = relative air density.

Now, we can write the expression for reduced productivity of the crane helicopter:

$$\tilde{\Pi}_{cre} = \bar{\Pi}_{cre}/\bar{G}_{fu/h} = k_T\bar{G}_{pl}/(G_{fu/h}/G_{gr}). \tag{1.27}$$

Substituting Eq (1.26) for $\bar{G}_{fu/h}$, we can represent the reduced productivity in the following form:

$$\tilde{\Pi}_{cre} = 37.5\eta_o\xi k_T\bar{G}_{pl}\sqrt{\Delta}/c_e\sqrt{P}. \tag{1.28}$$

When the specific operating conditions of the crane helicopter are unknown; on the basis of the accumulated statistical data, we can assume that $k_T = 0.5$. Then,

$$\tilde{\Pi}_{cre} = 18.75\eta_o\xi\bar{G}_{pl}\sqrt{\Delta}/c_e\sqrt{P}. \tag{1.29}$$

The higher the reduced productivity of crane helicopters, the larger the relative load which it can lift; the higher the Figure-of-Merit of the main rotor, the smaller the power losses, specific fuel consumption, and disc loading of the rotor(s).

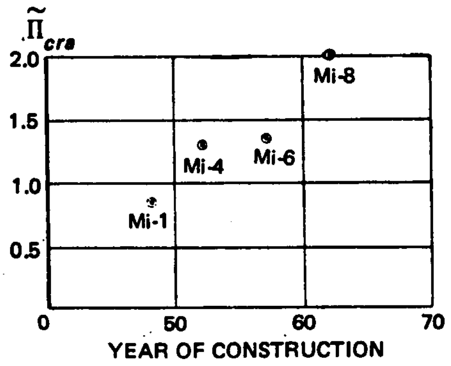

Figure 1.7 Values of relative productivity of Soviet crane helicopters vs years of their creation

By using an external sling, conventional transport helicopters can perform crane operations. Computed reduced productivity for the helicopters previously shown in Fig 1.4 is given in Fig 1.7 as a function of the year of their creation. These calculations were performed under the following assumptions: hovering with load at takeoff power; duration of hover with the load, 10 minutes; duration of flight without load, 10 minutes; and fuel reserve for 20 minutes of hover.

1.2.8 Criterion for Evaluating Operational Effectiveness of Agricultural Helicopters

The use of helicopters in agriculture in the USSR is expanding all the time. While in the beginning, their use was limited to treating vineyards and orchards, helicopters have recently been used extensively in the application of herbicides to the field and for fertilization of winter crops. The application of fertilizing at times considered optimal from the viewpoint of agrotechnology; i.e., in the spring when there is a lot of moisture in the soil and use of surface vehicles is not feasible, results in a considerable increase in the yield.

The experience of the helicopter industry in the USSR and abroad shows that as yet there is no serious need for the development of a special agricultural helicopter. Multipurpose transport helicopters are modified for this work by externally installing additional equipment. This approach does not provide an optimal helicopter for a given type of work, and this appears to be a significant drawback of the established practice. On the other hand, the present approach does have some advantages, primarily associated with the fact that agricultural operations are performed seasonally and consequently, the specialized helicopter would be destined for long down-times with the corresponding problems: how to occupy the crews during idle times, and how to utilize the quite extensive supply of specialized equipment, especially in light of the existing calendar limitations for their applications.

Use of the universal helicopters makes it possible to utilize them in the intervals between agricultural applications for liaison, transport, and other operations. Moreover, the universal helicopters are always produced in larger quantities than specialized rotorcraft and consequently, are cheaper, which is also very important, since the cost per hectare treated determines in considerable measure the advisability of using the helicopter for this type of operation.

The following discussion is equally related to the modified universal helicopter and specialized agricultural helicopters.

When conducting agricultural operations, it is very important to accomplish the required scope of work in short calendar periods as dictated by the growing cycle. Therefore, it is very important that expenditures of time associated with servicing the helicopter, preflight preparation, and routine inspections are as small as possible, at least during their seasonal utilization. On the basis of these considerations, it is best to take absolute productivity as the primary criterion for the operating effectiveness of agricultural helicopters, and to use relative productivity as a secondary criterion.

Absolute productivity of agricultural helicopters can be defined as the area in hectares (one hectare = 2.47 acres) treated by the helicopter per hour, while relative productivity is defined as the absolute productivity divided by the gross weight.

When determining productivity in the following considerations, we shall examine the time associated with performing four basic forms of operation which define the operating cycle of agricultural helicopters.

First is the time T_1 expended on dusting or spraying; i.e., operations associated with applying chemicals to fields. This is considered useful time since it is spent in performing functions which are essential to the helicopter mission.

Second is the time T_2 expended by the helicopter on turn-arounds after passing the strip being treated. As a rule, treated fields are represented by parallel strips, one after another.

Third is the time T_3 required for takeoff, acceleration, and flight from the servicing area to the field being worked and return, followed by deceleration and landing.

Fourth is the time T_4 required for supplying the chemicals to the helicopter.

Here, we have not mentioned the time expended on fueling, as we are assuming that this is accomplished with the engines not operating; i.e., with no expenditure of resources while, in contrast, loading of chemicals is performed with the engines running.

On this basis, agricultural helicopter productivity can be defined as the ratio of the area treated to the time expended for actual operation.

$$\Pi_{agr} = S/T = S/(T_1 + T_2 + T_3 + T_4) \quad (1.30)$$

where S is the area treated by a helicopter dispensing a complete load of chemicals (in hectares); T is the time expended (in hours) on loading the helicopter with chemicals, takeoff, and flight to the field being worked; working the field itself, and return for the next servicing; and Π_{agr} is the productivity in ha/hr.

Area S can be expressed as the ratio of the helicopter load including chemicals, G_{ch} (in tons), to the so-called chemical application norm, H, thus giving the quantity of applied chemicals in tons per hectare:

$$S = G_{ch}/H. \quad (1.31)$$

As the helicopter traverses the field it treats a strip of length L_p, usually termed a pass. The overall length L_Σ of the strips treated by the helicopter per servicing is

$$L_\Sigma = 10S/B \quad (1.32)$$

where L_Σ is the overall length in km; B is the width of the treated strip, or swath width in meters.

It is obvious that the number of passes over the field per servicing is

$$n = L_\Sigma/L_p. \quad (1.33)$$

Having these relationships, we can obtain expressions for the components of operating time T.

Time T_1 in hours spent applying the chemicals can be expressed in the following form:

$$T_1 = L_\Sigma/V = 10S/VB = 10G_{ch}/VHB. \quad (1.34)$$

At first glance, one could come to an unexpected conclusion that productivity of agricultural helicopters, calculated only on the basis of time T_1, is independent of the chemical load G_{ch} and the application norm H. Indeed, by substituting the above expression for T_1 into Eq (1.30), and assuming that $T_2 = T_3 = T_4 = 0$, then

$$\Pi_{agr} = 0.1\,VB. \quad (1.35)$$

In determining T_2—the time spent on turns—we shall assume that after passing the strip, the helicopter performs a turn with a bank angle of 45° without reducing its speed. This means that the load factor is $n = 1.41$. In this case, the centripetal force is equal to the weight, while the time for a complete turn in hours is

$$T_2 = (1/3.6)(1/3600)(2\pi/9)V(L_\Sigma/L_p) = 0.494 \cdot 10^{-3}(SV/BL_p) = 0.494 \cdot 10^{-3}(G_{ch}V)/HBL_p. \quad (1.36)$$

The time spent in flight from the service area to the field and back can be defined as

$$T_3 = 2L_{fi}/V_{ft} \quad (1.37)$$

where L_{fl} is the distance in km from the service area to the field; V_{ft} is the average flight speed in km/hr, determined taking into account the time lost in hovering, acceleration, and deceleration.

For simplicity, we shall assume that $V_{ft} = \frac{1}{2}V$.

Finally, the time lost in loading the chemicals is determined by the amount of material loaded and the productivity of the loading mechanism:

$$T_4 = G_{ch}/\Pi_3 \tag{1.38}$$

where Π_3 is the productivity of the loaders in tons/hr.

Substituting Eqs (1.34), (1.36), (1.37), and (1.38) into Eq (1.30), and making simple transformations, we obtain the following expression for productivity of the agricultural helicopter:

$$\Pi_{agr} = 1/[(10/VB) + 0.49 \cdot 10^{-4}(V/BL_p) + (4L_{fl}H/VG_{ch}) + (H/\Pi_3)]. \tag{1.39}$$

The relative productivity of the agricultural helicopter is obtained as the ratio of Π_{agr} and the gross weight, G_{gr}:

$$\overline{\Pi}_{agr} = \Pi_{agr}/G_{gr}. \tag{1.40}$$

It is possible to take the individual quantities appearing in Eq (1.39) and evaluate their influence on productivity. Increasing the flight speed leads to a reduction in the time expended on chemical application and on ferrying from the loading area to the field and therefore, the productivity increases. On the other hand, increasing the flight speed also increases the time expended on turns, resulting in decreased productivity. Calculations show that the optimal velocity from the viewpoint of productivity is higher than the usual helicopter speed and therefore, an increase in speed improves productivity.

Further, the wider the swath width B, the higher the productivity. The total productivity also becomes higher with an increase in the pass length L_p, weight G_{ch} of the chemicals, and productivity Π_3 of ground-based loaders.

Productivity decreases with an increase of the chemical norm H and the distance (L_{fl}) from the loading area to the field.

The results of calculations based on Eqs (1.39) and (1.40) are shown in Fig 1.8. In these calculations, the helicopter gross (takeoff) weight varied from 1 to 20 tons. The pass length was assumed to be $L_p = 1$ km. Ferry distance from the base was 3 km, and fertilizer application norm was 0.3 ton/ha. Speeds were taken as 120, 130, 150, 170, and 200 km/h respectively, for weights of 1, 2, 6, 12, and 20 tons. Productivity of agricultural helicopters, Π_{agr}, as calculated from Eq (1.39) is shown in Fig 1.8a for the above-indicated weights and speeds; using three values of the swath width (B = 20, 30, and 40m), and with the assumption that the loader productivity Π_3 = 50 ton/h. Fig 1.8b shows the relative productivity for B = 40 meters. It can be seen from Figs 1.8a and 1.8b that absolute productivity steadily increases with gross weight, while the relative productivity has a maximum gross weight of about 4 tons.

If, with an increase of the gross weight, we assume that the width of the swath and ground loader productivity also increase in such a way that the following values of B; B = 14, 16, 25, 40, and 59m; and Π_3 = 25, 50, 150, 300, and 500 ton/h correspond to the previously indicated gross weights, then the absolute productivity of agricultural helicopters

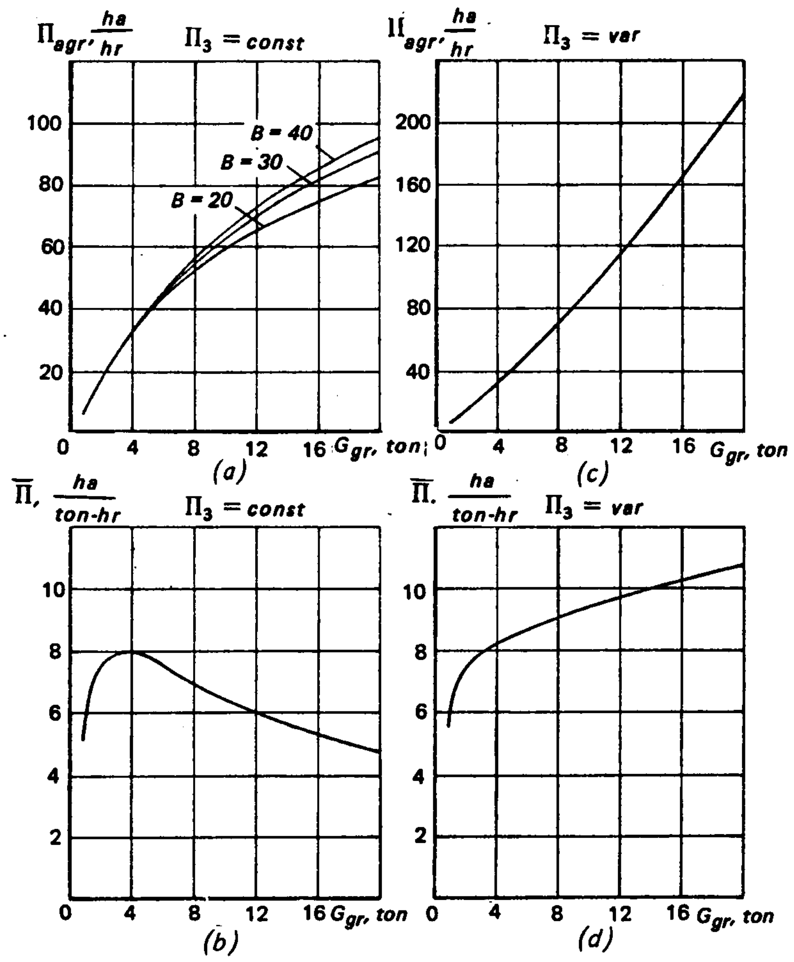

Figure 1.8 Influence of gross weight on absolute and relative productivity of agricultural helicopters

increases with an increase in G_{agr} as shown in Fig 1.8c. In this case, the relative productivity Π_{agr} (Fig 1.8d) also increases with an increase in the gross weight. However, for gross weights higher than four tons, the rate of increase in relative productivity diminishes.

1.3 Production Effectiveness

The concept of technological effectiveness of any manufactured object contains production effectiveness as one of its components. GOST 18831-73 defines the technological effectiveness of a manufactured object as an assembly of such construction characteristics as manifested by the possibility of optimal expenditure of labor, funds, materials, ant time expended for technical preparation of production, manufacture, operation, and overhaul. This is done by comparing the studied object with corresponding representatives of the same type. This definition includes the qualities characterizing production effectiveness (during preparation for production and fabrication) and operational effectiveness (during operation and repairs).

When examining productive effectiveness of a specific design, it is generally necessary to evaluate the labor, capital, and material requirements along with the time expended in preparation for production, and duration of the production cycle. In the preliminary design stage, most attention should be devoted to reducing the required labor and increasing the planned coefficient of material utilization.

Each of the aforementioned factors is well known and widely used in practice. The primary difficulty in using these quantities in the preliminary design stage or when selecting an optimal version of the design lies in the fact that at this particular time all the data and small details necessary for concrete calculations are not yet known.

It is obvious that if we could develop simplified quantitative criteria for evaluating the product, we could also develop (even in the early design stages) a sufficiently accurate technique for selecting the optimal version from all possible variants.

1.3.1 Approximate Method for Determining Labor Requirements

In the design process of a flight vehicle, the designer must constantly resolve the conflict between the requirements for obtaining minimal weight and ensuring acceptable labor expenditure in the series of production and operation. In analyzing different variants of any part or component, it is important to compare them from the viewpoint of labor requirements during manufacture.

We shall assume that the approximate relationship expressing the conditional labor requirement T_c for any helicopter component is

$$T_c = \sum_{n=1}^{n=N} k_{co} m_n \sqrt[4]{G_n} \tag{1.41}$$

where N is the number of individual parts of the given component; n is the part identification number; k_{co} is the coefficient of complexity of the given part; m_n is the number of required machining operations (turning, milling, etc.) of the given part; and G_n is the weight of the part.

Of all the quantities appearing in Eq (1.41), only k_{co}—the complexity coefficient—is arbitrarily selected. It is recommended that its value be taken between 1 and 10, depending on the complexity of machining operations and possible degree of mechanization and automation of the machining cycles which can be incorporated in the design, and on the technological process selected by the production engineer and designer.

The influence of size or weight of the component on the manhours required for its production is examined in detail in Ch 4. Consequently, in Eq (1.41), we have used the result obtained in Ch 4 without presenting any special proof at this time.

An approach such as that described above does not permit one to precisely determine the component manhours required, but is quite acceptable for a comparative analysis of different design variants.

1.3.2 Material Requirements

In all flight vehicle design stages, the designer must strive for the most economical use of materials and the highest possible coefficient of their utilization. This coefficient is determined from the formula

$$k_{m.u} = G_{f.p}/G \tag{1.42}$$

where $G_{f.p}$ is the weight of the finished part; G is the weight of the rough forging or casting; and $k_{m.u}$ is the coefficient of material utilization.

The correct form for a solution of this problem depends in considerable degree on the stage of development. As a rule, the manufacture of production articles is preceded by the construction of experimental articles on which the correctness of the proposed design solution is verified and finishing of parts and components is also accomplished. Therefore, the technical documentation generated at the beginning of development is often directed toward the experimental technological process since only a few specimens of the article are constructed. At this stage, it is not always possible to achieve high values of the material utilization coefficient. It should be noted, however, that major expenditures of material associated with the development of a given helicopter will occur later; namely, when the machine enters full-scale production. Therefore, during the design phase and particularly during the early stages, it is very important that a careful examination be made of the future series production conditions and that plans be made to incorporate the most progressive and efficient technological and manufacturing processes.

The use of prefabricated parts obtained by precision castings or forgings, and other technological methods which do not require subsequent major machining operations, the use of plastic parts in noncritical and nonstructural components, the use of glass and carbon reinforced plastic materials in structural components, and many other approaches makes it possible to obtain high values of the material utilization coefficient.

1.4 Operational Effectiveness

The service life of any flight vehicle far exceeds the time required for its design or construction. During its operational period, the helicopter or airplane performs the useful work for which it was developed. However, the labor expenditures associated with operation are also quite significant. For this reason, the problems related to improving operating conditions and methods have recently received increased attention.

In examining the questions of design optimization in the early stages of design, it is advisable to select, from the large number of criteria proposed by various authors, only those which the designer can use to evaluate the operational efficiency of the new product, whether it be an entire helicopter or individual components.

The concept of specific manhour expenditures for maintenance and overhaul satisfies this requirement better than other criteria. In accordance with GOST 16503-70, this specific maintenance labor requirement can be defined as manhours expended in conjunction with a definite period of operation of a given article. When applied to helicopters, this criterion can be refined by referring the required average labor expenditure in manhours per one flight hour. The smaller this quantity, the better the considered helicopter has been designed from an operational viewpoint.

The labor expenditure associated with operation can be arbitrarily divided into three groups. The first group represents those tasks which can be scheduled in advance; the second includes those for which time of performance cannot be planned in advance; and finally, the third includes those tasks for which the time of performance is known, but the actual extent of the work and associated manhours can only be approximated in advance, and further refined in the actual process of performing the subject operations.

In the present standard practice of aeronautical operation and maintenance, some definite tasks are performed as a means of assuring reliable function of the aircraft. These operations include preflight and postflight inspections, and postflight servicing, lubrication, and various routine checks.

The distinctive feature of these operations is the fact that the labor requirements can be determined in advance, even during design. Moreover, this labor expenditure is, in conisderable degree, predetermined in the very design process.

Thus, the above-mentioned operations—directed toward keeping the helicopter in a flight-ready condition through proper maintenance—constitutes the first "plannable" group in-service operations. The number of manhours required to perform maintenance can be established on a mockup of the helicopter by time-motion studies of the individual operations which must be performed in accordance with the operational documentation. By taking into consideration the specified frequency of the individual operations, we can calculate the specific maintenance labor output in manhours per flight hour:

$$U_{sme} = \sum_i t_i n_i / P_{tbo} \tag{1.43}$$

where U_{sme} is the specific maintenance labor expenditure in manhours per flight hour; t_i is the time required (in hours) to perform the i-th operation; P_{tbo} is the helicopter TBO in hours; and i is the sequential number of all maintenance operations performed between major overhauls during time P_{tbo}.

In the process of both operation and maintenance, one may discover various kinds of deformations or damaged elements of the components, parts, systems, and equipment. These discrepancies can be eliminated through adjustments, reworking, or replacement of the damaged elements.

The process of eliminating these problems is termed repairs. The primary feature of these operations is the fact that they cannot be planned in advance and therefore, we include the manhours spent on such operations in the second group of labor expenditures. It is evident that these labor expenditures can be defined specifically only through an operational analysis. Therefore, in the design process, it is not possible to determine the specific labor requirements for repairs.

At the present time, there is a tendency in airplane and helicopter development practice to specify the manhours required to replace the primary components and engines. This is based on the practice that in the case of detection of a serious malfunction or significant deviation of the system parameter from the accepted norm, it becomes advisable to remove the malfunctioning part or component and correct the problem at a specified facility rather than to try to perform the required repairs on the flight vehicle.

In this connection, particular attention is devoted to developing so-called modular designs which can be broken down into relatively simple and easy to replace individual units or modules.

Thus, in order to achieve maximum design efficiency from the viewpoint of ensuring minimal repair labor expenditure, it is very important to accomplish the design so that the manhours involved in replacing individual parts or modules will be minimal.

The third group of functions associated with vehicle operation consists of major overhauls. While the operations involving replacement of components can be specified a priori, the restoration of worn parts and similar tasks cannot be determined in advance.

In the process of designing a part or component, it is necessary to make provisions for the special measures necessary to perform the operations associated with major overhauls. This includes proving the clearance margins necessary for installation of repaired parts having dimensions larger than nominal, provisions for the replacement of bearings, and so on.

It should be particularly emphasized that the manhours required for maintenance, routine repairs, and major overhauls depend in considerable degree on such seemingly minor aspects as convenience of the location of the access panels and the means for fastening them, the convenience and simplicity of checking fluid levels, assurance of access to subassemblies, the possibility of removing one unit without disassembly of other units, and so on.

Thus, to ensure high operational effectiveness of the design, it is necessary to strive to obtain the minimal specific labor requirements for maintenance, reduce the manhour expenditure for replacement of primary components and systems, and also to reduce the manhours required for major overhauls.

1.5 Economic Effectiveness of Helicopter Operation

The criteria examined above makes it possible to evaluate both projected and already constructed helicopters (transport for example) from the viewpoint of the individual functional, production, or operational qualities. However, an overall evaluation of the design on a unified basis, taking into account all the qualities of the machine, can be obtained only by using an economic evaluation which determines the operating cost of the flight vehicle. By calculating the cost of the work performed by a given helicopter, whether this be the cost per ton-km for transport operations or the cost of treating one hectare by an agricultural helicopter, we obtain a unified result—on one hand, reflecting the costs of manufacturing, major overhauls (amortization costs), and operation (costs of fuel and lubricants, routine maintenance, and flight crew pay) and on the other hand, useful work performed.

Therefore, the cost of operations performed by helicopters appears as a generally accepted criterion of the effectiveness of their utilization. This approach is not new. Even at the beginning of passenger air transportation in the 1930s, this was clear to many authors who devoted their efforts to the task of developing a relatively simple formulae reflecting the basic laws governing cost variation and at the same time, establishing basic laws for calculating their cost. The problem was posed in this way because of the fact that an exact calculation of the cost was quite cumbersone and difficult to realize, especially when the task was directed toward evaluation of several variants of a design in order to select an optimum version.

At the present time, the solution of this problem becomes much easier, thanks to the use of electronic digital computers for engineering calculations. This makes it possible to perform direct calculations of helicopter operating costs. The accuracy of such calculations depends directly on the accuracy of the input data used. If, in practice, discrepancies are found between the values predicted in the design process and those obtained as a result of actual operation, the reason for these discrepancies is most often associated with inaccurate assumptions in regard to the service life used in the calculation. They also may be partially due to the variation in prices and wages with time, and refinements of some details of the maintenance process and overhaul periods.

However, when we perform optimization of the parameters of a new helicopter design, all the factors causing the aforementioned inaccuracies are the same for all the variants being examined and consequently, have no effect on the comparison results.

The cost-per-hour of operation forms the basis for the cost-based evaluation of the aircraft. It is customary to divide (or group) the operating costs into two parts: direct and indirect. As indicated by E.A. Ovrutskiy[7], such grouping is a result of the fact that the level of certain costs depends directly on the technical and flight characteristics of the aircraft (weight, engine power, cargo-carrying capacity, fuel consumption, type of structure, and so on). Other costs are determined only in part by the type of airplane being operated (for example, amortization and maintenance of runways); they depend more on the overall volume of transport, traffic density, and other factors not directly associated with airplane characteristics. Consequently, in developing a new design, the designer can basically influence only the first group; i.e., the direct operating costs. Furthermore, in most cases the indirect costs are determined as a definite percentage of the basic costs and therefore, only the direct operating costs can be used for design optimization.

Knowing the hourly operating costs, we can obtain the cost-per-unit of the useful work performed by dividing the costs per flight hour by the helicopter productivity;

$$C = C_{hr}/\Pi, \tag{1.44}$$

where C = cost of the work performed; C_{hr} = operating cost per flight hour; and Π = productivity.

Procedures for calculating direct operating costs are presented in Ch 4. The need for developing these procedures specifically for helicopters was caused by the significant differences in operating conditions and methods of calculating service life peculiar to rotary-wing aircraft and its components (as opposed to airplanes).

1.6 National Economic Effectiveness

In the preceding section we examined the economic effectiveness of operation of an individual helicopter. But what is the effectiveness of application of all the helicopters of a given type in the framework of the entire national economy as a whole. The criteria of the highest (third) level give the answer to this question.

The methods used in solving problems of this sort have been examined in detail by S.A. Sarkisyan and E.S. Minayev[18], and A.V. Glichev[6]. The integrated economic evaluation method has as its objective the determination of the most complete and rational utilization of national economic resources to achieve the posed objectives. This approach takes into consideration the following:

- prospects for advancement of the state-of-the-art, its technical effectiveness, and influence on productive capacity,
- time required for design, construction, and utilization of new articles,
- production capabilities of industry and prospects for the development of production methods and technology,
- duration of manufacturing cycle of new vehicles, production volume, and labor requirements for their construction,
- achievement level and tendency for further changes in the areas of concentration, specialization, subcontracting, and distribution of production,
- resources and production prospects of structural materials,
- rational utilization of the material, and manpower resources available to industry,
- level of, and prospects for, development of the technical means and conditions of operation and utilization of new articles, and
- rational utilization of the material and manpower resources in the sphere of technology applications.[6]

It appears to us that such problems are not among those which can be resolved in the preliminary design office. They should be resolved by the customer's scientific research organization. For example, questions may be asked regarding the development of optimal types and sizes of flight vehicles forming a particular transport system, and then the performance requirements for each type of aircraft belonging to the so-developed system.

1.7 Fields of Application of Criteria at the Various Levels

To obtain the optimal parameters of a new helicopter and to evaluate the influence on its efficiency of any design changes taking place in the process of development, construction, and "debugging", it is necessary, in the course of the entire operation, to monitor the basic parameters of the machine and to select specific criteria for each step of the development.

The choice of the level of criteria, or selection of a particular criterion of a given level for evaluating the degree of efficiency in performing the assigned task is determined in considerable degree by the development stage of the project. In examining the period of development and construction of any aircraft, starting from the moment of conception of the idea of such a vehicle and terminating with the completion of flight testing, we can identify three basic stages in this process.

The first stage involves determination of the requirements for the new flight vehicle and justification of its basic characteristics. In this stage, as applied to the helicopter, one formulates and specifies such important characteristics as the load capacity, flight range, cabin size, cruise and maximum speeds, hovering and forward-flight ceilings, number and type of engines, reliability level, operational characteristics (for example, the required life of primary components), maintenance manhours, and frequency of basic overhauls. The first stage terminates with formulation of the tactical/technical specifications for the new flight vehicle.

Since, in this period, all the requirements are formulated by the organizations responsible for ordering, buying, and then operating the helicopters, these organizations are primarily responsible for developing techniques which make it possible to optimize any posed problem.

In the early stage of flight vehicle development when the idea of building a machine of a particular size is generated, and the future transportation system is planned taking into account the total number of such helicopters, the proposed annual production rate, the operational load factors, and the depreciation life, it is best to use the criteria of the third and highest level which takes into account the maximum possible number of basic factors determining the effectiveness of the system in the framework of the overall economy of the country.

However, in the present study, when examining the problems facing the design office in developing a new flight vehicle, we shall not consider the third-level criteria—assuming that they have been developed and used in the customer's scientific-research organizations.

The second stage begins with formulation of the tactical-technical requirements in the experimental (preliminary) design office. This period of the study is characterized by very close interaction between the experimental design office and the customer. In order to ascertain that the requirements are attainable and based on concrete studies, the design office works out the preliminary design—usually called the technical proposal. In the process of this design analysis, the basic structural, aerodynamic, and weight parameters of the new helicopter and its components and systems are established. On this basis, some aspects of the tactical-technical requirements are refined, taking into account the realistic industrial capabilities at the given time frame. This phase terminates with formulation of the final tactical/technical requirements. Then begins the period of preliminary design and mockup of the vehicle. At this time, the final values of the basic parameters of the helicopter are worked out, and individual systems are refined. This work terminates with construction of a full-scale mockup in which final integration is accomplished. The mockup makes it possible to evaluate the suitability of the cargo cabin for loading and placement of the planned cargos, convenience of passenger seat arrangements, cockpit evaluation, placement of the instruments and controls, visibility, and so on. The mockup can also be used to work out solutions extremely important for future operation design; e.g., location of access panels. It is also possible to determine the time required for replacement of the various components, and the relative positioning and operating conditions of these basic components and systems can be checked out.

Optimization of the parameters of the future machine is performed during the second stage of design. It appears that the following sequence of calculations and project-design studies is most advantageous.

First of all, using methods and analytical relationships presented in Ch 2, it is necessary to determine the parametric ranges which will satisfy the performance characteristics specified in the tactical/technical requirements. The most suitable criterion for resolution of this problem in the case of the transport helicopter is the magnitude of the payload for a given flight range and takeoff weight, or the weight ratio based on transportable load for a given range.

Calculations show that the variation of the payload as a function, for example, of the main rotor diameter for constant takeoff weight and different number of blades is, in many cases, described by a quite-flat curve near the optimal payload load value. Thus, we can see in Fig 2.72 that for a tandem-rotor helicopter with a takeoff weight of 12 tons and a 370-km flight range, the payload load varies from 2.45 tons for 13-m diameter and 5 or 6 blades, to 2.65 tons for 16-m and 5 blades and finally, to 2.4 tons for 20-m and three blades. Therefore, we can examine diameters differing in both directions from that corresponding to the extremum.

In this respect, for the transport machine, for example, it is advisable to examine the possible solutions by using the previously proposed transport effectivensss criterion. As a rule, in such an examination, different results are obtained for solutions located on opposite sides of the extremum representing the useful load ratio. Thus, the region of admissible solutions can be narrowed. For this narrowed region, it is advisable to calculate the cost of the performed operations in order to obtain the final optimal solution.

It is advisable to perform these computations according to the indicated sequence during the preparation of technical proposals and preliminary design, as well as when refining the design during the mockup stage.

As a result of the mockup study performed by the experimental design office and the customer, a document is formulated which defines as completely as possible the basic characteristics of the future helicopter. This document enables the designer to begin work on the detail design leading to the third and final stage in the development of the new machine.

The third stage includes the release of final drawings, construction, and flight tests of the new machine.

The working design must take into consideration the results of verification tests of the individual critical elements of the structure and systems. Experience in the Soviet and foreign helicopter industry confirms the necessity of creating various facilities and stands on which tests of various types are performed.

In the working design process the designer, on one hand, relies on the scientific and experimental data accumulated prior to initiating the design and on the other hand, where assumed solutions have been made, he attempts to obtain experimental confirmation of the validity of the assumptions as quickly as possible. In this connection, the first-fabricated parts and components are, as a rule, stand-tested to verify their load-carrying capacity and to discover any weak spots which must be reinforced prior to their use in the first-flight article. Figs 1.9, 1.10, and 1.11 show typical stands for dynamic tests of a blade segment, pitch-bearing housing, and wear tests of the swashplate assembly of the Mi-6 helicopter.

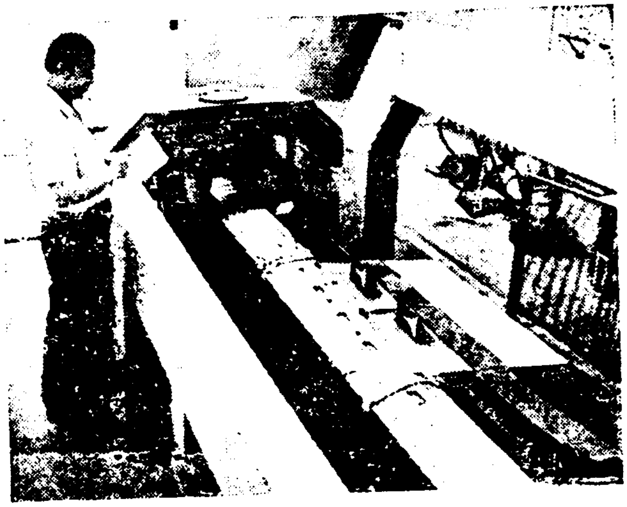

Figure 1.9 Stand for dynamic testing of the Mi-6 helicopter main rotor-blade segments

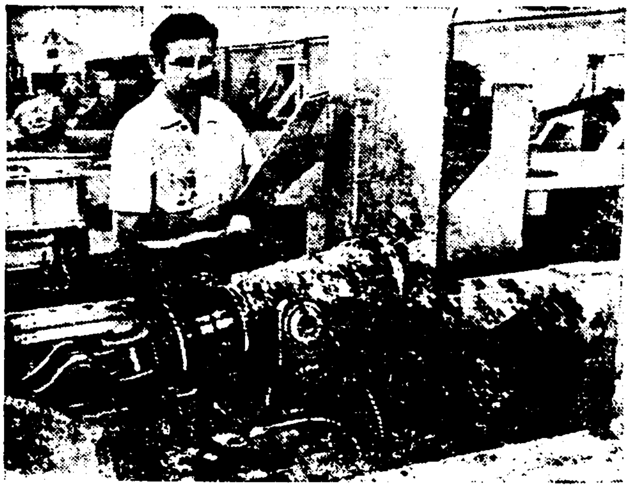

Figure 1.10 Stand for dynamic testing of the pitch-bearing housing of the Mi-6 helicopter main rotor hub

It has recently become obvious that it is necessary to construct a replica of the entire helicopter in order to conduct the fatigue tests necessary to ensure the required service life of the entire airframe; not just of the components which are subjected to the highest dynamic loads.

The results of such comprehensive tests are used as the basis for issuance of the final drawings, from which the first experimental models of the helicopter are constructed for flight testing.

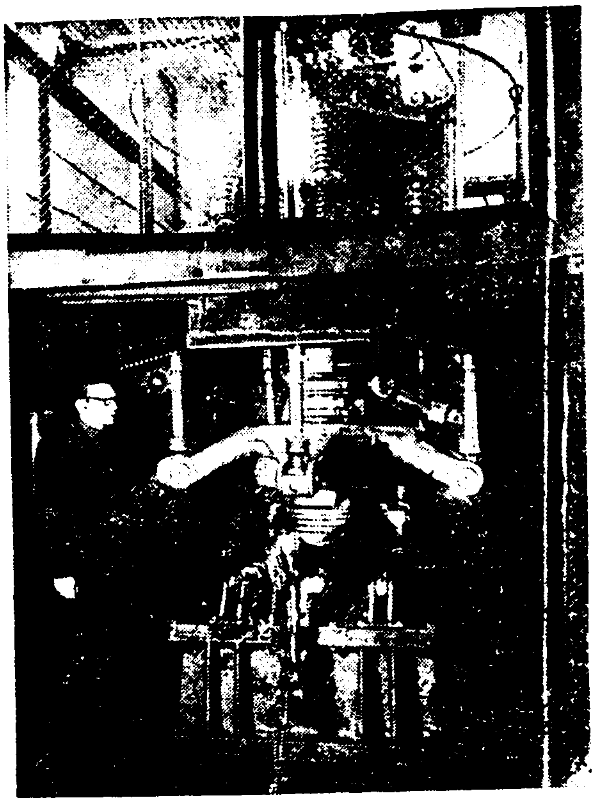

Figure 1.11 Stand for testing swashplate wear

In the process of flight testing, additional detail problems which could not be foreseen in advance, may appear. It is necessary to update the loads on the individual components; look for solutions to new problems associated with aerodynamics, stability and control, operating conditions; and so on. All of these factors again lead to the necessity for refinement of the drawings and basic specifications of the aircraft.

At this stage, the designers cannot alter the basic parameters of the helicopter under development. The primary objective of this period is to assure that the previously determined basic technical and flight characteristics, primarily weight, are met. Consequently, in order to assure that this all-important parameter of the aircraft does not exceed the previously established limits, weight control and accountability for weight changes, etc., are established.

During work on the third stage, it is necessary to assure that the requirements of the tactical/technical specifications or internal decisions by the design office management regarding values characterizing the technical and operational effectiveness of future helicopters are fulfilled.

And, finally, since it is only toward the end of the third stage in the development of the flight vehicle that its final technical characteristics are known, it is advisable, at this stage, to make a series of additional calculations in order to more precisely determine the previously obtained operating costs. This would permit one to incorporate all of the previously performed work in the final results.

2

SELECTION OF OPTIMUM TRANSPORT HELICOPTER PARAMETERS AND CONFIGURATION BASED ON MAXIMUM USEFUL (TRANSPORTED) LOAD

2.1 Introduction

The primary objective of this chapter is to present a procedure for selecting the optimum parameters and configuration of a transport helicopter on the basis of maximum useful payload. This procedure is illustrated by several examples related to the questions most often encountered in design practice such as selection of main and tail rotor diameter and number of blades, helicopter configuration, and comparison of the pure helicopter with the compound. It should be noted that the conclusions drawn on the basis of the calculations related to these examples are also of interest in themselves.

In solving the problem of selecting optimal parameters and configuration of the flight vehicle, it is necessary to precisely define which of the parameters vary, which configurations are examined and which factors remain constant.

In comparing helicopter configurations, the authors have limited themselves to only those types with the development of which they have definite experience. Other configurations; for example, helicopters with convertible rotors—although possibly quite interesting—are not considered here.

The possible variation of flight vehicle parameters is usually restricted to a quite narrow range by their upper and lower constraints. Quite often, the optimal parameter value may be obtained at the maximum or minimum limits determined by existing constraints. In this case, there is no point in varying this parameter, and we limit ourselves to explanation and confirmation of the fact that the optimal value of the given parameter coincides with its allowable limit.

In addition, many aircraft parameters depend on other variable parameters and on the specified flight and other technical characteristics. In particular, the required installed power of the engines is treated as a dependent parameter in all the considered examples, and examples related to a selection of aircraft parameters around a given engine are not studied.

Thus, the problem reduces to a comparative evaluation of helicopter configurations and parameters with variation of the rotor diameters (with corresponding variation of their mutual positioning) and number of blades. Also included in a selection of the optimal parameters are design schemes and structure of the individual helicopter components and systems within specified technical and flight requirements.

When varying these helicopter parameters, we take into account all of the associated changes. For example, when the main rotor diameter is changed, it is necessary to account, not only for the variation of blade and hub weights which are related to the magnitude of centrifugal force, but also to take into consideration changes in dimensions and consequently, the weight of the airframe, main gearboxes, and other helicopter components.

In addition to the specified flight and technical characteristics, the following invariants are assumed: technical level of design, range of applicable materials, skill, and quality of the production facilities which determine the possibility of manufacturing helicopter parts and components on a determined technical level.

The design and fabrication of modern aircraft can be accomplished at different levels of structural weight efficiency. The use of new and stronger materials, and transition to more modern, but at the same time more complex, technological processes may yield marked structural weight savings.

However, we must keep in mind that there is a definite inter-relationship between weight efficiency and structural cost: the more advanced the structure in regard to weight, the more expensive the structure, and the helicopter becomes more complex and costly to operate.

Therefore, it appears that the most rational helicopter designs are those which use modern, but not very expensive materials which do not require the creation of highly specialized series production facilities.

This approach, although leading to the development of helicopters with moderate weight ratios no higher than 40 to 45 percent, does not create significant difficulties in production nor a marked increase in the helicopter cost. Consequently, this is the approach taken in this chapter.

2.2 Weight Analysis Formulae and Brief Justification for Helicopter Weight Determination of Basic Components and Systems

Regardless of the criteria used when selecting optimal helicopter parameters, the magnitude of the useful load (payload) which the helicopter can transport over the required distance must be determined. This quantity cannot be obtained without a weight analysis. Therefore, weight analysis is a basic ingredient of any method for determining optimal flight vehicle parameters.

To this end, weight calculations should be made in the initial stage in the development of the preliminary design. Experience shows that it is not possible at this stage to bring the design to a level where detailed weight calculations of the components and systems are possible. This can be done only after releasing working drawings which have been thoroughly checked, both from the viewpoint of manufacturing feasibility, and strength. Therefore, in the preliminary design stage, the weight is determined using simplified relationships usually called weight prediction formulae.

Development of such weight formulae is based on the fact that knowing the overall helicopter dimensions defined by the layout, the weight of any component or system is determined either by the loads acting on the component—associated with the selection of the cross-sections required for strength or stiffness—or by other known relationships which can also be represented by formulae.

In this weight estimate, it is very important that the weight formulae reflect all the basic conditions and limitations encountered in the actual design in spite of the fact that the weight formulae as a rule do not include all the factors influencing the weight, but only the characteristic dimensions and the primary loads that determine the cross-sections of the parts. In addition, the obtained formulae are quite simple, yet still reflect the similarity laws for components of different dimensions.

It should be noted that weights of the same type components depend on their layout, successful or unsuccessful design, selection of component dimensions which are not necessarily related to the overall helicopter size, but are still influenced by the type of materials and loads. However, in the weight-prediction formulae structured as previously described, all of these factors can be accounted for only through proper values of the coefficients appearing in the formulae. These coefficients will be called weight coefficients.

Consequently, in this approach, the weight coefficients become a measure of the weight efficiency of a given component. However, in order to use the weight coefficients in this fashion, it is necessary to determine the scale effect on the weight of the component.

It is important to establish whether it is possible to design a new component of different dimensions—but still similar to its prototype—using the same specific loads and stresses. It turns out that this can not be done since the stiffness characteristics associated with component wall thickness does not vary proportionally to the scale. Consequently, the critical buckling stresses, which obviously vary approximately as the square of the wall thickness, will not remain the same. Therefore, with reduction of the overall component dimensions, we can not vary the wall thickness by the same factor. In a small part, the walls must always be relatively thicker than in a larger part. The manufacturing and operational limitations have the same influence and do not permit a reduction in the wall thickness below definite limits.

Consequently, the similarity laws do not apply, and the small component is, as a rule, relatively heavier than the large one. This effect must be taken into account in the weight formulae; thus leading to deviation of their structure from that resulting from the similarity laws. The magnitude of these deviations can be evaluated on the basis of refined calculations, one of which is presented as an example in Ch 3, or on the basis of statistical weight analyses of components having different dimensions, but designed on the basis of the same principles and fabricated under the same conditions.

Therefore, we propose a dual approach in the weight calculations: in one case, the scale effect is taken into account only by specifying different values of the weight coefficients depending on the size; while in the other case. account for this effect is achieved by changing the power to which the parameter defining the component size is raised, but the weight coefficients remain constant regardless of the size of the component.

Only the basic characteristic dimensions of the component and the primary loads that determine the cross-section areas of the parts appear in the weight formulae; consequently, when changing the other dimensions and loads, and also when introducing some specific features into the component which alter certain secondary functions, the weight of the component may change. However, these possible changes would not show up on the weights determined from the weight formulae. In this sense, we can speak of accuracy of the weight formulae associated with incomplete accounting for all the factors which influence the weight. However, in many cases, these factors can be taken into account on the basis of existing experience through suitable correction of the weight coefficients. Therefore, analysis of the possible calculation errors with account for all influencing factors and the available design experience convinces us that the weight calculation is quite accurate. It appears hence, that the presented formulae need hardly any serious refinements as far as selecting the optimal helicopter parameters and configuration is concerned.

We note in passing that judging weight formula accuracy on the basis of the scatter in the values of the component weight coefficients is not justified. This is due to the fact that those components were developed at different times and by different design offices according to different configurations with the use of different materials and fabrication methods. This scatter is associated primarily with the differences in the component developmental conditions and not with the accuracy of the formulae.

Sufficiently accurate weight formulae open up broad possibilities for varied applications.

The helicopter industry has been around for a long time. About a hundred different helicopter types have been produced with components and systems which are similar in purpose and construction whose weights are known. Following the advances in design and the general development of technology, the weight of helicopter components is continuously decreasing. By using the weight coefficients appearing in the formulae, we can observe the dynamics of the variation of weight characteristics of the components and systems as a function of the year of their introduction and indicate what their weight should be for the contemporary design.

This provides a very necessary guideline, directing the designer toward the development of components and systems having up-to-date weight characteristics.

The possibility of evaluating helicopter weight using weight formulae permits one to conduct broad studies in selecting the optimal parameters of new helicopter designs and to perform a comparison of the various configurations of rotary-wing aircraft.

It is quite obvious that the weight calculations can be made only in combination with the development of specific helicopter configurations, taking into account those requirements which result from aerodynamics, structural strength, necessary stiffness, and advances in allied fields of technology which determine the possibility of developing certain helicopter components. Specifically, in the preliminary layouts one determines the dimensions which are necessary for calculating the structural characteristics and weights. Therefore, when examining specific examples we, as a rule, use a specific configuration which appears to us as the most suitable of all the considered ones, and point out those limitations which this configuration encounters.

In addition to the weight formulae and their justification, we shall present in this section some statistical data on the weights of several basic helicopter components and systems in order to evaluate the achieved weight level and to illustrate the possible scatter in the weight values.

We shall examine the weight formulae and present a brief justification of these formulae for all the basic helicopter components and systems.

2.2.1 Main and Tail Rotor Blades

Just as in the design of all other helicopter components, the designer strives for maximum reduction of the blade weight. This effort is especially justified in the present case since the centrifugal force acting on the rotor hub and consequently, the hub weight, depends on the weight of the blade.

However, on the way to blade weight reduction, definite limitations appear which depend on blade dimensions: its chord and the rotor radius. One limitation is determined by the allowable values of blade mass characteristic γ_0 (Lock number); the other is determined by the minimal achievable structural and technological weight of the blade.

The level of the alternating stresses acting on the blade and the margins available in certain unstable modes (torsional–flapping and inplane flutter, divergency, and so on) depend on the blade mass characteristic

$$\gamma_0 = c_y^{\alpha} \rho_0 b_{0.7} R^4 / 2 I_{f.h} \qquad (2.1)$$

where c_y^{α} = slope of the lift-coefficient curve; ρ_o = air density at sea-level standard; $b_{o.7}$ = blade chord at the relative radius, $\bar{r} = 0.7$; R = rotor radius; and $I_{f.h}$ = blade moment of inertia about the flapping hinge.

Other conditions being the same, retention of the γ_0 values guarantees the same level of alternating stresses in the blade and therefore, becomes a very important criterion in evaluating blade weight.

If we express $I_{f.h} = k_I \; G_{bl} R^2$ where G_{bl} is the blade weight, we can write

$$\gamma_0 = c_y^{\alpha} \rho_0 b_{0.7} R^2 / 2 k_I G_{bl}, \qquad (2.2)$$

hence, the overall weight of all the blades is

$$\Sigma G_{bl} = k_{bl} \sigma R^3 \qquad (2.3)$$

where

$$k_{bl} = c_y^a \rho_0 \pi / 2 k_I \gamma_0 .$$

The weight of a single blade is given by the following formula:

$$G_{bl} = (1/\pi) k_{bl} b_{0.7} R^2 . \tag{2.4}$$

We note that the weight coefficient k_{bl} appearing in Eqs (2.3) and (2.4) is, for instance, inversely proportional to the blade mass characteristic γ_0. A constant relationship between them is maintained for the same laws of weight distribution along the blade length when

$$k_l = \bar{l}^2_{f.h}/g = const, \quad \text{where } \bar{l}_{f.h} = l_{f.h}/R,$$

and $l_{f.h}$ = the blade radius of inertia.

In determining γ_0, the values of c_y^a are assumed to be constant and equal to c_y^a = 5.75/rad.

The values of the weight coefficient k_{bl} for several existing blades are shown in Fig 2.1. The corresponding values of the blade mass characteristic γ_0 are also indicated. From a comparison of the values of k_{bl} and γ_0, we can draw a conclusion as to the degree of their nonproportionality.

Since normal operation of the main rotor, with the exclusion of the aforementioned unstable modes, can be ensured only with values of the mass characteristic no larger than γ_{0max}—at the present time, this value is assumed to be $\gamma_{0max} \approx 7.0$ for the main rotor blades—one can also introduce the concept of a minimum possible value of the weight coefficient k_{blmin}. Then Eqs (2.3) and (2.4) must be supplemented with the constraint that

$$k_{bl} > k_{blmin} . \tag{2.5}$$

For the main-rotor blades, we shall assume that $k_{blmin} = 5.5$ corresponds to γ_{0max}.

However, with few exceptions (see Fig 2.1), the weights of nearly all production blades are higher than those determined from the above-given k_{blmin} value. This can be explained both by the desire to reduce the alternating stresses acting in the blade spar which decrease with reduction of the γ_0 value, and by the fact that another limitation—the structural-technological limitation—becomes more critical. This limitation is associated with the minimal allowable wall thickness of the blade parts. The thickness of the spar walls can not be reduced below definite limits for both manufacturing reasons and because of loss of wall stability resulting from the blades hitting the stops. The wall thickness of the other blade elements also cannot be reduced because of operational and strength considerations. These, and several other constraints of a structural and technological nature lead to a relative increase in the weight of the small blades. Therefore, the value of the k_{bl} coefficient is usually higher for small, and lower for large blades (see Fig 2.1 and Table 2.1).

This question is examined in more detail in Ch 3, where the minimal achievable structural-technological weight of the blade is determined from analysis of the weight breakdown of two types of construction.

It follows from this analysis that for the blade with tubular steel spar and fiberglass shell in the chord range of $b \approx 0.45$ to $1.0 m$, and those with extruded aluminum spar in the

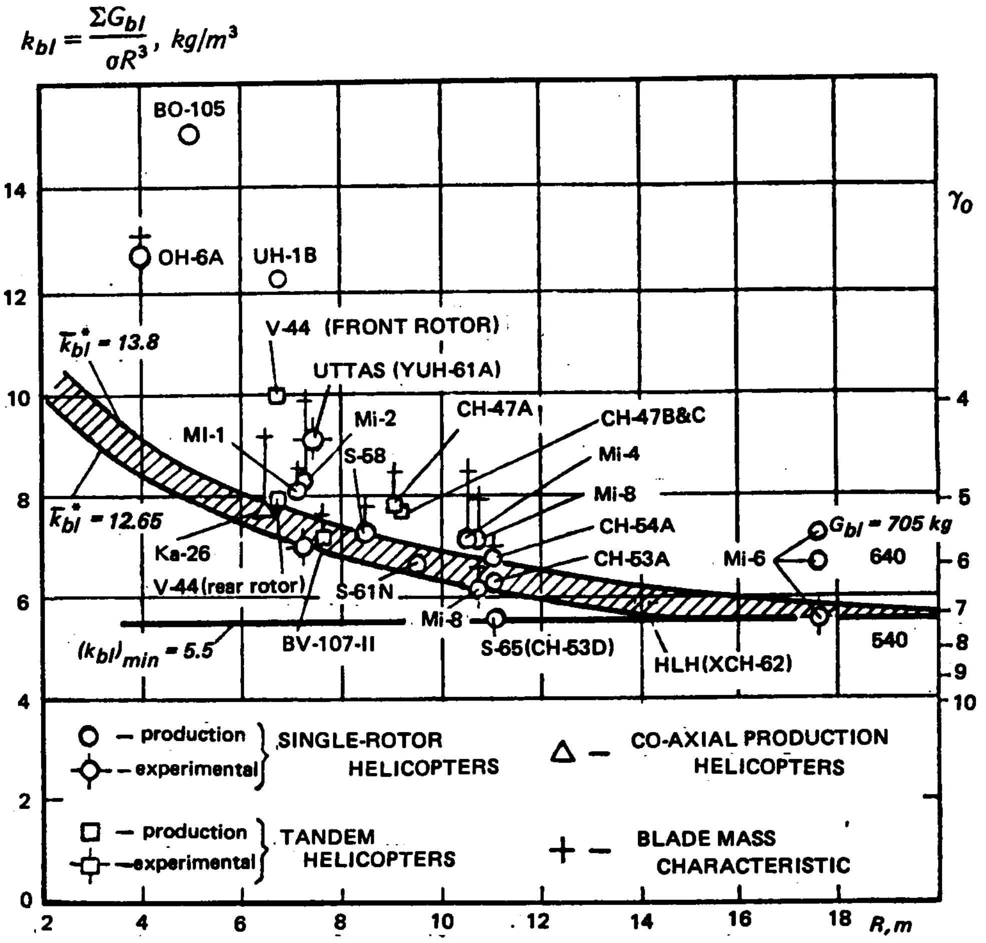

Figure 2.1 Variation of the blade weight coefficient k_{bl} and mass characteristic γ_0 as a function of the main-rotor radius (hatched area corresponds to more favorable weight relationships of modern helicopters in large-scale operations)

HELICOPTER	$R_{m.r.}$, m	$b_{0.7}$, m	λ	G_{bl}, kg	$I_{f.h}$, kg·m·s^2	γ_0	k_{bl}, kg/m^3	$\bar{k}^{\circ}_{bl}$, kg/m$^{2.7}$	k°_{bl}, kg/m$^{2.7}$	$\bar{r}_{c.g}$	n, rpm	N_{bl}, ton	G_{hub}, kg	k_{hub}, kg/ton$^{3/2}$	k°_{hub}, kg/ton$^{1.35}$	DESIGN FEATURES
Mi-1	7.15	0.400	17.86	53	82.6	4.60	8.15	14.80	14.71	0.485	235	11.30	123	1.080	1.54	– – –
Mi-2	7.25	0.400	18.12	55	98.5	4.04	8.25	15.00	15.12	0.50	246	13.55	132	0.885	1.31	– – –
Mi-4	10.50	0.520	20.19	130	460	4.52	7.12	14.36	15.60	0.48	165	20.00	425	1.190	1.82	– – –
Mi-8	10.65	0.520	20.50	134	487	4.90	7.13	14.30	15.70	0.48	192	29.50	605	0.720	1.20	Blades w/Duralumin extruded spar
				116	458	6.10	6.15	12.40	13.60	0.50		25.40				Glass-fibre—plastic blades
Mi-6	17.50	1.000	17.50	705	6236	5.34	7.20	17.00	16.80	0.45	120	96.00	33.25	0.673	1.33	– – –
				640	5650	5.90	6.50	15.40	15.25			86.00	–	–	–	
				540	4770	7.00	5.50	13.00	12.87			72.50				
Ka-26	6.50	0.250	26.00	26	37.2	4.26	7.75	13.35	17.20	–	–	–	–	–	–	– – –
OH-6A	4.0125	0.172	23.30	10.95	5.28	2.83	12.70	19.10	22.90	0.48	485	5.60	28.8	0.550	0.72	– – –
V-44	6.72	0.457	14.70	52	75	4.44	7.90	14.00	12.20	0.50	258	13.00	149	1.060	1.56	Aft Rotor
				65	95	3.50	10.00	17.50	15.20			16.50		0.740	1.13	Front Rotor
V-107-II	7.62	0.480	15.90	63.5	110	5.20	7.20	13.25	12.14	0.50	264	18.80	204	0.837	1.31	Hub w/manual blade folding
UH-1B	6.70	0.533	12.60	91.8	–	–	12.20	21.50	16.80	0.50	324	29.00	164.4	0.527	0.88	Two-bladed teetering rotor
CH-47A	9.01	0.583	15.45	118	298	4.60	7.79	15.00	13.56	0.47	230	31.30	326	0.622	1.04	– – –
CH-47B	9.145	0.640	14.30	130	335	4.80	7.70	14.85	12.60	0.50	230	35.20	369	0.585	1.06	– – –
CH-47C											243	39.00	382	0.514	0.89	– – –
CH-47C	9.14	0.820	11.20	169	435	4.74	7.80	14.90	10.70	0.47	230	42.80	–	–	–	Glass-fibre—plastic blades
S-58	8.53	0.420	20.30	71	159	5.00	7.36	13.75	15.00	0.47	220	16.60	298	1.102	1.68	– – –
S-61N	9.45	0.460	20.50	87	264	4.95	6.70	13.20	14.50	0.50	200	18.50	440	1.060	1.64	– – –
S-65 (CH-53A)	11.01	0.660	16.70	160	579	5.40	6.28	12.96	12.30	0.456	185	34.00	897	0.685	1.15	Steel hub w/some titanium production version w/automatic blade folding
S-65 (CH-53A)	11.01	0.660	16.70	160	579	5.40	6.28	12.96	12.30	0.456	185	34.00	1210	0.925	1.56	Steel hub, w/automatic blade folding (project)
													660	0.505	0.85	Titanium hub (project)
S-65 (CH-53D)		0.740	14.90			6.06	5.60	11.50	10.10				–	–	–	Blade w/tubular titanium spar
S-64 (CH-54A)	11.01	0.600	18.40	156.5	542	5.85	6.68	13.60	13.80	0.50	185	–	–	–	–	– – –
HLH (XCH-62)	14.02	1.016	13.80	366	2120	6.70	5.80	12.80	10.62	–	156	77.20	1404	0.524	1.00	Titanium hubs w/elastomeric bearings
UTTAS (YUH-61A)	7.465	0.600	12.40	97	–	–	9.15	16.70	–	–	–	–	–	–	–	Rigid-rotor blades (w/o horizontal and vertical hinges)
BO-105	4.91	0.270	18.20	30.8	–	–	14.90	23.80	23.70	–	424	–	–	–	–	

TABLE 2.1 MAIN ROTOR BLADE AND HUB DATA

chord range of $b \approx 0.25$ to $0.8\,m$, the dependence of the minimal achievable weight on the parameters can be approximately described by the following formula:

$$G_{bl_{min}} = q^*_{bl} b^{1.7} R [1 + \alpha_\lambda \bar{R}(\lambda - \lambda_o)] \tag{2.6}$$

where q^*_{bl} is a coefficient that depends on the type of blade structure, $\bar{R} = R/R_o$; and the value of R_o is arbitrarily taken as $R_o = 16m$.

For aspect ratio $\lambda < \lambda_o$, the expression in the square brackets is arbitrarily taken as equal to one.

It will be seen from Ch 3 that the values of the quantities appearing in this formula can be taken as follows: $\bar{R}\lambda_o = 20$, $\alpha_\lambda = 0.015$ for the steel-spar blades, and $\bar{R}\lambda_o = 12.4$, $\alpha_\lambda = 0.011$ for extruded-aluminum-spar blades.

For blades having the same aspect ratios

$$\lambda = R/b = const, \tag{2.7}$$

this formula can be transformed into the following formulae:

$$(\Sigma G_{bl})_{min} = \bar{k}^*_{bl} \sigma R^{2.7} [1 + a_\lambda \bar{R}(\lambda - \lambda_o)] \tag{2.8}$$

and

$$G_{bl_{min}} = (1/\pi) \bar{k}^*_{bl} b_{0.7} R^{1.7} [1 + a_\lambda \bar{R}(\lambda - \lambda_o)] \tag{2.9}$$

where

$$\bar{k}^* = k_{bl} R^{0.3} / [1 + a_\lambda \bar{R}(\lambda - \lambda_o)]\,. \tag{2.10}$$

It is obvious that for the same values of $\bar{k}^*_{bl}$, the blade mass characteristic γ_o of larger diameter rotors will be larger. Both the alternating stresses and the tendency of the blades toward various types of instabilities associated with the larger values of γ_o will be correspondingly greater in such blades. Therefore, when using Eqs (2.8) and (2.9), as well as Eqs (2.3) and (2.4), the conditions of Eq (2.5) should be fulfilled. It follows that

$$\bar{k}^*_{bl} \geqslant k_{bl_{min}} R^{0.3} / [1 + \alpha_\lambda \bar{R}(\lambda - \lambda_o)]\,. \tag{2.11}$$

Eqs (2.8) and (2.9), obtained from the consideration of only two types of blades and developed under the assumption that $\lambda = const$, sufficiently well reflect the general tendency of reducing the weight of the blade with increasing diameter of the rotor as can be seen from examination of various blade constructions (Fig 2.2) having not exactly the same aspect ratio, but varying within the approximate range of $\lambda = 16$ to $\lambda = 20$ and, in particular cases, even exceeding that range (see Table 2.1). This is apparently explained by the fact that, as a rule, the optimal construction is selected for the assumed blade size and aspect ratio. Therefore, the differences in blade weight associated with the influence of aspect ratio are, in large measure, concealed.

Hence, it follows that when comparing helicopter designs and selecting the optimal blade type for each dimension, Eqs (2.8) and (2.9) can be used. However, if we examine blades of only one particular type, we must take into account the differences in their aspect ratios

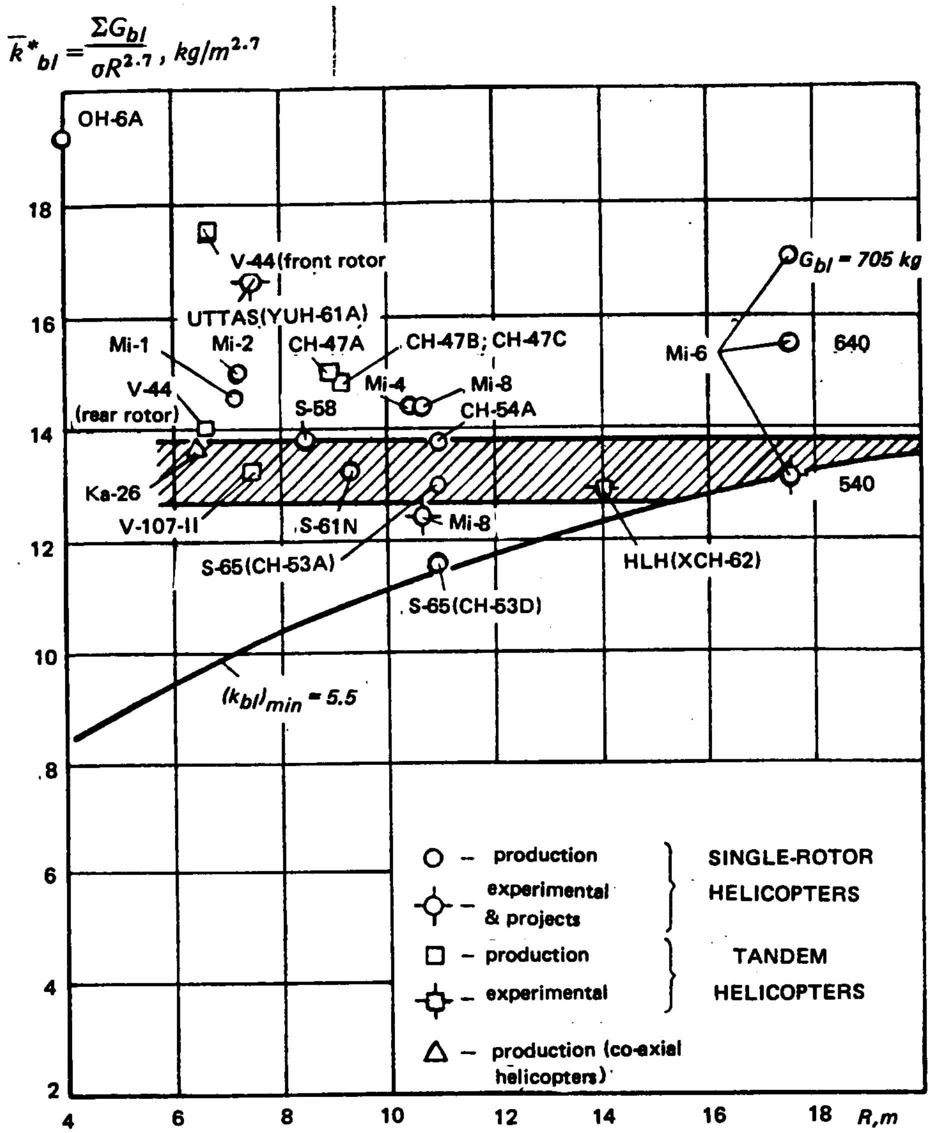

Figure 2.2 Lifting-rotor blade weight coefficient, $\bar{k}^*_{bl}$, without consideration of differences in blade aspect ratios (hatched area corresponds to the best blades from the weight point-of-view for large-scale operations)

which have a definite influence on their weight. In this case, it is necessary to use the more precise formulae which follow from Eq (2.6):

$$\Sigma G_{bl} = (k^*_{bl}/\bar{\lambda}^{0.7})\sigma R^{2.7}[1 + a_{\lambda}\bar{R}(\lambda - \lambda_o)] \qquad (2.12)$$

and

$$G_{bl} = [k^*_{bl}/\pi(\bar{\lambda})^{0.7}]b_{0.7}R^{1.7}[1 + a_{\lambda}\bar{R}(\lambda - \lambda_o)], \qquad (2.13)$$

where

$$\bar{\lambda} = \lambda/\lambda_{av}, \text{ while } \lambda_{av} = 18, \text{ and } k^*_{bl} = \pi q^*_{bl}/18^{0.7}. \qquad (2.14)$$

Just as Eqs (2.3), (2.4), (2.8), and (2.9); Eqs (2.12) and (2.13) are valid only for the region where $k_{bl} \geqslant k_{bl_{min}}$. Therefore, the coefficient k^*_{bl} can not be smaller than the value obtained from the condition given by Eq (2.5) and determined as

$$k^*_{bl} \geq \bar{\lambda}^{0.7} R^{0.3} k_{bl_{min}}/[1 + a_\lambda \bar{R}(\lambda - \lambda_o)] . \qquad (2.15)$$

The values of the blade weight coefficients with account for the difference in their aspect ratios are shown in Fig 2.3. Here the hatched lines represent the values of the weight coefficients k^*_{bl} corresponding to the condition $k_{bl_{min}} = 5.5$ for the indicated blade aspect ratios.

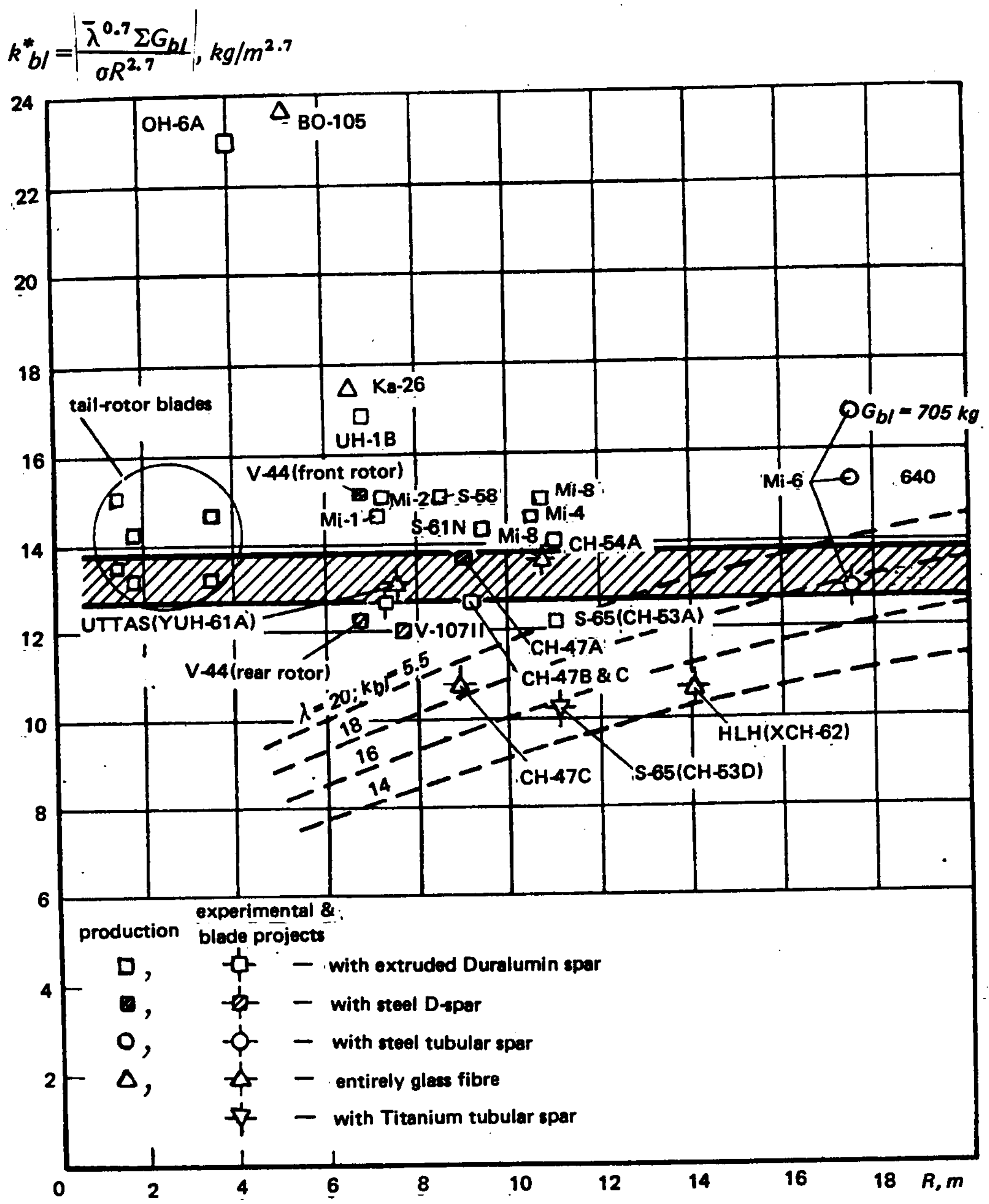

Figure 2.3 Lifting-rotor blade-weight coefficients k^*_{bl} considering the variation in blade aspect ratio. Hatched area denotes improved (weight-wise) blades having either extruded Duralumin or tubular-steel spars with fiberglass envelope; broken lines indicate bounderies of the minimum permissible blade weight resulting from the $\gamma_0 \approx 7$ condition ($k_{bl} = 5.5$). Tail-rotor k^*_{bl} values are also shown.

It is interesting to note that a large part of the operational blades with steel-tube and extruded-Duralumin spars have weight coefficients k^*_{bl} no smaller than those defined as corresponding to the contemparary level. Only the S-65 helicopter blade is somewhat lighter.

Attention should be called to the fact that using advanced materials, several experimental blades of relatively small aspect ratios that are markedly below this level have recently been constructed (Fig 2.3). We note that it was not possible to achieve a similar weight reduction for the Mi-6 blade since, in blades weighing 540 kg, a value for the mass characteristic has already reached a value of $\gamma_0 = 7$. Hence, it follows that the blade design with a steel-tube spar and fiberglass envelope used in this case is optimal for this blade size.

One may hence conclude that taking advantage of already-realized blade projects and analysis of the data presented in Fig 2.3 for blade designs with steel-tube and extruded Duralumin spar and fiberglass envelopes—manufactured at the modern level—the following weight coefficients can be achieved:

$$k^*_{bl} = 12.6 \dots 13.8 \qquad (2.16)$$

which corresponds to

$$k_{bl} = 5.5 \dots 6.0 \text{ at } R = 16m \text{ and } \lambda = \lambda_{av}.$$

It is obvious that blade weight is influenced by the selected rotor tip speed, $U_t = \omega R$.

With an increase in the tip speed, the centrifugal force increases, and an increase in wall thickness in the central part of the spar (loaded in tension) may be required. Some beefup of the blade envelope may also be necessary.

The techniques discussed in Ch 3 lead to the conclusion that for the blade types examined in Ch 3, the weight of lifting-rotor blades increases markedly as tip speed exceeds the normal value of $U_{t.n} = 220\ m/s$.

In order to account for this effect for $U_t > U_{t.n}$, Eq (2.12) is rewritten as follows:

$$\Sigma G_{bl} = (k^*_{bl}/\bar{\lambda}^{0.7})\ \sigma R^{2.7} [1 + a_{\lambda} \bar{R}(\lambda - \lambda_0)]\ [1 + 0.5(\bar{U}_t^2 - \bar{U}_{tn}^2)] \qquad (2.17)$$

where

$$\bar{U}_t = U_t/U_{t_o},\ \bar{U}_{tn} = U_{tn}/U_{t_o},\ \ U_{t_o} = 220\,m/s.$$

If $U_{t.n} = U_{t_o}$, then $\bar{U}_{tn} = 1$, and the expressions in the square brackets can be used only when $\bar{R}\lambda = \bar{R}\lambda_0$ and $U_t > 220\ m/s$. Eq (2.17 is also valid only when the condition of Eq (2.5) is satisfied.

Detailed comments on the use of these formulae will be presented in Sect 2.5.1.

2.2.2 Main Rotor Hubs

The main (articulated) rotor hubs consist of the centerbody and the "arms" components which, in turn, consist of pitch-bearing housings with other hinges and blade-attachment joints. The weight of the arms usually amounts to more than 85 percent of the hub weight. Therefore, it is important to determine the arm weight, and then the centerbody weight can be taken as approximately proportional to the pitch-bearing housing weight. In determining the pitch-bearing housing weight, it is important to establish which of the loads acting on the hub (centrifugal force or bending moments) determine the cross-section areas of the parts forming the housing.

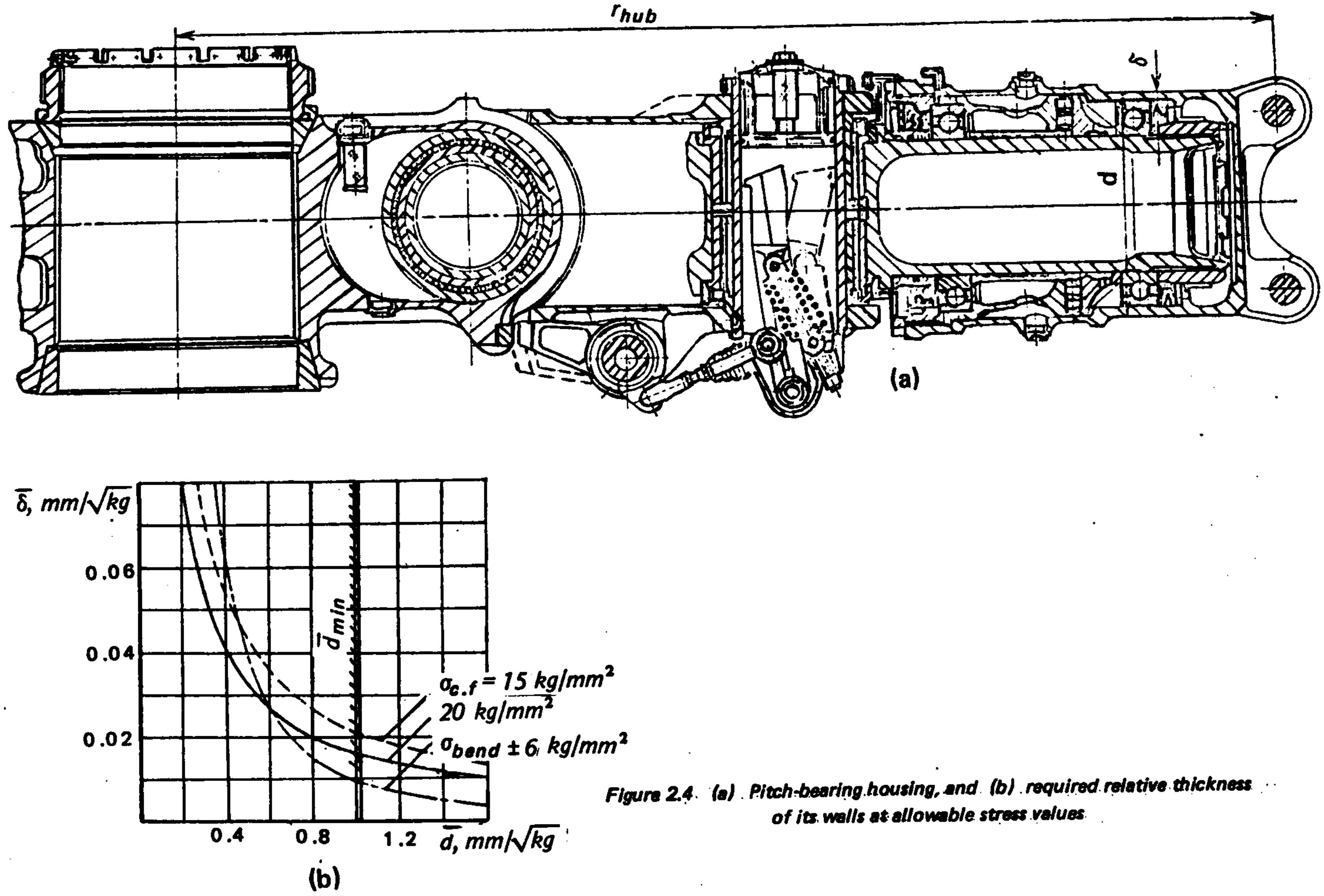
r_{hub}
δ
d
(a)
$\bar{\delta}$, $mm/\sqrt{kg}$
0.06
0.04
0.02
$\bar{d}_{min}$
$\sigma_{c.f} = 15\ kg/mm^2$
$20\ kg/mm^2$
$\sigma_{bend} \pm 6\ kg/mm^2$
0.4
0.8
1.2
$\bar{d}$, $mm/\sqrt{kg}$
(b)

Figure 2.4 (a) Pitch-bearing housing, and (b) required relative thickness of its walls at allowable stress values

In comparing these loads it is convenient to represent the alternating bending moment in the form of the product of the centrifugal force and the arm e. In this case, the stresses from the centrifugal force can be found from the formula:

$$\sigma_{c.f} = 1/a_1 \bar{\delta} \bar{d} \tag{2.18}$$

and the stresses from the bending moment, from the formula:

$$\sigma_{bend} = \pm \bar{e}/a_2 \bar{\delta} \bar{d}^2 \tag{2.19}$$

where $\bar{\delta}$ and $\bar{d}$ respectively, are the relative wall thickness and the relative overall dimension of the pitch-bearing housing section (Fig 2.4a);

$$\bar{\delta} = \delta/\sqrt{N_{bl}}, \ \bar{d} = d/\sqrt{N_{bl}}; \tag{2.20}$$

where N_{bl} = blade centrifugal force; a_1 and a_2 are coefficients accounting for the shape of the cross-section.

For a cylindrical section,

$$a_1 = \pi, \text{ and } a_2 = \pi/4. \tag{2.21}$$

The relative arm of centrifugal force characterizing the magnitude of the alternating bending moment is

$$\bar{e} = e/\sqrt{N_{bl}}. \tag{2.22}$$

Statistical values of $\bar{e}$ for various helicopters usually show that $\bar{e} < 0.045$.

In Fig 2.4b, the values of the minimum allowable relative wall thickness $\bar{\delta}$ and the overall dimension $\bar{d}$ are shown by assuming that the maximum allowable centrifugal force due to stress is $\sigma_{e.f} = 15 \ldots 20\ kg/mm^2$, and the maximum allowable alternating bending stress is $\sigma_{bend} = \pm 6\ kg/mm^2$.

A supplemental condition in hub design is that the hub parts must enclose the pitch bearing (see Fig 2.4a).

If we assume that the supporting surface of the bearing is approximately equal to one-half of the area enclosed by the outer contour of the pitch-bearing housing section,

$$F_{sup.bear} = \xi F_{cross}$$

where $\xi \approx 0.5$, then the relative outside dimension of the section must not be smaller than

$$\bar{d} = 1\sqrt{a_3 \xi q} \tag{2.23}$$

where a_3 is a coefficient which depends on the section shape (for a cylindrical section, $a_3 = \pi/4$); q = allowable specific load on the supporting surface of the thrust bearing.

In Fig 2.4b, the minimum value of $\bar{d}$ is shown for the case when $q = 300\ kg/cm^2$.

It can be seen from this graph that stresses due to the centrifugal force become the governing factor for the parts enclosing the bearings.

Therefore, the section areas of these parts and their weight-per-unit length are proportional to the centrifugal force, while the pitch-bearing housing weight is proportional to $N_{bl} r_{hub}$; i.e.,

$$G_{arm} = k_{arm} N_{bl} r_{hub} \tag{2.24}$$

where r_{hub} is the length of the arm along the blade radius.

Consequently, to reduce the hub weight we must reduce the arm length as much as possible.

Two constraints are encountered here. First of all, it is obvious that the arm length cannot be shorter than the overall dimension of the hinge fittings when the latter are located as close as possible to the body. In addition, for the assumed angle ξ_{max} of blade deflection about the lead-lag hinge, the offset of this hinge ($\ell_{l.h}$) cannot be reduced and must be kept unchanged for constant values of ωR and t_y, and be proportional to the maximum main-rotor torque ($M_{Q_{m.r}}$):

$$\ell_{l.h} = kM_{Q_{m.r}}. \tag{2.25}$$

In the case of hinges which are as close together as possible, the hub arm length is determined by the overall dimensions of the hinge brackets, proportional to

$$r_{hub} = k_{r_{hub}}\sqrt{N_{bl}}. \tag{2.26}$$

In this case, the hub weight can be determined from the well-known Leikand formula,

$$G_{hub} = k_{hub} z_{bl} N_{bl}^{3/2} \tag{2.27}$$

where N_{bl} = blade centrifugal force in tons.

However, realization of near-perfect closeness of the hinges is not possible for several reasons. There is not enough experience in operating helicopters with hubs having reduced vertical hinge offsets and large angles, ξ_{max}. There is also a lack of flight experience with hubs exhibiting nontraditional (for Soviet helicopters) hinge sequence, which markedly reduces the arm length for given $\ell_{l.h}$, as has been done in the hubs of the Chinook (flapping hinge, feathering hinge, and lead-lag hinge) (Fig 2.5) and Flettner (feathering hinge, flapping hinge, lead-lag hinge) helicopters.

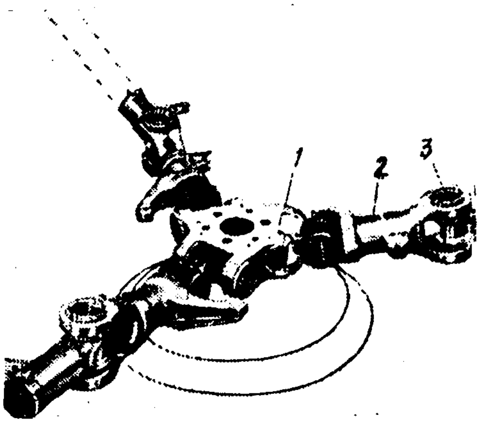

Figure 2.5 Hub of Chinook Helicopter[23]: (1) flapping hinge; (2) feathering hinge; (3) lead-lag hinge

In addition, shortening of the arm, particularly for multibladed rotor hubs, involves difficulties of a configurational nature. To illustrate this, Fig 2.6 shows two main rotor hubs having a different number of blades, but with the same values of the overall centrifugal force $z_{bl}N_{bl}$, and designed for the same torque $(M_Q)_{m.r}$.

In spite of a reduction (by a factor of 5/8) in the centrifugal force acting on each blade of the main rotor with $z_{bl} = 8$, the arm length could not be reduced both because of the necessity to maintain the same value of $\ell_{l.h}$, and because of the lack of space for the hub arms as the hinges are moved closer to the body of the hub. Therefore, the hub arm length obtained

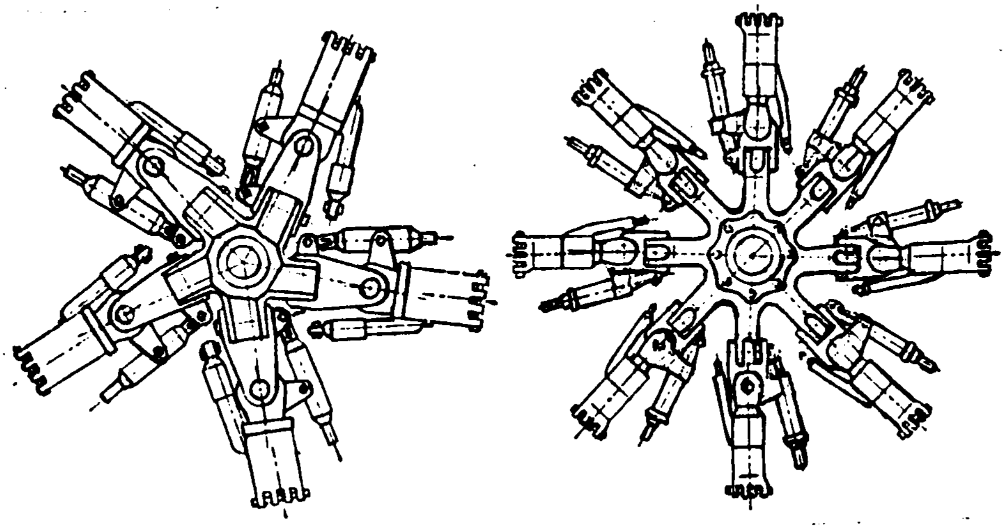

Figure 2.6 Schemes of multibladed rotor hubs with 5 and 8 blades having the same $\ell_{l.h}$ and designed for the same torque and overall value of centrifugal force

as a result of design efforts would depend on the general level of knowledge and experience of the helicopter manufacturer, as well as on the qualifications and skill of the designer.

Consequently, in evaluating the achieved design level, we can use the coefficients appearing in the following formula:

$$G_{hub} = k'_{hub} z_{bl} N_{bl} R \tag{2.28}$$

which was obtained from Eq (2.24) by expressing the arm length in terms of blade radius.

However, if one considers determination of hub weight for different values of the centrifugal force where the magnitude of the main-rotor torque does not prevent the hinges from being quite close together, we can use Eq (2.27).

It follows from this equation that for a given value of blade centrifugal force N_{bl}, the hub weight is directly proportional to the number of main rotor blades z_{bl}, or the number of hub arms. However, design experience shows that for multibladed rotor hubs, this dependence is violated somewhat and the hub weight per arm does not remain constant, but rather increases with an increase in the number of arms. In order to take this circumstance into consideration, we can introduce the coefficient $k_{z_{bl}}$ into the formula for calculating the hub weight in the form suggested by Leikand:

$$G_{hub} = k_{hub} k_{z_{bl}} z_{bl} (N_{bl})^{3/2} \tag{2.29}$$

where

$$k_{z_{bl}} = 1 \text{ for } z_{bl} \leqslant 4;$$

and

$$k_{z_{bl}} = 1 + \xi_{z_{bl}}(z_{bl} - 4) \text{ for } z_{bl} > 4. \tag{2.30}$$

The coefficient $\xi_{z_{bl}}$ can be taken as equal to 0.05, although several studies indicate that it may be smaller.

The weight coefficients k_{hub} for various Soviet and foreign helicopter hubs are presented in both Fig 2.7 and Table 2.1. For hubs with $z_{bl} > 4$, the weight coefficients are determined by Eq (2.30) in which the value $\xi_{z_{bl}} = 0.05$ was taken.

$$k_{hub} = \frac{G_{hub}}{z_{bl}[1 + 0.05(z_{bl} - 4)]N_{bl}^{3/2}}, \; kg/ton^{3/2}$$

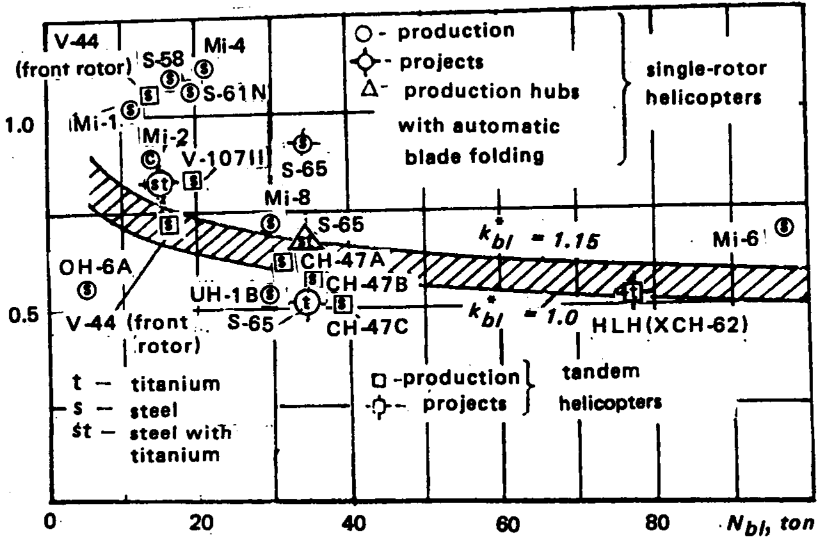

Figure 2.7 Character of variation of weight coefficient k_{hub} of main rotor hubs for a wide range of centrifugal force values N_{bl} (hatched area corresponds to the better designs (weight-wise) of fully-articulated blades now in extensive operational use

Analysis of data on hubs of the same type shows that because of the relative increase in wall thickness, the hubs designed for lower centrifugal force are relatively heavier. To account for this effect, we propose the use of the following formula:

$$G_{hub} = k^*_{hub} k_{z_{bl}} z_{bl} N_{bl}^{1.35} \tag{2.31}$$

The values of the coefficient k^*_{hub} are shown in Fig 2.8. It may be assumed that for modern Soviet hubs, $k^*_{hub} \approx 1.15$.

For the centrifugal force $N_{bl} = 60$, the corresponding value of the hub weight coefficient becomes $k_{hub} = 0.061$.

2.2.3 Helicopter Controls

To evaluate the weight we divide the helicopter control system into two parts: the boosted control system of the main rotor (or rotors, including the tail rotor), and the control links from the stick or pedals to the primary boosters. This latter part of the system is called the preboost or manual control linkage. The difference between these parts of the control system lies in the fact that the boosted control system is designed for the loads from the rotor blades which increase with rotor size, while the preboost linkage system is designed only for

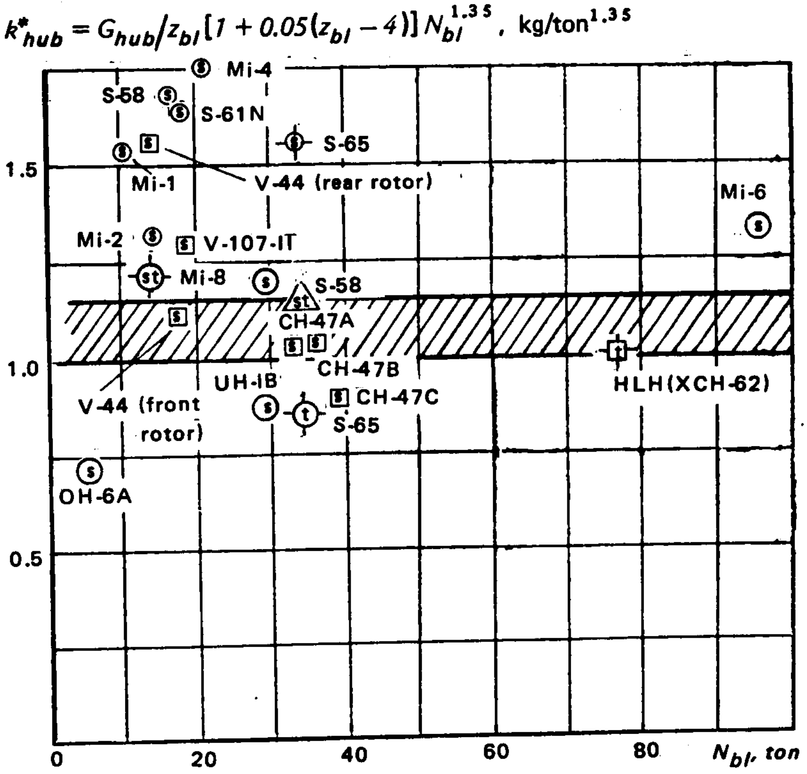

Figure 2.8 Main-rotor hub weight coefficients k^*_{hub}
(for other notations, see Fig 2.7)

the pilot forces of the single-step control system, and for the pilot forces and small boosters in the two-step control system. A schematic of the latter system is shown in Fig 2.9.

The boosted control system should include all the control elements that are computed for the loads transmitted from the blades. This system includes the swashplate assembly, primary boosters and their attachments, control system from the boosters to the swashplate assembly, and the primary hydraulic system; the output of which is directly associated with the power required by the primary boosters.

If we consider that the boosted control system weight is proportional to the sum of the blade feathering moments, this weight can be found from the formula

$$G_{b.cont} = k_{b.const} z_{bl} b^2 R \bar{U}_t^2 \bar{\mu}_{des} \qquad (2.32)$$

where

$$\bar{U}_t = \omega R/U_{t_o};\ \bar{\mu}_{des} = \mu_{des}/\mu_{cr_o};\ U_{t_o} = 220 m/s, \text{and } \mu_{cr_o} = 0.3.$$

Here, it is arbitrarily assumed that the design feathering moments are directly proportional to the design advance ratio, μ_{des}. Although this relationship may actually be more

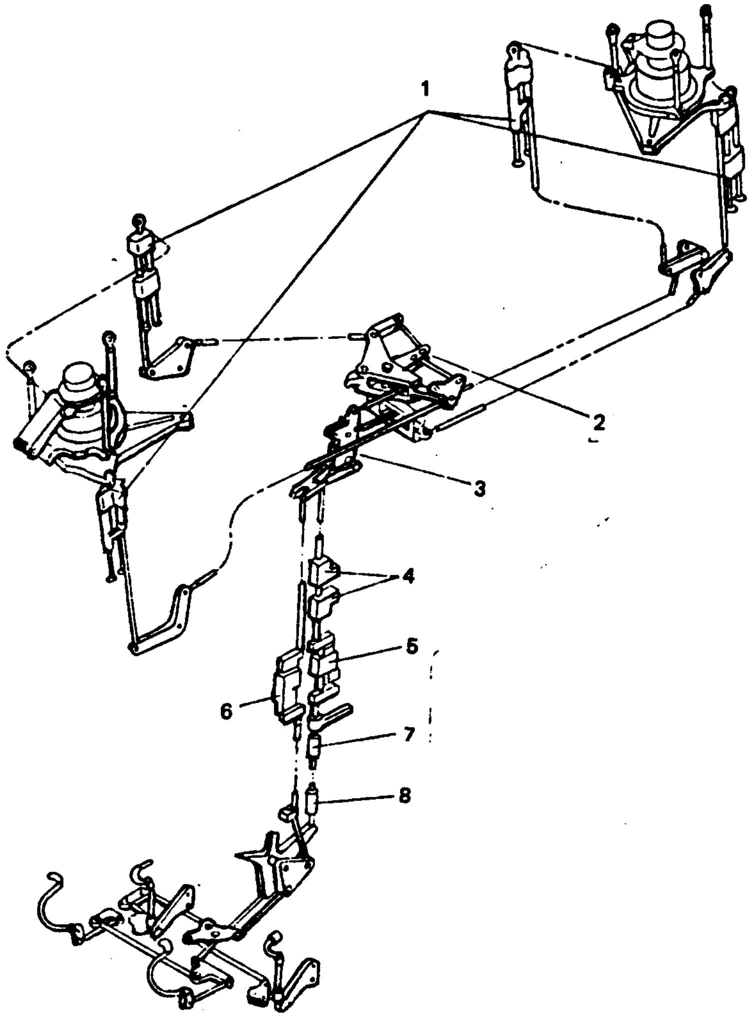

Figure 2.9 Scheme of two-step control system of the Chinook helicopter: 1 - basic hydraulic boosters (2nd step); 2 - second step of mechanical mixing; 3 - first step of mechanical mixing; 4 - SAS actuators; 5 - hydraulic boosters of longitudinal control system (1st step); 6 - hydraulic boosters of collective control system (1st step); 6 - hydraulic boosters of collective control system (1st step); 7 - upper control actuator of differential collective pitch control; 8 - lower control actuator of differential collective pitch control

complex, it permits one to at least partially account for the influence of the flight speed on the forces in the control system and therefore, on the system weight.

Figure 2.10 shows the specific boosted control weight coefficients for several Soviet helicopters where, for simplicity, it was assumed that $\overline{U}_t = \overline{\mu}_{des} = 1.0$. The weight coefficients of the swashplate assembly have been separated in order to evaluate its share in the overall weight of the boosted control system.

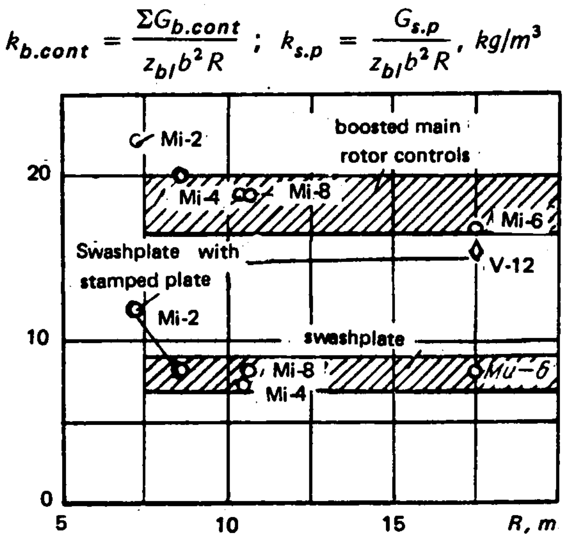

Figure 2.10 Weight coefficient of boosted controls and swashplates

Evaluating the above data, the achieved weight level of boosted controls can be expressed by the coefficient $k_{b.cont} = 16 \ldots 19\, kg/m^3$, and for swashplates by $k_{sw.pl} = 7 \ldots 8\, kg/m^3$.

However, recent analyses of modern boosters showed that the boosted control weight coefficient can be reduced to $k_{b.cont} = 13 \ldots 14 kg/m^3$.

Going ahead to Eq (2.132) and assuming that $t_{y_0} = 0.155$, we can transform Eq (2.32) for the boosted control weight to the following form:

$$G_{b.cont}/G_{gr} = (1/470) k_{b.cont}\, b\, \bar{\mu}_{des}\, \bar{U}_t^2 . \tag{2.33}$$

Consequently, for fixed values of $\bar{\mu}_{des}$ and $\bar{U}_t$, the relative boosted control weight, determined using Eq (2.33), is proportional to the blade chord b, and is independent of any other helicopter parameter.

In the context of manual control linkages, in addition to the controls up to the primary booster, we incorporate all other forms of controls, including those to the engines and stabilizers, and the auxiliary control systems for actuating the cargo doors, entry ladders, and cowlings. It also includes landing-gear retraction and the auxiliary hydraulic system used for this purpose.

In the single-rotor helicopter, all the control linkages, except for those to the tail rotor, are short and therefore, as a rule, we can use a simple single-step mechanical control system. The weight of the manual linkage of such control system is only about 20 to 30 percent of the weight of the entire control system and, in practice, depends only on its overall length. Assuming that the overall approximate length of the control linkage is proportional to the blade radius R,

$$G_{m.cont} = k_{m.cont}R. \tag{2.34}$$

For transport helicopters having no auxiliary control system, the value of the weight coefficient $k_{m.cont}$ (Fig 2.11) can be taken as $k_{m.cont} = 7 \ldots 10.5$ *kg/m*.

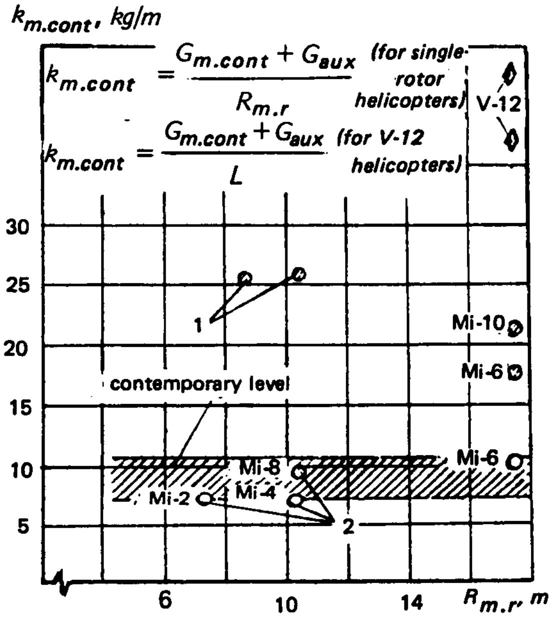

Figure 2.11 Weight coefficients of manual (pre-boost) controls
1 - helicopters with retractable L/G; 2 - helicopters without auxiliary control systems (hatched symbols refer to weight coefficients of manual and auxiliary controls, together with auxiliary hydraulic system)

For single-rotor helicopters having auxiliary controls for actuating the cargo doors, entry ladders, cowlings, and landing-gear retraction, this coefficient increases to $k_{m.cont} = 18 \ldots 25$ *kg/m*. Here, as already mentioned, the weight of the auxiliary control and its hydraulic system is included in the weight of the manual (pre-boost) controls.

The linkage length markedly increases for the twin-rotor helicopters and, because of the increased friction forces in the linkage, it is necessary to introduce additional small boosters; thus leading to a two-step control system which significantly increases the weight.

Assuming that the length of such linkage is proportional to the distance *L* between the rotors, we can evaluate the linkage weight from the formula

$$G_{m.cont} = k_{m.cont}L. \tag{2.35}$$

In the V-12 helicopter, the weight of the manual and auxiliary control together with the small boosters and their hydraulic system is 1360 kg (compared with the 350 kg for the Mi-6 helicopter). Consequently, $k_{m.cont} = 42.7$ *kg/m*.

In the tandem helicopters, the length of the overall control linkage is somewhat shorter. Therefore, the weight coefficient of manual and auxiliary controls for these helicopters should also have somewhat smaller values.

Considering that the development of the V-12 helicopter control system was the first experience of this sort, we believe that it is possible to lighten the preboost control linkage of twin-rotor helicopters. Therefore, we can take $k_{m.cont} = 30\ kg/m$ for the tandem, and $k_{m.cont} = 35\ kg/m$ for side-by-side rotor helicopters.

Considerable weight reduction can be achieved in twin-rotor helicopters with use of a fly-by-wire control system, whose weight coefficient $k_{m.cont}$ can be reduced by a factor of 1/1.5 to 1/2.0.

2.2.4 Main Gearbox

The dimensions of all the gears, bearings, and shafts of the main gearbox are determined basically by loads which depend on the torque transmitted by the gearbox. Therefore, the main gearbox weight can be expressed by the following formula:

$$G_{m.g.b} = k_{m.g.b} M_{Q_{m.r}} \tag{2.36}$$

where the coefficient $k_{m.g.b}$ can be considered as similar for all gearboxes of the same size, like configurations, and comparable gear ratios.

However, in analyzing the existing gearbox data shown in Fig 2.12 and Table 2.2, one may note that with a reduction of torque transmitted by the gearbox, the weight coefficient $k_{m.g.b}$ increases. This is explained by the fact that the wall thicknesses of the basic parts in the small gearboxes are relatively larger; both as a result of manufacturing difficulties, and because of the necessity of having wall thicknesses ensuring the required rigidity and static stability.

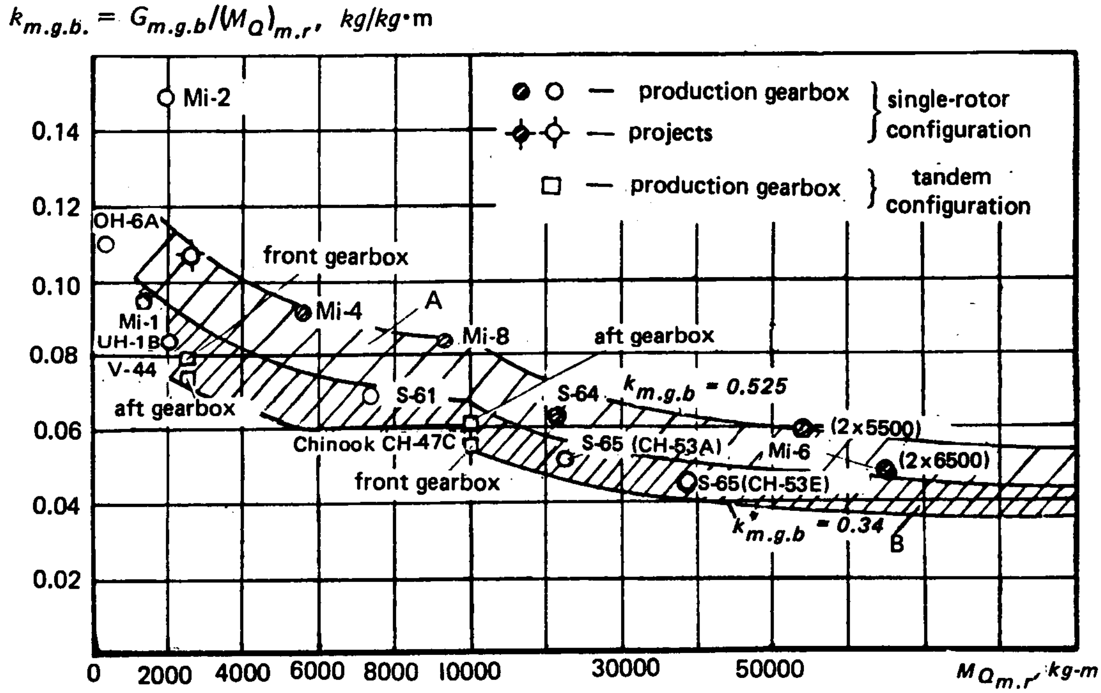

Figure 2.12 Variation of weight coefficients $k_{m.g.b}$, of gearboxes as a function of main-rotor torque (weight of the aft gearbox of Chinook helicopter is with extended rotor shaft). A - configurations with single main gearbox; B - configurations with several gearboxes in main-rotor transmission

HELICOPTER		N_{eng} h.p.	N_{tr} h.p.	ξ	$n_{m.r}$ rpm	$(M_Q)_{m.r}$ kg-m	$G_{m.g.b}$ kg	$k_{m.g.b}$	$k^*_{m.g.b}$
Mi-1		575	575	0.800	250	1320	135	0.102	0.427
Mi-2		2X400	800	0.810	246	1890	284	0.150	0.682
Mi-4		1700	1700	0.800	192	5110	471	0.092	0.510
Mi-8		2X1500	3000	0.830	192	9290	782	0.084	0.528
Mi-6 (2X5500 h.p.)		2X5500	11000	0.835	120	54800	3200	0.058	0.529
Mi-6 (2X6500 h.p.)		2X6500	13000	0.835	120	64800	3200	0.049	0.452
OH-6A		317	275	0.830	475	350	36	0.102	0.346
UH-1B		1100	1100	0.835	324	2030	173	0.084	0.386
S-61		2X1250	2500	0.830	203	7300	503	0.069	0.409
S-64		2X4050	6500	0.825	185	20900	1330	0.063	0.470
S-65(CH-53A)		2X3925	7000	0.815	185	23000	1200	0.0521	0.389
S-65 (CH-53E)		3X4390	11570	0.830	177	38900	1714	0.0442	0.363
CH-47C	Front gear bearing	2X3750	6000 3600 hp per rotor	0.940	258	10292	570	0.055	0.352
	Aft gearbox						627	0.074	0.387
V-44	Front gearbox	1425	855 hp per rotor	0.940	258	2370	175	0.079	0.370
	Aft gearbox						165	0.074	0.350

(a) MAIN GEARBOXES

HELICOPTER	Equivalent power through transmission N_{eq}, hp	$n_{t.r}$, rpm	$(M_Q)_{t.g.b}$ kg-m	$G_{t.g.b}$, kg	$k^*_{t.g.b}$	$n_{i.sh}$, kg-m	$(M_Q)_{i.sh}$, kg-m	$G_{i.g.b}$, kg	$k^*_{i.g.b}$	n_{sh}, rpm	L_{sh}, m	$(M_Q)_{ult}$, kg-m	G_{sh}, kg	k_{sh}
Mi-1	46	1350	24	18	1.42	2263	14.3	14	1.70	2263	8.95	–	21.2	–
Mi-2	73	1450	36	18	1.03	2462	21.5	14	1.21	2467	8.10	–	24.2	–
Mi-4	163	1040	112	48	1.09	2400	48.6	19	0.85	2400	12.40	330	54.4	0.091
Mi-8	280	1130	177	48	0.77	2596	79	22	0.67	2596	12.40	330	49.3	0.084
Mi-6 (2X5500 hp)	1200	675	1274	286	0.95	2006	430	114	0.89	2065	20.40	1490	214	0.082
Mi-6 (2X6500 hp)	1500	675	1591	297	0.81	2006	537	114	0.74	2065	20.40	1830	231	0.076
V-12	8200	–	–	–	–	2755	2139	354	0.76	2755	32	6000	650	0.063

(b) TAIL & INTERMEDIATE GEARBOXES, AND TRANSMISSION SHAFTS

TABLE 2.2 HELICOPTER TRANSMISSION DATA

Because of this, the weight of the parts of the small gearboxes is relatively higher. In order to somewhat offset this effect, such gearboxes should be made using simpler configurations; specifically, with transmission of the output torque through a smaller number of engagement points; for example, using two points as in the Lynx (Fig 2.13) and the Mi-2 helicopters, or even through only a single point as in the gearbox of the Mi-1 and Hughes OH-6A helicopters.

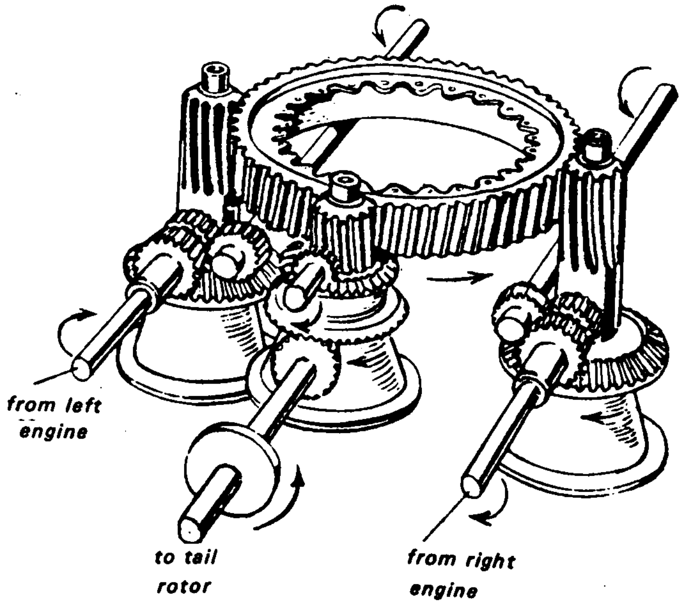

Figure 2.13 Scheme of the Lynx helicopter transmission[22]

However, in the R-7 gearbox of the Mi-6 helicopter, the bell gear output torque is collected from 18 satellites (planets) (Fig 2.14b). The use of a large number of engagement points was primarily dictated by the fact that when transmitting larger torques, circumferential loads must be restricted because of limited single-gear strength. Therefore, in small gearboxes, in order to account for the scale effect resulting from nonproportional reduction in wall thickness and to partially account for the influence of simplification of the configuration, the following formula is usually used both in Soviet practice and abroad·

$$G_{m.g.b} = k^*_{m.g.b} M_{Q_{m.r}}^{0.8} \qquad (2.37)$$

where

$$k^*_{m.g.b} = k_{m.g.b} M_{Q_{m.r}}^{0.2} .$$

Values of the $k^*_{m.g.b}$ coefficients for several existing gearboxes are shown in Fig 2.15. It can be seen from this figure that the weight coefficients for many existing gearboxes vary in the range $k^*_{m.g.b} = 0.34 \dots 0.525$, with a quite wide variation in the torque transmitted by the gearbox. It should be noted that the point corresponding to the Mi-2 gearbox lies outside

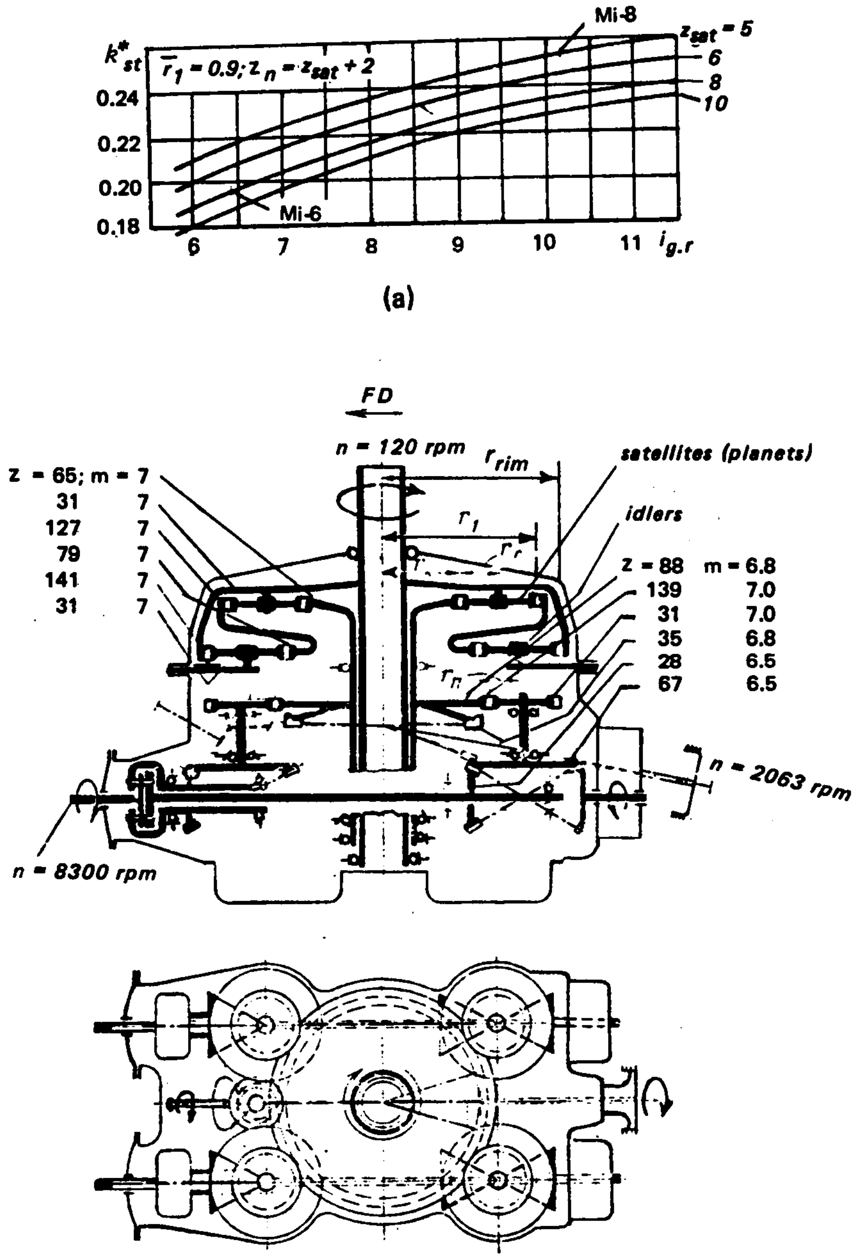
Mi-8
$z_{sat} = 5$
6
8
10
k^*_{st}
$\bar{r}_1 = 0.9; z_n = z_{sat} + 2$
0.24
0.22
0.20
0.18
Mi-6
6
7
8
9
10
11
$i_{g.r}$
FD
n = 120 rpm
r_{rim}
satellites (planets)
r_1
r_r
idlers
r_n
z = 65; m = 7
31 7
127 7
79 7
141 7
31 7
z = 88 m = 6.8
139 7.0
31 7.0
35 6.8
28 6.5
67 6.5
n = 2063 rpm
n = 8300 rpm

(a)

(b)

Figure 2.14 (a) Calculated weight coefficients of main gearbox planetary stage (working according to closed differential mechanism scheme) shown as a function of gear ratio $i_{g.r}$ and number of satellites z_{sat}; (b) kinematic scheme of the R-7 gearbox

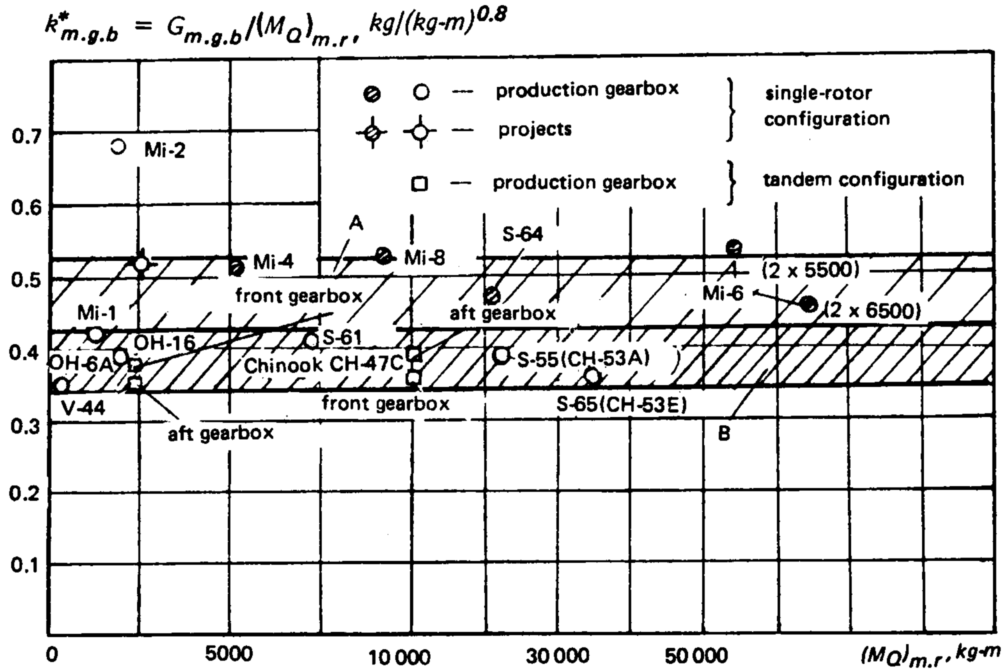

Figure 2.15 Weight coefficients $k^*_{m.g.b}$ of helicopter main gearboxes (weight of the Chinook aft gearbox is with extended rotor shaft): A - configuration with single gearbox; B - configurations with several gearboxes in the main rotor transmission

this range. The excessive weight of this gearbox can be explained by its configuration and the use of the basic gears from the Mi-1 helicopter.

A large influence on the main-gearbox weight is exerted by its configuration, which depends in large measure on the overall gearbox transmission ratio, since this ratio determines the number of main gearbox stages.

If, in addition to the main gearbox, the engine-to-main-rotor drive system has several other gearboxes including an engine-mounted reducer, then the gear ratio as well as the weight of the main gearbox itself decreases, while the overall weight of the whole rotor drive system may even increase. Correspondingly, the weight of a single main gearbox designed for the entire transmission ratio from the engine to the main rotor is usually higher, as can be seen from Fig 2.15 where the points relating to such gearboxes are hatched. From a weight standpoint, the best main gearboxes of helicopters with turboshaft engines have coefficients $k^*_{m.g.b} = 0.43 \dots 0.45$. This level is specifically achieved in the R-7 gearbox of the Mi-6 helicopter with an engine power 2×6500 *hp*.

Particular attention should be given to the main gearbox weight coefficients of tandem helicopters. In Figs 2.12 and 2.15, the main gearbox weights of the CH-47 and V-44 helicopters are referred to the maximum torque:

$$M_{Q_{max}} = a_Q M_{Q_{av}}$$

where a_Q = coefficient of nonuniformity of torque distribution between the main rotors — taken by Boeing Vertol as $a_Q = 1.2$, and $M_{Q_{av}}$ is the main average rotor torque

$$M_{Q_{av}} = 716.2\Sigma N_{tr}\xi/2n_{m.r}$$

where ΣN_{tr} = maximum engine power transmitted by the helicopter transmission; ξ = power utilization coefficient, and $n_{m.r}$ is the main rotor rpm.

It can be seen from Figs 2.12 and 2.15 that the CH-47C and V-44 main gearbox weight is at the weight level of modern gearboxes of single-rotor helicopters with turboshaft engines having a built-in engine gearbox, although one would expect that the gearboxes of tandems of such dimensions would be relatively lighter than the gearboxes of single-rotor helicopters. This assumption is based on the fact that (a) power input in these gearboxes is accomplished through a single synchronizing shaft and a single pair of bevel gears (Fig 2.16b), which is possible with this load level ($N_{max} \leqslant 4500$ hp), and (b) the total number of main gearbox reduction stages can be reduced to three.

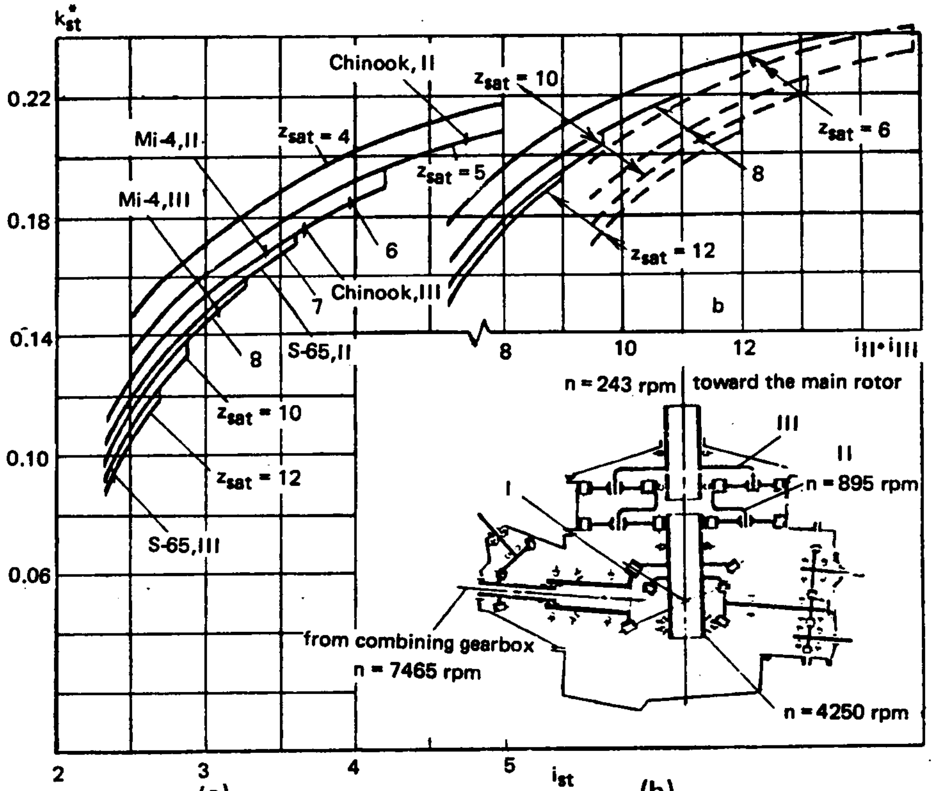

Figure 2.16 (a) Calculated weight coefficients of main gearbox planetary stage, and (b) two-stage planetary gearbox, shown as functions of their gear ratios and number of satellites, z_{sat}, (c) Scheme of Chinook helicopter gearbox: I - first stage; II - second stage; and III - third stage

In order to account for the influence of gearbox configuration on its weight, the following approach is proposed: We assume that Eq (2.37) can be used to estimate the weight of each gearbox stage individually, and the overall gearbox weight is determined as the sum of the weights of its stages. Then we can obtain the following approximate formula for comparing the weight coefficients of gearboxes of different configurations:

$$k^*_{m.g.b} = \Sigma\,[z_{p_j}^{0.2}\,k^*_{st_j}/(i_j\xi_j)^{0.8}] \tag{2.38}$$

where $k^*_{st_j}$ = weight coefficient of the j-th gearbox stage; i_j = gear ratio from the output of the j-th gearbox stage to the main rotor; z_{p_j} = number of independent paths along which power is transmitted from the output of each stage; ξ_j = coefficient accounting for the additional power transmitted by the j-th stage, not to the main rotor, but elsewhere (to the tail rotor, for example). If an examined stage transmits power to the main rotor, then $\xi_j = 1$. If the stage transmits all the incoming power into the gearbox—including the tail-rotor power in single-rotor helicopters—then, neglecting the other small power requirements we can assume that the coefficient ξ_j coincides with the power utilization coefficient $\xi_j = \xi_{m.r}$ (in the USA, called transmission efficiency). For the single-rotor main-gearbox stages that transmit power to the tail rotor, this coefficient should be taken equal to $\xi_j = \xi_{t.r}/\bar{N}_{t.r} \approx 7...8$, where $\bar{N}_{t.r} = N_{t.r}/N_{m.r}$; and i_j is the gear ratio up to the gear transmitting the highest torque in the considered stage.

If, on multiengine helicopters, the power input from each engine is based on emergency power N_{emer}, which is higher than takeoff power N_{to}—usually selected on the basis of the specified conditions at the hover ceiling—then we must introduce the coefficient $\xi^*_j = \xi_j/k_{emer}$, where $k_{emer} = N_{emer}/N_{to}$ instead of ξ_j into Eq (2.38). This should be done for all the stages transmitting power from a single engine, including the power-combining stage for whose gears the emergency power also becomes the design power.

The values of the weight coefficient $k^*_{st_j}$ of the main gearbox stages can be determined using the technique given below.

If the weight coefficients, $k^*_{st_j}$, are known, we can use Eq (2.38) to obtain the weight coefficient $k^*_{m.g.b}$ for the gearbox of any scheme; when the weight efficiency of each stage is the same, we call this coefficient the configuration weight efficiency coefficient. Then the gearbox weight can be found from the formula

$$G_{m.g.b} = k_{w.ef}k^*_{conf}(M_Q)_{m.r}^{0.8} \tag{2.39}$$

where $k_{w.ef}$ = coefficient of gearbox weight efficiency; and k^*_{conf} = weight coefficient that depends only on the selected gearbox configuration determined from Eq (2.38).

In order to determine the weight coefficient of nonplanetary type stages, we assume that the structural weight of each stage can be broken down into individual parts, the weight of which is proportional to the 0.8 power of torque transmitted by each gear in this stage. For stages which receive power from several power transmission paths, we shall consider that the weight of that part of the stage which includes the driven gear depends on the torque transmitted only by one driving pinion, and does not change as the number of pinions increases. Then the weight coefficients of these stages can be found from the following formula

$$k^*_{st} = k_{pi}[(z_{pi}^{0.2}/i_{st}^{0.8}) + (1/z_{pi}^{0.8})]$$

where z_{pi} is the number of driving pinions of the given stage which are connected with a single driven gear; $i_{st} = n_{in}/n_{out}$ is the gear ratio of the stage in question.

Similarly, for the stage with power division among z_{pi} pinions, we can use the formula

$$k^*_{st} = k_{pi}[1 + (1/z_{pi}i_{st}^{0.8})].$$

For the better (weightwise) helicopter gearboxes, we can take $k_{pi} = 0.25$ for spur gears, and $k_{pi} = 0.35...0.4$ for bevel gears.

It should be noted that for gearboxes constructed at the modern level, these formulae yield weight coefficients which are quite close to the actual values. However, the k^*_{st} coefficients obtained in this way will be higher than the actual weight coefficients of the spur gear stages of the Mi-1 and Mi-2 gearboxes which were designed with stresses higher than those allowed today. In the spur gear stages of these helicopters, $k_{pi} = 0.15 \ldots 0.22$.

Taking the same approach to the planetary gearbox stages, we obtain the approximate formulae for determining their weight coefficients.

For the conventional planetary stage,

$$k^*_{st} = k_{pi} \left\{ (1/z_{sat} i_{st}) + [(1/2) - (1/i_{st})]^{0.8} z_{sat}^{0.2} + [(i_{st} - 1)/i_{st} z_{sat}]^{0.8} \right\}$$

where z_{sat} = number of satellites (planets) used in the planetary stage; and $i_{st} = 2[1 + r_{sat}/r_{dr}]$ is the planetary gear ratio, where r_{sat} = satellite radius; and r_{dr} = driving (sun) gear radius.

The calculated weight coefficients of a planetary stage of a two-stage planetary gearbox with different values of the penultimate second stage—obtained using this formula— are presented in Fig 2.16a and b.

We see from these curves that the planetary stage weight can be significantly reduced with increase in the number of satellites (planets) used. However, in this case, the planetary stage gear ratio decreases. Therefore, in the two-stage planetary gearbox having a final stage with a larger number of satellites, it is better to have as high a gear ratio as possible in the penultimate stage with a correspondingly smaller number of satellites and larger weight coefficients k^*_{II} (see Fig 2.16b).

For the planetary stage based on the closed differential mechanism scheme, the analogous formula is somewhat more complex:

$$k^*_{st} = k_{pi} \left\{ \frac{1}{(z_{sat} i_{st})^{0.8}} + z_{sat}^{0.2} \left[\frac{\bar{r}_{sat} \bar{M}_{inp}}{2(r_1 - r_{sat})} \right]^{0.8} + \right.$$

$$\left. + \bar{M}_{rim}^{0.8} \left[\left(\frac{\bar{r}_1}{z_{sat}} \right)^{0.8} + \left(\frac{1 - 2\bar{r}_{id}}{z_{id}} \right)^{0.8} + z_{id}^{0.2} \bar{r}_{id}^{0.8} + \frac{1}{z_{id}^{0.8}} \right] \right\}$$

where z_{sat} and z_{id} are the number of satellites and idlers; $\bar{M}_{inp}$ and $\bar{M}_{rim}$ are the fractions of the torque transmitted through the satellite yoke (planet carrier) and through the rim of the bell gear.

$$\bar{M}_{inp} = 1/(1 + m); \quad \bar{M}_{rim} = m/(1 + m)$$

where

$$m = \bar{r}_1 / 2(\bar{r}_1 - \bar{r}_{sat})(1 - 2\bar{r}_{id})$$

The $\bar{r}_{sat}$ of satellites (planets), $\bar{r}_{id}$ of idlers, and the intermediate ring gear $\bar{r}_1$ appearing in these formulae are referred to the rim radius of the bell gear r_{rim} (Fig 2.14b).

The relationship given by this formula between the weight coefficients and the gear ratio i_{st}, and the number of satellites z_{sat} (Fig 2.14a) was obtained under the condition that there are two more idlers than satellites, and the intermediate ratio $\bar{r}_1 = r_1 / r_{rim} = 0.9$.

For somewhat higher values of the weight coefficients, but for the same circumferential loads on the gears, the planetary stage of the closed-differential-mechanism scheme makes it possible to transmit torques of higher absolute magnitude.

When computing gearbox weight coefficients $k^*_{m.g.b}$ from Eq (2.38), the main rotor shaft and the complex of clutches, couplings, and mechanism at the input to the gearbox should be considered as separate steps of the calculation.

A weight coefficient $k^*_{st} = 0.07$ can be achieved for shafts of modern articulated main rotors, although for many existing gearboxes, this coefficient is larger—often equal to $k^*_{sh} \approx 0.1$. For the overruning clutch and equalizing mechanism of the type used in the R-7 gearbox, the weight coefficient, $k^*_{st.o} = 0.5$. Without the equalizing mechanism, this coefficient may be equal to $k^*_{st.o} = 0.2 \ldots 0.3$. After determining the weight coefficient k^*_{conf}, which depends on the gearbox configuration, we can then determine the gearbox weight efficiency coefficient on the basis of the actual gearbox weight:

$$k_{w.ef} = G_{m.g.b}/k^*_{conf}(M_Q)_{m.r}^{0.8} \tag{2.40}$$

The data required for, as well as the results of, the calculation of the configuration weight coefficients for several existing gearboxes is given in Table 2.3. We see from these calculations that the configuration weight coefficients for the Mi-6 gearbox and the Chinook forward gearbox (without the extended main rotor shaft) are: $k^*_{conf} = 0.423$ for the R-7 gearbox, and $k^*_{conf} = 0.387$ for the Chinook gearbox.

Consequently, for the same weight efficiency level, the forward gearbox of the tandem-rotor helicopter (Chinook type), because of its greater simplicity (single-bevel pair) and fewer stages is about 10 percent lighter than the R-7 gearbox.

In comparing the transmission weights of helicopters of different configurations, it is possible, from Eq (2.38), to determine the overall weight coefficients of all helicopter main rotor-drive gearboxes shown in Table 2.3. From this data, it can be seen that if we compare the weight coefficients of all the main rotor-drive gearboxes, this coefficient is somewhat higher for the Chinook gearbox (without accounting for the extended aft rotor shaft) than for the Mi-6 gearbox.

In calculating the weight of the gearbox, it is convenient to include the weight of lubricants, and at least part of the weight of the gearbox fuselage attachments. When comparing the weights of Soviet and foreign gearboxes which usually do not have a gearbox frame, half of the weight of the gearbox frame and the weight of its attachments to the main gearbox should also be included in the gearbox weight. When using this approach, the coefficient for the best (weightwise) Soviet gearboxes, computed for the overall transmission ratio from the engine to the main rotor, is equal to about 0.465.

2.2.5 Intermediate and Tail Gearboxes

The intermediate and tail gearboxes of nearly all helicopters have very low gear ratios and consist of only two (usually bevel) gears. One example of intermediate gearbox design is shown in Fig 83, and that of a tail gearbox, in Fig 84 of Ref 11. Their weight coefficients, just as those of the main gearbox bevel gear stages are higher than the main gearbox coefficients in general. This aspect is most important for the twin-rotor helicopters, particularly for the tandems, which usually have several intermediate gearboxes (Fig 2.17), designed for continuous transmission of engine power. For the side-by-side configurations, the situation is somewhat better, since the synchronizing shaft is loaded comparatively briefly, only during lateral control application and in case of engine failure.

The weight of the intermediate and tail gearboxes can be estimated using a formula similar to Eq (2.37).

STAGE IDENTIFICATION		P-7 ($k_{ol} = 1$)			CHINOOK CH-47C (front gearbox) ($k_{ol} = 1.25$)			S-65 ($k_{ol} = 1.12$)		
		$z_{r.gj}$ i_j ξ_j, ξ^*_j	k^*_{stj}	$\frac{z_{r.gj}^{0.2} k^*_{stj}}{(i_j \xi_j)^{0.8}}$	$z_{r.gj}$ i_j ξ_j, ξ^*_j	k^*_{stj}	$\frac{z_{r.gj}^{0.2} k^*_{stj}}{(i_j \xi_j)^{0.8}}$	$z_{r.g}$ i_j ξ_j, ξ^*_j	k^*_{stj}	$\frac{z_{r.gj}^{0.2} k^*_{stj}}{(i_j \xi_j)^{0.8}}$
Lifting-rotor shaft	–	–	0.07		–	0.07		–	0.07	
Stage III	$z_{r.gj}$ i_j ξ_j	1 1 1	0.195 "differential planetary" $z_{sat} = 8; z_{id} = 10$		1 1 1	0.177 $z_{sat} = 6$		1 1 1	0.095 $z_{sat} = 12$	
Stage II	$z_{r.gj}$ i_j ξ_j	1 6.45 0.83	0.182 spur	0.047	1 3.65 1	0.206 $z_{sat} = 5$	0.0734	1 2.39 1	0.163 $z_{sat} = 7$	0.081
Stage I	$z_{r.gj}$ i_j $\xi_j; \xi^*_j$	4 29 0.83	0.6 "bevel"	0.062	1 17.44 1	0.56 "bevel"	0.066	1 8.15 0.728	0.378 "bevel"	0.091
Couplings and mechanisms at gearbox input	$z_{r.gj}$ i_j $\xi_j; \xi^*_j$	2 69.3 0.83	0.5	0.0224	– – –	–	–	2 32.6 0.728	0.2	0.018
Outlet to tail rotor IV	$z_{r.gj}$ i_j ξ_j	1 6.45 7.0	0.58 "bevel"	0.0276	– – –	–	–	1 11.2 7.8	0.73 "bevel"	0.02
Outlet to tail rotor V	$z_{r.gj}$ i_j ξ_j	– – –	–	–	– – –	–	–	1 14.2 7.8	0.476 "spur"	0.011
Configuration weight coefficient for main gearbox		–	–	0.423	–	–	0.387	–	–	0.386
Combining gearbox	$z_{r.gj}^{0.2}$ i_j $\xi_j = a_j k_{ol}$	– – –	–		1/2 30.7 1.2/1.25	0.65 "bevel"	0.021	– – –	–	
Engine gearbox	$z_{r.gj}$ i_j ξ^*_j	– – –	–		1 52.2 0.8	0.74 "bevel"	0.0374	2 32.6 0.728	0.61	0.056
Configuration weight coefficient of engine main-gearbox drive			–	0.423	–	–	0.446	–	–	0.442

TABLE 2.3 CALCULATION OF SCHEME WEIGHT COEFFICIENTS OF MAIN GEARBOXES FOR THREE TYPES OF HELICOPTERS

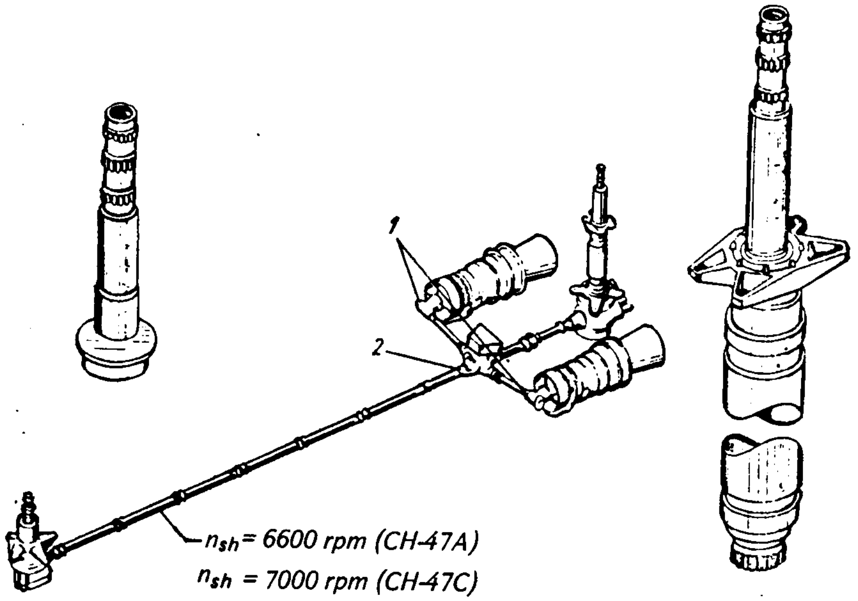

Figure 2.17 Transmission of the Chinook helicopter: (1) intermediate gearboxes (engine gearboxes); and (2) intermediate or combining gearbox

In evaluating intermediate and tail gearbox weights, difficulties often arise in determining the design torques, since the torques transmitted by these gearboxes often vary within very wide limits. Therefore, it is advisable to introduce the equivalent torque, $(M_Q)_{eq}$, into the formula for determining the weight of these gearboxes.

$$G_{int.g.b} = k^*_{int.g.b} (M_Q)_{eq}^{0.8} . \tag{2.41}$$

The $(M_Q)_{eq}$ value is established for loads exceeding the fatigue strength limit based on $6X10^6 \ldots 10X10^6$ cycles.

Calculations show that with an adequate degree of accuracy, the equivalent torque can be taken equal to the torque of the drive-shaft gearbox at the hover ceiling H_h for the single-rotor helicopter, and to the torque corresponding to the maximum power transmitted from the engines with account for nonuniformity of the distribution of this power between the main rotors for the tandem-rotor helicopter:

$$M_Q = 716.2\, a_Q \Sigma N_{eng}/\alpha n_{sh}\, z_{sh} \tag{2.42}$$

and to the torque corresponding to the power transmitted by the synchronizing shaft when controlling the side-by-side rotor helicopter, which can be taken as approximately

$$N_{sync.sh} \approx 1/4\, \Sigma N_{eng} . \tag{2.43}$$

In Eq (2.42) α = coefficient depending on the transmission scheme ($\alpha = 1$ if the gearbox transmits the power of all the engines, and $\alpha = 2$ if it transmits the power of half the engines);

n_{sh} = rpm of the shaft driving the intermediate gearbox; and z_{sh} = number of synchronizing shafts.

Figures 2.18 and 2.19, and table 2.2 show the weight data for several intermediate and tail gearboxes, calculated according to the described method.

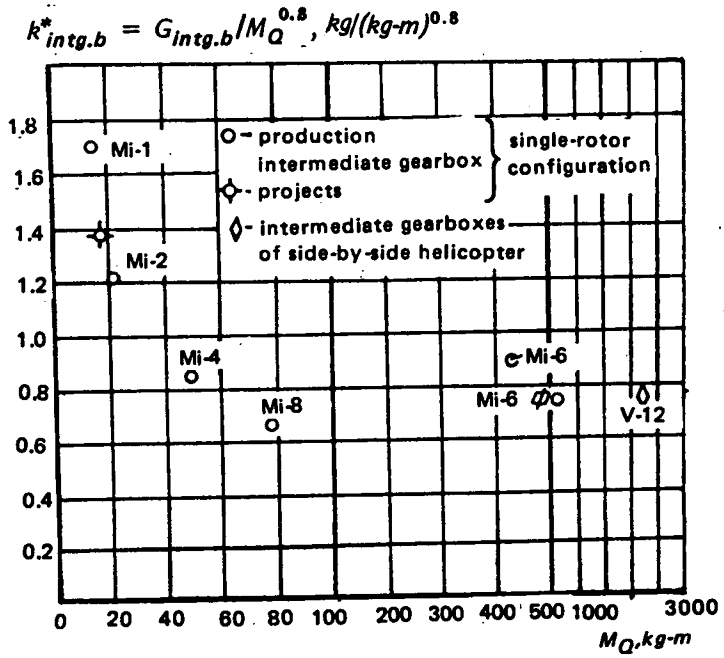

Figure 2.18 Weight coefficients of intermediate gearboxes

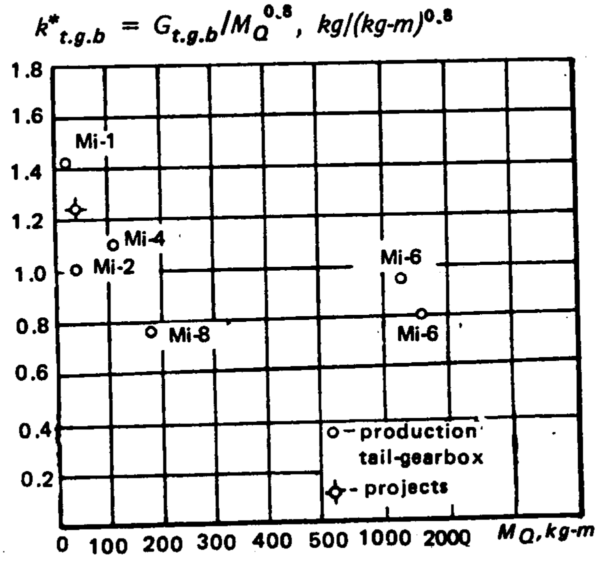

Figure 2.19 Tail-rotor gearbox weight coefficients of single-rotor helicopters

The weight coefficient for the central intermediate gearbox of the V-12 helicopter is given for the equivalent power $N_{sync.sh} = 8000\ hp$ for which it was designed; i.e., for a somewhat greater value than that obtained from Eq (2.43).

For modern intermediate and tail gearboxes, we can assume that $k^*_{i.g.b} = 0.7 \ldots 0.9$, and that $k^*_{t.r.g.b} = 0.65 \ldots 0.8$.

Some differences between the weight coefficients of intermediate and tail gearboxes is explained by the fact that the gear ratio for intermediate gearboxes is usually smaller than for tail gearboxes. If the tail gearbox is constructed using the two-stage scheme with bevel gearing at the input and a planetary gear at the output, then $k^*_{t.r.g.b}$ can be reduced in accordance with Eq (2.38)

2.2.6 Transmission Shafts

While the transmission shaft weight for the single-rotor helicopter is low, for the side-by-side and particularly for tandem helicopters, it is so large that it significantly influences the overall helicopter structural weight.

The weight of the transmission shaft is primarily determined by the weight of the shaft tube—representing 60 to 70 percent of the total (Fig 2.20)

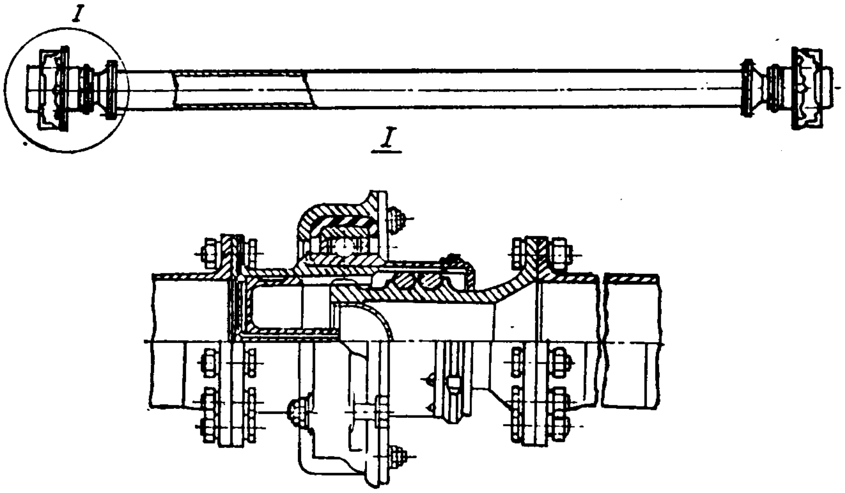

Figure 2.20 Cross-section of the transmission shaft of the Mi-6 helicopter

Selection of the shaft tube size is based on loss of stability, which can occur at the torque-breaking value $(M_Q)_{brea}$.

In order to minimize the shaft tube weight, it is very important to select the optimal relationship between the tube diameter and wall thickness $\bar{d} = d/\delta$.

The required shaft-section modulus in torsion can be expressed as

$$W_{req} = \tfrac{1}{2}\pi\bar{d}^2\delta^3 = M_{Q_{brea}}/\tau_{all}$$

from which

$$\delta = \sqrt[3]{2M_{Q_{brea}}/\pi\bar{d}^2\tau_{all}}. \qquad (2.45)$$

Substituting the value of δ into the formula for the shaft tube weight,

$$G_{sh} = \pi \bar{d} \delta^2 \gamma L_{sh}, \tag{2.46}$$

we obtain

$$G_{sh} = k_{sh} L_{sh} M_{Q_{brea}}^{2/3} \tag{2.47}$$

where

$$k_{sh} = 2.32\gamma / \sqrt[3]{\bar{d} \tau_{all}^2}.$$

The values of τ_{all} are determined from either the well-known graphs of allowable steel-tube torsional stresses (as, for instance, in Fig 2.21, where L_0 = distance between shaft supports), or from the following formula proposed by Golubtsov for Duralumin tubes:

$$\tau_{all} = 24.6 - 0.06(L_0/d) - 0.035(\bar{d})^2. \tag{2.48}$$

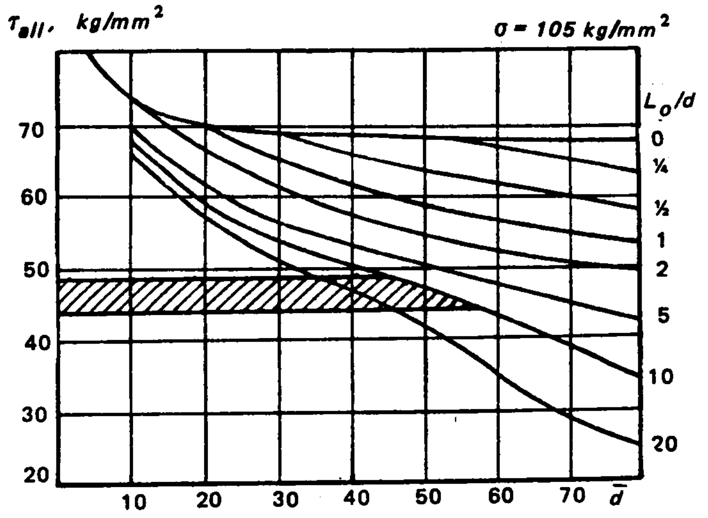

Figure 2.21 Allowable torsional stresses in shaft tubes as a function of tube diameter to wall thickness ratio ($\bar{d} = d/\delta$) for various shaft-length (L_0) values (shaded area corresponds to breaking stresses of optimal shafts)

The values of k_{sh} determined for steel tubes heat-treated to $\sigma = 105 kg/mm^2$ are shown in Fig 2.22. Here, it can be seen that for the steel tubes normally used with $\sigma = 105 kg/mm^2$, the optimal value is $k_{sh} = 0.038 \ldots 0.04$, and for Duralumin tubes, $k_{sh} \approx 0.027$.

If we assume that the structural weights of shaft supports and couplings constitute a definite percentage of the tube weight, then the weight of the shaft as a whole can be determined by th same equation, (2.47), except that now the weight of supports and couplings must be reflected in the value of the coefficient, k_{sh}.

Figure 2.23 and Table 2.2 show the values of k_{sh} for several Soviet helicopter transmission shafts. Most interesting is the weight data for the synchronizing shaft of the V-12 helicopter ($k_{sh} = 0.063$) for which the values of $\bar{d}$ are close to optimum.

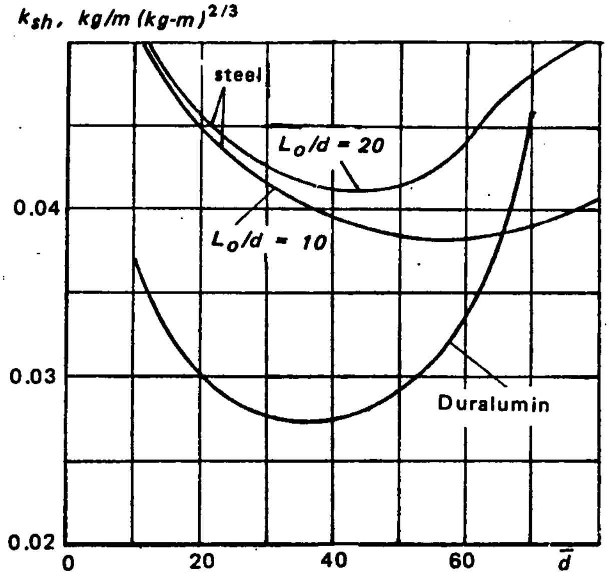

Figure 2.22 Calculated values of shaft tube weight coefficients shown as a function of $\bar{d}$

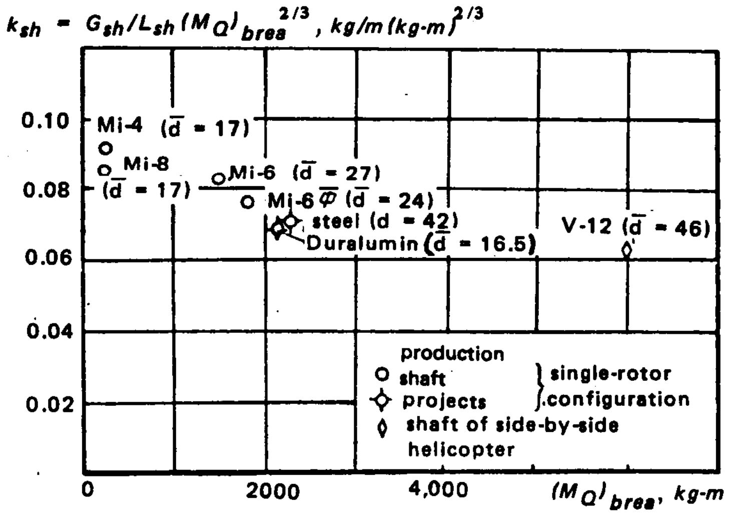

Figure 2.23 Shaft weight coefficients for several Soviet helicopters

Frequently, however, particularly in light helicopters, the tube dimensions differ from the optimal values in the direction of smaller $\bar{d}$ ratios. Therefore, their weight coefficients are somewhat larger: $k_{sh} = 0.076 \ldots 0.085$ for the Mi-4, Mi-8, and Mi-6 shafts.

For a proper selection of shaft dimensions and evaluation of shaft weight, it is very important to determine the maximum torque transmitted by the shaft.

For the single-rotor helicopter transmission shaft, this torque is known quite accurately from the results of many flight tests involving turns near the ground. For the helicopters tested in such turns, this torque did not increase by more than a factor of 2:2 to 2:6, in comparison with the torque in the hover regime at $H = H_h$.

It will be shown in Sect 2.3 that for twin-rotor helicopters, the maximum possible operational overloads—as far as torque on a single lifting rotor is concerned—may be equal to $n_{M_Q} = 1.8 \ldots 2.2$ from which it follows that

$$M_{Q_{max}} = 716.2 n_e (\Sigma N_{eng})/2n_{sh} \tag{2.49}$$

where $n_e = 1.8 \ldots 2.2$ if all the engines are located at the same place, as in the case of tandem-rotor helicopters; and $n_e' = 0.8 \ldots 1.2$, if the engines are separated into two groups, each with its own main rotor, as is customary in the side-by-side configuration.

When making the calculation using Eq (2.49), the obtained maximum operational torque $M_{Q_{max}}$ must be increased by a safety factor—usually taken as $f = 1.5$. As a result—bearing in mind that there may be z_{sh} rather than a single transmission shaft—we can write

$$G_{sh} = k_{sh} z_{sh} L_{sh} (n_e f M_{sh})^{2/3} \tag{2.50}$$

where M_{sh} is the torque transmitted by the shaft under no-overload conditions,

$$M_{sh} = 716.2 \Sigma N_{eng} / 2n_{sh} z_{sh}$$

for twin-rotor helicopters; and

$$M_{sh} = 716.2 N_{t.r} / n_{sh}$$

for single-rotor helicopters.

2.2.7 Tail Rotor

The details of tail-rotor construction can be found in Ref 8, Figs 62 and 64, while those of its hub are shown in Fig 2.24.

However, since the tail rotor operates under significantly more severe conditions (in a wider range of thrust and angle-of-attack variation, and also under conditions of turns with high angular velocities ω_y when hovering near the ground), the maximum usable value of $\gamma_{o_{max}}$ for its blades should be significantly lower than for the main-rotor blades. It can be assumed that γ_o should be no higher than

$$(\gamma_o)_{max} = 3.0 \tag{2.51}$$

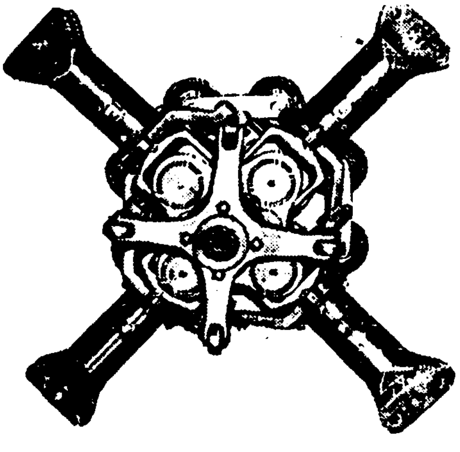

Figure 2.24 Tail rotor of the Mi-8 helicopter with flapping and lead-lag hinges

which approximately corresponds to

$$(k_{bl.t.r})_{min} = 13. \qquad (2.52)$$

In addition, tail-rotor blades experience large loads if an unmoored blade strikes the flapping stop in case of a strong wind gust.

For blades of similar basic dimensions and identical construction, the stresses which arise in the blade attachment in case of such impact are proportional to the blade aspect ratio $\lambda_{t.r}$. Because of this, tail-rotor blades are not usually made with aspect ratios higher than $\lambda_{t.r} \approx 8$ (see Table 2.4), and the value of the mass characteristic γ_o is usually lower than $(\gamma_o)_{max}$. Therefore, the limitation of Eq (2.51) usually has no effect on the parameters of the tail-rotor blades.

The weight coefficients for the tail-rotor blades $k^*_{bl.t.r}$, shown in both Fig 2.25 and Table 2.4 were calculated for several helicopters using Eqs (2.12) and (2.14) in which λ_{av} was taken equal to 18, just as for the main rotor. We see from this figure that the lowest weight coefficients $k^*_{bl.t.r}$ achieved in the best modern tail-rotor blade designs coincide with the same coefficients for the main-rotor blades. This is an indirect indication of the validity of the proposed formulae which appears to be applicable over the wide range of variation of the parameters encountered in transition from the main-rotor blades to the tail -rotor blades.

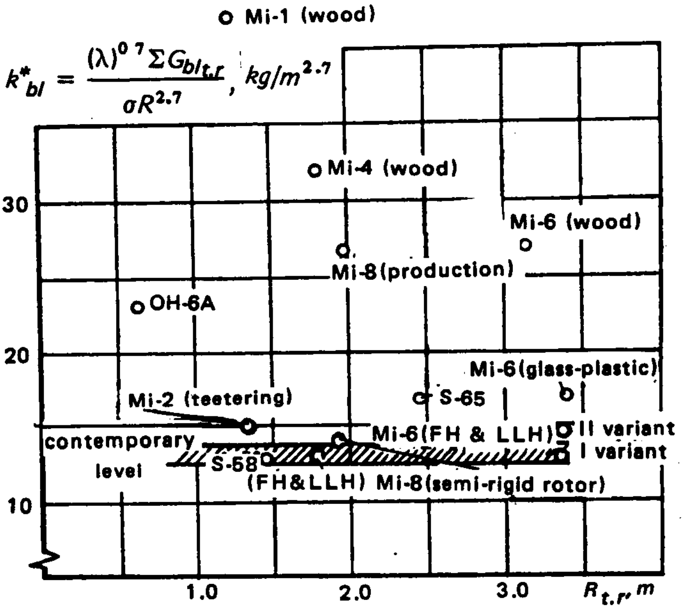

Figure 2.25 Weight coefficients of tail-rotor blades (FH – flapping hinge; LLH – (lead-lag hinge)

Figure 2.26 and Table 2.4 present the data and weight coefficients for tail-rotor hubs. It is interesting that the tail-rotor hubs have approximately the same weight coefficients as the main-rotor hubs, although in certain designs the tail-rotor hubs are markedly lighter. This is explained primarily by the fact that hubs without lead-lag hinges can be made relatively lighter.

HELICOPTER	R_{tr} m	b m	λ	$G_{bl.tr}$ kg	z_{bl}	$k^{\circ}_{bl.tr}$ kg/m$^{2.7}$	r_{eq}	n rpm	N_{bl} ton	$G_{hub.tr}$ kg	$k^{\circ}_{hub.tr}$ kg/ton$^{1.35}$	DESIGN FEATURES
Mi-1	1.260	0.123	10.16	3.60	3	42.20	0.42	1350	3.90	20.8	1.100	Tapered wooden blades
Mi-2	1.350	0.220	6.14	3.94	2	15.00	0.45	1450	5.60	17.0	0.850	Constant chord, metal production blades
Mi-4	1.800	0.242	7.40	12.60	3	32.50	0.32	1080	9.60	48.2	0.760	Tapered wooden blades
Mi-8	1.800	0.220	8.18	4.43	4	13.20	0.53	1130	6.05	50.3	1.110	Hub w/horizontal & vertical hinges, metal blades
	1.925	0.230	8.14	5;40	5	14.20	0.47		6.95	88.0	1.225	Semirigid hub, metal blades w/glass-plastic envelope
	1.954	0.270	7.24	13.70	3	27.10	0.40		15.40	76.5	0.637	Universally suspended hub, metal production blades w/glass-plastic envelope
Mi-6	3.150	0.500	6.30	64.00	4	27.40	0.30	675	32.00	322.0	0.745	Wooden tapered production blades
	3.350	0.450	7.40	27.40		13.20	0.46		21.80	400.0	1.560	Hub w/horizontal & vertical hinges (II variant), constant-chord metal blades
				30.40		14.65	0.49		25.30	480.0	1.540	Hub w/horiz. & vert. hinges (I variant) constant-chord metal blades w/glass-plastic envelope
	3.400	0.435	7.81	34.60		17.10	0.36		21.43	–	–	Glass-plastic tempered blades
S-58	1.450	0.185	7.84	2.63	4	13.50	0.50	1318	3.70	21.2	0.910	All-metal constant-chord blade
S-65 (CH-53A)	2,440	0.344	7.10	17.00	4	17.80	0.50	790	14.50	98.0	0.660	Hub w/horizontal hinge, all-metal, constant-chord blades w/extruded spar
Huey Cobra AH-1G	1.295	0.213	6.10	7.50	2	33.20	0.50	1654	14.80	44.0	0.580	Teetering hub, constant-chord metal blades w/extruded spar

TABLE 2.4 TAIL-ROTOR BLADE AND HUB DATA

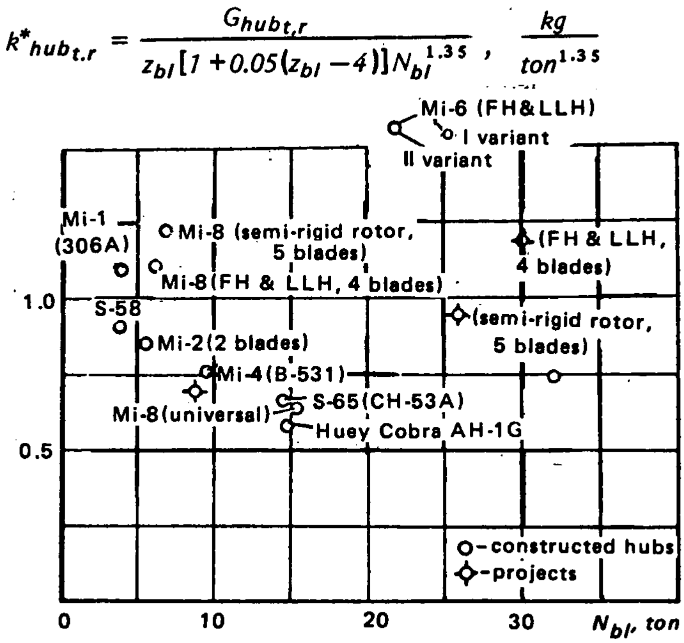

Figure 2.26 Weight coefficients of tail-rotor hubs (FH – flapping hinge; LLH – lead-lag hinge)

2.2.8 Propeller for Conventional or Compound Helicopters

Until very recently, solid Duralumin blades were most widely used in propeller construction. The weight of such blades usually considerably exceeds the weight required for normal operation of the blade.

Therefore, in accordance with the considerations of Ch 3, the propeller blade weight can be determined from the formula

$$G_{bl} = q_{bl} b^{\beta} R. \qquad (2.53)$$

Figure 2.27 shows data on the weight of several airplane propeller blades. It can be seen that the value of β for solid Duralumin blades can be taken equal to 1.4 and $q_{bl} = 86 \ldots 91$ $kg/m^{2.4}$.

It can be seen from the data presented in Fig 2.27 that the propeller tip speed is much higher than for helicopter tail rotors. In addition, propellers are made without flapping and lead-lag hinges, which leads to the appearance of both constant and alternating high bending moments in the propeller blade roots. These circumstances lead to an increase in the propeller blade weight in comparison with the helicopter tail-rotor blade weight which was calculated using Eq (2.12) with $k^*_{bl.t.r} = 13.8$, and referred to bR as indicated in Fig 2.27.

We note, however, that modern propeller blades may be made from glass-reinforced or carbon-reinforced plastic which results in a much lighter construction. This aspect must be considered in evaluating the weights of propellers for modern conventional and compound helicopters.

Figure 2.28 shows the hub weights of several propellers referred to the product $z_{bl}N_{bl}$, with curves corresponding to $G_{hub}/z_{bl}N_{bl}^{1.35} = const.$ We see that the formulae used for helicopter main-rotor hubs are also suitable for propeller hubs:

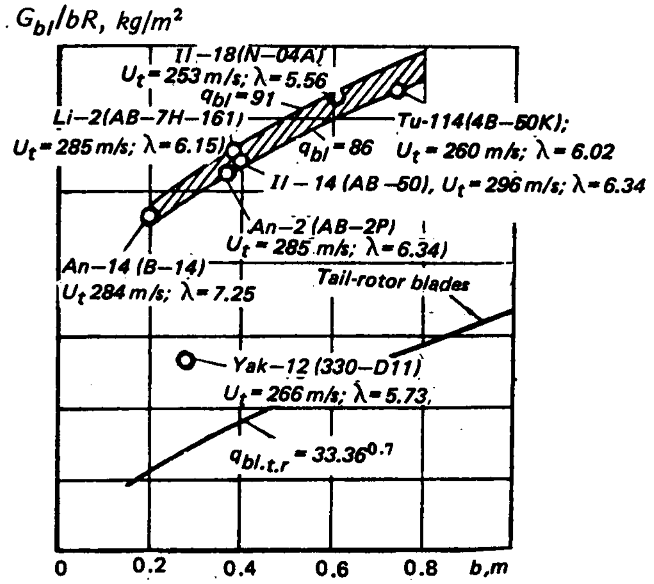

Figure 2.27 Weight coefficients of propeller blades (hatched area corresponds to weight level represented by Duralumin propeller blades weighing $G_{bl} = (86 \ldots 91)b^{1.4}R$

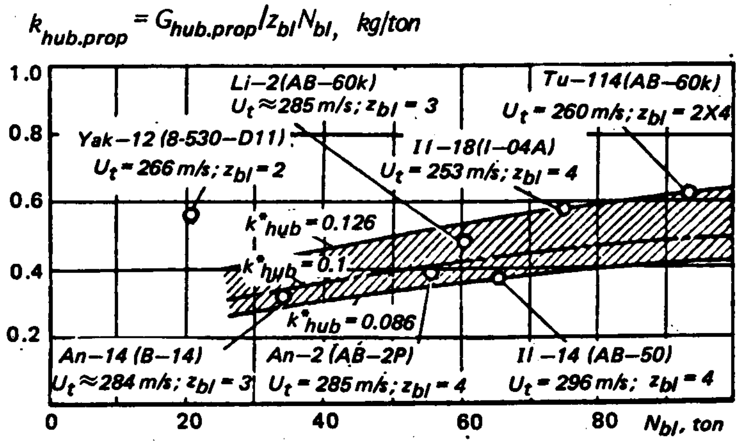

Figure 2.28 Weight coefficients of propeller hubs (hatched area corresponds to the achieved weight level)

$$G_{hub} = k^*_{hub} k_{z_{bl}} z_{bl} N_{bl}^{1.35}. \tag{2.54}$$

It should be noted that the weight coefficients are somewhat smaller because of the absence of articulated hinges in the propeller hubs, and because of the simpler hub configuration. The available data indicates that the weight coefficient of the propeller hub can be taken as $k^*_{hub} = 0.1$, $kg/ton^{1.35}$.

Unfortunately, there is no statistical data on multibladed propellers which would make it possible to evaluate the magnitude of the coefficient $k_{z_{bl}}$.

The weight of the propeller as a whole can be found from the formula

$$G_{prop} = [q_{bl} b^{1.4} R + k^*_{hub} k_{z_{bl}} N_{bl}{}^{1.35}] z_{bl} . \qquad (2.55)$$

2.2.9 Powerplant

In order to ensure necessary flight characteristics of helicopters throughout the whole range of altitudes and ambient temperatures encountered in operation, oversized engines are usually installed. The power available from these engines exceeds that required at sea-level, standard conditions. In order to avoid overloading the helicopter transmission; especially the main gearbox, and also to avoid unnecessary difficulties in the design and development of the engine itself, the engine power is limited by a governor to the magnitude necessary to ensure the required helicopter flight performance. This is usually determined on the basis of hovering under specified conditions of altitude and ambient air temperature. The so-obtained power represents the permissible power limit for all altitudes—from $H = 0$ to that where power available becomes equal to the limit value.

However, since the power limitations have practically no effect on engine weight, the engine specific weight is usually evaluated on the basis of the maximum power which would be obtained at $H = 0$ if no restrictions were imposed. This power is termed the *referred maximum engine power.*

In helicopter weight calculations it is more convenient to refer the engine weight to the maximum power referred, not to $H = 0$, but rather to the altitude where $H = 500 m$. Verification flights for helicopter ranges are usually performed at this altitude.

In this case,

$$G_{eng} = \gamma N_{ref} \qquad (2.56)$$

where the values of γ depend significantly on the absolute design engine power. This dependence, just as for most other mechanical systems, is explained by the fact that the wall thickness of parts can not be reduced below some limit because of both stiffness and manufacturing, and/or operational constraints. For instance, with a reduction in the blade height (particularly in the last compressor stages) of small engines, the relative tip losses increase. This, in turn, reduces the engine efficiency which leads to a higher specific fuel consumption. Therefore, for small engines it is better to use centrifugal stages in the compressor, and reduce the total number of stages, resulting in a simplification of the engine configuration; however, the relative weight of the small engine increases.

To illustrate this tendency, schemes of turboshaft engines of low and high power are shown in Fig 2.29.

The specific weight of various modern engines as a function of engine power is shown in Fig 2.30. We see from this figure that regardless of engine size, its weight can be found from the expression

$$G_{eng} = k_{eng} (N_{ref})^{0.7} \qquad (2.57)$$

where the values of the weight coefficient k_{eng} for modern (weightwise) engines can be taken as $k_{eng} = 1 \ldots 1.2$.

Curves corresponding to constant values of k_{eng} are shown in this figure, indicating that for modern helicopter engines of moderate and high power, the engine specific weight can be taken as $\gamma = 0.9 \ldots 0.11$. However, the specific weight of the installed powerplant is significantly higher.

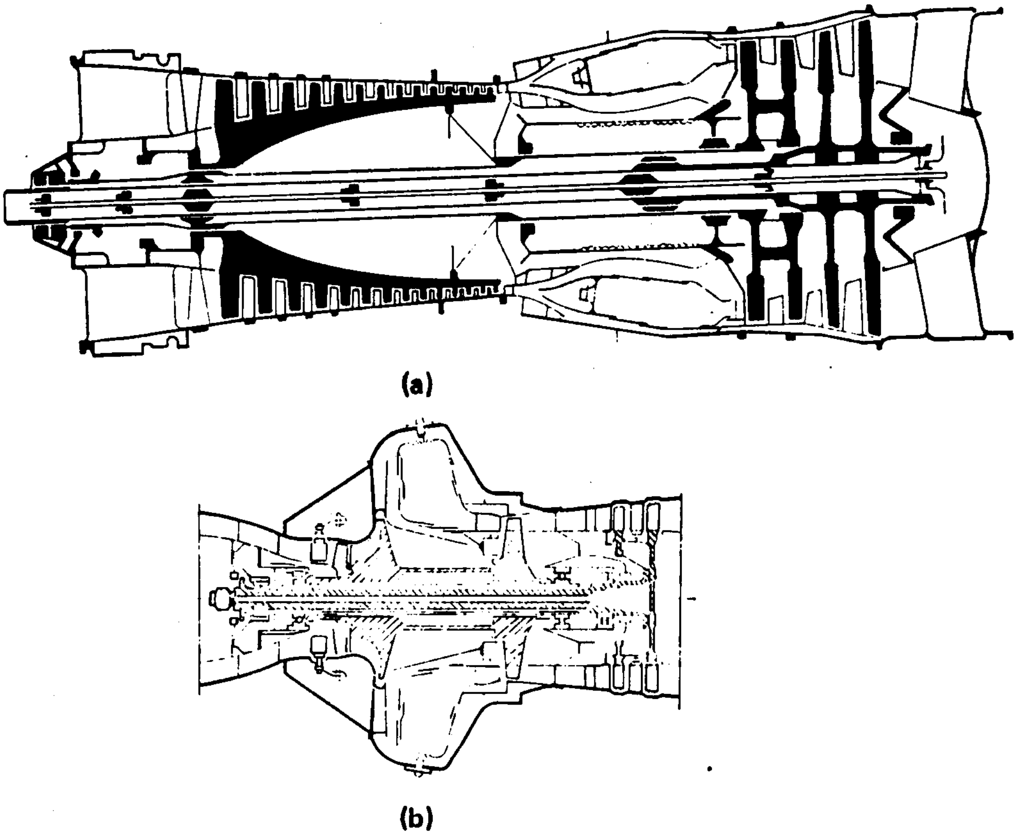

(a)

(b)

Figure 2.29 Cross-section of (a) high, and (b) low power helicopter engines

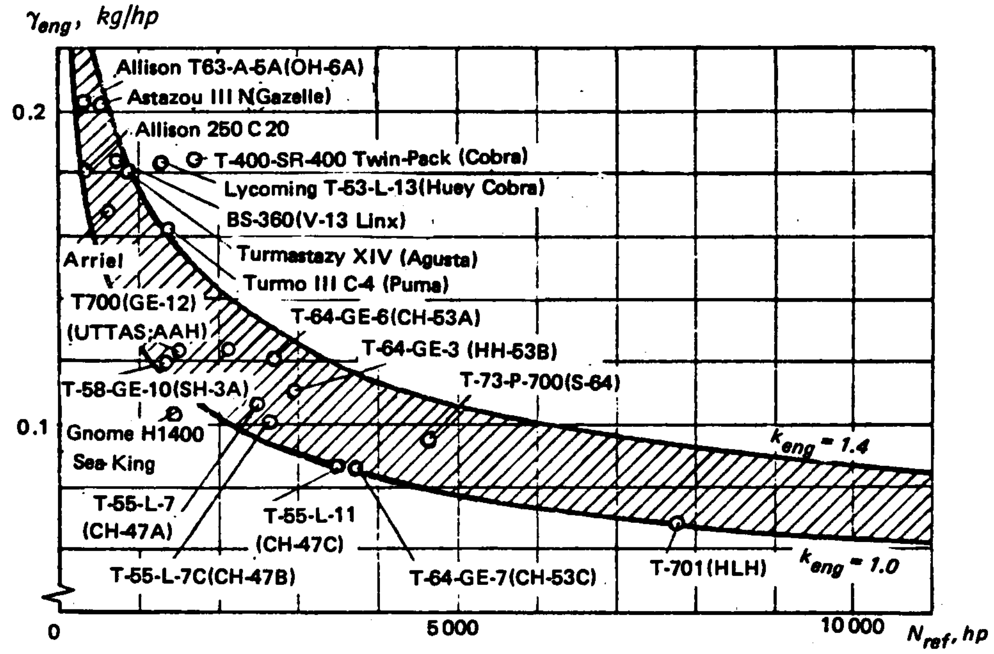

Figure 2.30 Specific weight of helicopter engines vs referred power

In calculating the weight of the powerplant, it is convenient to include the weight of the cooling and lubrication system of the engine and main gearbox as well as the oil itself, since the weight of all these items is usually directly proportional to the maximum usable engine power.

In addition, it is suggested that the installed powerplant weight include the weight of the intake and exhaust system, starting system, engine mounts, and fire extinguishing system; although their weight is not necessarily directly proportional to the engine power. The error will not be large if, by analogy with the engine weight calculations, the weight of all the aforementioned systems which we shall call powerplant installation systems are also expressed in terms of the referred power of the engines installed in the helicopter

$$G_{p.i.s} = k_{p.i.s} \Sigma N_{ref}. \qquad (2.58)$$

The weight coefficients of the powerplant installation systems of some helicopters are shown in Fig 2.31. We see that the coefficient $k_{p.i.s}$ can be taken as *0.04...0.05*.

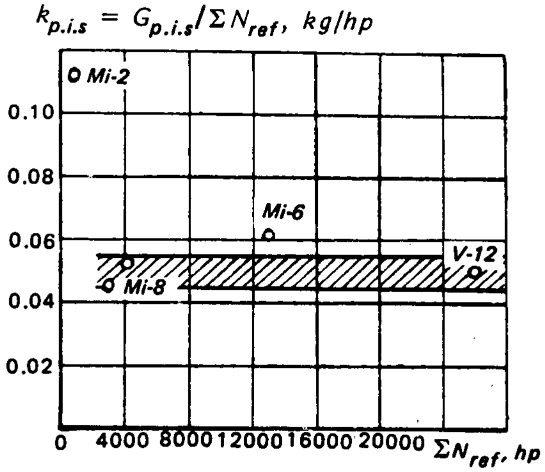

Figure 2.31 Weight coefficients of powerplant installation (hatched area corresponds to better (weightwise) powerplant installations)

For the powerplant as a whole, we write

$$G_{eng.ins} = \gamma_{eng.ins} \Sigma N_{ref} \qquad (2.59)$$

where the specific weight of the installed powerplant can be defined as

$$\gamma_{eng.ins} = k_{p.i.s} + k_{eng}/N_{ref}{}^{0.3}$$

2.2.10 Fuel System

The fuel system weight is defined as a percentage of the total fuel weight capacity for which this system is designed

$$G_{fu.s} = k_{fu.s}(G_{fu})_{tot}. \qquad (2.60)$$

For the fuel system of the single-rotor helicopter with self-sealing fuel tanks, a coefficient $k_{fu.s} = 0.07 ... 0.09$ can be assumed. For the system without self-sealing tanks, this coefficient can be reduced to $k_{fu.s} = 0.06 ... 0.07$.

The fuel-system weight for the twin-rotor helicopter increases if the tanks are located quite far from the engines.

The use of integrated tanks whose weight is usually included in the airframe structure weight may lead to a reduction of the fuel system weight coefficient to $k_{fu.s} \approx 0.035 ... 0.04$.

Figure 2.32 shows the weight coefficients $k_{fu.s}$ for some existing helicopters.

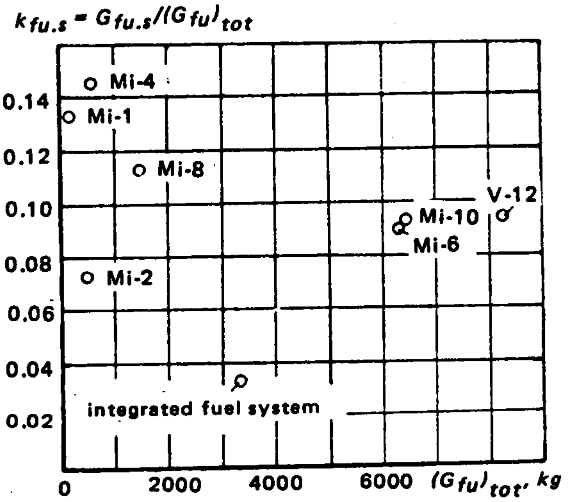

Figure 2.32 Weight coefficients of helicopter fuel systems

2.2.11 Cantilever Wing of Side-by-Side Helicopter (or Compound Helicopter)

In most cases, if the wing of the side-by-side rotor configuration (Fig 2.33) is designed for static loads, the wing would not be rigid enough to avoid the ground resonance type of self-excited vibrations of the main rotors on the elastic support (wing). The wing must be made considerably stiffer in order to eliminate these vibrations. The weight of the wing increases due to the fact that stiffness requirements now become the determining factor.

The natural vibration frequency of the cantilever wing in the plane of least stiffness (Fig 2.33) cannot, in practice, be made higher than the main rotor rotational frequency at operational rpm. Therefore, during rotor acceleration, the range of ground resonance rotor rpm must be passed through without permitting the development of self-excited vibrations. This is accomplished by providing the required damping margin. Suppression of this mode of self-excited vibrations is facilitated by two circumstances; the airframe mass referred to the main rotor hub in this vibration mode is quite large ($\epsilon < 0.006$ – see Ref 12), and the overall vibration damping increases significantly because of the main-rotor aerodynamic damping.

However, elimination of ground resonance is not ensured only through suppression of this mode of self-excited vibrations. It is also necessary to eliminate self-excited oscillatory modes in the plane of greater stiffness of the wing and in torsion as well (Fig 2.34). The airframe mass referred to the main-rotor hub with respect to these modes is not very large (from $\epsilon \approx 0.03$ in bending, up to $\epsilon \approx 0.08$ in torsion), and elimination of ground resonance through

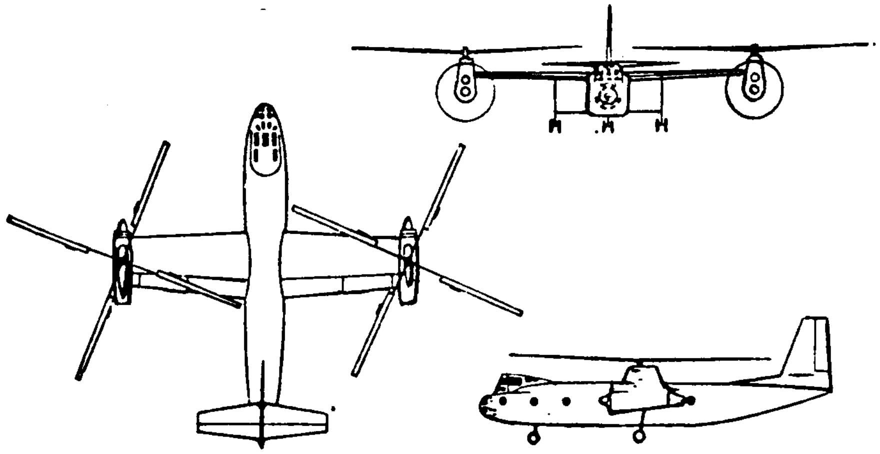

Figure 2.33 Side-by-side helicopter with a wing (Ka-22)

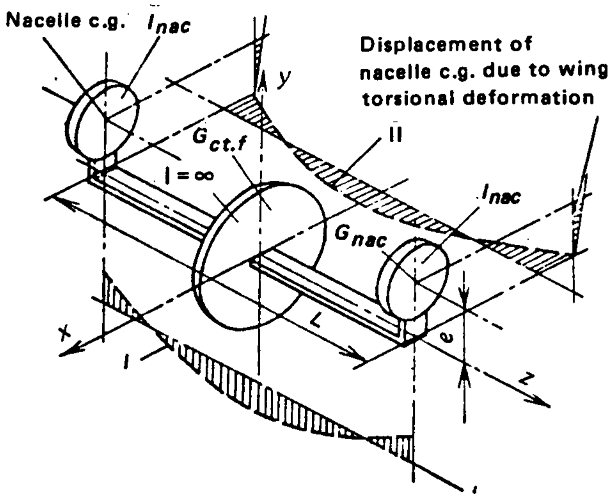
Nacelle c.g.
I_nac
Displacement of nacelle c.g. due to wing torsional deformation
y
II
G_ct.f
I = ∞
I_nac
G_nac
x
L
e
I
z

Figure 2.34 Simplified model of the side-by-side winged helicopter for evaluation of margins with respect to self-excited vibrations of the ground resonance type

provision of damping margins is very difficult in this case. Therefore, the most reliable approach is to shift the frequencies of these self-excited modes outside the operating frequency range of the rotor.

In this case, partial frequencies of the wing's natural modes P_x and P_{tor} must be higher than ω_{max}:

$$P_x \geqslant n_x \omega_{max}; \quad P_{tor} \geqslant n_{tor} \omega_{max} \tag{2.61}$$

where ω_{max} = the maximum main-rotor angular velocity at which the helicopter operates for a time sufficient for development of dangerous vibrations (15 to 20 sec). For existing Soviet helicopters, we can take $\omega_{max} \approx 1.07\omega$, where ω is the nominal angular velocity of the main rotor; n_x and n_{tor} are coefficients accounting for both the width of the instability zone and the position of its lower boundary in relation to the frequencies P_x and P_{tor}, as well as for the necessity of separation of the main rotor rotational speed from conventional resonance.

In selecting the values of the coefficients n_x and n_{tor}, one must also take into consideration the inaccuracy of the approximate formulae given below from which P_x and P_{tor} values will be determined as well as calculation errors associated primarily with lack of knowledge—in the preliminary design stage—of all the pliabilities of the actually constructured machine.

In the case of relative weak coupling between bending and torsional modes when $e \approx 0$ (Fig 2.34), we take $n_x = n_{tor} = 1.6$.

It should be noted that when designing the V-12 helicopter, these coefficients were taken as $n_x = n_{tor} = 2.0$ but, as one might expect, for various reasons they decreased markedly in the actually constructed helicopter.

If the coupling between bending and torsional modes of the wing is quite strong, coefficients n_x and n_{tor} can be taken as

$$n_x = n_{P_1}/\overline{P}_1 \quad \text{and} \quad n_{tor} = n_{P_1}/\widetilde{P}_1 \tag{2.62}$$

where $n_{P_1} = 1.5$ and $\overline{P}_1$ and $\widetilde{P}_1$ are the values of the lowered coupled wing natural frequencies referred to P_x and P_{tor}, respectively. For the symmetric vibration modes shown in Fig 2.34, these frequencies can be found from the following:

$$\overline{P}_1 = \sqrt{\frac{1+\overline{P}^2{}_{tor}}{2(1-\overline{e}^2)} - \sqrt{\frac{(1+\overline{P}^2{}_{tor})^2}{4(1-\overline{e}^2)^2} - \frac{\overline{P}^2{}_{tor}}{1-\overline{e}^2}}}; \quad \widetilde{P}_1 = \sqrt{\frac{1+\overline{P}_x^2}{2(1-\overline{e}^2)} - \sqrt{\frac{(1-\overline{P}_x^2)^2}{4(1-\overline{e}^2)^2} - \frac{\overline{P}_x^2}{1-\overline{e}^2}}}$$

Here, $\overline{e}$ = the vertical elevation of the nacelle center-of-gravity over the wing elastic axis referred to the nacelle radius of inertia (Fig 2.34).

The required natural vibration frequencies can be obtained by reducing the weight of the nacelle located on the tip of the wing, and reducing the nacelle mass moment of inertia relative to the wing elastic axis, and also by selecting the required wing stiffness.

Let us examine a constant chord, two-spar wing of the stressed-skin type with widely spaced spars and constant wing section. The wing is shown in Fig 2.35. There is no good reason to examine other wing configurations.

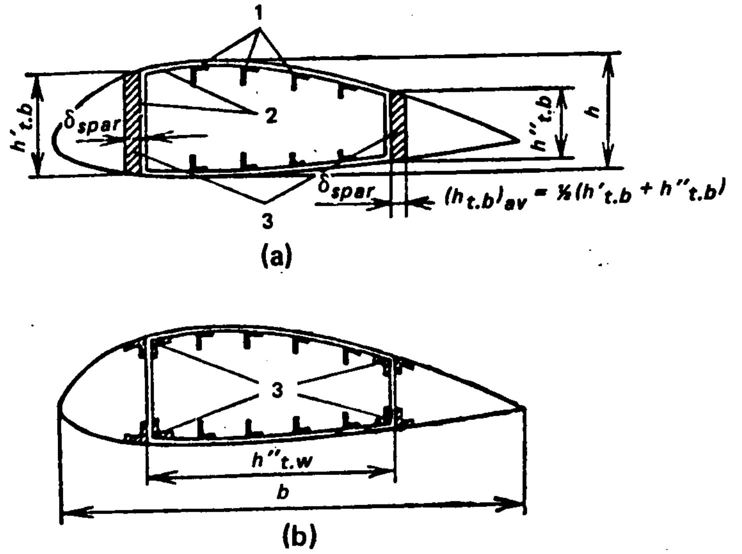

Figure 2.35 Scheme of a cross-section of stressed-skin type wing

Since the wing of trapezpidal shape has lower torsional stiffness, it is inferior weightwise. The use of spars with variable cross-section along the wing span may yield some weight improvement, but it will be no higher than 6 percent.

The weight of the wing and its sectional moments of inertia in bending in the x-z plane and in torsion can be determined from the following formulae:

$$I_x = k_{I_x} \delta h b^2, \tag{2.63}$$

$$I_{tor} = k_{I_{tor}} \delta h^2 b, \tag{2.64}$$

$$G_{wg} = k_G \gamma \delta h L. \tag{2.65}$$

Here, δ, h, and b are the skin thickness, wing height, and chord; γ = specific material weight; and L = wing span, equal to the distance between the lifting rotors if they are mounted at the wing tips.

The coefficients in these formulae can be found from the expressions:

$$k_{I_x} = \frac{\bar{b}_{t.b}^{\,3}}{6h} + \frac{(\bar{h}_{t.b})_{av}\,\bar{b}_{t.b}^{\,2}}{2\bar{h}} + \bar{h}\sum \bar{F}_{str_i}\bar{b}_i^{\,2} + \frac{\eta_{spar}}{1-\eta_{spar}} \times$$

$$\times \left[2\bar{b}_{t.b} - 2(\bar{h}_{t.b})_{av} + \bar{F}_{str}\right] \frac{\bar{b}_{t.b}^{\,2}}{4\bar{h}}; \tag{2.66}$$

$$k_{I_{tor}} = \frac{4\bar{F}_{t.b}^{\,2}}{[2(\bar{h}_{t.b})_{av}/\delta_{spar}] + 2\bar{b}_{t.b}}; \tag{2.67}$$

$$k_G = \frac{[2\bar{b}_{t.b} + 2(\bar{h}_{t.b})_{av} + \bar{F}_{str}]}{1-\eta_{spar}} \left[1 + \frac{\Delta G_{wg}}{G_{str}}\right]. \tag{2.68}$$

where $\bar{b}_{t.b}$ and $(\bar{h}_{t.b})_{av}$ respectively, are the torsion box width and average spar height, both referred to wing chord; $\bar{h}$ = relative height of wing airfoil section; $\bar{F}_{str}$ and $\bar{F}_{str_i}$ respectively, are the total area of section stringers and area of a single stringer, both referred to the skin thickness δ and wing chord: $\bar{F}_{str} = F_{str}/\delta b$ and $\bar{F}_{str_i} = F_{str_i}/\delta b$; $\bar{F}_{t.b}$ is the torsion box section area, referred to the wing profile height and chord; and η_{spar} is the fraction of the spar section area F_{spar}, of the total section F_Σ of all the elements working in tension and compression:

$$\eta_{spar} = F_{spar}/F_\Sigma. \tag{2.69}$$

$\bar{\delta}_{spar}$ = spar thickness referred to skin thickness. If the spar material weight is uniformly distributed along the spar height, then,

$$\bar{\delta}_{spar} = 1 + \bar{F}_{spar}/2(\bar{h}_{t.b})_{av}. \tag{2.70}$$

Here,

$$\bar{F}_{spar} = \frac{F_{spar}}{\delta b} = \frac{\eta_{spar}}{1-\eta_{spar}}\left[2\bar{b}_{t.b} + 2(\bar{h}_{t.b})_{av} + \bar{F}_{str}\right]; \tag{2.71}$$

ΔG_{wg} is the weight of the wing structural elements not participating in the general bending and torsion of the wing; G_{stru} is the wing structural weight, determined using the coefficient k_G when we set $\Delta G_{wg} = 0$ in Eq (2.68); and $1 + (\Delta G_{wg}/G_{stru})$ is the coefficient of wing-weight increase because of the non-load carrying elements ot the wing.

For the wing of optimal dimensions with skin stiffened by stringers, this coefficient can be taken as 1.8; for the honeycomb wing, it is 1.9.

In the case of nonoptimal wing dimensions, the weight of the elements which do not participate in the general bending and torsion of the wing is more accurately determined by setting

$$\Delta G_{wg} = q_{wg} S_{wg}$$

where

$$q_{wg} = 14...16 \ kg/m^2.$$

The values of the coefficients k_{I_x}, $k_{I_{tor}}$, and k_G are shown in Fig 2.36 as a function of relative spar-section area, characterized by the coefficient η_{spar}. The coefficients were calculated for the following values of the quantities appearing in the formulae

$$\bar{b}_{t.b} = 0.605; \ \bar{h} = 0.25,$$

$$(\bar{h}_{t.b})_{av} = 0.175; \ \bar{F}_{str} = 0.52,$$

$$\bar{F}_{t.b} = 0.495; \ 1 + (\Delta G_{wg}/G_{stru}) = 1.8.$$

We introduce the wing area $S_{wg} = bL$ into Eq (2.63) and (2.64) since, for the side-by-side configurations, it is desirable to have this area as small as possible because of download in hovering and rotor unloading in autorotation while still providing the required stiffness.

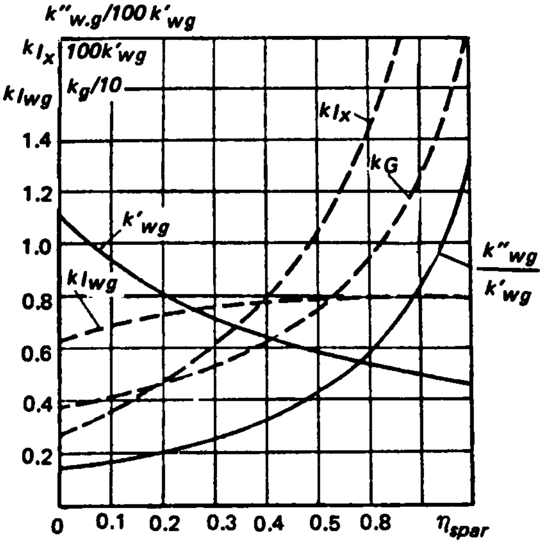

Figure 2.36 Variation of wing weight and rigidity coefficients as a function of the relative area of the spar, η_{spar}

Thus, using Eq (2.65), the formulae for the wing moments of inertia can be rewritten as follows:

$$I_x = k^*_{I_x} G_{wg} S_{wg}^2 \bar{h} / L^3 \qquad (2.72)$$

and

$$I_{tor} = k^*_{I_{tor}} G_{wg} \cdot S_{wg}^2 \bar{h}^2 / L^3 \qquad (2.73)$$

where

$$k^*_{I_x} = k_{I_x} / k_G \gamma, \; k^*_{I_{tor}} = k_{I_{tor}} / k_G \gamma, \; \bar{h} = h/b.$$

In the case of the symmetric oscillations shown in Fig 2.34, the natural frequencies P_x and P_{tor} of the airframe with rectangular wing can be found from the following approximate formulae:

$$P_x = \sqrt{(24gE\, I_x / G_{nac} L^3)[1 + (2G_{nac}/G_{ct.f})]} \qquad (2.74)$$

and

$$P_{tor} \sqrt{2GI_{tor}/I_{nac} L} \qquad (2.75)$$

where G_{nac} = total weight of one nacelle located at the wing tip, including the main-rotor weight; $G_{ct.f}$ = weight of all the helicopter systems and components. and the transported load located in the center-section of the fuselage. If the fuel is located in the fuselage, it should also be included in $G_{ct.f}$; and I_{nac} is the nacelle mass moment of inertia relative to the wing elastic axis. It can be written in the form:

$$I_{nac} = i^2 (G_{nac}/g).$$

Here, i = nacelle radius of inertia.

The nacelle weight can be approximately determined from the formula

$$G_{nac} = \tfrac{1}{2}[\Sigma G_{bl} + G_{hub} + G_{cont} + G_{m.g.b} + G_{i.g.b} + G_{eng.ins} + G_{cow} + G_{el.inst} + 0.3G_{wg}]. \qquad (2.76)$$

In the case of antisymmetric airframe vibration mode, the frequencies P_x and P_{tor} do not usually differ markedly from the values calculated using Eqs (2.74) and (2.75), although for certain designs there may be exceptions to this rule.

Substituting the values of the elastic moments of inertia from Eqs (2.72) and (2.73) into Eqs (2.74) and (2.75), and considering the conditions expressed by Eq (2.62), we obtain the formulae for the weight of the constant-chord cantilever wing of the side-by-side rotor helicopter, based on the stiffness requirement.

In order to satisfy the bending stiffness requirements, the weight of the wing should be found from the formula

$$G'_{wg} = k'_{wg} (L/2R)^2 (\bar{U}_t)^2_{max} L^4 G_{nac} / \bar{h} S_{wg}^2 [1 + (2G_{nac}/G_{ct.f})] \qquad (2.77)$$

where

$$k'_{wg} = n_x^2 k_G \gamma U_{t_o}^2/6gEk_{I_x};\ (\bar{U}_t)_{max} = \omega_{max}R/U_{t_o};\ U_{t_o} = 220\,m/s.$$

Based on the torsional stiffness requirements, the wing weight should be found from the formula

$$G''_{wg} = k''_{wg}(L/2R)^2(\bar{U}_t)^2_{max}L^2 i^2 G_{nac}/\bar{h}^2 S^2_{wg} \tag{2.78}$$

where

$$k''_{wg} = 2n_{tor}^2 k_G \gamma U_{t_o}^2/gGk_{I_{tor}}.$$

Depending on the helicopter parameters, the weight determined by the stiffness requirements in either bending or torsion may be larger. Therefore, we take the larger of the G'_{wg} and G''_{wg} values obtained from these two formulae. For

$$(L/l)_o = \sqrt{k''_{wg}[1 + (2G_{nac}/G_{ct.f})]/k'_{wg}\bar{h}}, \tag{2.79}$$

the wing weights determined by the stiffness requirements in bending and torsion will be the same. For $L/l > (L/l)_o$, the wing weight will be determined by the bending stiffness, while for $L/l < (L/l)_o$, it will be governed by the torsional stiffness.

When designing the wing, the value of $(L/i)_o$ can be varied—depending on the distribution of the material between the torsion-box spars and skin. In the case of weak bending-torsion coupling, the lowest wing weight is obtained for such η_{spar} when $G'_{wg} = G''_{wg}$. Therefore, after determining the required ratio of the coefficients

$$k''_{wg}/k'_{wg} = \bar{h}(L/i)^2/[1 + (2G_{nac}/G_{ct.f})], \tag{2.80}$$

we can use Fig 2.36 to find the η_{spar} value which corresponds to the lowest wing weight.

If we take $\bar{h} = 0.25$, $1 + (2G_{nac}/G_{ct.f}) = 1.85$, and $L/l = 16.7$; from which $k''_{wg}/k'_{wg} = 37.7$, then from Fig 2.36 we obtain $\eta_{spar} = 0.43$, $k_G = 6.9$, $k'_{wg} = 0.006$, and $k''_{wg} = 0.226$. After finding the weight from Eq (2.77), we must also check, from Eq (2.65), whether the obtained skin thickness is not lower than the allowable value. Usually, $\delta_{all} = 0.8$ to 1 mm.

In The case of a quite strong coupling between bending and torsion, the minimal wing weight is obtained for $P_{tor} > P_x$. In this case, the minimal wing weight coefficient can be obtained from curves analogous to those in Fig 2.37 which were plotted for the case when $\bar{e} = 0.45$, and $\bar{F}_{str} = 0.52$ ($\delta = 1.2\,mm$).

If we present the main-rotor thrust losses due to the wing download as

$$\Delta\bar{T}_{m.r} = c_{wg}\bar{S}_{wg},\ \text{where}\ \bar{S}_{wg} = S_{wg}/2\pi R^2_{m.r}$$

and assume that $c_{wg} = 0.9$ for the wing without flaps which can be deflected in hover, then the optimal wing area can be obtained from the condition that sum $\Delta T_{m.r} + G_{wg}$ is a minimum. From this, we find that

$$(\bar{S}_{wg})_{opt} = 2\left(\frac{L}{2R}\right)^2 \sqrt[3]{\frac{k'_{wg}k_{d.w}(\bar{U}_t)^2_{max}\bar{G}_{nac}}{c_{wg}\pi^2\bar{h}[1 + (2G_{nac})G_{ct.f})]}}. \tag{2.81}$$

where $\bar{G}_{nac} = G_{nac}/G_{gr}$.

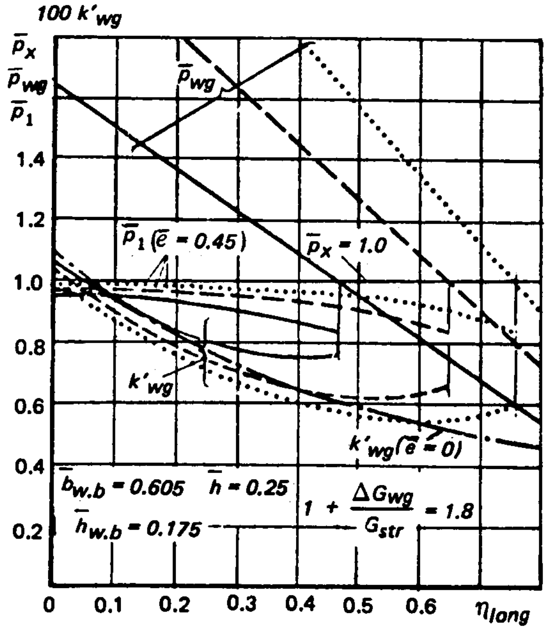

Figure 2.37 Weight coefficients k' of the wing and its vibratory frequencies depending on relative spar area η_{spar} at various values of L/i: ——— $L/i = 15$; – – – $L/i = 20$; -····· $L/i = 25$

If we use the values obtained above for the coefficients appearing in this formula and take $L/2R = 0.913$ and the nacelle relative weight $\bar{G}_{nac} = 18\%$—just as for the V-12 helicopter—then for the optimum value $(\bar{S}_{wg})_{opt} = 0.105$, the weight of the wing having area $S_{wg} = 200\ m^2$ and chord $b = 6.3\,m$ would be $5400\ kg$, while the download losses due to flow over the wing would amount to $\Delta T \approx 9000\,kg$.

In the actual design of the cantilever wing for the V-12 helicopter, its weight was found to be 7.5 to 8 tons. Consequently, the values given here of the k'_{wg} and k''_{wg} coefficients should be considered optimistic.

We note in passing that the use of a multi-strutted wing with inverted taper for supporting the main rotors on the V-12 helicopter made it possible—with a somewhat lower weight of the outer-wing panel—to reduce the download losses to 3.4 tons ($\Delta\bar{T} = 3.5\%$). This represents a gain of about six tons with much greater safety in regard to the ground resonance instabilities.

2.2.12 Truss-Mounting of Main Rotors in Side-by-Side Helicopter Configurations

The use of truss-type (multi-strut) construction for support of lifting rotors (Fig 2.38) makes it possible to shift the airframe natural vibration frequencies represented by the mode dominated by vertical displacements of the main rotors outside the operational rotational frequency band. This solution will please the designer since the possibility of the occurrence of ground resonance-type oscillations in flight now disappears. In addition, the truss-type construction is somewhat lighter than the cantilever wing construction, and also makes it possible to reduce the thrust losses due to wing download.

On the basis of these and many other considerations, the decision was made to use truss-type construction for the outriggers of the V-12 helicopter.

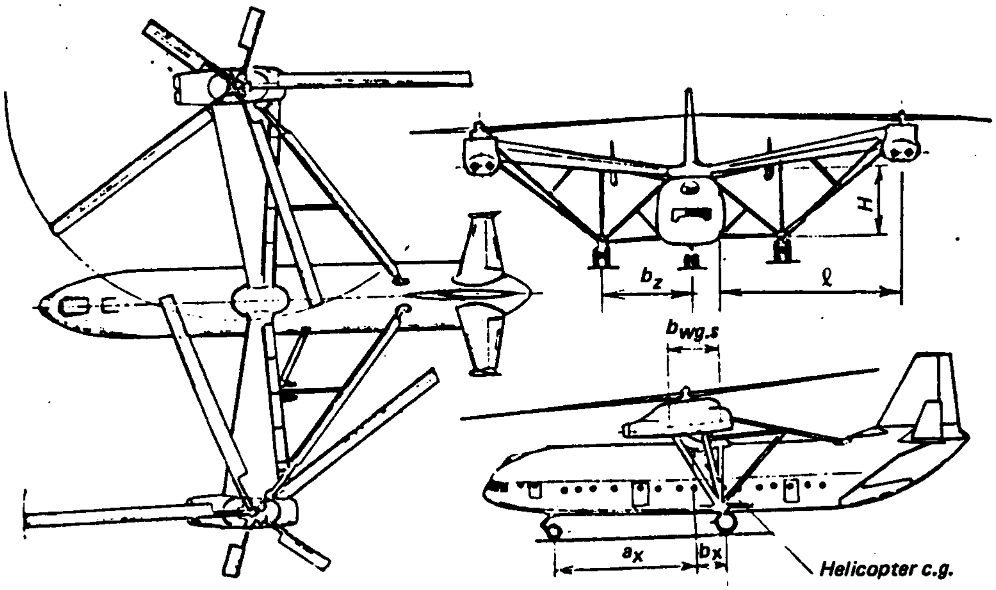

Figure 2.38 General view of a multi-strutted side-by-side type helicopter (V-12)

The vertical stiffness of the truss at the point of rotor attachment can be found from the following approximate formula

$$c_{vert} = k_c(EFH^2/\ell^3) \tag{2.82}$$

where EF = stiffness of the truss members in tension and compression; H = truss structural height at the point of attachment to the fuselage (see Fig 2.38); ℓ = length of the truss outriggers.

The truss weight can be defined as

$$G_{truss} = k_G \ell F \gamma \tag{2.83}$$

and natural frequency in the vertical oscillations as

$$p_y = \sqrt{(gc_{vert}/G_{nac})[1 + (2G_{nac}/G_{ct.f})]}\,. \tag{2.84}$$

Assuming that

$$p_y = n_y \omega_{max} \tag{2.85}$$

and using Eqs (2.82) and (2.83), and assuming that $1 + (2G_{nac}/G_{ct.f}) = const$, we obtain

$$G_{truss} = k_{truss}(\ell/R)^2(\ell/H)^2(\bar{U}_t)^2_{max}\,G_{nac} \qquad \text{(2.86}$$

where

$$k_{truss} = k_G\gamma U_{t_o}^2 n_y^2/k_c gE\,[1 + (2G_{nac}/G_{ct.f})];\; U_{t_o} = 220\,m/s. \tag{2.87}$$

Substituting the parameters of the V-12 outriggers: $G_{truss} = 7870\ kg$ (with wing but without the landing gear struts); $G_{nac} = 17\,500\ kg$; $\ell = 15\ m$; $R = 17.5\ m$; $H = 4.8\ m$; and $(\bar{U}_t)_{max} = 1.07$ into Eq (2.86), we obtain $k_{truss} = 0.0545$.

Assuming that in the new designs it would be possible to reduce the weight of the outrigger structure for side-by-side helicopters, we can take $k_{truss} = 0.05$.

We will also examine the truss outrigger regarding the requirements for ensuring the needed stiffness in torsion:

$$c_{tors} = \tfrac{1}{2} c_{vert} b^2_{wg.s} \tag{2.88}$$

where $b_{wg.s}$ = distance between the vertical wing-tip struts which take the loads from the moment M_z twisting the outrigger (see Fig 2.38).

The natural vibration frequency with respect to the outrigger torsion can be defined as

$$p_{tors} = \sqrt{c_{tors} g / i^2 G_{nac}}\,. \tag{2.89}$$

Taking into account the necessity for providing the required margin for torsional frequency, we find that b_k should be determined from the expression

$$b_{wg.s} = k_{b_{wg.s}} [\ell^2 i (\bar{U}_t)^2_{max}/HR] \sqrt{G_{nac}/G_{truss}}\,. \tag{2.90}$$

This expression is important for determining the area of the inverse-taper wing for truss-type helicopters of side-by-side configuration.

2.2.13 Strutted Wing of Side-by-Side Helicopter

A wing of skin-stressed type (monocoque) (Fig 2.39) can provide the required stiffness for main-rotor attachment in the longitudinal direction (along the x-axis) as well as in torsion while the use of a strut can shift the frequency P_y of wing vibrations in the plane of least stiffness outisde the main-rotor operating speed range.

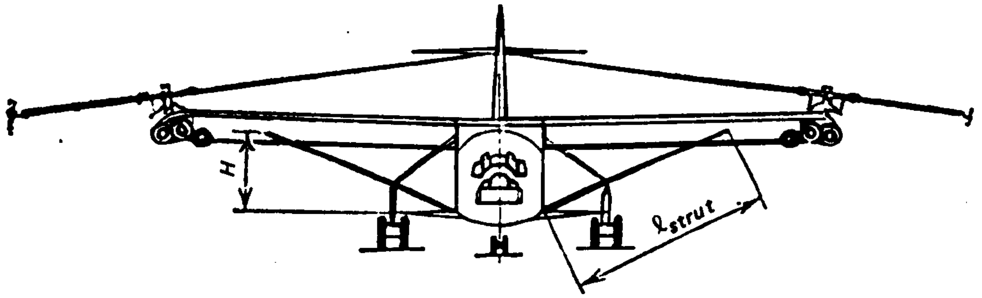

Figure 2.39 Side-by-side helicopter with strutted wing

In this case, the wing weight can be found from Eqs (2.77) and (2.78), and the overall weight of the struts can be found from a formula analogous to Eq (2.86):

$$G_{strut} = k_{strut} (\ell_{strut}/R)^2 (\ell_{strut}/H)^2 \bar{U}^2_{t_{max}} G_{nac}\,, \tag{2.91}$$

where ℓ_{strut} = strut length (Fig 2.39); and H = structural height of the strutted wing.

Calculations show that the value of the k_{strut} coefficient may be taken equal to *0.005*. The total weight of the outriggers is

$$G_{outr} = G_{wg} + G_{strut}. \tag{2.92}$$

2.2.14 Wing of Single-Rotor or Compound Helicopter

The cross-section at areas of the structural elements of the cantilever wing of the single-rotor transport helicopter are determined by the aerodynamic forces acting on the wing, and by the wing dimensions: chord, relative profile thickness, and wing span.

Assuming that the wing bending moments are proportional to the wing lift Y_{wg}, and wing span L; i.e.,

$$M_{bend} = k_M Y_{wg} L$$

and the wing-section resisting moment can be determined—as in Eqs (2.63) and (2.64) from an expression of the form

$$W = k_w \delta h b$$

and considering that the weight of the wing structural elements is defined as

$$G_{wg.s.e} = k_G \gamma \delta b L$$

from the condition of constant wing bending stresses, we obtain

$$G_{wg.s.e} = k^*_{wg} L^2 Y_{wg}/h .$$

Assuming then, as in Sect 2.2.11, that the weight per square meter of the wing elements which do not carry external loads is independent of the wing dimensions, and expressing the quantities in the above formula in terms of the wing aspect ratio λ_{wg} and area S_{wg}, we obtain the following formula for the cantilever wing weight

$$G_{wg} = k_{wg} [(\lambda_{wg} S_{wg})^{3/2} / \bar{h}] V_{des}{}^2 + q_{wg} S_{wg}$$

where V_{des} = design flight speed in km/hr.

The value of k_{wg} may be taken as $k_{wg} = 0.12 \times 10^6$, and the value of q_{wg}, as before, equal to *14* to *16 kg/m²*.

2.2.15 Helicopter Fuselage

The helicopter fuselage weight does not depend strongly on the loads acting on the helicopter, but is basically related to the surface area enclosing the fuselage structure.

Therefore, in the preliminary calculation of fuselage weight, a suitable approach is based on the following:

$$G_\phi = \sum_i q_i S_i \tag{2.93}$$

where S_i is the surface area of the various fuselage elements; q_i = weight per meter squared of the corresponding structural element.

If the relationship between the various areas S_i remains approximately constant, this formula can be still further simplified, setting

$$G_\phi = q_{av} S_\phi . \tag{2.94}$$

where q_{av} = average weight per square meter of the fuselage surface.

However, Eqs (2.93) and (2.94) do not reflect the weak, but still significant influence of the external loads on fuselage weight.

In order to take this influence into account, we can use the following approach, which was used previously by V.V. Kronshtadtov in a somewhat different form. We shall determine the parameters on which the weight of the fuselage longitudinal structure depends, and the form of this relationship in the case when the normal stresses from the fuselage bending moment are equal to the allowable stresses for this structure. Then in the same way, we determine the weight of the structural elements resisting the shearing force. We shall term these weights the partial structural weights of the fuselage.

The partial structural weight necessary to ensure allowable normal stresses in the longitudinal structure from the fuselage bending moments can be found from the approximate formula

$$G_M = k_M G_{gr} L \ell_\phi / h$$

where G_{gr} = helicopter design gross weight; L = some linear dimension defining the magnitude of the bending moments acting on the fuselage. For single-rotor and tandem helicopter configurations, this is the distance between the rotor axes. For the fuselages of side-by-side helicopters, this is the distance along the x-axis from the line connecting the lifting rotor axes to the point of application of the forces on the empennage; ℓ_ϕ = length of the working part of the fuselage, having transverse dimensions determined by the given transverse dimensions of the cargo cabin. For single-rotor helicopters, this is the length of the fuselage minus the tail boom; h = structural height of the working part of the fuselage.

The partial fuselage weight required to ensure allowable tangential stresses from the shearing forces can be found from the analogous formula,

$$G_Q = k_Q G_{gr} \ell_\phi .$$

However, the structural element section areas will be determined by the external loads only in certain segments of the fuselage. In the largest part of the fuselage, the component section areas determined by the external loads are much smaller than those resulting from manufacturing and technological considerations as well as the need to ensure local strength. Therefore, the fuselage weight is always greater than its various structural weights and, as we have already mentioned, depends to a considerable extent on the fuselage outer surface area S_ϕ.

In addition, the overall fuselage weight of transport helicopters is influenced considerably by the cargo floor weight which is usually proportional to the weight of the payload $G_{p.l}$ transported by the helicopter and the cargo floor width b_{flo}.

If we assume that all the aforementioned factors have a definite influence on fuselage weight but that the degree of their influence is different, we can represent the fuselage weight in the form

$$G_\phi = \bar{k}_\phi (S_\phi)^s [G_{g.w} L \ell_\phi / h]^m (G_{gr} \ell_\phi)^q (G_{p.l} b_{flo})^g$$

where the exponents s, m, q, and g will determine the degree of influence of the forementioned factors on fuselage weight.

Transforming this formula somewhat, we obtain

HELICOPTER	G_ϕ kg	NORMAL GROSS WEIGHT G_{gr}, kg	S_ϕ m^2	L m	$\tilde{\ell}_\phi$	k_ϕ	k^*_ϕ
Mi-1	341	2470	32	8.55	0.620	2.29	1.75
Mi-2	445	3700	40	8.77	0.526	2.22	1.73
Mi-4	936	7500	70	12.64	0.563	2.39	1.74
Mi-8	1465	11100	105	12.64	0.900	2.23	1.61
Mi-6	6070	41000	295	21.08	1.110	2.86	1.72
Mi-10	5100	43000	254	21.24	2.100	2.71	1.47
V-12	12750	96000	566	17.90	1.120	2.73	1.69
S-51	370	2500	37	9.10	0.520	2.18	1.70
S-52	208	1650	28	6.80	0.503	1.73	1.42
S-55	450	3270	56	11.00	0.550	1.72	1.29
S-58	570	5900	75	10.00	0.620	1.45	1.08
S-61B	930	8190	114	10.65	0.850	1.51	1.06
S-61R	1310	8845	126	11.50	0.920	1.91	1.31
S-56	1400	14060	140	16.50	0.520	1.66	1.17
S-65 (CH-53A)	2140	15200	175	13.37	0.920	2.04	1.36
S-64 (CH-54A)	1200	17240	120	13.60	1.830	1.55	0.92
CH-46A	1160	8800	103	10.16	0.940	2.02	1.41
CH-47A	2040	12950	180	11.94	0.960	1.98	1.34
CH-47B	2480	14970	180	12.04	0.960	2.32	1.56
CH-47C	2100	14970	180	12.04	0.960	1.96	1.32

TABLE 2.5 HELICOPTER FUSELAGE DATA

$$k_\phi = \frac{G_\phi}{G_{gr}^{0.25}\,S_\phi^{0.88}},\quad \frac{kg}{kg^{0.25}\,m^{1.76}}$$

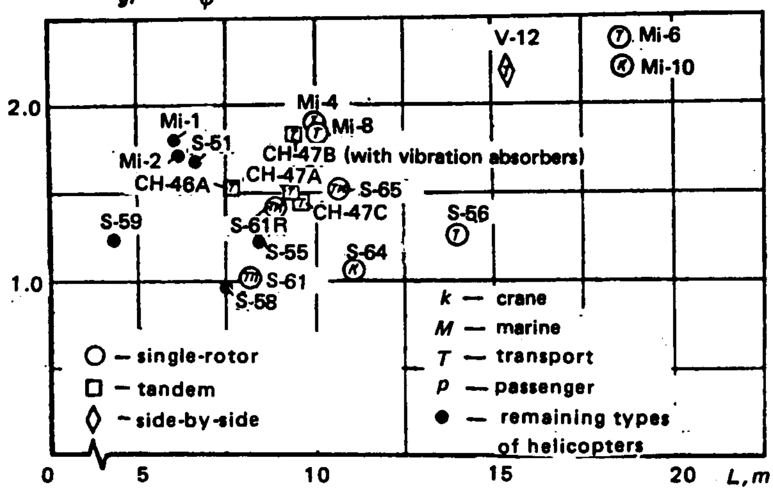

Figure 2.40 Fuselage weight coefficients k_ϕ used in Eq (2.96), not accounting for fuselage length

$$G_\phi = \bar{k}_\phi G_{p.l}^{\,g} (\ell_\phi G_{gr}\ )^{m+q} S_\phi^{s} (L/h)^{m} b_n^{\,g} . \qquad (2.95)$$

The values of the exponents in this formula can be determined by making more detailed calculations of the weight of various fuselage designs in which only certain of the parameters influencing the weight are alternately varied.

For example, by varying only the cargo weight transported by the helicopter, or only the helicopter weight, and leaving the fuselage dimensions unchanged, we can determine q and $m+q$. By varying the dimensions of the fuselage cross-section only by alternating its height and width, while keeping $G_{p.l}$, G_{gr}, ℓ_ϕ, and L unchanged, we can determine $s-m$ and $s+g$. The exponent m can be evaluated by examining designs with different L and ℓ_ϕ, varying them both jointly and independently. The results of such calculations by various authors, especially by V.V. Kronshtadtov, lead to the following approximate values of these exponents: $s = 0.67 \ldots 0.88$; $m = 0.1 \ldots 0.16$; $g = 0.09 \ldots 0.16$; and $q < 0.05$.

Various simplifications of the formula for G_ϕ are possible. The cargo weight $G_{p.l}$ can be taken proportional to the helicopter gross weight.

The value of the exponent q can be set equal to zero and we can thus exclude the influence of the shearing forces on fuselage weight. It is also possible to assign constant values to the other exponents, but within the scatter limits obtained in the various calculations.

We take: $g + m = 0.25$; $s = 0.88$; $m = 0.16$; and $q = 0$.

Then, neglecting the influence of ℓ_ϕ, L/h, and b_{flo}, we obtain the following quite frequently used formula:

$$G_\phi = k_\phi G_{gr}^{\,0.25} S_\phi^{\,0.88} . \qquad (2.96)$$

In determining the optimal main and tail rotor diameters, it is very important to account for the influence of the distance L between the rotor axes on the fuselage weight while, if possible, maintaining the fuselage working section length constant. In this case, the following formula is more exact:

$$G_\phi = k^*_\phi G_{gr}^{\,0.25} S_\phi^{\,0.88} (\tilde{\ell}_\phi L)^{0.16} . \qquad (2.97)$$

Here,

$$\tilde{\ell}_\phi = \bar{\ell}_\phi / \bar{\ell}_{av}, \text{ where } \bar{\ell}_\phi = \ell_\phi / h; \ (\bar{\ell}_\phi)_{av} = 6.$$

The value of $\tilde{\ell}_\phi$ usually changes along with the variation of the dimension L. We can assume that approximately, $\tilde{\ell}_\phi = \xi L$ or $\tilde{\ell}_\phi = L^\alpha$ where, in the calculations presented in Sect 2.5, we have taken $\alpha \approx 0.2$.

This approach makes it possible to take the same values of the weight coefficients k^*_ϕ when comparing different transport helicopter configurations.

The value of the coefficients k_ϕ and k^*_ϕ for several well-known helicopters are shown in Table 2.5 and Figs 2.40 and 2.41. In calculating these coefficients for helicopters with engines which are not located in individual nacelles, the weight of the powerplant installation is included in the fuselage weight. Correspondingly, the fuselage outer surface area S_ϕ also includes the cowlings.

Since Eq (2.97) and the exponents used therein were obtained from calculations based on transport helicopters (with cargo floors, doors, and ramps), this formula should be used with some care in application to other types of helicopters. The weight coefficients for these helicopters are presented in Figs 2.40 and 2.41 for information only.

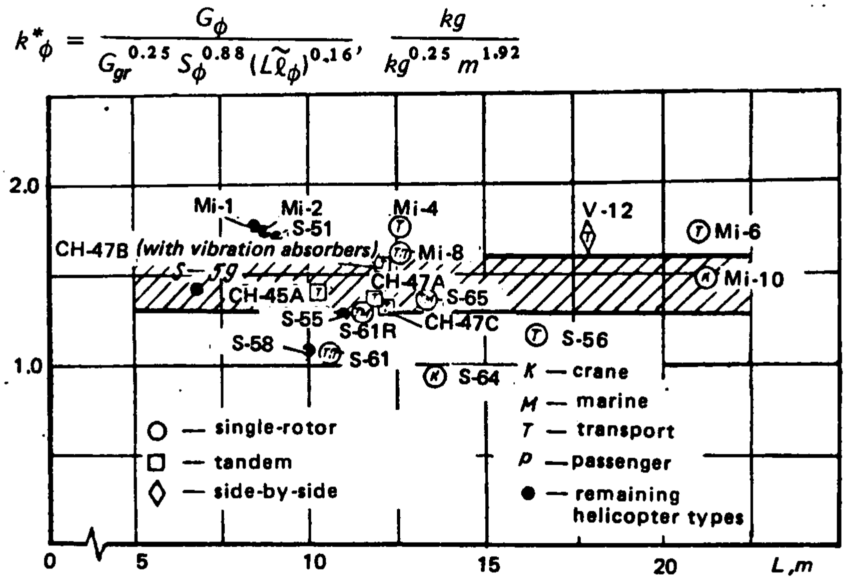

Figure 2.41 Fuselage weight coefficients k^*_ϕ used in Eq (2.97) which take into account the influence of parameters characterizing fuselage length ℓ_ϕ and distance L between rotor axes on fuselage weight (hatched area corresponds to the contemporary level of transport helicopters)

It should be noted that in design calculations and in the selection of fuselage weight coefficients, we should use only the data related to Soviet helicopters, since the requirements for operation in more severe climatic conditions which affect the fuselage weight, are reflected in their design. In addition, there is no assurance that all of the elements which we include in the fuselage weight are included in the published data on foreign helicopter fuselage weights.

Analysis of this data and later developments show that for modern Soviet helicopters, we can count on building fuselage with weight coefficients of $k^*_\phi = 13 \ldots 16$.

During the more advanced design stages, the fuselage weight estimate can be broken down into a detailed investigation of the individual major fuselage components which should obviously result in an improvement in the accuracy of the calculations.

2.2.16 Cowlings of Side-by-Side Helicopters

For single and tandem rotor helicopters, the cowling weight is most conveniently included in the fuselage weight. In side-by-side helicopters, the cowlings are far removed from the fuselage. As a result, their surface area markedly increases. In addition, the cowling construction becomes much more complex because of the necessity for ensuring safe servicing of the engines at a considerable height above the ground and of all the equipment located in the nacelles. As a result, the cowling weight increases correspondingly, reaching about 1.8 percent of the gross weight for the V-12 helicopter.

Separation of the cowling weight from the fuselage weight of the side-by-side helicopter is also necessary for more accurate determination of the nacelle weight which is required in calculating the weight of the main-rotor outriggers.

The weight of internally stiffened cowlings can be determined from a formula which is normally used in weight calculation practice:

$$G_{cow} = k_{cow} S^{\alpha}_{cow} \tag{2.98}$$

where S_{cow} = cowling surface area in m^2; k_{cow} = cowling weight coefficient—recommended by Kronshtadtov as 4.5 to 5.5; he also recommended that $\alpha = 1.25$.

In those cases when the cowlings have not yet been designed and their surface area is difficult to determine, we can use an approximate formula in which this area is related to engine dimensions which, in turn, depends on the engine power

$$G_{cow} = 2k'_{cow}[(\Sigma N_{eng})/2]^{2/3} \tag{2.99}$$

where, considering the compactness of modern engines and new nacelle structural configurations, the value of k'_{cow} should be taken as equal to 1.0, instead of 1.6 as in the case of the V-12 helicopter.

2.2.17 Main Rotor Mount

The weight of the gearbox frame of single-rotor and tandem helicopters is usually no more than 0.6 percent of the gross weight and, in calculations in the preliminary design stage, it can be combined with the gearbox and fuselage weights. In truss-type side-by-side helicopters, the main rotor mount weight increases and, in the V-12 helicopter, the so-called gearbox compartment weight amounts to 1.6 percent of the gross weight. Therefore, in calculations of this helicopter configuration, it is recommended to take

$$G_{g.b.c} = k_{g.b.c} G_{gr} \tag{2.100}$$

where $k_{g.b.c} = 0.015$.

In side-by-side helicopters with a wing, the gearbox compartment weight is included in the wing weight.

2.2.18 Helicopter Landing Gear

The landing gear weight is usually defined as a percentage of the helicopter gross weight

$$G_{l.g} = k_{l.g} G_{gr}. \tag{2.101}$$

However, for the same gear configuration and equal level of design skill, the gear weight will depend on the magnitude of the forces acting on the gear struts during landing. It is well known that these forces depend on the helicopter mass referred to the wheel. Therefore, we can consider that the gear weight is proportional to the sum of the maximum values of the masses referred to all the landing-gear wheels.

$$\Sigma(\overline{m}_{ref})_{max} \tag{2.102}$$

where $\overline{m}_{ref} = m_{ref}/m_{hel}$.

For helicopters of all configurations, the design case will be the one-leg landing. In such a landing, the referred mass will be maximum.

The mass referred to the wheels of one leg can be determined from the following approximate formulae:

when landing on the main gear,

$$\overline{m}_{ref} = 1/[1 + (b_x^2/i_z^2) + (b_z^2/i_x^2)]; \qquad (2.103)$$

and when landing on the nose gear,

$$\overline{m}_{ref} = \overline{V}_y^2/[1 + (a_x^2/i_z^2) + (a_z^2/i_x^2)], \qquad (2.103)$$

where the coefficient $\overline{V}_y^2 = (0.85)^2 = 0.72$ (accounting for the lower contact velocity of the nose wheels, usually taken as equal to 0.85 of the main gear touchdown speed); a_x, a_z, b_x, and b_z are the distances of the nose and main gear wheels from the helicopter c.g. (see Figs 2.38, 2.57, and 2.75); a_x is determined for the most forward, and b_x for the most aft c.g. position; i_x and i_z respectively, are the helicopter radii of inertia about the x and z axes.

Typical values of the quantities appearing in these formulae and the referred masses are shown in Table 2.6.

HELICOPTER CONFIGURATION	"One-Leg" Landing, Main Landing Gear			One-Leg" Landing, Nose Landing Gear			$\Sigma(m_{ref})_{max}$
	b^2_x/i^2_z	b^2_z/i^2_x;	Masses referred to wheels of of main landing gear leg	a^2_x/i^2_z;	a^2_z/i^2_x	Masses referred to wheels of of nose landing gear leg	
Single-Rotor	0.05	1.00	0.49	1.7	0	0.27	1.25
Tandem	0.20	1.00	0.45	0.5	0.91	0.30	1.50
Side-by-Side	0.12	0.21	0.75	2.3	0	0.22	1.72

TABLE 2.6 DETERMINATION OF THE SUM $\Sigma(\overline{m}_{ref})_{max}$ OF RELATIVE MASSES REFERRED TO ALL THE GEAR LEGS

Thus, on the basis of the fact that for the same design scheme, the gear weight is proportional to the sum of the maximum values of the masses referred to all helicopter gear legs, we find that the landing-gear weight of the tandem should be 1.2 times, and the side-by-side, 1.4 times higher than that of the single-rotor configuration. Consequently, if we assume that $k_{l.g} = 0.02$ for the single-rotor helicopter, then for the tandem, it should be taken as $k_{l.g} = 0.024$, and as $k_{l.g} = 0.028$ for the side-by-side configuration.

It should be noted, however, that the gear weight depends, to a large extent, on the configuration of the gear itself, which may lead to a considerable deviation of the weight from that determined from the above-presented coefficients. Thus, for the V-12 helicopter gear, $k_{l.g} = 0.045$. The values of the weight coefficients for various helicopters are shown in Fig 2.42.

We see from this figure that the skid landing gears are lightest ($k_{l.g} \approx 0.01$), and the heaviest are the gears of cranes designed for external transport of loads between the gear struts, as in the Mi-10 helicopter ($k_{l.g} = 0.06$). As a rule, the landing gears of tandem helicopters are heavier ($k_{l.g} \geqslant 0.033$) than those of single-rotor configurations for which, in many production machines, the weight coefficient $k_{l.g} = 0.028$ has been obtained, and even lower values have been achieved in the latest designs.

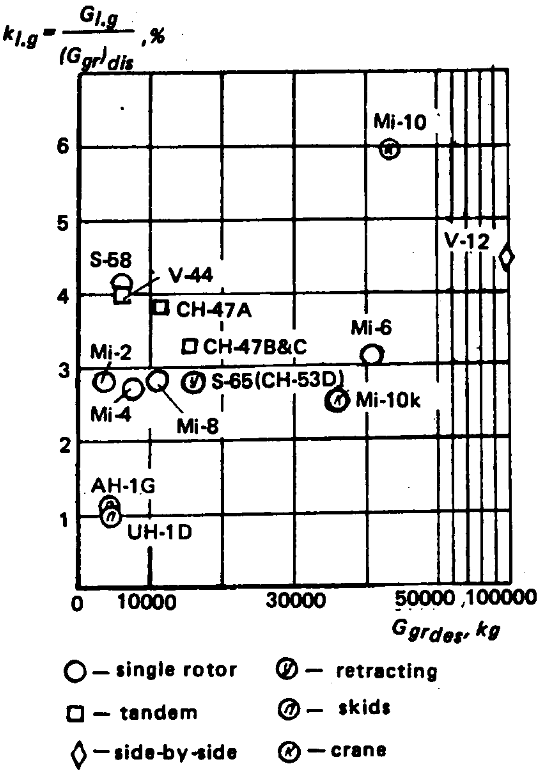

Figure 2.42 Weight coefficients of helicopter landing gears

2.2.19 Helicopter Equipment

In the equipment weight, we include the weights of the flight navigational and cockpit instrumentation, and such items as radio equipment, electrical equipment, cockpit equipment, cabin equipment, and various special equipment systems:

$$G_{\text{eqp}} = G_{p.n} + G_{rad} + G_{el} + G_{c.e} + G_{spec}\,. \qquad (2.105)$$

The composition of nearly all forms of equipment depends on the helicopter mission and therefore, it is very difficult to estimate the weight using a general formula without listing all of the elements of this equipment.

However, there is a definite relationship between the equipment weight and the helicopter parameters and configuration, which may influence their comparative values in a definite fashion. Therefore, it is advisable to select, from the overall equipment weight, those elements whose weight does not depend on the mission or on the helicopter parameters or configuration. One such element is the helicopter electrical system.

It is possible to make a preliminary estimate of the weight of the electrical system in its modern form when the primary power sources are AC Generators, the power of which is determined by anti-icing system requirements. In this case, the weight of that part of the electrical equipment which is determined by the overall power of the electrical power sources installed aboard the helicopter can be found by the formula

$$\Delta G_{el.ice} = k_{el.ice} F_{bl} \qquad (2.106)$$

where F_{bl} = total blade area proportional to the blade heated-surface area. Relationships presented in Eq (2.106) are justified by the fact that the power generated on board is consumed by the blade anti-icing system.

It is also very important to consider the weight of the increased wiring in twin-rotor helicopters. On the V-12 helicopter, the electrical equipment weight amounts to 2630 kg, which includes 1360 kg for the weight of the wiring. On the Mi-6, the electrical equipment weighs 1050 kg, including 400 kg for wiring. This situation can be dealt with by setting

$$G_{el} = k_{wir} L + k_{el.ice} F_{bl} \tag{2.107}$$

where, for the single-rotor helicopter configuration, we can take $k_{wir} = 22$ to $24\ kg/m$. For the twin-rotor types, we set $k_{wir} = 35$ to $40\ kg/m$, while L represents the distance between the rotor axes.

The value of $k_{el.ice}$ can be taken equal to about $5 \ldots 6\ kg/m^2$ for medium helicopters of all configurations. It should be noted that for light helicopters, the coefficient $k_{el.ice}$ increases to $12 \ldots 16\ kg/m^2$, while the coefficient k_{wir} decreases to about $10\ kg/m$.

For correct selection of the optimal helicopter size, it is very important to consider the fact that the equipment weight is related in a definite fashion to the helicopter gross weight; and with an increase of the latter, the relative equipment weight fraction decreases. In order to account for this dependence, we propose that the weight of the equipment for general-purpose helicopters, excluding the electrical equipment, be found from the following formula

$$G_{eqp_o} = k_{eqp} G_{gr}^{0.6}$$

where, as we see from Fig 2.43, the weight coefficient k_{eqp} for general-purpose helicopters may vary within the range of $(k_{eqp})_{min} \approx 1.6$ to $(k_{eqp})_{max} \approx 2.65$, depending on customer requirements. It should be noted that $(k_{eqp})_{min}$ determines the minimal equipment weight necessary for conventional helicopter operation under simple flight conditions, and $(k_{eqp})_{max}$ corresponds to the maximum weight of the equipment that the customer may require.

The following formula is suggested for determining the weight of all the helicopter equipment

$$G_{eqp} = k_{eqp} G_{gr}^{0.6} + k_{wir} L + k_{el.ice} F_{bl}. \tag{2.108}$$

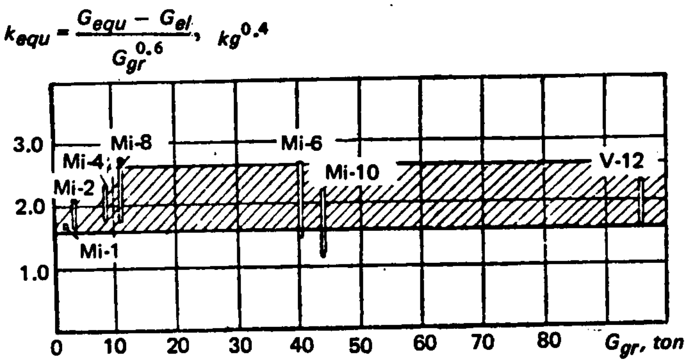

Figure 2.43 Weight coefficients of equipment (without electrical installation) vs gross weight for general-purpose helicopters

2.2.20 Vibration Absorbers

When selecting the helicopter configuration and the number of main-rotor blades, it is necessary to consider the magnitude of the vibration that may occur in the fuselage and cockpit.

In order to equalize the various helicopter designs in regard to this aspect, it is advisable to assume that if the vibrations exceed the allowable norms, special devices should be installed for vibration absorption, and their weight should be included in the structural weight.

If conventional inertial absorbers are considered, one must determine the active mass required to provide the necessary reduction of the vibration amplitudes, as well as the corresponding overall absorber weight which is proportional to its active mass.

The active mass can be determined only as a result of helicopter vibration calculations which are very difficult to perform in the preliminary design stage when helicopter parameters are being selected. Therefore, at this stage, various approximate estimates are normally used.

On the basis of experience in the development of single-rotor helicopters, it is known that if everything possible has been done to achieve separation from resonant modes, vibrations usually increase with an increase in takeoff weight and flight speed, and decrease with an increase in the number of main-rotor blades. For single-rotor helicopters having more than five blades and maximum speeds up to 300 km/hr, it may be expected that the vibrations will be within the allowable limits, even for very large helicopters.

The problem of reducing vibration is particularly severe for tandem helicopters in which the main-rotor forces that excite the vibrations are applied at the antinodal points; while increasing the number of bladse above four practically excludes the possibility of reducing the fuselage length by overlapping the rotors.

Therefore, the following expression is proposed for tandem-rotor helicopters in the parameter selection stage

$$G_{v.ab} = k_{v.ab} G_{gr} \tag{2.109}$$

where $k_{v.ab} = 0.015$ for four bladed, and $k_{v.ab} = 0.025$ for three-bladed, rotors.

The construction of the vibration absorbers for the Chinook CH-47C helicopter for which $k_{v.ab} = 0.026$ is shown in Fig 2.44. The location of the vibration absorbers on this helicopter is shown in Fig 2.45.

The side-by-side helicopter rotor mount outriggers can be used as vibration suppressors to achieve separation from resonant conditions and thus significantly reduce fuselage vibrations. Therefore it is not necessary to use inertial vibration absorbers in this configuration.

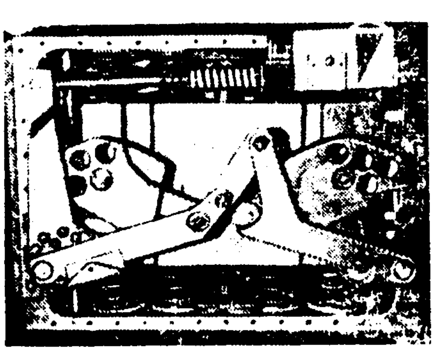

Figure 2.44 Vibration absorber of the CH-47C Chinook helicopter[24]

2.3 Some Constraints Encountered in Design

Those who point out design constraints run the risk that with the passage of time, they may be proved wrong since, due to technical progress, existing constraints constantly change, shift, or can often be surmounted. Nevertheless, constraints do exist. However, in the below enumeration of those constraints with which we must contend today, we must keep in mind the possibility of overcoming them in the very near future.

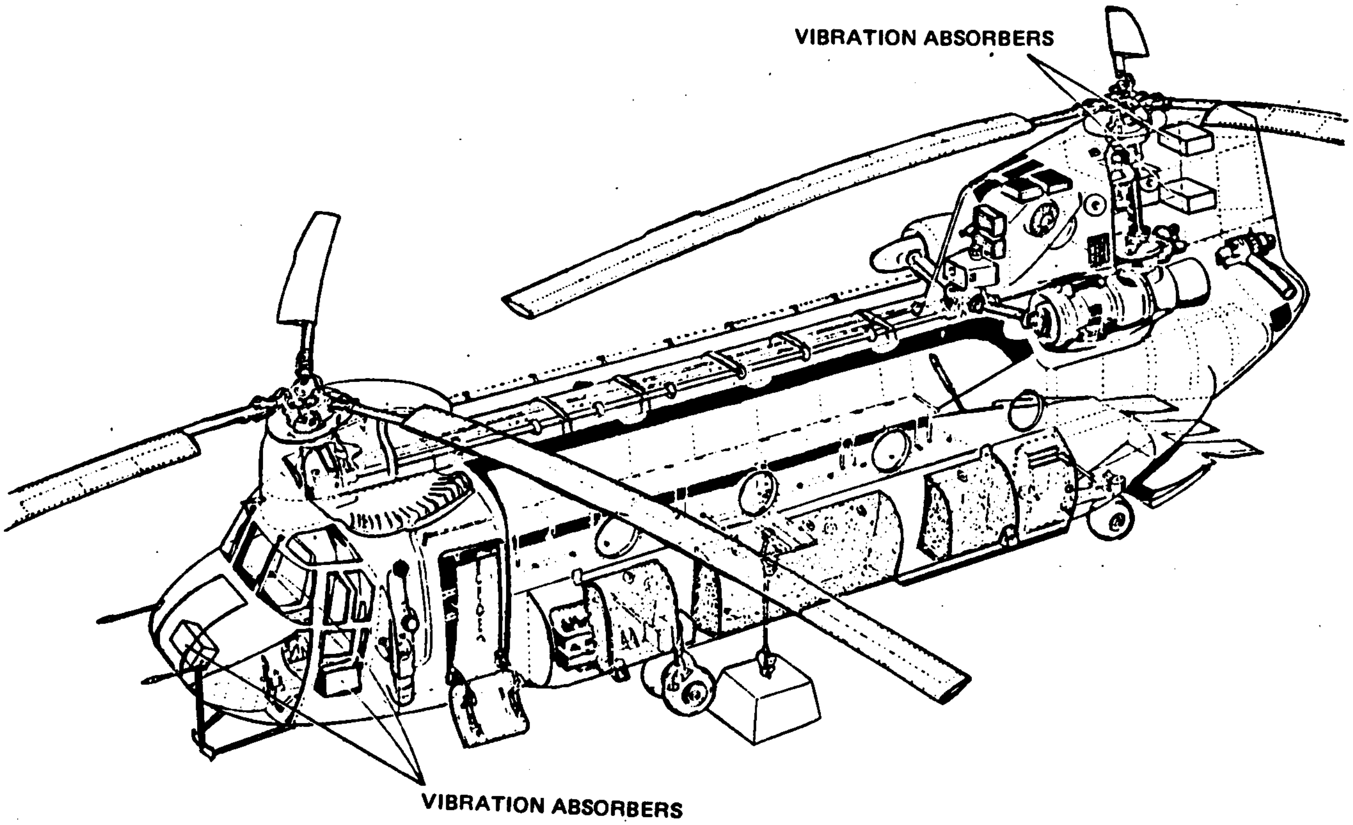
VIBRATION ABSORBERS
VIBRATION ABSORBERS

Figure 2.45 Location of vibration absorbers on the Ch-47C Chinook helicopter

However, these limitations do not disappear by themselves, but rather as a result of the general development of technology. They can be overcome only with the application and verification of new approaches which are not known today; new design principles, new materials with improved characteristics, introduction of more advanced technological processes, etc., which is possible only as the result of long and serious research.

2.3.1 Constraints Presented by Average Disc Loading of Lifting Rotors

Since all types of general-purpose helicopters must operate in hovering near the ground, the average main-rotor disc loading that governs the rotor downwash velocity must be strictly limited.

For transport helicopters which are not destined to perform installation or other crane-type operations during which personnel are located below the helicopter disc, loading should not exceed 70 to 80 kg/m^2.

For crane helicopters used for installation and other operations during which regular and specially equipped personnel are located beneath the hovering helicopter, the average disc loading should not exceed 50 to 60 kg/m^2.

For helicopters used in rescue and other operations during which people must be hoisted into the hovering helicopter, disc loading should not exceed 30 to 35 kg/m^2.

We note that for twin-rotor helicopters with overlapping rotors, the disc loading in the overlap zone located immediately above the area where the operations are performed approximately doubles in comparison with the average disc-loading value. As a result, the downwash velocity in this region increases by a factor of about $\sqrt{2}$ in comparison with the average induced velocity.

However, considering the limited dimensions of the overlap area, the disc loading in this zone can be allowed to be about 15 percent higher than the above-indicated values. Consequently, for twin-rotor transport helicopters with overlap, the overall rotor area loading should be no higher than 45 kg/m^2.

2.3.2 Stall Constraints

The approach of main-rotor blade stall manifests itself, first of all, in the growth of alternating loads in the boosted control system, and then, in a growth of the alternating loads in the other components, and increased helicopter vibrations.

In order to avoid flight in such regimes on the single-rotor helicopter, it is customary to not exceed the thrust coefficients $(t_y)_{all}$ shown in Fig 2.46. These limitations are considered valid for the blade airfoil sections in present use, and are not reduced up to rotor tip speeds of $\omega R = 230\ m/s$. The same constraints are valid in determining the flight characteristics of the side-by-side rotor configuration. For $\omega R < 200\ m/s$, the values of $(t_y)_{all}$ may be somewhat increased (but no more than 5 to 7 percent).

Somewhat more restrictive stall limits are established for the tandem-rotor configuration because of the fact that at maximum flight speeds, the forward rotor of this helicopter operates at more negative angles-of-attack (which leads to the earlier appearance of stall), while the aft rotor is in the field of alternating induced velocities from the forward main rotor. This is confirmed in part by the limitations established for the Chinook helicopters—shown in Fig 2.46—although it is not certain they correspond to the same degree of penetration into stall as in the case of the single-rotor configuration.

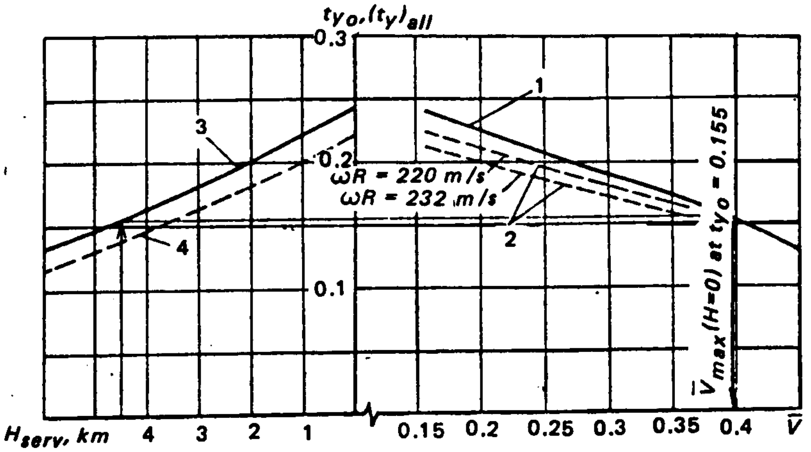

Figure 2.46 Maximum allowable values of thrust coefficients $(t_y)_{all}$ as a function of the rotor advance ratio $\bar{V}$. Limits established by an increase in alternating loads in the control system resulting from incipient stall. Recommended values of t_{y_0} as a function of required service ceiling are shown on the left side of this graph. (1) $(t_y)_{all}$ for single-rotor helicopter, (2) $(t_y)_{all}$ for tandems, (3) $(t_{y_0})_{max}$ for single-rotor helicopter at $(\omega R)_0 = 220$ m/s, and (4) $(t_{y_0})_{max}$ for tandems with $(\omega R)_0 = 220$ m/s.

Nevertheless, considering these limitations, and assuming that the optimal flight regime is that where $\bar{V} = 0.2$, we find that at altitude $H = H_s$ and $\omega R = 230$ m/s, the thrust coefficient should not be higher than $t_{y_H} = 0.0225$ for the single-rotor, and no more than $t_{y_H} \approx 0.2$ for the tandem configuration.

If we assume that the forward-flight (service) ceiling for these helicopters is $H_s = 4500$ m (relative air density $\Delta = 0.634$), we find that for a main-rotor tip speed at sea level of $(\omega R)_0 = 220$ m/s, the thrust coefficient for $H = 0$ should not exceed $t_{y_0} = 0.155$ for the single-rotor, and $t_{y_0} = 0.14$ for tandem helicopters.

For other values of the given H_s, and accounting for the required values of $\bar{V}$ at $H = 0$, the allowable coefficients t_{y_0} can be determined from the curve on the left side of Fig 2.46.

2.3.3 Constraints Due to Twin-Rotor Helicopter Overlap

In designing twin-rotor helicopters, it is very important to reduce the distance between the lifting rotor axes as much as possible because this makes it possible to reduce the dimensions of the wing (or truss) in the side-by-side, and the fuselage length in the tandem configurations. Reduction of these dimensions reduces the structural weight and increases the weight efficiency of the helicopter.

The most effective means for reducing the distance between the rotors is rotor overlap which, however, generates a new problem—the possibility of blade strike in the course of their opposing motion in the rotor-rotation plane.

It is pointless to try to avoid blade strikes by limiting blade motion through stops since the stops would not restrict blade motion if, under the influence of external forces, the blade deflects beyond established limits. The blade will continue its movement through bending and, if the stop does not yield, the blade will eventually break upon reaching ultimate stresses.

Rotor blade strike becomes most probable when the differential collective pitch is applied, as then the torque on one rotor increases while that on the other rotor decreases.

In general, the possibility of blade strike depends on the magnitude of the overlap, the possible difference in the torques on the rotors, the nature of the variation in time of these torques, blade parameters, blade retention at the hub, and finally, stiffness of the transmission which synchronizes rotor rotation.

We shall consider the contact of the blade axes in the plan projection as inadmissible since, in this case, the probability of strike is very high and depends only on the mutual positioning of the blades in their respective flapping planes (Fig 2.47).

For tandem helicopters with the aft rotor plane of rotation elevated above that of the forward rotor, blade strike is most probable when the control stick is moved aft, when the forward coning angle increases and that of the aft rotor decreases.

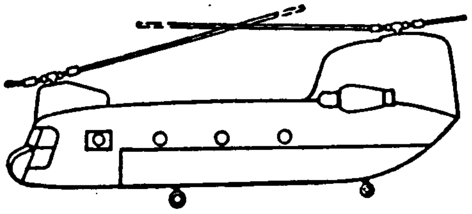

Figure 2.47 Mutual position of Chinook helicopter blades in their respective flapping planes

For the side-by-side rotor configuration with symmetric arrangement of the rotors, interference may not occur when the control stick is moved to the side, even if the blade axes contact each other in the plan projection. This is due to the fact that the blades may be at different elevations in their flapping planes.

However, it is easy to show that in the case of quick deflection of the control stick and return to the neutral position, the coning angle of the lifting rotors will follow the collective pitch change with a very small time lag. By contrast, because of the low natural frequency of the system, the blades will still be near their extreme positions in the plane of rotation as the control stick is returned to neutral. Consequently, the blades may actually come into contact if their centerlines touch in the plan projection.

We see from Fig 2.48 that with deflection of the blades of both rotors in different directions thorugh angles of the same absolute magnitude of $\Delta\xi_{all}$, the blade axes will touch each other in the plan projection if the overlap

$$\bar{P} = 2 - \cos(\Delta\xi_{all} + \Delta\psi) - \sin(\Delta\xi_{all} + \Delta\psi)/\tan\left[(\pi/z_{bl}) - \Delta\xi_{all} + \Delta\psi\right] \qquad (2.110)$$

where $\bar{P} = P/R$ is the rotor overlap; z_{bl} = number of main rotor blades; $\Delta\xi_{all}$ = maximum allowable blade deflection angle in the plane of rotation for which the blade axes contact each other in the plan projection; $\Delta\psi$ = azimuth angle of the initial blade position of one of the rotors measured from the line joining the rotor axes.

Eq (2.110) can be used to determine the allowable angles $\Delta\xi_{all}$ for different initial blade azimuthal positions $\Delta\psi$. The minimum allowable values of the $\Delta\xi_{all}$ angles corresponding to different $\Delta\psi$ values are shown in Fig 2.49 as a function of overlap $\bar{P}$ and number of main rotor blades. The points corresponding to the parameters of several widely known helicopters are also indicated on the curves.

With change in the differential blade collective pitch, the aerodynamic torque on one rotor increases and that on the other rotor decreases. In this case, the mutual position of the rotor blades changes, both because of blade deflection about the vertical hinge and the angular rotation of the rotors about their axes caused by torsional deformations of the synchronizing shafts.

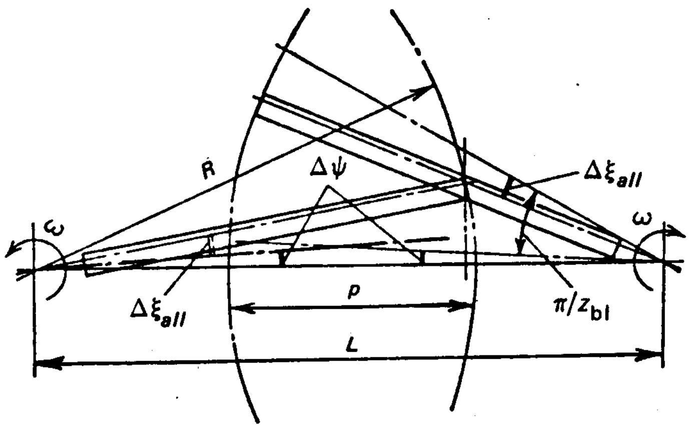

Figure 2.48 Scheme for determining maximum permissible blade deflection in the plane of rotation resulting from the no-blade-strike condition

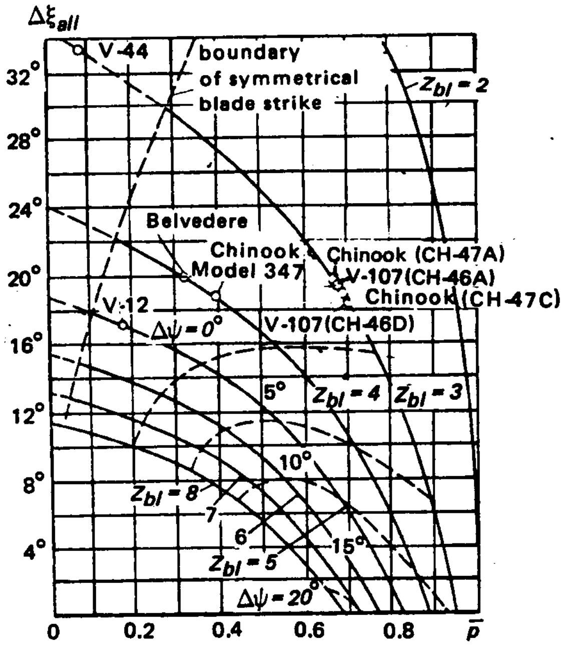

Figure 2.49 Minimal allowable azimuthal blade deflection angles, depending on overlap P, and number of blades

$$\Delta\xi = \lambda_d \left\{ [1 - (\ell_{l.h}/r_{aer})] / z_{bl}\,\omega^2 S_{l.h}\,\ell_{l.h}\,k_{a_0}] + (1/c_{s.tr}) \right\} \Delta M_Q \qquad (2.111)$$

where $\Delta\xi$ = blade deflection angle increment in the plane of rotation resulting from both blade rotation about the lag hinge, and by deformations of the synchronizing transmission; λ_d = dynamic response coefficient depending on the nature of the torque variation with time; $\ell_{l.h}$ = distance from the rotor axis to the lead-lag (vertical) hinge; $S_{l.h}$ = static mass moment of the blade relative to the lead-lag hinge; ω = rotor angular velocity; r_{aer} = radius of application of the resultant aerodynamic forces acting on the blade in the plane of rotation. We can take $r_{aer} \approx 0.7R$ where R = blade radius; $c_{s.tr}$ = torsional stiffness of the synchonizing transmission (one-half) referred to the main rotor axis; ΔM_Q = average differential increment of the aerodynamic torque

$$\Delta M_Q = (M_{Q_1} - M_{Q_2})/2; \tag{2.112}$$

M_{Q_1} and M_{Q_2} are the aerodynamic torques on the main rotors; k_{α_o} = the coefficient accounting for reduction of the restoring moment from the centrifugal forces relative to the vertical hinge because of rotation of the vertical hinge because of rotation of the vertical hinge axis relative to the horizontal hinge axis through the angle a_o. The value of this coefficient can be most accurately obtained from tests on the helicopter.

On the basis of existing theoretical considerations, the value of k_{a_o} can be determined from the formula

$$k\alpha_o = \frac{2[1 - (a_{o_1}{}^2/\nu_o^2)][1 - (a_{o_2}{}^2/\nu_o^2)]}{\Delta\bar{M}_{Q_1}[1 - (a_{o_1}{}^2/\nu_o^2)] + \Delta\bar{M}_{Q_2}[1 - (a_{o_1}{}^2/\nu_o^2)]}. \tag{2.113}$$

Here, $\nu_o = \sqrt{\ell_{l.h}\, S_{l.h}/I_{l.h}}$ is the relative natural frequency of blade oscillations in the plane of rotation; and a_{o_1} and a_{o_2} are the main rotor coning angles,

$$\Delta\bar{M}_{Q_1} = \Delta M_{Q_1}/\Delta M_Q; \ \Delta\bar{M}_{Q_2} = \Delta M_{Q_2}/\Delta M_Q$$

where

$$\Delta M_{Q_1} = M_{Q_1} - M_{Q_o}; \ \Delta M_{Q_2} = M_{Q_o} - M_{Q_2}.$$

M_{Q_o} = torque in the initial stage prior to control stick deflection.

The value of the coefficient k_{α_o} decreases as the stabilizing moment relatve to the vertical hinge diminishes. In the regimes examined below with abrupt control stick deflection while maneuvering the overloaded helicopter, this coefficient, determined from Eq (2.113), amounted to 0.86* for the Chinook and to 0.67 for the V-12 helicopter.

One can visualize two different cases of control applications which lead to reaching the maximal values of $\Delta\xi$: during abrupt maneuvering of the helicopter with use of differential collective pitch when the maximal value of ΔM_Q is reached but the dynamic response coefficient λ_d is not large; or during such control applications when, in order to maintain the required attitude, the pilot must periodically deflect the control stick, unintentially causing resonant oscillations of the blades with large dynamic response coefficient.

For evaluation of the operating conditions of synchronizing transmission in regimes that are critical with respect to blade strike, it is convenient to use the concept of main rotor differential overload with respect to the torque:

$$n_{M_Q} = 1 + [M_{s.tr}/(M_Q)_{max}] \tag{2.114}$$

---

*For the Chinook helicopter, the k_{α_o} coefficient was calculated without accounting for variation in the vertical hinge inclination resulting from the blade rotation about the pitch axis.

where $(M_Q)_{max}$ = rotor torque corresponding to maximum engine power with uniform power distribution between the rotors; and $M_{s.tr} = \lambda_d \Delta M_Q$ is the maximum torque transmitted by the synchronizing (transmission) shaft.

Calculations made for several helicopters, and presented below in part, show that the critical value (with respect to blade strike) of the average differential torque increment coefficient can reach values of $\Delta m_Q = 0.01$. From this, we can also define ΔM_Q as

$$\Delta M_Q = \tfrac{1}{2}\rho\sigma F(\omega R)^2 R \Delta m_Q.$$

Consequently, if the torque coefficient corresponding to maximum engine power amounts to $m_Q = 0.012$, then for $\lambda_d = 1.8$, the differential main-rotor torque overload may reach $n_{M_Q} \approx 2.5$, and the power transmitted by the synchronizing shaft may become 1.5 times higher than one-half of the maximum power of the engines.

In selecting the allowable rotor overlap for the twin-rotor helicopter, we must assume that in some (perhaps, very rare) cases in performing a maneuver, the pilot will use the entire differential collective pitch range, deflecting the control stick to the stop.

In this case, the differential torque rotor increment ΔM_Q varies as a function of flight speed and becomes maximum at V_{max}. However, it may also reach a significant magnitude in hover.

At high flight speeds, the differential torque increment ΔM_Q increases very markedly if, in performing the maneuver, one of the rotors (with high collective pitch angle) enters the stall regime.

The possibility of encountering stall when controlling the helicopter depends very strongly on the rotor load defined by its thrust coefficient t_y and the range of rotor collective pitch increment $\Delta\varphi_{c.p}$ used for control.

It would appear that the twin-rotor helicopter should be designed so that at full displacement of the control stick, the rotor would not encounter stall. But this means that the stall margin of the rotor must be very large. Practice indicates that it is not rational to design twin helicopters in this way. For this reason, all twin-rotored helicopters are designed in such a way that with control inputs restricted to very small displacements, the rotor would not enter into stall at the maximum flight speed. The stall margin is no more than 2 to 2.5 degrees with respect to collective pitch angle, while the control range of the differential pitch alone is usually at least $\Delta\varphi_{c.p} = \pm 4^\circ$. Therefore, at maximum flight speed with full control stick deflection, one rotor of the twin-rotor helicopter generally encounters stall.

The possibility of blade strike becomes particularly likely when the control stick is deflected to the stop in the process of maneuvering the helicopter and at the same time, the rotor collective pitch is briefly increased so that the power required for flight becomes larger than the available engine power and the rotor rpm begins to decay. In this case, the rotor whose pitch increases when the control stick is deflected will enter a particularly deep stall.

Figure 2.50 shows the calculated torque coefficients for a helicopter having parameters close to those of the Chinook at maximum flight speed. In order to simplify the analysis, the calculation was made only for the forward rotor with flapping compensator (delta-three) $\chi = 0.5$.

The delta-three coupling for the aft rotor of this helicopter is $\chi = 0$, but during control displacement, its collective pitch varies correspondingly more. Therefore, the characteristics of the aft rotor remain approximately the same as for the forward one.

It can be seen from Fig 2.50 that at the maximum flight speed with aft deflection of the control stick, the forward rotor immediately enters into the stall regime as a consequence of the collective pitch increase, and also because of the increase in the helicopter angle-of-attack.

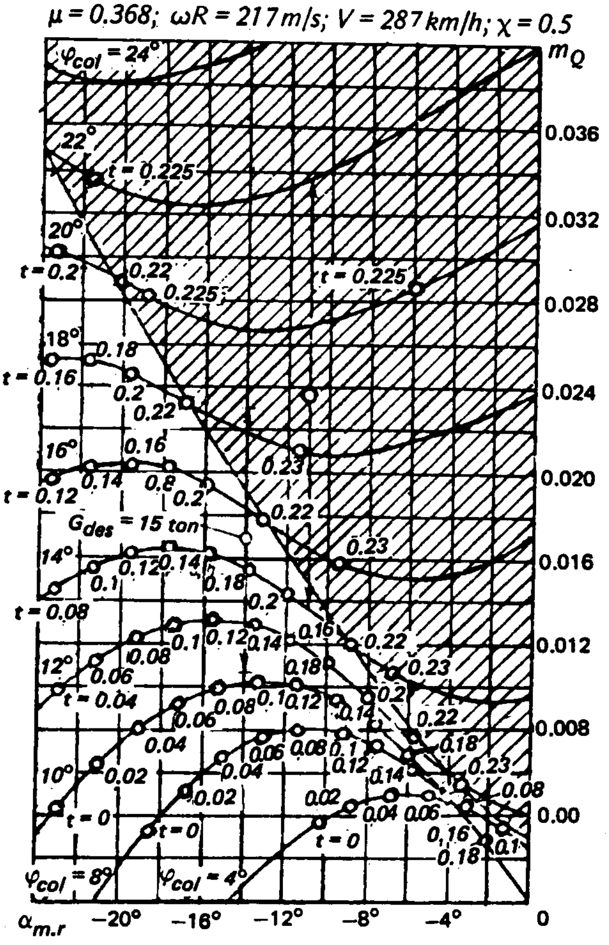

Figure 2.50 Dependence of rotor torque coefficients on angle-of-attack of the front rotor at various values of the blade collective pitch for a helicopter with parameters similar to those of the Chinook CH-47A at maximum speed-of-flight (hatched area defines stall regime)

If the control stick is deflected abruptly to the stop* then even with accounting for the angle-of-attack change, the torque coefficient difference becomes $2\Delta m_Q = m_{Q_1} - m_{Q_2} \approx 0.013$.

If, in this case, the rotor collective pitch angle is increased by only 3 degrees, and a load factor of $n \approx 1.2$ is obtained while at the same time the control stick is deflected to the stop, the difference in the torque coefficients increases to $2\Delta m_Q \approx 0.02$.

If, during a maneuver at maximum speed, the collective pitch is increased still further and, in addition, the control stick is moved to the aft stop, it is possible to obtain $m_{Q_1} - m_{Q_2} > 0.02$. However, the probability of such a maneuver is very remote.

---

*Differential pitch variation of $\Delta\varphi_{c.p} = \mp 4^\circ$ was assumed in analogy to other tandem helicopters.

Figure 2.51 shows the same relationships for the V-12 helicopter. With full lateral deflection of the control stick in level flight at 240 km/hr, the difference in the torque coefficients for this helicopter is $2\Delta m_Q = m_{Q_1} - m_{Q_2} = 0.0115$.

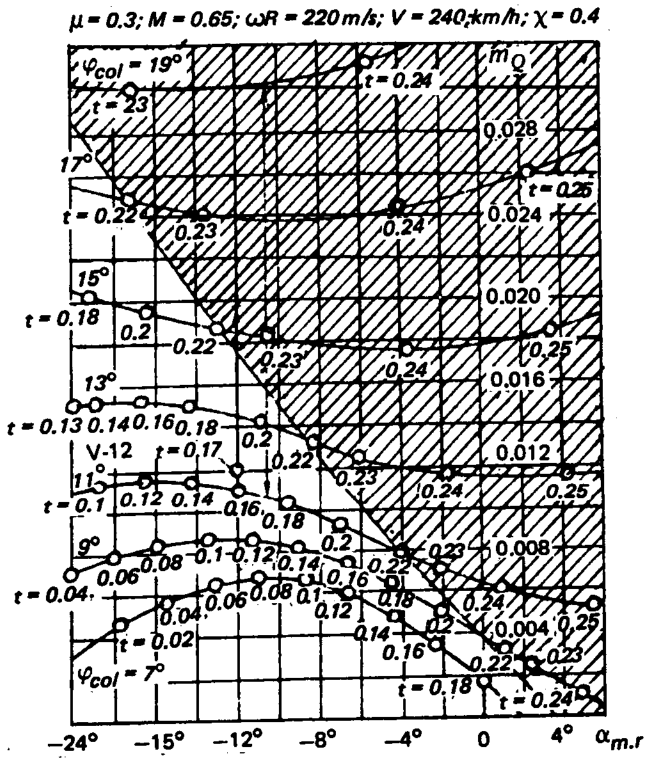

Figure 2.51 Dependence of rotor torque coefficients from rotor angle-of-attack at various collective pitch values for the V-12 helicopter in flight at V = 240 km/hr (hatched area defines stall region)

But if this stick deflection is performed simultaneously with increase of the average collective pitch (as shown on the indicator) from $\varphi_{indc} = 11.5^\circ$ to $\varphi_{indc} = 15^\circ$ (overload $n = 1.35$), the difference in torque increases so that $m_{Q_1} - m_{Q_2} = 0.02$. This latter figure was used for this helicopter as the maximal possible value in selecting parameters needed to prevent blade strike. In this case, the collective pitch of one of the rotors reaches the stop as $\varphi_{indc} = 19^\circ$.

Comparison of the charactersitics presented in Figs 2.50 and 2.51 shows that the parameters of the considered helicopters were selected using approximately the same approach to the stall margin. With sharp deflection of the control stick to the stop, one of the rotors in these helicopters enters the stall regime. However, if the control stick is deflected simultaneously with an increase of the collective pitch, one of the rotors enters a very deep stall.

No less important in studying rotor-blade strike is another possible and hazardous helicopter control regime.

Systems incorporating twin rotors connected through the synchronizing transmission exhibit a natural oscillation mode in which all blades of each rotor deflect simultaneously relative to the vertical hinge so that the torques—arising, in this case, from the inertial forces of the blades of the two rotors—are mutually equalized through the transmission.

As a consequence of synchronizing transmission elasticity, the natural oscillation frequency of such a system is somewhat lower than the partial natural oscillation frequency of the blade relative to the vertical hinge. On the V-12 helicopter, this frequency is about 0.5 Hz (oscillation period $T = 2\ sec$).

When controlling the helicopter—particularly during flight in rough air—the pilot may quite unintentionally deflect the control stick at a frequency coinciding with that of the natural oscillations of the main rotor system and thus, excite resonant rotor oscillations from the aerodynamic forces arising on the blades due to periodic variation of the rotor differential collective pitch.

In the case of periodic main-rotor excitation at the frequency of the described mode, the blade oscillation amplitude may strongly increase, particularly in the case of a step-like characteristic of the vertical-hinge damper (friction-type) when the relative damping coefficient decreases with an increase of the blade oscillation amplitude.

However, in the V-12 helicopter, the possibility of inadvertent excitation of such oscillations by the pilot is, in considerable measure, limited by the maximum possible rate of displacement of the small first-stage booster of the control system. This does not permit oscillation of the collective pitch at 0.5 Hz with an amplitude greater than one-quarter of the full control stick displacement since, in this case, oscillatory damping force in the control system reaches a value of $P_{da} \approx 200\ kg$ at the small booster piston, and booster speed can not exceed $V_{boo} = 60$ to $70\ mm/s$ (at $P_{da} = 0$, $V_{boo} = 95\ mm/s$).

Inadvertently created resonant oscillations excited by the pilot have been recorded several times in V-12 helicopter flight tests. However, their amplitudes did not exceed $\Delta\xi \approx 7^\circ$, and the corresponding power transmitted through the synchronizing shaft reached $\Delta N = 5300\ hp$.

It is not difficult to see that with an increase of the control-stick oscillation amplitude to one-half its full travel in one direction, the blade oscillation amplitude would reach $\Delta\xi = 15^\circ$. However, further increase of this angle is limited by the maximal rate of displacement of the small booster piston. Thus, there is no possibility of resonant blade strike on the V-12 helicopter.

The danger of the occurrence of resonant blade strike also exists in tandem helicopters where opposing blade oscillations may be excited by control-stick oscillations in the fore-and-aft direction.

Particular attention should be devoted to studying the possibility of reducing the dynamic response coefficients of the main-rotor control system.

The dynamic response coefficient for the case of a single abrupt control-stick deflection while maneuvering the helicopter can be determined using routine calculation methods.

If the control system permits one to perform abrupt control-stick deflection all the way to the stop in a time equal to, or even somewhat lower than, the system oscillation period, then the dynamic response coefficient λ_d may be equal to 1.8.

Due to the restricted control stick displacement rate used on the V-12 helicopter, the duration of the impulsive (sinusoidal) control-stick deflection to the stop can not be lower than 1.6 to 1.8 times the system oscillation period. In this case, the dynamic response coefficient is equal to or about 1.4. In the design of twin-rotor helicopters, particular attention should be devoted to increasing the torsional rigidity of the synchronizing transmission.

For the specific examples given in Table 2.7, it is shown that the allowable angle of blade deflection relative to the vertical hinge significantly decreases because of transmission torsional deformations.

HELICOPTER	z_{bl}, number	$\bar{P}$, %	$\Delta\varphi_{c.p}$, deg	$m_{Q_1}-m_{Q_2}$	$n_{m.r}$, rpm	$l_{l.h}$, %	$S_{l.h}$, kg·s^2	c_{tor} kg·m/rad	k_{Q_0}	λ	$\Delta\xi_{t.r}$, rad	$\Delta\xi$, rad	$\Delta\xi_{all}$, rad	$\Delta\xi_{all}-\Delta\xi$, rad	$(m_Q)_{max}$	n_{mQ}
Vertol CH-46A Model 107	3	66.6	∓4	0.02	265	4.6 at $l_{l.h}$ = 0.35 m R = 7.62 m	25	0.03J10^6	0.80	1.8	7.6	20.9	19.6	–1.3	0.0152	2.180
Vertol CH-46D Model 107	3	69.2	∓4	0.02	260	4.5 at $l_{l.h}$ = 0.35 m R = 7.77 m	25	0.03J10^6	0.80	1.8	8.2	23.1	18.6	–4.5	0.0162	2.125
Chinook CH-47A	3	66.4	∓4	0.02	230	8.0 at $l_{l.h}$ = 0.72 m R = 9.01	49	0.06J10^6	0.86	1.8	7.3	14.6	20	5.4	0.0162	2.110
Chinook CH-47C	3	68.3	∓4	0.02	243	7.9 at $l_{l.h}$ = 0.72 m R = 9.135 m	56	0.06J10^6	0.86	1.8	9.4	16.8	19	2.2	0.0202	1.886
Chinook Model 347	4	38.8	∓4	0.02	220	8.5 at $l_{l.h}$ = 0.8 m R = 9.38 m	49	0.055J10^6	0.87	1.8	11.8	19.6	19	–0.6	0.0192	1.935
V-12	5	17.2	∓4	0.02	120	4.8 at $l_{l.h}$ = 0.84 m R = 17.5 m	529	10^6	0.67	1.4	3.7	18.9	17.5	–1.4	0.0168	1.825

TABLE 2.7 DETERMINATION OF BLADE STRIKE MARGINS IN TWIN–ROTOR HELICOPTERS

It is very important to emphasize that the major portion of the main-rotor twist angle is explained by torsional deformations of the components of the main shafts rotating at the same angular velocity as the main rotors. In the V-12 helicopter, this angle amounts to about 60 percent of the overall transmission twist angle; while on the Chinook helicopter (we estimate), it is more than 80 percent. The main rotor twist angle resulting from torsional deformations of the synchronizing shaft proper is relatively small because of the fact that the synchronizing shaft turns at a high rotational speed and its stiffness referred to the main rotor should be multiplied by the square of the gear ratio. Therefore, on the Chinook helicopter; in spite of the fact that the synchronizing shaft is of Duralumin, its stiffness referred to the main rotor is quite high (the shaft speed is $n = 6600\,rpm$, and the gear ratio is $i \approx 29$).

At the same time, the configuration of this helicopter (with very long aft-rotor shaft) leads to a marked reduction in transmission torsional stiffness which should probably cause major difficulties in ensuring the required margin with respect to blade strike. According to our estimates, the angle of opposing rotation of the main rotors as a consequence of transmission deformation in the Chinook helicopter is even larger than the angle-of-blade rotation relative to the lead-lag (vertical) hinges (see Table 2.7).

From a comparison of the possible blade deflection in the plane of rotation $\Delta\xi$, determined using Eq (2.111), and the maximum allowable value based on blade-strike conditions (Fig 2.49), one can evaluate the available margin with respect to blade strike. The results of the evaluation of this margin for various helicopters are summarized in Table 2.7.

The value of $\Delta\xi$ determined from Eq (2.111) depends directly on the one-half difference of the ΔM_Q torques of the lifting rotors. As shown above, the value of ΔM_Q depends on many parameters, but primarily on the actions of the pilot in an unforeseen situation which requires unusually abrupt control inputs.

Considering all of this and desiring to obtain comparable estimates for various helicopters, $m_{Q_1} - m_{Q_2} = 0.02$ was taken as the most likely maximum value for all of the machines listed in Table 2.7; although it is quite possible that for some helicopters, even higher values of the difference in those coefficients can be encountered.

For all of the helicopters, the dynamic response was taken equal to $\lambda_d = 1.8$. For the V-12 helicopters with two-step control systems which limit the maximum possible control-stick movement rate to the small booster piston displacement rate, this coefficient was taken equal to $\lambda_d = 1.4$.

The data presented in this table show that on the CH-46 (Model 107) helicopter, the blade strike margins were right at the acceptable limit, or even somewhat insufficient.

The development of the Chinook helicopter with more than twice the engine power and correspondingly increased main-rotor size with use of the same types of hub and transmission construction as in the CH-46 (Model 107) helicopter would have led to a deficit in the allowable blade deflection angles in the plane of rotation amounting to more than 6°. It is probably for this precise reason that Boeing used a special hub configuration on the Chinook helicopter with the vertical hinge located outside the feathering hinge, thus significantly increasing the offset of the vertical hinges. The Company took this step in spite of the fact that this hub configuration leads, in general, to an increase in the hinge moments. In addition, in order to increase the transmission stiffness, the aft rotor diameter of the vertical shaft was made equal to $d_{sh} = 300\,mm$ for over 70 percent of the shaft length, which is nearly twice the value of $d_{sh} = 160\,mm$ required for power transmission.

As a result, an excess margin with respect to blade strike was created on the Chinook CH-47A helicopter which turned out to be very useful in later modifications of the helicopter in which this margin was utilized.

Of interest is the fact that when changing over to a four-bladed rotor on the Model 347, Boeing did not reduce the blade strike margins, but rather reduced the rotor overlap, which required stretching the fuselage by about three meters.

Comparison of the blade-strike margins on the V-12 helicopter with analogous margins on foreign tandem helicopters shows that the overlap on this helicopter was selected properly, although at the limit of the allowable value. The foregoing analyses, calculations, and data on existing machines show that in selecting the parameters of twin-rotor helicopters with conventional sequencing of hub hinges and rotational speed of the synchronizing shaft, $n_{sh} \leqslant 3000$ *rpm*, one cannot count on the possibility of increasing the overlap to more than $\overline{P} = 0.63$ at $z_{bl} = 3$; $\overline{P} = 0.4$ at $z_{bl} = 4$; and $\overline{P} = 0.17$ at $z_{bl} = 5$.

It should be noted that in order to assure flight safety with such overlaps, special steps should be taken which would guarantee the required blade-strike margins. This would include the following: increase of the vertical hinge offset, achievement of a very rigid-rotor synchronizing transmission, and limitation of the rate and range of control stick travel when varying the differential collective pitch of the rotors.

With number of blades $z_{bl} \geqslant 6$, rotor overlap becomes unacceptable.

2.3.4 Maximum Engine Power Utilizable by the Helicopter Because of Beveled-Gear-Pairs Limitations

Constraints of the power transmitted by bevel gears is important in selecting the parameters and configuration of heavy-lift helicopters. This limitation can be avoided in configurations with vertical free-turbine shafts but, to date, no acceptable design of such a scheme has been realized. Therefore, we shall not examine this scheme.

In accordance with the Gleason technique, we shall determine the torque transmitted by a bevel gear based on allowable tooth bending stresses σ_{bend}, using the formula

$$(M_Q)_{bend} = 5(bYk_v/k_s k_m)\sigma_{bend}\, m\, d_{p.c} \qquad (2.115)$$

and on allowable contact stresses σ_{cont}, using the formula

$$(M_Q)_{cont} = Ik_v b\, \sigma_{cont}^2\, d_{p.c}^2/109.5\, k_m \qquad (2.116)$$

where Y and I are coefficients which depend on the tooth shape. We shall take the following values of the coefficients and allowable stresses in these formulae: $k_m = 1.0$ (coefficient accounting for nonuniform load distribution over the tooth); $k_v = 0.9$ (coefficient accounting for dynamics of meshing); k_s = coefficient depending on the tooth size ($k_s = 0.725$ for $m = 7\ mm$; $k_s = 0.78$ for $m = 10\ mm$; $k_s = 0.89$ for $m = 16\ mm$); $(\sigma_{bend})_{all} = 21\ kg/mm^2$; and $(\sigma_{cont})_{all} = 140\ kg/mm^2$. Then for a gear ratio of $i = 2.5$ selected for examination, and the maximum possible tooth width b, usually no greater than $b = 85\ mm$, and no greater than $b = 0.3A$ (where A = length of the generatrix of the principal gear-cone), we obtain the maximum allowable circumferential load P_{all} as a function of pitch circle diameter $d_{p.c}$ for three values of the tooth modulus m, shown in Fig 2.52.

For a gear peripheral speed of $V_{max} = 100\ m/s$, which normally is the maximum value permitted for such transmissions, we obtain the maximum power which can be transmitted by a bevel stage. This power is shown in the left-side ordinate in Fig 2.52. In this figure, rotational speeds corresponding to this peripheral speed are also indicated.

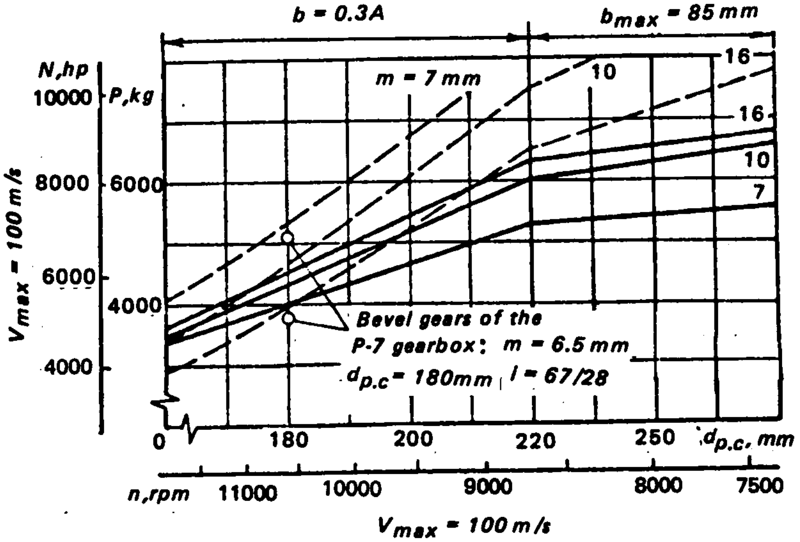

Figure 2.52 Maximum circumferential loads P and maximum permissible power N transmitted by a pair of bevel gears at peripheral speed V_{max} = 100 m/s, depending on the pitch diameter of the smaller gear $d_{p.c}$ at i = 2.5
– – – permissible load from contact stress; ——— permissible load from bending stress

It can also be seen from this figure that for the allowable stress σ_{bend} = 21 kg/mm^2, and peripheral speed V_{max} = 100 m/s, the maximum power which can be transmitted by the bevel gear pair is $N_{bevel} \approx 8000$ hp, with a small bevel gear pitch diameter of $d_{p.c}$ = 220 mm, and the large one of $d_{p.c}$ = 550 mm; i.e., with dimensions which seem acceptable with respect to gearbox layout.

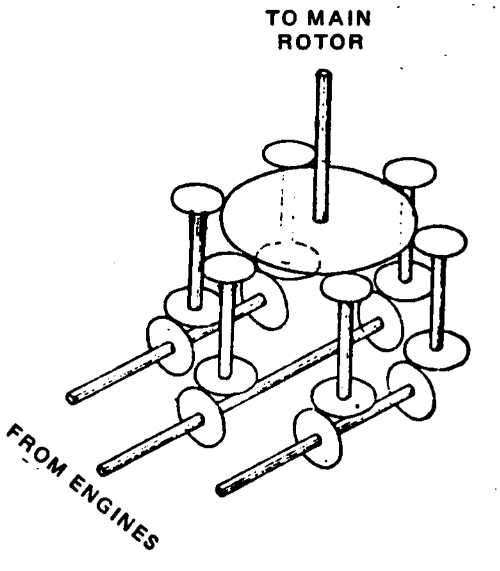

Figure 2.53 Possible scheme of the first step of the main gearbox of a three-engine, single-rotor helicopter

There is no doubt that as a result of new technical advances it will be possible to increase both the allowable gear stresses and maximum rotational speeds. Therefore, these constraints are evaluated only from the viewpoint of today's technology.

We can consider that the Soviet gear industry is ready for the production of bevel gears capable of transmitting up to 5000 hp per pair. If we examine the near future, we can assume that this power will increase to 8000 hp.

Therefore, in examining heavy-lift helicopters we must consider the following.

The single-rotor, heavy-lift helicopter may be a three-engine machine. In this case, it is possible to develop a gearbox with transmission of power from the engines through six bevel gear pairs (Fig 2.53) and consequently, the maximum utilizable engine power can be equal to 48 000 hp.

The tandem-rotor helicopter can have two synchronizing shafts. In this case, the maximum power transmitted to one of the lifting rotors through two bevel gear pairs can be 16 000 hp. Accounting for nonuniformity of rotor loading amounting to 15 percent, the overall usable engine power in the tandem helicopter can not be higher than 28 000 hp.

With the known transmission schemes it appears impossible to transmit power in the tandem helicopter to both main rotors through four bevel gear pairs.

It appears to us that the development of a helicopter with three synchronizing shafts is too complex, less reliable, and therefore, unacceptable.

The side-by-side rotor helicopters can be conceived with four engines, and with the power transmitted to the lifting rotors through eight bevel gear pairs. Therefore, the maximum usable power for such a helicopter can be equal to 64 000 hp, which does not appear to represent a constraint to the helicopter parameters in the immediate future.

Considerable power loading of the bevel gears which drive the synchronizing shaft in the side-by-side helicopter will be encountered for very brief periods only in conjunction with rapid lateral deflections of the control stick as well as in case of engine failure and therefore, will not limit the installed engine power.

2.3.5 Requirements Resulting from Balance Considerations of the Tandem Helicopter

Sometimes it is considered that longitudinal balancing of the tandem-rotor helicopter does not cause any problems. Actually, if the tandem-rotor helicopter is well balanced; i.e., if, at maximum loading, the forward and aft rotors have approximately the same thrust, then small variations of the c.g. location is easily compensated by a small difference in the thrust of the rotors.

However, balancing of the helicopter during design becomes a difficult task. The engines and their systems, two or more gearboxes, aft pylon, and doors with their ramps are located on a long arm below the aft rotor and must be balanced by the cockpit and the helicopter equipment. Therefore, in the layout of the tandem helicopter, it is necessary to try to shift the engines toward the middle of the helicopter as much as possible.

This can be accomplished in such transmission schemes as that of the Chinook helicopter where the engines can be located at any point along the length of the helicopter as may be required for balancing (see Fig 2.17). However, the use of this layout with a long shaft of the aft rotor is possible only for helicopters having a load capacity up to that of the Chinook, but no larger. In helicopters having higher lifting capacity, the use of such a shaft would lead to very high weight penalties.

It is apparently for this reason that Boeing went to a different transmission layout in the HLH helicopter (Fig 2.54); i.e., without the shaft extension of the aft rotor (Fig 2.55).

However, this scheme is suitable only for the crane helicopter. In the transport version of the helicopter with the required cargo-cabin dimensions, the engines and the combining gearbox located at the cargo cabin ceiling level would interfere with loading the helicopter. Thus, resolution of the problem of balancing the tandem helicopter with a lifting capability greater than that of the Chinook involves serious difficulties of a configurational nature.

2.3.6 Constraints Influencing Tandem-Helicopter Transmission Selection

It has been quite clear for a long time that when using shaft turbines, we can not use the tandem-engine arrangement scheme, as was proposed in the original design of the V-12 helicopter shown in Fig 2.56. In this case, the exhaust gases from the forward engines can easily

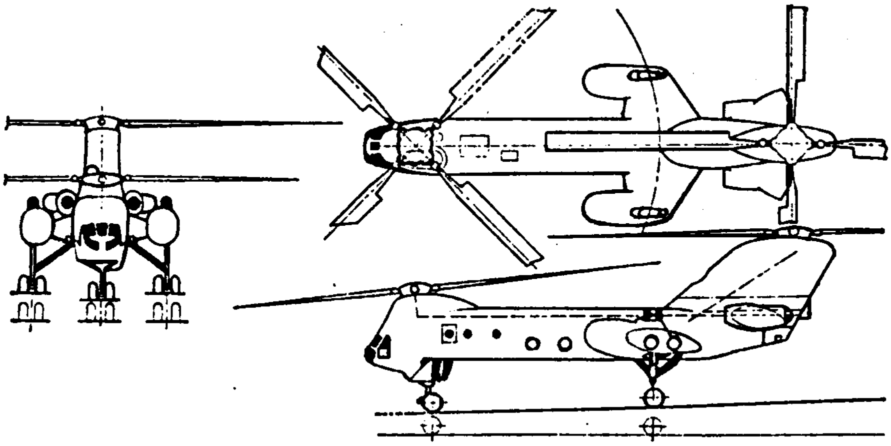

Figure 2.54 Project of the Heavy-Lift Helicopter (HLH) by Boeing[27]

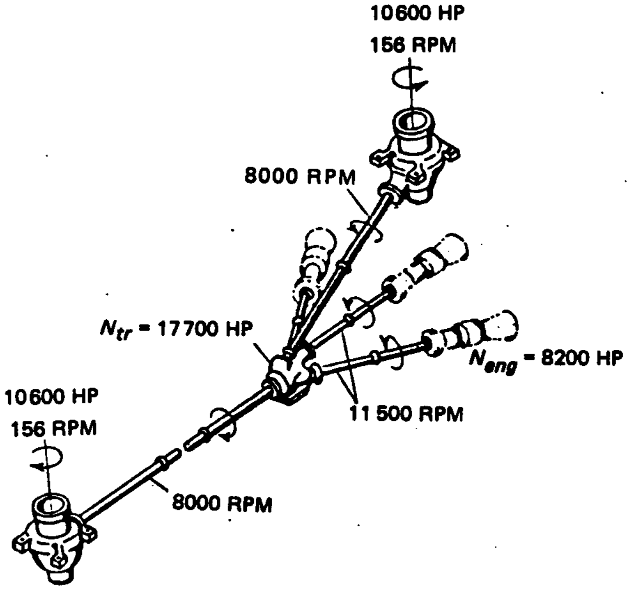
10600 HP
156 RPM
8000 RPM
N_{tr} = 17700 HP
N_{eng} = 8200 HP
10600 HP
156 RPM
11 500 RPM
8000 RPM

Figure 2.55 Scheme of the HLH Transmission[22]

enter the engine intakes located near the aft rotor and cause engine surging, with all the associated unpleasant consequences.

In the tandem-rotor helicopter, all the engines should be located together and preferably, close to the middle of the helicopter.

The transmission scheme with a single synchronizing shaft can be used up to a power of 8000 hp per main rotor, which seems to be the limit for a transmission by a single-bevel gear pair (see Subsection 2.3.4). At higher powers, input to the main gearboxes is possible only by using a two-shaft scheme with angle drive through no less than two bevel gearsets. It follows from this that there must also be two synchronizing shafts, since development of gearboxes which combine the power of two engines and then divide this power at the input to the main gearboxes would lead to weight losses exceeding gains from a single synchronizing shaft.

In the HLH proposal (see Fig 2.55), Boeing intends to transmit 10 600 hp through a single bevel gearset. It seems to us that this may lead to serious difficulties in main gearbox development.

Therefore, the configuration shown in Fig 2.57 with two synchronizing shafts is proposed for tandem-rotor helicopters with heavy-lift capability.

2.3.7 Constraints to Rotational Speed of Transmission Shaft

Increase of transmission shaft rotational speed runs into constraints represented by the maximum permissible circumferential velocity of the inner race of bearings using grease lubrication.

Usually, it is considered that for such bearings, the circumferential speed is

$$U_{inn} \leqslant 16 m/s$$

which is approximately equivalent to the well-known condition

$$n_{sh} \times d_{inn} \leqslant 300000$$

where d_{inn} = bearing inner race diameter in mm; and n_{sh} = shaft rotational speed in rpm.

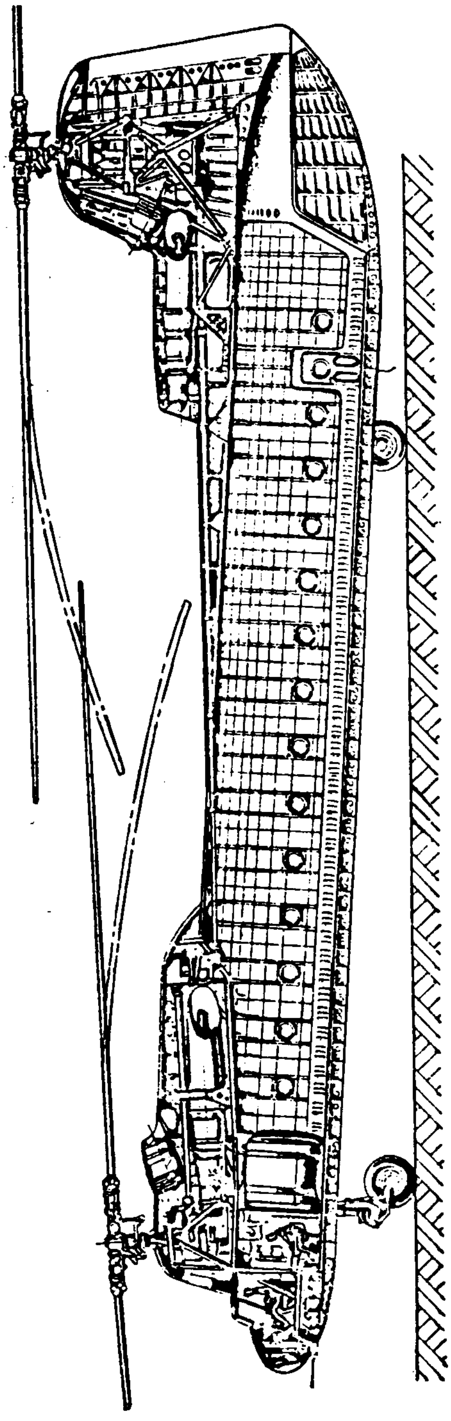

Figure 2.56 An old project of a tandem helicopter with a tandem arrangement of the engines

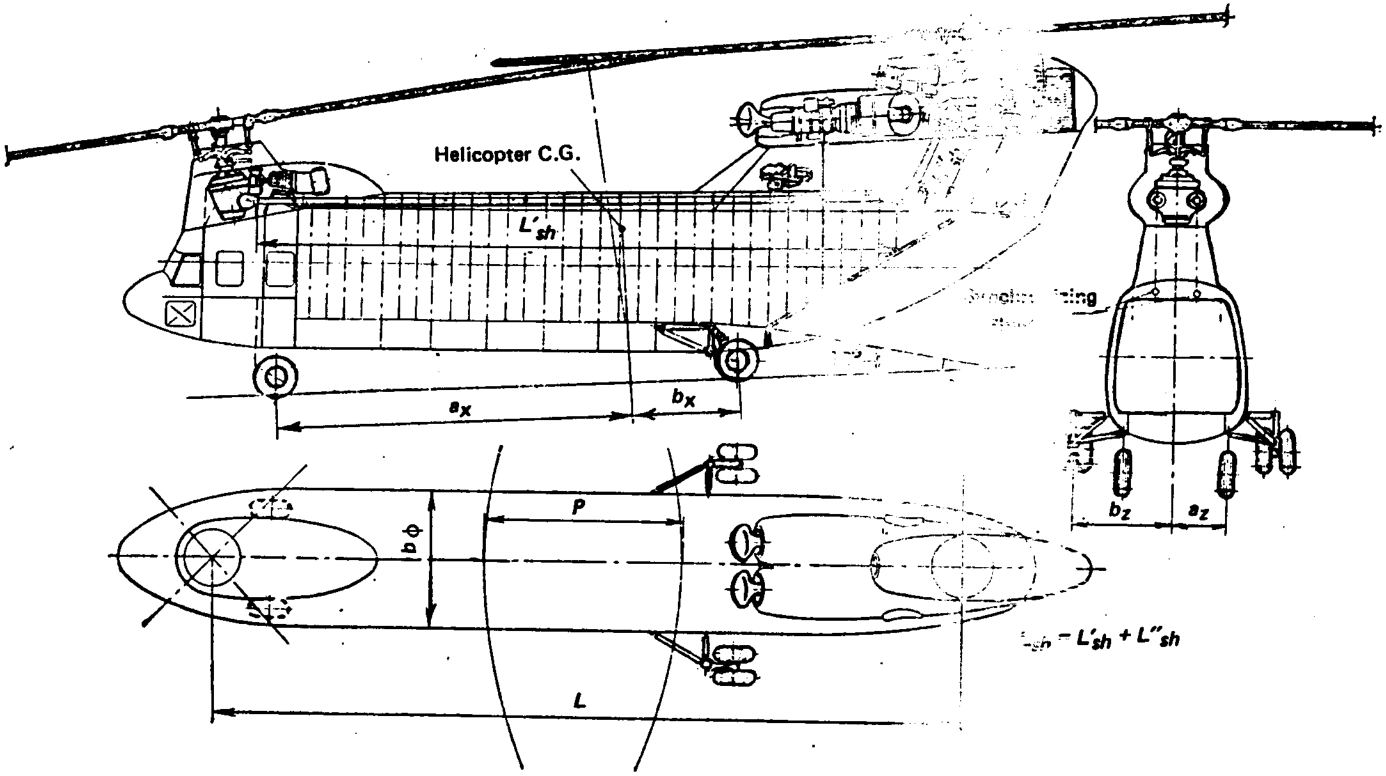
Helicopter C.G.
L'_{sh}
a_x
b_x
Synchronizing shaft
P
ϕq
L
b_z
a_z
$L_{sh} = L'_{sh} + L''_{sh}$

Figure 2.57 Three-view drawing of a tandem helicopter with [illegible]izing shafts

Practical experience shows that exceeding these limitations actually leads to serious difficulties and to reduced bearing operational reliability.

Therefore, with an increase of the circumferential speed U_{inn} above 16 m/s, it is advisable to change over to liquid bearing lubrication. However, the development of liquid lubrication systems for 10 to 12 support bearings increases operational difficulties of such shafts (monitoring oil level, replenishing and changing the oil), and also reduces bearing reliability. In addition, because of the necessity for providing bearing housings (sumps) and possibly, boost pumps, the use of a liquid lubrication system increases the transmission shaft weight which makes questionable the practice of saving weight by increasing shaft speed.

Therefore, in the tail transmissions of both Soviet and foreign single-rotor helicopters, the shaft speed is usually no higher than $n_{sh} = 3000\ rpm$, and grease-lubricated bearings are used.

The rotational speed of the synchronizing shaft on twin-rotor helicopters with rotor overlap is selected on the basis of entirely different considerations. On these helicopters, increase of the rotational speed of synchronizing shafts is necessary in order to increase their torsional stiffness (referred to the main rotor shaft) in order to avoid blade strike.

Therefore, the increased rpm of synchronizing shafts used by Boeing are not so much the result of technical progress, as a forced measure, resulting from the necessity of avoiding rotor-blade serike.

2.3.8 Constraints Based on Blade Static Deflection

With an increase in blade radius, aspect ratio, and weight, blade static deflection due to gravity increases.

If no special measures are taken to improve the helicopter configuration, the blade tip deflection becomes severely limited because of the possibility of the blade striking the helicopter structure. It is obvious that the exact value of the allowable blade tip deflection depends on the specific configuration of the considered helicopter. However, the relative blade tip deflection does not vary markedly from helicopter to helicopter in each helicopter weight class. Most often, the relative deflection is lower for small helicopters and higher for large helicopters. Therefore, the problem of limiting blade tip deflection is particularly serious for large helicopters.

Normally, for configurational reasons, the relative blade tip deflection in such heliccopters should not exceed the value

$$(\bar{y}_R)_{all} = (y_R)_{all}/R = 0.12 \tag{2.117}$$

where $(y_R)_{all}$ = absolute allowable tip droop.

If we assume that the blade section moment of inertia is proportional to the fourth power of the blade chord, then the blade tip droop can be found from the following expression:

$$y_R = k_{y_R} G_{bl} R^3/b^4 \tag{2.118}$$

where the coefficient of proportionality k_{y_R} characterizing the efficiency of blade design with respect to the achieved reduction of blade droop, depends on the blade construction, including both the spar material and the distribution of the moment of inertia and running weight along the blade length. The values of this coefficient for several production blades are shown in Fig 2.58. This same figure shows the achieved values of $(k_{y_R})_{min}$ for two blade construction types.

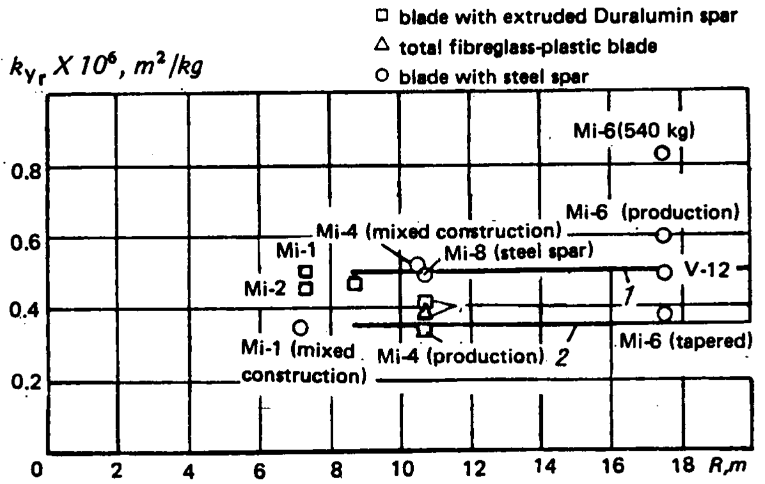

Figure 2.58 Values of the k_{y_R} coefficient characterizing the magnitude of tip deflection under the blade's own weight. 1 – $(k_{y_R})_{min}$ for blades with steel spars 2 – $(k_{y_R})_{min}$ for blades with extruded Duralumin spars

If we assume that the blade weight can be determined from the following formula for $\lambda < \lambda_o$ (see Eq (2.6)):

$$G_{bl} = q^*_{bl} b^{1.7} R \tag{2.119}$$

then, substiutting this value of the blade weight into Eq (2.118), we obtain the expression for the relative blade tip deflection

$$\bar{y}_R = k^*_{y_R} R^3/b^{2.3} \tag{2.120}$$

where, with account for Eq (2.14),

$$k^*_{y_R} = k_{y_R} q^*_{bl} = 2.41\, k^*_{bl} k_{y_R}\,. \tag{2.121}$$

If we assume that

$$\bar{y}_R = (\bar{y}_R)_{all}, \tag{2.122}$$

we can obtain the maximum allowable blade radius R_y from Eq (2.120). Substituting the blade chord from Eq (2.165) into Eq (2.120), we obtain the value of R_y for a given helicopter gross weight G_{gr}, and thrust coefficient, t_{y_o}:

$$R_y = 0.0585[(\bar{y}_R)_{all}/k_{y_R} k^*_{bl}]^{0.189}\,[G_{gr}/\bar{t} z_{bl_\Sigma}]^{0.435}\,. \tag{2.123}$$

The dependence of R_y on the parameters appearing in this formula is shown in Fig 2.59, and the values of the allowable blade aspect ratios λ_y equal to $\lambda_y = (\bar{y}_R/k^*_{y_R})^{0.435} \times (1/R_o^{0.304})$ are shown in Fig 3.14. When designing helicopters of all configurations, this constraint must be considered and the main rotor radius must not be greater than R_y. This condition usually becomes the governing factor in selecting the main rotor radius for heavy-lift helicopters, while for light helicopters it is satisfied without any particular effort.

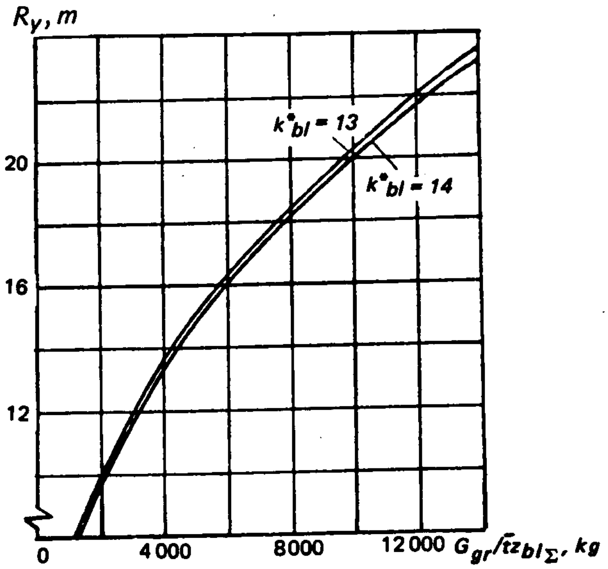

Figure 2.59 Maximum allowable blade radii resulting from droop condition

2.4 Determination of Data Required for Calculating Structural Weight, and Selection of Helicopter Parameters

When determining the structural weight and payload, it is convenient to make these calculations with variation of the various helicopter parameters while keeping the gross weight constant. Upon completion of the calculations made for different gross weights we can select the one which satisfies the specified helicopter performance.

The most important variable parameters are the main rotor diameter and number of blades. The calculations which follow will be devoted to this problem. It would appear that no less important is the determination of the optimal rotor tip speed U_t and thrust coefficient t_{y_0}. However, experience in helicopter design and testing shows that although increasing the rotor tip speed above $U_t = 220\,m/s$ yields a gain in structural weight, it also leads to power losses in level flight and increases the required fuel supply which, in the final analysis, is unfavorable because of the reduction in transportable payload. In addition, this leads to a significant increase in the external noise of the helicopter. Consequently, the optimal value of U_t, coinciding with its maximum acceptable value, is already known from helicopter test experience and can not be substantially improved by further calculations.

Nor is it possible to increase the main rotor thrust coefficient. Its value for blades with the best available airfoil sections is limited by the service ceiling and maximum flight speed as shown in Fig 2.46. Increase of t_{y_0} above the values determined by the stall constraints can not be justified.

Therefore, the optimal value of t_{y_0} coincides with the limiting allowable value of this parameter required to ensure the specified flight performance.

We shall examine in more detail the entire sequence of operations required for determining the values which are necessary for helicopter weight calculation and parameter selection.

Since this requires knowledge of many quantities which are computed in the aerodynamic analysis, we shall examine those aspects for single-rotor, tandem, and side-by-side helicopter configurations.

2.4.1 Selection of Wing Area for Side-by-Side Helicopters

In determining helicopter lift in hover, it is important to know the losses associated with main-rotor downwash flow over the helicopter airframe. In comparison with other configurations, the side-by-side helicopter experiences the largest losses from flow over the wing. Therefore, when designing the side-by-side rotor helicopter, it is necessary to reduce the wing area as much as possible. In the scheme with a cantilevered wing, this is limited by the stiffness requirements which were mentioned in Sect 2.2.

If we use a wing with a trailing-edge flap which can be deflected in hover, and reduce the wing area exposed to the downwash by about 20 percent, then the optimal wing with respect to the overall helicopter lift loss of $(\Delta T + G_{wg})$ in hover will be the wing with relative area $(\bar{S}_{wg})_{opt}$ determined from Eq (2.81) where the value of c_{wg} for the wing with trailing-edge flaps deflected 90° can be taken as

$$c_{wg} \approx 0.70 \ldots 0.75. \qquad (2.124)$$

When performing the computation using Eq (2.81), the nacelle relative weight must be assumed in the first approximation, and then refined after determining the outrigger weight from Eq (2.76).

For a V-12-type helicopter of the side-by-side rotor configuration with truss-type outriggers (see Fig 2.38), the area of the inverse taper of the wing can be defined as

$$S_{wg} = \alpha \ell b_{wg.s} \qquad (2.125)$$

where ℓ = length of the truss-type outrigger; and $b_{wg.s}$ = distance between the struts at the wing tip (see Eq (2.90)).

The basis for selection of the α coefficient can be provided by the V-12 helicopter where $\alpha = 1.7$.

2.4.2 Determination of Thrust Loss Due to Downwash Over the Airframe in Hover

In calculating the thrust loss due to downwash flow over the helicopter airframe, we normally use the formulas derived from the ideal rotor theory, but with coefficients which have been refined through experiments on models and in flight tests of existing helicopters. When using this approach, the downwash losses can be determined as follows:

a) for the single-rotor helicopter without wing

$$k_{dw} = 1 - \Delta\bar{T}_o (R_o/R)^2 \qquad (2.126)$$

where $\Delta\bar{T}_o$ = thrust loss due to downwash flow over the fuselage for a lifting-rotor with radius R_o. The value of $\Delta\bar{T}_o$ is best determined from model tests. It usually amounts fo 0.015 to 0.020 and sometimes even reaches a value of 0.03;

b) for the tandem-rotor helicopter without a wing,

$$k_{dw} = 1 - 0.34\bar{S}_{\phi}^{*}[1 + (\bar{P}/\bar{L}_{\phi})(2f - 1)] \qquad (2.127)$$

where

$$\bar{S}_{\phi}^{*} = S_{\phi}^{*}/2\pi R^2, \qquad (2.128$$

S_ϕ^* = fuselage plan-view area exposed to downwash flow from the main rotor; $\bar{P}$ and $\bar{L}_\phi$ respectively, are rotor overlap and helicopter fuselage length referred to the main rotor radius; $2f$ = ratio of the average area loading in the overlap zone to the average disc loading of isolated rotors. The approximate values of this parameter will be indicated in Subsection 2.4.7;

c) for the side-by-side rotor helicopter,

$$k_{dw} = 1 - \Delta\bar{T}_{wg} - \Delta\bar{T}_\phi . \qquad (2.129)$$

The thrust loss due to downwash flow over the wing can be determined as

$$\Delta\bar{T}_{wg} = c_{wg}\bar{S}_{wg} \qquad (2.130)$$

where $\bar{S}_{wg} = S_{wg}/2\pi R^2$.

The value of the coefficient c_{wg} can be taken equal to 0.9 for the rectangular wing, and 0.7 for the V-12 helicopter wing with inverse taper.

If we only examine rotors with overlap $\bar{P} \leqslant \bar{b}_\phi$ where $\bar{b}_\phi = b_\phi/R$, then the thrust loss due to downwash flow over the fuselage for side-by-side rotor helicopters can be found from the formula

$$\Delta\bar{T}_\phi = 0.34(2f\bar{S}_{ov} + \bar{S}_{dw}) \qquad (2.131)$$

where $\bar{S}_{ov} = S_{ov}/2\pi R^2$; $\bar{S}_{dw} = S_{dw}/2\pi R^2$,

while S_{ov} and S_{dw} respectively, are the rotor overalpped area and the helicopter fuselage area outside the overlap region that is exposed to the downwash.

The fuselage and wing drag coefficients in these formulae were taken from Ref 4.

2.4.3 Rotor Solidity Determination

The required rotor solidity is calculated from the formula

$$t_{y_0} = 2G_{gr}/\rho z_{rot}\,\sigma F_{m.r} U_t^2 \qquad (2.132)$$

where the value of U_t is determined on the basis of existing experience with account for the arguments stated at the beginning of this section, and t_{y_0} is taken in accordance with Subsection 2.2.2.

For known solidity σ and given R and z_{bl}, we can determine the blade chord.

2.4.4 Main-Rotor Thrust Increase Ejector Effect of the Engine Exhaust Flow

The stream of gas exhausted from engines centrally located under the main rotors and directed downward has an ejector effect on the air flow in the main-rotor hub region, and may increase the main-rotor thrust. This effect is most probable in the side-by-side helicopter with engines located beneath the main rotors, and where exhaust gases are directed downward for configurational reasons.

It is very difficult to obtain an exact experimental value of the thrust augmentation from this effect. However, when comparing helicopters of different configurations, it is advisable to take this effect into account for the side-by-side rotor helicopter with the engine exhaust directed downward.

According to our estimates, the main-rotor thrust may increase by 2 to 4 percent because of this effect. Therefore, in comparative calculations, it is suggested that this thrust augmentation be taken into consideration by introducing the special coefficient k_T.

2.4.5 Accounting for Engine-Lift Force

For helicopters in which the engine exhaust is directed downward at some angle α to the vertical, we introduce a coefficient accounting for the engine lift force

$$k_{eng} = 1 - T_{eng}/G_{gr} = 1 - \bar{T}_{eng}(N_h/G_{gr}), \tag{2.133}$$

where T_{eng} = engine lift force; and $\bar{T}_{eng}$ = engine lift force referred to engine power.

The engine lift force can be found from the following formula:

$$T_{eng} = (V_{exh}/g\bar{N})(N_h/G_{gr})\cos\alpha \tag{2.134}$$

where V_{exh} = exhaust velocity of gas discharged from the engine nozzle ($V_{exh} \approx 150\ m/s$); $\bar{N}$ = engine power obtained with air flow rate equal to 1 kg/s (for modern engines, one can take $\bar{N} \approx 260\ hp/kg/s$). N_h = power required at hovering ceiling; α = angle between the exhaust direction of the engine and the vertical (for the V-12 helicopter, $\alpha = 45°$).

For the cited parameters, the engine lift force referred to engine power is $\bar{T}_{eng} = 0.0415$, and the coefficient k_{eng} can be equal to about 0.98.

2.4.6 Determination of Main Rotor Efficiency (F.M. – Figure-of-Merit)

On the basis of the aerodynamic calculations for the selected U_t, blade planform, geometric twist, and selected airfoil sections, we determine the isolated rotor efficiency η at the helicopter hover ceiling for

$$t_y = t_{y_0} k_{eng}/k_{dw} k_T \Delta.$$

On the basis of such calculations for rotors having solidity $\sigma_o = 0.127$ and rectangular planform blades with about 6° twist and with the Soviet helicopter airfoil sections, $U_t = 220\ m/s$; and the thrust coefficients normally used in the range of $t_y = 0.15$ to 0.22, the following approximate formula for determining the Figure-of-Merit as a function of the thrust coefficient t_y can be proposed:

$$\eta_o = \eta_o^* - 0.3(t_y - 0.185)$$

where the achievable value of η_o^* at $t_y = 0.185$ can be within the range of 0.69 to 0.72, depending on fabrication quality and aerodynamic characteristics of the selected airfoil sections.

From the same calculations, we can determine the dependence of η on rotor solidity. However, with an adequate degree of accuracy, we can take

$$\eta = 1/[I + (1 - I\eta_o)\sqrt{\sigma_o/\sigma}/\eta_o] \tag{2.135}$$

where the value of η_o is determined for the solidity σ_o, and I = coefficient of the actual induced power in comparison with the ideal induced power. For rectangular blades having a twist of 6° to 9°, we can consider that $I \approx 1.06$ to 1.10. With an increase in the twist, the value of I decreases, while with a reduction of the twist, it increases.

The F.M. curve (η) vs rotor solidity (σ), as calculated from Eq (2.135) at $t_y = 0.185$, is shown in comparison with model test results in Fig 2.60.

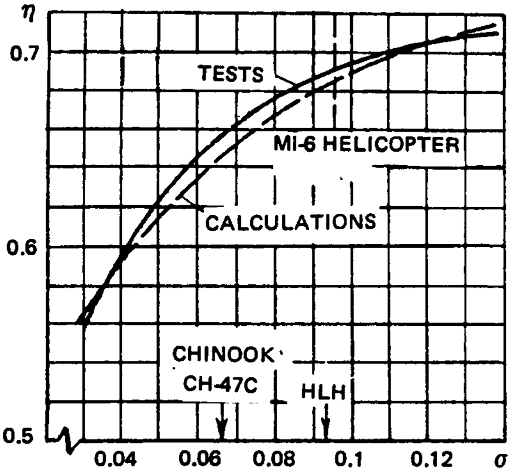

Figure 2.60 Comparison of experimental results with those computed from Eq (2.135) for rotor F.M. vs solidity ratio at $t_y = 0.185$

2.4.7 Rotor Overlap Losses in Hover

For the twin-rotor helicopters with rotor overlap, the losses due to overlap can be found from the formula

$$\xi_{ov} = 1/[1 + \eta m(\sqrt{2} f^{3/2} - 1)] \tag{2.136}$$

where

$$m = S_{ov}/\pi R^2.$$

(for the limiting overlap values of $\bar{P} = 0.63$, 0.4, and 0.17 indicated in Sect 2.3, the values of m are 0.202, 0.105, and 0.03 respectively); f = ratio of average isolated rotor disc loading over the overlap area, to the average disc loading over the entire isolated main-rotor area.

The magnitude of the parameter f depends on the character of the load distribution and the induced velocities along the blade radius.

For uniform disc loading and induced velocity distribution, $f = 1$.

For distribution of the induced velocities along the main-rotor radius following the law that $v_i = \alpha\sqrt{r}$, the parameter f can be found from the approximate formula

$$f \approx 3/2(1 - 0.375\bar{P}).$$

If we take a linear combination of these two laws for which

$$f = 1.1 - 0.1125\bar{P}, \tag{2.137}$$

then the value of ξ_{ov} obtained from Eq (2.136) will agree well with the experimental data.

The values of $k_{ov} = (\xi_{ov})^{2/3}$ calculated from Eq (2.136), taking into account Eq (2.137) and the corresponding experimental values obtained on models, are shown in Fig 2.61.

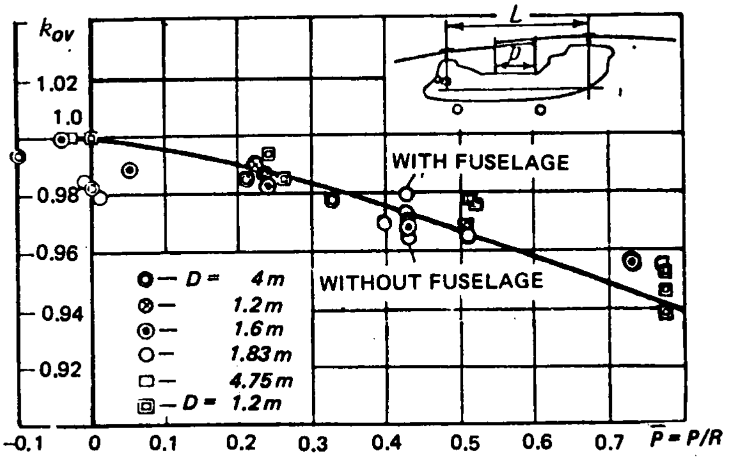

Figure 2.61 Dependence of the thrust loss coefficient k_{ov} on overlap values $\bar{P}$ computed from Eq (2.136), and corresponding values of that coefficient obtained from various model tests

2.4.8 Determination of Torque and Power Transmitted to Main Rotors in Hover

For known coefficients η, ξ_{ov}, k_{dw}, k_{eng}, and k_T, the average torque on one lifting rotor required for helicopter hovering at the static ceiling H_h can be found from the formula

$$(M_Q)_{av} = 1.13(G_{gr}k_{eng}/z_{rot}k_{dw}k_T)^{3/2}/\xi_{ov}\eta U_t\sqrt{\Delta}. \qquad (2.138)$$

The torque $(M_Q)_{m.r}$ of the main rotor for the single-rotor helicopter can be determined from this formula by taking $z_{rot} = 1$.

The horsepower required by all rotors will be

$$\Sigma N_{m.r} = z_{rot}(M_Q)_{av}U_t/75R. \qquad (2.139)$$

Substituting Eq (2.138) into Eq (2.139), we obtain

$$\Sigma N_{m.r} = (G_{gr}k_{eng}/k_{dw}k_T)^{3/2}/66.5\sqrt{z_{rot}}\,\xi_{ov}\eta R\sqrt{\Delta}. \qquad (2.140)$$

2.4.9 Torque and Power Required by the Tail Rotor

For the single-rotor helicopter, the above-listed operations must also be performed for the tail rotor.

In the final stage of the calculation, the optimal tail-rotor diameter must be selected (see Subsection 2.5.6). However, considering that the tail-rotor weight cannot markedly influence the overall helicopter structural weight, the tail-rotor disc loading $P_{t.r}$ can be specified a priori and its parameters (not necessarily optimal) determined.

The tail rotor radius can be found from the equation

$$R_{t.r}^3 + (R_{m.r} + \delta)R_{t.r}^2 - [(M_Q)_{m.r}/\pi P_{t.r}] = 0 \qquad (2.141)$$

where δ = clearance between the main and tail rotors. Usually, this clearance is taken as $\delta \geqslant 0.25\,m$ in order to provide some margin in case the main and tail-rotor diameters vary.

The tail rotor solidity is selected with consideration for the possibility of performing required helicopter maneuvers; especially, hovering turns near the ground.

Experience indicates that in order to satisfy these requirements, the tail-rotor thrust coefficient in hovering out-of-ground effect at normal gross weight and altitude $H = 0$ should be no higher than $(t_{t.r})_o$ = 0.15 for helicopters having engines that were not designed for operating at high altitudes. When the critical altitude for the engine is 1500 to 2000 m, the value of this coefficient should not exceed $(t_{t.r})_o = 0.14$.

The tail-rotor F.M. at the hovering ceiling for the selected blade shape and defined solidity σ_o is determined either on the basis of aerodynamic calculations or from tests on a prototype rotor. With a change in solidity, the F.M. can be calculated from Eq (2.135), just as for the main rotor.

The tail-rotor thrust losses due to flow over the helicopter fin can be determined as

$$k_{dw_{t.r}} = 1 - c_{fin}\bar{S}_{fin} \tag{2.142}$$

where

$$\bar{S}_{fin} = S_{fin}/\pi R_{t.r}^2 . \tag{2.143}$$

Here, S_{fin} = fin surface area blocking the tail rotor. The value of the coefficient c_{fin} for the usual relative location of the pusher tail rotor and fin section can be taken equal to 0.32.

With variation of the tail-rotor diameter, the area blocked by the fin can be defined as

$$S_{fin} = S_{fin_o} + b_{fin}\Delta R_{t.r} . \tag{2.144}$$

Here, S_{fin_o} = initial tail rotor area blocked by the fin; b_{fin} = fin chord in the tail-rotor blade-tip region; $\Delta R_{t.r}$ = variation of the tail-rotor radius $\Delta R_{t.r} = R_{t.r} - (R_{t.r})_o$, where $(R_{t.r})_o$ is the initial tail-rotor radius.

The tail-rotor torque and power required can be found from the formulae

$$(M_Q)_{t.r} = 1.13[(M_Q)_{m.r}/L_{t.r}k_{dw_{t.r}}]^{3/2} k_{t.r}/\eta_{t.r}(U_t)_{t.r}\sqrt{\Delta} \tag{2.145}$$

and

$$N_{t.r} = (M_Q)_{t.r}(U_t)_{t.r}/75R_{t.r} , \tag{2.146}$$

where

$$L_{t.r} = R_{m.r} + R_{t.r} + \delta \tag{2.147}$$

and the coefficient $k_{t.r}$ takes into account the tail-rotor power-required increase because of the influence of the main rotor. It is very difficult to obtain the exact values of this coefficient; therefore, in some calculations, it is taken conservatively as $k_{t.r} = 1.1$.

2.4.10 Engine Power and Power Utilization Coefficient

The engine power required at the input to the single-rotor helicopter main gearbox or the power transmitted by the twin-rotor helicopter transmission in hovering at $H = H_h$ can be defined as

$$N_h = (z_{rot}N_{m.r}/\xi_{m.r}) + (N_{t.r}/\xi_{t.r}) + N_{acc} + z_{prop}(N_{prop})_h \tag{2.148}$$

where $\xi_{m.r}$ and $\xi_{t.r}$ are the coefficients of power loss in the main and tail rotor drives (it is usually considered that the losses are equal to 1 percent of the power in each reduction stage); N_{acc} = power required to drive all the other accessories, $(N_{prop})_h$ = power expended in the hover regime to drive the propeller—if there is one on the helicopter; z_{rot} and z_{prop} = the number of lifting rotors and propellers.

Hence, the coefficient $\xi = N_{m.r}/N_{eng.inst}$ of power utilization by the helicopter main rotors can be obtained as

$$\xi = 1/[(1/\xi_{m.r}) + (\overline{N}_{t.r}/\xi_{t.r}) + \overline{N}_{acc} + (\overline{N}_{prop})_h] \qquad (2.149)$$

where $\overline{N}_{t.r} = N_{t.r}/N_{m.r}$; $\overline{N}_{acc} = N_{acc}/N_{m.r}$; $(\overline{N}_{prop})_h = z_{prop}(N_{prop})_h/N_{m.r}$.

For single-rotor helicopters, usually, $\xi_{m.r} = 0.96$; $\xi_{t.r} = 0.94$; and $\overline{N}_{acc} = 0.01$ to 0.015 for medium helicopters; while for light helicopters, $\overline{N}_{acc} = 0.015$ to 0.025.

The power going to the tail rotor in cruise flight depends on the degree of unloading of the rotor by the fin. For modern fin shapes, it may be assumed that $(N_{t.r})_{cr} \approx 0.3(N_{t.r})_h$.

The power transmitted in level flight to the propeller is usually determined separately, and the power utilization coefficient ξ, in this case, is determined from the same Eq (2.149) in which $\overline{N}_{prop} = 0$ is taken.

For the tandem and side-by-side helicopters with a number of speed reduction stages $(n_{st})_{tan} = 5$ (on the average), and $(n_{st})_{s.b.s} = 4$; we take $\overline{N}_{t.r} = 0$, $(\xi_{m.r})_{tan} = 0.95$, and $(\xi_{m.r})_{s.b.s} = 0.96$ for both hover and cruise.

For known values of ξ, one can determine the helicopter engine power required at the hovering ceiling

$$N_h = (\Sigma N_{m.r})/\xi. \qquad (2.150)$$

2.4.11 Determination of Maximum Rated Engine Power Required for All Specified Helicopter Flight Regimes

For determination of powerplant weight, it is important to determine the maximum rated power required to meet all the specified helicopter flight characteristics.

As was previously mentioned, it is convenient to evaluate the powerplant weight by referring it to the rated power at $H = 500\,m$, and not at $H = 0$ as is usually done.

It is well known that the maximum rated power can be determined by three specific helicopter operating regimes. These are: hovering at the static ceiling H_h at a given temperature, flight at the service ceiling H_s, at which $V_y = 0.5\,m/s$, and at the maximum speed of flight.

In addition, the one-engine-out condition where the other engines operate at contingency power may be the governing factor in selecting the installed rated engine power. Included here are both level flight with one engine inoperative, and continued takeoff. The flight altitude up to which the definite helicopter flight performance should be met after failure of one engine may also be specified as a design requirement. But since such a requirement is seldom used in practice, it will not be considered here.

For the modern general-purpose helicopters, the quantities listed above are usually specified as follows: hover ceiling $H_h = 1000$ to $1500\,m$ (in certain cases, at ambient temperature $t = t_{std} + 10°$); service ceiling $H = 4500$ to $5000\,m$; and maximum speed $V_{max} = 250$ to $300\,km/h$ at the altitude $H = 500\,m$ and, in special cases, even higher.

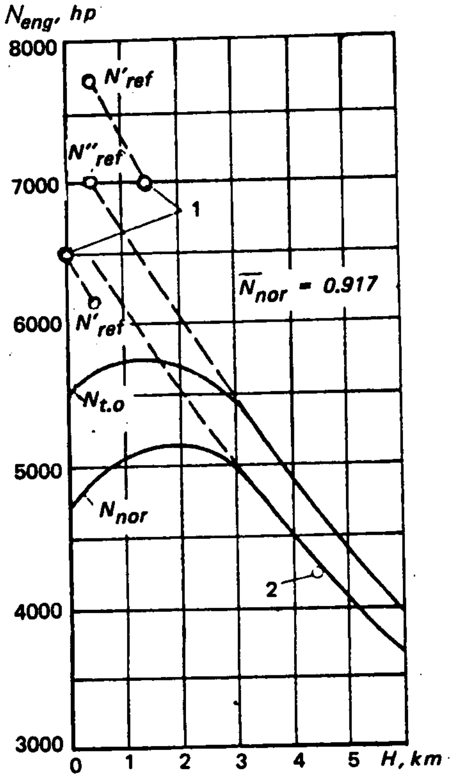

Figure 2.62 Power variation with altitude of the Mi-6 helicopter engines and values of referred rated power. (1) power required in hover; (2) power required for flight at $H = 4500 m$.

It is important to specify the flight duration at the service ceiling. If the required duration is an hour or more, as is usually the case, flight at the service ceiling should be conducted at maximum continuous (normal rated), rather than at takeoff, power.

All Soviet single-rotor helicopters perform flight at the prescribed service ceiling using only normal rated power.

Depending on the helicopter configuration and parameters as well as the specified takeoff performance, the rated installed engine power is defined by different flight regimes.

For the single-rotor helicopter the rated installed engine power is most often determined by the requirement for flight at the service ceiling at normal rating, although in the case of more severe requirements for time spent in hover, this regime may become the determining factor for the magnitude of power installed.

Figure 2.62 shows the altitude characteristic of the powerplant for the Mi-6 helicopter. Even if the helicopter were required to hover out-of-ground effect at $H = 0$ (usually the Mi-6 helicopter takes off with use of the ground effect), the referred rated installed engine power would still be determined by flight at the service ceiling ($N''_{ref} = 2 \times 7000$ hp). Only with the requirement for hovering out-of-ground effect at $H_h = 1500$ m would the referred rated installed engine power be determined by the hover regime.

With an increase of the disc loading to $p = 60\ kg/m^2$ for the single-rotor helicopter without a wing, the referred rated installed engine power will be determined by flight at the service ceiling and the required hover ceiling of $H_h = 1500 m$ (Fig 2.63).

We see from this figure that for the same values of hover and service ceilings, the critical altitude of the tandem-rotor helicopter engines must be significantly higher than for the single-rotor helicopter. In the examined case, the critical altitudes are $H_{s.r} = 2000\ m$ and $H_{tan} = 4300\ m$; i.e., the engine critical altitude for the tandem-rotor helicopter must be nearly the same as the required service ceiling.

If the thrust losses due to flow around the airframe in the hover regime amount to more than 7 to 10 percent as may be the case for the side-by-side helicopter with the rotors mounted on the wing, the referred rated installed engine power will most likely be determined by the hover regime. In the case of a specified maximum speed of more than 280 km/hr for the truss-type side-by-side rotor helicopter, and more than 320 to 340 km/hr for helicopters of other configurations, the high-speed regime may become a determining factor for selection of the referred rated installed engine power.

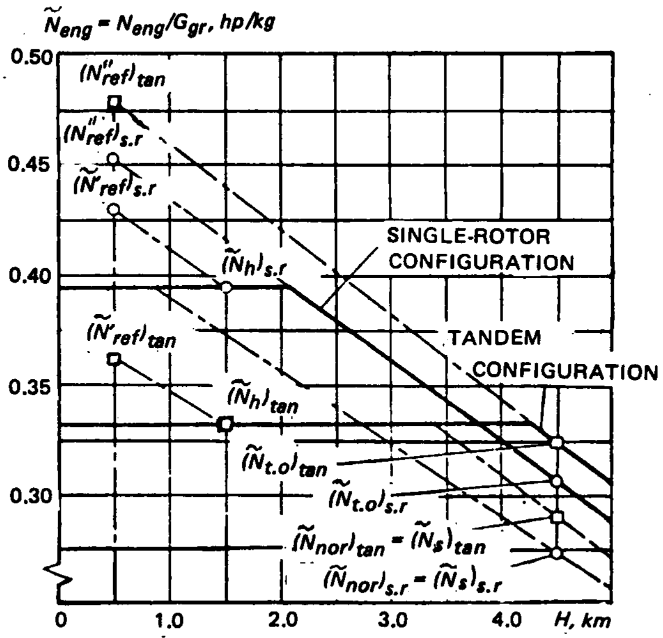

Figure 2.63 Required altitude characteristics of powerplant installation for single-rotor helicopters ($p = 60\ kg/m^2$) and tandems ($p = 42.5\ kg/m^2$) shown as power per kg of gross weight

In weight calculations, we must consider a powerplant that provides the necessary power required in all specified helicopter flight regimes. To this end, the power required at hover and service ceilings should be referred to the height $H = 500\ m$; i.e.,

$$N'_{ref} = A_h N_h;\ N''_{ref} = A_s\ N_s\ / \bar{N}_{nor} \qquad (2.151)$$

where N_h = engine power at the hover ceiling as determined from Eq (2.150); N_s = power required for flight at the optimal speed with the rate of climb at $V_y = 0.5\ m/s$, and at the specified service ceiling H_s; $\bar{N}_{nor}$ = ratio of engine normal-rated (maximum continuous) power to takeoff power. For altitudes higher than 3000 to 4000 m, this ratio is usually 0.89 to 0.92; A_h and A_s respectively, are coefficients obtained from the engine altitude characteristics. For $H_h = 1500\ m$ and $H_s = 4500\ m$, these coefficients can be taken as follows: $A_h \approx 1.1$, and $A_s \approx 1.5$. One also determines the power required for flight at maximum speed at the altitude $H = 500\ m$. In selecting the engine and calculating the powerplant weight, we take the highest referred rated power required for these three regimes. If the installed engine power required for flight at maximum speed is higher than N'_{ref} and N''_{ref}, then it is advisable to analyze whether or not incrasing the installed engine power in order to obtain the required speed is justified. It may be better to reduce this speed and obtain a less expensive aircraft.

2.4.12 Dimensions of Transport Helicopter Cargo Compartment

In addition to the transportable cargo weight, each transport helicopter weight category is defined by the dimensions of the cargo compartment. The fuselage dimensions and weight depend on the cargo compartment size. Therefore, when making the weight analysis, we must determine the standard dimensions of the cargo compartment.

Figure 2.64 shows transverse and longitudinal sections of cargo cabins of various types of helicopters. In Fig 2.64, we identify the standard cargo-cabin sizes by capital letters with corresponding subscripts.

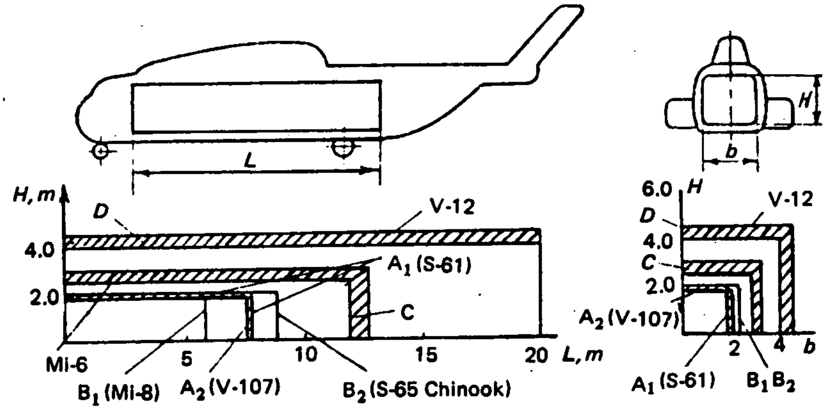

Figure 2.64 Typical dimensions of helicopter cargo compartments

2.4.13 Helicopter Preliminary Layout

Before making the weight analysis, we must make a very preliminary general layout of the helicopter, taking into account the required dimensions of the cargo compartment in order to determine from this layout the basic design data for the helicopter and its fuselage, as well as the powerplant and transmission configuration. One example is the three-view shown in Fig 2.57. It is necessary to determine from this layout the fuselage outer surface (wetted area) $(S_\phi)_o$; the plan projected area S_ϕ^* of the main fuselage section in order to determine the download losses due to rotor downwash; the length L_{sh} of the shafts; the dimensions ℓ and H in the truss outriggers of the side-by-side rotor; the moment of inertia I_{nac} of the side-by-side rotor helicopter nacelles; and so on.

When changing the rotor diameters, in certain cases it is not always necessary to redo the layout. It is possible to scale the basic dimensions using approximate formulae which, for tandem and single-rotor helicopters, can be as follows:

$$S_\phi = (S_\phi)_o + \Delta L S_\pi, \tag{2.152}$$

$$S_\phi^* = (S^*)_o + \Delta L b_\phi, \tag{2.153}$$

and

$$L_{sh} = (L_{sh})_o + \Delta L \tag{2.154}$$

where ΔL = change in the distance between the rotor axes; S_π = fuselage perimeter for the tandem-rotor helicopter and some equivalent perimeter of the tail boom for the single-rotor helicopter.

When the main-rotor diameter is reduced, it is necessary to examine whether the cargo compartment would still have the required length.

For the side-by-side rotor helicopter, we can consider that the fuselage dimensions remain unchanged as the rotor diameter is changed, while the length of the synchronizing shaft must be determined from Eq (2.154).

2.4.14 Parasite Drag of Nonlifting Helicopter Components

It is necessary to make an element-by-element calculation of the parasite drag of all the nonlifting components of the helicopter and determine its equivalent flat-plate area.

When changing the main-rotor diameter of the single-rotor and tandem helicopters, we must take into account the change of the parasite drag of the rotor hubs whose drag-reference area is usually proportional to the blade centrifugal force. For side-by-side rotor helicopters, we must also consider the change of drag of the rotor support outriggers.

If we assume that all the geometric dimensions of the components of the side-by-side trussed configuration vary similarly, the equivalent flat-plate area can be found from the following formula

$$c_x S = (c_x S)_o + 0.023 G_{truss}/\ell \qquad (2.155)$$

where the numerical coefficient is taken on the basis of wind-tunnel tests of a model of the V-12 helicopter.

This coefficient can be significantly reduced by installing fairings on the truss members, but studies have shown that the fairings increase the truss weight by 15 to 20 percent. Therefore, it was decided not to install such fairings.

2.4.15 Variation of Main-Rotor Rotational Speed Depending on Flight Regime

In order to increase the helicopter flight range at cruise speed, it is advisable to somewhat reduce the rotor rotational speed. By contrast, at maximum speed and with an increase in the flight altitude, it is better to somewhat increase the rpm in order to delay blade stall. However, existing helicopter engines do not usually permit variation of the rotational speed by more than 10 to 12 percent; i.e., $n_{max}/n_{min} = 1.1$ to 1.2.

Therefore, in our calculations $\omega R = 220\ m/s$ was used in hover and maximum speed flight; $\omega R = 210\ m/s$ in cruise at $H = 500 m$; and $\omega R = 230 m/s$ in flight at the service ceiling.

2.4.16 Determination of Power Required in Forward Flight

The determination of helicopter power required is usually made in the following sequence: We first determine all the rotor characteristics, including rotor power for the given thrust $T_{m.r}$ and propulsive force T_x equal to the difference between the parasite drag of the helicopter with given value of $c_x S$ and the thrust of the propulsor if the latter is installed on the helicopter, but without account for the power expended on the mutual lifting-rotor interference and wing drag. Therefore, when analyzing the tandem helicopter without wing and auxiliary propulsion, we add the following increment to the obtained power of the two main rotors

$$\Delta N_{m.r} = \chi_{co} G_{gr}^2 / 300 \rho \pi R^2 V \qquad (2.156)$$

where G_{gr} = helicopter flight weight, and χ_{co} = coefficient of main-rotor interference.

The values of the interference coefficients depend on the relative elevation of the aft rotor above the forward rotor $\bar{y} = y/R$. These coefficients are shown in Fig 2.65.

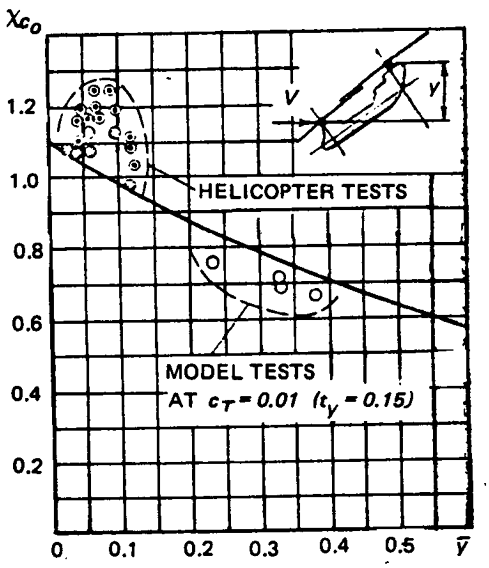

Figure 2.65 Dependence of the rotor interference coefficient χ_{co} from relative elevation, $\bar{y}$, of the rear rotor over the front rotor in tandems

For flight at the optimal speed, including flight at the service ceiling where the power expended on mutual rotor interference plays a particularly significant role, the elevation of the aft rotor above the forward rotor (for the usual average rotor tilt of about 6°) is practically zero. Therefore, in these regimes, we should take $\chi_{co} \approx 1.1$ (see Fig 2.65).

When analyzing the side-by-side rotor helicopter with a wing, we add the following increment to the computed main-rotor power:

$$\Delta N_{m.r} = (Y_{wg} V/75K'_{wg}) + [2\chi_{m.r} Y_{wg}(G_{gr} - Y_{wg})/75\rho\pi R^2 V] + [\chi_{co}(G_{gr} - Y_{wg})^2/300\rho\pi R^2 V] \qquad (2.157)$$

where Y_{wg} = wing lift and K'_{wg} its L/D ratio; $\chi_{m.r}$ = coefficient of main rotors inductive influence on the wing which, according to Ref 11, can be taken equal to $\chi_{m.r} = 0.12$. The value of χ_{co} can be taken as $\chi_{co} \approx 0.35$.

The wing L/D ratio with account for the inductive influence of the main rotors can be determined from the expression

$$(1/K'_{wg}) = (1/K_{wg}) + (\chi_{wg} c_T/4\mu^2) \qquad (2.158)$$

where K_{wg} = L/D ratio of the isolated wing. For the inversely tapered wing, as in the V-12 helicopter, $K_{wg} \approx 10$; χ_{wg} = the coefficient of inductive influence of the main rotors on the wing which, for the side-by-side rotor helicopter in accordance with Ref 11, can be taken as $\chi_{wg} = 0.8$.

The total engine power required for flight can be defined as

$$N_{tot} = (N_{m.r}/\xi_{m.r}) + (N_{prop}/\xi_{prop}), \text{ where } N_{prop} = T_{prop} V/\eta_{prop}. \qquad (2.159)$$

The calculation of the power required for flight should be made for the service ceiling, as well as with maximum and cruise speed conditions at different flight weights with account for fuel consumption in order to determine the helicopter flight range.

2.4.17 Difference Between the Power Transmitted by the Forward and Aft Gearboxes of Tandem Helicopters

It is well known that because of mutual rotor interference, the power transmitted by the forward and aft gearboxes of tandem helicopters is the same only in certain flight regimes. Power equalization during long-duration flights is accomplished by selecting the built-in tilt of the rotor axes or by suitable deflection of the swashplates. In many other flight regimes, the power transmitted by the gearboxes is significantly different. For this reason, Boeing designs the main gearboxes for a power exceeding by 20 percent the average power transmitted by the transmission.

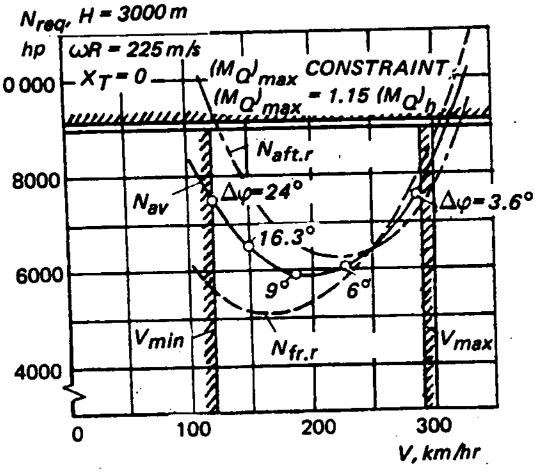

Figure 2.66 Power consumed by the front and aft rotors of a tandem helicopter in horizontal flight at altitude $H = 3000$ m and rotor dihedral $\Delta\varphi$ required for equalization of those powers

Figure 2.66 shows, as an example, the power required by the forward and aft rotors for a tandem-rotor helicopter at various flight speeds at the altitude $H = 3000$ m. Also shown are the rotor dihedral angles required to equalize this power.

It is obvious that achieving such dihedral angles for main-rotor tip-path planes by tilting the swashplate is not practical. At the same time, it appears to us that 20-percent main-rotor loading nonuniformity is excessive. Therefore, in our calculations, we have taken this nonuniformity as equal to 15 percent.

2.4.18 Fuel Weight

In calculating the fuel weight for flight over the required distance, it is assumed that the whole flight is performed at altitude $H = 500\,m$ at the same speed V_{cr} and the same main-rotor rotational speed, corresponding to the selected value of ωR.

In approximate calculations, the fuel weight can be determined using the power required corresponding to the average flight weight.

$$G_{av} = G_{t.o} - \tfrac{1}{2} G_{fu} . \tag{2.160}$$

The power required calculation should be made for several flight speeds. We take the cruise speed as that corresponding to minimal fuel consumption per kilometer; however, this speed can not exceed that determined by main rotor strength. Usually, for a helicopter without a wing, increasing the cruise speed above $V = 270\ km/hr$ is limited by main-rotor strength.

If the necessary engine characteristics are not available, the horizontal flight specific fuel consumption can be determined as a function of the power used from the following formula

$$(c_e)_{h.f} = [(c_e)_{t.o} - 0.16(1 - \bar{N}_{h.f})] / \bar{N}_{h.f} \tag{2.161}$$

where $\bar{N}_{h.f} = N_{h.f}/(N_{ref})_{max}$, and $(c_e)_{t.o}$ = sfc of the engine operating at takeoff power. $N_{h.f}$ = power required by the helicopter in horizontal flight at the cruise speed.

For modern engines, we can take

$$(c_e)_{t.o} = k_{c_e}/(N_{ref})^{0.1}{}_{max}$$

where $k_{c_e} = 470$ to $520\,gr/(hp^{0.9}hr)$.

It should be noted that sfc is usually higher for low-power engines, and lower for high-power engines.

The fuel weight is found from the formula

$$G_{fu} = k_{fu} (c_e)_{h.f} N_{h.f} L/V \tag{2.162}$$

where L = assumed helicopter flight distance. Here, the coefficient k_{fu} accounts for the 5 percent navigational reserve, the fuel consumption in transition regimes, and also includes a margin for possible calculation inaccuracies. It is usually assumed that $k_{fu} = 1.19$.

2.4.19 Allowance for Structural Weight Growth

Experience in helicopter development shows that the structural weight will inevitably increase from the preliminary design stage to the series production stage. This is an absolute law of engineering development, associated with the continuous appearance of new requirements, new concepts, and new circumstances in the course of more profound analysis, study, and testing of the hardware. Therefore, a margin for structural weight growth must be introduced into helicopter weight estimates in the preliminary design stage. We propose that this margin be about 10 percent of the overall helicopter structural weight, calculated using the previously presented formulae.

In order to account for possible blade-weight growth, the hub should be designed for centrifugal force from blades whose weight is increased by 10 percent.

2.5 Comparison of Different Helicopter Configurations Selection of Optimal Main-Rotor Diameter and Number of Blades

To illustrate the previously examined technique for selecting the optimal helicopter parameters on the basis of maximum payload, we shall present the results of calculations of the cargo weight transported by single-rotor and tandem helicopters with takeoff weights from 12 to 24 tons; and single-rotor, tandem, and side-by-side trussed helicopter configurations with takeoff weights from 40 to 44 tons, and then up to 60 or more tons.

We shall perform the helicopter weight estimates under the assumption that for helicopters of all sizes and configurations, blades having the same design will be used, and their weights determined from Eq (2.12).

Before presenting the calculation results, we shall examine how the blade and hub weight varies with change of the main-rotor diameter and number of blades for constant helicopter gross weight.

2.5.1 Overall Blade Weight Dependence on Main-Rotor Diameter and Number of Blades for Constant Helicopter Gross Weight

Assuming that the selected value of t_{y_o} does not change with variation of the main-rotor diameter, we obtain the relationship between blade chord and main-rotor radius from Eq (2.132):

$$b = 2G_{gr}/\rho_o R t_{y_o} U_t^2 z_{bl_\Sigma} \tag{2.163}$$

where z_{bl_Σ} = total number of blades of all the helicopter main rotors.

We introduce the relative parameter,

$$\bar{t} = t_{y_o} U_t^2/0.155\, U_{t_o}^2; \quad U_{t_o} = 220\, m/s. \tag{2.164}$$

Then Eq (2.163) becomes

$$b = (1/469R)(G_{gr}/\bar{t} z_{bl_\Sigma}), \tag{2.165}$$

Substituting this value into Eq (2.12) we will find that for $R\lambda < R\lambda_o$, the blade weight varies according to the following law:

$$\Sigma G_{bl} = [k^*_{bl}/(z_{bl_\Sigma} R)^{0.7}](G_{gr}/279\bar{t})^{1.7}, \tag{2.166}$$

i.e., it decreases with an increase of the rotor radius and number of blades.

However, the blade weight reduction indicated by Eq (2.166) continues only until the weight coefficient k_{bl} reaches its minimum value which we have taken as $(k_{bl})_{min} = 5.5$, or when the reduced blade aspect ratio reaches the value $\bar{R}\lambda_o$.

If, during the main-rotor radius increase, the following condition is reached,

$$k_{bl} = (k_{bl})_{min} \tag{2.167}$$

then, with a further increase in the radius, the blade weight will follow a law which can be obtained by substituting Eq (2.165) into Eq (2.3). In this case,

$$\Sigma G_{bl} = (k_{bl})_{min} G_{gr} R/\pi 469\bar{t}; \tag{2.168}$$

i.e., the blade weight will increase proportionately with an increase in the rotor radius, regardless of the number of main-rotor blades.

An example of this blade weight dependence on the main-rotor radius is shown in Fig 2.67. The blade weight is minimal for some radius R_γ, which can be found by equating the right sides of Eqs (2.166) and (2.168)

$$R_\gamma = 0.263[k^*_{bl}/(k_{bl})_{min}]^{0.588}(G_{gr}/\bar{t}z_{bl\Sigma})^{0.411} \tag{2.169}$$

or, for blade aspect ratio equal to

$$\lambda_\gamma = [k^*_{bl}/(k_{bl})_{min}]^{1.43}\lambda_{av}/R^{0.429}.$$

Values of aspect ratios λ_γ for those cases when $\lambda_\gamma < \lambda_o$ are shown in Fig 3.14.

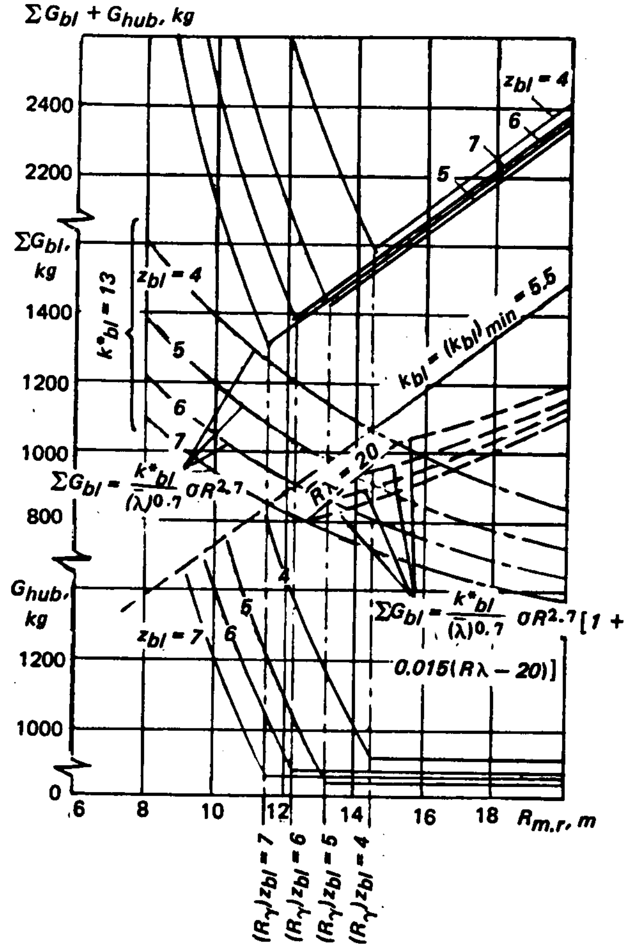

Figure 2.67 Dependence of blade and hub weights and their collective weight on the main rotor radius of a single-rotor helicopter of constant gross weight G_{gr} = 20 ton, operating at t_{yo} = 0.155

For certain values of coefficients k^*_{bl}, $G_{gr}/\bar{t}z_{bl\Sigma}$ and $\bar{R}\lambda_o$, the blade-weight variation law given by Eq (2.166) is violated earlier with increase of R because the blade reaches a reduced aspect ratio equal to $\bar{R}\lambda_o$; i.e., when $\bar{R}\lambda = \bar{R}\lambda_o$ or, as follows from the explanatory remarks regarding Eq (2.6), when $R^2/16b = \bar{R}\lambda_o$.

Substituting herein the value of b from Eq (2.165), we obtain the blade radius R_λ at which the blade begins to acquire additional weight resulting from the growth of the blade aspect ratio. Up to this point, there was no increase in blade weight caused by the increasing aspect ratio.

$$R_\lambda = 0.325\sqrt[3]{\bar{R}\lambda_o G_{gr}/\bar{t}z_{bl_\Sigma}} \; . \tag{2.170}$$

Figure 2.68 shows the values of R_γ and R_λ as functions of $G_{gr}/\bar{t}z_{bl_\Sigma}$ at $(k_{bl})_{min} = 5.5$ for several values of the coefficient k^*_{bl} and the reduced aspect ratios $\bar{R}\lambda_o = 20$, and $\bar{R}\lambda_o = 12.4$. We see from these curves that for small $G_{gr}/\bar{t}z_{bl_\Sigma}$, the radius R_γ is smaller. With an increase of $G_{gr}/\bar{t}z_{bl}$ beginning with certain values of this parameter, the radius R_λ is smaller.

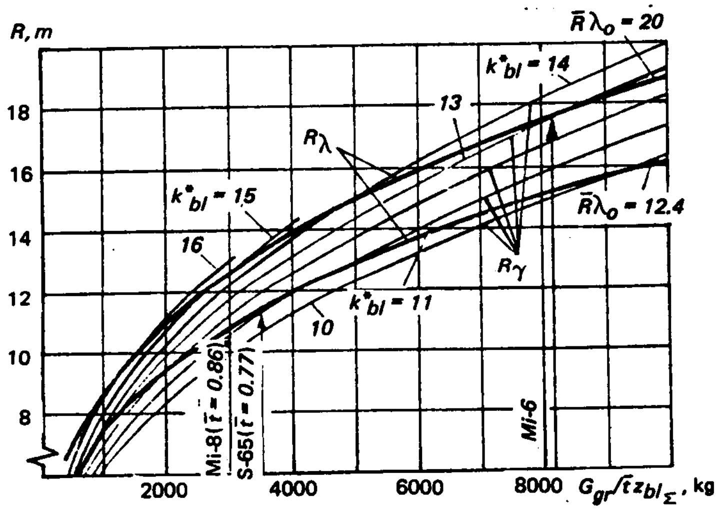

Figure 2.68 Dependence of optimal radii of main rotors with steel-tube spar and glass-fiber envelope ($\bar{R}\lambda$ = 20) and with Duralumin extruded spar ($\bar{R}\lambda_o$ = 12.4) on parameter $G_{gr}/\bar{t}z_{bl_\Sigma}$ at various levels of weight effectiveness defined by coefficient k^*_{bl}

Thus, for the blade with steel spar and glass-plastic envelope for which $\bar{R}\lambda_o = 20$, increase in blade weight resulting from its larger aspect ratio begins earlier than the appearance of blade increments resulting from the constraint given by the condition $k_{bl} = (k_{bl})_{min}$:

at $G_{gr}/\bar{t}z_{bl} \geqslant 3100\,kg$ if $k^*_{bl} = 15$
at $G_{gr}/\bar{t}z_{bl} \geqslant 4750\,kg$ if $k^*_{bl} = 14$
at $G_{gr}/\bar{t}z_{bl} \geqslant 8800\,kg$ if $k^*_{bl} = 13$

and does not occur at all for the values—encountered in practice—of parameter $G_{gr}/\bar{t}z_{bl_\Sigma}$, if $k^*_{bl} < 12.5$.

For the blade with extruded Duralumin spar for which $\bar{R}\lambda_o = 12.4$ at $G_{gr}/\bar{t}z_{bl} \geqslant 2000\,kg$ and $k^*_{bl} \geqslant 12$, weight increases resulting from the high aspect ratios always begin earlier than for the steel-spar types.

The minimum blade weight always occurs at the smaller of the two radii, R_γ or R_λ, and it will be shown in the below calculations that the smaller of these radii, which satisfies the allowable blade deflections in accordance with Subsection 2.3.8 is, in many cases, the optimal main rotor radius for the selected total number of blades for single-rotor, tandem, and side-by-side configurations. In these cases, Figs 2.59 and 2.68 can be used as graphs for selecting the optimal main-rotor radius.

In the aforementioned cases, the described citcumstance could significantly simplify optimal helicopter parameter selection since the problem would reduce to simply selecting the number of blades z_{bl} for which the weight estimates could be made only for several values of z_{bl} and main rotor radii selected from Figs 2.59 and 2.68. However, because of the fact that the curves showing the influence of certain helicopter parameters on the magnitude of transported payload become quite flat near the optimum, it is better, in this case, to select a main-rotor diameter that is somewhat smaller than its optimal value. While this would lead to a slight loss in the cargo weight, it would still facilitate the development of smaller-diameter blades. Therefore, as a rule, in the initial stage of helicopter parameter selection, it is still necessary to plot the entire curve of transported cargo weight as a function of the main-rotor diameter.

2.5.2 Dependence of the Hub and Entire Main-Rotor Weight on the Rotor Diameter and Number of Blades for Constant Helicopter Gross Weight

The blade centrifugal force can be determined by the following formula:

$$N_{bl} = (G_{bl}/g)(U_t^2/R)\bar{r}_{c.g} \qquad (2.171)$$

where $\bar{r}_{c.g}$ = the relative radius of the blade c.g., which is usually $\bar{r}_{c.g} = 0.49$ to 0.51.

If we substitute the expression for the blade weight from Eq (2.166) into Eq (2.171), we obtain

$$N_{bl} = k^*_{bl}\,\bar{r}_{c.g}\,\bar{U}_t^2\,[0.537G_{gr}/z_{bl_\Sigma}R\bar{t}\,]^{1.7}. \qquad (2.172)$$

Then, in accordance with Eq (2.31), the hub weight can be found from the following formula:

$$G_{hub} = k^*_{hub}(k_{z_{bl}}/z_{bl_\Sigma}^{1.29})(k^*_{bl}\bar{r}_{c.g}\bar{U}_t^2)^{1.35}[0.537G_{gr}/R\bar{t}\,]^{2.29}. \qquad (2.173)$$

Consequently, as long as the blade weight decreases with an increase of R, the hub weight decreases even more strongly; as it varies inversely proportionally to $R^{2.29}$. This relationship will no longer be valid as the main rotor radius becomes equal to R_γ. Beginning with this value, the blade weight increases in accordance with Eq (2.168), while the blade centrifugal force no longer varies with an increase in the main-rotor radius. This force is now defined as

$$N_{bl} = 3.35(k_{bl})_{min}\bar{r}_{c.g}\,\bar{U}_t^2\,G_{gr}/\bar{t}z_{bl_\Sigma}. \qquad (2.174)$$

In addition, in accordance with Eq (2.31), the hub weight remains constant, and equal to

$$G_{hub} = k^*_{hub}(k_{z_{bl}}/z_{bl_\Sigma}^{0.35})\,[(k_{bl})_{min}\bar{r}_{c.g}\,\bar{U}_t^2\,G_{gr}/\bar{t}\,]^{1.35}. \qquad (2.175)$$

The hub weight is shown in Fig 2.67 as a function of main-rotor radius. This figure also shows the total weight of the main rotor, consisting of the blades and hub.

We can see from these curves that as far as the weight dependence on radius is concerned, the transition from weight reduction to weight increase is more marked in the case of the main rotor as a whole than for the blades alone.

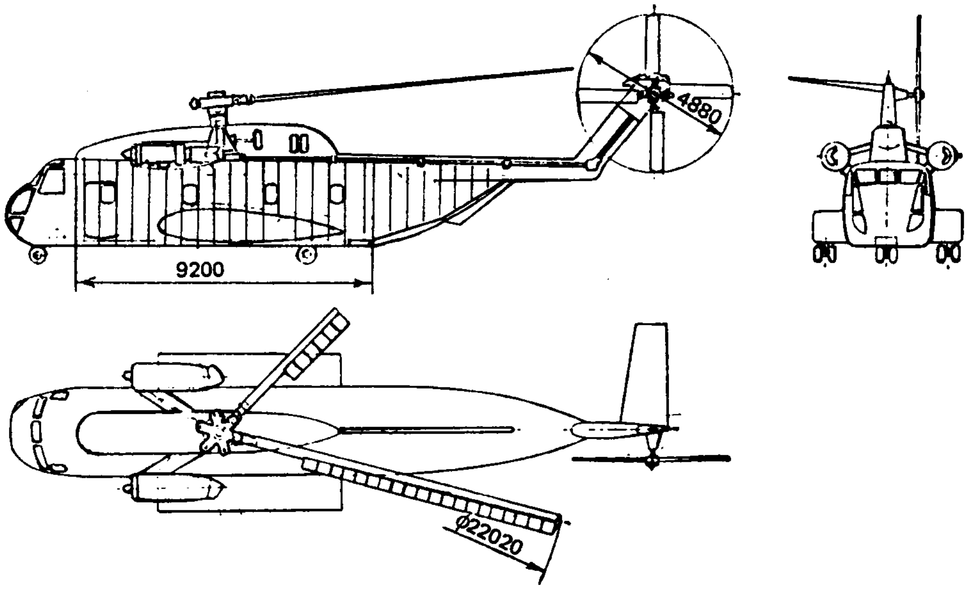
4880
9200
φ22020

Figure 2.69 Three-view drawing of the S-65 helicopter

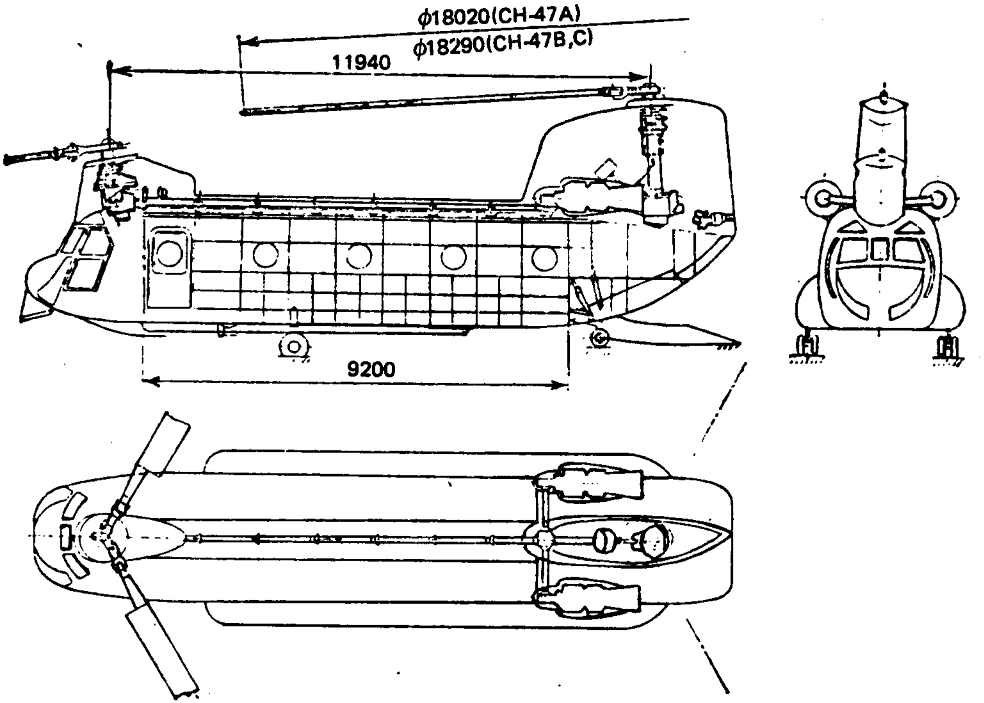
φ18020(CH-47A)
φ18290(CH-47B,C)
11940
9200

Figure 2.70 Three-view drawing of the Chinook helicopter

2.5.3 Comparison of Cargo Weights Transported by Single-Rotor and Tandem Helicopters of the 12 to 24-Ton Gross-Weight Class

We shall use the technique just described to make comparative calculations of the cargo weights carried by single-rotor and tandem helicopters with cargo compartment dimensions B_2 (see Fig 2.64). The S-65 (Fig 2.69) and Chinook (Fig 2.70) helicopters have such cabins. For the single-rotor helicopter, we shall examine the Mi-8 and Mi-6-type layouts while, for tandems, we shall examine that of the Chinook.

In order to properly compare helicopter configurations (not the actual aircraft), it is necessary to reduce the data of the helicopters being compared to the same weight efficiency levels, and impose the condition that these helicopters have the same flight performance.

We shall consider that the helicopters of both configurations have the same hover ($H_h = 1500\,m$) and service ($H_s = 4500\,m$) ceilings. The results of the comparison are presented in Tables 2.8 and 2.9.

The first columns of Tables 2.8 and 2.9 show data for the Chinook helicopter with an alternative gross weight of $G_{gr} = 20\,703\,kg$. The helicopter transmission and powerplant installation were selected for flight at this gross weight; however, the maximum fuselage and landing-gear loads required by the airworthiness (or strength) standards cannot be met at this gross weight, and the helicopter does not have hovering capability, and the service ceiling is $H_s \approx 2000\,m$.

At the normal gross weight of $G_{gr} = 14970\,kg$ (see Table 2.8 and 2.9), the Chinook helicopter has the required service ceiling of $H_s = 4500\,m$, but a large part of its components such as the blades, hubs, transmission, and powerplant are oversized. Therefore, for the tandem helicopter having a layout of the Chinook type, we take the thrust coefficient as $t_{y_0} = 0.145$ and not $t_{y_0} = 0.126$ as for the Chinook helicopter with normal gross weight, and specify, for this helicopter, the aforementioned hovering and service ceilings.

In addition, for valid comparison of these helicopter configurations, the following assumptions were made:

1) the blade tip speed $\omega R = 220\,m/s$, and all the other aerodynamic parameters of the main rotors which determine their efficiency are the same for these layouts;

2) for the tandem helicopter, we shall assume the hub scheme with the traditional sequence of hinge locations and consequently, with the same weight efficiency level as for the single-rotor helicopter schemes although, as a result of this, the tandem-rotor hub weight must be somewhat increased;

3) we take the maximum transmission shaft speed as $n_{sh} = 3000\,rpm$ which is usual for single-rotor helicopters for the reasons discussed in Subsection 2.3.7;

4) as a result of these changes, we shall assume that the rotor overlap will be somewhat smaller, and equal to the values determined in Subsection 2.3.3;

5) we assume that the weight coefficients for all the helicopter components are the same except for the main gearboxes, where a smaller weight coefficient is taken for the main gearbox of the tandem configuration (see Table 2.8). This is done, recognizing that this weight reduction represents a peculiarity of the Chinook helicopter transmission layout which we discussed earlier in Subsection 2.2.4.

Taking these refinements into account for the compared configurations with various gross-weight values, Figs 2.71 and 2.72 depict the magnitude of transportable cargo over a distance of 370 km as a function of the lifting-rotor diameter and number of blades. In developing these relationships, it was assumed in the calculations that in contrast to Table 2.8, both configurations will experience a 10-percent growth in structural weight.

HELICOPTER COMPONENTS	CHINOOK CH-47C ALTERNATIVE GROSS WEIGHT		CHINOOK CH-47C AT NORMAL GROSS WEIGHT		COMPARATIVE DATA OF HELIC. W/CARGO-LIFTING CAPACITY OF CHINOOK		ASSUMED DATA OF SINGLE-ROTOR HELICOPTER OF Mi-8 CONFIGURATION	
	WEIGHT COEFFICIENTS	WEIGHT KG	WEIGHT COEFFICIENTS	WEIGHT KG	WEIGHT COEFFICIENTS	WEIGHT KG	WEIGHT COEFFICIENTS	WEIGHT KG
Lifting Rotor Blades	12.55	780	12.55	780	13	768	13	616
Lifting Rotor Hubs	0.8900	764	0.890	764	1.15	846	1.15	538
Controls	–	793	–	793	–	759	–	609
Boosted Controls with Hydraulic System	18	(398)	18	(398)	18	(383)	18	(279)
Manual Controls (together with Auxiliaries)	33	(395)	33	(395)	30	(376)	30	(330)
Main Gearboxes (with Lubricating System)	0.4150	1340	–	1340	0.415	1026	0.465	1053
Intermediate Gearbox of Single-Rotor Helicopter & Engine Gear-Boxes (with Lubricating System) of Tandem Helicopters	0.9200	112	0.920	112	0.700	100	0.700	38
Combining Gearbox of Tandem Helicopter & Tail-Rotor Gearbox of Single-Rotor Helicopter (with Lubricating System)	0.6100	97	0.610	97	0.650	184	0.650	80
Tail-Rotor Blades	–	–	–	–	–	–	17	37
Tail-Rotor Hubs	–	–	–	–	–	–	1	120
Transmission Shafts	0.0625	118	–	118	0.070	124	0.070	64
Engine Installation	0.1060	795	–	795	0.140	940	0.140	790
Fuel System	0.0900	325 $(G_{fu} = 3550)$	–	325	0.090	135	0.090	130

Fuselage W/Cowlings & Engine Nacelles	—	2092	1.2	2092	1.2	2181	1.2	1916
Landing Gear	—	492	0.033	492	0.030	450	0.030	450
Equipment	—	1089	—	1089	—	1062	—	1048
Vibration Absorbers at $z_{bl} = 3$	—	388	0.026	388	0.025	375	—	—
Weight Empty	—	9194	—	9194	—	8953	—	7490
Crew	—	270	—	270	—	270	—	270
Fuel Supply (*L* = *370 km* Range)	—	2150	—	1850	—	1500	—	1450
Payload	—	9125	—	3675	—	4276	—	5890
Gross Weight	—	20730	—	14970	—	15000	—	15000

NOTE: Weights shown in parentheses enter into overall weight of controls.

TABLE 2.8 WEIGHT DATA OF CHINOOK HELICOPTER, AND SINGLE-ROTOR AND TANDEM HELICOPTER WEIGHT DATA REDUCED TO THE SAME CONDITIONS

BASIC DATA	CHINOOK CH-47C AT ALTERNATIVE GROSS WEIGHT	CHINOOK CH-47C AT NORMAL GROSS WEIGHT	COMPUTATIONAL DATA OF HELICOPTER WITH CARGO-LIFTING CAPABILITY OF CHINOOK	ASSUMED DATA OF Mi-8 SINGLE-RCTOR HELICOPTER CONFIGURATION
Lifting-Rotor Diameter, *m*	18.29	18.29	18,29	22.00
Tip Speed of Lifting Rotor, *m/s*	232	232	220	220
t_{yo}	0.175	0.126	0.145	0.155
H_h, *m*	0	4400	1500	1500
H_s, *m*	2000	4500	4500	4500
$\bar{p}$	0.70	0.70	0.63	–
Rotational Speed of Transmission Shaft *rpm*	12690/7465	12690/7465	10000/3000	3000
Sequence of Lifting-Rotor Hub Hinges	HH, PH VH	HH, PH VH	HH, VH PH	HH, VH PH
Fuselage Area Assumed in Computations of Initial Variant, m^2;	–	–	185	185
Assumed $c_x S$	–	–	4.27	4.27
$(c_e)_{to}$, *kg/(hp.hr)*	0.236	0.236	0.210	0.210

TABLE 2.9 BASIC DATA OF COMPARED HELICOPTERS

The calculations were performed, also assuming that the blades have tubular steel spars for which $\bar{R}\lambda_o = 20$.

For both configurations, it should be noted that the optimum rotor diameters appear to agree with those in Figs 2.59 and 2.68 for the same number of blades, differing only because coefficients $\bar{t}$ are assumed equal to *1.0* for the single-rotor helicopter, and $\bar{t} = 0.935$ ($t_{y_o} = 0.145$) for the tandem. As a consequence of the difference in these coefficients, somewhat larger diameters are optimal for the tandem-rotor helicopter for the same number of blades.

The weight of cargo transported by the single-rotor helicopter increases with increase of the number of main-rotor blades. However, with increase of the number of blades above $z_{bl} = 5$, the gains are not significant.

For tandem helicopters, main rotors with number of blades $z_{bl} = 5$ appear optimal. With a smaller number of blades, as well as with the number of blades greater than $z_{bl} = 5$, the transportable cargo weight decreases.

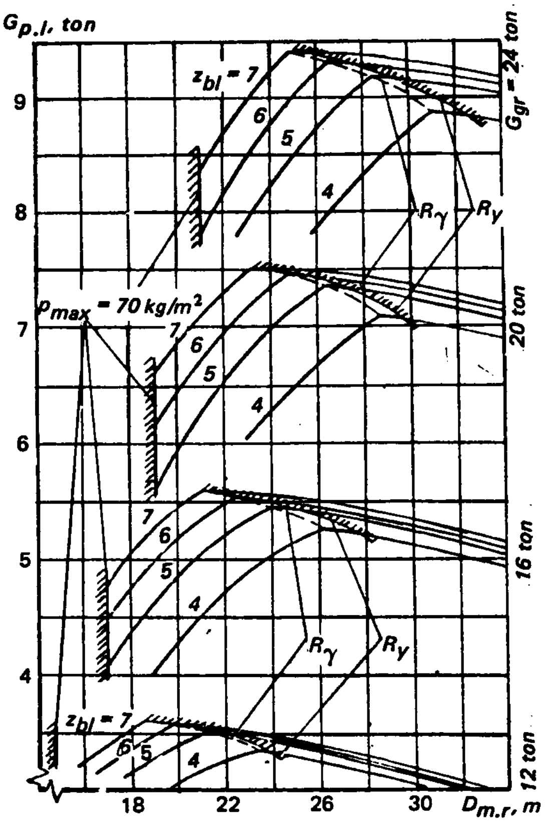

Figure 2.71 Dependence of cargo weight transported by single-rotor helicopters over distance L = 370 km on diameter of main rotor $D_{m.r}$ at various number of blades z_{bl} and for different helicopter gross weights G_{gr}

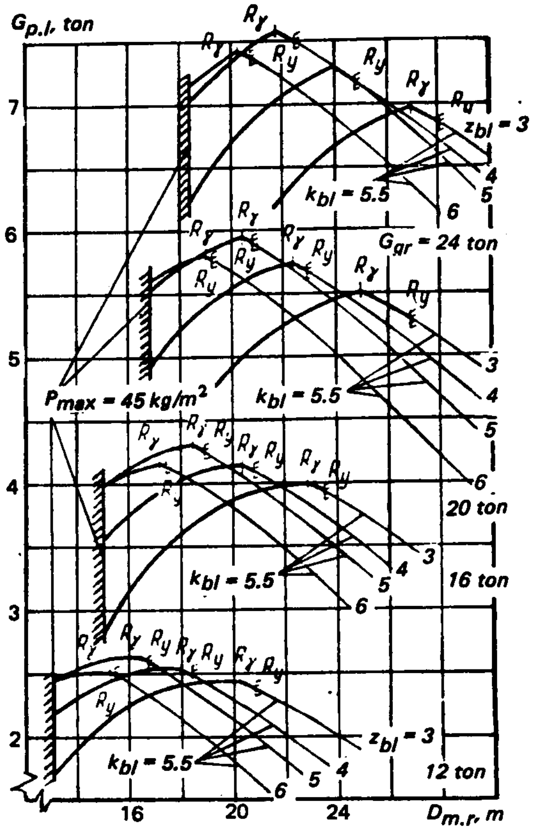

Figure 2.72 Dependence of cargo weight transported by a tandem helicopter over distance L = 370 km on diameter of lifting rotors $D_{m.r}$ at various number of blades z_{bl} and for different helicopter gross weights G_{gr}

For the single-rotor helicopter, the cargo weight transported increases markedly with an increase of the main-rotor diameter until this increase becomes limited as the k_{bl} coefficient reaches the value of $k_{bl} = (k_{bl})_{min}$. It should be noted that the gradient of cargo weight increments increases with the helicopter gross weight.

For tandem helicopters, the curves of transported cargo weight variation with reduction of the diameter below its optimal value, especially for lower gross weights, are very flat. This is especially visible for the curves of $G_{gr} = 12$ *tons*, and $z_{bl} = 3$ (see Fig 2.72). In such cases, therefore, it is better to select main-rotor diameters smaller than the optimal value in order to simplify blade development.

In all cases, the main-rotor radius constraint R_y based on allowable blade droop is beyond the point corresponding to the optimum of the cargo weight transported. Therefore, the optimal main-rotor radius coincides with R_γ. The value of R_λ for helicopters of this lift capability at the assumed coefficient $k^*_{bl} = 13$ is larger than R_γ and, therefore, the weight increase associated with excessive blade aspect ratio does not show up in the calculations.

Figure 2.73 shows, as a function of gross weight, the cargo weight transported over the distance $L = 370\ km$ by the optimal variants of the considered helicopters. It can be seen from these relationships that for the specified service ceiling—which represents a particularly difficult requirement for the tandem helicopter, and the same weight efficiency of the components and systems, the single-rotor helicopter is capable of transporting 1.0 to 1.5 tons more cargo weight than the tandem.

Such large differences are not observed in the cargo weights transported by existing helicopters because of the higher weight efficiencies of the tandem helicopter components; primarily the Boeing main-rotor hubs and blades, and also due to the lighter powerplant of this helicopter. In addition, Boeing has been able to solve such important problems as the use of very high rotational speeds of transmission shafts and avoidance of rotor blade strike in spite of large values of the rotor overlap, which also leads to some gain in structural weight.

However, for the same weight efficiency as assumed in the above calculations, the weight ratio $\bar{G}$ and the weight ratio based on payload $\bar{G}_{pl}$ for the tandem-rotor helicopter of the considered gross-weight class are 6 to 8 percent lower than for the single-rotor helicopter (Fig 2.74).

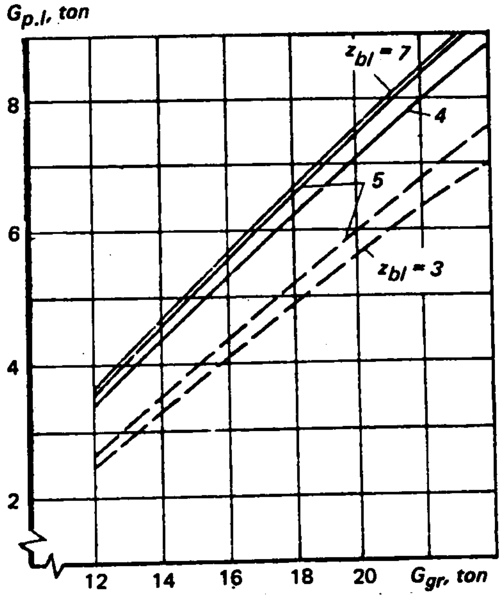

Figure 2.73 Dependence, on gross weight G_{gr}, of the cargo weight (payload) $G_{p.l}$ transported over a distance of $L = 370$ km by single-rotor and tandem helicopters: —— single-rotor; and – – – tandem

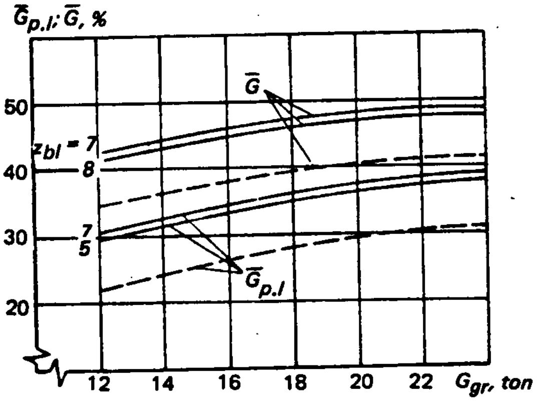

Figure 2.74 Payload and useful weight ratios for single-rotor and tandem helicopters: —— single-rotor, – – – tandem ($z_{bl} = 5X2$)

2.5.4 Comparison of Cargo Weights Transported by Single-Rotor, Tandems, and Side-by-Side Rotor Helicopters of the 44 to 60-Ton Gross-Weight Class

We shall present the results of calculations of the cargo weight transported over specified flight ranges by single-rotor, tandem, and trussed side-by-side rotor helicopters having the indicated gross weights. The data for the side-by-side rotor helicopter with a wing will be presented later in Sect 2.6 in conjunction with a comparison of pure and compound helicopters.

It is interesting to see how the optimal helicopter parameters vary with flight range. Therefore, calculations of the cargo weight transported were made for the minimal possible range of 50 km and for the maximum range which can be realistically specified for the transport helicopter. We consider this range to be 800 km. For the single-rotor helicopter, we also made calculations for an intermediate range of 400 km.

We shall examine helicopters whose layouts are similar to the Mi-6 for the single-rotor helicopter (Fig 2.75), to the V-12 for the side-by-side rotor helicopter (see Fig 2.38); and for the tandem whose three-view drawing is shown in Fig 2.57. We will assume that for all helicopters, blades of the same construction will be used; incorporating a steel spar and glass-plastic envelope, for which $\bar{R}\lambda_o = 20$ and therefore, we will determine blade weights from Eq (2.12).

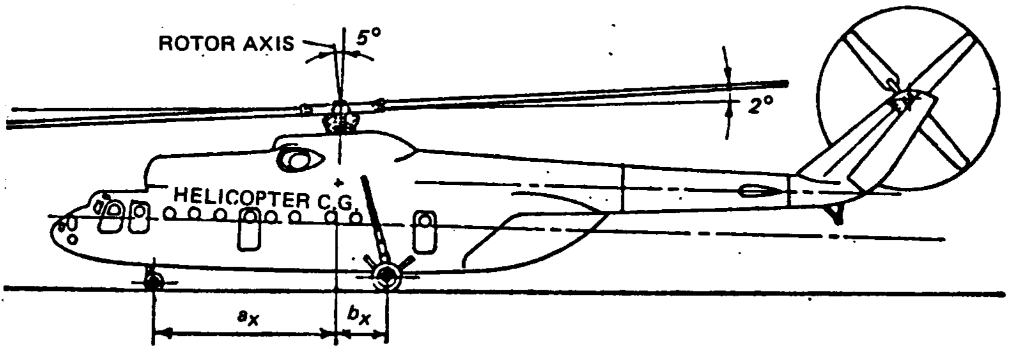

Figure 2.75 Side-view drawing of the Mi-6 helicopter

Table 2.10 presents the weight formulae and the weight coefficients used in the calculations, and Table 2.11 shows the basic data for the compared helicopters.

Dependence of some data and the cargo weight transported by the considered helicopters on main-rotor diameter and number of blades are shown for several helicopter gross weights in Figs 2.76 to 2.84.

Single-Rotor Helicopter. The cargo weight transported by the single-rotor helicopter over distances of 50, 400, and 800 km as a function of main-rotor diameter, are shown in Figs 2.76, 2.77, and 2.78. The curves are given for three gross weights and different numbers of main-rotor blades. The region of considered helicopter parameters is constrained on the left by the maximum allowable main-rotor disc loading of $p = 70\,kg/m^2$ and on the right by the maximum allowable blade deflection, taken as $(\bar{y}_R)_{all} = 0.12$.

We see from these graphs that for the single-rotor helicopters with the selected number of blades it is advantageous to increase the main-rotor diameter as much as possible until any of the applicable constraints is reached. Regardless of which constraint is reached first, we can confirm the previously drawn conclusion that for each number of blades there is a corresponding particular optimal main rotor diameter, coinciding with the diameter determined by the constraint which first becomes effective.

As we shall see later, we can include among the constraints the blade radius $\bar{R}\lambda$ at which the blade weight begins to increase because as the aspect ratio exceeds the value of $\bar{R}\lambda_o$, although, in contrast to the other constraints, it is quite feasible to develop blades with higher aspect ratios.

HELICOPTER COMPONENT	FORMULAE FOR WEIGHT CALCULATIONS (at $U_t = 220\ m/s$)	WEIGHT COEFFICIENTS		
		SINGLE-ROTOR HELICOPTER	TANDEM HELICOPTER	SIDE-BY-SIDE HELICOPTER
Lifting-rotor blades	$\Sigma G^*_{bl} = [k^*_{bl}(\sigma R^{2.7}/(\bar{\lambda})^{0.7}] [1 + \alpha_{\lambda} \bar{R}(\lambda - \lambda_o)]$	$k^*_{bl} = 13.8$	$k^*_{bl} = 13.8$	$k^*_{bl} = 13.8$
Lifting-rotor hubs	$G_{hub} = k^*_{hub} k_{z_{bl}} z_{bl} N_{bl}^{1.35}$	$k^*_{hub} = 1.15$	$k^*_{hub} = 1.15$	$k^*_{hub} = 1.15$
Boosted controls (swashplate, controls from boosters, hydraulic system of lifting rotors)	$G_{b.cont} = k_{b.cont} z_{bl} b^2 R$	$k_{b.cont} = 13.2$	$k_{b.cont} = 13.2$	$k_{b.cont} = 13.2$
Manual controls (including auxillary boosts)	$G_{m.cont} = k_{m.cont} R$ (single-rotor configuration) $G_{m.cont} = k_{m.cont} L$ (twin-rotor configuration)	$k_{m.cont} = 25$	$k_{m.cont} = 30$	$k_{m.cont} = 35$
Main gearboxes (with; attachment & lubricant)	$G_{m.g.b} = k^*_{m.g.b} z_{m.r} (a_Q M_{av})^{0.8}$	$k^*_{m.g.b} = 0.465$	$k^*_{m.g.b} = 0.465$	$k^*_{m.g.b} = 0.465$
Angular intermediate gearboxes (including lubricant)	$G_{i.g.b} = k^*_{i.g.b} z_{i.g.b} (a_Q M_{eq})^{0.8}$ For twin-rotor helicopters $M_{eq} = 716.2 (\Sigma N_{eng}/z_{sh} n_{sh} a)$ For single-rotor helicopters $M_{eq} = 716.2 (N_{t.r}/n_{sh})$	$k^*_{i.g.b} = 0.85$	$k^*_{i.g.b} = 0.85$ $a_Q = 1.15 \quad a = 1$	$k^*_{i.g.b} = 0.85$ Without middle intermediate gearbox, $a = 2z_{eng}$, $z_{i.g.b} = 4$; With middle intermediate gearbox, $a = 1.7z_{eng}$, $z_{i.g.b} = 5$
Tail-rotor gearbox (with lubricant)	$G_{t.r.g.b} = k^*_{t.r.g.b} M_Q^{0.8}$ where $M_Q = 716.2 (N_{t.r}/n_{t.r})$	$k^*_{t.r.g.b} = 0.65$	--	--
Transmission shaft	$G_{sh} = k_{sh} L_{sh} (M_Q)^{2/3}_{ult}$	$k_{sh} = 0.07$	$k_{sh} = 0.07$	$k_{sh} = 0.07$
Tail-rotor blades	$\Sigma G_{bl,t.r} = k^*_{blt.r}(\sigma R^{2.7}/(\lambda)^{0.7})$	$k^*_{bl.t.r} = 13.8$	--	--
Tail-rotor hub	$G_{t.r.b} = k^*_{t.r.h} k_{z_{bl}} z_{bl} N_{bl}^{1.35}$	$k^*_{t.r.h} = 1.15$	--	--
Powerplant installation (with engine mounts, cooling system lubricant, lubrication system and fire-suppression system)	$G_{eng.ins} = \gamma_{eng.ins} \Sigma N_{ref}$	$\gamma_{eng.ins} = 0.143$	$\gamma_{eng.ins} = 0.143$	$\gamma_{eng.ins} = 0.143$

Fuel System	$G_{fu.s} = k_{fu.s}(G_{fu})_{tot}$	$k_{fu.s} = 0.09$	$k_{fu.s} = 0.09$	$k_{fu.s} = 0.09$
Wing of side-by-side helicopter	$G'_{wg} = k'_{wg}\dfrac{(L/2R)^2[(\bar{U}_t)^2_{max}L^4]}{\bar{h}S_{wg}^2[1 + (2G_{nac}/G_{ct.f})]}G_{nac}$ at $L/i > (L/i)_o$	—	—	$k'_{wg} = 0.006$
Frames for rotor attachments	$G_{att} = k_{att}(l/R)^2(l/H)^2G_{nac}$	—	—	$k_{att} = 0.05$
Fuselage (with cowlings)	$G_\phi = k_\phi^* G_{gr}^{0.25} S_\phi^{0.88} L^{0.16(1+\alpha)}$	$k_\phi^2 - 1.36 \quad a = 0$	$k_\phi^* = 1.36 \quad a = 0.2$	$k_\phi^* = 1.36 \quad a = 0.05$ (without cowlings)
Cowlings of side-by-side helicopter	$G_{cow} = k_{cow}S_{cow}^{1.25}$ or $G_{cow} = 2k'_{cow}(\Sigma N_{eng}/2)^{2/3}$	—	—	$k'_{cow} = 1.0$
Lifting-rotor attachment	$G_{g.b.c} = k_{g.b.c}G_{gr}$	—	—	$k_{g.b.c} = 0.015$
Landing gear	$G_{l.g} = k_{l.g}G_{gr}$	$k_{l.g} = 0.02$	$k_{l.g} = 0.025$	$k_{l.g} = 0.03$
Electrical equipment	$G_{el} = k_{wir}L + k_{el.ice}F_{bl}$	$k_{wir} = 25$ $k_{el} = 6.5$	$k_{wir} = 40$ $k_{el} = 6.5$	$k_{wir} = 40$ $k_{el} = 6.5$
Other equipment	$G_{eqp_o} = k_{eqp}G_{gr}^{0.6}$ For fixed-helicopter mission: $G_{eqp_o} = const$	$k_{eqp} = 0.036$	$k_{eqp} = 0.036$	$k_{eqp} = 0.036$
Vibration absorbers;	$G_{v.ab} = k_{v.ab}G_{gr}$	—	$k_{v.ab} = 0.015$ $z_{bl} = 4$ $k_{v.ab} = 0.025$ $z_{bl} = 3$	—

TABLE 2.10 ASSUMED WEIGHT FORMULAE AND COEFFICIENTS

BASIC PARAMETER USED IN CALCULATIONS	HELICOPTER		
	SINGLE-ROTOR	TANDEM	SIDE-BY-SIDE
Main-rotor diameter of baseline variant, m	32.0	26.8	22.0
Tip speed of main and tail rotors, m/s, at			
H_h	220	220	220
V_{cr}	210	210	210
H_s	230	230	230
$t_{yo} = 2G_{gr}/\rho_o \sigma F U^2_t$	0.155	0.155	0.171
Airframe download coefficient for baseline version of configuration $(k_{d.w})_o$	0.970	0.967	0.940
Rotor thrust augmentation coefficient, k_T	1.00	1.00	1.04
Engine vertical thrust augmentation coefficient k_{eng}	1.00	1.00	0.99
Thrust coefficient at $H_h = 1500m$. In baseline variant, $t_y = (t_{yo} k_{eng}/k_{d.w} k_T \Delta)$	0.185	0.185	0.200
F.M. of isolated rotor at $H = H_h$ and solidity $\sigma_o = 0.217$	0.707	0.707	0.689
Coefficient of losses due to overlap, ξ_{ov} at $z_{bl} = 3$	–	0.930	Rotors without overlap
$z_{bl} = 4$	1.0	0.963	
$z_{bl} = 5$	–	0.990	
Coefficient of power utilization in hover; ξ	0.83	0.94	0.95
Coefficient of power utilization at V_{cr}, ξ_{cr}	0.89	0.94	0.95
Coefficient of unequal loading of main-gearboxes, α_Q	1.00	1.15	1.00
Number of intermediate gearboxes, including tail-rotors, $z_{i.t.b}$	2	4	3
Number of transmission shafts, z_{sh}	1	2	1
Rotational speed of transmission shaft, n_{sh}, rpm	2700	2700	2700
Coefficient of operational shaft overload, n_e	2.6	2.2	1.2
Shaft length in the original layout, L_{sh}, m	20.25	21.40	20.80
Rotor overlap $\bar{P}$ for			
$z_{bl} = 3$	–	0.63	Rotors without overlap
$z_{bl} = 4$	–	0.40	
$z_{bl} = 5$	–	0.17	
Distance between rotor shafts in the original layout, L, m	20.25	21.40	22.00
External area of fuselage in the original layout S_ϕ, m^2	320 with cowlings	356 with cowlings	240 with cowlings
Parasite drag equivalent flat-plate area, $c_x S$, m^2	7.50	8.95	12.40

TABLE 2.11 DATA ASSUMED IN WEIGHT CALCULATIONS

Assuming values of $(k_{bl})_{min} = 5.5$, $\overline{R}\lambda_o = 20$, $(\bar{y}_R)_{all} = 0.12$, and $k^*_{bl} = 13.8$, and increasing the gross weight of the considered helicopter while decreasing the number of blades in the lifting rotor, the character of the dependence of the transported cargo weight changes as a result of an increase in the referred aspect ratio above $\overline{R}\lambda_o$. However, the transported cargo weight continues to increase for the single-rotor helicopter which, in many cases, places in question the advisability of using high aspect-ratio blades because the small improvement in the transported cargo weight must be weighed against significantly greater difficulties in developing blades of high aspect ratios.

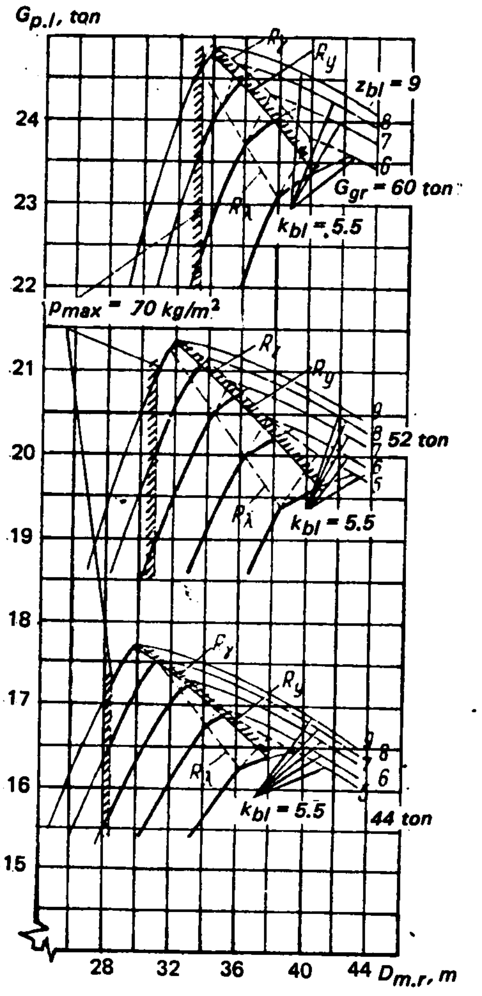

Figure 2.76 Dependence of cargo weight transported by a single-rotor helicopter over a distance of L = 50 km on main-rotor diameter

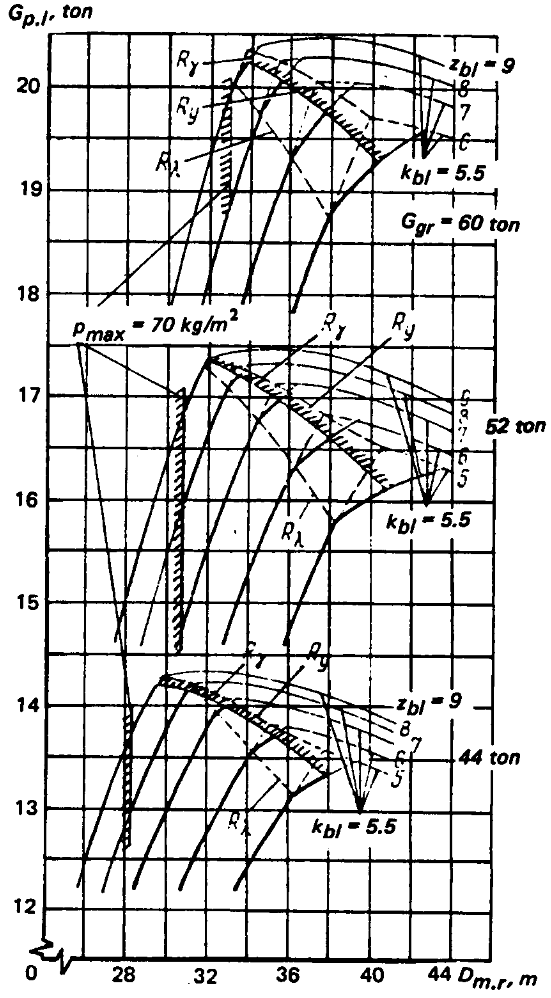

Figure 2.77 Dependence of cargo weight transported by a single-rotor helicopter over a distance of L = 400 km on main-rotor diameter

Therefore, bearing in mind the entire complex of problems requiring solutions, we can conclude that in spite of the increase in the transportable cargo weight with increase of the diameters above $2R$, diameters equal to $2R_\lambda$ when $R_\lambda < R_y$ and $R_\lambda < R_\gamma$ are still optimal for single-rotor helicopters.

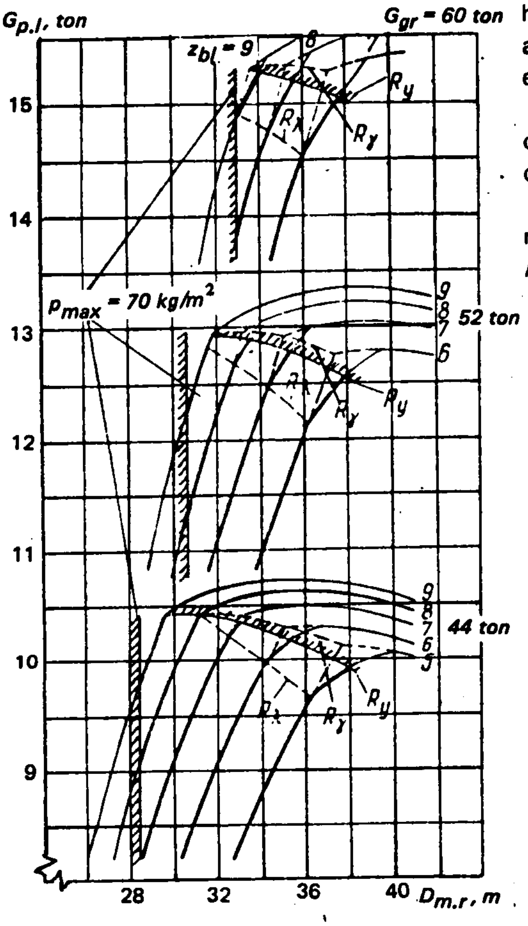

Figure 2.78 Dependence of cargo weight transported by a single-rotor helicopter over a distance of L = 50 km on main-rotor diameter

In nearly all of the cases for the considered helicopters, the constraint reflecting the maximum allowable blade deflection R_y appears somewhat earlier than the coefficient $(k_{bl})_{min}$.

Consequently, for these helicopters, the optimal main-rotor diameter is determined by only two constraints: $\bar{R}\lambda_0$ and $(\bar{y}_R)_{all}$.

For a flight range of 800 km and gross weights no higher than 44 tons considering the $(\bar{y}_R)_{all}$ and $\bar{R}\lambda_0$ constraints, one finds a weak optimum of the transportable cargo weight as a function of the number of main-rotor blades. Thus, the optimal number of blades is $(z_{bl})_{opt} = 8$, for $G_{gr} = 44$ *tons*.

The payload transportable by the single-rotor helicopter over short flight ranges ($L = 50$ *km*) increases with the number of blades (for all considered z_{bl} values) and a corresponding decrease in rotor diameter.

Thus, it turns out that for short ranges, multibladed rotors of smaller diameters are always more favorable, while for long ranges, this is true for rotors with somewhat fewer blades equal to $(z_{bl})_{opt}$ and larger diameters.

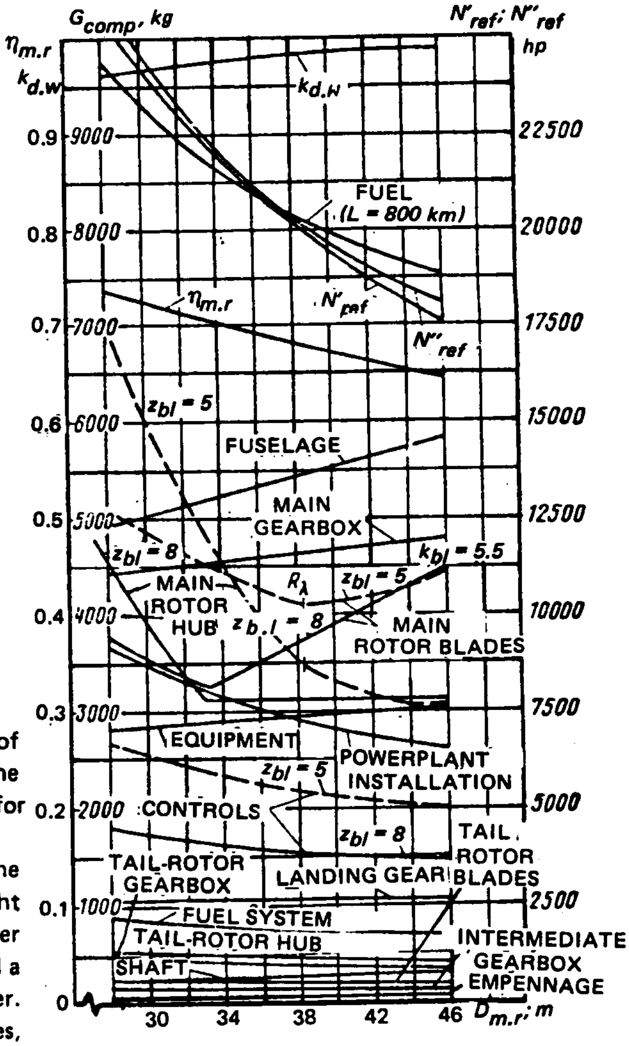

Figure 2.79 Various data for single-rotor helicopter of 52-ton gross weight, shown vs main-rotor diameter

The influence of the main-rotor diameter value on the various data required for calculations of single-rotor helicopters with 5 and 8 blades is shown in Fig 2.79.

Tandem-Rotor Helicopter. Figures 2.80 and 2.81 show the cargo weight (payload) transported by the tandem-rotor helicopter over ranges of 50 and 800 km as a function of the diameter of the main rotor with three, four, five, and six blades for three gross weights. The examined parametric region is bounded on the left by the allowable main-rotor disc loading $p = 45\ kg/m^2$, and on the right by the maximum allowable blade deflection, $(\bar{y}_R)_{all} = 0.12$.

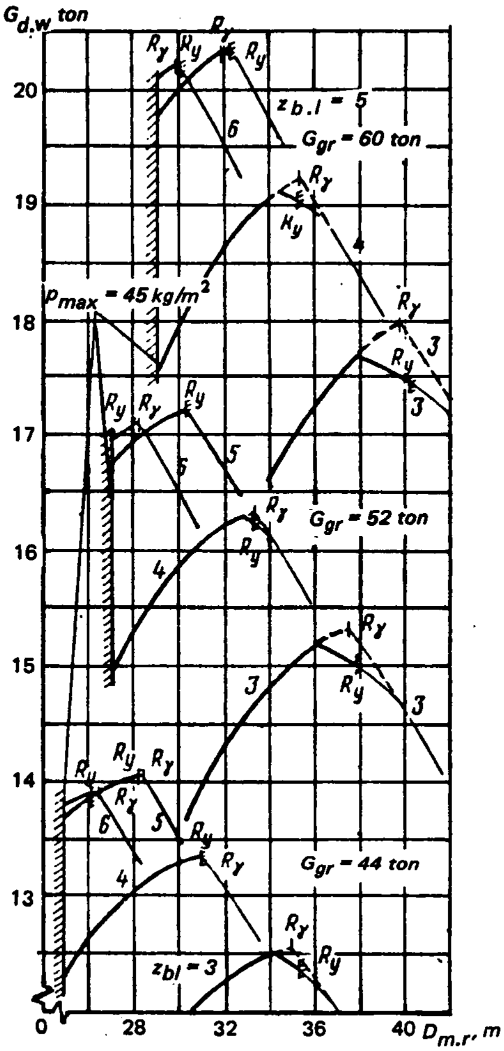

Figure 2.80 Dependence of the tandem-rotor payload on rotor diameter when transported over range L = 50 km

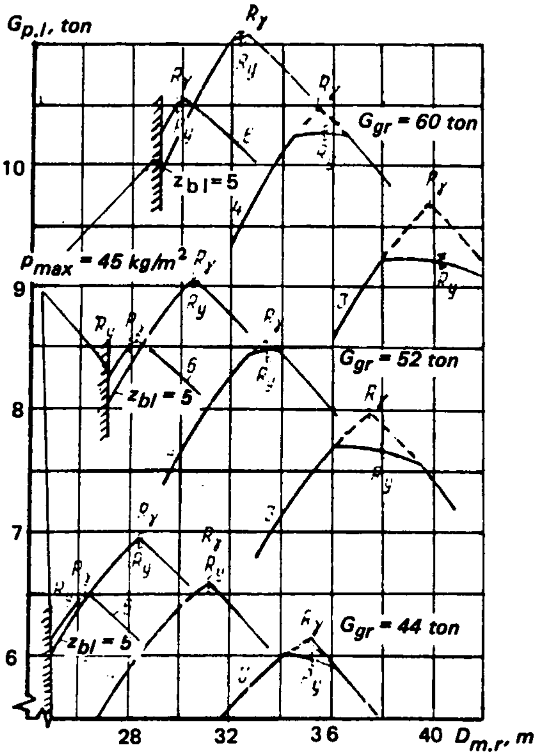

Figure 2.81 Dependence of the tandem-rotor payload on rotor diameter when transported over range L = 800 km

We see from these figures that main rotors with five blades are optimal for the tandem-rotor transport helicopter of the considered lifting capability. The cargo load (payload) which can be transported decreases with both larger and smaller number of blades, including the configuration with six blades.

In contrast with the single-rotor helicopter, the curves of cargo weight transported for diameters lower than optimal are flatter, although they are quite steep near the optimum, and become steeper as the gross weight of the helicopter increases.

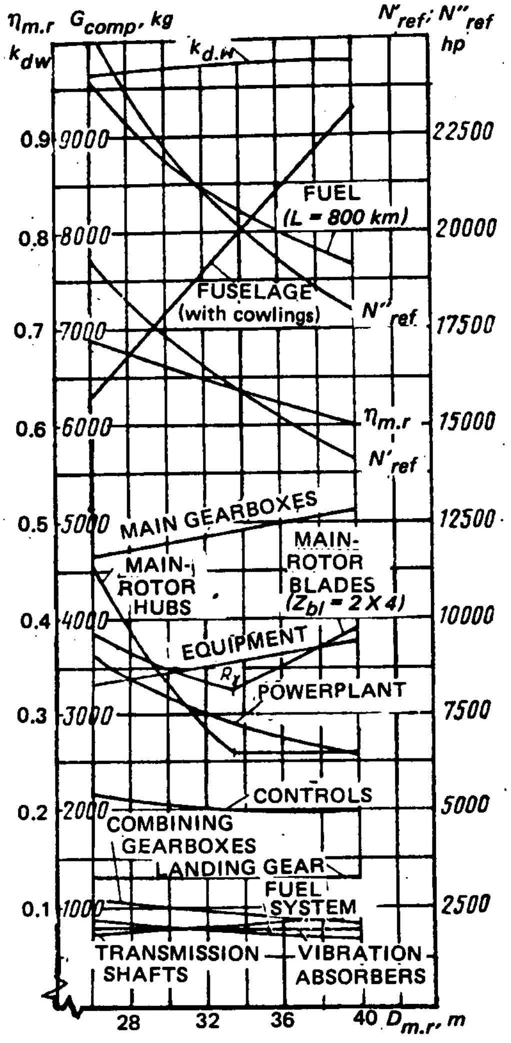

Figure 2.82 Various data for 52-ton gross weight tandem helicopter, shown vs rotor diameter

In practically all cases, transported cargo weight maximum coincides either with the reduced aspect ratio $\bar{R}\lambda_o$, or with the constraint resulting from the maximal allowable blade deflection R_y. the constraint with respect to $(k_{bl})_{min}$ comes into effect for radii greater than the optimal values.

Since, in order to provide more comparable results, the same values of t_{y_o} and U_t (see Table 2.11) were assumed for the single-rotor and tandem configurations, the optimal values of rotor diameters of those helicopters (excluding blades having increased aspect ratio) for each gross weight would occur at the same overall number of blades; for instance at $(z_{bl})_{s.r} = 8$ — $(z_{bl_\Sigma})_{tan} = 2 \times 4$; or at $(z_{bl})_{s.r} = 6$ — $(z_{bl_\Sigma})_{tan} = 2 \times 3$ independent of acting constraints, as all constraints depend on the $G_{gr}/\bar{t} z_{bl_\Sigma}$ parameter only.

Nevertheless, since the considered tandem lifting rotors have a higher number of blades than the single-rotor helicopter—for instance, the optimal parameter $z_{bl_\Sigma} = 10$—consequently, the diameter of the lifting rotors for the optimal variants of tandem helicopters appear to be smaller.

The variation of the quantities used as a function of the rotor diameter are shown in the calculations for the tandem helicopter in Fig 2.82.

Trussed Side-by-Side Rotor Helicopter. The same relationship for a side-by-side rotor helicopter similar to the V-12 with truss-type main-rotor supports and inversely tapered wing, but with multiblade main rotors without overlap are shown in Figs 2.83 and 2.84.

It should be noted that the cargo weight which can be transported by this configuration increases strongly with an increase in the number of main-rotor blades, even for $z_{bl} = 8$ or more.

In nearly all cases, the maximum allowable blade deflection represents the first constraint encountered; although, just as in many of the cases examined earlier, the differences in the main rotor radii corresponding to the different constraints are very small.

Because of the increased weight of the truss-type rotor mounting and the constraint associated with $(k_{bl})_{min}$, the cargo weight (payload) which can be transported decreases very sharply for main-rotor radii larger than the optimal value.

In calculating the truss-type side-by-side rotor helicopter, we used the value $t_{y_0} = 0.171$. Therefore, the optimal main-rotor diameters of this helicopter are somewhat smaller than for the single-rotor and tandem helicopters for the same total number of lifting rotor blades.

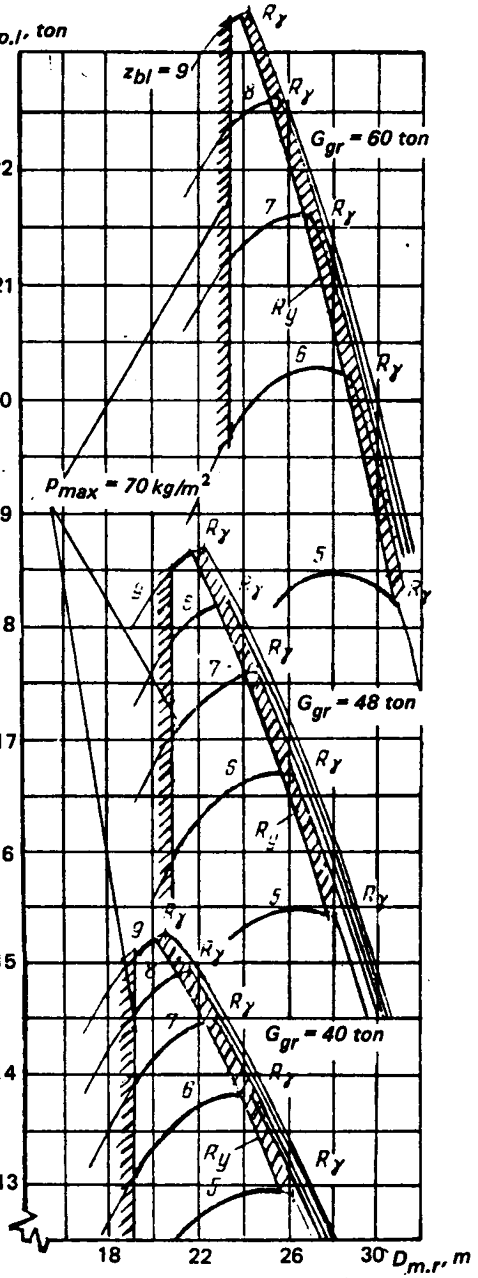

Figure 2.83 Truss side-by-side helicopter payload for 50-km range as a function of main-rotor diameter

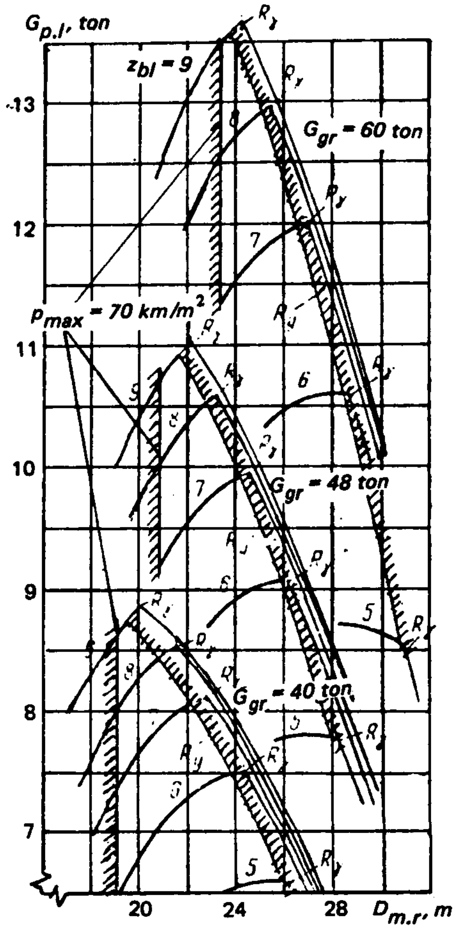

Figure 2.84 Truss side-by-side helicopter payload for 800-km range as a function of main-rotor diameter

The variation of the quantities used as a function of rotor diameter in the calculation for the trussed side-by-side rotor helicopter is shown in Fig 2.85.

Comparison of Cargo Weight Transported by Optimal Variants of Various Helicopter Configurations. Fig 2.86 shows as a function of the gross weight the cargo weight which can be transported over distances of 50 and 800 km by the considered optimal helicopter variants. It can be seen from this figure that the single-rotor helicopter can transport the largest load.

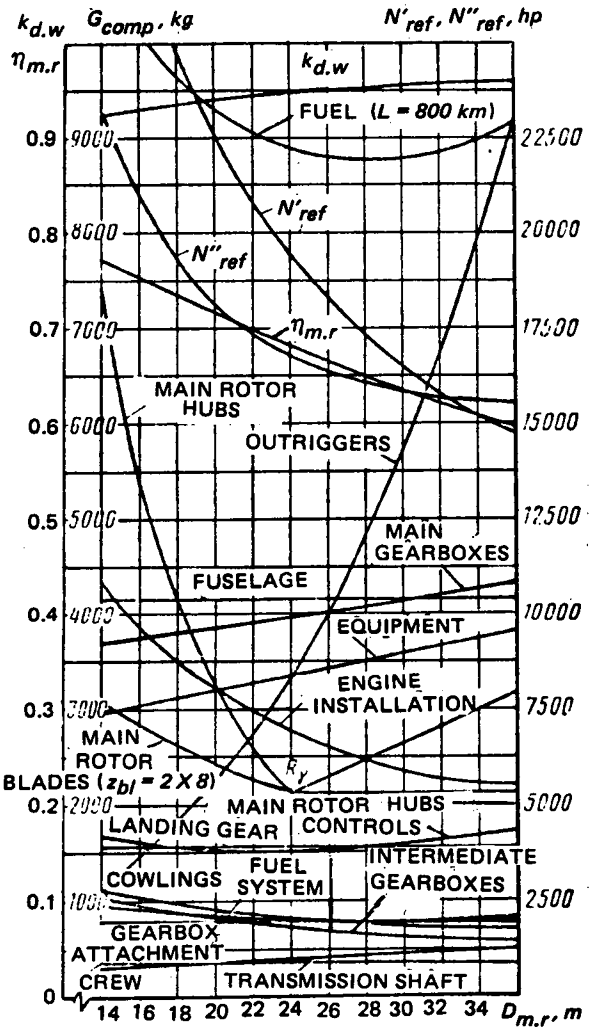

Figure 2.85 Various data for 52-ton gross-weight, truss-type, side-by-side helicopter shown vs rotor diameter

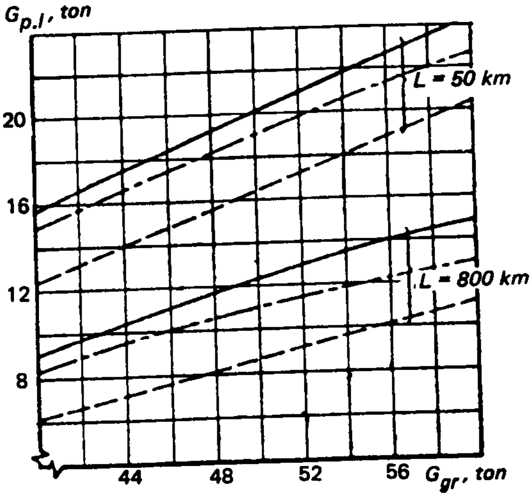

Figure 2.86 Dependence of payload transported by optimal variants on gross weights of various helicopter configurations: ——single-rotor helicopter (z_{bl} = 8); — — —tandem (z_{bl} = 5X2); — - — - side-by-side (z_{bl} = 8X2)

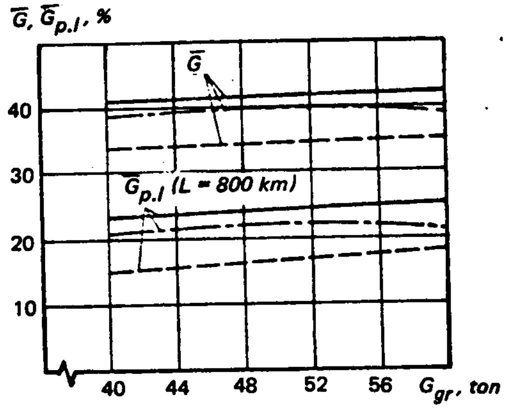

Figure 2.87 Weight output $\overline{G}$ and payload weight efficiency ($\overline{G}_{p.l}$) for optimal variants of various helicopter configurations shown as a function of gross weight: ——single-rotor helicopter (z_{bl} = 8);— — —tandem (z_{bl} = 5X2); — - — —side-by-side (z_{bl} = 8X2)

For the same weight efficiency, the tandem helicopter will transport 3 to 4 tons less cargo over the same distance. The truss-type side-by-side rotor helicopter occupies an intermediate position between the aforementioned configurations—approaching cargo weight transport capabilities of the single-rotor helicopter.

Figure 2.87 shows $\overline{G}$ values and payload weight ratios $\overline{G}_{p.l}$ for optimal variants of the examined helicopter as a function of gross weight. It can be seen from this figure that for the assumed weight coefficients—allowing 10 percent for structural overweight—the weight ratio $\overline{G}$ lies within the limits of 41 to 42 percent for the single-rotor, 39 to 40 percent for the side-by-side, and about 34 to

36 percent for tandem helicopters. In the weight outputs of the examined configurations, we observe the same approximate relationships as in the cargo weights (payload) transported by these helicopters.

In conclusion, it should be noted that helicopter configurations are sometimes compared exclusively or primarily on the basis of their aerodynamic aspects. It is obvious from the calculation results presented here that incorrect conclusions will be reached from such an approach, since the most marked differences between the helicopter configurations show up in the structural weights, and not in the aerodynamic data.

2.5.5 Estimate of Helicopter Maximum Lifting Capability

It is interesting to evaluate the maximum capabilities with respect to the cargo weight which can be transported by the helicopters considered above when constructed at the modern level of weight and aerodynamic efficiency, and under the constraints discussed in Sect 2.3. To evaluate this capability, we shall make calculations of helicopters having gross weights greater than 60 tons using the basic data shown in Tables 2.10 and 2.11. It is obvious that for such a lift capability, the fuselage dimensions should be taken in accordance with the standard fuselage size D (see Fig 2.64). However, in this case, the fuselage weight increases very markedly to the detriment of the cargo weight which can be carried. Therefore, in order to obtain data comparable with that presented above, we shall also make calculations for helicopters with fuselages corresponding to standard fuselage size C. In examining helicopters with standard fuselage size D, we will also make allowance for the increase in equipment weight by determining it from Eq (2.108) for a gross weight of 100 tons.

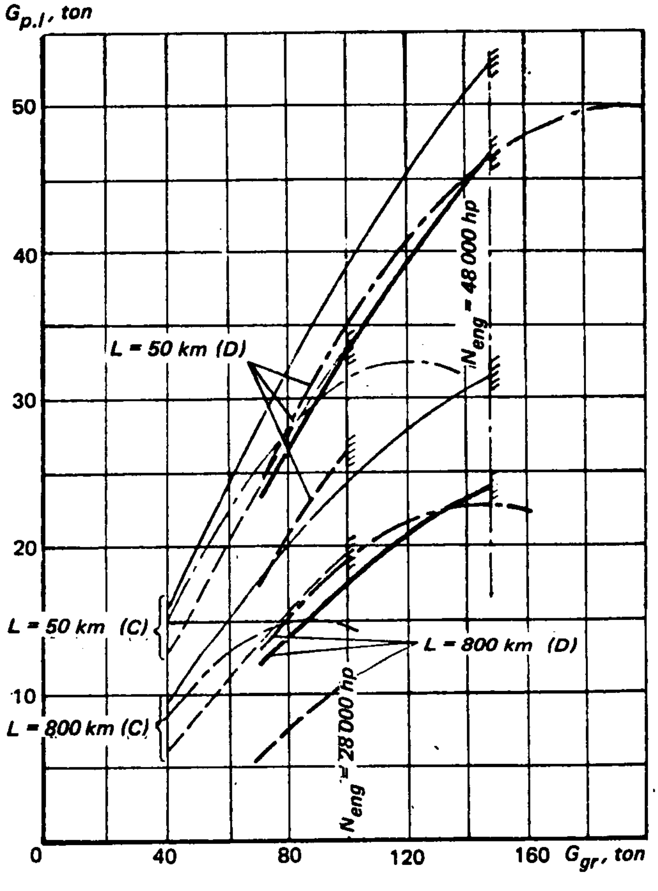

Figure 2.88 Dependence on gross weight of cargo weight transported over distances of 50 and 800 km by single-rotor, tandem, and trussed side-by-side configuration helicopters having fuselages of the C and D types. ——single-rotor, — — —tandem, — · — · —trussed side-by-side

Fig 2.88 shows the absolute cargo weights which can be transported by such helicopters over ranges of 50 and 800 km, and Fig 2.89 shows their weight output $\bar{G}$ and payload weight ratios $\bar{G}_{p.l}$ as functions of the helicopter gross weight. We see from these figures that the maximum gross weight of the single-rotor helicopter cannot be higher than approximately 145 tons since, in this case with three-shaft power input to the main gearbox, the power

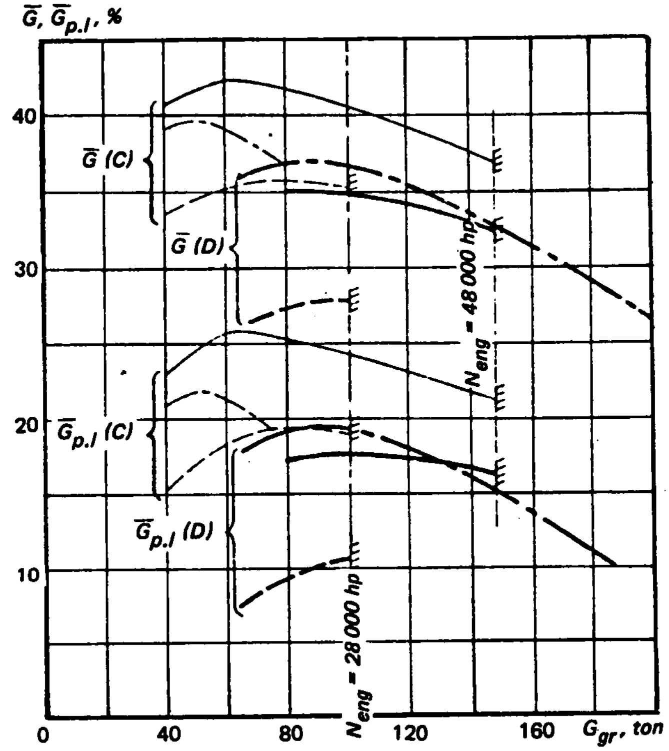

Figure 2.89 Weight ratios $\bar{G}$ and $\bar{G}_{p.l}$ shown vs gross weights for single, tandem, and trussed side-by-side configuration helicopters having E and D type fuselages

transmitted by each of the six bevel gear pairs reaches 8000 hp; i.e., the magnitude which we have assumed to be maximum for transmission by a single bevel gear pair (see Sect 2.3).

The weight ratio of this helicaopter with standard fuselage size C and with the assumed performance decreases by about 5 percent in comparison with the maximum weight ratio achieved for the gross weight class of 60 to 65 tons. For the standard fuselage size D and the corresponding increase in equipment weight, the weight ratio additionally decreases by approximately 5 to 6 percent.

Thus, the single-rotor helicopter with the assumed basic data is capable of hovering out-of-ground effect at $H = 1500\,m$, transporting cargo weighing 53 tons over a distance of 50 km with standard fuselage dimension C, and cargo weighing 47 tons with standard fuselage D. Over a range of 800 km, it could transport 31.5 tons with standard fuselage size C and 24 tons with standard fuselage D. Such a helicopter will have the following parameters: eight-bladed 52-m diameter main rotor with blades having high aspect ratio—for this diameter, $\lambda = 17.7$; blade chord $b = 1.47m$; and its tail-rotor diameter will be about 13 meters.

The weight output of the tandem-rotor helicopter appears about 6 to 8 percent lower than that of the single-rotor helicopter. In addition, because of the limitation of the power transmitted by the bevel gear pairs, the gross weight of the tandem-rotor helicopter with two synchronizing shafts cannot be higher than approximately 100 tons. With this gross weight, the tandem can transport cargo weighing 34 tons over a distance of 50 km with standard fuselage size C, and 26.5 tons with standard fuselage D. For a distance of 800 km, the payload will amount to 19.5 tons with standard fuselage C and 10.5 tons with standard fuselage size D; i.e., significantly less than for the single-rotor helicopter.

The truss-type side-by-side helicopter with standard fuselage size C and truss structural height at $H = 3$ m has a maximum weight output for a gross weight of about 50 tons. The weight output of the helicopter of this configuration decreases quite rapidly at higher gross weights because of the increase in the main-rotor diameters and the corresponding increase in both the dimensions and weight of the outriggers.

With standard fuselage size D and truss structural height $H = 4.3\,m$, the maximum weight output of the truss-type side-by-side rotor helicopter is achieved at gross weights of 80 to 100 tons. As for the constraints with respect to power, they turned out to be higher than for the single-rotor helicopter for all of the examined gross weights. However, because of the higher parasite drag, the cargo weight which can be transported by such a helicopter over a range of 800 km is higher than for the single-rotor helicopter, but only up to gross weights of about 130 tons. At higher gross weights, the single-rotor helicopter has payload advantages.

We note that the performance of the truss-type side-by-side rotor helicopter for takeoff weights over 100 tons could be somewhat improved by increasing the truss structural height above $H = 4.3$ meters.

The constraint resulting from the power transmitted by the bevel gear pairs has practically no influence on the characteristics of this helicopter.

The truss-type side-by-side rotor helicopter with standard fuselage size D, capable of transporting the greatest load over a range of 800 km, would have multibladed ($z_{bl} = 8$ or more) main rotors of about 35 to 36-m diameter.

We see from this data that using the contemporary design approaches and the currently achievable component weight level, the greatest cargo-lifting capability can be reached by single-rotor and truss-type side-by-side helicopters.

2.5.6 Selection of Optimal Single-Rotor Helicopter Tail-Rotor Parameters

The parameters of the tail rotor exert a relatively small influence on the overall helicopter performance; nevertheless, just as the parameters of all the other helicopter components, they should be optimal, since every possibility for structural weight reduction, no matter how slight, must be utilized.

Just as for the main rotor, we shall examine various diameters and numbers of blades, while retaining unchanged the tail-rotor thrust coefficient in hovering out-of-ground effect at $H = 0$. However, the value of the thrust coefficient will be assumed lower than for the main rotor, $(t_{t.r})_o = 0.14$.

When varying the tail-rotor diameter and number of blades, we shall take into account the changes in the weight of the tail-rotor blades, hub, tail and intermediate gearboxes, transmission shafts, fuselage (as a consequence of variation of the distance between the axes of the main and tail rotors) and the tail-rotor control system. We separate the weight of the latter from the overall weight of the control system and then determine its weight by the following formula:

$$G_{t.r_{cont}} = k_{t.r_{cont}}\, z_{t.r}\, b_{t.r}^{2}\, R_{t.r}, \quad \text{assuming } k_{t.r_{cont}} = 40\ kg/m^{3}.$$

We also consider all the other small changes in the weight of the other helicopter components and systems, and the fuel supply in connection with the change in engine-power required because of the difference in the power required by the tail rotor resulting from the $D_{t.r}$ variation.

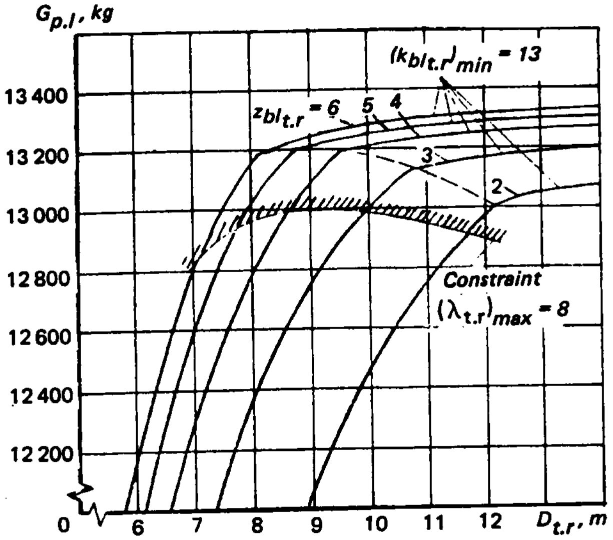

Figure 2.90 Dependence of payload transported over a distance of 800 km on the tail-rotor diameter and number of blades by a 52-ton gross weight, single-rotor helicopter, assuming that the other helicopter parameters remain unvaried ($R_{m.r} = 16.75\,m$)

As an example, the results of one such calculation are shown in Fig 2.90 where, for a helicopter of 52-ton gross weight with constant main-rotor parameters and selected fuselage cargo compartment dimensions, the values of the cargo weight (payload) transported by such a helicopter over a distance of 800 km are shown as a function of tail-rotor diameter and number of blades.

We see from this figure that with an increase of $D_{t.r}$, the cargo weight transported by the helicopter becomes constrained by the maximum allowable tail-rotor blade aspect ratio, which we took as $(\lambda_{t.r})_{max} = 8$ (see Subsection 2.2.7).

We see from these calculations that for tail rotors with different number of blades, the cargo weight transported by the helicopter increases quite rapidly with increase of the tail-rotor diameter and the corresponding increase in the tail-rotor blade aspect ratio up to and including $\lambda_{t.r} = 8$.

Consequently, the optimal tail rotor will always be that with the maximum allowable aspect ratio of its blades.

The optimal number of blades depends on the tail-rotor thrust required. In the considered case (see Fig 2.90), the cargo weight transported by the helicopter is practically the same for a number of blades from $z_{bl_{t.r}} = 3$ to $z_{bl_{t.r}} = 5$, and decreases somewhat for $z_{bl_{t.r}} > 5$ and $z_{bl_{t.r}} = 2$; i.e., the payload optimization aspects do not impose serious constraints on the selection of the number of tail-rotor blades.

The constraint determined by the maximum blade mass characteristic $(\gamma_o)_{max} = 3$ appeared everywhere outside the $\lambda_{t.r} = 8$ constraint.

2.6 Comparison of Pure and Compound Transport Helicopter

Increase in the helicopter flight speed is limited by main-rotor blade stall. In order to delay stall through unloading of the main rotor, a wing can be installed on the helicopter which, at high speeds, would share in the generation of the flight vehicle lift force. Unfortunately, the unloaded main rotor cannot provide the propulsive force necessary for flights at high speed. Therefore, special propulsors must be installed on such a flight vehicle—either airplane-type propellers, or turbofans. This type of flight vehicle is termed a compound helicopter.

In the hover regime, both the propulsors and the wing represent not only unnecessary ballast which reduces the useful load, but is also a source of additional power losses: the wing because of download losses, and the propellers because of their operation in idling. In hover, up to 3 to 5 percent of the power transmitted to the main rotor is expended in rotating the propeller at zero thrust.

In forward flight when the lift is generated by the wing, and the specially installed powerplants are used to obtain the propulsive force, the main rotor with its controls and transmission becomes a parasitic component which increases the parasite drag of the compound helicopter. Therefore, for the same weight efficiency of the components and the same gross weight, but for different flight speeds, the cargo weight transported by the compound helicopter will always be smaller than that transported by the pure helicopter.

The question is: can the compound helicopter, in spite of its smaller useful load but thanks to its higher flight speed, provide greater productivity than the pure helicopter and, if so, how much higher?

Since we are considering only transport aircraft. we shall compare their productivity in cruise over a given range.

It is not difficult to imagine compound helicopters developed on the basis of helicopters of all the known configurations. But if we recall that the additional components installed on the pure helicopter to convert it into a compound would significantly reduce the useful load transported by the vehicle, the most logical approach appears to begin with a configuration showing the highest weight output; namely, with the single-rotor helicopter (Fig 2.91).

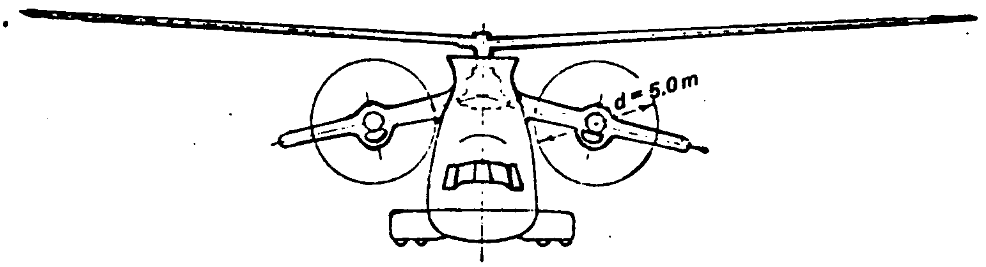

Figure 2.91 Scheme of a compound helicopter of single-rotor configuration

However, conversion of the side-by-side helicopter with a wing into a compound has certain advantages since it already has a wing which need not be added (Fig 2.92). Consequently, it can be shown that its weight increase will be less than for the other configurations. However, calculations show that this advantage is not decisive, since the use of very powerful and consequently, quite heavy, powerplants and propulsors which, for configurational reasons are best located at the wing tips, leads to further increase of the wing weight, which is already heavy in the pure helicopter of this configuration because of the necessity for ensuring the required stiffness of the main-rotor supports located at the wing tips (see Subsection 2.2.8). For the same reason—as will be discussed later—it is not possible to achieve a very high wing L/D ratio in this compound helicopter configuration.

The development of a compound helicopter from the pure tandem-rotor helicopter is least favorable, both with respect to weight considerations and because of difficulties of a configurational nature. It is not advisable to install the wing in the middle of the helicopter—the region of highest downwash velocities arising in the rotor overlap region. Installation of two wings below the forward and aft rotors would complicate the configuration of the compound

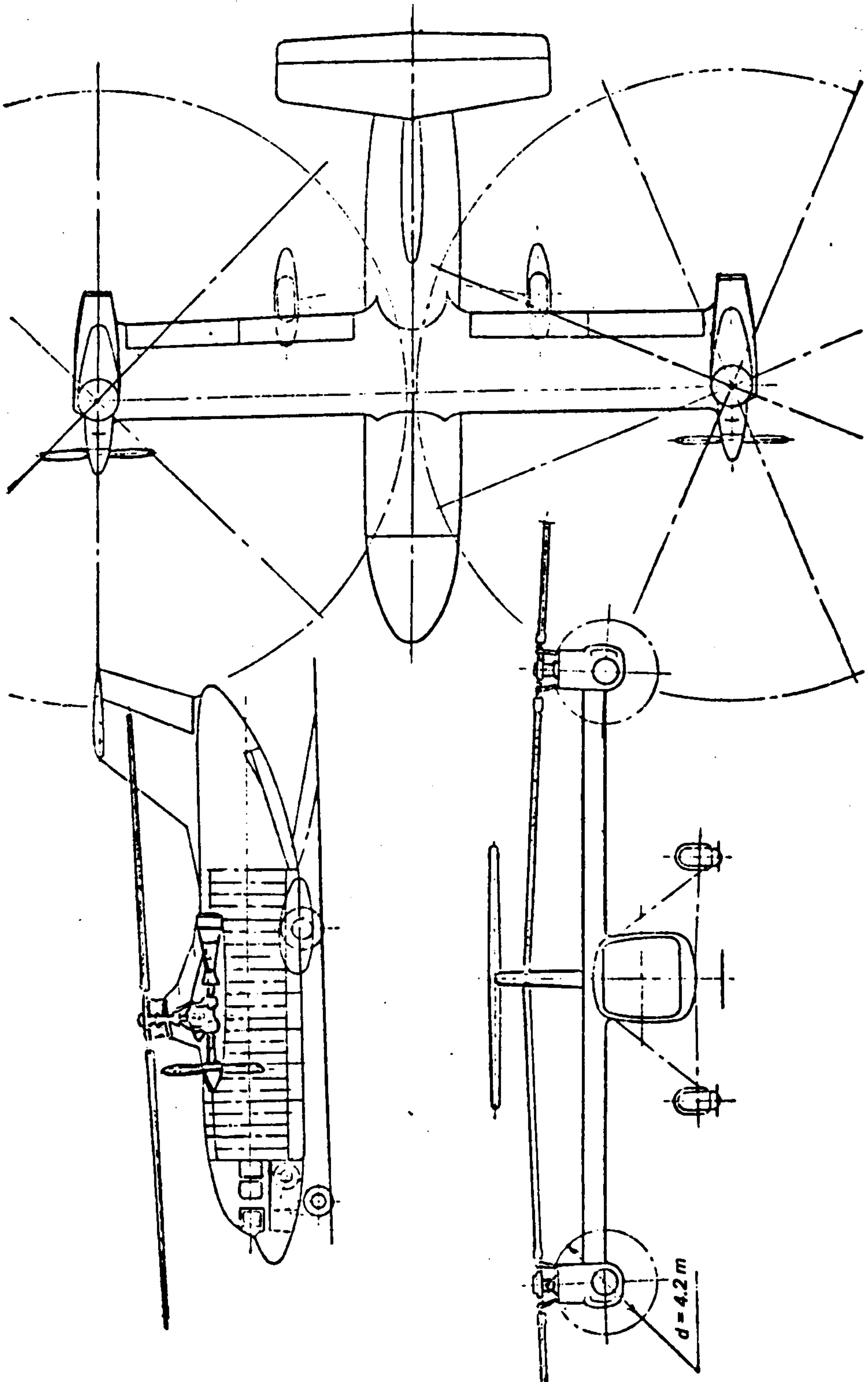

Figure 2.92 Three-view drawing of a side-by-side compound helicopter configuration

helicopter still further. In addition, major difficulties may arise because of the very complex transmission required in this layout.

We a priori exclude the schemes with independent powerplants for main rotors and propulsion from consideration since, in this case, either in hover or at high forward speeds, one of the two powerplants is entirely parasitic, in addition to the previously-mentioned components, which further increases the compound helicopter structural weight.

We shall examine compound helicopters with cruise speeds from 350 to 450 km/hr, bearing in mind that flight speeds up to 350 km/hr can be achieved with lower weight penalties on the helicopter with a wing.

2.6.1 Determination of t_{y_o} with Account for the Compounding Effect

In selecting the parameters of the compound helicopter, we must take into account the so-called "compounding effect" which leads to the possibility of using lifting rotors with reduced solidity in comparison with the pure helicopters. Such rotors can have somewhat lower power required in hover, and the required stall margin in level flight, thanks to rotor unloading by the wing lift force. Use of the "compounding effect" makes it possible to lighten the lifting rotors of the compound helicopter. In the design process, this approach is reduced to specifying a higher value of the rotor thrust coefficient t_{y_o}, based on the vehicle gross weight in hover at $h = 0$.

If it is required that the compound helicopter be able to fly at the service ceiling of $H = 4500\ m$ within some speed range, beginning with a speed of about 160 km/hr, it should be realized that even at such a low velocity ($\overline{V} = 0.2$), the wing can generate a lift which makes it possible to reduce the rotor thrust coefficient by $\Delta t_y = 0.03$, and, in accordance with Fig 2.46, the value of t_{y_o} can be determined as

$$t_{y_o} = (0.225 + 0.03)\Delta[(\omega R)_s / (\omega R)_o]^2 = 0.18;$$

i.e., the value of this coefficient can be assumed as somewhat higher than that for helicopters.

Even if we do not impose the requirements noted above with respect to minimal flight velocity at $H = 4500$ meters, t_{y_o} cannot be increased above 0.18 for many other reasons. The main rotor efficiency in hover at the specified hover ceiling, or under similar air density conditions in hot weather at $H = 0$, would decrease markedly with a further increase of t_{y_o}. By the same token, in flight at low speed, when the wing develops a small, or even negative, lift force, the helicopter can easily encounter main-rotor stall in the case of small overloads; for example, in deceleration prior to landing.

2.6.2 Compound Helicopter Main-Rotor Tip Speed and Its Variation as a Function of Flight Conditions

Several studies have been made of compound helicopter designs in which it is proposed to reduce the main-rotor rotational speed $(\omega R)_{m.r}$ at high flight speeds in order to reduce the parasite drag. In this case, the compound helicopter lift force is practically completely provided by the wing and the propulsive force by the propulsors. The power required to turn the main rotor decreases significantly in such designs.

Reduction of $(\omega R)_{m.r}$ makes it possible to reduce the engine power required and the fuel supply for flight over the specified range, but makes the main rotors with their transmissions nearly completely dead weight in flight at high speeds. The propulsor which, in this case, creates practically the entire propulsive force of the compound helicopter, must be more powerful and consequently, heavier, which reduces the possibility of obtaining a large improvement in useful load in this layout.

In realizing this scheme, significant technical difficulties arise in reducing the main-rotor rotational speed in flight at high speeds. Discarding as impractical the schemes with use of various clutches and gear shifts, we shall consider that this reduction is feasible only by regulating the rotational speed of the free-turbine engine. However, in this case, an obvious contradiction arises in the required laws of variation in the various flight regimes of the main-rotor and engine rotational speeds. The propulsor speed must be reduced in the hover regime and increased to the design value at the cruise speed of flight, while the main-rotor speed would vary in reverse order. This approach can be realized only with the use of combined engines with two free turbines.

When using engines with a single free turbine, this rotational speed reduction cannot be more than 10 to 15 percent. It is not possible to count on the marked change of the compound helicopter characteristics in this case. Therefore, in the present section, we shall examine only compound helicopters with small variation of the main-rotor speed for which, just as for the helicopters, $(\omega R)_{m.r}$ increases by 5 percent (in comparison with the hover regime) at moderate flight speeds and high altitudes, including flight at H_s; and decreases by 5 percent at V_{cr}. The absolute magnitude of the $(\omega R)_{m.r}$ increase is limited by the Mach number because of the appearance of the wave drag on the tip sections of the advancing blade. However, considering that the lifting rotor weight increases significantly with reduction of the tip velocity, the Mach number at the tip of the advancing blade should be as high as possible. Therefore, we take the values of $(\omega R)_{m.r}$ shown in Fig 2.93 as a constraint for the main-rotor tip speeds.

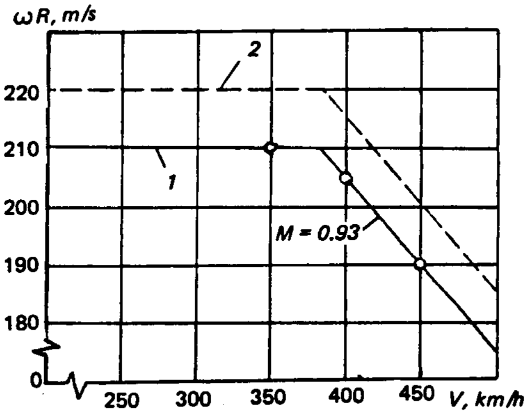

Figure 2.93 Assumed main-rotor tip speeds of compounds designed for (1) various cruise speeds, and (2) corresponding tip speeds in hover.

2.6.3 Number of Blades, Diameter, and Possible Lift of Main Rotors of Compound Helicopters

In the preceding section, it was shown that the optimal main-rotor diameter for the pure helicopter corresponds to the minimum rotor weight. To achieve this goal, it was advantageous to use main rotors with the maximum number of blades. It is obvious that this conclusion also applies to compound helicopters. However, considering the increased complexity of the main-rotor hubs, we introduce a constraint regarding the number of blades, assuming that there cannot be more than $z_{bl} = 8$ blades.

Then, assuming $z_{bl} = 8$, and taking into consideration the fact that for the sizes considered below, the main-rotor radius is first constrained by the allowable blade deflection y_R, we find that radius either from Eq (2.123) or Fig 2.59.

It follows from the calculations presented below that the most advantageous flight regime of a compound, from the point-of-view of transported cargo weight, is when the lifting rotor develops lift as close as possible to its maximum value as given by the blade stall limit.

It is obvious that this regime cannot be used in practice since, under rough air conditions, and when maneuvering the compound helicopter, the main-rotor angle-of-attack continuously varies, and a small increase in the thrust will trigger blade stall, as a result of which, the alternating loads in many components of the compound helicopter will increase markedly. Therefore, it is necessary to have a definite stall margin with respect to the main-rotor thrust. However, in this respect, we shall not specify any definite values in the following calculations, considering that the introduction of such requirements would be premature and not sufficiently justified experimentally.

2.6.4 Requirements to Ensure Main-Rotor Blade Fatigue Strength

With an increase in the flight speed, the alternating stresses in the main-rotor blades increase markedly. This increase becomes still more intense because of the need for reducing the rotor tip speed (see Subsection 2.6.2). Therefore, the development of main rotor blades for the compound helicopter designed for high flight speeds is a much more difficult problem than for the pure helicopter.

The most effective way to reduce the alternating stresses in the blade is to unload the main rotor of the compound helicopter by a wing. To ensure fatigue strength of the blade designs used at the present time, the degree of main-rotor unloading should be considerably higher than that which is optimal with regard to maximum cargo weight transported. Therefore, in order not to depart too far from the optimal flight regimes, we shall consider that the blade strength under high alternating stresses is ensured through use of modern high-strength materials.

However, we shall avoid all other aerodynamic performance improvement techniques which lead to an increase in the alternating stresses in the blades; increased blade twist, for example.

2.6.5 Aerodynamic Characteristics of Compound Helicopter Main Rotor

In selecting the aerodynamic parameters of the compound helicopter main-rotor blades, we are guided by the same considerations used in designing transport helicopter blades.

For the compound helicopter, just as for the pure helicopter, it is important to have an adequate margin with respect to main-rotor blade stall. This margin must be provided at moderate flight speeds up to the maximum usable altitude, when main-rotor unloading by the wing is slight. Therefore, it is not recommended to use airfoil sections with relative thickness lower than 10 to 11 percent for the blade tip region, since thinner sections have lower $c_{y_{max}}$ values.

In spite of main-rotor unloading by the wing, the problem of ensuring blade strength, particularly at high flight speeds, remains even more serious for the compound helicopter than for the pure helicopter and, in order to reduce the alternating stresses in the blade, it is necessary to use blades with moderate aerodynamic twist. Calculations show that increasing the twist above 6 to 8 degrees leads to definite difficulties in ensuring blade strength.

Therefore, for the compound helicopter, we shall examine conventional main rotors with the same aerodynamic parameters as for the pure helicopters.

Figs 2.94, 2.95, 2.96, and 2.97 show the aerodynamic coefficients m_Q and t_x for such rotors as a function of the ratio of the main rotor thrust to compound helicopter gross weight $\bar{T}_{m.r} = T_{m.r}/G_{gr}$ for four flight speeds: 260, 350, 400, and 450 km/h.

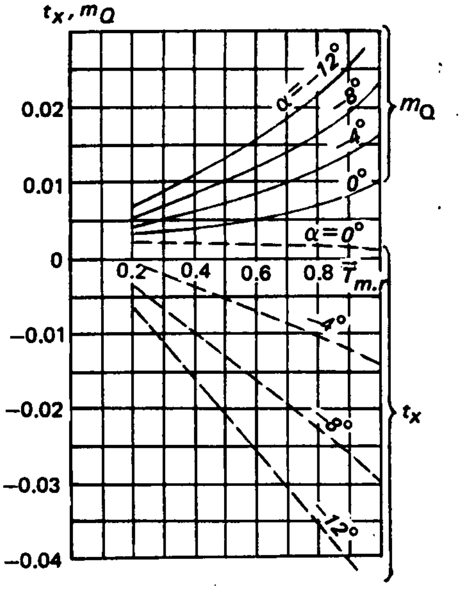

Figure 2.94 Aerodynamic coefficients m_Q and t_x as a function of the main-rotor relative thrust defined by the coefficient $\bar{T}_{m.r}$ for 260 km/h speed with ωR = 210 m/s, H_{cr} = 500 m std., and σ = 0.116.

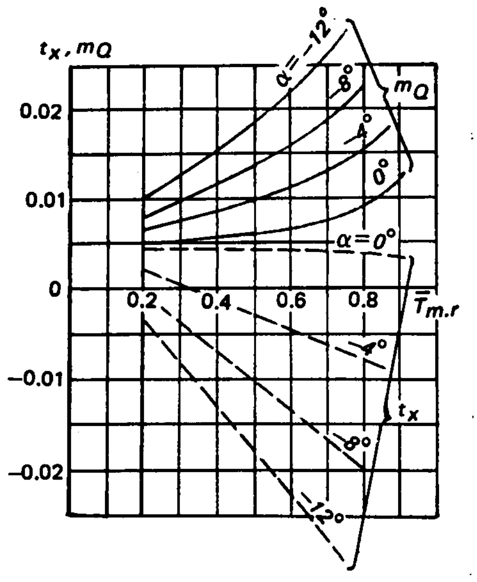

Figure 2.95 Aerodynamic coefficients m_Q and t_x as a function of the main-rotor relative thrust defined by the coefficient $\bar{T}_{m.r}$ for 350 km/hr speed with ωR = 210 m/s, H_{cr} = 500 m, std, and σ = 0.116

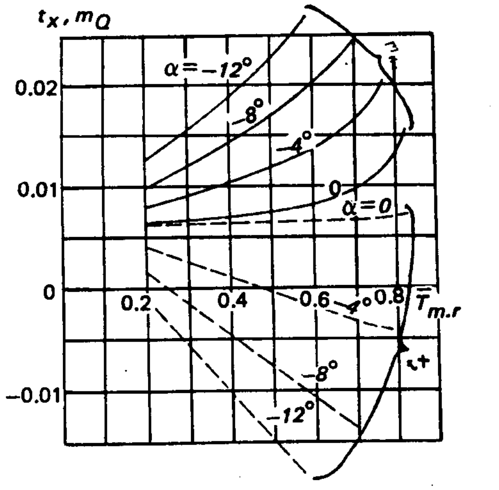

Figure 2.96 Aerodynamic coefficients m_Q and t_x as a function of the main-rotor relative thrust defined by the coefficient $\bar{T}_{m.r}$ for 400 km/hr speed with ωR = 190 m/s, H_{cr} = 500 m, std., and σ = 0.121

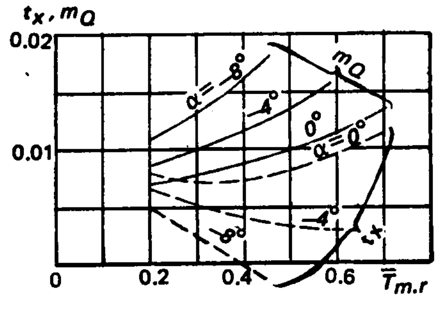

Figure 2.97 Aerodynamic coefficients m_Q and t_x as a function of the main-rotor relative thrust defined by the coefficient $\bar{T}_{m.r}$ for 450 km/hr speed with ωR = 205 m/s, H_{cr} = 500 m, std., and σ = 0.14

For a selected value of t_{y_o}, the quantity $\overline{T}_{m.r}$ can be found from the formula

$$\overline{T}_{m.r} = (\rho_{cr}/\rho_o)\,[(\omega R)_{cr}/(\omega R)_h]^2\,(t_y/t_{y_o});$$

where ρ_o and ρ_{cr} are the ISA densities for $H = 0$ and at the altitude used for cruising flight. We shall take this altitude as 500 meters, just as for the pure helicopter.

Since trimming of the compound helicopter at high flight speeds is best accomplished with the aid of airplane-type control surfaces, the angles-of-attack on the characteristic curves are given from trimmed main rotors, for which the moments $(M_{hub})_x$ and $(M_{hub})_z$ on the hub are made equal to zero by tilting the swashplate.

The main rotor L/D calculated from these characteristics

$$K_{m.r} = t_y / [(m_Q/\overline{V}) + t_x] \qquad (2.176)$$

has a maximum $(K_{m.r})_{max} = 7.5$ at $V = 260$ *km/hr*, and $(K_{m.r})_{max} = 4.6$ at $V = 450$ *km/hr*.

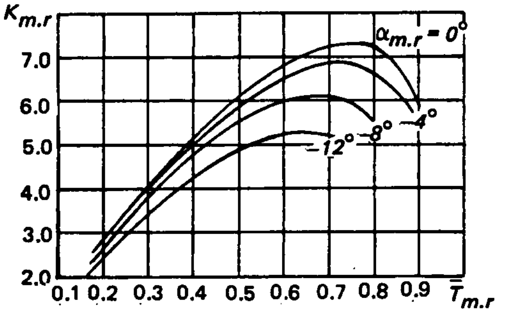

Figure 2.98 Main rotor L/D plotted from the aerodynamic characteristics shown in Fig 2.95 for V = 350 km/hr and ωR = 210 m/s

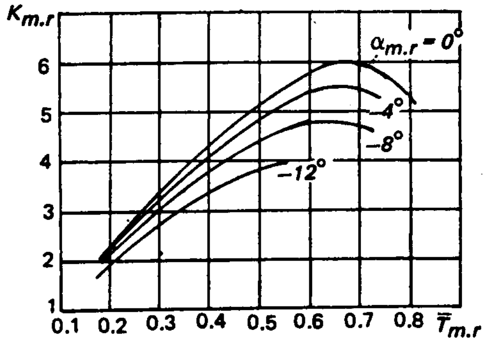

Figure 2.99 Main rotor L/D plotted from the aerodynamic characteristics shown in Fig 2.96 for V = 400 km/hr and ωR = 205 m/s

The dependence of $K_{m.r}$ on the ratio of the main rotor thrust to the gross weight $\overline{T}_{m.r}$ for several main-rotor anglesof-attack and flight speeds of $V = 350$ and 400 *km/h* as shown in Figs 2.98 and 2.99. The maximum L/D values for various flight speeds are shown in Fig 2.100.

Figure 2.100 Maximum main-rotor L/D as a function of flight speed for the aerodynamic characteristics shown in Figs 2.94 through 2.97

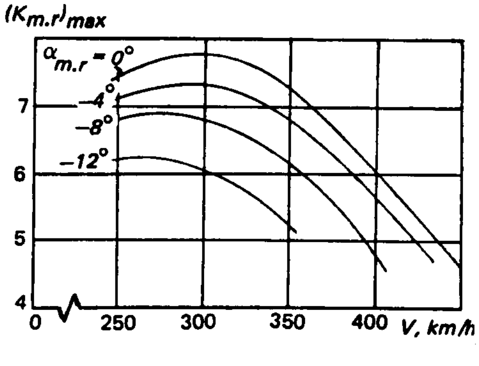

2.6.6 Method for Selecting Optimal Distribution of Lift Between the Main Rotor and the Wing, and Power Between the Main Rotor and Propulsor

The optimal relationship between main-rotor lift and wing lift, and the corresponding distribution of power between the main rotor and the propulsor are often found from the condition of minimizing the power required by compound helicopters. In many cases, this approach yields quite satisfactory results since, at high flight speeds, the power required increases sharply and consequently, the weight of the powerplant installation as well as the fuel. Both of these factors become of prime importance in determining the payload of the compound helicopter.

However, the weight of the propulsor, particularly if this is a propeller requiring transmission for its rotation, constitutes a significant fraction of the overall structural weight. Consequently, it is important to know the fraction of the overall propulsive force provided by the propulsor since its weight and therefore, the payload, depends on this relationship which was not considered when selecting the design parameters on the basis of minimum engine power required.

Therefore, the optimal relationship between the main rotor and wing lift, as well as the power distribution between the main rotor and the propulsor, can be determined only as a result of calculations culminating in the determination of the cargo weight that can be transported by the compound helicopter. This problem will be discussed below.

2.6.7 On Selection of Wing Dimensions and Characteristics for Side-by-Side Type Compound Helicopters

If the wing of the side-by-side compound helicopter is selected solely on the basis of aerodynamic considerations, it will turn out to be either insufficiently rigid to prevent "ground-resonance" type vibrations in the air, or will be excessively heavy.

Therefore, the wing dimensions, especially area S_{wg} and relative airfoil thickness $\bar{h}$, should be selected taking into account the requirements of stiffness and minimal weight of the wing. If, in attempting to increase the wing L/D, its airfoil relative thickness $\bar{h}$ is taken equal to 0.12 ... 0.14, then in accordance with Eq (2.81), the optimal wing area (selected on the basis of minimizing $G_{wg} + \Delta T_{m.r}$) would be too large and, because of the low value of the c_y coefficients, the obtained wing L/D ratio would be inadequate.

Therefore, in order to reduce the weight of the wing and improve its L/D by reducing the wing area and approaching optimal values of c_y, the relative thickness of the wing section must be increased. However, considering that an excessive increase in the relative thickness of an airfoil also leads to a reduction in its maximum L/D, we establish the value of $\bar{h} = 0.2$ as a limit.

Taking the above arguments into consideration, the wing aspect ratio which was selected on the basis of the $G_{wg} + \Delta T_{m.r}$ minimization, does not come out higher than $\lambda_{wg} = 4 ... 4.5$.

For configurational reasons, it is desirable to reduce the wing incidence angle as much as possible. Therefore, a profile with the highest possible α_o value would be selected for the wing.

Figure 2.101 shows K_{wg} as a function of c_y for a wing with aspect ratio $\lambda_{wg} = 4.5$, and one of the acceptable airfoil sections with relative thickness $\bar{h} = 0.2$.

We see from this figure that the maximum L/D of this wing is no higher than $(K_{wg})_{max} = 14.5$, which constitutes a well-known drawback of the side-by-side compound helicopter configuration.

For the single-rotor helicopter, it is possible to develop a wing with $(K_{wg})_{max} = 21$ to 25.

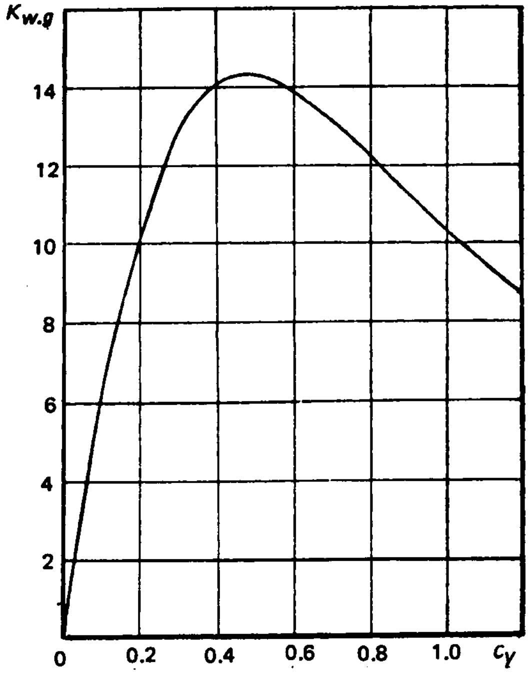

Figure 2.101 $(L/D)_{wg}$ as a function of c_y for a wing with characteristics ($\lambda_{wg} = 4.5$, $\bar{h} = 0.2$) suitable for a side-by-side compound helicopter

2.6.8 Propulsor Thrust

The propulsor thrust in flight at the cruise speed can be found from the expression:

$$T_{prop} = T_x + T_y \Delta\alpha_{m.r} + X_{wg} + Y_{wg}\,\Delta\alpha_{wg} + Q_{par} \tag{2.177}$$

where T_x and T_y respectively, are the main rotor drag and lift along the axes of flow deflected because of wing-rotor interference; X_{wg} and Y_{wg} respectively, are the wing drag and lift, also along axes fixed with respect to the deflected flow; Q_{par} is the parasite drag of non-lifting compound helicopter components; and $\Delta\alpha_{m.r}$ and $\Delta\alpha_{wg}$ respectively, are the increments of downwash angles at the main rotor and wing because of the mutual main-rotor and wing interference. We find the values of $\Delta\alpha_{m.r}$ and $\Delta\alpha_{wg}$ from the following formulae:

$$\Delta\alpha_{m.r} = [\chi_{m.r}(c_y)_{wg}/\pi\lambda_{wg}] + (\chi_{co}\sigma t_y/4\mu^2) \tag{2.178}$$

and

$$\Delta\alpha_{wg} = \chi_{wg}c_T/4\mu^2 \tag{2.179}$$

in which we take $\chi_{m.r} = 0.12$, $\chi_{wg} = 0.8$, and $\chi_{co} = -0.35$ for the side-by-side compound helicopter configuration.

2.6.9 Propulsor-Type Selection

Two types of propulsors can be considered for the compound helicopter; namely, airplane-type propellers, or fans which have a smaller disc area than propellers with correspondingly higher solidity and an outer cowling, or shroud as it is sometimes termed.

Designs incorporating the fan built into the engine itself which, in this case, is termed a bypass turbofan engine, are better from an installation and weight viewpoint.

When the fan is separated from the engine, the powerplant configuration becomes more complicated because additional angle gearboxes with high-speed connecting shafts are required. The weight of such a powerplant is significantly higher. Therefore, we shall not examine this propulsor version. Use of the turbofan propulsor makes it possible to obtain a more compact aircraft, and facilitates a solution of the vibration problems which often develop in vehicles with a propeller; but, as will be shown later, is unfavorable from the viewpoint of weight.

The primary difference between the fan and the propeller from the aerodynamic viewpoint is the much higher disc loading and correspondingly higher velocity of the airstream discharged by the fan. While for the optimal parameters of the propeller for the compound helicopter, the disc loading is about $p = 200\ kg/m^2$ and no more than $p = 300\ kg/m^2$; for the modern bypass turbofan engines, a loading on the order of $p = 3000$ to $4000\ kg/m^2$ is used. This high loading reduces the propulsive efficiency in spite of the fact that in compound helicopters this efficiency improves somewhat more than for the propeller because of the influence of the shroud which prevents contraction of the slip-stream discharging from the fan or even somewhat increases its cross-section.

If we assume that the section-area of the slip-stream leaving the fan remains constant, the ideal thrust efficiency of the fan can be found from the formula

$$(\eta_T)_{fan} = 1/(\tfrac{3}{4} + \tfrac{1}{4}\sqrt{1 + 4p/\rho V^2}). \tag{2.180}$$

The ideal propeller thrust efficiency is found from the formula

$$(\eta_T)_{prop} = 1/(\tfrac{1}{2} + \tfrac{1}{2}\sqrt{1 + 2p/\rho V^2}). \tag{2.181}$$

The relative efficiency of the propeller and fan can be written as

$$\eta_{rel} = 1/[1 + (c_x/4t\overline{V})\eta_T] \tag{2.182}$$

where $\overline{V} = V/U_t$.

The values of c_x for a propeller with tip speed $U_t = 285\ m/s$ and solidity $\sigma \approx 0.2$ are shown in Fig 2.102.

The overall propulsive efficiency of the propulsor can be found from the formula

$$\eta_{pr} = \eta_T \eta_{rel}. \tag{2.183}$$

The efficiencies obtained from these formulae are shown in Fig 2.103. From the performed calculations it was found that the optimal parameters for the propeller are $t_{prop} \approx 0.175$ and $c_x = 0.025$. For the fan we take $t_{fan} = 0.25$ and $c_x \approx 0.075$.

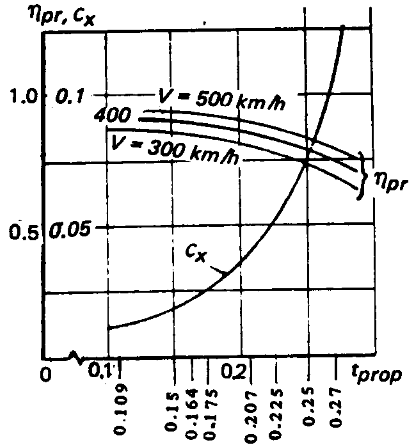

Figure 2.102 Dependence of coefficient c_x on thrust coefficient t_{prop}, obtained from characteristics of a propeller with tip speed $\omega R = 285\ m/s$ and solidity $\sigma \approx 0.2$, and corresponding efficiencies calculated using Eq (2.183)

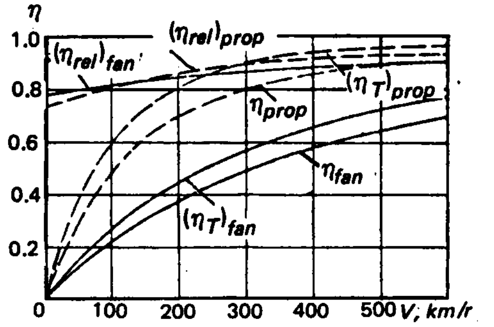

Figure 2.103 Thrust $(\eta_T)_{prop}$, relative $(\eta_{rel})_{prop}$, and overall propulsive efficiencies η_{pr} for propellers; and analogous efficiencies of the fan with $p_{fan} = 3000\ kg/m^2$

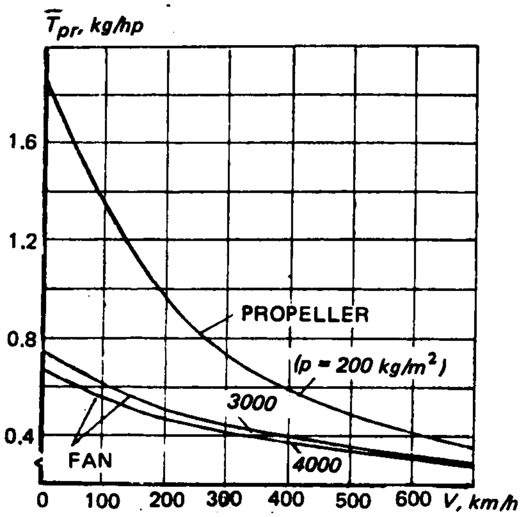

Figure 2.104 Ratio of thrust to power expended as a function of flight speed for propeller and fan

The ratio of the obtained propulsing thrust to the power expended can be defined as

$$\overline{T}_{pr} = T_{pr}/N_{pr} = 75\eta_T\eta_{rel}/V \qquad (2.184)$$

Figure 2.104 shows $\overline{T}_{pr}$ as a function of flight speed for a propeller with $p = 200\ kg/m^2$ and a fan with $p = 3000$ to $4000\ kg/m^2$.

From this graph, we see that for the same power available, the fan thrust is significantly lower than for the propeller, and according to this data, the fan approaches the propeller only at speeds near 700 km/hr.

However, the fan is much lighter than the propeller. Therefore, the final decision on the optimal propulsor type can be made by examining the sum of the weights of all the compound-helicopter elements which depend on the propulsor type.

Let us examine how the ratio of the overall weight of these elements (i.e., weight of the propeller, increment of the powerplant installation, and fuel required for flight over a given distance) to the propulsor thrust will vary with the speed of flight.

The magnitude of this ratio can be calculated from the following approximate formula:

$$\Delta\overline{G}_{psor} = \overline{G}_{psor} + [\gamma_{eng.ins} + k_T(c_e)_{cr}(L/V)]\ V/270\eta_T\eta_{rel}. \qquad (2.185)$$

Here, $\Delta\overline{G}_{psor}$ = the ratio of overall weight of all the compound helicopter elements which depend on the propulsor type, to its thrust; and $\overline{G}_{psor}$ = the ratio of the propulsor weight to its thrust. For the optimal propeller variants examined below, consisting of blades, hub, and reduction gearing, this quantity varies as a function of propeller power within the limits of $\overline{G}_{psor} = \overline{G}_{prop} = 0.2$ to 0.21. In the case of turbofans, we shall set $\overline{G}_{psor} = 0$; and consider the fan weight as part of the engine weight as defined by the powerplant weight coefficients, $\gamma_{eng.inst}$. In the propeller case, we take this coefficient as equal to $\gamma_{eng.inst} = 0.143$ in accordance with Table 2.10. In modern turbofan engines for compound helicopters, we assume that it is possible to achieve specific weights of such engines corresponding to the coefficient $\gamma = 0.14$ to $0.15\ kg/hp$. With account for the weight of the powerplant installation (see Subsection 2.2.9), we take $\gamma_{eng.inst} = 0.19$. With respect to engine sfc at the cruise-flight speed $(c_e)_{cr}$, we take it to be the same in the versions being compared and equal to $(c_e)_{cr} = 0.21\ kg/hp.hr$, although the fuel flow rate may be somewhat higher for the turbofan engines with two free turbines. The flight velocity V in Eq (2.185) should be in km/hr.

We note that the changes in the powerplant cowling weight, and wing weight of the side-by-side helicopter which depend on the installed engine power, are assumed as small and thus, do not appear in Eq (2.185).

Values of $\Delta\overline{G}_{psor}$ are shown in Fig 2.105 for the powerplant types being compared for two compound helicopter flight ranges. We see from this figure that the propeller is better on the basis of weight for both the 400-km and 800-km ranges. Therefore, we shall examine only airplane-type propellers as propulsors in application to transport compound helicopters.

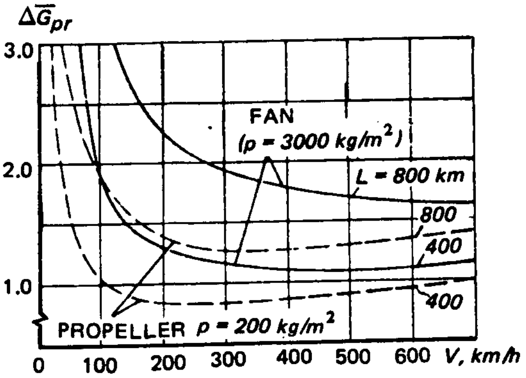

Figure 2.105 Relative overall weight of compound helicopter components whose weight depends on the propulsor type is shown as a function of flight speed for a propeller and fan

2.6.10 Selection of Propeller Parameters

The propeller parameters may have a serious influence on the cargo weight transported by the compound helicopter, particularly for the side-by-side rotor configuration. In this configuration, the weight of the propeller together with its reduction gearing is included in the weight of the nacelle located at the wing tip which influences the wing weight. Consequently, the weight of the propeller together with its reduction gearing not only contributes directly to the empty weight of the side-by-side compound helicopter, but also indirectly through the increase of the wing structural weight.

The propeller efficiency η_{prop} also influences the value of the cargo weight carried by the compound helicopter. The installed power and the overall weight of the fuel on board required for the specified flight range depend on this coefficient. Therefore, we shall find the optimal propeller parameters for each variant of the compound helicopter. To accomplish this task, we make calculations for several values of the propeller thrust coefficient t_{prop}, and blade aspect ratio λ_{prop}, assuming that in all cases, the number of propeller blades is $(z_{bl})_{prop} = 4$.

We find the propeller radius from the following:

$$R_{prop} = \sqrt{2\,T_{prop}\lambda_{prop}/\rho(z_{bl})_{prop}\,t_{prop}\,U_t^2}$$

where the propeller tip speed is assumed as $U_t = 285\ m/s$. The propeller efficiency is determined from the following formula

$$\eta_{prop} = \frac{1}{\tfrac{1}{2}[1 + \sqrt{1 + (c_T/\overline{V}^2)}] + (c_x/4t_{prop}\overline{V})} \qquad (2.186)$$

which yields results in agreement with Eq (2.183). Here, $c_T = \sigma t_{prop}$ where

$$\sigma = b_{prop}(z_{bl})_{prop}/\pi R_{prop}.$$

The value of c_x for the propeller with tip speed $U_t = 285\ m/s$ is determined from Fig 2.102. This figure also shows the efficiency of a propeller with solidity $\sigma \approx 0.2$ for various compound helicopter flight speeds. We see that the propeller used in the analysis has quite high efficiency.

Knowing η_{prop}, we find the propeller power required from the formula

$$N_{prop} = TV/75\eta_{prop}. \tag{2.187}$$

After determining the propeller parameters, we introduce a constraint on the maximum propeller diameter, which is established for the particular compound helicopter configuration on the basis of considerations of difficulties associated with mutual positioning of the propellers and the main rotors.

We determine the propeller blade and hub weights from Eqs (2.53) and (2.54).

2.6.11 Powerplant Power Required for Compound Helicopter Flight at Cruise Speed

The powerplant power required for the compound helicopter flight at cruise speed can be found from the formula

$$(N_{eng.ins})_{cr} = N_{m.r}/\xi + N_{prop}/\xi_{prop} \tag{2.188}$$

where ξ and ξ_{prop} respectively, are coefficients of power utilization by the main rotor and propeller.

We assume the ξ_{prop} coefficient equal to 0.98 and determine the coefficient ξ in accordance with Subsection 2.4.10.

2.6.12 Relationship Between Engine Power Used in Long-Range Flight and Takeoff Engine Power. Determination of Powerplant Weight

Usually, the engine power used in cruise as determined at an altitude of $H = 500\,m$ standard, represents about 60 percent of the takeoff engine power. We shall assume that the compound helicopter begins a long-range flight at normal gross weight and at higher power, closer to normal rated power, equal to

$$(N_{eng.ins})_{V_{cr}} = 0.7N_{t.o}$$

where $(N_{eng.ins})_{Vcr}$ is the compound helicopter engine power required for flight at the cruise speed at which it begins long-range flight with the normal gross weight.

Consequently, the takeoff engine power corresponding to that required for flight at cruise speed with the normal gross weight can be determined as

$$N_{t.o} = (N_{eng.ins})_{V_{cr}}/0.7. \tag{2.189}$$

It was shown in Sect 2.4 that the level of helicopter takeoff engine power is usually determined by the necessity for ensuring either flight at the service ceiling at continuous engine power or hovering at the prescribed altitude.

For pure transport helicopters and compound helicopters intended for flight at high speeds as indicated by some prescribed cruise speed, the takeoff engine power will be determined by the power required for flight at this cruise speed in accordance with Eq (2.189).

For the side-by-side compound helicopter examined below, this speed is $V_{cr} \approx 350$ *km/h*. For the single-rotor compound helicopter, $V_{cr} \approx 380$ *km/h* because of the lower drag of the nonlifting elements and lower wing drag.

2.6.13 Power Transmitted by Main Gearboxes to the Main Rotor in Steady Cruise Flight. Possibility of Reducing Main Gearbox Weight of Compound Helicopters

The design power for which the compound helicopter main gearboxes are designed is the power required for hover at the specified altitude, H_h.

This is a short-term operating condition, and its duration is usually taken at 10 percent of the overall gearbox service life. Therefore, in steady long-range flight, lower power will be transmitted through the main gearboxes. We assume that this power will be no higher than

$$(N_{m.r})_{V_{cr}} = 0.7(N_{m.r})_h . \tag{2.190}$$

This constraint must be considered in selecting the optimal power distribution between the main rotor and the propulsor.

It sometimes happens that the compound helicopter configuration permits reduction of main gearbox weight because of the rotor unloading in level flight. This weight saving can be achieved if one assumes that the duration of hover, which is the most strenuous regime for the main gearbox, is shorter for the compound than for the pure helicopter. However, if we consider that the compound helicopter is a vertical takeoff vehicle (just as the pure helicopter) and the percentage of flights in the hover regime is the same for both aircraft; i.e., at most, about 10 percent of the operating time, then it is not difficult to find that for a design service life on the order of 3000 hours, even the slowest rotating gear in the main gearbox (regardless of the gearbox configuration, but under the condition that this gear has no less than four engagement points), the number of tooth loading cycles in the hover regime alone would exceed $N = 10^7$. Therefore, hovering becomes the design condition for both pure and compound helicopters, and for the same duration of operation in hover, it is not possible to reduce the gearbox weight in spite of unloading the rotor in other, less critical, regimes.

2.6.14 Parasite Drag of Compound Helicopter Nonlifting Elements

With an increase in the flight speed of the compound helicopter, it is particularly important to reduce the parasite drag of the nonlifting elements as much as possible. There are definite difficulties in accomplishing this task, especially for transport compound helicopters.

Table 2.12 shows the typical c_xS values of the components of some previously examined helicopters, and the possible corresponding c_xS values for the single-rotor and side-by-side compound helicopters which have been streamlined as much as possible.

Here, we assume that the landing gear of the single-rotor compound helicopter can be retracted into special pods which form part of the fuselage. We shall consider the drag of these pods to be included in the fuselage drag. For the side-by-side rotor compound helicopter, retraction of the landing gear is very difficult because of the necessity for a wide track (see Fig 2.92). Therefore, for this configuration, we examine only the possibility of reducing the landing gear drag with the aid of fairings.

The use of retracting landing gear for the single-rotor compound helicopter and fairings for the side-by-side rotor version leads to an increase in the gear weight. Therefore, considering the difference in the gear weights for the various helicopter configurations (see Subsection 2.2.18), in the calculations, we take $(k_{l.g})_{s.r} = 0.03$ and $(k_{l.g})_{s.b.s} = 0.035$.

AIRCRAFT COMPONENT	HELICOPTER		COMPOUND	
	SINGLE-ROTOR	TANDEM	SINGLE-ROTOR	SIDE-BY-SIDE
AIRFRAME:				
FUSELAGE	2.5	1.8	2.5	1.5
FRONT PYLON	–	0.45	–	–
AFT PYLON	0.5	0.65	0.5	0.3
FIN, NACELLE STABILIZER	–	–	0.2	0.3
AIRFRAME AS A WHOLE	3.0	2.9	3.2	2.1
LANDING GEAR & TAIL SKID	1.8	2.0	RETRACTABLE	FAIRED 1.5
LIFTING-ROTOR HUBS WITH SWASHPLATES & TAIL-ROTOR HUB	1.5+0.3	3.0	1.5+0.3	2.8
OTHER COMPONENTS	0.2	0.2	0.2	0.2
Σ	6.8	8.1	5.2	6.6
c_xS, INCLUDING INTER-INTERFERENCE	7.5	8.95	5.7	7.2

TABLE 2.12 TYPICAL PARASITE VALUES, c_xS in m^2, OF NONLIFTING ELEMENTS OF PURE AND COMPOUND HELICOPTERS WITH 52–TON GROSS WEIGHT

2.6.15 Load Transported by the Side-by-Side Rotor Compound Helicopters with Propellers

We shall examine the results of analysis of the side-by-side rotor compound helicopter with a takeoff weight of 52 tons, whose configuration is shown in Fig 2.92. This compound helicopter has the same weight efficiency as previously adopted for pure helicopters, with the weight coefficients shown in Table 2.10 (except for the coefficient $k_{l.g}$, which was discussed in Subsection 2.6.14).

For calculation of the main-rotor aerodynamic characteristics, we use the coefficients shown in Figs 2.94 to 2.97 with suitable scaling of the coefficients to the required different main-rotor solidity. For selection of the optimal parameters of the compound helicopter designed for a particular cruise speed, we calculate the cargo weight (payload) transported by the vehicle for various values of $\overline{T}_{m.r}$ and $\alpha_{m.r}$. For each combination of these parameters, we select the optimal propeller parameters, examining three propeller blade aspect ratios, $\lambda_{prop} = 4$, 6, and 8, and the values of t_{prop} noted in Fig 2.102. Here, we introduce a configurational constraint restricting propeller diameters to $d = 4.2 m$ (see Fig 2.92).

When calculating the fuel weight required for flight over the specified range, we shall consider that as fuel is consumed, and the compound helicopter flight weight decreases, the wing lift also decreases, while the main-rotor lift remains unchanged. We make the calculations only for a range of $L = 800 km$.

For the sake of comparing compound and pure helicopters, the cargo weight carried by the compound at a cruise speed of $V_{cr} = 260\ km/h$ is shown in Fig 2.106. The curves are plotted for the four $\alpha_{m.r}$ angles-of-attack with different distributions between the main rotor and the wing up to the value of $\overline{T}_{m.r}$ at which the propeller thrust $T_{prop} = 0$. These values of $\overline{T}_{m.r}$ are also true for the side-by-side helicopter with a wing. The cargo weight transported by this helicopter is somewhat higher than the values obtained earlier for the trussed side-by-side helicopter, since here we have taken a somewhat higher thrust coefficient of $t_{y_0} = 0.18$ instead of $t_{y_0} = 0.171$ for the helicopter. This makes the main rotor lighter, but introduces definite limitations on the flight speed as a function of altitude because of earlier main-rotor blade stall. In addition, we have assumed considerably lower parasite drag of the nonlifting elements of the helicopter with a wing.

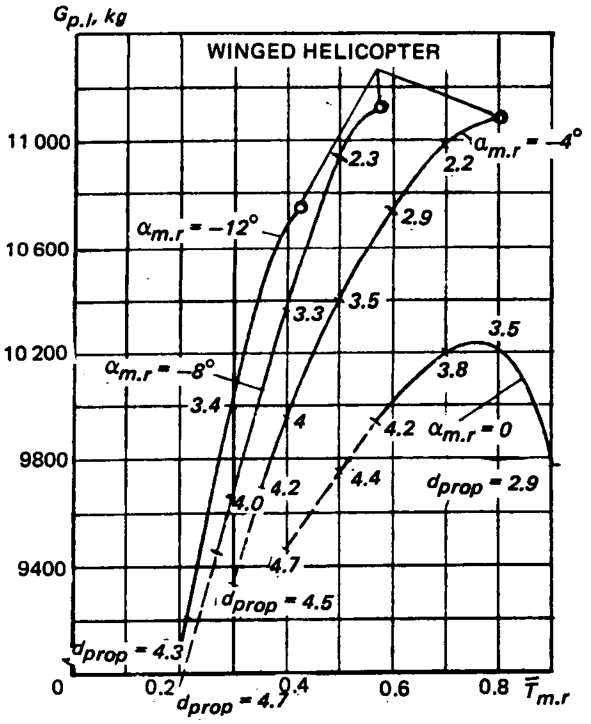

Figure 2.106 The cargo weight transported over 800 km by a side-by-side compound helicopter of $G_{gr} = 52$ tons at a cruise speed of $V_{cr} = 260$ km/h is shown as a function of $\overline{T}_{m.r}$ for various angles-of-attack $\alpha_{m.r}$. In all cases, $\lambda_{prop} = 6$, and $t_{prop} = 0.164$.

As we would expect, it follows from these curves that for a cruise speed of $V_{cr} = 260\ km/hr$, the pure helicopter is always superior to the compound.

Figure 2.107 shows the same curves for the compound helicopter with a cruise speed of $V_{cr} = 350\ km/h$. The points corresponding to the side-by-side helicopter with a wing are also indicated on these curves. We see that for the cruise speed of 350 km/h, the pure helicopter at $\alpha_{m.r} = -12°$, and the compound helicopter at $\alpha_{m.r} = -8°$, are capable of transporting approximately the same loads. Consequently, these configurations are equivalent in regard to this parameter. However, the compound helicopter has more favorable main-rotor operating regimes (lower negative values of $\alpha_{m.r}$), which facilitates trimming, but because of the presence of the propeller, it is a more complex aircraft.

Figure 2.108 shows the cargo weights transported by the side-by-side compound helicopter as a function of lift distribution between the main rotor and wing for various given

Figure 2.107 The cargo weight transported over 800 km at a cruising speed of V_{cr} = 350 km/h by the side-by-side G_{gr} = 52 ton compound helicopter is shown as a function of $\overline{T}_{m.r}$ for various rotor angles-of-attack, $\alpha_{m.r}$.

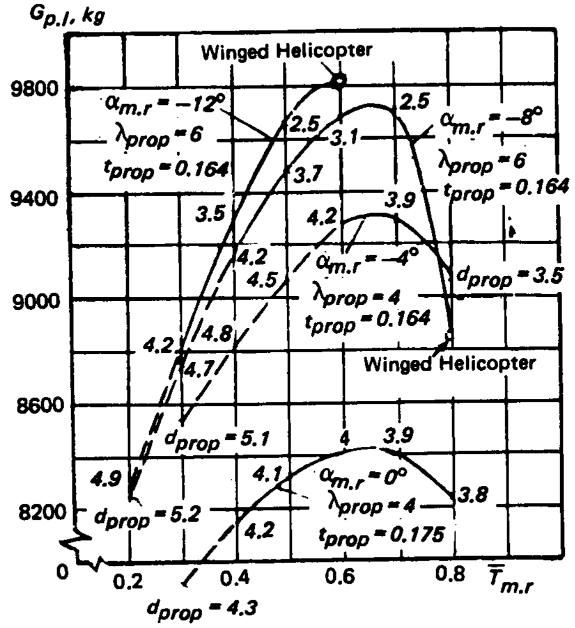

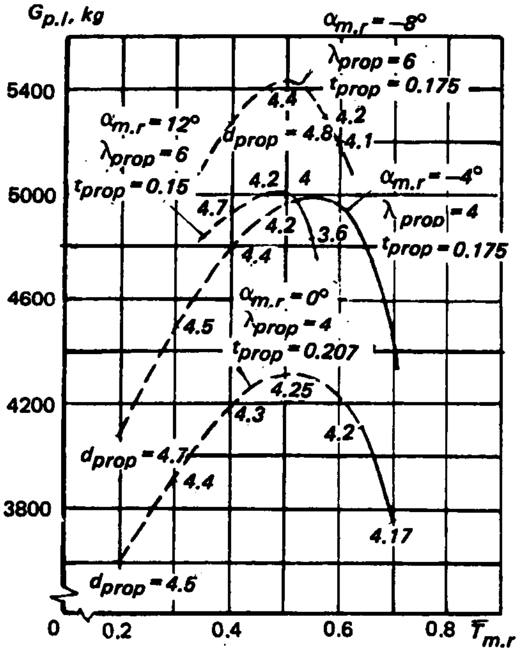

Figure 2.108 Cargo weight transported over 800 km at a cruising speed of 400 km/h by side by-side G_{gr} = 52-ton compound helicopter is shown as a function of $\overline{T}_{m.r}$ for various rotor angles-of-attack $\alpha_{m.r}$.

main-rotor angles-of-attack at the cruise speed of $V_{cr} = 400\ km/h$. We see from these curves that with account for the constraint of $(d_{prop})_{max} = 4.2\,m$, the optimal parameters associated with this flight speed will be

$$\overline{T}_{m.r} = 0.57 \text{ and } \alpha_{m.r} = -8°.$$

At a cruise speed of V_{cr} = 400 km/h, the helicopter regime of flight is not possible for the aircraft with the considered parameters. However, it can be seen from Fig 2.108 that the cargo weight which can be carried by the optimal variant of the compound helicopter decreases quite markedly.

We see from Fig 2.109 that for a cruise speed of 450 km/hr, the cargo weight which can be transported becomes negative.

The data for the optimal side-by-side pure and compound helicopter variants are shown in Tables 2.13 and 2.14.

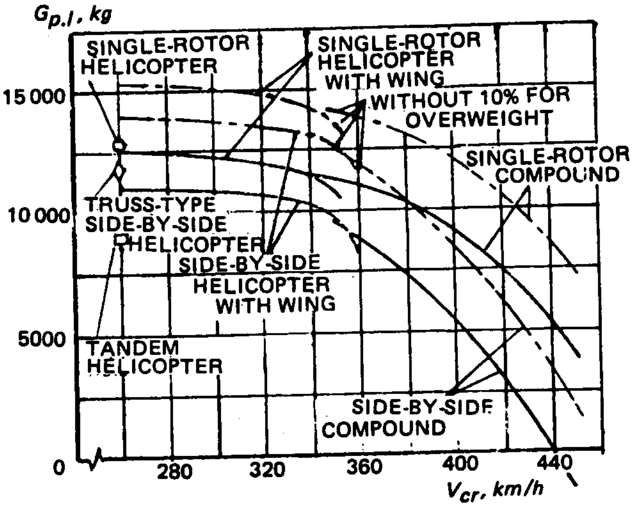

Figure 2.109 Cargo weight transported over 800 km by optimal variants of 52-ton gross weight pure and compound helicopter is shown as a function of cruising speed

PARAMETER	SIDE-BY-SIDE HELICOPTER AND COMPOUND DESIGNED FOR CRUISE SPEED, V_{cr}, km/h				
	WINGED HELICOPTER		COMPOUND		
	260	350	350	400	450
$D_{m.r}$, m	23.1	23.1	23.1	23.6	25.1
$T_{m.r}$	0.575	0.600	0.600	0.565	0.400
T_x, kg	–2000	–2850	–1670	–1200	–3
X_{wg}, kg	1140	1380	1388	1750	2510
Q_{par}, kg	2235	4050	4050	5290	6690
T_{prop}, kg	–	–	2190	4730	9300
λ_{prop}	–	–	6	6	4
t_{prop}	–	–	0.164	0.175	0.225
d_{prop}, m	–	–	3.05	4.20	4.20
η_{prop}	–	–	0.863	0.873	0.818
$(N_{m.r})_{V_{cr}}$, hp	8420	15580	11510	12980	10250
$(N_{eng.ins})_{to}$	25110	25110	25120	31820	43750

TABLE 2.13 BASIC PARAMETERS OF OPTIMAL SIDE–BY–SIDE, PURE, AND COMPOUND HELICOPTER VARIANTS WITH 52-TON TAKEOFF WEIGHT, DESIGNED FOR DIFFERENT CRUISING SPEEDS

HELICOPTER & COMPOUND COMPONENTS		WEIGHT, IN KG, OF COMPONENTS OF HELICOPTERS AND COMPOUNDS DESIGNED FOR CRUISE SPEED OF V_{cr}, km/h				
		WINGED HELICOPTER		COMPOUND		
		260	350	350	400	450
AIRFRAME WITH EQUIPMENT	FUSELAGE WITH EMPENNAGE	4190	4190	4190	4190	4190
	COWLINGS	980	980	980	1140	1400
	WING	3310	3310	3330	3350	3350
	LANDING GEAR	1820	1820	1820	1820	1820
	EQUIPMENT	3290	3290	3290	3330	3500
	Σ	13590	13590	13510	13830	14270
LIFTING ROTORS WITH CONTROLS	BLADES	2000	2000	2000	2130	2610
	HUBS	2090	2090	2090	2080	2070
	CONTROLS	1460	1460	1460	1530	1760
	Σ	5550	5550	5550	5710	6440
MAIN GEARBOXES WITH SYNCHRONIZING TRANSMISSION	MAIN GEARBOXES	4710	4710	4710	4800	5070
	SYNC SHAFT AND INTERMEDIATE GEARBOXES	1110	1110	1110	1240	1430
	Σ	5820	5820	5820	6040	6500
POWERPLANT INSTALLATION WITH FUEL SYSTEM	POWERPLANT INSTALLATION	3590	3590	3590	4550	6260
	FUEL SYSTEM	750	850	830	990	1210
	Σ	4340	4440	4420	5540	7470
PROPELLERS	BLADES	–	–	150	340	580
	HUBS	–	–	130	240	580
	PROPELLER GEARBOXES	–	–	160	390	770
	Σ	–	–	440	970	1930
10% RESERVE FOR OVERWEIGHT		2930	2940	2980	3210	3660
STRUCTURE W/OVERWEIGHT RESERVE		32230	32340	32820	35330	40270
FUEL FOR 800 KM RANGE		8290	9480	9170	14020	13490
CREW		360	360	360	360	360
CARGO TRANSPORTED OVER 800-KM DISTANCE		11120	9820	9650	5290	–2110

TABLE 2.14 COMPARABLE WEIGHTS OF OPTIMAL SIDE–BY–SIDE, PURE, AND COMPOUND HELICOPTER VARIANTS WITH 52-TON TAKEOFF WEIGHT, DESIGNED FOR DIFFERENT CRUISING SPEEDS

These data can be used to clarify the reasons for the nature of the variation of the cargo weight (payload) which can be carried by the compound helicopter as a function of cruise speed. These reasons are as follows:

- With increase in the cruise flight speed, the required engine power increases; consequently, the powerplant weight also increases, as well as the weight of the cowlings and intermediate synchronizing transmission gearboxes designed, in this case, for failure of one engine whose power becomes higher as flight speed increases;
- The fuel consumption per kilometer increases; consequently, the fuel supply required for a given range and the fuel system weight increases;
- The required thrust and power of propellers increase; therefore, their weight goes up, as well as that of the reduction gearing;
- Because of the necessity for maintaining low main-rotor tip speed at high-speed flight and a corresponding decrease of tip speed in hover, it is necessary to increase the main-rotor solidity which causes the main-rotor blade weight to also increase. Because of the increased blade chord, the blade pitching moments increase and the blade control system weight goes up. With reduction of the tip speed, the main-rotor torque required in hover increases, resulting in a higher main gearbox weight.

It is clear that the previously-obtained results apply only to compound helicopters with the component weight efficiencies assumed in the present calculations. At a higher level of weight efficiency, the cargo weight which can be carried by compound helicopters designed for the considered cruise speeds can be increased. Such a possibility is shown in Fig 2.109, where the 10-percent margin for structural weight growth was eliminated. However, this could apply equally well to pure helicopters. Therefore, there is no qualitative change in the presented data comparing the cargo weights which can be carried by both pure and compound helicopters.

2.6.16 Determination of Cargo Weight Transported by a Single-Rotor Compound and Comparison of Single-Rotor and Side-by-Side Rotor Compound Helicopters With Respect to This Parameter

We mentioned previously that the transport compound helicopter developed on the basis of the lightest single-rotor pure helicopter is the most favorable with regard to the cargo weight that can be carried.

In developing the single-rotor compound helicopter, no problem arises from avoidance of "ground-resonance-type" oscillation in the air. Consequently, there is no necessity to additionally increase the wing stiffness. By contrast, in the case of the side-by-side compound helicopter, as we have shown before, it is necessary to increase the wing transverse dimensions, the wing area, and thus, the wing weight.

Therefore, the single-rotor compound helicopter wing area can be selected to achieve maximum wing L/D, which leads to a reduction in the propeller thrust and power required, installed engine power, and in the final analysis, reduction in the structural weight and fuel supply needed for the aircraft to cover a given range.

Calculations show that the wing-lift coefficient at cruise speed should be no higher than $c_y = 0.55$. With this value of c_y, the compound helicopter can be flown at lower speeds, as well as at the specified altitudes without encountering wing stall. With wing aspect ratio $\lambda_{wg} = 6$ to 7, and wing-root relative airfoil thickness of $\bar{h} = 0.15$, the wing L/D of $K_{wg} \approx 21$ to 25 can be obtained without accounting for interference with the main rotor.

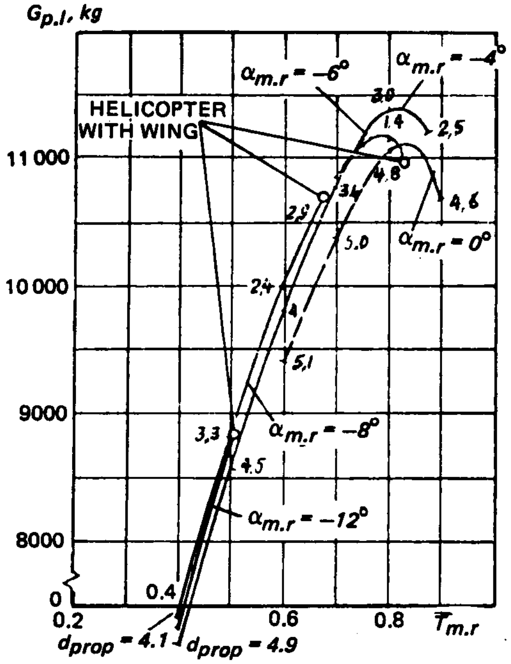

Figure 2.110 Cargo weight transported 800 km at a cruise speed of 350 km/h by a 52-ton single-rotor helicopter is shown as a function of various $\overline{T}_{m.r}$ and main-rotor angles-of-attack $\alpha_{m.r}$ (in all cases, λ_{prop} appeared as optimal).

The configuration with two propellers and engines mounted on the wing as close as possible to the fuselage (see Fig 2.91) is best for the single-rotor cargo transport compound helicopter.

In this case, the powerplants and propellers do not significantly increase the weight of the wing since the aerodynamic forces on the wing lead to higher loads in the wing elements than those from the powerplant and propeller. However, certain difficulties may arise in developing the transmission because of the limitations with respect to the power which can be transmitted by a single-bevel gear pair. Therefore, in consideration of power required in hover by the compound helicopters discussed below with a gross weight of G_{gr} = *52 tons*, the power from each powerplant must be transmitted to the main gearbox through two drive shafts for each engine, and two corresponding intermediate bevel gearboxes.

Use of an inverted-V wing makes it possible to increase somewhat the maximum allowable propeller diameter in comparison with the side-by-side rotor compound helicopter. We shall assume this diameter to be $(d_{prop})_{max} = 5\,m$.

Using the same approach as in Subsection 2.6.15, we obtain the cargo weight carried by the single-rotor compound helicopter of the same design cruise speed for a range of 800 km.

Figure 2.110 shows the cargo weight which can be carried by such a compound helicopter at a cruise speed of $V_{cr} = 350\ km/h$. The maximum useful load is obtained with relative main-rotor thrust $\overline{T}_{m.r} = 0.8$. The differences in the magnitude of the cargo weight carried by the helicopter with a wing and by the compound helicopter are very small. With reduction of $\overline{T}_{m.r}$, the wing lift and consequently, the wing area and weight increase, the required propeller thrust increases, and the cargo weight which can be transported decreases very markedly. Increase of $\overline{T}_{m.r}$ above $\overline{T}_{m.r} = 0.8$ is also unfavorable because of deterioration of the main-rotor aerodynamic characteristics associated with the approach to blade stall. The optimal rotor angles-of-attack are of the order of $\alpha_{m.r} = -4^\circ$ to -6°.

Figure 2.111 shows the useful loads (payload) which can be transported by the single-rotor compound helicopter at the cruise speed of $V_{cr} = 400\ km/h$. The useful load decreases significantly at this cruise speed; however, not as markedly as for the side-by-side compound helicopter. Unloading of the main rotor corresponding to $\overline{T}_{m.r} = 0.65$ at an angle-of-attack of about $\alpha_{m.r} = -4^\circ$, is optimal. At this speed, the pure helicopter regime of flight cannot be realized for the considered compound helicopter parameters.

At the cruise speed of 450 km/h, the cargo weight carried by the single-rotor compound helicopter (Fig 2.112) decreases still further. However, in contrast to the side-by-side compound helicopter, this weight is still positive.

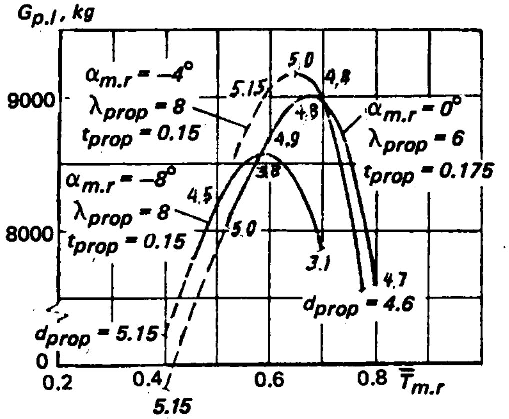

Figure 2.111 Cargo weight transported over 800 km at cruise speed of V_{cr} = 400 km/h by a single-rotor compound helicopter of G_{gr} = 52 tons is shown as a function of $\overline{T}_{m.r}$ for various main-rotor angle-of-attack values.

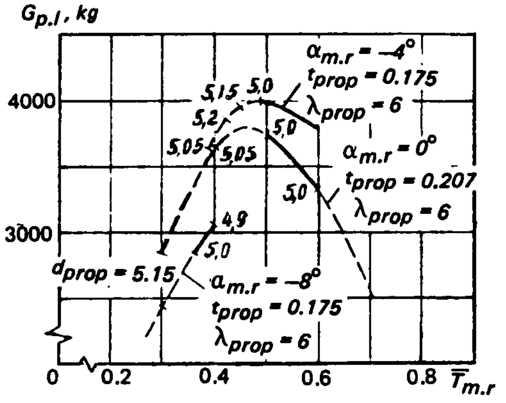

Figure 2.112 Cargo weight transported over 800 km at a cruise speed of 450 km/h by a single-rotor compound helicopter of G_{gr} = 52 ton is shown as a function of $\overline{T}_{m.r}$ for various main-rotor angle-of-attack values.

The optimal regime of flight corresponds to unloading of the main rotor equal to $\overline{T}_{m.r} = 0.45$ to 0.5, and angles-of-attack near $\alpha_{m.r} = -4°$.

The data for the optimal variants of the single-rotor compound helicopter is presented in Tables 2.15 and 2.16.

PARAMETERS	COMPOUND WITH CRUISE SPEED V_{cr}, km/n		
	350	400	450
$D_{m.r}$, m	31.2	31.9	33.9
$T_{m.r}$, kg	0.80	0.65	0.475
T_x, kg	−1860	−610	900
X_{wg}, kg	410	720	1080
S_{wg}, m^2	33.6	45	53.4
Q_{par}, kg	3200	4190	5300
T_{prop}, kg	2100	4620	7520
λ_{prop}	8	8	6
t_{prop}	0.175	0.150	0.175
d_{prop}, m	3.0	5.0	5.15
η_{prop}	0.86	0.91	0.89
$(N_{m.r})_{V_{cr}}$, hp	11090	10180	8300
$(N_{eng.inst})_{t.o}$	16350	27360	33920

TABLE 2.15 BASIC PARAMETERS OF OPTIMAL SINGLE–ROTOR COMPOUND HELICOPTER VARIANTS WITH 52-TON TAKEOFF WEIGHT, DESIGNED FOR VARIOUS CRUISE SPEEDS

COMPOUND COMPONENT		Component weight in kg, of compound designed for cruise speed V_{cr}, km/h		
		350	400	450
Airframe with Equipment	Fuselage with empennage & cowlings	5090	5130	5240
	Wing	820	1310	1920
	Landing Gear	1560	1560	1560
	Equipment	2750	2790	2920
	Σ	10220	10820	11640
Lifting rotor with Controls	Blades	2630	2810	3180
	Hub	2560	2570	2600
	Controls	1350	1430	1720
	Σ	6540	6810	7800
Transmission	Main Gearbox, engine gearboxes, and connecting shafts	4840	4980	5280
	Tail-Rotor Shaft, intermediate and tail-rotor gearbox	880	900	950
	Σ	5720	5880	6230
Powerplant installation with fuel system	Powerplant installation	3770	3910	4850
	Fuel system	840	860	950
	Σ	4610	4770	5800
Tail Rotor	Blades	215	235	300
	Hub	440	440	475
	Σ	655	675	775
Propellers	Blades	110	340	515
	Hubs	80	200	355
	Propeller Gearboxes	140	420	700
	Σ	330	960	1600
10% margin for structural overweight		2805	2990	3385
Structure with overweight margin		30880	32905	37230
Fuel for 800-km range		9380	9565	10440
Crew		360	360	360
Cargo transported over 800 km		11380	9170	3970

TABLE 2.16 COMPARATIVE WEIGHT DATA FOR OPTIMAL SINGLE-ROTOR HELICOPTER VARIANTS WITH 52-TON TAKEOFF WEIGHT' DESIGNED FOR VARIOUS CRUISE SPEEDS

From a comparison of compounds with winged helicopters of the single-rotor and side-by-side types (Fig 2.109), we see that the single-rotor configurations are better with respect to the cargo weight that can be carried. The superiority of this configuration shows up more strongly with an increase of the cruise flight speed.

2.6.17 Comparison of Pure and Compound Helicopters With Respect to Flight Productivity

From the previous discussion it can be seen that the cargo weight that can be transported by the compound helicopter decreases with increase of the cruising-flight speed. However, it is also of interest to investigate how the compound helicopter flight productivity varies in this case.

We find the flight productivity from the formula

$$\Pi_{p.l} = G_{p.l} V_b \qquad (2.191)$$

where V_b is the block speed.

The value of V_b can be found from the formula

$$V_b = 1/[(\tau/L) + (1/V_{cr})] \qquad (2.192)$$

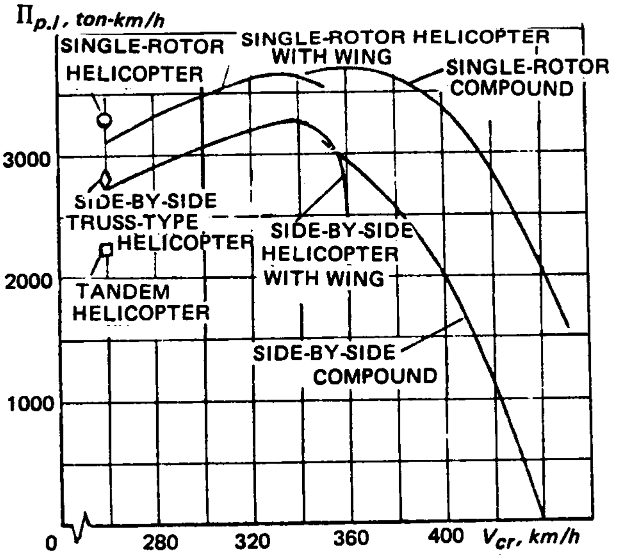

Figure 2.113 Dependence of flight productivity on cruise speed for optimal variants of 52-ton gross-weight, single-rotor and side-by-side pure and compound helicopters.

where τ = time expended in checkout hover, and maneuvering prior to takeoff and landing, as well as on the ground with the engine running. In addition, the quantity τ also includes the additional time loss in climb and descent because the flight speed corresponding to those regimes are lower than the cruise speed. For civil compound helicopters, we can take $\tau = 0.18$ *hr*; and L = the considered flight distance. Figure 2.113 shows the flight productivity of pure and compound helicopters having a gross weight of $G_{gr} = 52$ *tons*, capable of transporting the cargo weight shown in Fig 2.109.

We see from this figure that in the side-by-side configuration of cargo transports, both compounds and pure helicopters with a wing, and constructed at the same weight efficiency level as the pure helicopters examined previously in Sect 2.4, will have a maximum flight productivity at cruise speeds on the order of 330 to 350 km/h, while the same aircraft in the single-rotor configuration have maximum productivity at a cruise speed of 350 to 370 km/h. Both the compound and pure helicopters with wings will have approximately the same maximum flight productivity, although the winged helicopter is less favorable in regard to center-of-gravity travel.

The flight productivity of the transport compound helicopter decreases at high cruise speeds because of the reduction in the cargo weight that can be carried.

The single-rotor transport configuration, as represented by the pure winged and compound helicopters will, at the same cruise speed, have higher productivity than the side-by-side rotor types, thanks to the larger cargo weight that can be carried.

At a cruise speed of $V_{cr} = 260\ km/h$, the side-by-side pure and compound helicopters with wings are somewhat inferior in maximum productivity when compared with the single-rotor helicopter without a wing.

The single-rotor compound helicopter has about 12 percent higher maximum productivity than the single-rotor helicopter without a wing at a cruise speed of $V_{cr} = 260\ km/h$.

3

ANALYSIS OF WEIGHT—CONTRIBUTING STRUCTURE AND CALCULATIONS OF STRUCTURAL-TECHNOLOGICAL WEIGHT OF LIFTING-ROTOR BLADES

3.1 Some Relations Concerning Blade Weight

Blade design includes fulfillment of many different requirements which are conveniently divided into the following groups.

1. *Design strength requirements* which involve taking all possible measures during blade design and fabrication to avoid stress concentrations in the structural elements of the blade so that the dynamic (fatigue) strength of the structure will be adequate for reliable operation throughout the service life of the blade. In addition, all possible measures must be taken to reduce the alternating stresses in the structure to an acceptable level. The blade spar must also satisfy the static strength requirements which will be discussed later in more detail.

2. *Operational requirements* are represented by a reliable protection of blade structure against damage incurred during operation. Also included are provisions for easy repair of any damage that may occur, and a warning system which must be activated at the beginning of blade structural element failure resulting from either operational damage or because of undetected manufacturing defects.

3. *Requirements related to the assurance of normal main-rotor operation.* The main-rotor blade must be designed so that in all the permitted flight regimes, there is the required margin of safety with respect to the occurrence of any type of instability (all flutter modes, divergences reaching large amplitudes of oscillations because of flow separation which are sometimes related to stall flutter, and so on). This margin must be such that the forced oscillation amplitudes do not increase because of proximity to any of these instability modes. Blade deformations, particularly torsional ones, must not increase so as to lead to deterioration of rotor aerodynamics (earlier flow separation, marked increase in the required power), or trim and controllability of the helicopter.

While the first two groups of requirements are quite clear and the approaches to their satisfaction are well known, it is not possible, because of imperfect analytical methods, to guarentee that a new blade design will meet all the requirements of the third group, even if all the necessary structural changes resulting from the calculations are incorporated. Final verification of satisfaction of this group of requirements can be accomplished only in the process of flight tests where dangerous phenomena that were not foreseen in the design often show up.

In order to eliminate, in practice, all unforeseen deviations from normal operation, it is necessary to either alter the blade stiffness—most often, to increase the blade torsional rigidity; or incorporate, into the blade, additional weight in the form of ballast which does not carry any other functional load. Therefore, the blade weight determined during design often increases after flight tests, in the process of "debugging".

In this connection, it is convenient to introduce concepts of blade structural-technological weight, and blade weight required to ensure regular (dynamically undisturbed) operation of the main rotor.

The improvements in blade technology and construction, and the appearance of new and stronger materials and strength-increasing processes make it possible to more-and-more reduce the blade structural-technological weight, while still ensuring the required strength under the larger alternating stresses which arise; for example, with incresase in the blade mass characteristic γ_o. However, this weight reduction encounters difficulties resulting from the requirement of assuring regular operation of the lifting rotor.

Blade development experience shows that a large part of the phenomena which limit regular operation of the main rotor can be eliminated quite easily in the case of relatively heavy blades when the blade mass characteristic is not higher than $\gamma_o = 4$, and with much greater difficulty when the blades are relatively lighter; i.e., $\gamma_o = 6$ to 7.

It should be noted that it is easier to reduce the structural technological weight of blades with large dimensions and thus, obtain blades with high mass characteristics, but the same is not true for small blades. While for blades of large diameter rotors, the structural-technological limitations do not prevent the development of blades with $\gamma_o \approx 7$; for small-diameter main-rotor blades, the minimum achievable blade weight is such that their mass characteristic is $\gamma_o < 3...4$.

Consequently, in order to reduce the weight of small-diameter blades, it is necessary to primarily solve the structural-technological problem, while achievement of large-diameter blade reduction lies in solving the problem of ensuring regular main-rotor operation with blades having a mass characteristic on the order of $\gamma_o \approx 7$.

The gap between the minimal feasible blade weight and the blade weight required for regular operation becomes wider and wider for large-diameter rotors, and the weight "saved" in design does not result in lightening the structure, but rather leads to the application of ballast in the form of various weights and counter-weights, or increase of the blade structural element cross-section area above the values required by the strength considerations.

Therefore, attempts to reduce blade weight must be carried out in two directions. On the one hand, means must be found which would make it possible to achieve regular operation of a main rotor with light-weight blades; on the other hand, work must be continued on further reduction of the structural technological weight. All the measures taken to eliminate instability, which forces the designer to make the blade heavier than its required weight must not "cool" his ardor in the drive to achieve the minimal feasible structural-technological blade weight. Work in this direction must be continued regardless of the difficulties encountered in the application of its results.

In the present chapter, we shall present only the method for evaluating the minimal feasible structural-technological blade weight, and some results of the application of this method (means for ensuring regular main-rotor operation and evaluation of the resulting blade weight increases will not be examined).

3.1.1 Static-Strength Requirements

Among the many conditions dictated by blade strength, two very important requirements must be satisfied which, by convention, we will call the static-strength requirements.

The blade must be so designed that stresses $\sigma_{c.f}$ occurring in the spar due to centrifugal forces at the selected operational values of $n_{m.r}$, and σ_{bend} from bending by the blades own weight are within allowable limits; i.e., so that

$$\sigma_{c.f} \leqslant (\sigma_{c.f})_{all} \tag{3.1}$$

and

$$\sigma_{bend} \leqslant (\sigma_{bend})_{all}. \tag{3.2}$$

Satisfaction of these conditions, and especially those given by Eq (3.1) is also necessary in order to ensure blade dynamic (fatigue) strength and operational life; but no less important is the fact that the level of those allowable stresses depends on the maximum nonrecurring stress which determines the required blade static strength. Therefore, the selected values of $(\sigma_{c.f})_{all}$ and $(\sigma_{bend})_{all}$ must ensure spar strength during main-rotor overspeed and when the blade contacts the droop stop (Case II-h of the Helicopter Airworthiness Standards) although, in the latter case, it is also necessary to satisfy conditions of prevention of the loss of spar static stability.

The static-strength requirements lead to a division of the blade into three segments along the length, differing in nature of the loading from centrifugal force and blade weight. These are: the ballast segment at the blade tip, the middle fail-segment with corresponding allowable tensile stresses, and the root augmented-weight segment where additional structural weight is acquired because of the high blade-weight bending moments which predominate when the blade aspect ratios exceed some definite values.

We shall consider the weight of a blade which satisfies the first two groups of requirements presented in Sect 3.1, including the static-strength requirements, as minimal achievable blade weight.

Determining this weight from the sum of the weights of the three aforementioned segments, we can find the minimal realizable weight as a function of the various blade parameters. The solution of this problem is the basic objective of this chapter.

3.1.2 Assumptions

We shall examine an idealized, but quite realistic, blade scheme. For simplicity, we will consider that the blade is rectangular in planform. All the blade structural elements other than the spar will arbitrarily be considered part of the envelope, assuming that the counterweight is also an element of the envelope (Fig 3.1).

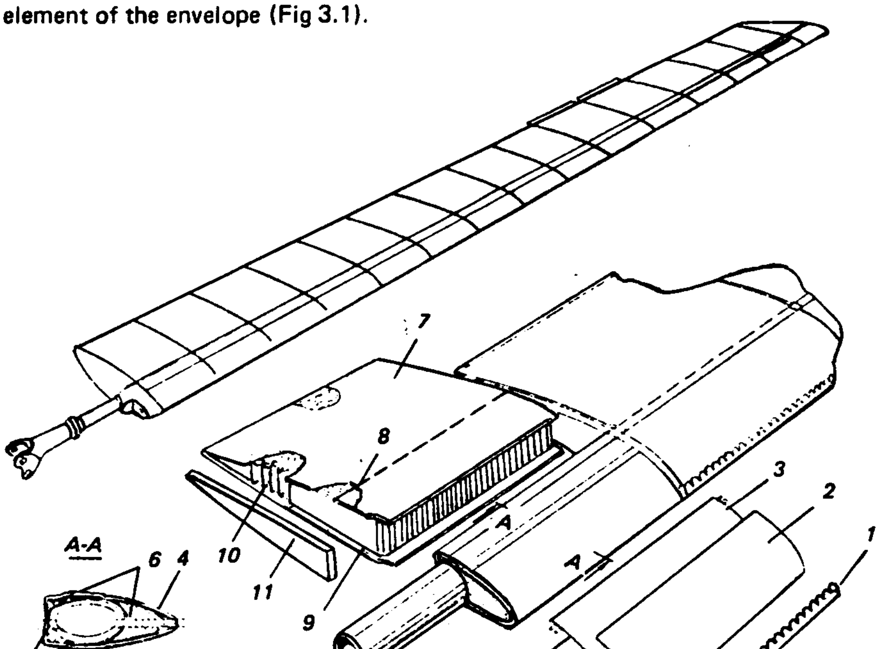

Figure 3.1 Blade scheme with tubular steel spar and glass-plastic envelope: (1) abrasion strip, (2) heating element protective strip, (3) heating element of the anti-icing system, (4) leading-edge skin, (5) compensators, (6) plastic-foam filler, (7) aft-section skin, (8) aft-section skin reinforcement, (9) rib, (10) honeycomb filler, and (11) inter-box insert

We assume that the loads acting on the blade are taken only by the spar. We shall consider the running weight q_{env} of the blade envelope to be constant along the blade length. In reality, the envelope running weight usually decreases somewhat toward the root. But, in most cases, this has practically no effect on the spar section dimensions and still less influence on the weight of the blade.

However, if a heavy counterweight with correspondingly higher running weight is located only in the tip part of the blade, this idealized blade scheme may lead to large errors. In this case, the running weight of the counterweights should be distributed over a larger length of the blade in the analysis.

3.1.3 Ballast Segment at the Blade Tip

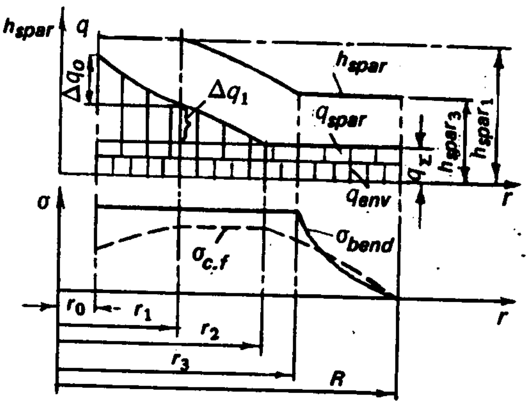

Figure 3.2 Running weight, spar height, and static stress as a function of blade radius

In order to maintain the stresses from the centrifugal forces at the constant allowable level, the spar section at the blade tip should be made so that the area decreases to zero at $\bar{r} = 1$. However, for technological and manufacturing reasons, the spar tip has constant section area over some length and consequently, the running weight q_{spar} is constant (see Fig 3.2).

In this way, an additional so-called ballast weight that is not dictated by spar strength requirements is introduced into the blade. With increasing distance from the blade tip, the stresses from the centrifugal forces also increase and become equal to the allowable stress at the relative radius $\bar{r}_2$, which is determined from the formula

$$\bar{r}_2 = \sqrt{1 - (1 - \bar{G}_{env})\alpha} \tag{3.3}$$

where $\bar{G}_{env}$ = ratio of the envelope running weight q_{env} to the overall running weight q_Σ at the blade tip segment: $\bar{G}_{env} = q_{env}/q_\Sigma$;

$$\alpha = (2g/U_t^2)[(\sigma_{c.f})_{all}/\gamma]. \tag{3.4}$$

For $U_t = 220\ m/s$, the values of α are taken as follows: $\alpha = 1.35\ [(\sigma_{c.f})_{all} = 26\ kg/mm^2]$ for steel; $\alpha = 1.2\ [(\sigma_{c.f})_{all} = 8\ kg/mm^2]$ for aircraft aluminim; and $\alpha = 2\ [(\sigma_{c.f})_{all} = 8\ kg/mm,$ $\gamma = 1.6\ kg/cm^3]$ for glass-reinforced plastic.

We shall call the blade segment from $\bar{r}_2$ to $\bar{r} = 1$ the ballast segment. Should it be technologically possible to reduce the spar-section area to zero at $\bar{r} = 1$ $(\bar{G}_{env} = 1)$, then the blade ballast segment overweight would be reduced to zero.

3.1.4 Middle-Fail Segment of Blade with Steel Spar

The spar section area must increase from $\bar{r} = \bar{r}_2$ toward the blade root in order to maintain constant stresses from the centrifugal forces

$$\sigma_{c.f} = (\sigma_{c.f})_{all} = const. \tag{3.5}$$

If one would make special tests, increasing the main-rotor rotational speed far in excess of its normal level, then the blade would fail within this segment. Therefore, this segment of the blade can be termed the fail segment.

The bending moment resulting from the weight of the blade itself also increases toward the root.

At radius $\bar{r}_3$, the bending stresses from the blade's own weight become equal to the allowable stresses $(\sigma_{bend})_{all}$. If $\bar{r}_3 > \bar{r}_2$, then the value of $\bar{r}_3$ can be found from the formula

$$\bar{r}_3 = 1 - \sqrt{\beta_3(1 - \bar{G}_{env})}. \tag{3.6}$$

Here,

$$\beta_3 = h_{eff_3}(\sigma_{bend})_{all}/R^2\gamma \tag{3.7}$$

where

$$h_{eff_3} = 2W_3/F_3 \tag{3.8}$$

is the effective spar height; W_3 is the spar section resisting moment in the plane of action of the blade-weight forces; F_3 is the area of the spar section loaded by the tensile centrifugal forces.

For a blade having a steel spar, it is possible to increase the structural height of the spar toward the root, beginning at radius $\bar{r}_3$ to satisfy the condition

$$\sigma_{bend} = (\sigma_{bend})_{all} = const \tag{3.9}$$

while the spar section area must be increased beginning only at the radius $\bar{r}_2$ to satisfy the condition of Eq (3.5).

For the blade with extruded aluminum spar, an increase of the section resisting moment W is possible only through an increase of its cross-section area F. Therefore, the nature of the section variation of the blade with extruded spar will be different.

But even for the blade with a steel spar, the structural height of the spar cannot be increased without limit. The maximum structural height at the root is determined by the diameter of the original spar tube which, in the central and tip parts of the blade, is squeezed down into an ellipse with the required structural height. The tube structural height must be such that the relative blade airfoil thickness would not exceed the magnitudes specified on the basis of aerodynamic considerations. Usually, the airfoil relative thickness is not increased above 10 ... 11 percent of the chord starting at the blade station $\bar{r}_{th.con}$, marking the beginning of the airfoil thickness constraint, to the blade tip, and is no higher than 20 percent of the chord in the root of the blade, up to a radius no larger than $\bar{r} = 0.15$. Between these points, the allowable airfoil section height can vary linearly (Fig 3.3). These conditions determine the spar height which, in the blade with a steel spar and glass-plastic envelope, cannot be larger than the relative thickness of the blade airfoil section (in percentage) minus two percent.

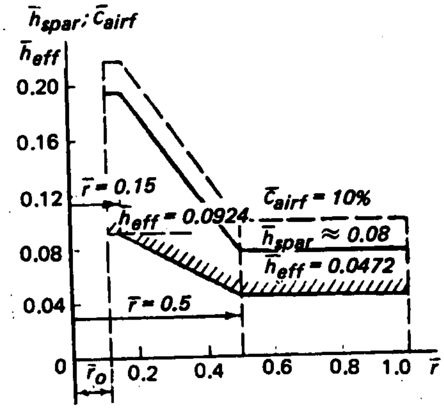

Figure 3.3 Distribution along the blade radius of (1) relative airfoil height $\bar{c}_{airf}$, and (2) relative $\bar{h}_{spar}$, and effective $\bar{h}_{eff}$ spar height for blades having steel-tube spars

We shall find the value of the relative blade radius $\bar{r}_1$ at which further increase in the structural height toward the blade root for satisfaction of the condition of Eq (3.9) is not possible because of violation of the allowable airfoil-section height. Down from this blade section, additional thickening of the spar walls is necessary to satisfy the condition of Eq (3.9).

The relative running blade weight increase $\Delta\bar{q}_1 = \Delta q_1/q_\Sigma$ as a consequence of an increase in the spar section area between radii $\bar{r}_2$ and $\bar{r}_1$ (see Fig 3.2) can be determined for the condition of Eq (3.5) from the following approximate formula

$$\Delta\bar{q}_1 = [1-\bar{r}_1^2-\alpha(1-\bar{G}_{env})]/[\alpha-(1/3)(\bar{r}_2^{\,2}+\bar{r}_1\bar{r}_2-2\bar{r}_1^{\,2})], \qquad (3.10)$$

obtained on the basis of the assumption that along the $\bar{r}_1$ to $\bar{r}_2$ segment, the running weight varies linearly. This formula could be refined by introducing the running-weight variation law corresponding exactly to the condition of Eq (3.5). However, calculations have shown that for the accuracy required in blade weight estimates, there is no need for this.

From the condition that at the radius $\bar{r}_1$, where running weight is $(q_\Sigma+\Delta q_1)$ and the maximum allowable spar height is h_{spar_1}, the bending stress resulting from the blade's own weight must be equal to $(\sigma_{bend})_{all}$, and we obtain

$$\beta_1 = [(1-\bar{r}_1^{\,2}) + (1/3)\Delta\bar{q}_1(\bar{r}_2+\bar{r}_1)^2]/(1+\Delta\bar{q}_1-\bar{G}_{env}). \qquad (3.11)$$

Here,

$$\beta_1 = (h_{eff_1}/R^2)(\sigma_{bend})_{all}/\gamma \qquad (3.12)$$

where $h_{eff_1} = 2W_1/F_1$ is determined for the spar with height h_{spar_1}.

For the circular cylindrical tube with thin walls,

$$h_{eff_1} = d_{spar}/2 \qquad (3.13)$$

where d_{spar} = spar tube outer diameter.

For actual wall thickness, we can take

$$h_{eff_1} = 0.95 d_{spar}/2. \qquad (3.14)$$

The value of β_1 can be related to the blade aspect ratio λ.

We introduce the concept of the reduced blade aspect ratio $\bar{R}\lambda$, where $\bar{R} = R/R_o$ and $R_o = 16m$.

Then,

$$\bar{R}\lambda = (\bar{h}_{eff_1}/\beta_1)/[(\sigma_{bend})_{all}/R_o\gamma] \qquad (3.15)$$

where

$$\bar{h}_{eff_1} = h_{eff_1}/b. \qquad (3.16)$$

The allowable bending stresses from the blade's own weight can be determined from the necessity for ensuring strength in case the blade strikes the flapping stop; i.e.,

$$(\sigma_{bend})_{all} = \sigma_{fail}/f\bar{\delta}$$

where σ_{fail} = bending stresses in the spar which lead to failure of the blade; $f = 1.5$ = safety factor; $\bar{\delta}$ = coefficient expressing the maximum stress ratio when the blade strikes the stop to the static stress corresponding to the blade's own weight.

Since $\bar{\delta}$ depends on the blade parameters and the angle of blade elevation from which it falls onto the stop, $(\sigma_{bend})_{all}$ will also be a variable quantity. However, to avoid overcomplicating the analysis, we shall assume that $(\sigma_{bend})_{all} = 26\,kg/mm^2$ for the steel-tube spar, and we obtain

$$\bar{R}\lambda = 208\bar{h}_{eff_1}/\beta_1.$$

Consequently, specifying various values of $\bar{r}_1$ and using Eqs (3.10), (3.11), and (3.15), we can obtain the reduced blade aspect ratio $\bar{R}\lambda$ as a function of $\bar{r}_1$ for various $\bar{G}_{env}$ values.

Such relationships for the steel-tube-spar blade are shown in Fig 3.4. Taking several integral values of the reduced blade aspect ratio, we can plot the radii $\bar{r}_1$ as a function of $\bar{G}_{env}$ (Fig 3.5).The values of the radius $\bar{r}_2$ are also shown in this figure.

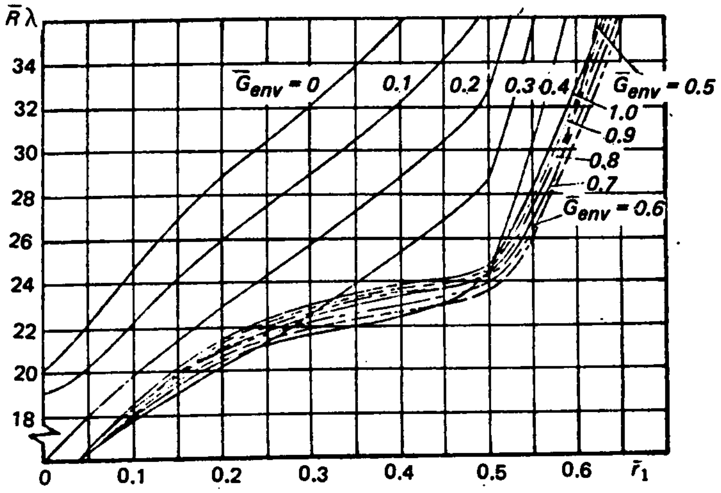

Figure 3.4 Reduced aspect ratio $\bar{R}\lambda$ of a blade with tubular steel spar as a function of the length of the weight-augmented root segment defined by the relative radius $\bar{r}_1$, is shown for various relative blade-envelope weights $\bar{G}_{env}$

We see from Fig 3.5 that for small relative envelope weights $\bar{G}_{env}$, the value of $\bar{r}_2$ determined from Eq (3.3) may be smaller than that of $\bar{r}_1$; i.e., the middle blade segment, just as the other segments, in other cases may disappear. In this case, we must set $\bar{r}_1 = \bar{r}_2$ and $\Delta\bar{q}_1 = 0$ in Eqs (3.10) and (3.11).

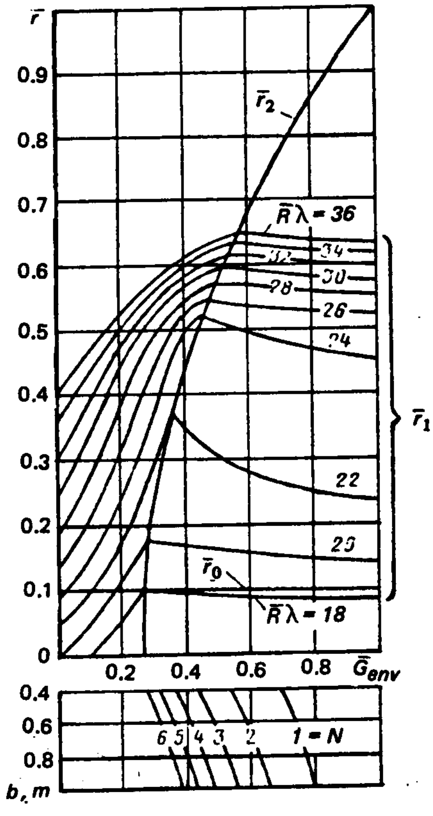

Figure 3.5 Boundary locations of ballast, middle fail, and weight-augmented root segments as a function of the relative envelope weight of the outer segment of a blade with tubular steel spar

3.1.5 Fail-Segment of the Extruded-Spar Blade

The extruded-spar blade is characterized by the fact that the spar resisting moment cannot be increased without changing the spar cross-section area, since the spar internal channel contour is constant along the blade length because of the extrusion process. Therefore, for this blade, the relative radius $\bar{r}_3$, at which one should begin to increase the section resisting moment (without increasing the cross-section area), coincides with the relative radius $\bar{r}_1$ from which the cross-section area begins to increase in order to ensure the required section resisting moment.

We shall examine the most general case, when the relative radius $\bar{r}_2$ determined by Eq (3.3) is larger than the relative radius $\bar{r}_1$.

In contrast with the steel-tube-spar blade, the value of the spar effective height h_{eff_1} at the radius $\bar{r}_1$ is completely defined by the spar height h_{spar_2}, the radius of inertia i of the added spar area ΔF_1, and the effective spar height h_{eff_2} in the blade end segment.

$$h_{eff_1} = [(1 - \bar{G}_{env})h_{eff_2} + \xi^2 (1 + ½\Delta\bar{F}_1/\xi)^2 h_{spar_2} \Delta\bar{q}_1]/[(1 - \bar{G}_{env} + \Delta\bar{q}_1)(1 + \Delta\bar{F}_1)] \quad (3.17)$$

where

$$\xi = 2i/h_{spar_2} ; \Delta\bar{F}_1 = \Delta F_1/h_{spar_2} b_{spar} = q^* \Delta\bar{q}_1,$$

$$q^* = \bar{q}_\Sigma/\gamma h_{spar_2} \bar{b}_{spar}. \quad (3.18)$$

Here, h_{spar_2} and b_{spar} respectively, are the spar height and width in the blade end segment, and $\bar{b}_{spar} = b_{spar}/b$. The value of q^* is usually about 0.35 to 0.45.

Just as for the steel-spar blade, in order to determine the boundary between the middle and root segments, we take various values of $\bar{r}_1$, and then use Eqs (3.10) and (3.11) to determine $\Delta\bar{q}_1$ and β_1.

From the obtained values of β and h_{eff_1}, we determine the reduced blade aspect ratio from Eq (3.15). Assuming that $(\sigma_{bend})_{all} = 8$ kg/mm² for the extruded Duralumin spar, we obtain

$$\bar{R}\lambda = 185 h_{eff_1}/\beta_1. \quad (3.19)$$

The values of $\bar{r}_1$ for several integral values of reduced aspect ratios and dependence of the boundary segment position on the quantity $\bar{G}_{env}$ for the blade with extruded Duralumin spar are shown in Fig 3.6.

In comparing Figs 3.5 and 3.6, we should note that for the blade with extruded Duralumin spar, the thickened root segment appears for significantly lower reduced aspect ratios $\bar{R}\lambda = 11$ to 12.

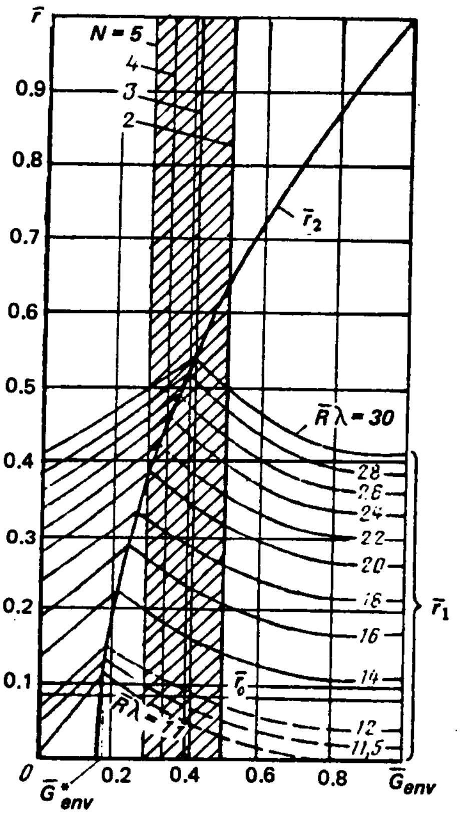

Figure 3.6 Location of boundaries of ballast, middle-fail, and reinforced root segments as a function of relative envelope weight of the outer blade segment with extruded Duralumin spar

In the particular case when $\bar{r}_1 > \bar{r}_2$, the middle fail segment for the extruded Duralumin spar blade disappears and the blade will consist of only two segments—the ballast segment and the thickened root segment.

3.1.6 Thickened Blade-Root Segment

The segment of the blade from its root end, located at the radius $\bar{r}_o$, to the radius $\bar{r}_1$ will be termed the blade thickened root segment (see Fig 3.2).

It follows from Fig 3.5 that the blade with a sufficiently high steel spar at the root (bounded by the heights indicated in Fig 3.3) does not have the augmented root segment for reduced aspect ratios up to $\bar{R}\lambda = 18.5$ to 19.

The variation in the blade running weight in the augmented root segment is associated with the increase in the wall thickness of the spar in accordance with the condition of Eq (3.9). The relative running weight increase in the radius range from $\bar{r}_1$ to $\bar{r}_o$ (see Fig 3.2) can be determined from the following approximate formula:

$$\Delta\bar{q}_o = 2\Delta\bar{r}\bar{G}_{\Sigma_1}/\beta_o[1-(\Delta\bar{r}^2/3\beta_o)] \tag{3.20}$$

where

$$\Delta\bar{q}_o = \Delta q_o/q_\Sigma;\ \Delta\bar{r} = \bar{r}_1 - \bar{r}_o;\ \bar{G}_{\Sigma_1} = G_{\Sigma_1}/Rq_\Sigma = 1 - \bar{r}_1 + ½\Delta\bar{q}_1(\bar{r}_2 - \bar{r}_1). \tag{3.21}$$

Here, G_{Σ_1} is the combined weight of the fail and ballast segments of the blade.

For the steel spar blade, the value of β_o is calculated from the formula

$$\beta_o = (\bar{h}_{eff_o}/\bar{R}\lambda)(\sigma_{bend})_{all}/R_o\gamma = 208\bar{h}_{eff_o}/\bar{R}\lambda \tag{3.22}$$

where $\bar{h}_{eff_o}$ is determined from the selected spar tube dimensions, while the reduced aspect ratio $\bar{R}\lambda$ has already been found from Eq (3.15).

For the extruded Duralumin spar blade, by analogy with Eq (3.17), we can write

$$\bar{h}_{\mathrm{eff}_o} = \frac{(1-\bar{G}_{env})h_{eff_1} + \xi_o{}^2 h_{spar_1}[1 + (1/2\xi_o)\Delta\bar{F}_o]^2\Delta\bar{q}_o}{(1-\bar{G}_{env} + \Delta\bar{q}_o)(1 + \Delta\bar{F}_o)} \tag{3.23}$$

where h_{eff_1} = the effective spar height at the relative radius $\bar{r}_1$ as determined from Eq (3.17); and h_{spar_1} = the spar height at the same radius, $h_{spar_1} \doteq h_{spar_2}(1 + \Delta\bar{F}_1)$; and

$$\Delta\bar{F}_o = q^*\Delta\bar{q}_o. \tag{3.24}$$

Eq (3.23) can be transformed to the form:

$$\beta_o = \frac{(1-\bar{G}_{env})\beta_1 + \beta_{spar1}[1 + (1/2\xi_o)\Delta\bar{F}_o]^2\Delta\bar{q}_o}{(1-\bar{G}_{env} + \Delta\bar{q}_o)(1 + \Delta\bar{F}_o)} \tag{3.25}$$

If we then substitute β_o into Eq (3.20), we obtain a quite complex fourth-degree equation for determining $\Delta\bar{q}_o$, and with certain refinements, the equation will be of an even higher degree.

This equation can be solved by successive approximations, setting $\Delta\bar{F}_o = 0$ in the first approximation, and then in subsequent approximations, determine its value from the obtained value of $\Delta\bar{q}_o$.

Then,

$$\Delta\bar{q} = A + \sqrt{A^2 + B} \tag{3.26}$$

where

$$A = \frac{1}{2}\left[\frac{1 + \Delta\bar{F}_o}{[1 + (1/2\xi_o)\Delta\bar{F}_o]^2}\;\frac{L}{\beta_{spar_1}} - \frac{1 - \bar{G}_{env}}{[1 + (1/2\xi_o)\Delta\bar{F}_o]^2}\;\frac{\beta_1}{\beta_{spar_1}}\right] \tag{3.27}$$

$$B = (1 - \bar{G}_{env})\,\frac{1 + \Delta\bar{F}_o}{[1 + (1/2\xi_o)\Delta\bar{F}_o]^2}\;\frac{L}{\beta_{spar_1}} \tag{3.28}$$

In these expressions,

$$L = \frac{2\Delta\bar{r}}{1 - (\Delta\bar{r}^2/3\beta_o)}\left[1 - \bar{r}_1 + \tfrac{1}{2}\Delta\bar{q}_1(\bar{r}_2 - \bar{r}_1)\right]$$

$$\beta_{spar_1} = (\xi_o^2\bar{h}_{spar_1}/\bar{R}\lambda)[(\sigma_{bend})_{all}/R_o\gamma] \tag{3.29}$$

where $\bar{h}_{spar_1} = h_{spar_1}/b$.

In the process of successive approximations, it is advisable to also refine the coefficient L, initially setting $\beta_o = 0$, and then refine β_o using Eq (3.25)

In the particular case when $\bar{r}_1 > \bar{r}_2$, and the middle fail segment is absent, we can set $\bar{r}_2 = \bar{r}_1$ and $\Delta\bar{q}_1 = 0$ in these formulae.

The spar sections in the augmented root segment must satisfy Eq (3.9). In this case, the stresses from the centrifugal forces fall below $(\sigma_{c.f})_{all}$ (see Fig 3.2).

3.1.7 Overall Weight of the Blade Plume

Representing the running weight variation along the blade length as shown in Fig 3.2, and using the values of $\Delta\bar{q}_1$ and $\Delta\bar{q}_o$, we can determine the weight of the blade plume from the formula

$$G_{pl} = Riq_{\Sigma 2}, \tag{3.30}$$

where i is a function depending on the dimensionless parameters α, β_1, β_o, and $\bar{G}_{env}$:

$$i = (1 + \Delta\bar{q}_1)\Delta\bar{r} + \left\{1 + \Delta\bar{r}^2/\beta_o[1 - (\Delta\bar{r}^2/3\beta_o)]\right\}[1 - \bar{r}_1 + \tfrac{1}{2}\Delta\bar{q}_1(\bar{r}_2 - \bar{r}_1)] \tag{3.31}$$

If we introduce the concept of the blade weight per square meter of the blade outer-segment area,

$$\tilde{q}_\Sigma = q_{\Sigma 2}/b, \tag{3.32}$$

the blade plume weight can be represented in the form

$$G_{pl} = i\tilde{q}_\Sigma bR. \tag{3.33}$$

Hence, it follows that i is th coefficient of average blade plume weight increase in comparison with the weight per square meter of its outer segment.

The values of i for various reduced aspect ratios of the steel-spar blade are shown in Fig 3.7.

It follows from Eq (3.33) that for a selected reduced aspect ratio, the blade weight is determined by the weight per square meter of its outer part and the overall blade area.

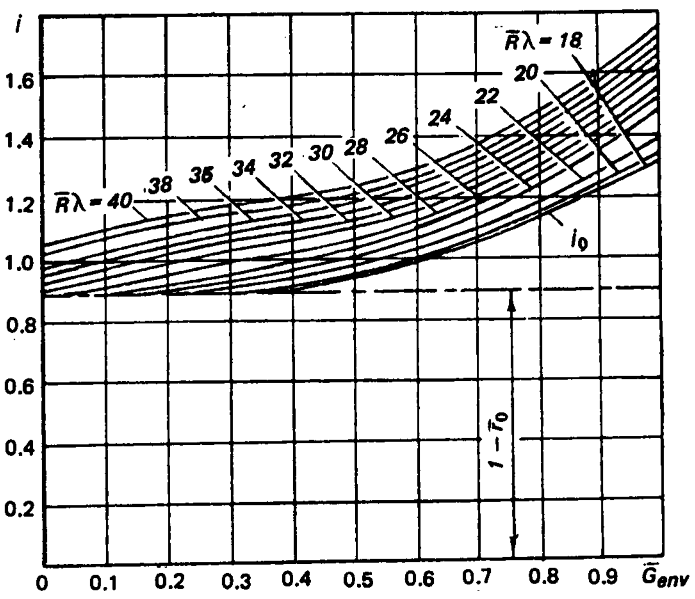

Figure 3.7 Blade weight increase coefficient i as a function of the relative envelope weight of the outer segment for various reduced aspect ratios

The weight per square meter of area or—as we shall refer to it hereafter—the specific weight of the outer blade segment, consists of the weight of the envelope (with counterweight) and the blade spar.

We shall examine the parameters on which this weight depends.

3.1.8 Specific Weight (Including Counterweight) of Envelope Structure in the Blade Outer Region

We shall examine a typical modern glass-reinforced plastic blade envelope construction. This design makes it possible to obtain minimal envelope weight for the blade with a steel tubular spar.

The construction of such an envelope is accomplished as follows (see Fig 3.1). The trailing edge sections (boxes) with honeycomb filler and glass-plastic skin are attached to the glass-plastic blade nose-box which, in turn, is attached to the spar through so-called compensators. The space between the blade nosebox and the spar is filled with plastic foam. The counterweights are located inside the nosebox. The blade anti-icing elements and abrasion strips are located along the outer contour of the nose.

For the subsequent analysis, it is important not only to determine the minimum possible specific envelope weight, but also the nature of its variation as a function of blade chord.

The running weights of the envelope elements used to fill any part of the blade airfoil section are proportional to the square of the chord. These elements include the plastic-foam and honeycomb filler, ribs, spacers, compensators, and the cement used for bonding and gluing the honeycombs and other elements of the envelope. For manufacturing reasons, the aft section skin for chords up to about one-half meter is no less than 0.3 to 0.4-mm thick and therefore, its weight is proportional to the blade chord. With increase of the chord, the skin thickness at the point of attachment to the nosebox must be increased because of strength requirements. The running weight of the skin stiffeners increase as the square of the chord. The running weight of the nose section skin stiffeners exhibits the same dependence on the chord.

A large part of the nosebox running weight and also the running weight of the blade anti-icing and abrasion protection, and the weight of the trailing-edge box spacers are proportional to the first power of the chord.

The running weight of the counterweights is proportional to the running weight of the envelope; therefore, it can be divided into two parts: one varying as the first power and another as the square of the blade chord.

The minimal possible running weight, which is the sum of the weights of all the above-listed envelope elements referred to the chord can be obtained as

$$\tilde{q}_{env} = b\sum_{i}(\Delta\tilde{q}_{env_i})/\Delta b + \sum_{j}\Delta\tilde{q}_{env}$$

where, for the elements whose specific weight is proportional to the chord, the values of $\Delta\tilde{q}_{env}/\Delta b$ are

	kg/m³
Plastic foam filler	1.6
Honeycomb	1.28
Compensators and spacers	1.88
Nose-section skin reinforcements	1.88
Aft-box skin reinforcements	1.2
Ribs	0.36
Adhesive	0.76
Changeable part of the counterweight	1.08
	$\sum_{i}(\Delta\tilde{q}_{env_i})/\Delta b \approx 10.1$

and for the elements with specific weight which does not change with variation of the chord, the values of $\Delta\tilde{q}_{env}$ are

	kg/m²
Icing and abrasion protection	1.36
Unvarying part of nose and aft skins	1.6
Inter-box inserts	0.22
Unchangeable part of the counterweight	2.00
	$\sum_{j}\Delta\tilde{q}_{env_j} = 5.2$

The actual weights of these elements are shown in Fig 3.8 for three blade sizes where, in the assumed relationships, account was taken of the necessary structural changes in accordance with modern concepts.

Thus, the minimal specific envelope weight of the glass-plastic blade with steel spar can be represented as

$$\tilde{q}_{env} = 5.2 + 10.1b. \tag{3.34}$$

In Fig 3.9, this relationship can be compared with the actual specific weight of the blade envelope. A similar analysis was made to obtain the specific weight of the envelope as a function of chord for blades with extruded Duralumin spars (Fig 3.10).

For blades of this construction, fabricated accounting for the latest achievements in weight reduction, this relationship can be presented in the following form:

$$\tilde{q}_{env} = 5.0 + 5.0b. \tag{3.35}$$

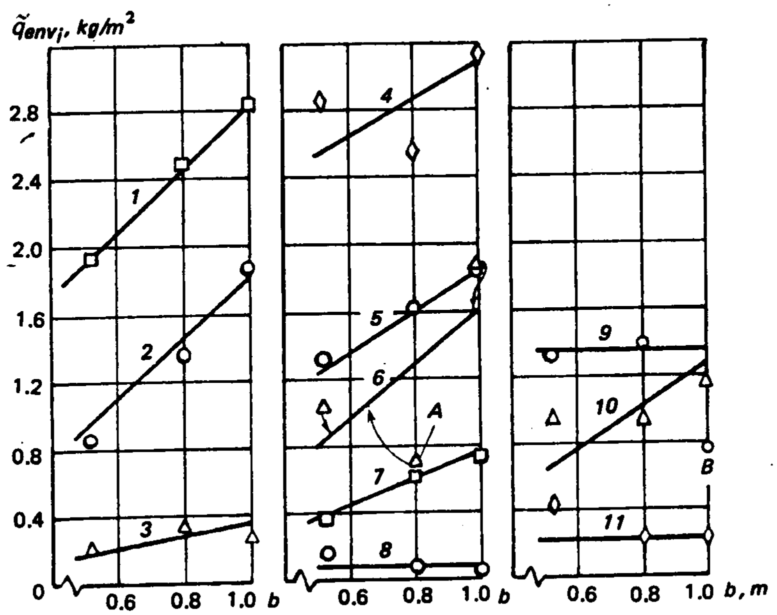

Figure 3.8 Specific weights versus blade chord of various envelope elements of a blade with tubular spar and glass-plastic skin and weight data of existing and projected blades: (1) leading-edge skin; (2) compensators and spacers; (3) ribs; (4) counterweight; (5) aft-section skin with reinforcement; (6) plastic foam; (7) adhesive; (8) aft stringer; (9) anti-icing and abrasion protection; (10) honeycomb filler; (11) inter-box inserts; and (A) point for a blade with reduced space between contour and spar; (B) point for a blade without protective strips

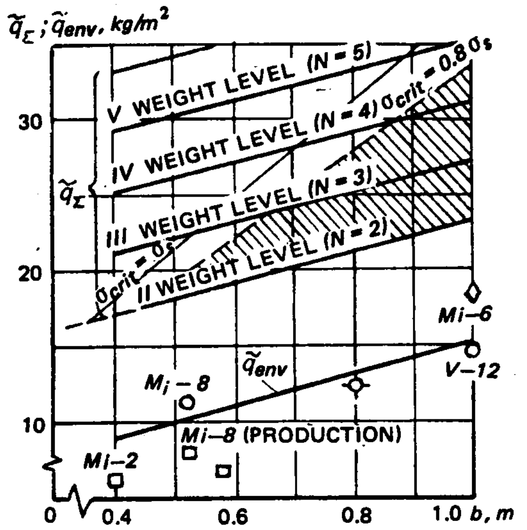

Figure 3.9 Specific weights of envelope $\tilde{q}_{env}$, and outer part $\tilde{q}_\Sigma$ of a blade with steel spar and glass-plastic shell corresponding to various weight levels (shaded region cannot be used because of loss of spar stability; circles represent specific weights of glass-plastic envelopes in blades with steel spars; squares mark specific weights of Duralumin envelope in blades with extruded spar; also shown is the envelope specific weight for the Mi-6 helicopter of mixed design)

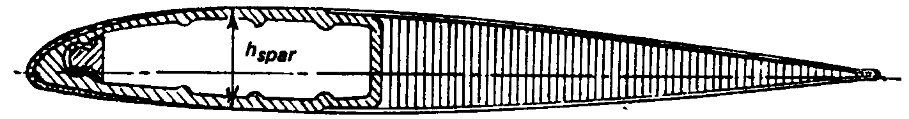

Figure 3.10 Cross-section of blade with extruded Duralumin Spar

For comparison, the specific envelope weight for several production blades with extruded aluminum spars are shown in Fig 3.9. Also shown is the specific envelope weight of the Mi-6 helicopter production blade which, as is well known, is fabricated according to a very complex structural scheme.

3.1.9 Specific Weight of Spar and Blade Outer Segment

In order to lighten the blade, the weight of the spar in its outer part should be reduced as much as possible. This would be the most effective weight reduction measure. Outside of the general requirements regarding the magnitude of the mass characteristic γ_o, blade stiffness in torsion, and possible loss of stability, such weight reduction encounters only technological (manufacturing) difficulties.

It is very difficult, although possible, to fabricate the spar tube with wall thickness of less than $\delta = 2mm$ at the tip. This constraint leads to a situation in which the specific weight of the steel spar at the tip cannot be less than $\tilde{q}_{spar} = 8\ kg/m^2$, if we assume that its perimeter is $S_{spar} = 0.512b$.

For blades with an extruded aluminum spar, the specific spar weight at the tip is somewhat lower in spite of the fact that its perimeter is usually about $S_{par} = 1.15b$. For a wall thickness of $\delta = 2mm$, it is about $\tilde{q}_{spar} = 6.1\ kg/m^2$.

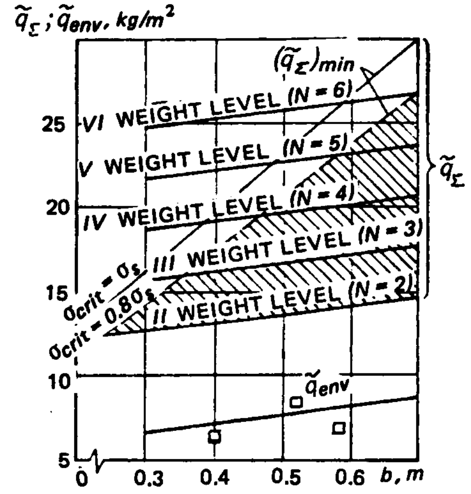

Figure 3.11 Weight per square meter of the outer part of blade with extruded Duralumin spar (hatched region cannot be used because of loss of spar stability at $\rho_{min}/b = 2.6$; squares represent specific weights of the extruded Duralumin spar blade envelope)

We introduce the concept of the blade-tip segment weight level, evaluating it on the basis of the spar wall thickness referred to a perimeter equal to $0.512b$ for the steel tube, and to a perimeter equal to $1.15b$ for the extruded aluminum spar. We take the sequential number N of each weight level to coincide with the wall thickness in millimeters; i.e., the blade with a spar tip wall thickness of 4 mm will belong to weight level IV.

Figure 3.9 shows the specific weights of blades with steel spar and glass-plastic envelope corresponding to various weight levels. These specific weights are described by the formula

$$\tilde{q}_\Sigma = 5.2 + 4N + 10.1b. \qquad (3.36)$$

In Fig 3.5, the values of $\overline{G}_{env}$ corresponding to these levels—varying with the blade chord—can be compared with the division of the blade into segments.

Similarly, the specific weights of the tip segment of the blade with extruded Duralumin spar can be described by the formula

$$\tilde{q}_\Sigma = 5.0 + 3.05N + 5.0b. \qquad (3.37)$$

The values of these specific weights are shown in Fig 3.11 as a function of the blade chord for various N.

3.1.10 Plume Weight of Unaugmented and Slender Blades

It follows from Figs 3.5 and 3.6 that up to definite values of the reduced aspect ratio, the blade consists only of the middle and ballast segments, while for $\bar{G}_{env} \leqslant \bar{G}^*_{env}$, the blade consists of the ballast segment only, and has no augmented root segment. We shall call such blades unaugmented and the maximum aspect ratio for which the augmented root segment does not yet appear, we call the maximum unaugmented blade aspect ratio λ_{una}. It follows from these figures that for the blade with steel spar and glass-plastic envelope, $\bar{R}(\lambda_{una})_{max}$ = 18.5 to 19, while for the blade with extruded aluminum spar, $\bar{R}(\lambda_{una})_{max}$ = 11 to 11.5.

For the unaugmented blades, the value of $i = i_0$ can be found from Eq (3.31), setting therein $\Delta\bar{r} = 0$ and $\bar{r}_1 = \bar{r}_0$,

$$i_0 = 1 - \bar{r}_0 + \tfrac{1}{2}\Delta\bar{q}_1(\bar{r}_2 - \bar{r}_1). \tag{3.38}$$

The values of i_0 are shown in Fig 3.7.

Consequently, the plume weight of unaugmented blades can be found from the formula

$$G_{pl} = i_0\tilde{q}_\Sigma bR. \tag{3.39}$$

In order to evaluate the plume weight of slender blades with reduced aspect ratios of $\bar{R}\lambda > \bar{R}(\lambda_{una})_{max}$, we construct a graph of the relative weight increase $\bar{i} = i/i_u$ as a function of the reduced aspect ratio $\bar{R}\lambda$. This relationship for the blade with steel spar and glass-plastic envelope is shown in Fig 3.12, and in Fig 3.13 for the blade with extruded Duralumin spar.

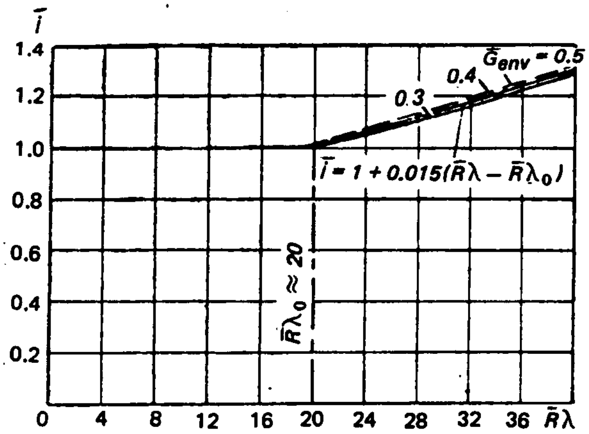

Figure 3.12 Coefficient $\bar{i}$ of the relative blade weight increase as a function of reduced aspect ratio $\bar{R}\lambda$ for blade with tubular steel spar and glass-plastic envelope

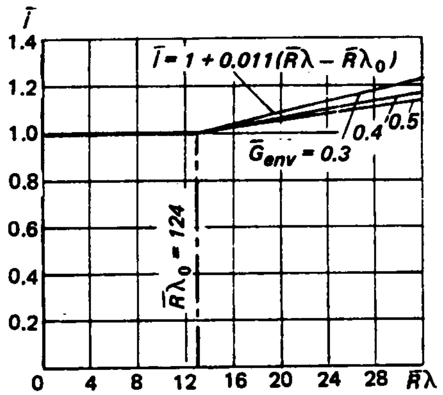

Figure 3.13 Coefficient $\bar{i}$ of the relative blade blade weight increase as a function of reduced aspect ratio $\bar{R}\lambda$ for blade with extruded Duralumin spar

For values of $\bar{G}_{env}$ corresponding to the usual blade-weight levels, these relationships can be represented in the form

$$\bar{i} = 1 + \alpha_\lambda \bar{R}(\lambda - \lambda_0) \tag{3.40}$$

where the coefficient $\alpha_\lambda = 0.015$ for the steel-spar blade, and $\alpha_\lambda = 0.011$ for the extruded Duralumin spar blade.

The value of the reduced aspect ratio $\bar{R}\lambda_0$ at which marked increase of the blade weight begins, is somewhat higher than $\bar{R}(\lambda_{una})_{max}$, and can be taken equal to $\bar{R}\lambda_u = 20$ for the steel spar blade, and $\bar{R}\lambda_0 = 12.4$ for the extruded Duralumin spar blade.

This approach makes it possible to evaluate the blade plume weight from the general formula

$$G_{pl} = i_o \bar{q}_\Sigma bR[1 + \alpha_\lambda \bar{R}(\lambda - \lambda_o)] \qquad (3.41)$$

where the expression in the square brackets is equal to one, except for blades with reduced aspect ratio $\bar{R}\lambda > \bar{R}\lambda_o$.

Calculations made taking (3.41) show that the weight of the blade plume increases insignificantly even for a very significant increase in the reduced blade aspect ratio. However, this weight increase may still have a noticeable influence on the selection of optimal helicopter parameters as shown earlier in Ch.2.

In addition to the constraints of blade aspect ratio on the blade mass characteristic λ_γ and tip deflection λ_y, λ_o values verus main rotor radius are shown in Fig 3.14 for blades with steel and extruded Duralumin spars.

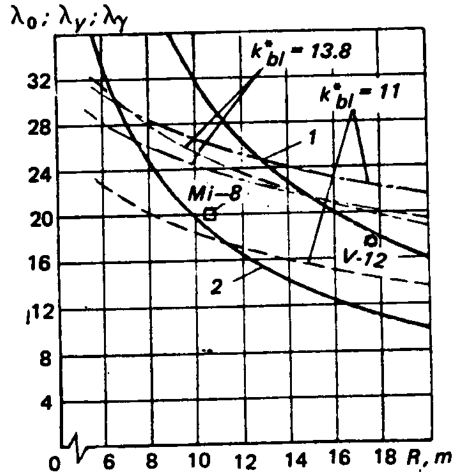

Figure 3.14 Maximum allowable blade aspect ratios constrained by: weight increase on the root part of the blade (λ_o); maximum allowable deflection of (λ_y) representing $\bar{y}$ = 0.12; and maximum allowable blade mass characteristic (λ_γ) corresponding to γ_o = 7 and k_{blmin} = 5.5. (1) blade with steel spar and glass-plastic envelope ($\bar{R}\lambda_o$ = 20); (2) blade with extruded Duralumin spar ($\bar{R}\lambda_o$ = 12.4)

——— λ_o; – · – · – λ_y; – – – λ_γ

3.1.11 Refinement of Formulae for Calculating Running Weight of Steel-Spar Blades with Very Large Aspect Ratios

If we examine steel-spar blades with reduced aspect ratios of $\bar{R}\lambda > 25$ for which the augmented root segment extends to the radius $\bar{r}_1 > \bar{r}_{i.lim}$, then refinement should be introduced into the calculation of $\Delta\bar{q}_o$.

We write

$$\Delta\bar{q}_o = \Delta\bar{q}'_o + \Delta\bar{q}''_o \qquad (3.42)$$

where $\Delta\bar{q}'_o$ = the relative increase in the blade running weight from the radius $\bar{r}_1$ to $\bar{r}_{i.lim}$; and $\Delta\bar{q}''_o$ from radius $\bar{r}_{i.lim}$ to $\bar{r}_o$.

Then,

$$\Delta\bar{q}'_o = 2\Delta\bar{r}'\bar{q}_\Sigma/\beta_1[1 - (\Delta\bar{r}')^2/3\beta_1] \qquad (3.43)$$

and

$$\Delta\bar{q}''_o = 2\Delta\bar{r}''/\beta_o[1 - (\Delta\bar{r}'')^2/3\beta_o]\ [\bar{G}_{\Sigma 1} + \Delta\bar{r}'(1 + \Delta\bar{q}_1) + \tfrac{1}{2}\Delta\bar{r}'\Delta\bar{q}'_o] \qquad (3.44)$$

where

$$\Delta\bar{r}' = \bar{r}_1 - \bar{r}_{i.lim},\quad \Delta\bar{r}'' = \bar{r}_{i.lim} - \bar{r}_o.$$

It is important that in determining β_1, here we have introduced the effective spar height within the segment where this height is limited by the relative airfoil thickness, $\bar{c}_{airf} \approx 10\%$.

The coefficient of the weight increase of such a blade can be defined as

$$i = 1 - \bar{r}_1 + (1 + \Delta\bar{q}_1)\Delta\bar{r} + \tfrac{1}{2}\Delta\bar{q}_1(\bar{r}_2 - \bar{r}_1)(\tfrac{1}{2}\Delta\bar{r}' + \Delta\bar{r}'')\Delta\bar{q}'_0 + \tfrac{1}{2}\Delta\bar{q}''_0\Delta\bar{r}''. \qquad (3.45)$$

3.1.2 Blade Size Constraints Determined by Loss of Spar Stability

With increase in the transverse dimensions of the spar section while keeping the same spar wall thickness, the critical buckling stresses for spar bending by forces acting in the same direction as the blade's own weight, decrease markedly.

If we assume as in the case for several existing blades, that the critical loss-of-stability stresses σ_{crit} must not be lower than the spar material yield stress σ_{yi}, we find that the spar wall thickness cannot be made smaller than a definite value δ_{min}, estimated from the curves shown in Figs 3.15 and 3.16. In these figures, the critical stresses for the steel-tube spar and for the extruded aluminum spar with the cross-section as shown in Fig 3.10 are plotted as a function of spar lower-flange radius of curvature ρ.

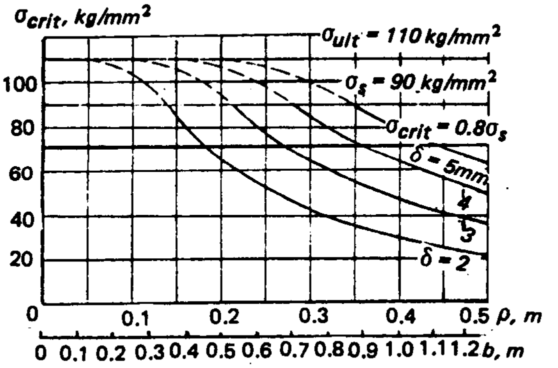

Figure 3.15 Critical buckling stresses in bending of tubular steel spar with oval section shape as a function of lower surface spar radius of curvature ρ and spar wall thickness δ. Corresponding blade chords which satisfy the condition ρ/b = 0.4 are also marked.

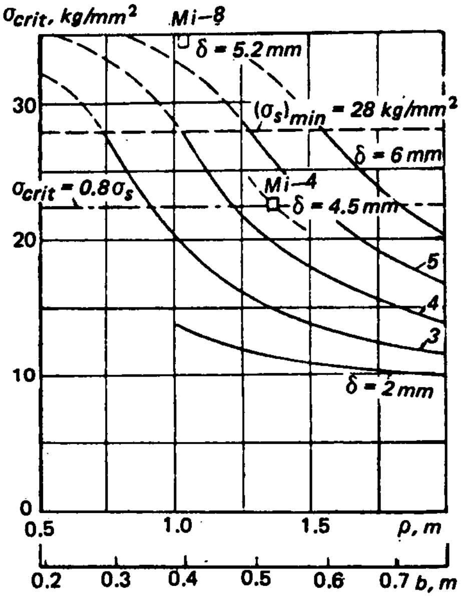

Figure 3.16 Critical buckling stresses in bending of extruded Duralumin spar as a function of spar lower-surface radius-of-curvature ρ and spar wall thickness δ . Corresponding blade chords which satisfy the condition ρ/b = 2.6 are also marked.

In determining σ_{crit} for the steel-tube spar, we used Eq (10) presented on page 421 of Ref 1, while for the extruded Duralumin spar, we used the formula for the critical compressive stresses in the aluminum plates given by Eq (13) presented on page 424 of the same reference. Fig 3.16 also shows the critical stresses for failure (from wall buckling) of the blade spars of the two helicopters.

On the basis of existing construction and those relationships of the spar and profile chord geometric dimensions which are, at the present time, considered optimal, we conclude that the maximum radius of curvature ρ at the relative blade radius $\bar{r}_2$ is related to the blade chord as follows: for the blade with steel spar and glass-plastic envelope, $\rho/b = 0.4$ (for example, for the blade of the V-12 helicopter), and for the blade with extruded Duralumin spar $\rho/b = 2.6$. Blade chords corresponding to these ρ/b ratios are shown in Figs 3.15 and 3.16.

Assuming that these relationships remain unchanged for blades of different dimensions, we can obtain from the curves of these figures, the maximum blade chords for the selected spar wall thickness.

However, we would like to indicate that it is not mandatory that the critical spar buckling stresses must be higher than the yield strength of the material. Thus, on the Mi-4 helicopter where, through many years of operating experience without a single case of buckling, the critical stress is

$$\sigma_{crit} = 0.8\sigma_{yi}. \tag{3.46}$$

Therefore, with suitable verification of blade strength for the case of blade impact on the stop, this magnitude of the critical stresses can be allowed for other blades as well.

3.1.13 Overall Blade Weight and Possible Approach to Determination of Minimal Obtainable Blade Weight

The overall blade weight consists of the weight of the blade plume and the weight of the root section for attaching the blade to the hub, which is usually termed the blade shank.

$$G_{bl} = G_{pl} + G_{shk}. \tag{3.47}$$

If we assume the values of p/b proposed above, then with satisfaction of the condition for $\sigma_{crit} = 0.8\sigma_{yi}$, some spar regions with small wall thicknesses would not be acceptable for use because of loss of spar static stability (see Figs 3.9 and 3.11). Consequently, the constraints with respect to spar stability do not permit having specific weight of the outer part of the blade below a definite minimal value of $(\tilde{q}_{\Sigma})_{min}$, and the blade plume weight cannot be made less than

$$(G_{pl})_{min} = i(\tilde{q}_{\Sigma})_{min} bR. \tag{3.48}$$

Upon evaluation of the minimal blade shank weight which can be determined only by taking into account the current technology development, we shall consider that the minimal blade weight can be defined as

$$(G_{bl})_{min} = (G_{pl})_{min} + (G_{shk})_{min}. \tag{3.49}$$

3.1.14 Approximate Formula for Determining Minimal Blade Weight

If we define the relative weight of the outer part of the blade envelope as

$$\bar{G}_{env} = \tilde{q}_{env}/(\tilde{q}_{\Sigma})_{min}$$

and determine i_o on the basis of these values using Eq (3.38) or Fig 3.7, then the value of $i_o(\tilde{q}_{\Sigma})_{min}$ for the adopted blade chord values is approximately

$$i_o(\tilde{q}_{\Sigma})_{min} = q_{\pi}\, b^{0.745} \tag{3.50}$$

where $q_{\pi} = 31.2$ for the blade with steel spar and glass-plastic envelope, and

$$i_o(\tilde{q}_{\Sigma})_{min} = q_{\pi} b^{0.785} \tag{3.51}$$

where $q_{\pi} = 32$ for the blade with extruded Duralumin spar.

The error will be small, if we assume that

$$l_o(\tilde{q}_\Sigma)_{min} = q^*_\pi b^{0.7} \tag{3.52}$$

where $q^*_\pi = 30.9$. Substituting this expression into Eq (3.48) with account for Eq (3.40), we obtain

$$(G_{pl})_{min} = q^*_\pi b^{1.7} R[1 + \alpha_\lambda \bar{R}(\lambda - \lambda_o)]\,. \tag{3.53}$$

Below, we shall analyze the possible blade shank weights, and their dependence on the magnitude of centrifugal force.

However, for an approximate weight estimate, we can assume that the shank weight is a fixed percentage of the blade plume weight. Then, for evaluating the weight of the blade as a whole, we can assume a formula analogous to Eq (3.53):

$$(G_{bl})_{min} = q^*_{bl} b^{1.7} R[1 + \alpha_\lambda \bar{R}(\lambda - \lambda_o)]\,. \tag{3.54}$$

This formula can be considered a general expression for evaluating the minimal possible weight of both blades with steel spar and glass-plastic envelope and blades with extruded Duralumin spar; only the values of q^*_{bl} will differ somewhat because of differences in the specific weights of the outer part of the blade and in the weights of the blade shanks.

3.1.15 Weight of Blade Shanks

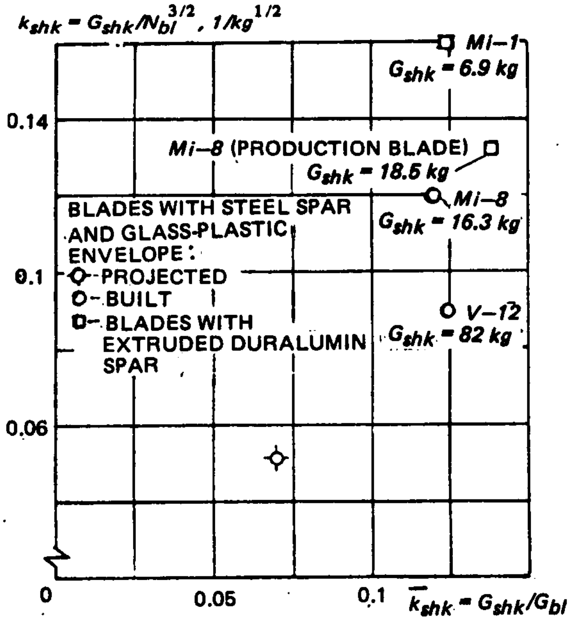

Figure 3.17 Statistical data on weights of blade attachments (shanks) for two types of construction

The weight of blade shanks in existing production main-rotor blades is usually from 10 to 17 percent of the blade weight; i.e., a significant fraction of the blade weight.

This weight is conveniently evaluated using the same formulae used for the main-rotor hub weight. We assume that

$$G_{shk} = k_{shk}(N_{bl})^{3/2} \tag{3.55}$$

where N_{bl} = blade centrifugal force in tons.

Figure 3.17 shows the values of k_{shk} for various existing blades and for a blade design with steel spar and single-bearing flanged attachment with the use of titanium. We see from this figure that at the modern level of tube fabrication technology, the shank of the blade with steel tubular spar can be made with a weight coefficient of $k_{shk} = 0.055$.

The weight coefficients of the shanks of blades with extruded Duralumin spars are considerably higher and, in the best case, may be equal to 0.135.

3.1.16 Refinement of Approximate Formula for Minimal Blade Weight

We shall determine the ratio of the shank weight to the blade plume weight. If we assume that

$$N_{bl} = (G_{pl}/g)(U_t^2/R)\bar{r}_{c.g}, \tag{3.56}$$

and determine the blade plume weight in accordance with Eq (3.53), examining only unaugmented blades, then

$$(G_{pl})_{min} = q^*_{pl}\, b^{1.7} R \tag{3.57}$$

then in accordance with Eq (3.55) and setting $\bar{r}_{c.g} = 0.5$, we obtain the blade attachment (shank) relative weight as

$$\bar{k}_{shk} = 3.87 k_{shk} b^{0.85} (\bar{U}_t/R)^3 \sqrt{q^*_{pl}} \tag{3.58}$$

where $\bar{U}_t = U_t/U_{to}$ $(U_{to} = 220\ m/s)$.

Taking $q^*_{pl} \approx 30$ and $k_{shk} = 0.055$ as approximates, we obtain the minimal values of the coefficient $\bar{k}_{shk}$ for the blade with steel spar and glass-plastic envelope shown in Fig 3.18. The same coefficient for the blade with extruded aluminum spar will be 2.5 times higher.

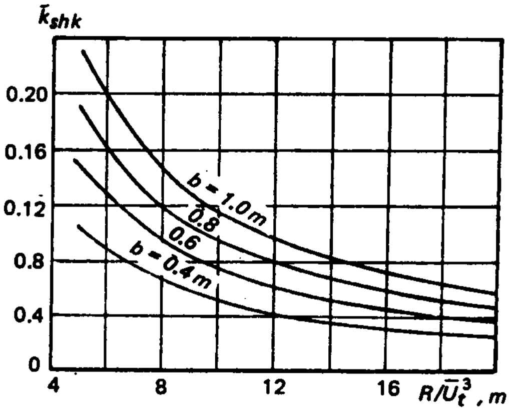

Figure 3.18 Approximate ratio of shank weight to plume weight $\bar{k}_{shk} = G_{shk}/G_{pl}$ of blades with tubular steel spar and glass-plastic envelope

With account for these results, the approximate blade weight formula of Eq (3.54) can be rewritten as follows:

$$(G_{bl})_{min} = (1 + \bar{k}_{shk}) q^*_{bl} b^{1.7} R\,[1 + \alpha_\lambda \bar{R}(\lambda - \lambda_o)]\,. \tag{3.59}$$

The value of the expression $(1 + \bar{k}_{shk})$ for the coefficients shown in Fig 3.18 and the blade parameters used can be approximately determined from the formula

$$1 + \bar{k}_{shk} \approx 1.38 b^{0.1(1.65\, -\, \log R)}/R^{0.091} \tag{3.60}$$

which makes it possible to somewhat refine Eq (3.54).

If we examine blades with radius $R \approx 16\,m$, then Eq (3.60) can be rewritten in the following form:

$$1 + \bar{k}_{shk} \approx 1.38 b^{0.045}/R^{0.091}\,. \tag{3.61}$$

Consequently, the formula for the minimum attainable weight of the blade with steel spar and glass-plastic envelope with account for Eqs (3.50) and (3.61) can be written as

$$(G_{bl})_{min} = 43b^{1.79} R^{0.091} [1 + \alpha_{\lambda} \bar{R}(\lambda - \lambda_o)] . \tag{3.62}$$

However, the refinements resulting in this formula in comparison with the weight estimates using Eq (3.54) are not significant enough to be taken into consideration in selecting helicopter parameters.

3.1.17 Minimal Lifting-Rotor Blade weight as a Function of the Blade Chord and Radius, Obtained Using the Approximate Formulae

If we determine the blade plume weight using Eq (3.48), then the minimal weight of the blade as a whole can be calculated from the following formula

$$(G_{bl})_{min} = (1 + \bar{k}_{shk}) i_o (\tilde{q}_{\Sigma})_{min} b R [1 + \alpha_{\lambda} (\lambda - \lambda_o)] . \tag{3.63}$$

Figure 3.19 shows the blade weight per square meter $(G_{bl})_{min}/bR$ as a function of main-rotor radius for several blade chord values.

The slight reduction of the blade weight per square meter on the region up to $\bar{R}\lambda = \bar{R}\lambda_o$ is explained only by the variation of the shank weight which, because of the reduction of the blade centrifugal force at $\omega R = const$, decreases with increase of R.

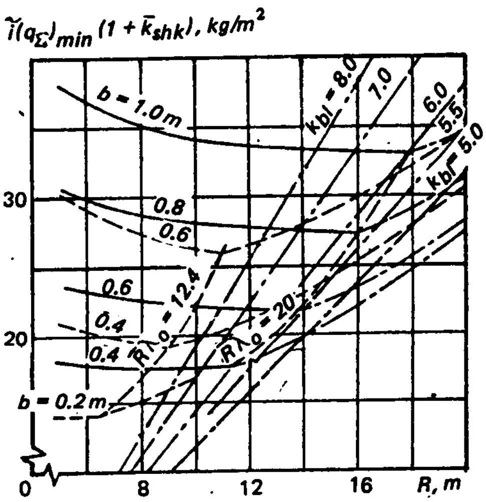

Figure 3.19 Minimal blade weight referred to bR versus main-rotor radius for various blade chords

The weight values shown can be compared with the coefficients k_{bl} indicated in the same figure. We see from this comparison that the blade-weight dependence on its chord and radius does not follow the $k_{bl} = const$ law. In order to compare these results with the calculations based on the use of Eq (2.8) of Ch 2, we establish the dependence of the coefficient k^*_{bl} on the main rotor radius.

$$k^*_{bl} = \pi(\bar{\lambda})^{0.7} G_{bl}/bR^{1.7} [1 + \alpha\bar{R}(\lambda - \lambda_o)] = i(\tilde{q}_{\Sigma})(1 + \bar{k}_{shk})/2.41 b^{0.7} . \tag{3.64}$$

These relationships are shown in Fig 3.20. For all the considered blade sizes, we see from these curves that when $R > 8\,m$, the coefficient k^*_{bl} lies in a quite narrow range of 12.8 to 14.6 for blades with steel spar and glass-plastic shell, and varies within $k^*_{bl} = 14$ to 16 for blades with extruded Duralumin spar. Consequently, the nature of the dependence of the weight of the considered blade designs on blade chord and radius is quite close to the law that $k^*_{bl} = constant$, which justifies the use of Eq (2.8).

3.1.18 Evaluation of Overall Blade Weight for Given Wall Thickness of the Spar Tip

In reality, for both technological and manufacturing reasons, blades which have actually been constructed have a weight greater than the minimal feasible value. Therefore, it is important to evaluate the weight of blades conceived with different weight levels of the outer part of the blade in order to present other possible constraints which are effective in blade design. We assume the blade envelope weight as determined in Subsection 3.1.8.

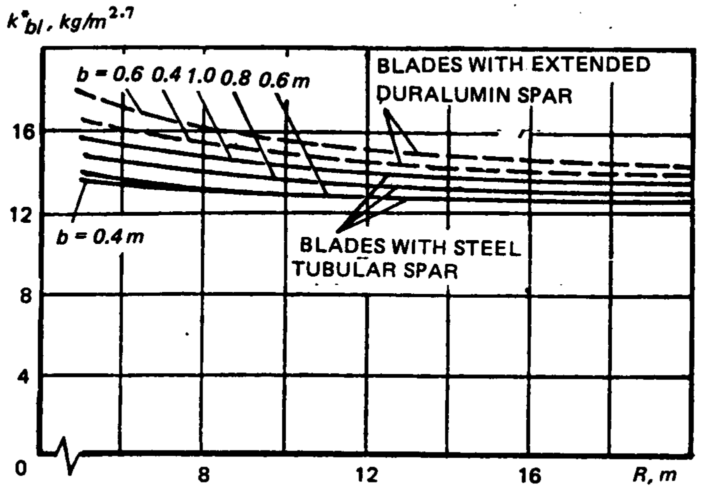

Figure 3.20 Variation of weight coefficient k^*_{bl} for the considered blade types throughout the range of examined values of b and R: – – – blade with extruded Duralumin spar; and ——— blade with tubular steel spar

We shall evaluate blade weight in terms of the coefficient k^*_{bl} (see Subsection 2.2.1). If, by analogy, the blade plume weight is written as

$$G_{pl} = k_{pl} b R^2 / \pi, \tag{3.65}$$

then the value of k_{pl} can be expressed in terms of the coefficient of Eq (3.33),

$$k_{pl} = \pi i \tilde{q}_\Sigma b / R. \tag{3.66}$$

Just as above, we obtain the blade weight by combining the plume weight with that of the shank by which the blade is attached to the hub link.

Assuming that the blade centrifugal force can be represented using Eq (3.56) and substituting the value of G_{pl} from Eq (3.65) into this formula, we find that the blade weight coefficient can be written as

$$k_{bl} = [1 + (k_{shk} \bar{r}_{c.g}{}^2 U_t{}^3 / g\, 10^{9/2}) \sqrt{k_{pl} / \pi g \bar{r}_{c.g} \lambda}\,] k_{pl}. \tag{3.67}$$

As an example, the values of the weight coefficient k_{bl} calculated using Eq (3.67) are shown in Fig 3.21 as a function of main-rotor radius for various weight levels of blades with aspect ratio $\lambda = 20$ and under the assumption that $\bar{r}_{c.g} = 0.49$ and $k_{shk} = 0.055$ for blades with steel spar, and $k_{shk} = 0.135$ for blades with extruded Duralumin spar.

We have already mentioned that these values of the coefficients were obtained for designs with the blade envelope weight which can be achieved at the modern level of construction and which should be considered to be very low. The spar cross-section dimensions were assumed to be as close as possible to the airfoil contour in order to reduce, as much as possible, the weight of the envelope forming this contour. This approach is justified by the fact that it leads to the maximum possible increase in the spar stiffness in torsion. But at the same time, because of the increase of the radii of curvature of the lower surface of the spar and reduction of the wall thickness, the critical spar buckling stresses decrease. As has been mentioned, this situation leads to a limitation of the minimal values of the weight coefficients k_{bl}.

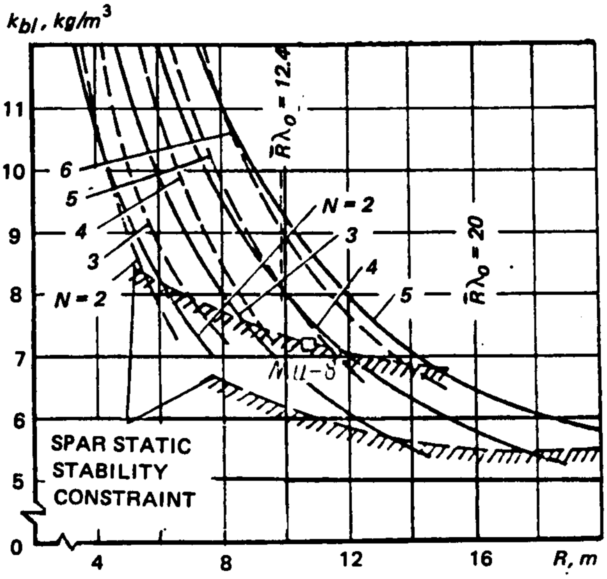

Figure 3.21 Calculated weight coefficients k_{bl} as a function of main-rotor radius for two blade constructions with aspect ratio $\lambda = 20$ for various weight levels, as determined by spar wall thickness: ——— blade with steel spar; and — — — blade with Duralumin spar

Figure 3.21 also shows the constraints associated with satisfaction of the condition that the critical buckling stresses in spar bending should not be lower than $0.8\sigma_{yi}$.

In addition, we see from Fig 3.21 that for small main-rotor radii and, therefore, small blade chords resulting from the assumed $\lambda = const$, the blade weight increases still more sharply because of the constraints associated with the difficulty of making spars with wall thicknesses lower than $\delta = 2\ mm$. Therefore, for such blades, we should examine other constructions; for example, with C-shaped spar.

3.1.19 Results and Conclusions of the Analysis

Our analysis of the weight-contributing structures of rectangular-planform blades and specifically, of two types of construction—with steel, and extruded Duralumin, spars—shows that the minimum feasible blade weight is proportional to the weight per square meter of the outer part of the blade and the overall blade area. Since the envelope weight per square meter at the blade outer region increases with increase of the blade chord, the weight of the blade as a whole also increases to the same degree with enlargement of the blade chord.

The blade weight is associated, in the same fashion, with the spar tip wall thickness. The thinner the spar in the outer blade region walls, the lower the weight of that part and the overall blade weight.

The blade weight does not depend directly on the blade aspect ratio, if this ratio is less than the reduced maximum "unaugmented-weight" aspect ratio $(\lambda_{una})_{max}$. This dependence shows up indirectly, since the weight per square meter of the outer blade segment depends on the blade chord; and with change of the chord and unchanged blade radius, the aspect ratio λ will change, and the blade weight will increase with increase of the chord and corresponding reduction of the blade aspect ratio. For an aspect ratio larger than the maximum "unaugmented-weight" aspect ratio $\bar{R}(\lambda_{una})_{max}$, the blade weight, in addition, increases directly with increase of its aspect ratio because of the necessity for reinforcing the root part of the spar.

It follows from these relationships that for constant rotor tip speed and constant chord ($\omega R = const$, and $b = const$), the minimum obtainable weight of the blade with an aspect ratio lower than $\bar{R}(\lambda_{una})_{max}$ increases proportionally to the blade radius, while the weight coefficient k_{bl} decreases inversely to the blade radius. Consequently, with increase of the main rotor radius, the blade can be made with a higher value of the mass characteristic γ_o; i.e., relatively lighter.

]

With increase of the chord, the blade weight increase is not proportional to the chord, but more rapid because of the increase of the blade outer envelope weight per square meter and the necessity—because of the large spar transverse dimensions—to increase the spar wall thickness in order to prevent buckling when the blade strikes the droop stop.

Consequently, when maintaining a constant overall blade area, the main rotor with a larger number of blades and smaller blade chord will always be lighter as long as the blade aspect ratio is no higher than the maximum unaugmented-weight aspect ratio.

Because of the constraint based on spar buckling, the weight coefficient of the blade with steel spar and glass-plastic shell with $\lambda = 20$ (see Fig 3.21) cannot be made lower than $k_{bl} = 5.4$. For the blade with extruded Duralumin spar, the minimal value of the weight coefficient of the blade with the same aspect ratio is $k_{bl} \approx 6.8$, although it is possible to obtain even lower values of this coefficient if we somewhat increase the height of the spar-wall stiffening fins (see Fig 3.10) and thereby increase the critical buckling stresses.

One's attention should also be called to the additional weight increase of the considered construction types when the chord becomes less than $b = 0.25\ m$ for blades with extruded aluminum spar, and less than $b = 0.45\ m$ for the blade with steel tubular spar and glass-plastic envelope, because of manufacturing aspects limiting spar wall thickness to no less than $\delta = 2\ mm$. In order to avoid this weight increase, we can either seek manufacturing techniques permitting reduction of the spar wall thicknesses to values lower than $\delta = 2mm$, or develop different designs; for example, with spar of open-section form. Otherwise, the blades of such dimensions will be significantly heavier.

Examination of the two blade construction types confirms the well-known—and obvious from general considerations— conclusion that for different main-rotor dimensions, different blade designs may be optimal from the viewpoint of minimum attainable weight.

Therefore, in the statistical data on the weights of blades of different designs, we do not observe the marked differences in the values of the weight coefficients which were obtained through the analytical calculations presented herein. However, the general tendency toward reduction of the coefficients k_{bl} with increase of the rotor radius and reduction of the blade chord and marked increase of this coefficient for small main-rotor radii can also be noted in examining the data for the existing blades presented in Ch 2.

There is no doubt that the described relationships, obtained from examination of the two construction types, will have approximately the same character for other types of blades as well. Therefore, the formulae presented in this chapter—with some refinements of the values of the coefficients appearing in the formulae—can also be used for other constructions. Naturally, we can expect that the use of various new technical approaches will make it possible to reduce the minimum obtainable weight in modern blade constructions, or will make it possible to expand the region of application of any particular type.

At the same time, there is no basis to expect that the weight of the blade types examined here can be changed significantly in comparison with the data obtained as a result of the calculations.

In concluding this chapter, it should be emphasized that the entire analysis presented here is made on the basis of manufacturing capabilities and static-strength requirements. The necessity for the satisfaction of many other conditions may have a significant effect on the conclusions drawn herein, although satisfaction of these conditions may be achieved without large weight expenditures.

4

SOME METHODS FOR CALCULATING HELICOPTER COSTS

4.1 Helicopter Production Costs

After making all the required calculations using the techniques presented in the preceding sections, one can be certain that the selected helicopter parameters will ensure the maximum possible weight efficiency of the designed aircraft. But, can we, at the same time, be equally certain that this vehicle will also be optimal from an economic viewpoint?

4.1.1 Basic Difficulties in Evaluating Economic Aspects of Helicopter Operations

The concepts of aircraft weight and economic efficiency are traditionally considered to be equivalent. Indeed, even a very simple analysis indicates a significant relationship between the weight of a structure and its cost (Fig 4.1). The higher the weight of the helicopter structure, the more expensive the machine. The higher its weight efficiency, the higher its productivity (other conditions being the same). Since the ratio of cost to productivity is considered to be the most universal criterion for evaluating the quality of any transport vehicle, the following conclusion seems obvious: Helicopter structural weight should be reduced whenever possible.

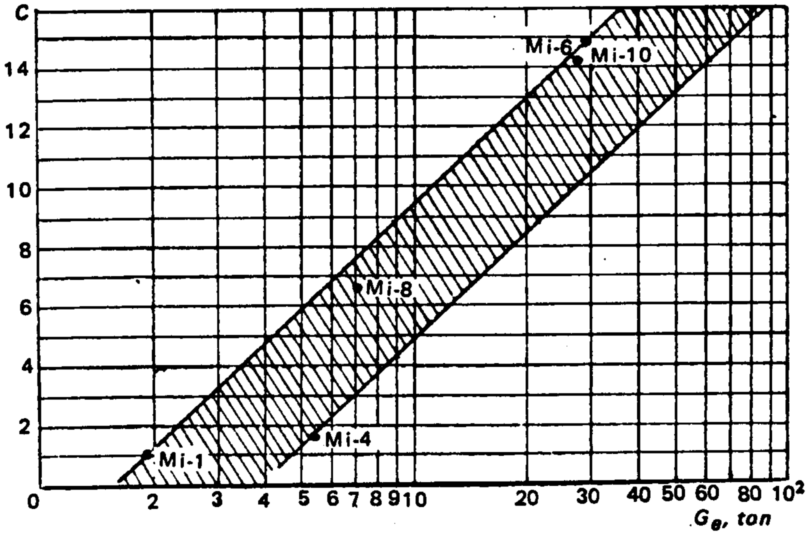

Figure 4.1 Helicopter cost as a function of structural weight (C = helicopter cost in fifth year of production, referred to the Mi-1 helicopter cost

Recently, however, it has been suggested that a helicopter may sometimes be heavier but, at the same time, more economical[28,30]. In order to make certain that the selected helicopter design variant is also optimal with respect to the economic criterion, it is necessary to have reliable methods of economic analysis. However, because of various difficulties, the accuracy of economic predictions based on the "weight-cost" hypothesis has not been high in the past. Errors reaching a factor of two or three were not unusual. We shall illustrate the complexity of the problem by some examples. Let us assume that we wish to determine the basic cost of manufacturing a helicopter having a gross weight of about 3.5 tons (34.4 kN), capable of transporting 900 kg (8.85 kN) of cargo over a distance of 100 km. We take, as 100 percent, the cost of the predecessor helicopter having a gross weight of about 7.5 ton (73.9kN), cargo capacity of about 2 ton (19.6 kN), and a 400-km range (both helicopters have piston engines). As an axiom, we take the statement: The heavier the machine, the more expensive it is. Let us assume that the helicopter cost is proportional to its weight. Then, the cost of the 3-ton helicopter in our problem should be about 40 percent of the cost of the 7-ton helicopter. However, the cost relationship of actual production machines may be quite different.

For example, we know of two helicopters similar to those being examined. The lightweight machine is more than twice as expensive as the heavy machine (for the same number of machines produced, and for the same service life). There are known cases in which helicopters of the same type built in different factories differed in cost by a factor of 1.5. If we wish to correctly compare machines with respect to their manufacturing cost, it is necessary to consider the differences in outfitting the manufacturing plants with modern equipment, in staffing with qualified personnel, in organizational efficiency and experience in helicopter production, in the time-varying costs of materials and labor, and we must also consider the differences in the geographic location of the manufacturing plants. But, as will be shown below, even this is not sufficient. For example, the plants of well-known American engine manufacturers such as Lycoming and General Electric—as far as we can judge by available information—are nearly equal with respect to their equipment level, personnel qualification, and experience in producing turboshaft engines for helicopters. Apparently, the other production conditions affecting the cost of their output are also approximately the same. Table 4.1 shows the characteristics of two types of helicopter engines of these firms that are in the same power class; have been in mass production for a long time, and compete with one another in the world market.

To the data of Table 4.1, we should add that at the time of comparison, the TBO's of the two engines were nearly the same and their production rates were also similar.

These data indicate first, that the widely-used method for estimating the cost of one machine purely on the basis of the cost per kg of another one may lead to large errors, even in those cases when the production conditions are the same for both models; second, price apparently has very little influence on the scale of application, as both engines are mass produced.

The first aspect is undoubtedly explained by the greater complexity of the T-58 design and the higher precision required in the manufacture of the components; consequently, the technology required is more complex. The second aspect seems to be explained by the fact that the additional costs of procuring the lighter weight, but more expensive, engines are balanced by the possibility of increasing the payload (productivity) while retaining the same design gross weights of such medium-size helicopters as the S-61 and BV-107* on which these engines were installed or, conversely, by the possibility of reducing their gross weights while maintaining a

---

*It is known that T-53 engines were installed on the BV-107 prototype.

CHARACTERISTICS	ENGINE TYPE	
	General Electric T-58 (installed on the following helicopters: Sikorsky S-61, Boeing-Vertol 107 Kaman HU2K, & on some modifications of Bell Iroquois; e.g., UH-1F)	Lycoming T-53 (installed on various versions of the Bell Iroquois)
Specific Fuel Consumption; kg/hp.hr	0.286	0.322
Maximum Power, hp	1280*	1100*
Weight, kg (N)	138 (1360)	220 (2160)
Average world-market price in1000-dollar units**	69	39
Price per kg of engine weight, $	500	177.5
Price of one hp, $	55	35.6

*Power of both engines was increased to 1500 hp in the Seventies

**According to late Sixties Data

TABLE 4.1 CHARACTERISTICS OF THE T-53 & T-58 ENGINES (1967 DATA)

given payload. This latter aspect involves reduction of certain forms of operating costs; specifically, an additional decrease in fuel costs (in addition to the fuel savings directly resulting from the lower specific fuel consumption of the T-58 engine). It is well known that in the stage of selecting basic helicopter parameters, a reduction by one kg of the weight of any helicopter component leads to a reduction in the gross weight by several kilograms[11]. The lower the weight class of the designed vehicle, the smaller this gain. It is therefore possible that for light helicopters of the Iroquois type, the increase of their cost because of installation of the expensive, but light, T-58 engines was not adequately compensated for by the increase of their productivity and a reduction of certain operating costs. In other words, in this case, it was economically better to develop a machine having obviously poorer weight characteristics than might otherwise have been achieved.

We note that the Iroquois helicopter with the relatively heavy T-53 engine was—at the time this book went to press—the most widely produced helicopter in the West. According to the foreign press, by 1974 more than 16,000 of these helicopters had been built (for comparison, the number of constructed helicopters of any other type did not exceed 4000 machines).

It is possible that the installation of the more expensive T-58 engine on certain modifications of the Iroquois helicopter (see Table 4.1) can be explained by the fact that such modifications were developed to perform special tasks which were not possible to accomplish with the aid of the T-53 engine; for example, because of the higher fuel consumption rates.

In any case, this example shows that evaluation of the component cost of a new helicopter, using statistical weight data without adequqte precise accounting for design differences, may not be reliable. This conclusion is confirmed by other examples as well. Thus, the engine characteristics of the well-known M-6 and Mi-8 helicopters are shown in Table 4.2. Here, again, the conditions at the manufacturing plants are approximately the same. At the time of comparison, about the same number of each engine had been produced. But we see from the table that the engine, which is several times heavier and more powerful, still has a much lower specific cost.

CHARACTERISTIC	ENGINE TYPE	
	TV-2-117 (installed on the Mi-8 helicopter)	D-25V (installed on the Mi-6 helicopter)
Maximum Power, hp	1500	5500–6500
Weight, kg(N)	325 (3200)	1300 (12800)
Cost in percentage of the D-25V engine cost	81.5	100
Cost per kg (percentage cost per 1 kg of the D-35V engine)	326	100
Cost of one HP (in percentage of 1-hp cost of the D-25V engine)	300	100
Note: At establishedmass production and equal-delivery rate.		

TABLE 4.2 CHARACTERISTICS OF D-25V AND TV-2-117 TURBOSHAFT ENGINES
(For established production level and equal rate of production)

Perhaps helicopter engines are an exception? Statistical data on the specific costs of some helicopters and their components are shown in Fig 4.2. The known actual specific costs of the basic components of certain production helicopters are marked along the ordinate axis; while the abscissas indicate their theoretical specific costs* computed, in the present case in accordance with the adopted hypothesis of proportionality between weight and cost; and expressed with respect to the specific costs of the corresponding helicopter components adopted as standard. If this hypothesis were ideally valid, all the points for the components of the considered helicopters should lie on the straight line of the reference helicopter. In actuality, we observe nearly random scatter of the points.

4.1.2 Basic Tendencies in Economics of Modern Helicopter Construction

Through more careful examination of Fig 4.2—knowing the year when the helicopters represented were developed—we can identify some temporal relationships. The ordinates representing the specific cost of those helicopters for which the data is given in Fig 4.2, are shown in Fig 4.3, along with that of other production machines. The time, in years, from the initiation of series of the oldest of these helicopters, is marked along the abscissa.

The cost per kg of the structure of each helicopter decreases from year to year as its series production is mastered and the output increases. This obviously does not require any special explanation, but the cost per kg of the structure of each helicopter of a later design is higher in the n-th year of production than that of its predecessor. This latter tendency is usually

---

*Specific cost is defined as the cost per kg of component weight.

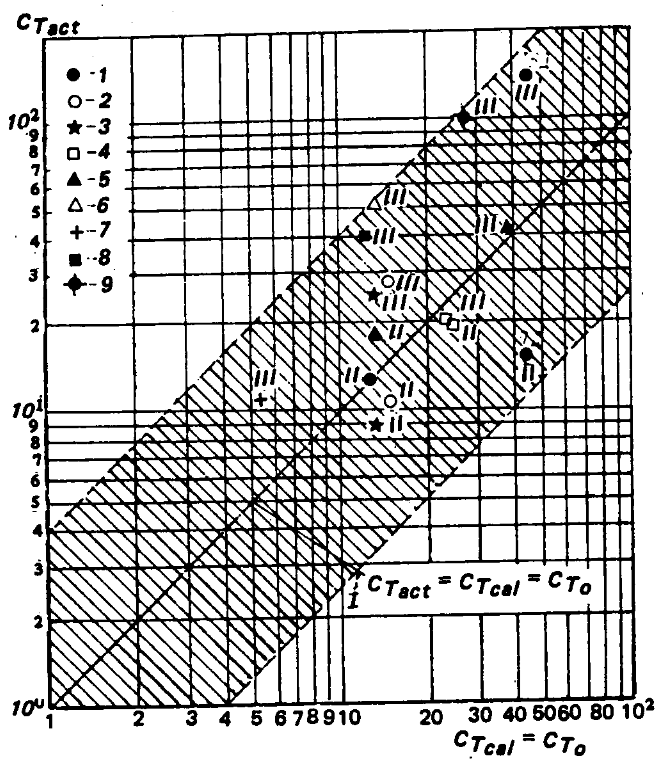

Figure 4.2 First regression analysis. Relationship between calculated and actual specific costs of basic components of some production helicopters: I) helicopter Model I; II) helicopter Model II; III) Helicopter Model III; 1) engines; 2) transmission; 3) hub; 4) blades; 5) fuselage; 6) tail rotor; 7) landing gear; 8) swashplate; 9) equipment. (C_{T_0} = specific cost of components of baseline helicopter Model I; values of C_T expressed in terms of specific equipment cost of helicopter Model III, taken as 100).

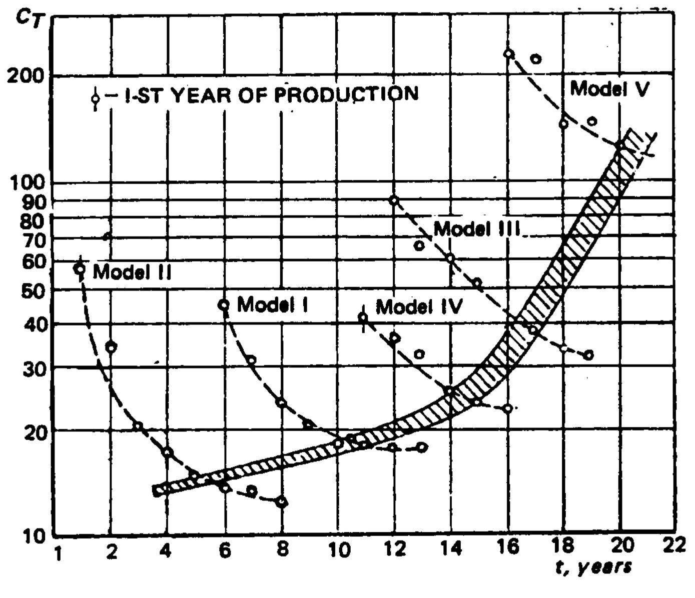

Figure 4.3 Variation of specific cost of structure C_T for some production helicopters as a function of time t from entry into series production of Model II; (C_T is expressed in terms of the specific equipment cost of helicopter Model III, taken as 100).

usually explained by the continuously increasing complexity of the design, more sophisticated production, and inspection methods which are the result of the necessity for improving the productivity and reliability of the new flight vehicle, and expanding its capabilities. The cost increases most steeply as a result of installing increasingly complex equipment on the helicopters, and also because of the use of better, but, as a rule, more expensive building materials. The modern helicopter, designed according to 1950 requirements would, of course, be more expensive today, but it would also be more efficient.

Can this statistical temporal relationship be used to solve the problem of selecting optimal parameters? Of course not, and precisely because this is a time-dependent relationship. Obviously, it is convenient for any sort of retrospective analysis, since it reflects the results of reducing to practice the concepts which dominated in the design of helicopters in the preceding period; especially the concept of structural weight reduction at any cost. But the absolute validity of this concept must be verified.

4.1.3 Some Drawbacks of Existing Methods for Calculating Helicopter Costs

There are several statistical formulae that are sometimes used for preliminary evaluation of aircraft costs. Unfortunately, the structure of these formulae does not always adequately reflect all the factors which determine vehicle cost. One such formula is the following relationship that is sometimes used in cost estimates of helicopter mechanical components:

$$C_n = k_m (G_n)^m \tau^{\ell} (N\underline{o})^{-t} k_{cor} \tag{4.1}$$

where C_n = cost of the n-th component; G_n = its weight; τ = service life; $N\underline{o}$ = serial number of components in series production; k_m, m, ℓ, and t = constants determined from statistics; and k_{cor} = coefficient correcting the temporal variations (also taken from statistical data).

There is no question as to the validity of the term $(G_n)^m$ in this formula. The term $(N\underline{o})^{-t}$ also appears valid. The cost reduction as a function of the number of articles produced has just such a nature (Fig 4.4) for practically all the industrial products. As for the real relationship, $C_n = f(\tau)$ is considerably more complex than that reflected by Eq (4.1). In actual practice, a considerable increase, or reduction, of helicopter component service life is frequently accomplished on the basis of operating experience without the introduction of any fundamental changes in design and manufacturing; and consequently, without additional expenditures (simply on the basis of operating experience and control testing results). Therefore, τ should be interpreted as assumed during the design "service life" potential of a component that is primarily determined by the component weight, fabrication precision, quality of the materials used, and so on. But in this case, how do we allocate the cost associated with change of the "service-life" potential between the terms $(G_n)^m$ and $(\tau)^{\ell}$ when determining the exponents m and ℓ in Eq 4.1?

At the same time (Eq (4.1) does not directly account for such cost factors influencing the improvements (complications or simplifications) which are not associated with increasing service life. Thus, in accordance with this formula, main rotor hubs having the same weights, service life, and production serial numbers, but differing in construction (one is the classical type with mechanical hinges, the other has elastomeric hinges) should have the same production cost. However, in reality, the difference in the cost of these hubs may be very significant.

But let us assume that we have in some way been able, with the use of stastics, to select values of the quantities k_m, m, ℓ, t, and k_{cor} in such a way that they would ensure satisfactory agreement of the calculated costs with the real costs for existing helicopters. Does this mean that we have obtained a correct basis for determining the cost of a component being designed

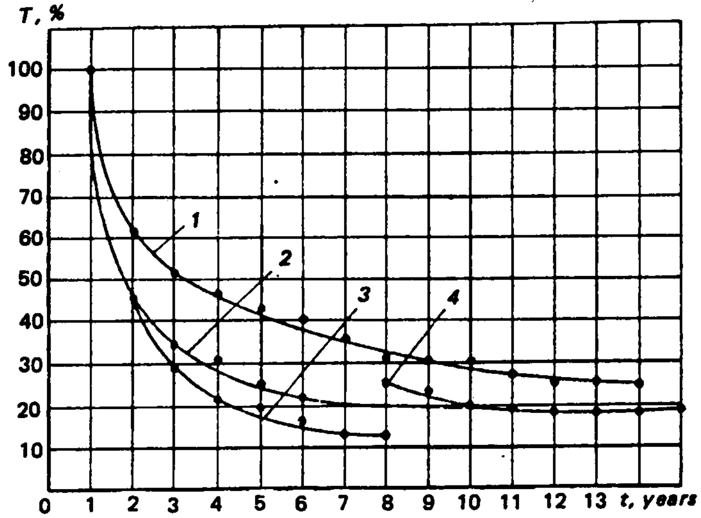

Figure 4.4 Part fabrication manhours T (in percent of manhours per part in the first year of series production) as a function of series production time t: 1) Model I (in plant A) 2) Model II (in plant B); 3) Model III (in plant B); 4) initial production of modified version.

for a new helicopter by using Eq (4.1)? Of course not. We have already seen that there are components with the same service life, produced in the same time period, belonging to the same class, and having the same serial number in series production, but differing in cost. Should one use this formula to calculate the costs of the engines in Table 4.1? The cost of the heavier engine would be approximately 1.5 times higher than that of the lighter engine; i.e., an error of more than a factor of 3 will be made. In this case, Eq (4.1) could not take into account the differences in the required fabrication accuracy. The influence of this factor on cost is illustrated in Fig 4.5, where the relationship between the required machining time and the established manufacturing tolerances are shown—with tightening of the tolerance from 0.05 to 0.025, the time required is increased by a factor of 4[30].

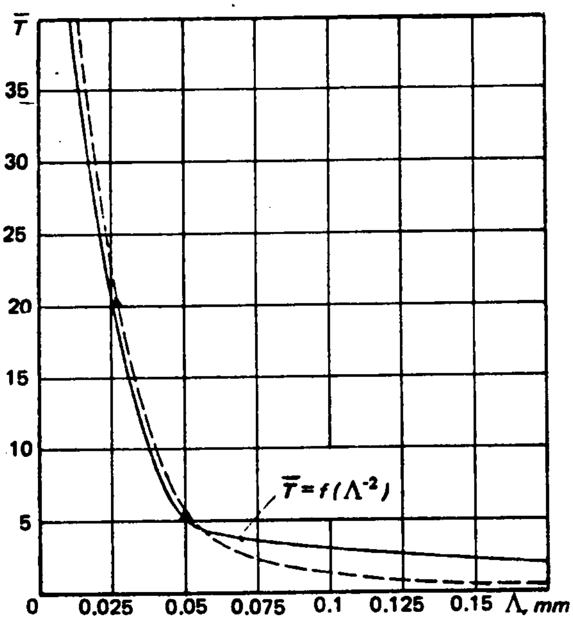

Figure 4.5 Influence of fabrication accuracy Λ on relative manhours $\bar{T}$.

A formula which meets all the requirements can be written in the form

$$C_{T_n} = k_{d.p} k_e C_{T_0} \tag{4.2}$$

where C_{T_n} = specific cost (cost per kg of structure) of the component of a new helicopter design; C_{T_0} = specific cost of an analogous production component which is very similar to the new design with respect to type of construction and size, and is taken as the baseline; $k_{d.p}$ = coefficient accounting for the design peculiarities of the considered component in comparison with the baseline unit; k_e = "economic" coefficient, accounting for the difference in material costs; labor productivity, and wages, in fabrication of the new and baseline components.

The problem obviously reduces to the determination of sufficiently reliable coefficients $k_{d.p}$ and k_e.

Knowing the conditions of the plant in which we intend to produce a series of new components, and comparing part-by-part on the basis of shop-released drawings the new and baseline components with respect to the manpower required for their production (we assume that the baseline article manpower requirement is known), we can quite reliably evaluate the influence of both the design peculiarities and the production conditions on the cost of the new component. This is correct under the assumption that all parts being compared are similar. Unfortunately, this technique is very tedious and is not suitable for evaluating helicopter cost in the initial and prelininary design stages, when working drawings are not yet available. In addition, new designs may incorporate new approaches which have not been previously used.

In the present chapter, we shall discuss a method which makes it possible to solve this problem with satisfactory accuracy in the early design stages. This method has some basic advantages: first, it takes into account all the important factors influencing helicopter costs, which is well confirmed by the results of regression analyses of helicopters for which the economic data are known; second, it is relatively simple. Both of these advantages make it possible to utilize this method in the initial phase of selecting the basic parameters and helicopter configuration.

4.1.4 Influence of Helicopter Production Conditions on Manufacturing Cost (Determination of Economic Coefficient k_e)

We shall examine the basic expenditure items involved in manufacturing any article.

A. Article fabrication cost – 100%.
   a. production personnel wages
   b. cost of materials (and semi-finished products)
   c. purchase cost of finished parts
   d. productione equipment amortization charges
   e. special equipment costs
   f. shop, and general-plant expenditures (electric power, heating, building maintenance, and so on)
   g. wages of inspectors and office personnel (in percent of production workers'pay)

B. Overhead expenditures (expressed in percent of article fabrication costs)

C. Article cost (article fabrication cost, plus overhead).

Since any form of work can be evaluated in terms of the money paid to the worker for his performance, all the items of this list could be reduced to a single item – wages. But, when making the calculations, we would have to know a lot of data on the hourly wages of the various categories of workers, including metallurgists and miners. Therefore, considering that production equipment amortization life is usually established as five years and that the overhead expenses are basically the wages of the various categories of factory personnel, the calculation of the expense items for a helicopter part, beginning with the sixth year of production, can be represented in simplified form.

Cost of manufactured object:

a. overall wages of all workers and factory and office personnel categories chargeable to the manufactured object
b. costs of purchased parts
c. costs of electric power and fuel for the plant, transportation costs, and so on
d. cost of special tooling materials
e. cost of the materials (and semi-finished products) used in the manufactured object.

Similar calculations can be made for the cost of each of the purchased items used in making the object. The expenditures for special tooling materials, electric power, fuel for the plant, transportation, and so on, which we term "other costs", represent a relatively small contribution to the overall cost, and can be taken into account by a constant coefficient $k_{o.c}$ in the expression for the cost of the object. This makes it possible to reduce the cost calculation to only three items: (a) wages – $\Sigma(T\theta)$, (b) materials (semi-processed items) – $\Sigma(G_{s.p}M)$; and (c) other costs.

Then, the cost of the object can be written as

$$C = [\Sigma(T_i\theta_i) + \Sigma(G_{s.p_i}M_i)]\,k_{o.c} \tag{4.3}$$

where T_i = labor expended in fabricating the i-th part used in the produced object in norm-hours (or the labor component of the i-th assembly operation); θ_i = norm-hour cost of performing the corresponding operation; $G_{s.p_i}$ = weight of the i-th semi-processed item in the finished object; and M_i = cost per kg of the material used in this part.

Then, the specific cost of the n-th component is

$$C_{T_n} = \frac{C_n}{G_n} = \left[\frac{\Sigma(T_i\theta_i)}{G_n} + \frac{\Sigma(G_{s.p_i}M_i)}{G_n}\right]k_{o.c} = \left[\frac{T_n\theta_n}{G_n} + \frac{G_{s.p_n}M_n}{G_n}\right]k_{o.c} \tag{4.4}$$

where C_{T_n} = average component cost per kg; G_n = weight of the component; T_n = overall component fabrication labor content in norm-hrs; θ_n = average factory norm-hr cost; $G_{s.p}$ = overall weight of the semi-processed parts used in the component; and M_n = average cost per kg of the semi-processed parts used in the component (average specific cost of the material).

Since T_n/G_n in norm-hrs per kg is associated with productivity (we denote this ratio by Πp_n*), and $k_{m.u_n}G_{s.p_n} = G_n$, where $k_{m.u_n}$ is the average coefficient of material utilization, the expression for the specific cost of the article can be written in the form

$$C_{T_n} = [\theta_n \Pi p_n + (M_n/k_{m.u_n})]\,k_{o.c}.$$

Similarly, for the baseline component

$$C_{T_o} = [\theta_o \Pi p_o + (M_o/k_{m.u_o})]\,k_{o.c}.$$

We denote the ratio of the expressions by

$$k_{co} = \frac{C_{T_n}}{C_{T_o}} = \frac{\theta_n\Pi p_n + (M_n/k_{m.un})}{\theta_o\Pi p_o + (M_o/k_{m.u_o})} = \frac{\theta_n\Pi p_n}{\theta_o\Pi p_o + (M_o/k_{m.u_o})} + \frac{M_n/k_{m.un}}{\theta_o\Pi p_o + (M_o/k_{m.u_o})}. \tag{4.5}$$

---

*Average value of norm-hrs required for each kg of component weight.

Then, we denote the ratio of the baseline component material cost and the overall sum of the wages paid for its fabrication by $k_{b.c}$:

$$k_{b.c} = \frac{M_o}{\theta_o \Pi p_o k_{m.un}}.$$

For the components of helicopters which have been built to date, the quantity $k_{b.c}$ is quite stable (Fig 4.6). In the calculations, we can take it as 0.52 to 0.66. Then,

$$k_{co} = \frac{C_{T_n}}{C_{T_o}} = \frac{\theta_n \Pi p_n}{\theta_o \Pi p_o (1 + k_{b.c})} + \frac{k_{m.uo} M_n}{k_{m.u_n} M_o [1 + (1/k_{b.c})]}$$

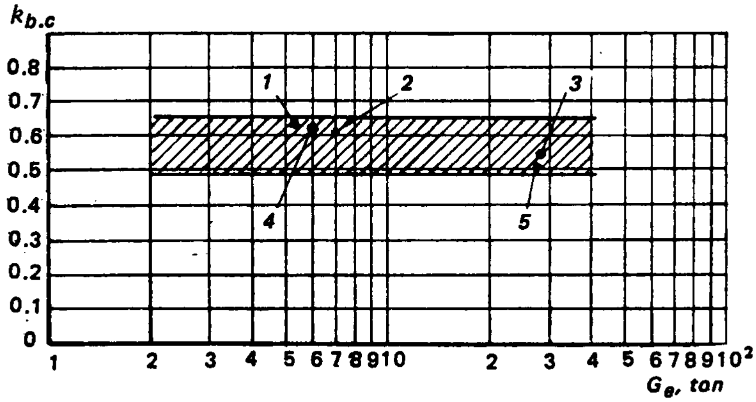

Figure 4.6 Ratio of material cost to overall wages as a function of helicopter structural weight: 1) Model II (in plant B); 2) Model III (in plant B); 3) Model I in plant A); 4) modification of Model II (in plant B); Model IV (in plant A)

Assuming the average utilization material coefficient to be the same for similar components, we obtain

$$k_{co} = \frac{1}{(1 + k_{b.c})}\left(\frac{\theta_n \Pi p_n}{\theta_o \Pi p_o} + k_{b.c}\frac{M_n}{M_o}\right). \qquad (4.6)$$

In order to reduce Eq (4.6) to a form more convenient for the subsequent analysis, we introduce new notations:

$$k_\theta = 1/(1 + k_{b.c}) \text{ and } k_M = k_{b.c}/(1 + k_{b.c});\text{ i.e., } (k_\theta + k_M = 1). \qquad (4.7)$$

Then, Eq (4.6) takes the following form:

$$k_{co} = k_\theta \frac{\theta_n \Pi p_n}{\theta_o \Pi p_o} + k_M \frac{M_n}{M_o}. \qquad (4.8)$$

This is essentially the expression in general form for the product $k_{d.p} k_e$ in Eq (4.2). If the new component is similar as far as its design is concerned to the baseline component (differing only with respect to materials used and production conditions), then $k_{d.p} = 1$ and consequently,

$$k_{co} = k_e = k_\theta \frac{\theta_n \Pi p_n}{\theta_o \Pi p_o} + k_M \frac{M_n}{M_o}. \qquad (4.9)$$

In those cases when it is necessary to determine the cost of the N_n-th component produced by a factory, the calculations are conveniently made with the condition $\Pi p_n = \Pi p_o$ or $T_n/G_n = T_o/G_o$; i.e., assuming that the required (on the average) amount of labor per kg of structural weight is unchanged.

It is assumed that the relative productivity does not change. It is clear that the shorter the time interval between the production of the components being compared, the smaller the possible calculation error. (The error can be reduced by introducing a suitable coefficient accounting for the planned labor productivity increase).

In this case,

$$k_e = k_\theta(\theta_n/\theta_o) + k_M(M_n/M_o). \qquad (4.10)$$

Since the ratio of the number of components (new and baseline) constructed during the same time period, on the same equipment, in the same production area, and with the same number of workers is inversely proportional to the required manhour ratio N where N = (the total manhours required to produce the series of components)/(manhours required to produce a single component).

This means that $N_n/N_o = T_o/T_n$, and for $\Pi p_n = \Pi p_o$,

$$N_o = N_n G_n/G_o. \qquad (4.11)$$

After determining N_o and consequently, the corresponding year of production of the baseline component, we can use relations of the type shown in Fig 4.4 for the calculation of θ_o and M_o.

If we wish to take into account the difference in the production areas and in the number of workers; as an example, we can use the ratio

$$S_{pro_n} n_{wo_n} / S_{pro_o} n_{wo_o}$$

where S_{pro} = production areas; and n_{wo} = number of workers. In this case, the condition $\Pi p_n = \Pi p_o$ is satisfied if

$$N_n G_n / S_{pro_n} n_{wo_n} = N_o G_o / S_{pro_o} n_{wo_o}. \qquad (4.12)$$

The specific material cost M_n is expressed in accordance with the following formula:

$$M_n = G_1 M_1/G_n + G_2 M_2/G_n + \ldots + G_i M_i/G_n \qquad (4.13)$$

where G_1, G_2, ..., and G_i are the weights of the component parts; and M_1, M_2, ..., and M_i are the corresponding specific material costs of these parts.

We shall consider that $M_n/M_o = 1$ if the basic elements of the baseline and new components are made from the same materials and in the same time period.

For example, if it is known that a new component has 15 percent of its weight in titanium and the remainder in steel, then in accordance with the above assumptions, we can take

$$M_n/M_o = 0.85 + (0.15 M_{ti}/M_{st}).$$

For the specific material cost of major elements such as blade spars for which special tubes and special extruded profiles are used, we must use specific costs of semi-finished products in the calculations.

The nature of the variation of the quantity θ_n, if not known, is taken from the latest data on the norm-hour cost in the plant in which production of the new machines is planned.

The effect of introducing the correction k_e into the calculation of the specific cost of a newly designed helicopter can be observed by comparing Figs 4.2 and 4.7, plotted for components of the same existing helicopters.

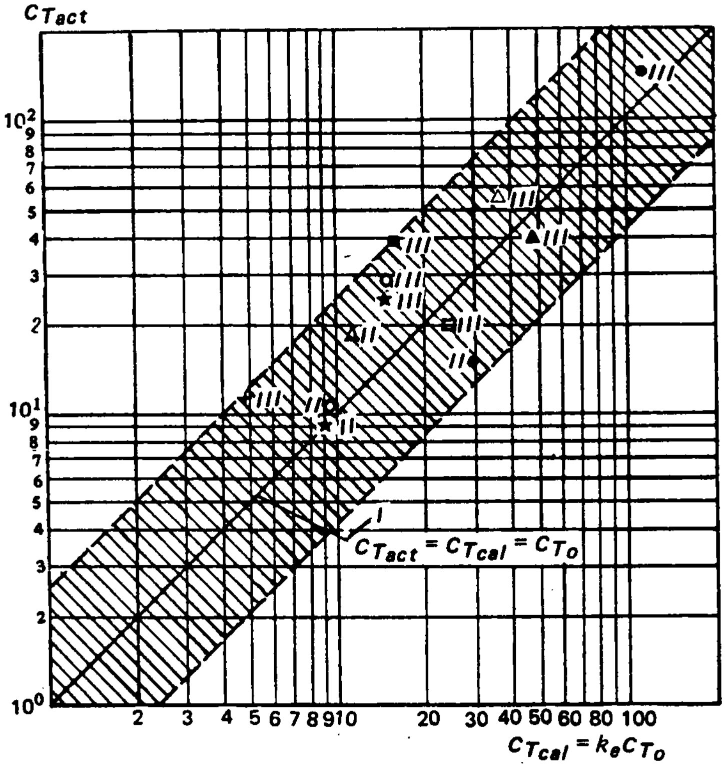

Figure 4.7 Second regression analysis. Relationship between calculated and actual specific component costs of some production helicopters (notations same as in Fig 4.2).

In Fig 4.7, which shows the results of this calculation (with use of the coefficient k_e), the point scatter zone is considerably narrower and the location of the points in this zone is more orderly in comparison with the similar zone in Fig 4.2. But the point scatter is still large because there was no complete structural similarity between the examined analogous components. However, all the calculations were made under the assumption that the coefficient accounting for the design difference (peculiarities) was $k_{d.p} = 1$.

4.2.5 Influence of Design Pecularities on Helicopter Component Manufacturing Cost

Analysis of the factors that determine the structural characteristics of helicopter components and systems shows that the manhours required for their fabrication are determined primarily by the number of detail parts used in these components. The number of production operations, number of assembly stations, riveted seam lengths, and so on, are directly or indirectly related to this parameter. Another parameter which influences the manhours is the required detail part fabrication accuracy and, naturally, the dimensions. Thus, the manhours required to fabricate the helicopter airframe depends—in addition to the materials—on the number of detail parts and their dimensions, length of riveted seams (number of rivets), number of production operations, and the required contour accuracy of the manufactured fuselage.

A considerable part of the main-rotor and tail-rotor blade manufacturing cost is associated with fabricating the spar blanks; the production of special extruded profiles made from aluminum (titanium) alloys and special steel tubes, which consist of highly labor-intensive operations (this labor expenditure is taken into account when determining the coefficient k_e). In spite of this, their cost is influenced by the number of detail parts and their dimensions, the number of production operations, and the required fabrication accuracy and surface quality.

The manhours involved in fabricating the main and tail-rotor hubs, swashplate assemblies, and hydraulic boosters are determined by the number and size of the detail parts, the number and size of the bearings, the number of production operations, and the required fabrication tolerances.

The manhours involved in manufacturing the transmission are influenced by the number of detail parts and their dimensions, the required fabrication tolerances, the number of production operations, and the number of assembly stations.

The manhours involved in fabricating the control system and the other systems are influenced by the number of detail parts, the number of production operations, the number of assembly stations, and the required tolerances.

The quantities T_n and T_o which enter through the quantities Πp_n and Πp_o into Eq (4.9) for the coefficient k_e represent only a part of the manhours required for manufacturing the entire assembly, since they do not include the manhours involved in fabricating the materials. Their values are determined from the condition that the newly designed and the baseline assembly are similar. The difference between these quantities basically depends on the production conditions (experience and qualification of personnel, equipment and efficiency of the machining tools, and so on), and on the size of the units. The overall manhours can generally be expressed as a function of the form

$$\Sigma T_n = f(z_n, \Lambda_n, Y_n)$$

where ΣT_n = overall manhours for fabrication of the n-th component; z_n = number of detail parts in the n-th component; Λ_n = average manufacturing tolerance of the detail parts of this assembly; and Y_n = parameter accounting for other factors which influence the magnitude of the required manhours (production conditions, choice of materials, and size). Since all of these parameters are practically independent of one another, and since $C_n = f(\Sigma T_n)$, the expression for the cost can be written in general form as

$$C_n = k_{c_n} (z_n)^n (\Lambda_n)^m (Y_n)^\ell$$

where k_{c_n} = proportionality coefficient characterizing the type of component; n, m, and ℓ = quantities characterizing the degree to which the corresponding structural and production factors influence the cost of the assembly. We shall examine each of these parameters in more detail.

Evaluation of aircraft assembly manhours (cost) on the basis of the number of detail parts is nothing new. This quantity has long been used in engineering practice (for preliminary calculations). However, components consist of detail parts which are not commensurate with respect to manufacturing manhours (and therefore, their cost). It is possible to evaluate the manhours on the basis of the number of detail parts if, in order to reduce the degree of noncommensurability, one introduces the ratio of the number of parts to the component weight z_n/G_n into the calculations*.

The use of this ratio as the basic criterion in evaluating design economic efficiency was initiated in the early 1970s.For example, the "design-to-cost" concept was introduced by Boeing Vertol in 1971 in developing helicopters under the new UTTAS and HLH programs. The previous Boeing Vertol philosophy—"Design it right, make it light"—was supplemented by the new concept—"Design to cost, or all is lost".[30] In this connection, in addition to weight, one of the primary indices measuring the quality of design work at Boeing Vertol became the number of detail parts in the unit being designed per pound of weight of each unit. The smaller this ratio, the lower the cost. This situation is illustrated in Fig 4.8 which shows the statistical dependence of the quantity A_M, characterizing the cost of the mechanical assemblies of the well-known Chinook and CH-46 helicopters, on the ratio z_n/G_n[30]. This relationship, defined for components having fundamental design differences (main rotor hubs and swashplate assembly elements) can be represented in the form

$$A_M = k_{A_M}(z_n/G_n)^{0.61}$$

where k_{A_M} = proportionality coefficient accounting for various factors influencing cost which do not vary within the scope of the given problem.

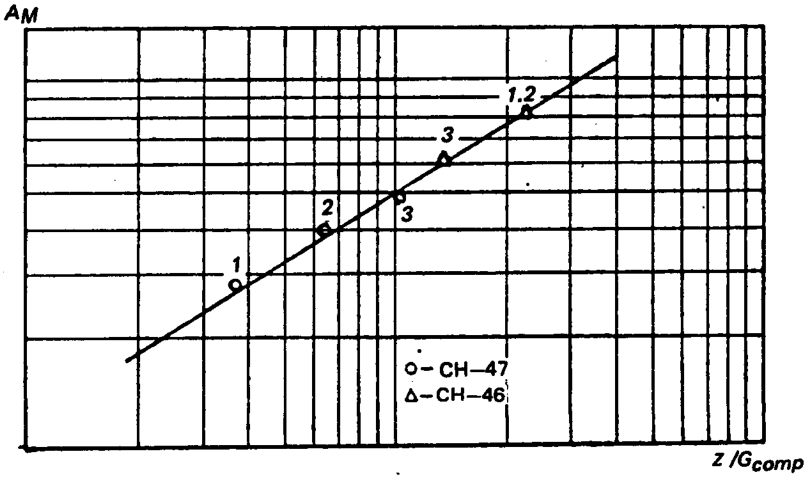

Figure 4.8 Component Cost parameter A_M as a function of the ratio of the number of component parts to their weight: (1) aft main-rotor swashplate with boosters, (2) forward main-rotor swashplate with boosters, and (3) main-rotor hubs

Figure 4.9 shows the relationship obtained by Boeing Vertol between the ratio z_n/G_n for the airframes of the production helicopters of this firm and their weight. It is claimed that if the traditional design approach was used, the airframe of the new UTTAS helicopter would have a detail-part "density" z_n/G_n of about 6.2 parts per kg. With the new approach (the design-to-cost concept), the reduction of the "density" by nearly a factor of 2 (to 2.85 parts per kg) made it possible to reduce the airframe cost by at least 40 percent[30].

---

*The question of detail part cost noncommensurability will be more thoroughly examined later.

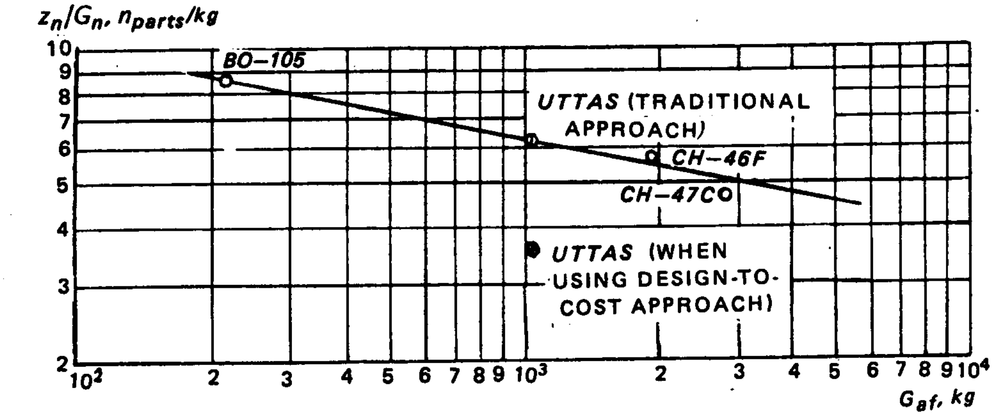

Figure 4.9 z_n/G_n ratio as a function of the airframe weight

The cost (manhours) of components fabricated from identical parts under identical production conditions is directly proportional to the number of detail parts used in these components. This is obvious. For example, with an increase of the main-rotor blade number from four to five, it is clear that the main-rotor cost increases approximately in the ratio 5/4 if the blade and hub link designs remain the same.* For such cases,

$$C_n = f[(z_n)^n] = k_{z_n} z_n$$

where k_{z_n} - proportionality coefficient, equal in magnitude to the cost of a single part.

It is obvious that if $G_n = const$, the expression $C_n = k_{z_n} z_n$ will be valid only for absolutely identical components manufactured under absolutely identical production conditions. However, let us imagine some structure; for example, of the shell type, consisting of identical detail parts, which is modified so that every two parts are replaced by a single part, while the weight of the structure as a whole remains unchanged. Let us assume that the detail parts of the original structure were obtained by stamping on a hydraulic press. We further assume that on this same press it is also possible to stamp the details for the modified structure.

It is clear that under these conditions, the manhours required to fabricate a single detail part of both the original and the modified structure will be of the same order. This is also valid for a structure of a different type. Accordingly, the costs of these operations will also be of the same order. It is also clear that when fabricating the modified structure, it is not necessary to expend any effort on joining the two detail parts with one another as was necessary with the old type.

Since we have assumed that the weight of the structure did not change during modification, we can assume that the material cost remains approximately the same. We neglect the cost of the attachment details "saved" upon changeover to the new structure (nor shall we consider the number of these parts). It is not difficult to see that if the material cost and the cost saved by reduction in the number of assembly operations are of the same order, then the cost of the modified structure will be less than the cost of the original structure by the ratio of the number of parts used in these structures; i.e., by a factor of 2 in the present case.

We further assume that our original design can be modified differently; namely, by reducing the number of parts by several fold, rather than by a factor of 2. It is clear that the cost of such a modified unit (assembly) can be expressed approximately as follows:

---

*Actually, the increase may be somewhat greater because of increased complexity of the hub housing.

$$C_n \approx (z_n/z_o)C_{part_o} + M_o - \Delta C_{part_o}$$

where C_{part_o} = cost of fabricating the detail parts of the original design; z_n and z_o are the numbers of detail parts used in the modified and original designs, respectively; M_o = material cost; and ΔC_{part_o} = cost saved in assembling the modified design.

It is convenient to transform this expression, dividing the number of parts of each component by its weight, which can be done since, by assumption, $G_n = G_o$.

Then,

$$C_n \approx \frac{z_n/G_n}{z_o/G_o} C_{part_o} + M_o - \Delta C_{part_o}.$$

Let us now suppose that the modification of the original design is accomplished both by combining identical parts into a single part and by replacing some portion of the detail parts of the original type by fundamentally new parts. In this case, the following basic conditions are again satisfied: $\Lambda = const$, and $Y = const$; consequently, $G_n = G_o$.

Although the costs of the individual parts of the modified design are not equal to one another, we find that as a result of averaging these costs (in terms of the number of detail parts per kg of overall weight), the expression derived above for a particular case is also valid in this more general case.

Assuming that on the average, for designs of different types in analogous problems, the value of $M_o/\Delta C_{part_o}$ is close to one, we will have

$$C_n \approx \frac{z_n/G_n}{z_o/G_o} C_{part_o};$$

i.e., the costs of analogous-type structures which are of the same size, and made from the same material and at the same level of accuracy and under identical production conditions are directly proportional to the number of detail parts used referred to weights of the structures. Therefore, we can consider that the exponent n in the function $C_n = f[(z_n)^n] = f[(z_n/G_n)^n]$ is approximately equal to one.

Now let us examine the next parameter influencing component cost. This is the average level of component accuracy Λ_n, required in fabrication of detail parts. Previously (see Fig 4.5), we examined the typical dependence of the required machining time on the established tolerances in detail part fabrication. It can be expressed approximately by the function

$$C_i = k_{\Lambda_i}(\Lambda_i)^{-2}$$

where C_i = cost of performing the i-th operation; Λ_i = maximum allowable deviation from the nominal dimension; k_{Λ_i} = coefficient accounting for other cost determining factors which, in the present case, do not change. (Approximately the same character of cost dependence also exists in the analogous case of streamlining of monocoque structures).

If the average level of component manufacturing tolerance is defined as

$$\Lambda_n = \Sigma\Lambda_i/\Sigma_i$$

where $\Sigma\Lambda_i$ = sum of the maximal tolerances on all the dimensions of the component parts being fabricated; and Σ_i = overall number of operations in manufacturing the detail parts; then for the entire component as a whole, we can write

$$C_n = f[(\Lambda_n)^m] \approx k_{\Lambda_i}(\Lambda_n)^{-2}$$

which is valid for designs differing only in the accuracy of their manufacture; i.e., here

$$k_{\Lambda_i} = k_{c_n}(z_n)^n(Y_n) = const.$$

The next cost parameter to be examined is the quantity Y_n.

The cost of components of the same design, but manufactured from different materials and under different production conditions can be expressed as

$$C_n = f[(Y_n)^\ell] = k_{Y_n}(Y_n)^\ell.$$

Here, $k_{Y_n} = const$, but on the basis of the analysis made in the previous section, we have, for the considered case,

$$C_n = k_{e_n}G_nC_{T_o}$$

from which

$$(Y_n)^\ell = (C_{T_o}/k_{Y_n})k_{e_n}G_n = k^*_{Y_n}k_{e_n}G_n$$

where $k^*_{Y_n} = const$, since here, C_{T_o} and k_{Y_n} are constant quantities.

Now let us turn to the general case, when the analogous designs differ in the number of detail parts, accuracy of their fabrication, materials, production conditions, and size; i.e., to the expression $C_n = k_{c_n}(z_n)^n(\Lambda_n)^m(Y_n)^\ell$. On the basis of the relations examined above, the expression for the component cost can be presented in the form

$$C_n = k_{c_n}z_n(\Lambda_n)^{-2}k_eG_n,$$

or

$$C_n = \bar{k}_{c_n}k_{e_n}G_n(z_n/G_n)(\Lambda_n)^{-2}.$$

The corresponding expression for the specific cost is

$$C_{T_n} = \bar{k}_{c_n}k_{e_n}(z_n/G_n)(\Lambda_n)^{-2}.$$

Similarly, for the baseline component,

$$C_{T_o} = \bar{k}_{c_o}(z_o/G_o)(\Lambda_o)^{-2} \quad (\text{since } k_{e_o} = 1),$$

then

$$\frac{C_{Tn}}{C_{T_o}} = \frac{\bar{k}_{cn}k_{en}(z_n/G_n)(\Lambda_o)^2}{\bar{k}_{c_o}(z_o/G_o)(\Lambda_n)^2}.$$

Let us assume that for components which are, in general, similar, the value of the ratio $\bar{k}_{c_n}/\bar{k}_{c_o}$ is close to one. On this basis, we write

$$C_{T_n} = k_e(z_n/z_o)(G_o/G_n)(\Lambda_o/\Lambda_n)^2C_{T_o} \tag{4.14}$$

from which

$$k_{d.p} = (z_n/z_o)(G_o/G_n)(\Lambda_o/\Lambda_n)^2. \tag{4.15}$$

We shall judge the degree to which this last, and all the other, assumptions and hypotheses used previously correspond to reality on the basis of the results shown in Fig 4.10 where our third regression analysis is presented of the cost data of all those production helicopter components which were used in the first two analyses of this sort (see Figs 4.2 and 4.7). Comparison of the results of these three regression analyses shows that Eq (4.14) provides the highest degree of agreement between the calculated and actual helicopter component costs. This accuracy can be considered quite satisfactory for solutions of the basic problem, which we have posed selecting the optimal parameters on the basis of the economic criterion. It is interesting to note that Eq (4.14), which was derived for similar designs, also yields (as can be seen from Fig 4.10), quite good agreement for components having fundamental design differences and, in principle, makes it possible to use this technique in more general cases.

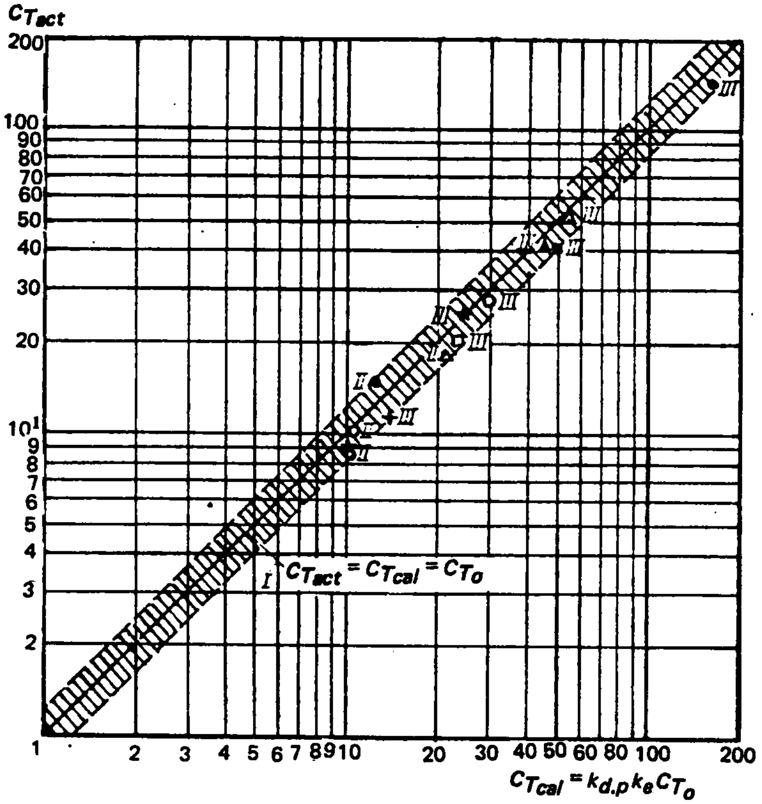

Figure 4.10 Third regression analysis. Relationship between calculated and actual specific costs (notation same as for Fig 4.2)

Becasue of the special importance of the number of detail parts in evaluating component cost, it is necessary to precisely determine which detail parts need to be considered in the calculations, and which do not. We have already mentioned the possible cost differences in the detailed parts in a single component. For example, the blade spar is much more expensive than the trailing-edge strip which, in turn, costs much more than a standard rivet. Or, in the case of the main-rotor hub, the pitch bearing housing is not comparable in regard to cost with a roller bearing or a standard bolt.

A still larger degree of difference may appear when comparing detail parts used in components which are being compared with one another, but are of fundamentally different design.

Because of such striking contrasts, it may appear that the averaging of the detail part costs introduced in Eq (4.14) through the ratios z_n/G_n and z_0/G_0 is not sufficient. We shall show that this is not so. We arbitrarily break down the numbers of detail parts in the components being compared into several groups such that in each group there are "combined" only those detail parts which are approximately comparable with one another in regard to cost. For the two components being compared, we write

$$z_n = z_o + \Delta z, \ z_n = A_n + B_n + M_n + Q + F_n,$$

$$z_o = A_o + B_o + M_o + E + F_o$$

where A = number of individual large detail parts whch are mandatory for a component of the given type (characteristic only for a structure of the particular type); for example, the main-rotor blade spar; B = comparatively small number of mandatory detail parts of smaller size; for example, the blade attachment or main-rotor pitch-bearing housing; M = number of mandatory detail parts of medium and small size; for example, the elements of the blade trailing-edge strip and the bolts which fasten the blade attachment to the spar; Q and E = numbers of parts characteristic only for a particular modification of the component of the given type; for example, in the case of blades with extruded Duralumin spar, the honeycomb blocks for one version and the ribs for another; F_n and F_o = numbers of small standard fasteners (which also include small nonstandard detail parts) with overall weight not exceeding 1 to 2 percent of the overall weight of the corresponding components (we included the large standard detail parts in the preceding groups).

We can exclude from further consideration the numbers of detail parts from the F_n and F_o groups. We have mentioned previously that the number of fastening details depends indirectly on the fundamental structural characteristics, which are determined by the basic detail parts. The influence of the detail parts from the F group on the structure or, so to speak, the reverse influence, is relatively weak. As a rule, the cost of these details in the overall balance is very slight and can be fully accounted for through their weight.

In analyzing component designs of modern helicopters, it is not difficult to see that the probability of "encountering"—in the Q and E groups—detail parts comparable in cost to those from groups A and B is small. However, the cost of the detail parts from groups Q and E is basically of the same order as those from group M. It is clear that the average cost per detail part in any particular group cannot differ as markedly from the cost of the individual detail parts of this same group, as the cost of the latter can differ from the average cost of a single detail part of the entire component.

Now, we shall examine some possible cases. If the newly designed component and the baseline component are similar in construction and nearly of the same size, then $A_n = A_o$, and $B_n = B_o$. If $z_o = z_n$, and $M_n = M_o$, and hence, $(z_n/z_o) = (Q/E)$; this means that we have a ratio of detailed parts approximately equal in cost. If $z_o = z_n$, but $M_n \neq M_o$; consequently, $Q \neq E$, and the conclusion still remains the same.

Indeed,

$$\frac{z_n}{z_o} = \frac{(A_n + B_n + M_n) + Q}{(A_o + B_o + M_o) + E} = \frac{(A_o + B_o + M_o) + M_n - M_o + Q}{(A_o + B_o + M_o) + E},$$

or $z_n/z_o = (M_n - M_o + Q)/E$; i.e., in this case also, the cost commensurability principle is not violated.

Now, we shall examine the case where $z_n \neq z_o$, but the components are similar in size. Let $z_n = z_n' + \Delta z$, where $z_n' = z_o$. In addition, let $Q \neq E$, and $M_n \neq M_o$ (but in accord with the general condition, $A_n = A_o$, and $B_n = B_o$). Then we can write $z_n/z_o = (z_n'/z_o) + (\Delta z/z_o)$. In accordance with the above-discussed example, $z_n'/z_o = (M_n' - M_o + Q')/E$, where M_n' and Q' are the numbers of detail parts arbitrarily taken from groups M_n and Q satisfying the condition $M_n' + Q' = M_o + E$ (in this case, $z_n' = A_n + B_n + M_n' + Q' = A_o + B_o + M_o + E$). Then,

$$\frac{\Delta z}{z_o} = \frac{(A_n + B_n + M_n + Q) - (A_o + B_o + M_o + E)}{A_o + B_o + M_o + E} = \frac{M_n - M_o + Q - E}{(A_o + B_o) + (M_o + E)}.$$

But the quantity $A_o + B_o$ is usually much smaller than the quantity $M_o + E$. Therefore, with some approximation

$$\frac{\Delta z}{z_o} \approx \frac{(M_n - M_o) + (Q - E)}{M_o + E}$$

and finally,

$$\frac{z_n}{z_o} \approx \frac{M_n' - M_o + Q'}{E} + \frac{(M_n - M_o) + (Q - E)}{M_o + E}$$

i.e., again, in this case, we have the ratio of commensurable, cost-wise, detailed parts.

We can visualize still other cases which may be encountered when making practical calculations.

Let us assume that due to special circumstances, it is not possible to select a baseline component which is completely similar to the new design. For example, a fresh design is being made of a seven-blade, main-rotor hub. Among the existing designs which are close in size and similar in the type of their pitch-housings, there are only five blade designs ($z_n = 7z_o/5$). It is obvious that with respect to this example, $z_n/z_o = 7/5$ or, in more general form, $z_n/z_o \approx z_{bl_n} Q / z_{bl_o} E$, where z_{bl_n} and z_{bl_o} are the numbers of blades of the compared main rotors.

We see that everything again reduces to the ratio of commensurable detail parts.

Another example: there are no baseline components that are similar in size. The existing component, which is similar in design, is only half the size (with regard to weight). Can we, in this case, take this component as the baseline unit? This is possible, since the ratio (z_n/z_o) appears in Eq (4.15) together with the ratio (G_o/G_n); i.e., we do not simply compare the numbers of detail parts, but rather the ratios of the numbers of parts per kg of component weight $(z_n/G_n)/(z_o/G_o)$. Thereby, the scale factor is taken into account.

In this case, we can obviously expect a larger calculation error. However, the analysis results shown in Fig 4.10 indicate that this error may not be excessive even if the compared components differ significantly (by several fold) both in size and, as mentioned above, in type of construction. This makes it possible to use this technique to calculate the specific cost of newly designed components (Eq (4.15)) for preliminary estimates even in the extreme case when we are comparing non-similar designs; for example, piston and turbine engines, main-rotor hubs having elastomeric bearings and hubs having conventional bearings, and so on.

Substituting the expression for k_θ from Eq (4.9) into Eq (4.15), we obtain the expanded expression for the specific cost of the n-th component

$$C_{T_n} = \frac{z_n/G_n}{z_o/G_o}\left(\frac{\Lambda_o}{\Lambda_n}\right)^2 \left(k_\theta \frac{\theta_n \Pi p_n}{\theta_o \Pi p_o} + k_M \frac{M_n}{M_o}\right) C_{T_o}; \tag{4.16}$$

In the subsequent sections, we will refine the limits in which this formula provides adequately valid calculation results.

The overall cost of the n-th component can be expressed as follows:

$$C_n = G_n C_{T_n} = \frac{z_n}{z_o}\left(\frac{\Lambda_o}{\Lambda_n}\right)^2 \left(k_\theta \frac{\theta_n \Pi p_n}{\theta_o \Pi p_o} + k_M \frac{M_n}{M_o}\right) C_o \tag{4.17}$$

If the average levels of accuracy of fabrication of the new and baseline components are the same, then

$$C_n = k_\theta (z_n/z_o) C_o. \tag{4.18}$$

If, in addition, they are manufactured in the same production areas, from identical materials, and in the same time period, then

$$C_n = (z_n/z_o)C_o. \tag{4.19}$$

However, it does not follow from this formula that by combining two simple detail parts into a single unit, we can always reduce the cost of the assembly, even when the new part is more complex than the original one. The reason is that in practical design, the combining of two parts into a single unit is accomplished on the basis of the accumulated technological experience, and replacement is not permitted if the overall cost of manufacturing the two parts is less than the cost of fabricating the single unit which is intended to replace them. For example, it is obviously advisable to replace a rib consisting of a web with stamped stiffeners and angle-profile flanges which are riveted to the web by another rib which is stamped integrally together with the stiffeners and flanges on a hydraulic press. But it was not advisable to mill, from a single blank, the swashplate for such a large helicopter as the Mi-6. Therefore, it was welded up from several elements.

4.1.6 Estimating the Number of Detail Parts of Helicopter Component in the Early Design Stages

The question now is how to obtain the ratio z_n/z_o for each component in the concept formulation and preliminary design stages. We shall consider this problem on an example.

In application to the designs of two similar main-rotor hubs, the ratio of the numbers of their detail parts can be expressed as follows:

$$z_n/z_o = 1 + (z_n - z_o)/z_o.$$

The numbers of large indispensable details of the new and baseline hubs are equal to, or represent multiples of, one another

$$A_n = (z_{bl_n}/z_{bl_o})A_o, \quad B_n = (z_{bl_n}/z_{bl_o})B_o$$

where z_{bl} = number of blades. This is also true for parts of small indispensable details from group M_n. We denote this number by M_n'

$$M_n' = (z_{bl_n}/z_{bl_o})M_o'.$$

The numbers of details of these groups are independent of the loads determining the dimensions of these details, and other design factors as well. In the subject case, the determining load is the blade centrifugal force.

The other factors include the necessity for ensuring adequate rigidity of the structure, reliable sealing of the hub hinges, and so on. With an increase of the main rotor size, the number of bearings also increases, because of the increase in centrifugal force, the sealing system becomes more complicated, and because of this, the new detail parts are introduced into the design. In other words, the numbers of remaining detail parts from groups M, Q, and E depend directly or indirectly on the centrifugal force, N_{bl}.

For the same number of main rotor blades,

$$z_n = A + B + M_n' + \bar{m}_{hub_n} N_{bl_n}; \quad z_o = A + B + M_o' + \bar{m}_{hub_o} N_{bl_o}$$

where A = hub core; B = pitch housings; and M_n' and M_o' = other indispensable elements of the hub structure, the number of which is independent of the centrifugal force (small standard joining elements are not considered in the calculations); $(\bar{m}_{hub} N_{bl})$ = numbers of detail parts of groups Q and E (bearings, seals, nonstandard and large standard joining elements, and other detail parts) which are determined by the scale factor; $\bar{m}_{hub}$ = coefficient of proportionality characterizing the particular hub type. Then

$$z_n/z_o = 1 + \bar{m}_{hub}(N_{bl_n} - N_{bl_o})/z_o .$$

For different number of blades in the new and baseline rotors

$$z_n/z_o = [1 + \bar{m}_{hub}(N_{bl_n} - N_{bl_o})/z_o](z_{bl_n}/z_{bl_o}) .$$

Analogous relationships can also be obtained for other similar components. For this, we must first consider the detail parts of the components by groups and then find the dependence of the number of details from groups Q and E and, in part, from groups M_n and M_o on the loads which determine the number of these parts. Having such relationships for all the basic components, we can calculate the cost of fabricating the helicopter as a whole. The coefficients of proportionality $\bar{m}_n$ are determined with the use of statistical data for each type of component design. The technique used to determine these coefficients will be examined in detail in the next chapter.

4.1.7 Dependence of Helicopter Component Manufacturing Cost on Machined Surface Area

Let us now determine the range of applicability of the family of formulae as given by Eqs (4.15) to (4.19). Specifically, will Eq (4.19) be valid if we take as the baseline component one which is similar to the one being designed (with the same number of detail parts) but significantly different in size from the latter? This, obviously, cannot be done without introducing a suitable correction. For example, if we take, as the baseline, the Mi-2 helicopter main-rotor blade extruded spar together with the root attachment, then in accordance with Eq (4.19) it should be nearly equivalent with regard to cost to the similar Mi-8 helicopter blade element which is analogous in construction and has nearly the same number of detail parts. In actuality, the Mi-8 helicopter spar has considerably more machined surface area, and thus, is more expensive for the same production conditions. For all designs consisting only of a fixed number of "independent" detail parts, the part "density" in the component decreases with increase in the component size to the same degree by which its weight increases and consequently, in accordance with Eq (4.19), the calculated cost of its fabrication will be independent of the size. It is obvious that in reality, in this case, the cost must incresse with increase of the size.

The question naturally arises of how was it possible to obtain satisfactory agreement of the calculation results with the actual data which was illustrated in Fig 4.10.

In the preceding subsection, we noted that with increase of the component size, even if the designer attempts to maintain complete similarity of the design, he is still forced to increase the number of detail parts because of the scale-factor effect to ensure adequate stiffness, strength, and so on. It is obvious that for certain subassemblies of this component, the increase in the number of detail parts cannot be expressed precisely as a continuous function of any parameter characterizing the size increase. Up to some point, we can obviously increase the size of the individual subassemblies of the component without increasing the number of detail parts. But for the component as a whole, if we are talking about the primary helicopter components, each having several thousand detail parts, we can consider approximately that the increase in size is accompanied by a continuous increase in the number of detail parts. It is difficult to imagine the design of any basic helicopter component for which it is possible to maintain the number of detail parts completely constant in case of any significant change in its dimensions. This obviously helps to explain the good agreement of the calculation with the actual data, which was demonstrated above.

Nevertheless, we shall attempt to improve the "mechanism" of the considered formulae which take into account the change in the cost of the assembly with change of its dimensions. We can see that this "mechanism" operates very simply (for example, see Eq (4.17)): the component unit cost, determined on the basis of the baseline component unit cost is multiplied by the weight of the new component. It would seem that all the factors which depend on size and influence the cost would be taken into consideration in this way. However, as we noted above, because of the influence of another "mechanism" of the proposed method, taking into account the unit cost variation with change of the detail part "density", for subassemblies with the same number of detail parts, we find that to the degree to which the first component is heavier than the second component, the unit cost of the second will be many times higher than the unit cost of the first. In order to compensate for the possible resulting calculation inaccuracy, we must introduce an additional correction. We denote it by ΔC_s.

We should point out that the importance of this correction in the overall cost balance will not be very large (see Fig 4.10).

It is obvious that the growth of the cost of a component with increase in its size, while retaining the same number of parts, will be associated primarily with increase of the machined surface area. Therefore, it is natural to take a quantity being a function of the following ratio as the correction:

$$\Sigma S_{mach_n}/\Sigma S_{mach_o}, \text{ where } \Sigma S_{mach_n} \text{ and } \Sigma S_{mach_o}$$

are the overall machined surface areas of the similar detail parts in the new and baseline assemblies, respectively. However, since, in the preliminary design stage, these values are not known and furthermore, the influence of the quantity ΔC_s is not significant, we can make a very rough approximation by assuming that

$$\Sigma S_{mach_n} = k_s S_n \text{ and } \Sigma S_{mach_o} = k_s S_o;$$

i.e., the overall machined surface areas of all the detail parts of the similar components are proportional to the sum of the side surface areas (S_n and S_o) of the considered components. Here, k_s is a coefficient of proportionality. Then

$$\Delta C_s = (\Sigma S_{mach_n}/\Sigma S_{mach_o})^h \approx (S_n/S_o)^h = C_{T_n}/k_e k_{d.p} C_{T_o}.$$

The exponent h obviously cannot be equal to one, since the quantity ΔC_s considers only the change in the required machine time. There is practically no change in the assembly operation manhours, overall number of operations performed (both machining and inspection) of preparatory operations manhours, preparation of the technical documentation, and so on (the material cost is taken into account by the coefficient k_e and the weight).

It follows from analysis of the statistical data that for most components, $h = 0.25$; i.e.,

$$\Delta C_s = \sqrt[4]{S_n/S_o}.$$

Then Eq (4.2) takes the form

$$C_{T_n} = k_e k_{d.p} \sqrt[4]{S_n/S_o}\, C_{T_o}. \tag{4.20}$$

Eqs (4.15) to (4.19) change correspondingly. We see from examination of Fig 4.10 that when developing new components based on the classical scheme, there is no need to introduce any corrections into the calculations.

However, when using the proposed method for nontraditional designs with a large percentage of "indispensable" detail parts, it is advisable to introduce the ΔC_s correction into the calculation.

4.2 Estimating Direct Operating Costs

By direct operating costs, we usually mean the expenses for amortization, maintenance, flight crew wages, and fuel plus oil costs. The amortization charges constitute a significant part of all costs (usually more than 60 percent). They are subdivided into the so-called replacement costs and major overhaul costs[2]. The replacement costs are practically equal to the helicopter manufacturing costs and constitute a large part of the amortization costs.

If we had an absolutely reliable method for calculating the manufacturing cost of components, we would have the "key" to overcoming the considerable difficulties which usually arise in estimating helicopter economic effectiveness. This will be shown below. It is convenient to calculate the operating costs by referring them to the total helicopter flight time; (i.e., per flight hour).

4.2.1 Annual Flight Time. Helicopter Amortization and Calendar Periods and Depreciation Period

The replacement cost is, in essence, that part of the helicopter that "disappears" per each hour of flight. By definition, upon complete retirement of the helicopter, its amortization is 100 percent, and the total replacement cost should be equal to the helicopter manufacturing cost (for the operational organization, the replacement cost will be equal to the helicopter price).

When helicopters were first introduced to Aeroflot for civil operation, in calculating the flight-hour cost, the replacement fraction was, by analogy with airplanes, defined in terms of the ratio of the helicopter airframe and engine price (minus the 5-percent representing residual cost – metal scrap cost, etc.) to the established overall service life (amortization period expressed in flight hours). In this case, by airframe we mean the entire helicopter with all the components other than the engines. This method has several drawbacks.

As a rule, the overall service life of the helicopter dynamic system elements is considerably lower than the service life of the entire hleicopter. These elements are replaced several times during the complete operating life of the helicopter. Expenditures for replacing these components (main and tail rotor blades and hubs, gearboxes, transmission shafts), the costs of which, although lower, are very roughly commensurate with the engine cost, and were considered part of the major overhaul costs, which were very roughly estimated.

Another drawback of this technique is that the calendar aspects were not taken into account in estimating the replacement costs. As is well known, in addition to the component service life in flight hours, their service life is also established in terms of years of operation (because of corrosion, aging, etc.). In practice, it is very likely that helicopter operation may have to be terminated because of the calendar time expiration, even though the established overall technical life in flight hours has not been used up.

In addition, the values of the overall technical service life used in the calculation did not reflect the full potential capabilities of the helicopter structure. [For many reasons, it is difficult to determine the full service life potential of the airframe at the time a new helicopter type is introduced into operation. The preliminary amortization and calendar lives are established for the airframe on the basis of similarity with a predecessor helicopter that has been in operation for a long time.] As a rule, these overall technical service lives are extended as operational experience is assimilated. For example, the preliminary overall technical service life for the airframe of one well-known helicopter initially did not exceed 5000 hours. At the present time, the fleet-leading helicopters of this type have flown approximately 12 000 hours each. Furthermore, they have been in operation for more than 15 years. But even these life extents do not appear to reach their limits from the viewpoint of potential capability of the structure.

A consequence of this approach is the fact that the average annual flight time of any new helicopter type is estimated without accounting for the actual capabilities of the machine in question. It seems obvious that the annual flight time should always be so-selected that the overall technical life of the particular helicopter will be used up before the calendar limitations come into play.

When using this approach, no specific account is taken for whether or not the helicopter can perform normal flights at night or under adverse weather conditions. These capabilities depend on the level of the radio-navigation equipment, automatic flight control, and anti-icing systems. Nor is consideration given to the time expended in loading and unloading operations, which depends on the efficiency of the loading and unloading equipment, and the time spent in performing various sorts of repairs and maintenance which, in turn, depends on the design of the given machine. For all of these reasons, the calculations made using this technique are of an arbitrary nature.

In the methodologies adopted by certain foreign aeronautical companies, such calculations are based on determining the number of years in the course of which the helicopter will justify all the costs and bring in a profit. This period is established with account for the service life and calendar limitations as a function of the planned flight rate, and usually amounts to 8–10 years. In this case, the residual value is taken, on the average, as 20 percent of the original cost. The customers require, from the helicopter manufacturers, technical and organizational guarantees ensuring the required helicopter operating rate; for example, 1500 hours a year. These guarantees consist of agreements to deliver spare parts at strictly established times, and provide the helicopter with special rigging equipment and tools which would make it possible to meet the helicopter servicing standards established by the manufacturer. The helicopter manufacturers also guarantee the corresponding service life of the components. The parts representing replacement costs are estimated as 80 percent of the initial helicopter airframe price, referred to the period of the service life established by the manufacturer in years, times the guaranteed annual flight time (in hours). The engine replacement costs are similarly determined. With the aid of this approach, the operating companies basically protect themselves against errors in estimating the cost per flight hour (at the expense of the manufacturers, who take a definite risk in establishing sufficiently long overall technical life of the airframes and other helicopter components in the initial operating stage).

However, in spite of some advantages of this method in comparison with the previously-considered one obtained specifically by introducing into the calculation a technically rational value of the maximal possible annual flight time (the actual time required for repair and maintenance is established on the basis of special tests of the new helicopter), this new technique cannot be used to solve our problem because of several arbitrary assumptions; for example, why should the helicopter, after 10 years of operation, be worth 20 percent of its original cost?

We shall use a technique which is a modification of the two methods just examined.

We will determine the magnitude of maximal possible annual flight utilization as follows. We take the maximum number of hours which the helicopter can fly under ideal operating conditions as this quantity. In the latter, we would consider such conditions under which the helicopter is on the ground only because of technical reasons which result from design peculiarities.

While the requirements of the purchasing agency with respect to flight hours may be higher than this quantity, the actual hours flown by the operating organization, because of their capability, may be lower. We denote this quantity as k_{util} (number of flight hours per year). T_{util} is the maximum number of operational flight hours (utilization) for the helicopter throughout its useful life, which we denote in calendar years as T_{cal}. Then,

$$k_{util} = T_{util}/T_{cal} \tag{4.21}$$

or, if T_{util} and T_{cal} are expressed in the same units of time, $k^*_{util} = T_{util}/T_{cal}$ becomes a nondimensional coefficient characterizing the complete utilization of the overall calendar time for flights.

The bar graphs in Fig 4.11a show the operation of one well-known cargo transport helicopter—the Mi-6 (related to the initial stage of operation of machines of this type). We see from this diagram that the time required for performing preflight and postflight operations, plus the time for scheduled maintenance occupies a considerable portion of the calendar time of operation. Even when considering the time limitations associated with night and bad weather, and the time expended in loading and unloading operations and on major overhauls (these time expenditures are not shown in Fig 4.11a), the flight time is only 12 percent ($k^*_{util} = 0.12$); i.e., T_{util} is an order of magnitude lower than T_{cal}. Fig 4.11b shows a diagram characterizing the typical relationship between flight time and the other time required to conduct the various operations needed to support this flight time.

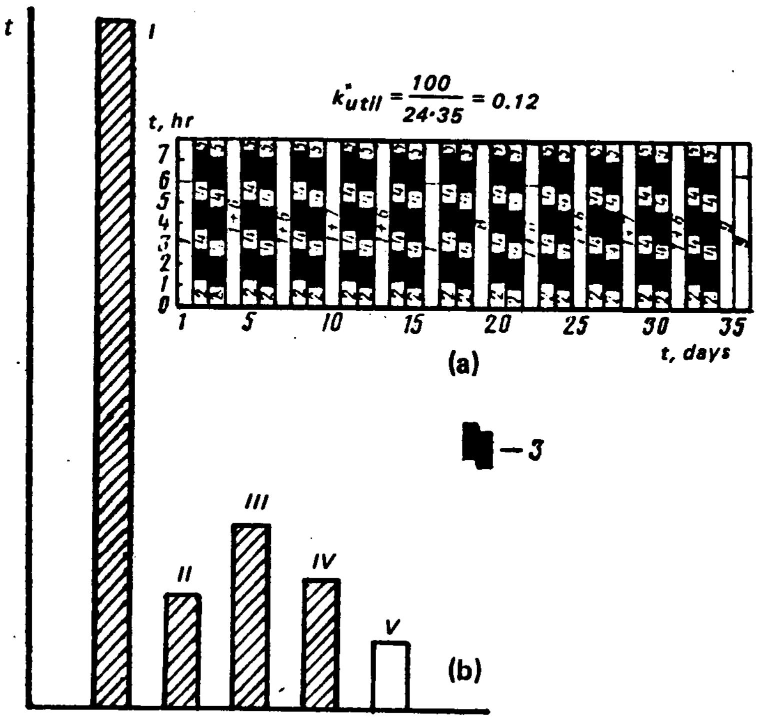

Figure 4.11 Breakdown of helicopter operating time: (a) program of Mi-6 helicopter operation; 1) preliminary preparation; 2) preflight preparation, 3) flights, 4) return flight preparation, 5) postflight servicing, 6) work through 10 ± 5 hrs, 7) work through 25 hrs, 8) work through 50 hrs, 9) work through 100 hrs; (b) typical relationship between flight time and time spent on routine maintenance, major overhaul, and downtime for modern helicopters: (I) routine maintenance, (II) major overhaul, (III) downtime because of weather and darkness, (IV) loading-unloading operations, and (V) flights.

In accordance with the definition of the quantity k_{util}, we can write

$$365 \cdot 24 = k_{util} + T_{m.o} + T_{s.m} + T_{insp} + T_{l.u} + T_{wea.n} \tag{4.22}$$

where $T_{m.o}$ = time expended on major overhauls of the helicopter in the course of the year, in hours; $T_{s.m}$ = time expended in the course of the year in performing scheduled maintenance, in hours; T_{insp} = time expended in the course of the year on technical inspection and servicing, in hours; $T_{l.u}$ = time spent on the ground in the course of the year for conducting loading and unloading operations, in hours; $T_{wea.n}$ = overall time spent during the year on the ground because of bad weather and nights, in hours.

The time expended on major overhauls can be expressed approximately by the relationship

$$T_{m.o} \approx \Sigma t_{m.o}/\eta_w m_{m.o} = (t_{m.o_{eng}} + t_{m.o_{hub}} + \ldots + t_{m.o_n}) n'_{m.o}/\eta_w m_{m.o} \tag{4.23}$$

where $\Sigma t_{m.o}$ = overall manhours required for major overhauls per year of operation; $t_{m.o_{eng}}$ = manhours needed for major engine overhauls; $t_{m.o_{hub}}$ = manhours required for major overhaul of main-rotor hubs; $t_{m.o_n}$ = manhours for major overhaul of the n-th component; $n'_{m.o}$ = number of major overhauls per year. [One of the primary requirements imposed on modern helicopters is that of equality (or multiplicity) of the TBOs for the basic components]; $m_{m.o}$ = overall number of factory, engineering, and technical personnel occupied with overhaul of the given helicopter; η_w = dimensionless coefficient expressing the relationship between the number of workers and the calendar hours per week (for example, for an 8-hr working day, two days off per week, and single-shift operation, $\eta_w = 8 \cdot 5/24 \cdot 7$).

The number of workers required is obtained from the data of any existing overhaul organization. Data on the manhours required to overhaul the individual components can be determined similarly to the evaluation of their manufacturing labor requirements. This question is examined in more detail in the following subsections of the present section.

Analogous to the determination of the quantity $T_{m.o}$, we can estimate the quantities $T_{s.m}$ and T_{insp}.

$$T_{s.m} \approx \Sigma t_{s.m}/\eta_w m_{s.m} \tag{4.24}$$

and

$$T_{insp} \approx \Sigma t_{insp}/\eta_w m_{insp} \tag{4.25}$$

where $\Sigma t_{s.m}$ = overall scheduled maintenance manhours per year; Σt_{insp} = overall manhours of preflight and postflight inspections per year; $m_{s.m}$ and m_{insp} = number of ground technical personnel involved in performing scheduled maintenance and technical inspections (taken in the calculations to be equal to the corresponding number of ground personnel servicing the existing helicopter selected as the baseline vehicle).

The method for estimating the technical servicing manhours will also be presented in the following subsections of this section.

In order to estimate $T_{l.u}$, we take as the basis some average transport operation. Let us assume that on the average, a numbers of workers equal to $m_{l.u}$ will participate in each such operation. We shall assume that for a single flight the helicopter is loaded completely with cargo weighing $G_{p.l_{max}}$. Then it flies a distance $L/2$ to the destination at a cruise speed of V_{cr}, is completely unloaded, then is loaded with another cargo whose weight is $\frac{1}{2} G_{p.l_{max}}$, and returns to the base airport where it is again unloaded. We shall also assume that only the cargo-loading equipment which is on board the helicopter is used in this operation (winches, portable ramps, conveyors, and so on). We denote the average value of manhours needed for loading and unloading operations for one such flight (out and back) as $t_{l.u}$. Then,

$$T_{l.u} \approx t_{l.u} n_{n.f}/\eta_w m_{l.u} = \Sigma t_{l.u}/\eta_w m_{l.u} \qquad (4.26)$$

where $n_{n.f}$ = average number of flight per year.

Finally, we discuss the quantity $T_{wea.n}$, which is determined for the average weather annual conditions in a particular geographic region. $T_{wea.n} = 365 \cdot 24 k_{wea.n}$, where $k_{wea.n}$ is a coefficient characterizing the effectiveness of the radio-navigation equipment, anti-icing system, autopilot, etc. For example, if the equipment installed aboard the helicopter makes it completely capable of "all-weather" operations, then $k_{wea.n} = 0$.

We assume that the quantity η_w is the same in Eqs (4.23) through (4.26). Then, substituting these equations into Eq (4.22), we obtain

$$24 \cdot 365 \approx k_{util} + \frac{\Sigma t_{m.o.h}}{\eta_w m_{m.o}} + \frac{\Sigma t_{s.m}}{\eta_w m_{s.m}} + \frac{\Sigma t_{insp}}{\eta_w m_{insp}} + \frac{\Sigma t_{l.u}}{\eta_w m_{l.u}} + 24 \cdot 365 k_{wea.n}$$

But, $\Sigma t_{mo.h}/k_{util} = t'_{m.o.h}$ is the major overhaul manhours per flight hour; $\Sigma t_{s.m}/k_{util} = t'_{s.m}$ is the scheduled maintenance manhours per flight hour; $\Sigma t_{insp}/k_{util} = t'_{insp}$ is the sevicing manhours per flight hour; and $\Sigma t_{l.u}/k_{util} = t'_{l.u}$ is the cargo handling manhours per flight hour. Then,

$$24 \cdot 365(1 - k_{wea.n}) = k_{util}\left(\frac{t'_{m.o.h}}{\eta_w m_{m.o}} + \frac{t'_{s.m}}{\eta_w m_{s.m}} + \frac{t'_{insp}}{\eta_w m_{insp}} + \frac{t'_{l.u}}{\eta_w m_{l.u}} + 1\right)$$

and

$$k_{util} = \frac{24 \cdot 365(1 - k_{wea.n})}{1 + \dfrac{t'_{m.o.h}}{\eta_w m_{m.o}} + \dfrac{t'_{s.m}}{\eta_w m_{s.m}} + \dfrac{t'_{insp}}{\eta_w m_{insp}} + \dfrac{t'_{l.u}}{\eta_w m_{l.u}}} \qquad (4.27)$$

The quantity $t'_{l.u}$ in this formula can be expressed as

$$t'_{l.u} = t_{l.u} V_{cr}/L,$$

since $n_{n.f} = k_{util}/(L/V_{cr})$ (see Eq (4.26)). Here, $t_{l.u}$ for the newly designed helicopter (we denote it by $t_{l.u_n}$) can be related to the analogous quantity for the baseline helicopter $t_{l.u_o}$ by the formula

$$t_{l.u_n} = \zeta_{l.u}(G_{p.l_n}/G_{p.l_o})\, t_{l.u_o}$$

where $\zeta_{l.u}$ = coefficient expressing the relationship between the manhours for loading and unloading operations when using different types of helicopter-installed cargo-handling mechanisms and devices. If the manhours used in manual unloading and loading cargo with a standard conveyor, for example, is taken as unity, then when using winches of a sufficient lifting capacity, this coefficient may be reduced to 0.5; when using winches and roll conveyors, it may be reduced to 0.3; and when using telphers and winches, it may be reduced to 0.15. For example, if only winches were installed on the baseline helicopter and both winches and telphers are installed on the newly designed helicopter, then $\zeta_{l.u} \approx 0.15/0.5$.

Data regarding productivity for cargo-handling operations when using various mechanisms and devices are taken either from the results of special tests or from statistics. The methods for estimating the remaining t' values in Eq (4.27) will be examined below in the corresponding subsections of this section.

Now, having a method for estimating the maximum possible annual flight time, we could easily solve the entire problem of the replacement cost share in the cost per flight hour, if we could predict, with sufficient accuracy, the total potential service life of the aircraft, both in flight hours and calendar years.

In principle, when starting the design of the new machine, we could take T_{util_n} equal to the known amortization period T_{util_0} established for the baseline helicopter and correspondingly take T_{cal_n} equal to the calendar limitation time, T_{cal_0}, of the baseline machine.

Then the requirement for satisfying the limitations of flight time and calendar time would be obtained under the condition

$$T_{util_n}/k_{util} = T_{util_0}/k_{util} < T_{cal_n} = T_{cal_0} \qquad (4.28)$$

However, with this approach, just as in the case of the methods examined at the beginning of this section, the question of the true overall service life for both new and baseline helicopters will remain unanswered. In order to avoid this difficulty, we proceed as follows. We divide the problem into two parts. We then remove from the system the following components which are traditionally considered as part of the airframe: rotor blades and hubs, swashplate assembly, gearboxes, transmission shafts, hydraulic boosters, and landing gear. As we have already mentioned, these assemblies (except for the landing gear), together with the engines, are customarily termed "dynamic components". Now, we shall solve this problem separately for the dynamic system and for the airframe. In the first case, on the basis of numerous dynamic tests and experience in operating several thousand helicopters, the overall potential service life may, in most cases, be determined quite precisely. Since the weight coefficients used to estimate the weights of such components (see Ch 2) are connected in a definite way with their service lives and since, in selecting these coefficients we begin with the fact that the service life level of new components will be at least as high as before, we can, in the early design stages, take the overall potential service lives of the new and baseline components to be equal. We can also take the calendar limitations to be the same.

As for modern helicopter airframes, on the basis of existing concepts, we can assume that their total service life potential is considerably higher than the maximum values which are known at the present time (on the order of 12 000 hours). Because of the higher vibration level, more frequent overhauls may be required for the compound helicopter airframe than for the airplane. However, the potential service life of the compound helicopter airframe may be significantly longer than that of the airplane because of the greater complexity and "criticality" of the structural airplane elements. For exemple, the airframe of the airplane includes the wing with all its mechanisms which, since it is the basic load-carrying system, determines flight safety. On the other hand, the wing which is sometimes installed on the helicopter is obviously not its primary lifting system. Even if the helicopter wing fails in flight, the probability of a serious accident is not very high. Nevertheless, the depreciation life established for helicopters have been shorter by a factor of 2 to 2.5 than those for airplanes. The annual flight time of modern helicopters, because of the nature of their operation, has not exceeded a few hundred hours on the average. Only a few machines in isolated years of operation had flight times exceeding 1000 hours. As to the calendar life for these helicopters, it has now reached 15 years. With this relationship of these numbers, it has not been possible to confirm, by actual operating experience, that the airframe of any helicopter has a depreciation life on the order of 30 000 hours; i.e., the same as for the passenger airplane. It is obvious that with time both the average annual flight time and the calendar life for helicopters can be increased. But then, in place of the calendar life, another constraint becomes effective – the helicopter obsolescence life. The operating life of helicopters of a given type will come to an end before reaching the depreciation life, since new, more efficient, and more productive helicopters will come into extensive operation. For example, it might become necessary to change over the production area used to make spare parts for older helicopter models to incorporate spares for the new model.

At the present time, we can consider that the calendar life and the obsolescence life are approximately equal.

On this basis, we take the calendar life as the governing constraint in estimating the airframe depreciation life. In so doing, we shall consider that $T_{cal_n} = T_{cal_o}$. Then the depreciation life (utilization time in hours) is

$$T_{util_n} = k_{util_n} T_{cal_o}.$$

This equality should be written more exactly in the form

$$T_{util_n} = \zeta_{c.c} k_{util_n} T_{cal_o} \tag{4.29}$$

where $\zeta_{c.c}$ = correction coefficient accounting for the true relationship between the potential service life of the baseline helicopter airframe (T_{util_o}), if it can be established, and the product ($k_{util_n} T_{cal_o}$) For $T_{util_o} \geqslant k_{util_n} T_{util_o}$, the quantity $\zeta_{c.c}$ is taken equal to one. Now, after finally obtaining the expression for the helicopter depreciation life, we can turn to the determination of replacement costs of helicopters.

4.2.2 Replacement Costs of Helicopter Airframe Dynamic System Components

We mentioned previously that since the weight of the helicopter dynamic system components is associated with the service life "postulated" during their design, the corresponding component service life is ensured by selecting the weight coefficients. The graphs considered in Ch 2 give the statistical weight data of modern helicopters having the service life of major components of the dynamic system reaching, on the average, 2500 to 3600 hours and, for particular components, up to 7000 hours. The calendar life established for these components is five years and longer. Therefore, even for relatively short annual flight times (several hundred hours), the governing limitation in estimating the replacement costs of these components is their potential service life. Consequently, the number of required components of a given type for the entire operating life of the new helicopter may be expressed in terms of the ratio of the overall flight time T_{util_n} to the potential service life of the component ($P_n^{O.T} = P_o^{O.T}$):

$$n_{comp} = T_{util_n}/P_o^{O.T} = \zeta_{c.c} k_{util_n} T_{cal_o}/P_o^{O.T} \tag{4.30}$$

where n_{comp} = total number of components of a given type, including those installed on the helicopter during manufacture (if T_{util_n} is not a multiple of $P_o^{O.T}$, n_{comp} should be increased to the closest integer).

It should once again be emphasized that in the present case, we are discussing the "postulated" service life (computed potential) of the component which is gradually achieved only after conducting various tests and after relatively extensive verification of the component during operation.

For example, the postulated service life of the main rotor blade must be at least 2000 hours. However, the first production blades of a given type delivered for operation are not likely to reach this service life immediately. The initial service life (only a few hundred hours) will be increased gradually if the results of operation of a considerable number of blades of this type are positive In the final analysis, the magnitude of the postulated service life of a component can be increased thanks to the introduction of improvements in its structure and technology of manufacturing processes. But in order not to complicate the problem, in evaluating the operating costs, we shall assume that the service life remains constant. We shall also assume that after complete amortization of the helicopter components, 5 percent of their original cost (scrap value) remains. Then the cost per flight hour for replacement of the dynamic system components can be expressed in the form

$$a_{d,c} = \frac{0.95(n_{eng}C_{eng} + n_{m.g.b}C_{m.g.b} + \dots + n_n C_n)}{\zeta_{c.c}k_{util_n}T_{cal_0}} \tag{4.31}$$

where $a_{d.c}$ = cost per flight hour for replacement of the dynamic system components; n_{eng}, $n_{m.g.b}$, n_n = number of dynamic system components (engines, main gearboxes, etc) used during the time T_{util_n}. The airframe replacement costs per flight hour is

$$a_{a.f} = \frac{0.95\,C_{a.f}}{\zeta_{c.c}k_{util_n}T_{cal_0}}. \tag{4.32}$$

The per-flight-hour replacement cost of the helicopter as a whole is

$$a_{hel} = a_{d.s} + a_{a.f} = \frac{0.95(C_{a.f} + n_{eng}C_{eng} + n_{m.g.b}C_{m.g.b} + \dots + n_n C_n)}{\zeta_{c.c}k_{util}T_{cal_0}} \tag{4.33}$$

Since, for the individual dynamic system component

$$a_n = \frac{0.95 n_n C_n}{\zeta_{c.c}k_{util}T_{cal}} = \frac{0.95C_n}{P_n^{0.T}} \tag{4.34}$$

then

$$a_{hel} = 0.95\;\frac{C_{a.f}}{\zeta_{c.c}k_{util}T_{cal}} + \frac{C_{eng}}{P^{0.T}_{eng}} + \frac{C_{m.g.b}}{P^{0.T}_{m.g.b}} + \dots + \frac{C_n}{P^{0.T}_n} \tag{4.35}$$

We see that Eq (4.35) for calculating this type of amortization cost takes into account both the flight and calendar service life of the helicopter components.

4.2.3 Major Overhaul Costs

The second component of the amortization costs are the costs for major overhaul of the helicopter components.

As is well known, the major overhauls for modern helicopters are, on the average, performed every 1000 to 1500 flight hours (if there are no earlier calendar limitations). This life will obviously increase significantly for helicopters of the future. With the exception of modern main and tail rotor blades, the structures of which are still considered unsuitable for overhaul, the dynamic system components can be subjected to major overhaul two, three, and in certain cases, more times. Minor blade repairs which are not of a major overhaul type are possible. The potential service life for the n-th component can be written as

$$P^{0.T}_n = (Z+1)P^{t.b.o} \tag{4.36}$$

where Z = allowable number of major overhauls; $P^{t.b.o}$ = time between overhauls in flight hours (TBO): $P^{t.b.o} \geqslant P_{guar}$ where the latter is the service life guaranteed by the manufacturer.

The times between overhaul established after each overhaul are not necessarily equal to one another. The time to the first overhaul may be longer than the TBO after the second and third. This is basically explained by the fact that at some overhaul facilities, it is, for many reasons, difficult to provide the same level of technological expertise as that supplied at the helicopter manufacturer's plant.

In some foreign firms, a mode of servicing the customer's helicopter is adopted in which the major overhaul is performed at the manufacturing facility. This makes it possible to establish identical TBOs for the components after every overhaul. We shall adopt this system for our problem, and shall consider that $P_n^{t.b.o} = const$ for all the examined cases.

In the well-known methods, the major overhaul cost is estimated on the basis of statistical data

$$C_n^{m.o} = \alpha_n C_n i_{m.o} \tag{4.37}$$

where $C_n^{m.o}$ = cost of major overhaul of the n-th component; α_n = constant statistical coefficient derived on the basis of actual overhaul expenditures for the corresponding components of helicopters which are in operation; and $i_{m.o} = Z$ allowable number of major overhauls.

However, this method does not assure that possible calculation errors will not be excessive. And this is so even when the "scatter" of the statistical data used to determine the coefficient α_n is small. Since this value is usually taken to be the same for all like components of different helicopters regardless of the degree of similarity of their construction, the calculation error when using this method may be so large that the method is not suitable for our purpose.

Let us examine, in somewhat more detail, the basic operations performed in major overhauls of the component. We shall consider the basic operations in main-rotor hub overhauls as a typical example:

(a) Complete disassembly,

(b) Cleaning of the parts,

(c) Thorough part inspection, during which the parts found defective are either scrapped and then replaced with new ones, or sent out for repairs. For existing hub designs, on the average, 0.3 to 0.6 percent of all the detail parts are scrapped after the first overhaul, and this increases to 1.5 percent (sometimes 2 percent) after the second overhaul. The number of repairable parts is greater by a factor of 3 or 4. As a rule, all rubber seals and safety elements are completely replaced, regardless of their condition. When overhauling certain types of hubs, some critical parts; for example, the pitch hinge trunnions, may be designated as mandatory replacement items.

(d) Repair of the parts – depending on the defects – with restoration of cadmium coating, elimination of traces of corrosion, individual surface defects, etc.

(e) Reassembly with corresponding checks.

It follows from this listing of the various overhaul operations that in the major overhaul process, the production operations used in manufacturing the component are repeated in considerable degree. The only difference is that during the major overhaul, the hub is "reassembled" from old parts. As we have mentioned, the percentage of repaired and newly manufactured parts is very low.

Therefore, it appears (on the basis of the previous discussion) that the most reliable formula for expressing major overhaul cost will be that analogous to Eq (4.2):

$$C_{T_n}^{m.o} = k'_e k_{d.p} \; C_{T_o}^{m.o} \tag{4.38}$$

where $C_{T_n}^{m.o}$ = unit cost of major overhaul of the n-th assembly (cost of major overhaul per unit weight of the assembly); $k'_e = \theta_n \Pi p_n / \theta_o \Pi p_o$, (provided that the percentage of new parts used is no more than 1 to 2 percent, the difference in cost of used materials can be neglected); and $C_{T_o}^{m.o}$ = unit cost of baseline component major overhaul (cost of major overhaul per unit weight of the component).

Thus, the cost of a single major overhaul is

$$C_n^{m.o} = k'_e k_{d.p} G_n C_{T_o}^{m.o}. \tag{4.39}$$

For the case when the overhaul of similar components of two different helicopters is accomplished in the same production facility during the same approximate time period ($k'_e = 1$), and the required manufacturing component tolerances are of the same order, Eq (4.39) takes a form analogous to Eq (4.19):

$$C_n^{m.o} = (z_n/z_o)C_o^{m.o}. \tag{4.40}$$

Therefore, the major overhaul cost per flight hour is analogous to the expression for the hourly replacement cost

$$c_n^{m.o} = C_n^{m.o}/P_n^{t.b.o} = k'_e k_{d.p} G_n C_{T_o}^{m.o}/P_n^{t.b.o} \tag{4.41}$$

or, for the particular case (see Eq (4.40)),

$$c_n^{m.o} = (z_n/z_o)(C_o^{m.o}/P_n^{t.b.o}). \tag{4.42}$$

The conditions for calculating the major overhaul cost are chosen similarly to the selection of the conditions under which the cost of manufacturing a new helicopter was determined (serial number, production capacity, and productivity level).

In order to determine the annual flight time of a new helicopter, we need to know the major overhaul manhours per flight hour:

$$t'_{m.o_n} = k'_e k_{d.p} G_n C_{T_o}^{m.o}/\theta_n P_n^{t.b.o}. \tag{4.43}$$

4.2.4 Routine Maintenance Costs

It is required that the TBOs of the components of modern helicopters be equal to, or a multiple of, the airframe TBO (mandatory requirement). However, we can imagine that a need may arise to replace an engine, blades, main rotor hub, tail rotor, or any other components under field conditions or, at best, in airfield facilities. In economic calculation practice, maintenance cost estimates are sometimes made using formulae in which terms accounting for the cost of such replacements are introduced.

One example is the following formula:

$$C_n^{r.m} = \Psi_o(n_{b.o}K_{b.o} + n_{50}K_{50} + n_{100}K_{100} + n_{200}K_{200} + n_{b.f}K_{b.f} + n_{p.f}K_{p.f} + K_{sh.t}) \tag{4.44}$$

where Ψ_o = standardized routine maintenance unit cost (we take the manhours required for routine servicing of the vehicle or component as the standardized unit); $K_{b.o}$ = manhours required for replacing engines and other components (in standardiaed units) during between-overhaul periods; $K_{50(100,200,400)}$ = manhours (in standardized units) required for 50, 100, 200, and 400-hour scheduled maintenance inspections (work), if required by regulations;

$K_{b.f}, K_{p.f}, K_{sh.t}$ = manhours (in standardized units) required for preflight and postflight servicing and also servicing during short-term layups (in the case of long-term layups, the helicopters are preserved (moth-balled) and the routine maintenance is minimal); $n_{b.o}$ = number of replacements of the corresponding components; $n_{50(100,200)}$ = number of corresponding scheduled maintenance inspections; $n_{b.f}$ and $n_{p.f}$ = number of corresponding preflight (before-flight) and postflight inspections; and $n_{sh.t}$ = number of routine maintenance cycles during short-term layups.

It would appear that we have taken into consideration everything that can influence helicopter routine maintenance costs. If we are calculating the economic characteristics of an existing helicopter, this is so. After making a preliminary time and motion study of all the operations involved with routine maintenance and thus, finding the required manhours, we can quite reliably determine $C^{r.m}$, if we know $n_{b.o}$ and $n_{sh.t}$. But how can we estimate the maintenance cost with the aid of this formula for a new helicopter design? In this case, it is recommended that we take the approximate manhour values from the statisticsl data of helicopters which are in operation; i.e., actually without accounting for the parameters of the new helicopter design. Consequently, the so-obtained accuracy would not be adequate for our problem. For the same reason, the other methods based on the assumption that routine maintenance costs are proportional to the wages paid to the flight crew are also not acceptable. In this case, the routine maintenance costs would appear to be completely independent of new helicopter parameters. Assuming that new helicopters must meet all mandatory requirements for modern aircraft, including the assurance that the TBOs of the airframe would be in multiples of the TBOs for the basic dynamic system components, we shall not include the time for unscheduled component replacements in the overall maintenance manhour routine, as scheduled replacement is accomplished only at the time of major overhaul. In reality, in the course of the entire operating period, situations may arise which lead to a necessity for premature replacement of some particular component, subassembly, or individual part. Such unscheduled repair will not be accomplished at the overhaul plant, but rather at the operating organization base, or even under field conditions.

We shall examine minor (unscheduled) repair costs separately. It is obviously impossible to foresee exactly the costs associated with these operations (manhours and spare parts), since they may be the result of piloting error, maintenance error, manufacturing defect, or design defect.

The largest number of defects and correspondingly, a considerable part of the minor maintenance cost is associated with the radio and electronic equipment. These are primarily malfunctions due to the relatively high vibration level in existing helicopters. Damages to the airframe structure rarely occur, but their repair is expensive. Powerplant failure occurs considerably more often than failure of the airframe elements, and is also very expensive. We have already mentioned that the causes of failure may vary. We are only interested in those causes that depend on the type of selected helicopter construction, and can be related in some way to the parameters being selected. For example, the eight-bladed main rotor, in principle, provides a lower level of airframe vibration than the four-bladed main rotor and consequently, we may expect fewer failures of the electronic equipment and certain other assemblies. According to statistical data, the average overall unscheduled repair costs for the existing helicopter fleet are estimated to be within the limits of 10 to 12 percent of the amortization costs;

$$C_n^{un.r} = \alpha\, a_{hel} \qquad (4.45)$$

where $\alpha = 0.1$ to 0.12.

We shall assume that the part of the helicopter minor repair costs $(\Delta C_n^{un.r} = \beta C_n^{un.r})$ basically depends on the vibration level. Then we can write

$$\Delta C_n^{un.r} = (n_{g_n}/n_{g_o})\Delta C_o^{un.r} \tag{4.46}$$

where n_g = quantity characterizing the vibration level in the region of the electronic equipment locations $\Delta C_n^{un.r}$ and $\Delta C_o^{un.r}$, incremental costs of unscheduled repairs of the n-th component, and the baseline component due to vibration. These same costs per flight hour are

$$\Delta c_n^{un.r} = \Delta C_n^{un.r}/P_n^{0.T} = (n_{g_n}/n_{g_o})(\Delta C_o^{un.r}/P_n^{0.T}) . \tag{4.47}$$

In spite of the fact that this type of expenditure depends on parameter selection, they can be ignored in further calculations, since they constitute a very small part of the overall operating costs. The major portion of the unscheduled repair costs $(C^{un.r} - \Delta C^{un.r})$ is independent of parameter selection.

Now we shall examine the question of manhours for scheduled maintenance and routine inspection. Analysis of scheduled works shows that their manhour content and consequently, their cost, are proportional to the number of basic operations performed. The scheduled work is cyclic. It is usually accomplished after accumulation of h hours of flight; for example, after every 50, 100, and 200 flight hours. During each subsequent interval, as a rule, all the operations of the preceding inspection plus some additional operations are performed. For early-model helicopters, maintenance procedures were also scheduled at 25-hour intervals. It is obviously advantageous to perform the scheduled maintenance as infrequently as possible. The 25-hour inspection cycles are no longer performed for recently produced helicopters. As a result of suitable design approaches, some aspects of the 25-hour maintenance schedule are incorporated into routine inspections. However, at the present time, inspection/maintenance intervals as long as 300 and 400 hours are scheduled. After 400 hours, the entire cycle of operations is repeated. There are also calendar inspections. But in the case of intensive operation, their extent is small in comparison with other forms of maintenance, and shall not be considered. Just as in the preceding cases, from the existing helicopters, we select a baseline helicopter which is closest to the new helicopter design with regard to size and mission. All the actual data of an operational nature must be known for this machine (results of time and motion studies of various operations during operational tests).

Let h (in flight hours) be the adopted maintenance cycle for the baseline helicopter; t_{sche_o} = labor expenditure in norm-hours for all maintenance of the complete cycle; I_o = overall number of operations during the cycle; $t'_o = t_{sche_o}/h$ = specific labor expenditure for maintenance operations in norm-hours per flight hour; $i_o = I_o/h$ = average number of operations per flight hour; and $\Delta t_{av} = t_{sche_o}/I_o = t'_o/i_o$ = average labor content of a single operation in norm-hours (quantity characterizing work productivity).

We shall assume that on the average, $\Delta t_{av} \approx const$ for the organizations operating helicopters. In selecting the parameters of a new helicopter when the characteristics are not yet known in detail, we usually assume that its primary components will be basically similar to those for the baseline helicopter (naturally, we take the machine which is to be replaced by the new design as the baseline). The possible differences can be taken into account by estimating, component-by-component, the difference in the number of required maintenance operations. For example, a tail-rotor gearbox in which the oil must be changed after a definite period can be replaced by a gearbox in which the lubricant is not replaced during the entire service life. It is evident that in this case, there is no great difficulty in estimating the reduction in the number of operations.

In reality, the labor content of individual operations may differ quite markedly from one another. However, use of the average labor content per operation in the present technique still makes it possible to obtain satisfactory accurate calculations.

For the newly designed helicopter we can write

$$\Delta t_{av} = t_{sche_n}/l_n = t'_n/i_n,$$

i.e., $t'_n/l_n = t'_o/l_o$ or $t'_n = (l_n/l_o)t'_o = (i_n/i_o)(t_{sche_o}/h) = (l_n/l_o)(t_{sche_o}/h)$

(since $l_o/h = i_o$, and $l_n/h = i_n$). Then, the maintenance costs per flight hour for the new helicopter can be written as

$$c_{sche_n} = \theta'_n(i_n/i_o)(t_{sche_o}/h) = \theta'_n(l_n/l_o)(t_{sche_o}/h) \tag{4.48}$$

where θ'_n = average cost per norm-hour maintenance operations.

The labor requirement of the preflight and postflight inspections can be similarly estimated as, in the present case, we do not consider inspections associated with layups for organizational reasons. The specific inspection manhours per flight hour for the newly designed helicopter can be expressed in terms of the baseline helicopter specific inspection manhours:

$$\Sigma t_{insp} = t_{insp.b.f} + t_{insp.p.f};$$

$$\Sigma t_{insp_n} = (l_{insp_n}/l_{insp_o})\Sigma t_{insp_o}$$

where $t_{insp.b.f}$ = preflight inspection labor content (in norm-hours); $t_{insp.p.f}$ = postflight inspection labor content (in norm-hours); Σt_{insp} = overall technical inspection manhours per flight (in norm-hours); and l_{insp} = number of inspection operations per flight.

We take the ratio of the maximum range to the cruise speed as the average duration of flight for cargo transport and passenger helicopters (ISA altitude 500 m, $G_{gr.des}$, $G_{fu.des}$, and 5 percent fuel reserve). Then, the specific routine maintenance manhours (in norm-hours per flight hour) can be expressed as

$$t'_{insp_o} = (V_{cr_o}/L_o)\Sigma t_{insp_o}$$

and

$$t'_{insp_n} = (V_{cr_n}/L_n)(l_{insp_n}/l_{insp_o})\Sigma t_{insp_o}. \tag{4.49}$$

Therefore, the inspection costs per flight hour are defined as

$$c_{insp_n} = \theta'_n t'_{insp_n} = \theta'_n(l_{insp_n} V_{cr_n}/l_{insp_o} L_n)\Sigma t_{insp_o} \tag{4.50}$$

where θ'_n = average maintenance costs per norm-hour.

4.2.5 Fuel and Lubricant Costs

Examining the costs of fuels and lubricants per flight hour, we can write

$$c_{fu} = C'_{fu} G_{fu} k_l V_{cr}/L \tag{4.51}$$

where C'_{fu} = fuel cost per kg; G_{fu} = normal (design) fuel capacity in kg; and k_l = coefficient accounting for lubricating material costs ($k_l = 1.05$).

4.2.6 Flight-Crew Wages

In accordance with the requirements of our problem, we shall consider that the annual flight time is determined only by helicopter performance. Therefore, for the calculations, we use a typical flight organization scheme in which, by introducing replacement crews we can ensure full utilization of the helicopter flight potential.

This specifically means that if the helicopter has all-weather capabilities, it can fly round-the-clock, and this requires several working shifts of pilots, flight engineers, navigators, and mechanics.

We shall not complicate the flight-crew calculation by introducing several coefficients accounting for operating condition peculiarities (geographic regions, and so on) as is usually done, since this will have very little influence on the final results of the analysis.

We specify the annual flight time norm for the crew as H (flight hours).Then, the required number of crews is determined as the ratio k_{util}/H. We denote the average cost per calendar hour (based on monthly pay) by θ'_{ℓ} ; and the number of crew members by m_{crew}. Then, the expression $\theta'_{\ell}\, m_{crew}\, T_{cal}\, k_{util}/H$ will be the cost of the conventional ("ground") part of the flight crew pay for the entire helicopter service period (here, T_{cal} is in hours). We denote θ''_{ℓ} as the average pay per hour of flight operation. Then, the expression $\theta''_{\ell}\, m_{crew}\, \Gamma_{util}\, k_{util}/H$ will be the cost of the "flight" part of the crew pay. Hence, the overall sum of the flight crew pay for the calendar period of helicopter service will be

$$C_{sal_{\ell}} = k_{util}\, m_{crew}(\theta'_{\ell}\, T_{cal} + \theta''_{\ell} T_{util})/H = k_{util}\, m_{crew}\, T_{cal}(\theta'_{\ell} + k^{*}_{util}\, \theta''_{\ell})/H. \tag{4.52}$$

Here, $k^{*} = T_{util}/T_{cal}$ where both T_{util} and T_{cal} are in hours; and $k_{util} = T_{util}/T_{cal}$ where T_{util} is in hours and T_{cal} is in years. The flight crew pay per flight hour is expressed as follows:

$$c_{sal_{\ell}} = \frac{C_{sal_{\ell}}}{k^{*}_{util} T_{cal}} = \frac{k_{util}\, m_{crew}}{k^{*}_{util} H}\left(\theta'_{\ell} + k^{*}_{util}\theta''_{\ell}\right) = \frac{24\cdot 365\, m_{crew}}{H}\left(\theta'_{\ell} + k^{*}_{util}\theta''_{\ell}\right) . \tag{4.53}$$

Since a crew having different qualifications than their predecessors may be required for the new helicopter, we should also introduce a correction for the required rating into the expression for the costs in these formulae. However, this will have very little influence on the final results of the economic calculation. Therefore, we shall not consider this factor.

4.3 Indirect Cost Estimation. Basic Relations for Estimating Operating Costs

4.3.1 Training Flight Costs. Airport and Other Costs

In economic calculation practice, we usually take into account the costs of training and service flights, and the costs of engine operation on the ground, as well as the per diem costs for crew during interruption of trips, and so on. At the present time, in calculations made by Aeroflot, these costs are taken on the order of 10 percent of the amortization, maintenance, and fuel and lubrication costs. The indirect costs also usually include other forms of "secondary" costs; specifically, the cost of airport upkeep.

It is obvious that for helicopters which do not require expensive runways, these costs should be much lower than for the airplane. In the calculations made by Aeroflot, these costs were previously taken as practically the same as for airplanes; i.e., 30 percent of the overall direct costs (without the amortization costs). Since these costs are essentially independent of the helicopter parameters, they may be ignored in our considerations.

4.3.2 Insurance Costs

We also include the insurance costs in the indirect category. In our calculations we must consider, during design, the different degrees of technical risk "inherent" in the new helicopter.

It is obvious that the use of proven configurations and technical approaches provides a basis for reducing the insurance costs and, vice versa, we must increase them if, in the design, we intend to use new technical solutions which have not been verified by many years of operation of hundreds of preceding helicopters. It is clear that this approach to estimating the insurance costs is applicable to helicopters of a given type which are in the initial stage of operation. As operating experience is accumulated and the designs in which fundamentally new technical approaches have been used is "debugged", the insurance costs can be reduced accordingly.

In foreign practice, the annual insurance costs for well-verified designs range from 5 to 16 percent of the initial helicopter cost (without account for life insurance for passengers and crew members). In our case, we must naturally assume that operation of the helicopters being compared will take place under the same conditions. Let the annual insurance cost of a newly designed helicopter having no fundamental difference in configuration or type of components from previously designed machines in extensive operation be a q fraction of the initial helicopter cost; for example, one percent. In reality, the design of such a machine is unlikely, as new and different qualities are required which can be achieved only by introducing new technical approaches into the design. However, when designing the new machine, the designers attempt to utilize previous solutions as much as possible, and striving for an optimal overall result with the introduction of the minimal number of new approaches and associated problems. Today, such new approaches include changeover from main-rotor hubs with steel housings to hubs with titanium housings, and from hubs of the conventional type to hubs with elastomeric bearings. Other examples include: changeover from conventional hinged rotors to "rigid" rotors, from gearboxes with conventional involute gears to gearboxes with conformal gears, and from the conventional mechanical flight control system to the fly-by-wire system, and so on.

We denote the number of such new technical innovations which are "introduced" into a particular project by $n_{t.inn}$. Then, the annual insurance cost for the new helicopter can be expressed as

$$C_{insu_n} = n_{t.inn} C_{i.c} q \qquad (4.54)$$

where $C_{i.c}$ = initial helicopter cost; q = insurance rate used for the helicopter of conven-optimal design and $n_{t.inn}$ = number of fundamentally new technical approaches (innovations) introduced into the critical elements of the helicopter structure. The insurance costs per flight hour are

$$c_{insu_n} = n_{t.inn} q C_{i.c} / k_{util}. \qquad (4.55)$$

4.3.3 Basic Formulae for Estimating Helicopter Operating Costs

On the basis of our analysis we have obtained several relationships which make it possible to estimate the operating costs for a new helicopter in the early stages of its design.

The unit cost of manufacturing the n-th assembly of the helicopter

$$C_{T_n} = k_{d.p} k_e C_{T_o} \tag{4.2}$$

$$C_{T_n} = k_e k_{d.p} \sqrt[4]{S_n/S_o}\, C_{T_o} \tag{4.20}$$

where

$$k_e = k_\theta \frac{\theta_n \Pi p_n}{\theta_o \Pi p_o} + k_M \frac{M_n}{M_o}. \tag{4.9}$$

$$k_{d.p} = (z_n/z_o)(G_o/G_n)(\Lambda_o/\Lambda_n)^2. \tag{4.15}$$

The cost of manufacturing the n-th component of the helicopter is

$$C_n = G_n C_{T_n} = \frac{z_n}{z_o}\left(\frac{\Lambda_o}{\Lambda_n}\right)^2 \left(k_\theta \frac{\theta_n \Pi p_n}{\theta_o \Pi p_o} + k_M \frac{M_n}{M_o}\right) C_o \tag{4.17}$$

$$C_n = k_e (z_n/z_o)(\Lambda_o/\Lambda_n)^2 C_o \sqrt[4]{S_n/S_o}. \tag{4.56}$$

Cost of manufacturing the entire helicopter

$$C_{hel_n} = \Sigma C_n. \tag{4.57}$$

Replacement costs per flight hour

$$a_{hel} = 0.95\left(\frac{C_{a.f}}{\zeta_{c.c} k_{util} T_{cal}} + \frac{C_{eng}}{P^{0.T}_{eng}} + \frac{C_{m.g.b}}{P^{0.T}_{m.g.b}} + \ldots + \frac{C_n}{P^{0.T}_n}\right) \tag{4.35}$$

Major overhaul costs (per flight hour for the n-th assembly

$$c^{m.o}_n = k'_e k_{d.p} G_n C^{m.o}_{T_o} / P^{t.b.o}_n \tag{4.41}$$

Overall major overhaul costs per flight hour

$$c^{m.o}_{hel_n} = \Sigma c^{m.o}_n. \tag{4.58}$$

Periodic maintenance costs per flight hour

$$c_{sche_n} = \theta'_n (l_n/i_o)(t_{sche_o}/h) = \dot{\theta}_n (l_n/l_o)(t_{sche_o}/h) \tag{4.48}$$

Inspection costs per flight hour

$$c_{insp_n} = \theta'_n t'_{insp_n} = \theta'_n (l_{insp_n} V_{cr_n} / l_{insp_o} L_n) \Sigma t_{insp_o} \tag{4.50}$$

Fuel and lubricant costs per flight hour

$$c_{fu} = C'_{fu} G_{fu} k_\ell V_{cr}/L \tag{4.51}$$

Flight crew costs per flight hour

$$c_{sal_\ell} = \frac{24 \cdot 365 m_{crew}}{H}\left(\theta'_\ell + k^*_{util} \theta''_\ell\right) \tag{4.53}$$

Insurance costs per flight hour

$$c_{insu_n} = n_{t.inn}\, q\, C_{i.c}/k_{util} \tag{4.55}$$

Cost per flight hour

$$c_{hel} = a + c^{m.o} + c_{s.m} + c_{insp} + c_{fu.\ell} + c_{sal.\ell} + c_{insu}\,. \tag{4.59}$$

5

OPTIMAL HELICOPTER PARAMETER SELECTION BASED ON MINIMAL COST CRITERIA

The formulae presented in the preceding chapter make it possible to examine the cost variation of both the individual components and the helicopter as a whole, as a function of gross weight, main-rotor diameter, and number of blades for helicopters of various configurations and different weight categories.

We shall present the calculations of the operating costs for some variants of one of the helicopters examined in Ch 2 (see Table 2.11). By analyzing the results of these calculations, we shall try to clarify the degree to which the optimum found on the basis of the minimal weight criterion coincides with the optimum determined on the basis of the minimal helicopter operating cost criterion.

5.1 Replacement Cost Dependence on Helicopter Parameters

5.1.1 Blade Replacement Costs

To obtain the weight of the n-th component, we substitute the blade-weight expression from Eq (2.8) (for $\lambda \leqslant \lambda_o$) into the general formula (Eq (4.17)):

$$\Sigma C_{bl_n} = k_{d.p} k_e C_{T_{bl_o}} k^*_{bl} \sigma_n R_n^{2.7} \tag{5.1}$$

where ΣC_{bl_n} = overall cost of a set of main-rotor blades.

In accordance with the discussion in Ch II, this relationship will be valid only for definite types of blade designs with aspect ratio varying in a relatively narrow range of $\lambda = 16$ to 20, and for chords of $b = 0.4$ to $1.0\,m$. Within this range, the constraints with regard to maximum allowable values of γ_o and blade droop need not be considered.

In spite of these narrow limits, Eq (5.1) makes it possible to quite reliably estimate the cost of the blade sets of most existing types, since their weight characteristics are within the limits that can be considered acceptable by contemporary designers (exceeding these limits in blade design may lead to the need for solving some new problems). On this basis, we have taken advantage of the approximate formula given by Eq (2.8) in our blade cost calculations.

In principle, we could take any weight formula to illustrate this cost analysis technique. The accuracy of the cost analysis calculation itself will not change as a result of this. It will be shown below that the assumptions made in order to simplify the cost calculation do not influence the final result. On this basis, the overall cost of the blade set (per flight hour) can be expressed as

$$\Sigma c_{bl_n} = 0.95 k_{d.p} k_e k^*_{bl} \sigma_n R_n^{2.7} C_{T_{bl_o}} / P_{bl_n}{}^{0.T} \tag{5.2}$$

or

$$\Sigma a_{bl_n} = 0.95 k_{d.p} k_e k^*_{bl} z_{bl_n} b_n R_n^{1.7} C_{T_{bl_o}} / \pi P_{bl_n}{}^{0.T} \tag{5.3}$$

After sequentially determining all the coefficients appearing in these expressions we can vary the values of z_{bl}, b, and R to evaluate the blade set costs for each considered helicopter variant.

We shall first calculate the cost of blade set replacement using Eq (5.3) only for a single initial variant (for example, for the single-rotor helicopter from Table 2.11), taking a blade set of the production helicopter of the corresponding class as the baseline. Then we replace the baseline. We now take the main-rotor blades of the original helicopter variant as the baseline and vary the indicated quantities. This is convenient in that it avoids the necessity of determining several intermediate quantities since, in this case, $k_e = 1$ and $\Lambda_o/\Lambda_n = 1$.

It is clear that when estimating replacement costs, the solution of the problem depends considerably on the design peculiarities ($k_{d.p}$), and the determination of this coefficient basically reduces to finding the corresponding detail part "densities" z_n/G_n in the component. In Fig 4.9, z_n/G_n was shown as a function of airframe weight for several Boeing Vertol helicopters. Fig 5.1 shows analogous relationships for the individual airframe components of the helicopters of that company. Examination of these figures leads to the obvious general conclusion that the part density decreases with an increase of the size of the article. If we could find similar relations for all the basic components, including the blades, we would be able to obtain a quantitative estimate of the cost of the new machine. An approach to the solution of this problem in application to the blades might be, for example, as follows.

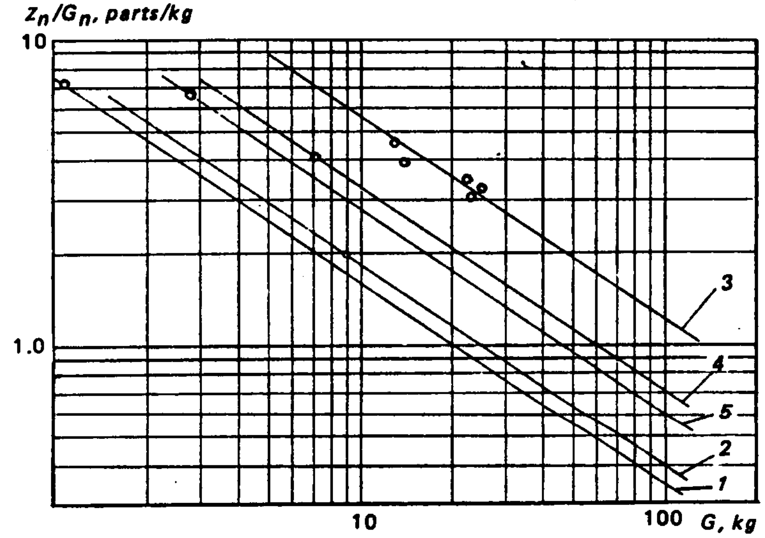

Figure 5.1 Ratio z_n/G_n as a function of fuselage component weights: (1) rib, (2) panel, (3) bulkheads, (4) beams, and (5) partitions

The main rotor blades of many modern helicopters are a typical example of aircraft "skeleton" construction, in which a specific set of elements is used repetitively. The number of such "repetitions" is proportional to the parameters characterizing the dimensions of the structure. For example, for blades consisting of a spar and "envelope" sections, this dimension is the blade radius. With change of the airfoil chord and thickness, the number of detail parts remains practically constant. Since we have assumed that the blade weight is proportional to the product of the chord and the radius to the 1.7-th power, the average density of the blade parts can be expressed approximately as

$$z_{blade}/G_{bl} \approx m_{bl} R/b R^{1.7} = (m_{bl}/b) R^{-0.7} \tag{5.4}$$

where z_{blade} = number of parts in the blade; and m_{bl} = coefficient of proportionality, which we shall consider constant for a given type of structure. In reality, this relationship should be more complex since specific optimal dimensions of the trailing-edge boxes correspond to each value of R. For small variations of R, the quantity z_{blade} may not change at all. However, this refinement is not significant for a quite wide range of variations of the blade parameters.

Knowing the actual relationships between the average structure density and the radius for the existing blades, we can use the corresponding logarithmic relations to determine the coefficients of proportionality m_{bl} for various types of structures. Taking the logarithm of Eq (5.4), we have

$$\log (z_{blade}/G_{bl}) = \log(m_{bl}/b) - 0.7 \log R.$$

In the logarithmic coordinate system, this relationship is represented by a straight line in the form $U = A - kX$.

In order to construct the graph of this relationship for any type of structure, we need only have the coordinates of a single point.

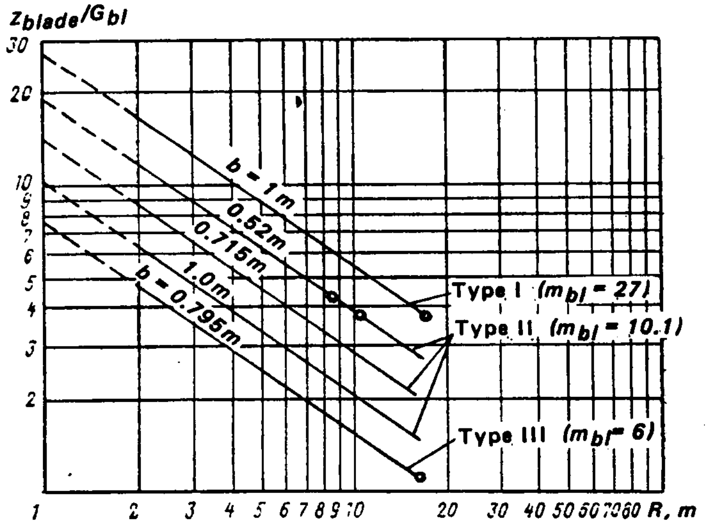

Figure 5.2 Density of the main-rotor parts as a function of the blade radius: Type I - steel tube spar, steel root end, and Duralumin envelope with metal honeycomb; Type II — extruded aluminum alloy spar, steel root end, Duralumin envelope with metal honeycomb; Type III — steel tube longeron, titanium root end, glass-plastic envelope.

Such relationships are shown in Fig 5.2. Using them, we have

$$k_{d.p} = m_{bl} G_{bl_o} \Lambda_o^2 / b_n R_n^{0.7} z_{blade_o} \Lambda_n^2 . \tag{5.5}$$

Substituting the expression for $k_{d.p}$ given by Eq (5.5) into Eq (5.3), we obtain

$$\Sigma a_{bl} = \left(\frac{0.95 k_e k^*_{bl} m_{bl} C_{T_{bl_o}} \Lambda_o^2}{\pi z_{blade_o} P_{bl.n}^{0.7} \Lambda_n^2} \right) R_n z_{bl_n} G_{bl_o} . \tag{5.6}$$

If the type of structure and the materials are not varied when selecting the parameters, then, in this equation, the expression in the parentheses is constant:

$$\frac{0.95 k^{*}_{bl} m_{bl} C_{T bl_o} G_{bl_o} k_e \Lambda_o^2}{\pi z_{blade_o} P_{bl_n}^{0.T} \Lambda_n^2} = const.$$

Denoting this expression by k_a^{bl}, we obtain

$$\Sigma a_{bl} = k_a^{bl} R_n z_{bl_n}. \tag{5.7}$$

Or, since in selecting the parameters of a helicopter with a constant gross weight, a definite value of σ corresponds to each value of R because of the necessity for satisfaction of the condition $t_{y_o} = const$. Then,

$$\Sigma a_{bl_n} = \pi k_a^{bl} \sigma_n R_n^2 / b_n. \tag{5.8}$$

Thus, in Eq (5.7), we have obtained relationships for the hourly costs of main-rotor blade replacement as a function of number of blades (z_{bl}) and blade radius. But it follows from Eq (5.7) that these costs do not depend on the blade chord. However, increase of the chord should lead to an increase in material costs; increase in the length of bonded, riveted, or other types of seams; and increase of the machined surface area of the spar, resulting in some associated increase in the blade cost. It was shown in the preceding chapter that in the technique which we have used for economic estimation, provision was made for accounting for an increase in the component cost because of an increase in its dimensions (while retaining the same number of parts). This was done by multiplying the component unit cost by the relative weight increment. But with the assumption we have made, it turns out that the single blade replacement cost, because of the increase in weight, increases to the same degree as its decrease because of the reduction in structure density. In other words, Eqs (5.7) and (5.8) are valid for the case when costs are compared for blades with chords which are similar in size. However, since the analysis should be made with a wide range of blade parameter variations, we shall use Eq (4.56), which takes into account the increase of the manhours with increase of the surface area of the parts being machined. Then,

$$\Sigma a_{bl_n} = \frac{0.95 k_{d.p} k_e C_{T_o} G_{bl_n} \sqrt[4]{S_n/S_o}}{P_{bl_n}^{0.T}},$$

where, in application to the blade structure $\sqrt[4]{S_n/S_o} = \sqrt[4]{R_n b_n / R_o b_o}$. After transformation, this formula takes the form

$$\Sigma a_{bl_n} = \frac{k_a^{bl}}{(R_o b_o)^{0.25}} z_{bl_n} R_n^{1.25} b_n^{0.25} \tag{5.9}$$

or

$$\Sigma a_{bl_n} = k_a'^{bl} z_{bl_n} R_n^{1.25} b_n^{0.25} \tag{5.10}$$

where

$$k_a'^{bl} = k_a^{bl} / (R_o b_o)^{0.25} = const.$$

We can rewrite Eq (5.10) in a different way;

$$\Sigma a_{bl_n} = \pi k_a'^{bl} \sigma_n R_n^{2.25} / b_n^{0.75}. \tag{5.11}$$

When we wish to estimate the economic advisability of using a particular type of blade structure or material, it is necessary to repeat the calculations several times, varying k_e and m_{bl} within the entire range of the examined main-rotor diameters.

However, if the type of structure and materials are determined from considerations of non-economic nature (for example, by the specific production capabilities), the first aspect of the parameter selection problem associated with estimating blade cost, reduces to finding the relationship between the main-rotor diameter and the quantity characterizing the relative cost of blade replacement. By this, we mean the ratio of replacement costs for the set of blades of given dimension to the corresponding costs for the set of blades taken as the baseline.

$$\Sigma\bar{a}_{bl} = \Sigma a_{bl_n}/\Sigma a_{bl_o}. \tag{5.12}$$

Taking the original helicopter blade as the baseline (see Table 2.11), we will have

$$\Sigma\bar{a}_{bl} = \frac{z_{bl_n}}{z_{bl_o}}\left(\frac{b_n}{b_o}\right)^{0.25}\left(\frac{R_n}{R_o}\right)^{1.25}. \tag{5.13}$$

In conjunction with the general formulation of the problem of finding the correspondence between the weight and the economic optima when selecting the parameters, it is interesting, even at this stage of the calculation, to compare the nature of blade weight and cost variation as a function of gross weight, main-rotor diameter, number of blades, and the corresponding blade chord. To this end, we write the expression for the relative blade weight similar to that of the quantity characterizing the relative replacement costs.

$$\Sigma\bar{G}_{bl} = \frac{G_{bl_n}}{G_{bl_o}} = \frac{z_{bl_n}}{z_{bl_o}}\,\frac{b_n}{b_o}\left(\frac{R_n}{R_o}\right)^{1.7}. \tag{5.14}$$

From comparison of the last two formulae, it follows that with a change in the radius and chord dimensions, the blade weight changes faster than its cost. However, we recall that due to the fact that the approximate expression for ΣG_{bl} appears in these relationships, they are valid only for the case where the aspect ratio does not exceed the maximum value up to which increases of λ do not increase the weight of the blade. In the more general case, we must introduce a correction in accordance with Eq (2.8):

$$\bar{I}_n = [1 + \alpha_\lambda \bar{R}(\lambda - \lambda_o)]$$

(see Ch 3). In this case, Eq (5.14) for the blade relative weight characteristics takes the form

$$\Sigma\bar{G}_{bl} = \frac{z_{bl_n}}{z_{bl_o}}\,\frac{b_n}{b_o}\left(\frac{R_n}{R_o}\right)^{1.7}[1 + \alpha_\lambda \bar{R}(\lambda - \lambda_o)]. \tag{5.15}$$

How does the expression for $\Sigma\bar{a}_{bl}$ vary in this case? After making the necessary transformations, it is not difficult to see that it remains unchanged, since the weight correction enters into Eq (5.13) to the same power in both the numerator and denominator.

Fig 5.3 shows Eqs (5.13) and (5.15) in graphical form. We see that for $\lambda > (\lambda_{n.y})_{max}$ the weight increases with increase of the main-rotor radius considerably faster than the relative replacement costs. When using the more general weight formula (Eq (2.12)) which is valid for $\lambda = var$ within a wide range, the relationship for blade replacement costs (as before), does not change.

In this case, the blade relative weight is

$$\Sigma\bar{G}_{bl_n} = \frac{z_{bl_n}}{z_{bl_o}}\,\frac{b_n}{b_o}\left(\frac{R_n}{R_o}\right)^{1.7}\left(\frac{\lambda_o}{\lambda_n}\right)^{0.7}[1 + \alpha_\lambda(\lambda - \lambda_o)] = \frac{z_{bl_n}}{z_{bl_o}}\left(\frac{b_n}{b_o}\right)^{1.7}\frac{R_n}{R_o}[1 + \alpha_\lambda(\lambda - \lambda_o)]. \tag{5.16}$$

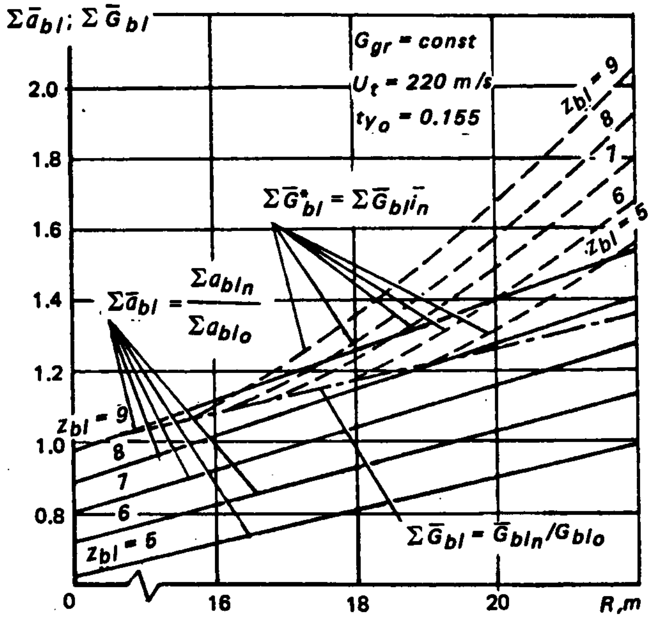

Figure 5.3 Example of relationship between the blade relative weight and cost characteristics vs main-rotor radius: — · — · $\Sigma\bar{G}_{bl}$; — — — — $\Sigma\bar{G}^*_{bl}$; ——— $\Sigma\bar{a}_{bl}$

This expression is valid with satisfaction of the conditions given by Eqs (2.15) and (2.122).

To find the dependence of $\Sigma\bar{a}_{bl}$ on the main-rotor radius, it is not necessary to first find the relationship of the type $z_{blade}/G_{bl} = f(R)$. As was shown in the preceding chapter, for this we need only know the relation of the type $z_{blade} = f(R)$. However, in many cases, it is more convenient to use the numerical part densities in the economic calculations. But the quantity z_{blade}/G_{bl} makes it possible to directly compare the cost levels of similar components (somewhat analogous to the weight ratio). Therefore, we will use this characteristic whenever possible when examining the replacement costs for certain other basic components.

5.1.2 Main Rotor Hub Replacement Costs

It was shown in Ch 2 that the hub weight is determined primarily by the centrifugal forces of the blade. With increase of the centrifugal forces, it becomes necessary to increase the characteristic dimensions, particularly of the pitch-bearing-housing cross-sections, because of the necessity to install bearings with increased supporting surface area and housings having higher load-carrying capacity. This naturally involves introduction of new detail parts into the structure (see Ch 4). In conjunction with the increase of the bearing dimensions, there is an increase in the number of rollers and needles, new elements appear in the sealing systems, as well as standard and nonstandard fasteners, the number of which is also determined by the increased cross-section area of the pitch-bearing housings. The number of bearings also increases. [The scale factor also leads to an increase in the number of detail parts in the hub mechanisms, which are not directly associated with the quantity N_{bl}; for example, in the centrifugal blade droop stop.] However, the cross-section areas, as was shown in Ch 2, are proportional to the centrifugal force N_{bl}. With an increase of the sleeve member length, the number of detail parts changes relatively little (however, with increase in the number of blades and the associated appearance of additional joints and other complications, the number of detail parts increases). For example, the Mi-8 medium helicopter hub consists of 2640 parts, and a similar Mi-6 heavy-lift helicopter hub has approximately 7500 parts.

On this basis, we can write

$$z_{hub} \approx z_{bl} m_{hub} N_{bl} \tag{5.17}$$

where m_{hub} = coefficient characterizing the hub type. Since the hub weight in accordance with Eq (2.31) is

$$G_{hub} = k^{*}_{hub} k_{z_{bl}} z_{bl} N_{bl}^{1.35}$$

we can write

$$z_{hub}/G_{hub} = (m_{hub}/k^{*}_{hub} k_{z_{bl}}) N_{bl}^{-0.35}. \tag{5.18}$$

To determine m_{hub}, we proceed similarly to the approach used in the preceding section when estimating m_{bl}; knowing the detail part densities of the existing helicopter hubs, and the exponent of the centrifugal force in the expression for z_{hub}/G_{hub}, we plot relations of the type of Eq (5.18) to logarithmic scale. Fig 5.4 shows examples of such relationships. Now substituting Eq (5.18) into Eq (4.17), we obtain

$$C_{hub_n} = k_e \left(\frac{\Lambda_o}{\Lambda_n}\right)^2 \frac{m_{hub}}{z_o} z_{bl_n} G_{hub_o} C_{T_{hub_o}} N_{bl_n}. \tag{5.19}$$

Then the hub replacement costs will be

$$a_{hub} = 0.95 \frac{C_{hubn}}{P_{hub}^{0.T}} = \frac{0.95 k_e}{P_{hub}^{0.T}} \left(\frac{\Lambda_o}{\Lambda_n}\right)^2 \frac{m_{hub}}{z_o} z_{bl_n} G_{hub_o} C_{T_{hub_o}} N_{bl_n}. \tag{5.20}$$

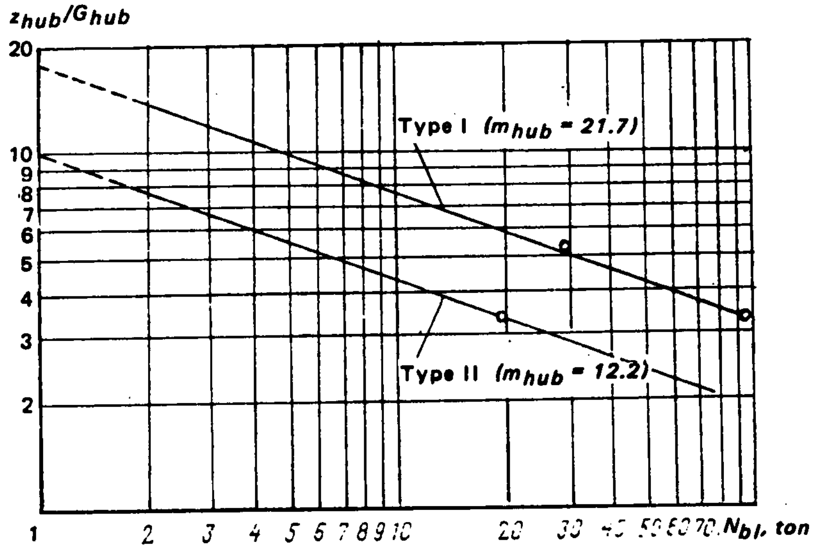

Figure 5.4 Density of main-rotor hub parts as a function of the blade centrifugal force; Type I — fully articulated with hydraulic dampers; Type II — fully articulated with friction dampers

If we wish to solve the problem of selecting the optimum material for the hub, we make a series of calculations in which we vary the quantity k_e.

By varying m_{hub}, we can solve the problem of selecting the optimal hub type on the basis of minimal cost. If the type of hub construction and the materials have been determined, the problem reduces to finding the relationship between the main rotor radius and the relative hub replacement costs. For the selected bype of hub and materials, the quantity

$$\frac{0.95k_e}{P_{hub}^{0.7}}\,\frac{m_{hub}}{z_o}\left(\frac{\Lambda_o}{\Lambda_n}\right)^2\ G_{hub_o}C_{T_o}=const.$$

Denoting this quantity by k_a^{hub}, we obtain

$$a_{hub} = k_a^{hub}\, z_{bl}N_{bl}. \tag{5.21}$$

Taking the main-rotor hub of the original helicopter as the new baseline (see Table 2.11), we can write the expression for the relative hub replacement cost as

$$\bar{a}_{hub_n} = \frac{a_{hub_n}}{a_{hub_o}} = \frac{z_{bl_n}}{z_{bl_o}}\,\frac{N_{bl_n}}{N_{bl_o}}. \tag{5.22}$$

The relative hub weight is

$$\bar{G}_{hub} = \frac{G_{hub_n}}{G_{hub_o}} = \frac{z_{bl_n}k_{zbl_n}}{z_{bl_o}k_{zbl_o}}\left(\frac{N_{bl_n}}{N_{bl_o}}\right)^{1.35} \tag{5.23}$$

From a comparison of Eqs (5.23) and (5.22), we can see that with an increase of the centrifugal force, the relative cost of the hub replacement increases; but somewhat more slowly than the hub weight. In order to account for the cost increase associated with an increase of the machined surface area of the parts (with no corresponding increase in the number of parts), we introduce the correction $\sqrt[4]{S_n/S_o}$ (see Ch 4). We shall consider an example. The special nuts with the system of seals of the horizontal and vertical hinges of the Mi-8 helicopter are basically similar in construction to the corresponding parts of the Mi-6 helicopter hub. They have the same number of parts and the same coefficient k_e, and they are fabricated from the same materials at the same production facilities. While differing in weight by a factor of 4.5 to 5, they differ in cost by only a factor of 1.7 to 2, which is proportional to the ratio $\sqrt[4]{S_{nut\ Mi\text{-}6}/S_{nut\ Mi\text{-}8}}$.

For the hubs

$$\sqrt[4]{S_{hub_n}/S_{hub_o}} \approx \sqrt[4]{d_n\,\xi_n\,R_n/d_o\,\xi_o\,R_o}$$

where ξ_n and ξ_o = relative length of the hub sleeve, counted from the axis of rotation and expressed as a percentage of the main-rotor radius; d_n and d_o = the effective pitch-bearing housing diameters (characteristic dimension). In accordance with Eq (2.10)

$$d_n = \bar{d}\sqrt{N_{bl_n}};\ d_o = \bar{d}\sqrt{N_{bl_o}}.$$

Assuming that for the same hub type, $\xi_n = \xi_o$, we have

$$\sqrt[4]{\frac{S_{hub_n}}{S_{hub_o}}} \approx \sqrt[4]{\frac{N_{bl_n}^{0.5}\,R_n\,z_{bl_n}}{N_{bl_o}^{0.5}\,R_o\,z_{bl_o}}} = \frac{N_{bl_n}^{0.125}\,R_n^{0.25}\,z_{bl_n}^{0.25}}{N_{bl_o}^{0.125}\,R_o^{0.25}\,z_{bl_o}^{0.25}};$$

then

$$a_{hub} = k_a^{hub} z_{bl_n} N_{bl}^{1.125} R^{0.25} \qquad (5.24)$$

and

$$\bar{a}_{hub} = \left(\frac{z_{bl_n}}{z_{bl_o}}\right)^{1.25} \left(\frac{N_{bl_n}}{N_{bl_o}}\right)^{1.125} \left(\frac{R_n}{R_o}\right)^{0.25} . \qquad (5.25)$$

Figure 5.5 shows the dependence of $\bar{a}_{hub}$ and $\bar{G}_{hub}$ on the main-rotor radius for various numbers of blades.

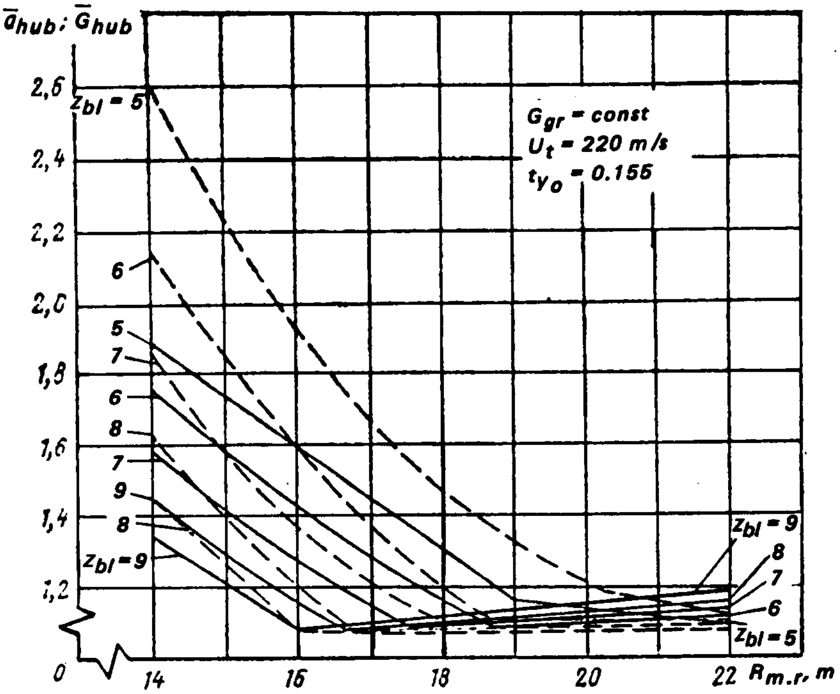

Figure 5.5 Example of relationship between main-rotor hub relative weight-and-cost characteristics, and main-rotor radius: – – – $\bar{G}_{hub}$ ——— $\bar{a}_{hub}$

5.1.3 Main Gearbox Replacement Costs

The basic data available to the designers of the main gearbox in the early design stage is the transmitted power and rotational speed of the main rotor, $n_{m.r}$, and input shaft n_Ii. These characteristics determine the number of reduction stages.

Using arguments analogous to those presented in the preceding subsection, we conclude that the number of detail parts for the i-th stage is $z_i = m_i \sqrt[3]{(M_Q)_i}$, since the number of detail parts increases in proportion to the shaft and gear diameters. The number of detail parts for the entire gearbox is

$$\Sigma z_{m.g.b} = m_I \sqrt[3]{(M_Q)_I} + m_{II} \sqrt[3]{(M_Q)_{II}} + \ldots + m_i \sqrt[3]{(M_Q)_i} + \ldots + m_n \sqrt[3]{(M_Q)_n}, \qquad (5.26)$$

where n = number of reduction stages.

If we take the main rotor as the n-th output stage, then

$$z_n = m_n \sqrt[3]{(M_Q)_n} = m_n \sqrt[3]{(M_Q)_{m.r}}$$

since

$$(M_Q)_i / (M_Q)_{m.r} = n_{m.r}/n_i = 1/i^*_i, \quad \text{then} \quad (M_Q)_i = (M_Q)_{m.r}/i^*_i$$

and

$$\Sigma z_{m.g.b} = \sqrt[3]{(M_Q)_{m.r}}\left(m_I \sqrt[3]{1/i^*_I} + \ldots + m_i \sqrt[3]{1/i^*_i} + \ldots + m_{n-1} \sqrt[3]{1/i^*_{n-1}} + 1\right). \quad (5.27)$$

For modern gearboxes, on the average,

$$i_i = n_{i-1}/n_i \approx 2.6 \text{ to } 2.8.$$

Then the overall gear ratio from the 1st to the n-th stage is $i = i^*_I = i_I i_{II} i_{III} \ldots i_i \ldots i_n \approx (i_i)^n \approx 2.7^n$. Correspondingly, $i^*_{II} \approx 2.7^{n-1}$, $i^*_{III} \approx 2.7^{n-2}$, $i^*_{n-1} \approx 2.7$, $i^*_n \approx 1$; i.e, for each gearbox type having a selected number of reduction stages, the quantity

$$\left(m_1 \sqrt[3]{1/i^*_I} + \ldots + m_i \sqrt[3]{1/i^*_i} + \ldots + m_{n-1} \sqrt[3]{1/i^*_{n-1}} + 1\right) \approx const.$$

Denoting this quantity by $m_{m.g.b}$, we can write for the single-rotor helicopter main gearbox

$$\Sigma z_{m.g.b} = m_{m.g.b} \sqrt[3]{(M_Q)_{m.r}}. \quad (5.28)$$

For the general case,

$$\Sigma z_{m.g.b} = m_{m.g.b} z_{rotor} \sqrt[3]{\alpha M_{av}}. \quad (5.29)$$

The density of the detail parts in the main gearbox is

$$\Sigma z_{m.g.b}/G_{m.g.b} = m^*_{m.g.b} (\alpha M_{av})^{-0.467}. \quad (5.30)$$

For the single-rotor helicopter,

$$\Sigma z_{m.g.b}/G_{m.g.b} = m^*_{m.g.b} (M_Q)_{m.r}^{-0.467}. \quad (5.31)$$

Knowing the actual data on the density of certain specific gearboxes, we can apply the method used in the preceding subsections to construct the dependence of the quantity $\Sigma z_{m.g.b}/G_{m.g.b}$ from $(M_Q)_{m.r}$.

These relations for several known types of helicopter gearboxes are shown in Fig 5.6. Substituting Eq (5.30) into Eq (4.17), we obtain

$$\Sigma C_{m.g.b} = k_e \left(\frac{\Lambda_o}{\Lambda_n}\right)^2 \frac{m_{m.g.b} \sqrt[3]{\alpha_n M_{av}}}{z_o} G_{m.g.b_o} C_{T m.g.b_o} z_{rotor}. \quad (5.32)$$

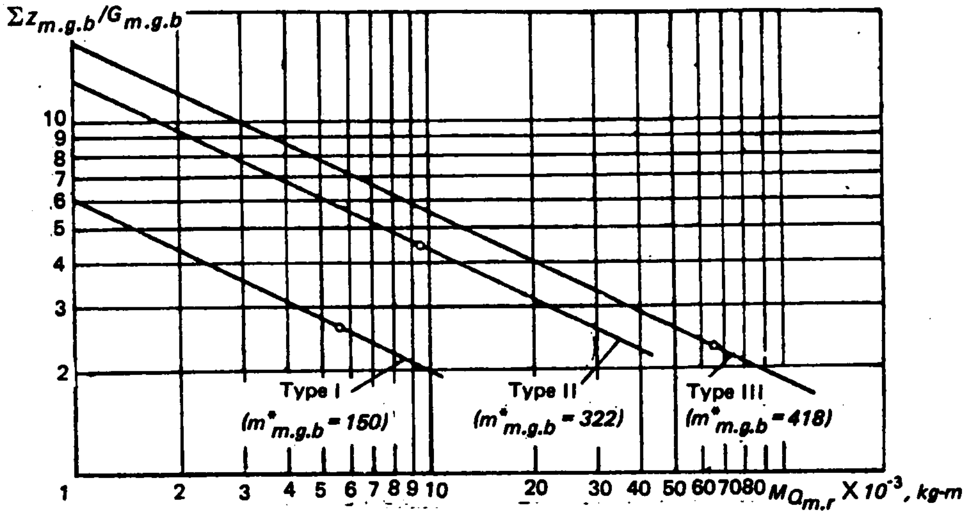

Figure 5.6 Density of main gearbox parts as a function of output shaft torque: I – three-stage planetary gearbox (two planetary gear sets, one input; outputs to main rotor, tail rotor, fan, accessories, and free-wheeling clutch); II – four-stage gearbox with closed planetary transmission (two planetary gear sets, two inputs; outputs to main rotor, tail rotor, fan and free-wheeling clutch); III – four-stage gearbox with closed planetary transmission (two planetary gear sets, two inputs, equalizing mechanism; outputs to main rotor, fan and accessories; free-wheeling clutch).

For the single-rotor helicopter

$$\Sigma C_{m.g.b} = k_e \left(\frac{\Lambda_o}{\Lambda_n}\right)^2 \frac{m_{m.g.b}\sqrt[3]{(M_Q)_{m.r}}}{z_o} G_{m.g.b_o} C_{T_{m.g.b_o}}. \tag{5.33}$$

Consequently, the main-gearbox replacement costs are

$$a_{m.g.b_n} = 0.95\,\frac{\Sigma C_{m.g.b}}{P^{0.T}_{m.g.b}} = 0.95\,\frac{k_e}{P^{0.T}_{m.g.b}} \left(\frac{\Lambda_o}{\Lambda_n}\right)^2 \frac{m_{m.g.b}\sqrt[3]{(M_Q)_{m.r}}}{z_o} G_{m.g.b_o} C_{T_{m.g.b_o}}. \tag{5.34}$$

In the general case,

$$a_{m.g.b_n} = 0.95\,\frac{k_e}{P^{0.T}_{m.g.b}} \left(\frac{\Lambda_o}{\Lambda_n}\right)^2 \frac{m_{m.g.b}\sqrt{(\alpha M_{av})_n}}{z_o} G_{m.g.b_o} C_{T_{m.g.b_o}}. \tag{5.35}$$

By varying the quantities k_e and $m_{m.g.b}$, we can select the optimal (from a cost viewpoint) type of main gearbox and materials. For the selected main-gearbox type and materials,

$$0.95(k_e/P^{0.T}_{m.g.b})(\Lambda_o/\Lambda_n)^2\,(m_{m.g.b}/z_o)G_{m.g.b_o} C_{T_{m.g.b_o}} = \text{const.}$$

Denoting this quantity by $k_a^{m.g.b}$, we have

$$a_{m.g.b} = k_a^{m.g.b}\sqrt[3]{\alpha M_{av}}. \tag{5.36}$$

Then, taking the main gearbox of the original single-rotor helicopter variant as the new baseline, we write the expression for the relative main-gearbox replacement costs:

$$\bar{a}_{m.g.b} = \frac{a_{m.g.bn}}{a_{m.g.b_o}} = \sqrt[3]{\frac{(M_Q)_{m.r.n}}{(M_Q)_{m.r_o}}}. \tag{5.37}$$

The relative main-gearbox weight is

$$\bar{G}_{m.g.b} = [(M_Q)_{m.g.b_n}/(M_Q)_{m.g.b_o}]^{0.8}. \tag{5.38}$$

In application to the main gearbox, the correction accounting for the cost change with variation of the overall machined surface area of the detail parts (for the same number of parts) can be expressed as

$$\sqrt[4]{S_n/S_o} = \sqrt[4]{d_n(\bar{m}_1 d_n + \bar{m}_2 n_{st_n})/d_o(\bar{m}_1 d_o + \bar{m}_2 n_{st_o})}$$

where d = characteristic gearbox dimension (case diameter); and $\bar{m}_1$ and $\bar{m}_2$ = coefficients of proportionality.

For a particular gearbox, type $\bar{m}_2 n_{st}/\bar{m}_1 d \approx const$, then

$$\sqrt[4]{\frac{S_n}{S_o}} = \sqrt[4]{\frac{\bar{m}_{m.g.bn} d_n^2}{\bar{m}_{m.g.b_o} d_o^2}} = \sqrt[4]{\frac{\bar{m}_{mg.b.n}\sqrt[3]{(\alpha M_{av})_n^2}}{\bar{m}_{m.g.b_o}\sqrt[3]{(\alpha M_{av})_o^2}}} \tag{5.39}$$

For the gearboxes of the single-rotor configuration,

$$\sqrt[4]{S_n/S_o} = \sqrt[6]{(M_Q)_{m.r_n}/(M_Q)_{m.r_o}}. \tag{5.40}$$

With this correction, Eqs (5.36) and (5.37) take the following form

$$a_{m.g.b} = \bar{k}_a^{m.g.b}(\alpha M_{av})^{0.5} \tag{5.41}$$

and

$$\bar{a}_{m.g.b} = [(M_{av})_n/(M_{av})_o]^{0.5}. \tag{5.42}$$

An example of the relationships expressed by Eqs (5.38) and (5.42) is shown in Fig 5.7 as a function of the main-rotor radius.

5.1.4 Replacement Costs of Intermediate and Tail Gearboxes

Using arguments similar to those in the preceding subsection 5.1.3, we can obtain the expression for the number of intermediate gearbox detail parts.

$$z_{i.g.b} = m_{i.g.b}\sqrt[3]{(M_Q)_{eq}}.$$

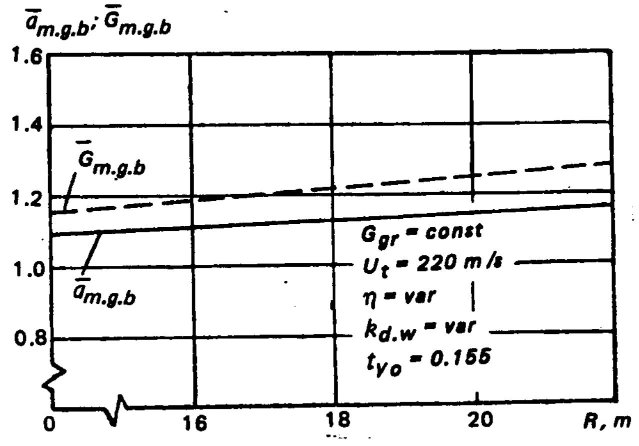

Figure 5.7 Example of the relationshipp between the main-gearbox relative weight and cost characteristics, and main-rotor radius

Consequently,

$$z_{i.g.b}/G_{i.g.b} = m^*_{i.g.b}(M_Q)_{eq}^{-0.467} \tag{5.43}$$

For single-stage intermediate gearboxes consisting of a single pair of gears (without a fan-cooling system), with single input and output shafts, $m^*_{i.g.b} \approx 127$. Most production helicopters have an intermediate gearbox of this type.

Similar to the above, we can obtain expressions for the quantities $C_{i.g.b}$, and $a_{i.g.b}$ and $\bar{a}_{i.g.b}$:

$$C_{i.g.b} = k_e\left(\frac{\Lambda_o}{\Lambda_n}\right)^2 \frac{m_{i.g.b}}{z_o} \sqrt[3]{(M_Q)_{eq}}\ G_{i.g.b_o} k^*_{i.g.b} C_{T_{i.g.b_o}};$$

$$a_{i.g.b} = 0.95\frac{k_e k^*_{i.g.b}}{P^{0.T}_{i.g.b}}\left(\frac{\Lambda_o}{\Lambda_n}\right)^2 \frac{m^*_{i.g.b}\sqrt[3]{(M_Q)_{eq}}}{z_o}\ G_{i.g.b_o} C_{T_{i.g.b_o}}; \tag{5.44}$$

$$a_{i.g.b} = k_e^{i.g.b}\sqrt[3]{(M_Q)_{eq}}. \tag{5.45}$$

where

$$k_e^{i.g.b} = 0.95\frac{k_e k^*_{i.g.b}}{P^{0.T}_{i.g.b}}\left(\frac{\Lambda_o}{\Lambda_n}\right)^2 \frac{m^*_{i.g.b} G_{i.g.bo} C_{T_{i.g.bo}}}{z_o};$$

$$\bar{a}_{i.g.b} = \sqrt[3]{(M_Q)_{eq_n}/(M_Q)_{eq_o}} \tag{5.46}$$

These expressions are valid if the gearbox in question and the baseline gearbox are similar in size. For the more general case, introduction of the correction $\sqrt[4]{S_n/S_o}$ alters the preceding expressions as follows:

$$a_{i.g.b} = \bar{k}_a \sqrt{(M_Q)_{eq}} \tag{5.47}$$

$$\bar{a}_{i.g.b} = \sqrt{(M_Q)_{eqn}/(M_Q)_{eq_o}} \; . \tag{5.48}$$

For comparison,

$$\bar{G}_{i.g.b} = [(M_Q)_{eq_n}/(M_Q)_{eq_o}]^{0.8} \tag{5.49}$$

Similarly, for the tail-rotor quantities, $C_{t.r_{g.b}}$, $a_{t.r_{g.b}}$, and $\bar{a}_{t.r_{g.b}}$ are expressed through M_Q. For the conventional single-stage gearboxes without forced cooling, $m^*_{t.r_{g.b}} = 66.5$.

5.1.5 Transmission Shaft Replacement Costs

For each transmission shaft segment with its supports, the number of detail parts is proportional to $\sqrt[3]{(M_Q)_{ult}}$. The number of segments is proportional to the characteristic helicopter dimensions (main-rotor radius for the single-rotor helicopter, and distances between the main rotors for twin-rotor machines).

$$n_{sh.seg} = L_{sh}/\ell_{av} \approx R/\ell_{av} \tag{5.50}$$

where ℓ_{av} = average segment length; and L_{sh} = overall shaft length. Then

$$\Sigma z_{sh}/G_{sh} = (m^*_{sh}/\ell_{av})(M_Q)_{ult}^{-1/3} \tag{5.51}$$

where $m^*_{sh} = 12$ for transmission shafts of the conventional ("subcritical") type. Further, making several transformations analogous to those made in the preceding subdivisions, we obtain

$$C_{sh} = k_e(\Lambda_o/\Lambda_n)^2 (m^*_{sh}/z_o) G_{sh_o} C_{T_o} k_{sh} (L_{sh_n}/\ell_{av_n}) \sqrt[3]{(M_Q)_{ult_n}} \tag{5.52}$$

and

$$a_{sh} = k_a^{sh} (L_{sh_n}/\ell_{av_n}) \sqrt[3]{(M_Q)_{ult_n}} \tag{5.53}$$

where $\ell_{av} \approx 1.2$ to $2.2m$ for rotational speed below the critical value, and

$$k_a^{sh} = 0.95\, k_e \left(\frac{\Lambda_o}{\Lambda_n}\right)^2 \frac{m^*_{sh} k_{sh}}{P_{sh}^{0.T}} G_{sh_o} C_{T_o} .$$

For the more general case, just as for the other components, we introduce the correction $\sqrt[4]{S_n/S_o}$. In application to transmission shafts,

$$\sqrt[4]{\frac{S_{sh_n}}{S_{sb_o}}} = \sqrt[4]{\frac{L_{sh_n}\sqrt[3]{(M_Q)_{ultn}}}{L_{sh_o}\sqrt[3]{(M_Q)_{ult_o}}}} .$$

With this correction, Eqs (5.52) and (5.53) change as follows:

$$C_{sh} = k_e \left(\frac{\Lambda_o}{\Lambda_n}\right)^2 \frac{m^*_{sh}}{z_o} G_{sh_o} C_{T_o} k^*_{sh} \frac{(L_{sh_n})^{1.25}}{\ell_{av_n}} (M_Q)_{ult_n}^{0.415} \tag{5.54}$$

and

$$a_{sh} = k^{*\,sh}_{a} \frac{(L_{sh_o})^{1.25}}{\ell_{av_n}} (M_Q)_{ult_n}^{0.415} . \tag{5.55}$$

In this case, the relative replacement costs are

$$\bar{a}_{sh} = \frac{a_{sh_n}}{a_{sh_o}} = \left(\frac{L_{sh_n}}{L_{sh_o}}\right)^{1.25} \left(\frac{M_{Q_n}}{M_{Q_o}}\right)_{ult}^{0.415}. \tag{5.56}$$

For comparison, the relative shaft weight is

$$\bar{G}_{sh} = G_{sh_n}/G_{sh_o} = (L_{sh_n}/L_{sh_o})(M_{Q_n}/M_{Q_o})_{ult}^{0.75}. \tag{5.57}$$

5.1.6 Tail-Rotor Replacement Costs

It is obvious that all of the basic expressions for the tail-rotor blade and hub replacement costs will be analogous to the corresponding expressions for the main-rotor blade and hub. The only difference is in the coefficients m_{hub} and m_{bl}. Thus, for tail rotors having blades with extruded spar and honeycomb-supported envelope construction, plus the hub with axial and horizontal hinges, we can take

$$m_{bl_{t.r}}/b_{t.r} = 3.78 \text{ and } m_{hub_{t.r}} = 11.4.$$

5.1.7 Engine Replacement Costs

The modern turboshaft helicopter engines represent a relatively modest fraction of the helicopter weight. However, at the same time, the engine is one of the most expensive components, the cost of which determines, in considerable degree, the cost per flight hour.

The number of detail parts for each compressor and turbine stage depends basically on their rotor-disc diameters. The number of combustion chamber elements varies in proportion to the engine diameter which, in turn, is determined by the first-stage compressor disc diameter. Therefore, the number of detail parts can be expressed in general form as follows:

$$z_{eng} \approx m_{eng} D_{c.st} n_{st}$$

where $D_{c.st}$ = average disc diameter of the compressor stages; n_{st} = total number of compressor and turbine stages; m_{eng} = coefficient characterizing the engine type. The disc diameters for various stages are basically determined by the airflow rates required to obtain the specified power.

$$D_{c.st} = f(\sqrt{G_{air}}) = f(\sqrt{N_{h.p}}).$$

The number of stages is proportional to the pressure ratio π_c. Since $N_{h.p} = f(\pi_c^{3.5})$, we can assume that for a particular engine type,

$$z_{eng} \approx m_{eng} N_{h.p}^{(0.785 + y)}.$$

The term y in the exponent of the quantity $N_{h.p}$ takes into account the influencce on the overall result of such factors as engine shaft diameter change $[\Delta z_{eng} = f(N_{h.p}/n_{rpm})]$ and certain other factors. To simplify the calculations, we assume that the number of detail parts and elements in the cooling system, oil system, fuel control system, and certain other engine accessories vary in proportion to the power for engines of the same type. This quite approximate assumption can be made specifically, because of the fact that this group of detail parts is quantitatively much smaller than the group of detail parts which depend on the diameter and number of the various stages. On this basis, we take

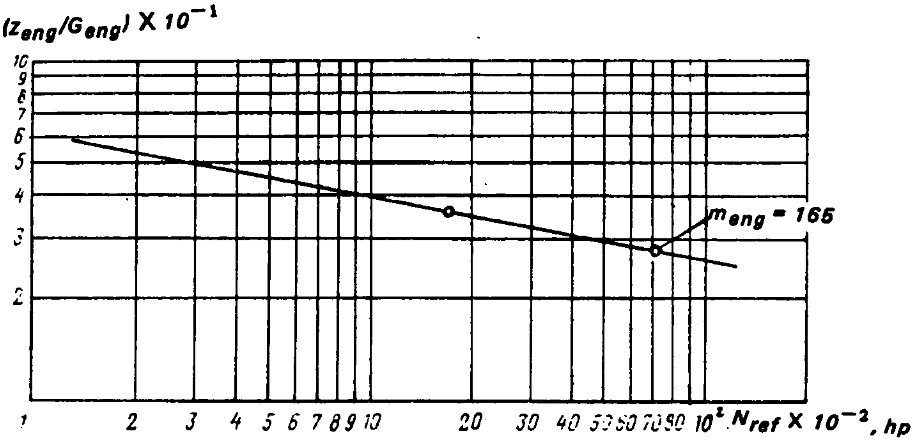

Figure 5.8 "Density" of helicopter powerplant parts as a function of power (referred to H = 500 m, std) for turboshaft engine (10-stage axial compressor, pivoting inlet, guide vanes, two-stage free turbine, annular combustion chamber)

$$z_{eng} \approx m^*_{eng} N_{h.p}^{0.8}. \tag{5.58}$$

In accordance with the previous discussion, we write the expression for the density of the detail parts in the engine in the form

$$\frac{z_{eng}}{G_{eng}} = \frac{m_{eng}}{\gamma_{eng.inst}} N_{h.p}^{-0.2} = m_{eng} N_{h.p}^{-0.2}. \tag{5.59}$$

This relationship is shown graphically in Fig 5.8. Just as in the preceding subsections, we make all the usual transformations beginning with the substitution of Eq (5.59) into Eq (4.17). As a result, we obtain the following expressions for a_{eng}, C_{eng}, and $\bar{a}_{eng}$ (with installation of a definite number of engines, n_{eng}, on the helicopter):

$$\Sigma C_{eng} = k_e \left(\frac{\Lambda_o}{\Lambda_n}\right)^2 \frac{m^*_{eng} N_{ref}^{0.8}}{z_o} G_{eng_o} C_{T_{eng_o}} n_{eng}; \tag{5.60}$$

$$\Sigma a_{eng} = 0.95 \frac{k_e}{P_{eng}^{0.7}} \left(\frac{\Lambda_o}{\Lambda_n}\right)^2 \frac{m^*_{eng} N_{ref}^{0.8}}{z_o} G_{eng_o} C_{T_{eng_o}} n_{eng} \tag{5.61}$$

For engines of similar construction, built to the same accuracy level using identical materials, and constructed in the same period and in the same production facilities,

$$k_a^{eng} = 0.95 \frac{k_e}{P_{eng}^{0.7}} \left(\frac{\Lambda_o}{\Lambda_n}\right)^2 \frac{m^*_{eng}}{z_o} G_{eng_o} C_{T_{eng_o}} = const.$$

In this case,

$$\Sigma a_{eng} = k_a^{eng} n_{eng} N_{ref}^{0.8}. \tag{5.62}$$

We introduce, into the calculation, the usual correction for the change of the component fabrication cost because of the change in the machined surface area of certain parts (primarily the "indispensable" parts), while retaining the same number of parts. In application to the engine,

$$\sqrt[4]{\frac{S_n}{S_o}} = \sqrt[4]{\frac{\bar{m}_1 D_{e_n}^2 + \bar{m}_2 D_{en} \ell_{eng_n}}{\bar{m}_1 D_{eo}^2 + \bar{m}_2 D_{eo} \ell_{eng_o}}}\ .$$

where ℓ_{eng} = engine length; $\bar{m}$ = coefficients of proportionality; and D_e = average engine external diameter. Since ℓ_{eng}/D_e for modern helicopter engines of the same class changes very little with changes in size, then

$$\sqrt[4]{S_n/S_o} \approx \sqrt[4]{\bar{m}_{eng_n} D_{e_n}^2 / \bar{m}_{eng_o} D_{e_o}^2}\ . \tag{5.63}$$

But $D_e = f(D_{c.st})$. Then for engines of the same type

$$\sqrt[4]{S_n/S_o} = \sqrt[4]{N_{ref_n}/N_{ref_o}}$$

and

$$\Sigma a_{eng_n} = k^{*eng}_{e} n_{eng} (N_{ref_n})^{1.05}\ . \tag{5.64}$$

Correspondingly,

$$\bar{a}_{eng} = (N_{ref_n}/N_{ref_o})^{1.05}. \tag{5.65}$$

For comparison, the engine relative weight is

$$\bar{G}_{eng.inst} = N_{ref_n}/N_{ref_o}\ . \tag{5.66}$$

The relationships expressed by Eqs (5.65) and (5.66) are shown graphically in Fig 5.9.

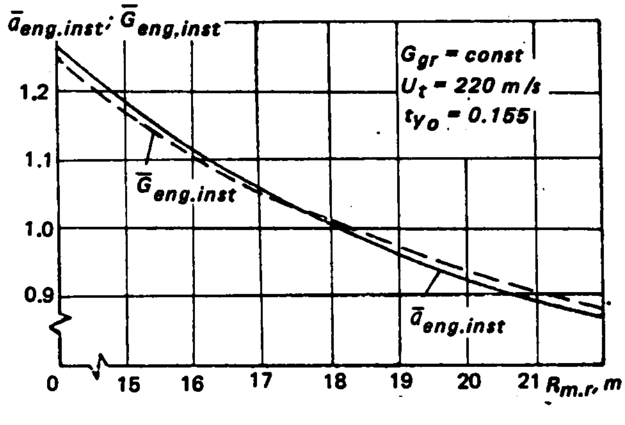

Figure 5.9 Example of relationship between relative weight and cost characteristics of powerplant installation shown vs main-rotor radius

—— $\bar{a}_{eng.inst}$, – – – $\bar{G}_{eng.inst}$

5.1.8 Replacement Costs of Monocoque Structures

In determining the number of detail parts for all basic helicopter monocoque structures (fuselage, cowlings, empennage, and wing), we shall start from the seemingly obvious assumption that on the average, there is a constant number of elements per unit of outer surface area for each structure and size.

$$\Delta z/\Delta S \approx const. \tag{5.67}$$

The statistical data basically confirms this assumption. But in this case, the number of fuselage detail parts, together with the cowlings and empennage, can be expressed as follows:

$$z_\phi = m_\phi S_\phi . \tag{6.68}$$

Since, in the general case,

$$G_\phi = k^*_\phi G_{gr}^{0.25} S_\phi^{0.88} L^a$$

then

$$z_\phi/G_\phi = m^*_\phi S^{0.12}/G_{gr}^{0.25} L^a$$

where

$$m^*_\phi = m_\phi/k^*_\phi .$$

For the single-rotor helicopter

$$z_\phi/G_\phi = m^*_\phi S_\phi^{0.12}/G_{gr}^{0.25} R^{0.16} .$$

Using Eq (2.152) and from it, expressing R in terms of S_ϕ, the following approximate formula can be written for the fuselage of a single-rotor helicopter.

$$z_\phi/G_\phi \approx m^*_\phi (S_\phi)^{-0.04}/(G_{gr})^{0.25} .$$

This relationship is shown graphically in Fig 5.10. Then

$$C_\phi = k_e (\Lambda_o/\Lambda_n)^2 (m_\phi/z_o) G_{\phi_o} C_{T_o} S_\phi \tag{5.69}$$

and

$$a_\phi = k_a{}^\phi S_\phi \tag{5.70}$$

where

$$k_a{}^\phi = 0.95 \frac{k_e}{P_\phi^{0.T}} \left(\frac{\Lambda_o}{\Lambda_n}\right)^2 \frac{m_\phi}{z_o} G_{\phi_o} C_{T_o} = const$$

where in accordance with Eq (4.29),

$$P_\phi{}^{0.T} = k_{util} T_{cal} .$$

The introduction of a correction for the difference in the machined areas (in this case, $\sqrt[4]{S_{\phi_n}/S_{\phi_o}}$) transforms Eq (5.70) as follows:

$$a_\phi = k^*_a{}^\phi S_\phi^{1.25} . \tag{5.71}$$

The relative replacement cost for fuselages of the same type

$$\bar{a}_\phi = (S_{\phi_n}/S_{\phi_o})^{1.25} . \tag{5.72}$$

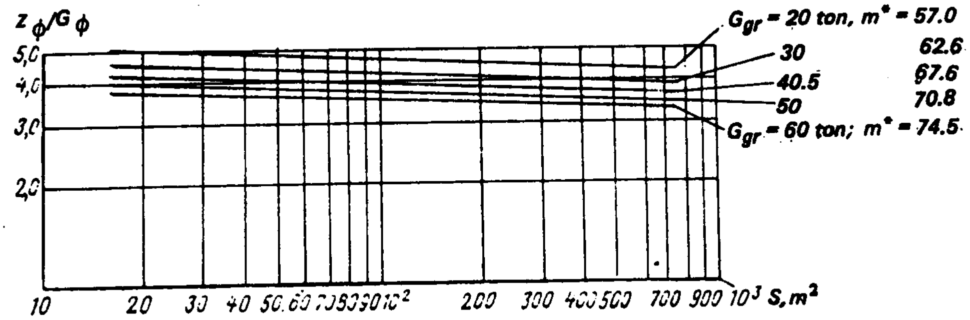

Figure 5.10 Density of fuselage parts (with cowlings, empennage, and cargo floor) of a single-rotor helicopter as a function of fuselage wetted surface

For comparison, the fuselage relative weight is

$$\bar{G}_\phi = (G_{gr_n}/G_{gr_o})^{0.25}\,(S_{\phi_n}/S_{\phi_o})^{0.88}. \tag{5.73}$$

These relationships are shown graphically in Fig 5.11. In the same way, we can obtain the analogous relations for the other monocoque-type helicopter structures.

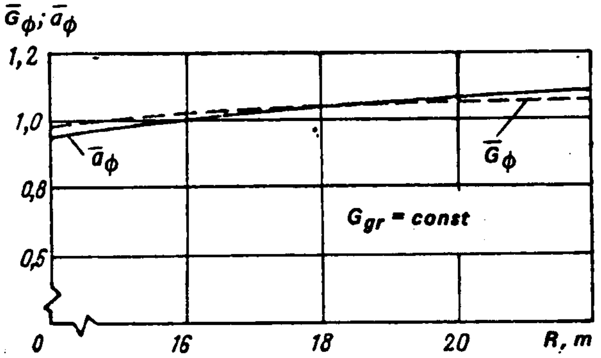

Figure 5.11 Example of the relationship between fuselage relative weight and cost characteristics vs rotor radius: – – – – $\bar{G}_\phi$; ——— $\bar{a}_\phi$

5.1.9 Replacement Costs of the Control System

In Ch 2, the control system was broken down into two parts for convenience of weight calculations; one part being the booster control, which includes the hydraulic boosters with the main-rotor hydraulic system, and the swashplate assembly with its post-booster rods and levers; the other part being the manual control system. It is convenient to use this same breakdown in calculations of the control system cost characteristics.

From the viewpoint of estimating the number of detail parts, the booster control system differs from other previously examined assemblies in that in the construction of its elements, the "indispensable" details constitute a significant part. The number of such parts either does not change at all, or changes very little with variation of the basic helicopter parameters. [In determining the dependence of the detail part density on the helicopter parameters for the previously examined components, it would have been more accurate to use relationships of the $z_n/G_n = my^n + A$ type, where A is the number of indispensable parts. But, since in the examined cases, $A \ll my^n$, we use the expression $z_n/G_n \approx my^n$]. For example, for the swashplate assembly of the type normally used in Soviet helicopters (for helicopters of the medium-weight category), the number of detail parts for this group usually constitutes about a quarter of the total number of parts. The number of detail parts which depend only on the number of main-rotor blades constitutes another quarter. About 40 percent of the detail parts depend on the diameter of the main-rotor shaft. Finally, only about 10 percent of the detail parts are determined by the pitching moments of the blade, while the weight of the swashplate assembly, as was shown in Ch 2, is basically determined by the pitching moments.

The overall number of detail parts for the swashplate assembly can be expressed as

$$z_{s.p} = \Delta z_{s.p_I} + \Delta z_{s.p_{II}} + \Delta z_{s.p_{III}}. \tag{5.74}$$

Here,

1. $\Delta z_{s.p_I} = A'_{s.p} + A''_{s.p} z_{bl}$, where $A'_{s.p}$ = number of indispensable Group I parts which is independent of the helicopter parameters; and $A''_{s.p}$ = number of indispensable Group II parts per blade. The ratio of these numbers can be taken as $A''_{s.p}/A'_{s.p} \approx 0.16$. Then $\Delta z_{s.p_I} = A'_{s.p}(1 + 0.16 z_{bl})$. In the calculations, we can take $A'_{s.p} \approx 150$ to 160.

2. $\Delta z_{s.p_{II}} = m'_{s.p} \sqrt[3]{(M_Q)_{m.r}}$ = the number of parts determined by the dimensions of the main-rotor shaft; i.e., those that depend on the torque, where $m'_{s.p} \approx 5.5$ to 6.0.

3. $\Delta z_{s.p_{III}} = m'' z_{bl} b^2 R$ = number of parts, depending on the magnitude of the blade pitching moments [$m''_{s.p} = 0.75$ to 0.8]. Then, the expression for the cost of the swashplate assembly can be written as follows:

$$C_{s.p_n} = k_e \left(\frac{\Lambda_o}{\Lambda_n}\right)^2 \frac{[A'_{s.p}(1 + 0.16 z_{bl}) + m'_{s.p}\sqrt[3]{(M_Q)_{m.r_n}} + m''_{s.p} z_{bl_n} b_n^2 R_n]}{z_o} G_{s.p_o} C_{T_{s.p_o}}. \tag{5.75}$$

We will introduce the usual correction accounting for the machined surface change area.

If we take the outside swashplate housing diameter $d_{s.p}$ as the characteristic dimension, then the housing height is about 0.8 to $0.85 d_{s.p}$.

For the same main-rotor hub axial hinge offset, the outer diameter of the "horns" and the swashplate disc and its height can be expressed with the aid of constant coefficients in terms of $d_{s.p}$.

Then, we can write

$$\sqrt[4]{\frac{S_n}{S_o}} \approx \sqrt[4]{\frac{\bar{m}_n^{s.p} d^2_{s.p_n}}{\bar{m}_o^{s.p} d^2_{s.p_o}}}$$

For designs of the same type

$$\sqrt[4]{\frac{S_n}{S_o}} = \sqrt{\frac{d_{s.p_n}}{d_{s.p_o}}} = \sqrt[6]{\frac{(M_Q)_{m.r_n}}{(M_Q)_{m.r_o}}} \tag{5 76}$$

After introducing this correction, Eq (5.75) takes the form

$$C_{s.p_n} = k_e\left(\frac{\Lambda_o}{\Lambda_n}\right)^2 \frac{[A'_{s.p}(1+0.16z_{bl}) + m'_{s.p}\sqrt[3]{(M_Q)_{m.r}} + m''_{s.p}z_{bl_n}b_n^2R_n]}{z_o} \times$$

$$\times \quad G_{s.p_o}C_{T_{s.p_o}} \sqrt[6]{\frac{(M_Q)_{m.r_n}}{(M_Q)_{m.r_o}}}\,. \tag{5.77}$$

Therefore, the hourly swashplate assembly replacement costs are expressed as

$$a_{s.p} = k_a^{s.p}\,[A'_{s.p}(1+0.16z_{bl_n}) + m'_{s.p}\sqrt[3]{(M_Q)_{m.r}} + m''_{s.p}z_{bl_n}b_n^2R_n] \times \sqrt[6]{(M_Q)_{m.r_n}} \tag{5.78}$$

where

$$k_a^{s.p} = \frac{0.95}{P_{s.p_n}^{\,0.T}}\;\frac{\Lambda_o}{\Lambda_n}\Big)^2\;\frac{G_{s.p_o}C_{T_{s.p_o}}}{z_o\sqrt[6]{(M_Q)_{m.r_o}}} = const$$

for assemblies of the same type, made from identical materials under the same production conditions.

For hydraulic boosters, the number of detail parts does not change significantly with change of the helicopter parameters. Therefore, the cost of boosters of the same type depends basically on the size of the machined surfaces of their elements. This correction can be represented by the expression

$$\sqrt[4]{S_n/S_o} = \sqrt[4]{\bar{m}_n^{bo}\,d_{bo_n}^2/\bar{m}_o^{bo}\,d_{bo_o}^2}$$

where d_{bo} = booster outside diameter. For boosters of similar design

$$\sqrt[4]{S_n/S_o} = \sqrt[4]{(d_n/d_o)^2} = \sqrt[4]{b_n^2R_n/b_o^2R_o}. \tag{5.79}$$

Then,

$$C_{bo_n} = k_e\left(\frac{\Lambda_o}{\Lambda_n}\right)^2 \frac{G_{bo_o}C_{T_o}}{\sqrt[4]{b_o^2R_o}}\sqrt[4]{b_n^2R_n} \tag{5.80}$$

or

$$C_{bo_n} = k^*_{bo}\sqrt[4]{b_n^2R_n} \tag{5.81}$$

where

$$k^*_{bo} = k_e\left(\frac{\Lambda_o}{\Lambda_n}\right)^2 \frac{G_{bo_o}C_{T_o}}{\sqrt[4]{b_o^2R_o}} = const$$

for boosters of the same type, constructed from the same materials under the same production conditions.

The number of detail parts in the main-rotor hydraulic system also changes very little with change of the helicopter parameters. The correction in the machined surface areas of the parts for all the basic hydraulic system elements is

$$\sqrt[4]{S_n/S_o} = \sqrt[4]{\Sigma m_{i_n}d_{i_n}/\Sigma m_{i_o}d_{i_o}}$$

where d_i = characteristic element dimensions; for example, the outside diameter of the hydraulic pump. For similar designs

$$\sqrt[4]{S_n/S_o} \approx \sqrt[4]{(N_n/N_o)^{1/2}} \approx \sqrt[8]{z_{bl_n}b_n^2R_n/z_{bl_o}b_o^2R_o} \tag{5.82}$$

where N_n and N_o = hydraulic pump powers. With the introduction of this correction, the main-rotor hydraulic system cost is

$$C_{h.s_n} = k^*_{h.s}\sqrt[8]{z_{bl_n} b_n^2 R_n} \tag{5.83}$$

where

$$k^*_{h.s} = k_e\left(\frac{\Lambda_n}{\Lambda_o}\right)^2 \frac{G_{h.s_o} C_{Th.s_o}}{\sqrt[8]{z_{bl_o} b_o^2 R_o}} .$$

Therefore, the hourly replacement costs of boosters and hydraulic systems can be expressed as follows:

$$a_{bo_n} = k_a^{bo} \sqrt[4]{z_{bl_n} b_n^2 R_o}; \quad a_{h.s_n} = k_a^{h.s}\sqrt[8]{z_{bl_n} b_n^2 R_n} \tag{5.84}$$

where

$$k_a^{bo} = 0.95k^*_{bo}/P_{bo_n}^{0.T}; \quad k_a^{h.s} = 0.95k^*_{h.s}/P_{h.s_n}^{0.T}.$$

The replacement costs for the entire booster part of the helicopter control system is

$$\Sigma a_{bo_{c.s}} = a_{s.p} + a_{bo} + a_{h.s} = k_a^{s.p}[A'_{s.p}(1 + 0.16 z_{bl_n}) + m'_{s.p}\sqrt[3]{(M_Q)_{m.r_n}} + m''_{s.p} z_{bl_n} b_n^2 R_n] \times$$
$$\times \sqrt[6]{(M_Q)_{m.r_n}} + k_a^{bo}\sqrt[4]{z_{bl_n} b_n^2 R_n} + k_a^{h.s}\sqrt[8]{z_{bl_n} b_n^2 R_n} . \tag{5.85}$$

The relative swashplate assembly replacement costs (for similar designs) will be

$$\bar{a}_{sp} = \frac{[A'_{s.p}(1 + 0.16 z_{bl_n}) + m'_{s.p}\sqrt[3]{(M_Q)_{m.rn}} + m''_{s.p} z_{bln} b_n^2 R_n]\sqrt[6]{(M_Q)_{m.rn}}}{[A'_{s.p}(1 + 0.16 z_{bl_o}) + m'_{s.p}\sqrt[3]{(M_Q)_{m.r_o}} + m''_{s.p} z_{bl_o} b_o^2 R_o]\sqrt[6]{(M_Q)_{m.r_o}}} . \tag{5.86}$$

For the hydraulic boosters,

$$\bar{a}_{bo} = \sqrt[4]{z_{bl_n} b_n^2 R_n / z_{bl_o} b_o^2 R_o} . \tag{5.87}$$

For the main-rotor hydraulic system,

$$\bar{a}_{h.s} = \sqrt[8]{z_{bl_n} b_n^2 R_n / z_{bl_o} b_o^2 R_o} . \tag{5.88}$$

For comparison, the corresponding relative weight characteristic of these elements is

$$\bar{G}_{contr} = z_{bl_n} b_n^2 R_n / z_{bl_o} b_o^2 R_o . \tag{5.89}$$

We can see from a comparison of this last expression with Eqs (5.86), (5.87), and (5.88) that with variation of the helicopter parameters, the cost of the booster part of the control system changes much more slowly in comparison with the corresponding change in its weight.

As for the cost of the manual part of the control system, we can, without large error, take it to be constant since the number of detail parts of this system does not change significantly with variation of the helicopter parameters for helicopters of the same configuration, and furthermore, the distances to the rotors change very little for all the variants. When comparing the costs of the manual control system of helicopter variants of different configurations, we can consider that they are approximately proportional to the control system length (see Eq (4.17)), assuming that $z_{m.con}/z_{m.coo} = L_n/L_o$, where L_n and L_o are the overall control system lengths leading up to the hydraulic boosters.

5.1.10 Landing Gear Replacement Costs

It is obvious that the landing gear replacement cost does not change with variation of the helicopter parameters for constant gross weight, since the number of detail parts and the dimensions of the structure do not change. With increase of the gross weight, the landing-gear weight increases proportionally. [It may also vary if the layout is changed.] However, the number of detail parts will increase much more slowly than the weight. We can consider that for a selected landing gear type, the number of detail parts will increase only because of the increase in the number of wheel detail parts, since the number of detail parts in the shock absorbers and struts remains nearly constant. One requirement imposed on a particular helicopter class is satisfaction of the condition that the footprint pressure should not exceed a given magnitude. The problem is resolved either by increasing the tire diameter or by increasing the number of tires. The maximum allowable footprint pressure can be expressed as

$$p = \xi_w G_{gr}/\Delta S_i$$

where ξ_w = coefficient accounting for the fraction of the gross weight supported by a single wheel; and ΔS_i = the tire area in contact with the ground, $\Delta S_i = 2b_w R_w tg\alpha$. Here, R_w = radius of the wheel; b_w = tire width ($b_w = f(R_w)$); and α = angle between the vertical and the line connecting the center of the wheel with the extreme point of the surface of tire contact with the ground, which depends on the gage pressure in the tire. Hence, $R_w = f(G_{gr}^{0.5})$.

Assuming that the change in the number of wheel parts is proportional to the wheel radius, we can write $z_{whe} = m_{whe}\sqrt{G_{gr}}$. Then, the total number of landing gear parts is

$$z_{l.g} = A_{l.g} + n_w m_{whe}\sqrt{G_{gr}}. \tag{5.90}$$

where $A_{l.g}$ = constant for given landing-gear construction type characterizing the number of indispensable parts; and n_w = number of wheels.

For the three-strut landing-gear scheme of the heavy and medium helicopters with pyramidial main-strut construction with dual-chamber, shock-absorbing struts, twin-wheel nose gear, and tail skid,

$$A_{l.g} \approx 800 \text{ to } 870; \quad m_{whe} = 6 \text{ to } 6.5.$$

Then, the gear cost can be written as

$$C_{l.g_n} = k_e\left(\frac{\Lambda_o}{\Lambda_n}\right)^2 \frac{(A_{l.g} + n_w m_{whe}\sqrt{G_{grn}})G_{l.go}C_{Tl.go}}{z_o}. \tag{5.91}$$

The hourly gear replacement costs will be

$$a_{l.g_n} = 0.95\frac{k_e}{P_{l.g}{}^{0.7}}\left(\frac{\Lambda_o}{\Lambda_n}\right)^2 \frac{(A_{l.g} + n_w m_{whe}\sqrt{G_{l.go}C_{Tl.go}}}{z_o} \tag{5.92}$$

or

$$a_{l.g_n} = k_a^{l.g}(A_{l.g} + n_w m_{whe}\sqrt{G_{gr_n}}) \tag{5.93}$$

where

$$k_a^{l.g} = 0.95 \frac{k_e}{P_{l.g_n}^{0.1}}\left(\frac{\Lambda_o}{\Lambda_n}\right)^2 \frac{G_{l.go}C_{Tl.go}}{z_o}.$$

Just as for the other components, we introduce the correction $\sqrt[4]{S_n/S_o}$. If we keep the gear shock absorbing characteristics constant for all the variants, we can consider that the shock-strut cylinder outside diameter change is proportional to the change in the quantity $\sqrt{G_{gr}}$. Taking the change of all the other dimensions to be proportional to this quantity, we can write, for the landing gear

$$\sqrt[4]{S_{l.g_n}/S_{l.g_o}} = \sqrt[8]{G_{gr_n}/G_{gr_o}}.$$

Correspondingly, Eqs (5.91) and (5.93) take the form

$$C_{l.g_n} = k_e\left(\frac{\Lambda_o}{\Lambda_n}\right)^2 \frac{G_{l.go}C_{Tl.go}}{z_o}\left(A_{l.g} + n_w m_{whe}\sqrt{G_{gr_n}}\right)\sqrt[8]{\frac{G_{grn}}{G_{gr_o}}}; \tag{5.94}$$

$$a_{l.g_n} = \frac{k_a^{l.g}}{\sqrt[8]{G_{gr_o}}}\left(A_{l.g} + n_w m_{whe} G_{gr_n}\right)\sqrt[8]{G_{gr_n}}. \tag{5.95}$$

The relative expenditure for replacement of the landing gear is

$$\bar{a}_{l.g_n} = (A_{l.g} + n_{w_n} m_{whe}\sqrt{G_{gr_n}})/(A_{l.g} + n_{w_o} m_{whe}\sqrt{G_{gr_o}}). \tag{5.96}$$

For comparison, the landing gear relative weight is

$$\bar{G}_{l.g} = G_{gr_n}/G_{gr_o}. \tag{5.97}$$

From a comparison of Eqs (5.96) and (5.97), we see that with an increase in the helicopter gross weight, the gear replacement costs vary much more slowly than the weight.

5.1.11 Fuel System Replacement Costs

For fuel systems of the same type of helicopters of the same class, we can consider that the same number of detail parts, on the average, will be used for each main fuel tank.

With the usual tank placement under the cargo cabin floor, the number of tanks can be approximately estimated from the formula

$$n'_{fu.t} \approx G'_{fu}/\gamma_{fu} t_{f.s} B_\phi H_{flr} \tag{5.98}$$

where $n'_{fu.t}$ = number of tanks under the cabin floor (rounded off to the next higher integer); G'_{fu} = basic fuel supply minus the portion of the fuel in the distribution tank and the external tanks (if used); γ_{fu} = fuel specific weight; $t_{f.s}$ = fuselage frame spacing in the region where the fuel tanks are located; B_ϕ = average width of the fuselage cabin at the floor; and H_{flr} = fuselage floor depth.

The quantities $t_{f.s}$, B_ϕ, and H_{flr} are determined from the preliminary layout of the helicopter. The total number of tanks is $n_t = n'_t + n''_t$, where n''_t is the number of distribution (usually one) and external tanks. Then the number of fuel system detail parts can be expressed as

$$z_{fu.s} = m_{fu.s}n_t = m_{fu.s}\left(\frac{G_{fu} - G''_{fu}}{\gamma_{fu} t_{f.s} B_\phi H_{flr}} + n''_t\right). \tag{5.99}$$

where G_{fu} = total fuel supply; and G''_{fu} = fuel in the distribution and external tanks.

For the case where there is a single distribution tank, and no external tanks, G''_{fu} expressed as a fraction of the total fuel supply becomes $G'' \approx 0.1 G_{fu}$.

$$z_{fu.s} = m_{fu.s}\left[(0.9G_{fu}/\gamma_{fu} B_{\phi} H_{flr}) + 1\right] \tag{5.100}$$

where $m_{fu.s} \approx 400$.

Then, substituting as usual, the expression for $z_{fu.s}$ into Eq (4.17) (assuming $\Lambda_o = \Lambda_n$),

$$C_{fu.s} = k_e m_{fu.s}\left(\frac{G_{fu} - G''_{fu}}{\gamma_{fu} B_{\phi} H_{flr}\, t_{f.s}} + n''_t\right)\frac{G_{f.s_o}}{z_o} C_{T_o} \tag{5.101}$$

For systems of the same type,

$$k_a^{fu.s} = k_e (G_{fu.s}/z_o)\, m_{fu.s} C_{T_o} = const$$

and

$$C_{fu.s_n} = k_a^{fu.s}\left(\frac{G_{fu} - G''_{fu}}{\gamma_{fu} B_{\phi} t_{f.s} H_{flr}} + n''_t\right). \tag{5.102}$$

Since the quantities B_{ϕ} and $t_{f.r}$ are constant for the considered helicopter class and H_{flr} can vary only slightly, the usual correction for difference in the size of the machined surfaces need not be introduced. The hourly fuel system replacement costs

$$a_{fu.s} = 0.95 \frac{k_a^{fu.s}}{k_{util} T_{cal}}\left(\frac{G_{fu} - G'_{fu}}{\gamma_{fu} B_{\phi} t_{f.s} H_{flr}} + n''_t\right). \tag{5.103}$$

For systems with no external tanks, and with a single distribution tank

$$a_{fu.s} = \bar{k}_a^{fu.s} \left.\frac{0.9 G_{fu}}{\gamma_{fu} B_{\phi} t_{f.s} H_{flr}} + 1\right). \tag{5.104}$$

where

$$\bar{k}_a^{fus} = k_a^{fu.s}/k_{util} T_{cal}.$$

The expression for the relative replacement costs for this case with variation of the helicopter parameters will have the form

$$\bar{a}_{fu.s} = \frac{0.9 G_{fu_n} + \gamma_{fu_n} B_{\phi_n} H_{flr_n} t_{f.s_n}}{0.9 G_{fu_o} + \gamma_{fu_o} B_{\phi_o} H_{flr_o} t_{f.s_o}}. \tag{5.105}$$

For comparison, the fuel system relative weight is

$$\bar{G}_{fu.s} = G_{fu_n}/G_{fu_o}.$$

5.1.12 Equipment Replacement Costs

The cost of most of the equipment does not change with variation of the helicopter parameters. The flight, navigation, and instrument panel equipment, radio equipment, cockpit and cargo cabin equipment, including the air-conditioning system, will be the same for all the variants. It is obvious that the cost of the portion of the electrical installation servicing the electric power consumers among the aforementioned systems also will not vary significantly. Only the portion of the electrical system which supplies current to the main-rotor blade anti-icing system can, in principle, have a direct influence on the selection of the helicopter parameters with respect to the cost criteria. We can assume that the variable portion of the number of electrical system detail parts is proportional to the number of blades and the number of electrical sections of the blade. Specifically, the number of junctions and certain other elements varies in this way. As the required electrical system power increases, the number of AC generator detail parts may change. However, these changes are very slight in comparison with the overall number of detail parts in the electrical system (for electrical systems and subassemblies of the same type).

Therefore, we can consider that for helicopters designed for a given mission, the equipment cost remains approximately constant with variation of the design parameters.

5.1.13 Replacement Costs of the Helicopter Structure as a Whole

Using the presented method for calculating helicopter cost characteristics, we can obtain all the required data on replacements for the primary components of the considered helicopter variant. Then, from the ratios of these data, we can find the relative replacement cost for the individual components.

An example of the results of such calculations is shown in Fig 5.12, in which the considered helicopter costs were determined with respect to those of a production helicopter which was taken as the baseline.

The relative costs for replacement of components were determined in dimensionless units. In the calculation, we used the replacement costs as a unit of the set of eight main-rotor blades for the baseline helicopter. From the curves in Fig 5.13, we can evaluate the nature of the dependence of the overall replacement costs on the main-rotor diameter for all the components for various numbers of blades, but for the same number of engines. But, at this stage, it would be premature to draw any conclusions on the optimal main-rotor diameter on the basis of minimal replacement costs. The fabrication cost of a particular helicopter variant in terms of cost-per-flight hour may be higher, while the cost-per-unit of work performed by the helicopter may be lower than for another variant.

It is also clear that with variation of the construction type and materials, the relationship between the replacement costs of the individual components and therefore, the main-rotor diameter for which the minimal structural cost is obtained may be completely different. The magnitudes of the potential service life has a large influence on the result. Proper evaluation of these characteristics should be given particular attention. In these calculations, attention should also be devoted to proper evaluation of the magnitude of the *m* coefficients. We must bear in mind that for each new type of construction, it is necessary to establish the particular pattern of the number of detail parts with the variation of the helicopter parameters.

In this chapter, we have not posed the problem of conducting an analysis of the laws governing the variation of detail parts in the components in as much detail as, for example, that carried out in Ch 2 for the weight analysis. Here, only one of the possible approaches to the solution of this problem was demonstrated on the example of the approximate methods of determining the densities of the detail parts in the components. For existing modern helicopters, these methods yield quite satisfactory agreement between calculated and actual costs. However, helicopter designs are being improved and new designs are appearing which have fundamentally different solutions requiring special analysis of the nature of the density variation of the detail parts. Using the above-presented formulae, it is necessary, in these cases, to

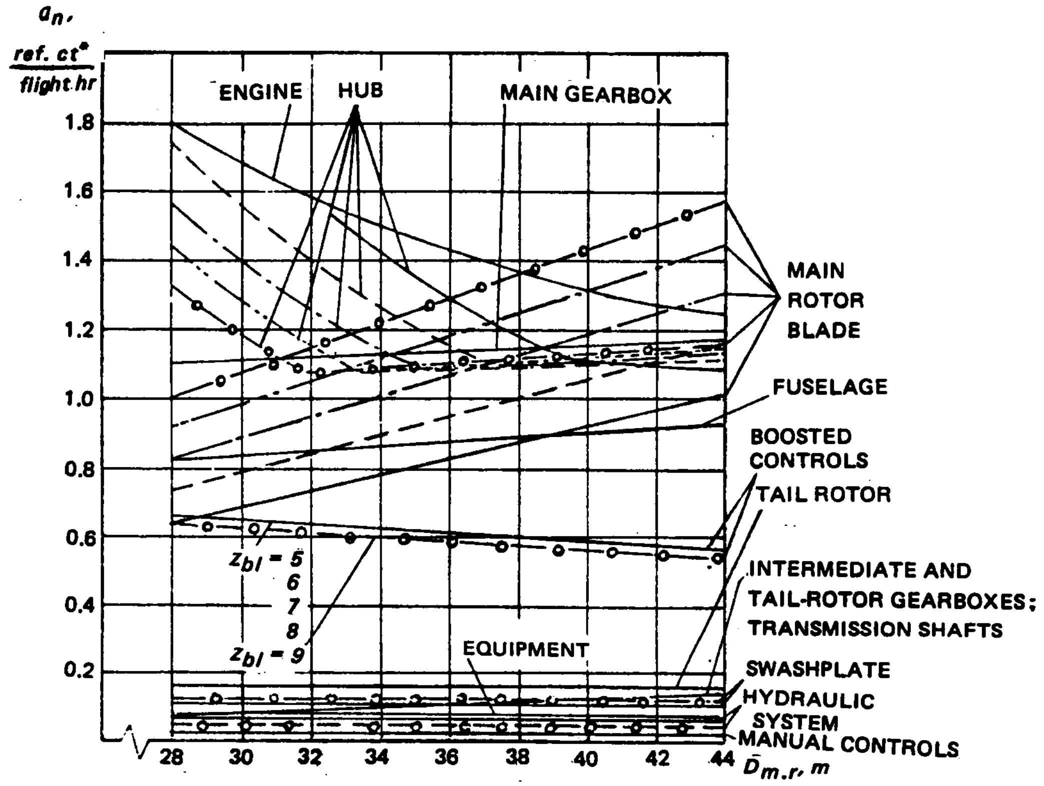

Figure 5.12 Replacement cost of basic helicopter components shown as a function of the main-rotor diameter: ——— $z_{bl} = 5$; – – – – $z_{bl} = 6$; — · — $z_{bl} = 7$; — · · — · · $z_{bl} = 8$; — o — o — $z_{bl} = 9$

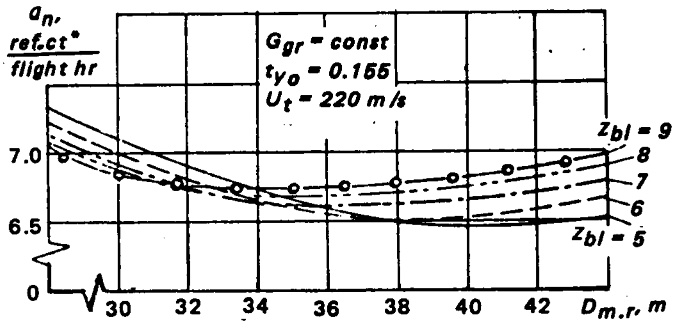

Figure 5.13 Replacement cost of a helicopter structure as a function of main-rotor diameter

introduce the appropriate corrections into the calculation. It is obvious that the replacement cost calculation for the various helicopter versions should not terminate at this point. It is necessary to repeat the entire cycle for several gross weights, just as was done in selecting the parameters based on the weight criterion.

5.2 Dependence of Direct and Indirect Costs on Helicopter Parameters

As we have already mentioned, replacement costs represent a very important cost item. They may amount to several tens of percent of the cost-per-flight hour. Together with the major overhaul costs, they constitute the primary portion of the direct operating costs.

5.2.1 Variation of Major Overhaul Costs

It is obvious that the nature of the helicopter major overhaul cost variation will be basically similar to the nature of the replacement cost variation. This follows from comparison of the expressions

$$C_n = k_{d.p} k_e C_{T_o} G_n \text{ and } C_n^{m.o} = k_{d.p} k'_e C_{T_o}^{m.o} G_n .$$

The only difference between these expressions is in the magnitude of the coefficients k_e and k'_e $[k'_e = k_e - 0.36(M_n/M_o)]$, and in the values of C_{T_o} and $C_{T_o}^{m.o}$ which equal the unit cost of structure manufacture, and the unit cost of major overhaul ($C_{T_o}^{m.o} = \xi_{m.on} C_{T_o}$, where $\xi_{m.on} \approx 0.2$ to 0.4).

Therefore, in evaluating the changes in costs of this type, we can use the relative cost relationships presented in the preceding section (without account for size corrections of the type $\sqrt[4]{S_n/S_o}$).

In evaluating the fraction of the operating costs per flight hour associated with major overhauls $C_n^{m.o}$, we can also use the analogous replacement cost relations presented in Ch 4. But here, in addition to the differences in the magnitude coefficients k_e and k'_e, as well as C_{T_o} and $C_{T_o}^{m.o}$, we must also consider the difference between the magnitudes of the overhaul and service lives which appear in these relations. For the dynamic system components (excluding the blades), $p^{0.T} \approx 3$ to $4 p^{t.b.o}$.

For main and tail rotor blades, usually $P^{0.T} = P^{t.b.o}$ (i.e., these assemblies are not subject to major overhaul). For the fuselage, cowlings, wing, empennage, and landing gear (except tires) for which $P^{0.T} = k_{util} T_{cal}$, the major overhauls are performed along with the major overhauls of the dynamic system components. For these components, the number of major overhauls is

$$n_{m.o} = [(k_{util} T_{cal}/P^{t.b.o}) - 1] .$$

where, for modern helicopters, $P^{t.b.o} \approx 1000$ to 1500 hours. The general expression for the major overhaul cost per flight hour for any component is modified as follows:

$$C_n^{m.o} = n^*_{m.o} k'_e k_{d.p} G_o C_{T_o}^{m.o} / P_n^{0.T} \tag{5.106}$$

where

$$n^*_{m.o} = (n_{m.o} + 1).$$

For comparison, we recall the general expression for the replacement costs of the n-th component (without correction for size):

$$a_n = 0.95 k_e k_{d.p} G_o C_{T_o} / P^{0.T}.$$

5.2.2 Variation of Periodic Maintenance Costs

The portion of operational cost associated with periodic maintenance is expressed by Eq (4.48). The influence of helicopter parameter variation on the number of operations performed during the periodic maintenance cycle will depend (for similar structures) on the number of components: main and tail rotor blades, number of engines, and so on. The quantity $C_{p.m_n}$ will vary only slightly with variation of the component dimensions, as long as we consider helicopters of the same class and designed for the same mission.

In this case, the number of installed components of the same type (including the engines) does not change with variation of the parameters. An exception is the number of main-rotor blades and the associated complication of the construction of the main-rotor hub and swashplate assembly. For a given specific case, the number of main-rotor blade servicing operations can be written as

$$l_{bl_n} = (z_{bl_n}/z_{bl_o})\,l_{bl_o}.$$

where l_{bl_o} = number of operations performed when servicing the main-rotor blades of the baseline helicopter variant. Similarly for the main-rotor hub and the swashplate assembly,

$$l_{hub_n} = (z_{bl_n}/z_{bl_o})\,l_{hub_o} \qquad l_{s.p_n} = (z_{bl_n}/z_{bl_o})\,l_{s.p_o}.$$

It is interesting to note that the number of periodic maintenance operations performed when servicing the classical main rotor with three-hinge hub and a swashplate assembly constitutes up to 30 percent of the total number of operations performed in conducting all forms of periodic maintenance for the helicopter as a whole.

5.2.3 Variation of Routine-Maintenance Costs

It is obvious that the nature of the variations of the cost of operations associated with routine maintenance of the helicopter (preflight and postflight inspections, and so on), should, in principle, be analogous to the nature of the variation of the periodic maintenance operations under the same conditions.

The operating costs associated with technical inspections and routine maintenance per flight hour are calculated from the formula

$$C_{insp} = \theta'_n\, t'_{insp} = \theta'_n \,\frac{l_{insp\,n}\, V_{cr\,n}}{l_{insp_o}\, L_n}\, \Sigma t_{insp_o}.$$

With variation of the helicopter parameters, the ratio V_{cr_n}/L_n will change very slightly. However, the l_{insp_n}/l_{insp_o} ratio basically depends on the number of components of the same type installed on the helicopter (in the considered example, on the number of rotor blades).

$$l_{insp_n} = l_{insp_o} + \Delta l_{insp_n}$$

where

$$\Delta l_{insp_n} = (z_{bl_n}/z_{bl_o})(l_{insp_o}^{\;hub} + l_{insp_o}^{\;bl} + l_{insp_o}^{\;s.p}).$$

$l_{insp_o}^{\;hub}$, $l_{insp_o}^{\;bl}$, and $l_{insp_o}^{\;s.p}$ respectively, are the number of operations associated with routine technical inspections of the main rotor hub, blades, and the swashplate assembly.

For single-rotor helicopters having five-bladed main rotors of the classical scheme (three-hinge hub), the number of operations involved with servicing the blades, hub, and swashplate assembly constitutes 25 to 30 percent of the total number of operations.

5.2.4 Variation of Fuel and Lubricant Costs

The fraction of the fuel and lubricant cost per flight hour is determined from Eq (4.51). In accordance with Eq (2.162), the fuel supply is

$$G_{fu} = k_{fu}(C_e)_{p.p} N_{p.p} L_n / V_{cr_n}.$$

Consequently,

$$C_{fu.l} = C'_{fu.l} k_{fu} k_M N_{p.p} (C_e)_{p.p}$$

Since $N_{p.p} = \overline{N}(N_{ref})_{max}$, then

$$C_{fu.l} = C'_{fu.l} k_{fu} k_M \overline{N}_{p.p} (N_{ref})_{max} (C_e)_{p.p}. \tag{5.107}$$

5.2.5 Crew Salaries and Indirect Costs

It is obvious that for a definite helicopter configuration, the flight crew costs do not change with variation of the helicopter parameters.

The calculation of these costs should be made as shown in Ch 4, using Eq (4.53). For the considered case,

$$C_{sal} = (24 \times 365/H)(\theta'_l + k^* \theta''_l) m_{crew}$$

When using a definite number of new technical approaches in helicopter design, the insurance costs will not change with variation of the helicopter parameter; therefore, in accordance with Eq (4.55), we can write

$$C_{ins_n} = n_{t.inn} C_{l.c} q = const.$$

As was noted in Ch 4, the fraction of the other indirect costs is usually evaluated as a fixed percentage of the direct operating costs; the indirect costs may reach 30 percent of the sum of the direct costs without replacement, and the major overhaul costs.

The costs of training and support flights, etc., is on the order of 10 percent of the amortization (replacement plus major overhaul), routine maintenance, and fuel and lubricant costs.

As mentioned before, these cost items need not necessarily be considered in conducting a parametric analysis.

5.2.6 Variation of Helicopter Cost per Flight Hour as a Function of Helicopter Parameter Variation

After determining the nature of the variations of the helicopter cost characteristics, we can summarize the most important results of the conducted study. Fig 5.14 shows the relationships for all forms of direct and indirect operating costs per flight hour as a function of main-rotor diameter. Fig 5.15 shows the overall relationships representing the nature of the flight-hour cost variation with variation of the main-rotor diameter, number of main-rotor blades, and engine power. We see from this latter figure that with increase of the main-rotor diameter for helicopters with the same gross weight, the cost per flight hour initially decreases and then increases again. The flight-hour cost is lowest for helicopters with the least number of blades in the large-diameter zone, while in the small-diameter zone, the cost is lowest for helicopters with the largest number of blades. However, the optimum is relatively weak. This is explained

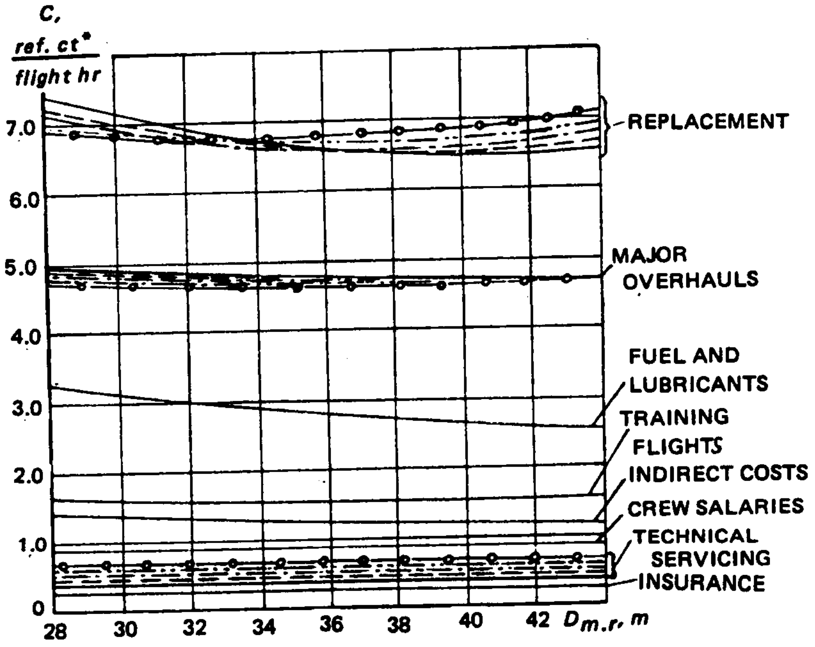

Figure 5.14 Direct and indirect costs as a function of main-rotor diameter (notation the same as in Fig 5.12)

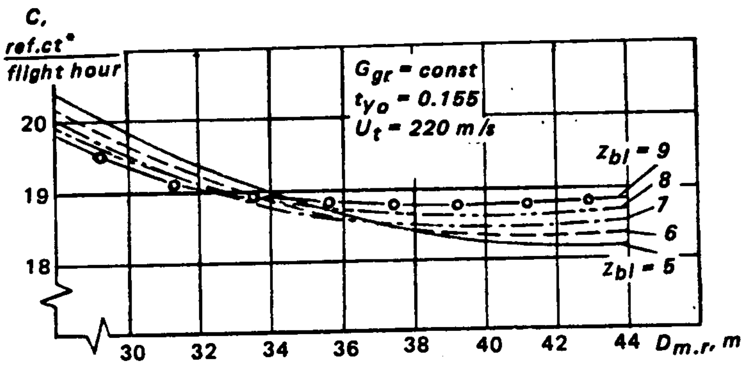

Figure 5.15 Flight-hour cost as a function of main-rotor diameter (notation same as for Fig 5.12)

for the given specific example by the fact that an increase in the main-rotor diameter leads to a considerable reduction in the costs for replacement of the powerplant and the main-rotor hub, as well as a corresponding reduction in the costs of major overhaul of these components, and also in the cost of fuel and lubricants. But these savings are accompanied by simultaneous increases in the main-rotor blade replacement costs, and in the costs of certain other items as well. However, it is clear that the picture may be different for a different relationship of the prices for materials, and fuel and lubricants, and also when using fundamentally new technical approaches.

For example, if the price of fuel incresaes several fold and simultaneously, $P_{eng}^{o.r}$ and $P_{eng}^{t.o.b}$ are halved, the minimum flight-hour cost will shift still further to the right. We note that the minimum flight-hour cost still does not completely define helicopter economic effectiveness, and therefore cannot be used as a criterion for parameter selection. An exception to this rule may be represented by helicopters which are primarily intended for long-duration flights of a patrol nature within a limited zone; for example, highway patrol.

5.3 Selection of Parameters Based on Cost Criteria for Helicopters With Different Missions

5.3.1 Selection of Optimal Cargo Transport Helicopter Parameters Based on Minimum Cost per Ton-Kilometer

We mentioned previously that the basic criterion of economic efficiency of the cargo transport operations performed by the helicopter is the cost per ton-km, defined as the ratio of the cost-per-flight hour to the productivity. By productivity, we mean the product of the payload $G_{p.l}$ and the helicopter block speed, V_{blk}.

In some methods of helicopter economic calculation, this quantity is termed the flight productivity. In order to account for the limitations with respect to calendar time, one introduces a new concept of calendar productivity. Since all the basic calendar limitations were taken into consideration in our economic analysis: in the following, we shall use only the flight productivity concept $\Pi = G_{p.l}V_{blk}$, where V_{blk} is the block speed.

Fig 5.16 shows, as an example, the productivity for one of the single-rotor helicopter variations examined in Ch 2. Here, V_{blk} = average flight speed from the time of engine start at the origin, to the time of engine shutdown at the destination .

$$V_{blk} = L_n/t_{blk}$$

where t_{blk} = block flight time,

$$t_{blk} = \tau_{gr} + \tau_h + \tau_m + \tau_{cl} + \tau_{dc} + \tau_{cr}; \qquad (5.108)$$

τ_{gr} = engine operating time on the ground (usually two to three minutes), τ_h = hovering time (usually one to two minutes); τ_m= maneuvering time (up to five minutes); τ_{cl}= time to climb to the specified flight altitude H; τ_{dc} = descent time, and τ_{cr} = flight time at cruising speed.

Now, let us see how the cost per ton-km will vary with change of the main-rotor diameter and number of blades

$$C_{ton\text{-}km} = C_{hel_n}/\xi_{l.f}\Pi_n$$

where $\xi_{l.f}$ = coefficient characterizing the average helicopter load factor (in Ch 4, we took $\xi_{l.f} = 0.75$ in estimating the annual flight time). It is convenient to make the analysis using the relative cost per ton-km:

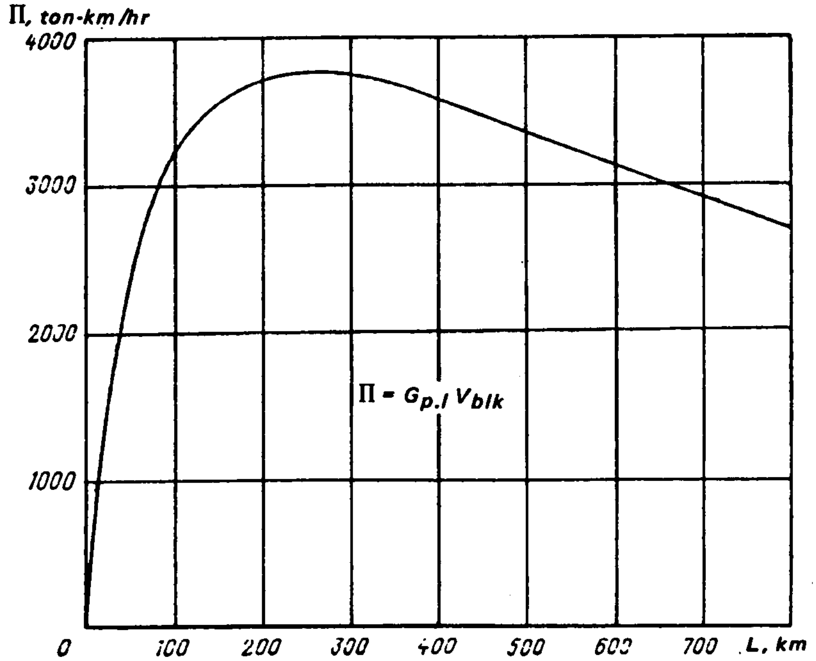

Figure 5.16 Maximum productivity as a function of stage length

$$\overline{C}_{ton\text{-}km} = C_{ton\text{-}km_n}/C_{ton\text{-}km_o} = C_{hel_n}\Pi_o/C_{hel_o}\Pi_n = \overline{C}_{hel_n}/\overline{\Pi}_n. \qquad (5.109)$$

Here, C_{hel_o} and Π_o respectively are the flight-hour cost and the productivity of the basic helicopter variant, where

$$\overline{C}_{hel_n} = C_{hel_n}/C_{hel_o} \text{ and } \overline{\Pi}_n = \Pi_n/\Pi_o.$$

Figures 5.17 and 5.18 show examples of $C_{ton\text{-}km}$ as functions of the main-rotor diameter. Analogous relations using the considered method can be obtained for the single-rotor helicopter variants with other gross weights and for helicopters of other configurations intended to perform quite different missions; differing in range, lift capability, cargo cabin dimensions, takeoff conditions, ceilings, and so on.

This technique makes it possible to include, if necessary, the variation of any other characteristic in the parametric analysis. We have already mentioned the possibility of varying the type of construction and the materials. This method also makes it possible to study how such an important parameter as the cruise speed influences the cost per ton-km of cargo-transport compound helicopters. At first glance, the advisability of increasing this speed to the maximum level possible from the technical point of view seems obvious, since it is inversely proportional to the cost per ton-km, but as we have already mentioned above, this will lead to a reduction in the annual flight time and the service life because of limitations resulting from the vibration level, etc., thus leading to an increase in the cost per flight hour.

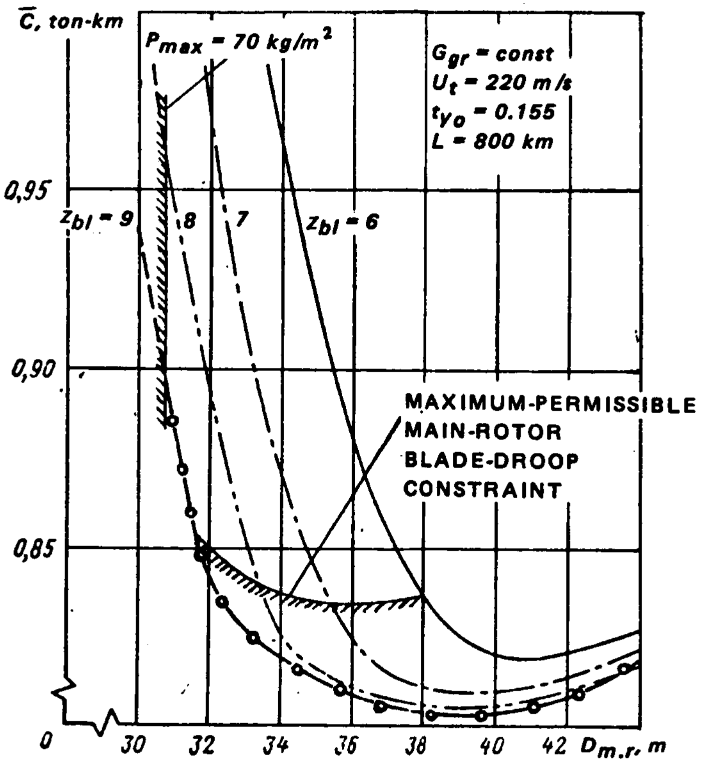

Figure 5.17 Relative cost per ton-km of single-rotor transport helicopter as a function of the main-rotor diameter

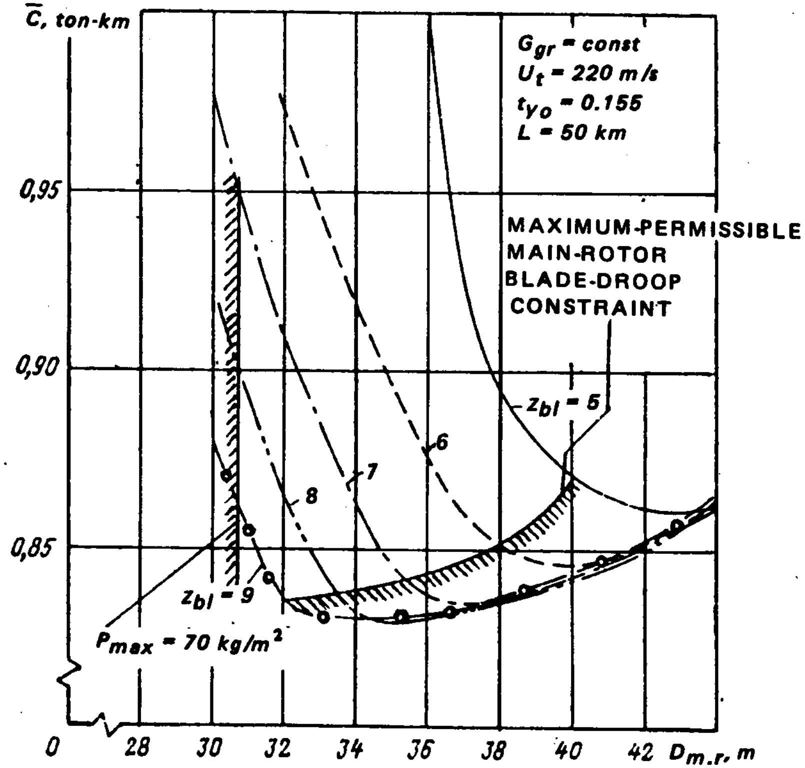

Figure 5.18 Relative cost per ton-km of a single-rotor transport helicopter as a function of the main-rotor diameter

5.3.2 Selection of Optimal Passenger Helicopter Parameters Based on Minimum Cost per Passenger-km

In modern helicopter construction practice, the passenger helicopters are developed, in principle, from previously constructed cargo-transport helicopters. Therefore, the problem of selecting the parameters for such a machine is usually replaced by the problem of selecting the cargo-transport helicopter which is most suitable for conversion into a passenger variant. This is explained by the relatively small (to date) volume of passengers traveling by helicopter.

As the basic economic criterion for selecting the parameters of such a machine, it is advisable to use the minimum cost per passenger kilometer. By this we mean the ratio of the flight-hour cost to the product of the number of passenger seats, block speed, and a coefficient accounting for the helicopter load factor.

Upon receiving the task of designing a passenger helicopter for a definite number of seats, the selection of the parameter based on this cost criterion is made by a method similar to that developed in the preceding subsection.

The nature of the variation of the cost characteristics of the basic passenger-helicopter components will be analogous to the variation of the corresponding characteristics of the cargo-transport helicopter.

The only difference will be an increase of the fraction representing the equipment cost (practically constant for all the variants): cabin interior, airconditioning system, heating, lighting, and so on.

5.3.3 Selection of Optimal Crane Helicopter Parameters Based on Minimum Cost per Ton

In designing flying cranes, the primary mission of which is the transportation of external loads, the optimal parameter selection technique is basically analogous to that examined above. Once again, the criterion is the minimum cost per ton-kilometer. However, if we wish to develop a helicopter in which the primary purpose is the assembly of various structures, then it is necessary to use different economic criteria. For example, we can, in many cases, select the parameters on the basis of the minimum cost per ton of weight of the structure being assembled with the aid of the helicopter. It is obvious that the types of structures being assembled may differ markedly in both weight and dimensions, which affects the productivity of the crane helicopter. In order to compare the different variants under the same conditions, we need to introduce the concept of the standard assembly structure. As such, we can take any of the most typical elements from which factory smokestacks, scrubbers, tall building roofs, towers, and so on, are assembled; for example, a steel-sheet tube, four meters in diameter, seven meters long, and weighing eight tons. The air purification structure was assembled from such elements with the aid of the Mi-10K flying crane in 1973 on the roof of the Sinarskiy Tubing Plant, see Fig 1.5. The design weight of the element being assembled will be equal to its own weight multiplied by a coefficient accounting for the aerodynamic download. In most practical cases, this coefficient is equal, or close to, one.

Other questions which arise in connection with the need to compare different modes of crane helicopter operations are the questions of distance from the plant being constructed to the pads on which the crane helicopter must be based and where the elements of the equipment being assembled must be located, the height of the facility being assembled, the time required for hovering with the load including installation time, the necessity for accuracy of installation, and so on. The basic data of this type (typical operation) is determined by the purchasers of the helicopter. The cost per flight hour for the various crane helicopter versions can be determined by a technique analogous to that examined above. But in evaluating the annual flight time and the costs of certain forms of maintenance, it is necessary to start with the conditions of this typical crane operation. In place of the ratio, L/V_{cr}, characterizing the part of flight service life expended in a single flight – which was used in evaluating these quantities for both cargo transport and passenger helicopters – in the corresponding formulae for the annual flight time and maintenance costs, we should use the magnitude of the overall time spent in hovering with and without the cargo, and the ferry flights from the base pad to the location of the construction and back, as determined by the normal fuel supply.

Then we evaluate the productivity for each of these variants, which is defined as the ratio of the total weight of the structure being installed to the total flight time spent directly on its installation. The optimal main-rotor diameter, number of blades, and engine power will correspond to the minimal ratio of the cost per flight hour to the crane productivity for a given cargo-lift capability.

5.3.4 Selection of Optimal AG Helicopter Parameters Based on Minimum Cost for Treating One Hectare of Cultivated Land

In selecting the optimal parameters with respect to the economic criterion of a specialized machine such as the AG helicopter, we can use the method developed above to calculate the cost per flight hour for several variants, differing in configuration, main-rotor diameters, number of main-rotor blades, installed power, and gross weight (with account for the peculiarities of the typical agricultural operation). It is natural to evaluate the AG machine productivity on the basis of time required to treat one hectare of fields, orchards, and vineyards. Obviously, the forms of treatment may be quite different. For example, one of the most promising tasks is the application of mineral fertilizers to fields.

It may not always be advantageous to modify conventional helicopters for such operations. In the case of large volumes of operations of this nature, the question arises of developing a specialized helicopter type. Considering the requirements imposed on such a helicopter, including requirements for flight speed and altitude from the viewpoint of effective field treatment, and also for productivity of the helicopter-borne agricultural equipment, we can evaluate the number of hectares treated by the helicopter per flight hour for all the variants being considered (see Ch 1). If we then divide the previously obtained corresponding costs per flight hour by these quantities, we obtain the cost of treating one hectare; and consequently, we can determine the helicopter variant with the lowest cost for treating one hectare. The problem of selecting the optimal helicopter variant used to combat agricultural pests and treat vineyards and orchards with chemicals is similarly accomplished. This approach also makes it possible to solve another interesting problem. Using this technique, we can determine the theoretical possibility of developing an AG helicopter for which the cost of treating one hectare when performing particular operations will be lower than when using ground-based equipment for this purpose. This can apply both to today's level of aircraft technology development and to that predicted for the future. Specifically, in these calculations, we can take into account the difference between the quality of the treatment of a hectare from the air and from the ground. It is well known that thanks to the higher effectiveness of field treatment with chemicals dispersed from a helicopter, increased yield will be obtained from the fields thus treated.

5.3.5 Selection of Optimal Parameters for Specialized and Universal Helicopters

It is possible that the intensive development of the national economy will require the development of still other types of specialized helicopters, for example, special fire-fighting helicopters, tanker helicopters used to refuel ground-based vehicles operating far from their bases, special helicopters for servicing off-shore oil fields, and so on.

In all of these cases, we can use the above-developed method to evaluate, with an adequate degree of accuracy, the cost per flight hour of different versions of any particular helicopter. Depending on the stated requirements, the notion of productivity can be formulated for this, or other, specialized helicopters.

The ratio of the flight-hour cost to this productivity is the criterion which makes it possible to solve the problem of selecting optimal parameters for such a machine. However, it should be noted that the development of highly specialized machines will be justified only if the following conditions are satisfied: (1) the volume of operations performed by a single helicopter guarantees sufficient utilization of the machine throughout the year; (2) the overall volume of anticipated operations is sufficient for the purchase of a significant quantity of helicopters of the given type; (3) the production capabilities of the industry make it possible to put the specialized helicopter type into series production without loss of output of other, no less important, types.

Otherwise, it will be necessary to develop a multipurpose helicopter for two or more missions. It is clear that such machines may be less effective than the specialized helicopter when performing the individual missions (including economic aspects as well). However, the use of a single universal type may be more profitable than the use of several specialized machines.

If necessary, how do we select the parameters based on the economic criterion for such a helicopter? It is clear that if the requirements for performance of the operations are divided into primary and secondary tasks, then the parameter selection is made for the primary mission using the above-described technique. If all the missions have equal importance, it is proposed that we use the ratio of the flight-hour cost to the planned benefit obtained from operation of the helicopter per flight hour as the primary criterion in selecting the parameters. The cost per flight hour is determined by the technique examined above.

By specifying the maximum allowable specific cost of performing any particular operation from the viewpoint of earning capability at the initiation of the design of a multipurpose machine, we can use the proposed technique to evaluate how the problem can be successfully solved by particular design improvements and the use of particular materials.

5.3.6 Comparson of Selected Parameters Using Weight and Minimal Operating Cost Criteria

The analysis performed in the preceding sections makes it possible to answer the following question which was posed at the beginning of these considerations: To what degree does the weight efficiency of the helicopter reflect its economic efficiency? It was shown above that if the comparison of the economic characteristics of different helicopter variants designed to the same requirements is made under the same conditions,including,((a) the same average wage level in the plants where production of the new helicopters is planned; (b) the same materials and type of structure for similar components; (c) the same helicopter production schedule, and (d) the same level of productivity, then the results of this analysis will depend only on the nature of the variation of the quantity $k_{d.p}$. These conditions are satisfied if the basic economic calculation coefficients are held constant for all the considered variants

$$k_e = const; \quad k_e' = const; \quad C' = const; \quad \text{and} \quad m_n = const.$$

The results of the weight and economic calculations made using the techniques described above make it possible to draw the following conclusions: (1) With satisfaction of the above-cited conditions, the optimum civil helicopter parameters determined using the weight criteria, correspond to the optimum parameters of these machines determined using the cost criteria if the coefficient accounting for the design difference is $k_{d.p}$ = *const* for all the considered variants. (2) With satisfaction of the indicated conditions, but with $k_{d.p} \neq$ *const*, correspondence of the "weight" and "economic" techniques for solving the basic problem of parametric analysis is possible, but not certain. In this case, in order to evaluate the degree of correspondence, it is necessary to perform special verifying economic calculations using the proposed technique. (3) If, in addition to $k_{d.p} \neq$ *const*, still other necessary conditions are not satisfied; for example, if $k_e \neq$ *const*, there may be a significant degree of noncorrespondence between the parameters selected on the basis of minimum cost of the performed operation and minimum structural weight.

The first case is very unlikely to arise in actual vehicle design practice. It is difficult to imagine how, while varying the parameters over a wide range, we can, at the same time, maintain constancy of the m_n coefficients that are determined by the type of structure of the primary components, and satisfy the condition, $k_{d.p}$ = *const*; i.e., keep the number of detail parts in each component constant.

The second and third items represent usual cases. The examples at the beginning of Ch 4 show that when comparing helicopters for which the basic coefficients are not equal, the heavier helicopter may be more economical. In application to the cargo transport helicopter, this may mean that the heavier helicopter will have a lower cost-per-flight hour, and lower cost per ton-km.

Such results of calculations made to select the optimum single-rotor cargo-transport helicopter parameters according to cost and weight criteria are compared in Figs 5.19 and 5.20. We see from the curves that, in this specific case, the results of these calculations for the 50-km range are in practically complete agreement; however, there is some discrepancy for the 800-km range.

A careful examination of the figures shows that the costs per ton-km corresponding to the optimal main-rotor diameters differ slightly with different numbers of blades.

Increasing this difference to more significant magnitudes in other cases is possible. But in the considered example $k_{d.p} \neq$ *const*, this difference cannot be very large because of factors which we have already mentioned: the increased cost of the main-rotor blades, and several other components with increase of the diameter was balanced, in considerable measure, by a simultaneous decrease in the powerplant and fuel costs.

In other words, in the calculations for one gross weight and helicopter configuration, the minimum cost per ton-km for a constant number of lifting rotor blades is, in principle, determined by the maximum cargo-lifting capacity of the helicopter. This is due to the fact that with the assumed average relationships between the basic cost items, the cost per flight hour changes very little with rotor diameter, and the change in cruise speed for all helicopter variants is also slight. This essentially explains the agreement of the obtained results.

But we should point out once again that the picture may change markedly if, in addition to varying the main-rotor diameters and number of blades, we also vary the helicopter configuration, number of control rotors, engines, gearboxes, transmission shafts, tail rotors, and other components; and also the types of their materials and structures. The change may be still more noticeable if we significantly alter the average relationship of the costs for the individual items; for example, the fuel cost is significantly increased or reduced.

When examining the variants of the cargo-transport compound helicopter, there is particular interest in the relationship between the cost per ton-km and the cruise speed. The following specific results were obtained when solving this problem in accordance with the proposed technique in application to a single-rotor compound helicopter with one lifting rotor

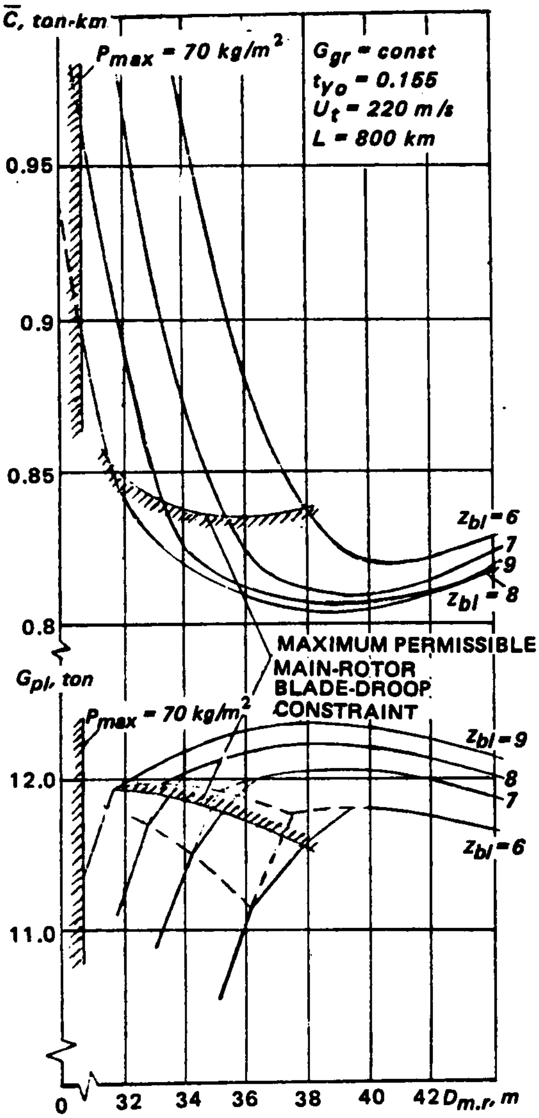

Figure 5.19 Relative cost per ton-km and maximum cargo capacity of a single-rotor helicopter as a function of main-rotor diameter

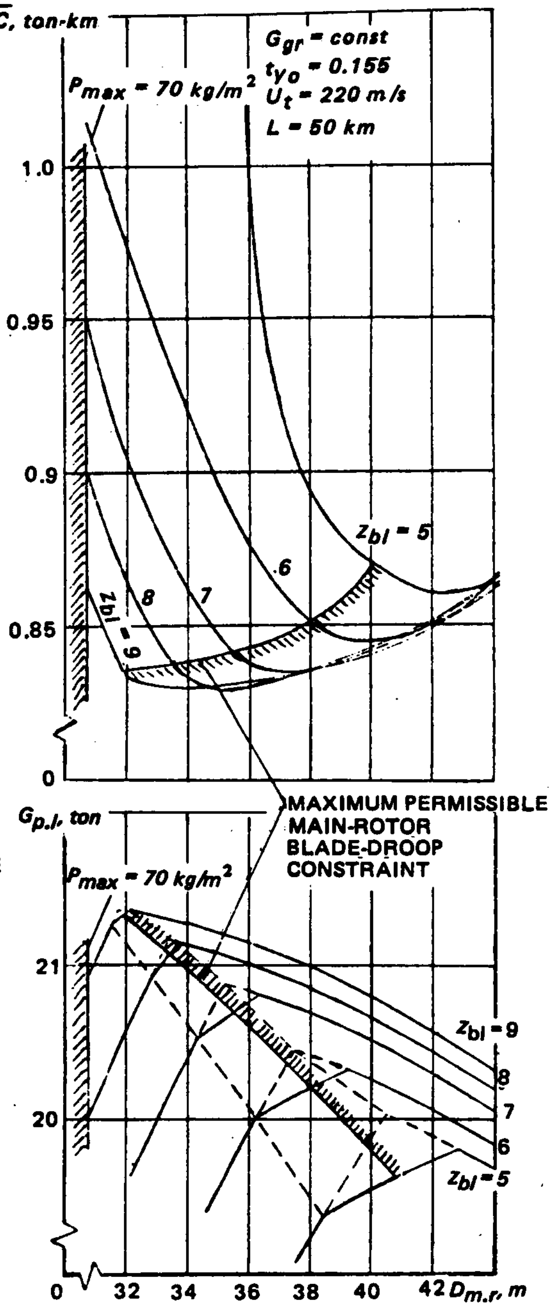

Figure 5.20 Relative cost per ton-km and maximum cargo capacity of a single rotor helicopter as a function of the main-rotor diameter

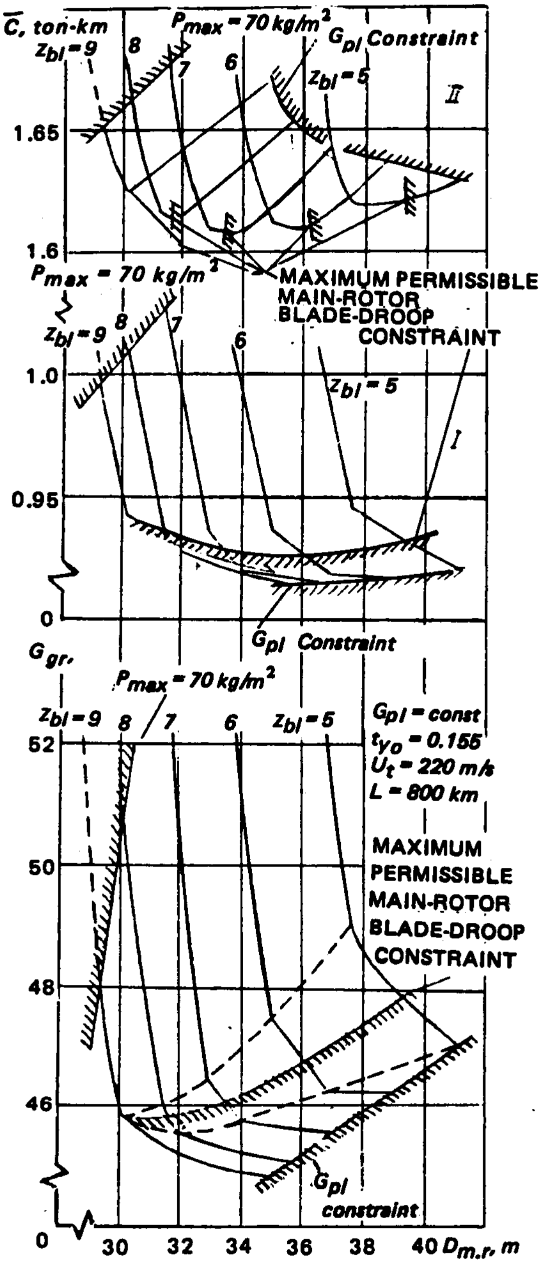

Figure 5.21 Gross weight and relative cost per ton-km as a function of main-rotor diameter (cases I and II differ in relationship as to specific material costs for the basic components):

$M_{m.g.b_{II}} = 10 M_{m.g.b_I}$; $M_{bl_{II}} = 10 M_{bl_I}$;

$4 M_{eng_{II}} = M_{eng_I}$; $M_{\phi_{II}} = 3.75 M_{\phi_I}$;

$7.5 M_{hub_{II}} = M_{hub_I}$); G_{pl} – *payload*

and two tractor propellers (see Fig 2.91). The characteristics of this aircraft were examined in Sect 2.6. The optimal variant of this compound helicopter has a cruise speed of 350 km/hr. Its productivity is 12 percent higher than that of the optimal (with respect to weight efficiency) cargo-transport pure helicopter having a speed of 260 km/hr and the same gross weight (for *L = 800 km*). The economic analysis of the compound helicopter shows that as a result of the installation on this vehicle of a wing, tractor propellers, additional gearboxes with transmission shafts, and more powerful engines, as well as due to other design peculiarities, the cost per flight hour for this machine was 11.8 percent higher than for the pure helicopter. It is obvious that the relative compound helicopter cost per ton-km is of the same order as for the pure helicopter. However, for shorter flight ranges and particularly when operating with external loads, the pure helicopter is preferable with regard to the economic characteristics.

In order to get a complete picture of the relationship between the weight and cost optima for the compound helicopter variants being compared, it is necessary to plot graphs of the type shown in Figs 5.19 and 5.20 for several gross weights, and then determine from them the range of gross weights for which it is possible to satisfy the basic requirement with regard to transporting the specified cargo over the specified distance without exceeding these quantities, and replot the graphs of aircraft weight and economic characteristics for these gross weights. In the lower part of Fig 5.21, an example is shown of the gross weight of the single-rotor cargo-transport helicopter as a function of the main-rotor diameter with different number of blades for constant payload (the curves are plotted on the basis of Fig 2.78). Obviously, the helicopter variants which are optimal with respect to weight efficiency are represented on the curves by the lowest possible gross weights; the corresponding coordinate points lie on the boundary representing the payload constraint.

The upper part of Fig 5.21 shows the relative cost per ton-km as a function of the main-rotor diameter for the entire examined range of gross weights for which transportation of the specified cargo load is possible.

Specifically, we see from a comparison of the upper and lower curves that the minimal costs for helicopter variants differing in number of main-rotor blades do not, in all cases, correspond to their weight efficiency maxima.

This is seen more clearly in Fig 5.22, which presents the relative cost per ton-km as a function of gross weight for the same helicopter variants (case II). For example, we see that for the variants with a five-bladed rotor, the minimum cost per ton-km is achieved for gross weights higher than those for which the maximum weight efficiency is obtained.

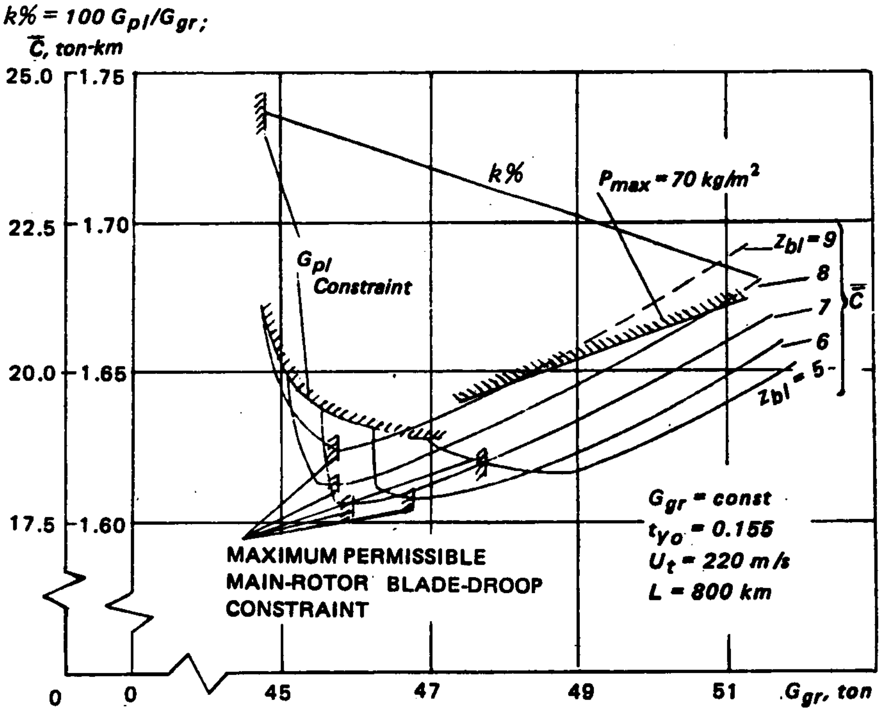

Figure 5.22 Relative cost per ton-km as a function of gross weight

The best variant from the viewpoint of economic efficiency is the helicopter with a seven-bladed main rotor having a gross weight of 46.2 tons; while from the viewpoint of weight efficiency, the optimal is the variant with a nine-bladed main rotor having a gross weight of 45.7 tons, i.e., a difference of 0.5 tons. If we ignore the blade-droop constraint, this difference increases to one ton. In other words, the calculations confirm the statements made above regarding the possibility of developing, under certain conditions, a helicopter that has the best of all possible economic indices, but which is, at the same time, far from optimal in regard to weight efficiency. To what degree do these analytical results correspond to the known actual data?

We gave several examples at the beginning of Ch 4 which confirm the presented deviations. We shall discuss another example. The first flight of the French SA350 helicopter was made in 1974. According to the foreign press[28], the basic concept of this machine was to develop a helicopter having the best possible economic characteristics. This objective was achieved by the use of several design approaches which made it possible to reduce, by a factor of two, the total number of bearings and gears in the helicopter, and also made possible the use of heavier (but at the same time, several times less expensive) automotive accessories. For example, the aircraft fuel pump weighing 0.8 kg was replaced by a heavier auto pump weighing 1.35 kg, but the latter was one-eighth as expensive. In spite of the fact that the helicopter structural weight increases when using this approach, its economic efficiency is 30 percent higher than that of any other helicopter in production at the present time.

Since, when developing new machines, the helicopter designers cannot be certain that the basic parameters which they have selected with respect to maximum weight efficiency or maximum productivity criteria, or any other effectiveness criterion (see Ch 1) also provide, in all possible cases, the maximum economic efficiency of the newly designed rotary-wing aircraft, it is necessary to verify, at definite stages in the design of the new machine as to whether the so-selected parameters meet the economic criteria as well. For this assessment, the techniques examined in Chs 4 and 5 can be used.

REFERENCES

1. M.F. Astakhov, A.V. Karavaev, S. Ya. Makarov, et al. *Airplane Stress Analysis Handbook* (in Russian). Oborongiz, Moscow, 1954.

2. A. A. Badyagin and E. A. Ovrutskiy. *Design of Passenger Aircraft with Account for Economy of Operations* (in Russian). Mashinostroyeniye, Moscow, 1964.

3. I. P. Bratukhin. *Helicopter Design and Construction* (in Russian). Oborongiz, Moscow, 1955.

4. L. S. Vil'dgrube. Account for the Influence of Twin-Rotor, Side-by-Side, or Tandem Helicopter Bodies in Determining the Main-Rotor Blade Configuration which is Optimal for the Hovering Regime. *Uchenyye zapiski TsAG*, Vol 3, No 5, 1972.

5. L. S. Vil'dgrubee. Study of Helicopter Flight Characteristics. *Helicopter Design.* Thematic Collection of Scientific Studies of Moscow Institute (in Russian), No. 302, Moscow, 1974.

6. A. V. Glichev. Economic Effectiveness of Technical Systems (in Russian). *Ekonomika*, Moscow, 1971.

7. N. N. Gromov, E. V. Mukhordykh, E. A. Ovrutskiy, et al. Air Transport Economics (in Russian). *Transport.* Moscow, 1971.

8. V. I. Dalin. *Helicopter Design* (in Russian). Mashinostroyeniye, Moscow, 1971.

9. I. S. Dmitriev and S. Yu. Esaulov. *Single Rotor Helicopter Control Systems* (in Russian), Mashinostroyeniye, Moscow, 1969.

10. M. M. Maslennikov, Yu. G. Bekhli, and Yu. L. Shal'man. *Gas Turbine Engines for Helicopters* (in Russian), Mashinostroyeniye, Moscow, 1969.

11. M. L. Mil, A. V. Nekrasov, A. S. Braverman, et al. *Helicopters. Analysis and Design*, Vol 1 (in Russian), Mashinostroyeniye, Moscow, 1966.

12. M. L. Mil, A. V. Nekrasov, A. S. Braverman, et al. *Helicopters. Analysis and Design*, Vol 2 (in Russian), Mashinostroyeniye, Moscow, 1967.

13. R. A. Mikeyev. *Helicopter Stress Analysis* (in Russian, MAI, Moscow, 1972.

14. R. A. Mikeyev. *Helicopter Stress Analysis* (in Russian), MAI, Moscow, 1974.

15. E. A. Ovrutskiy. Economic Evaluation of Transport Airplanes. *Aeroflot.* Moscow, 1940.

16. P. R. Payne. *Helicopter Dynamics and Aerodynamics* (Russian Translation). Oborongiz, 1963.

17. V. P. Petruchik. Selection of Crane-Helicopter Optimal Configuration and Basic Parameters. *Helicopter Design.* Thematic Collection of Scientific Studies of MAI, No. 302 (in Russian), Moscow, 1974.

18. S. A. Sarkisyan and E. S. Minaev. *Economic Evaluation of Flight Vehicles* (in Russian). Mashinostroyeniye, Moscow, 1972.

19. V. M. Sheynin and V. I. Kozlovskiy. *Problems of Passenger Airplane Designs* (in Russian), Mashinostroyeniye, Moscow, 1972.

PAGE 280 INTENTIONALLY BLANK

20. V.M. Sheynin, *Weight and Transport Effectiveness of Passenger Airplanes* (in Russian), Oborongiz, Moscow, 1962.

21. Tencer, Ben and J.P. Cosgrove, Heavy Lift Helicopter Program: An Advanced Technology Solution to Transportation Problems, *Journal of Aircraft*, No 11, 1972, p. 753_758.

22. By the Technical Editor, A Look at Lynx, *Flight*, No 3222, 1970, p. 908–910.

24. Hooper, W.E., Some Technical Aspects of Boeing Helicopters, *The Aeronautical Journal of the Royal Aeronautical Society*, No. 700, Vol. 73, April 1969, p. 347–354.

25. *L'Aeronautique et l'-Astronautique*, No. 47, 1974, p. 24.

26. Les helicopteres, *Aviation Magazine*, No. 661, July 1975, p. 43.

27. Longer Life Sought for CH-46, CH-47, *Aviation Week & Space Technology*, No. 10, September 1974, p. 43–46.

28. Marchinski, L.J. *Design to Cost at Work for Helicopter Systems*. The 30th Annual National Forum of AHS, Preprint No. 810, p. 1–10.

29. Peck, W.B., Binder, S., and Bieber, R.D. High-Speed Gearing and Shafting. Problem in Helicopter Design, *SAE Journal*, October 1962, p. 84–88.

30. Plaks, A., Metzger, R.F., MacDonald, H.I., Meier, R.S., *Improved Cost Effectiveness of Helicopters Through a Two-Point Design Criterion*, The 30th Annual National Forum of AHS, Preprint No. 811, p. 1–10.

31. Rowe, N.E., *Complexity and Progress in Transport Aircraft*, RAS, No. 11, p. 787–788.

32. *Turboshaft Engine T64-MTU-7.*

33. Vertol: premiers détails–sur le futur HLH de l'US Army, *Air & Cosmos*, No. 441, 1972, p. 26.